LA-13110-PR
Progress Report

1995 LABORATORY-DIRECTED RESEARCH AND DEVELOPMENT

RECEIVED
APR 0 1
OSTI

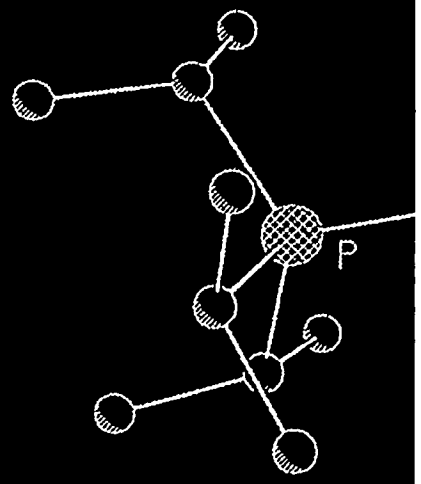


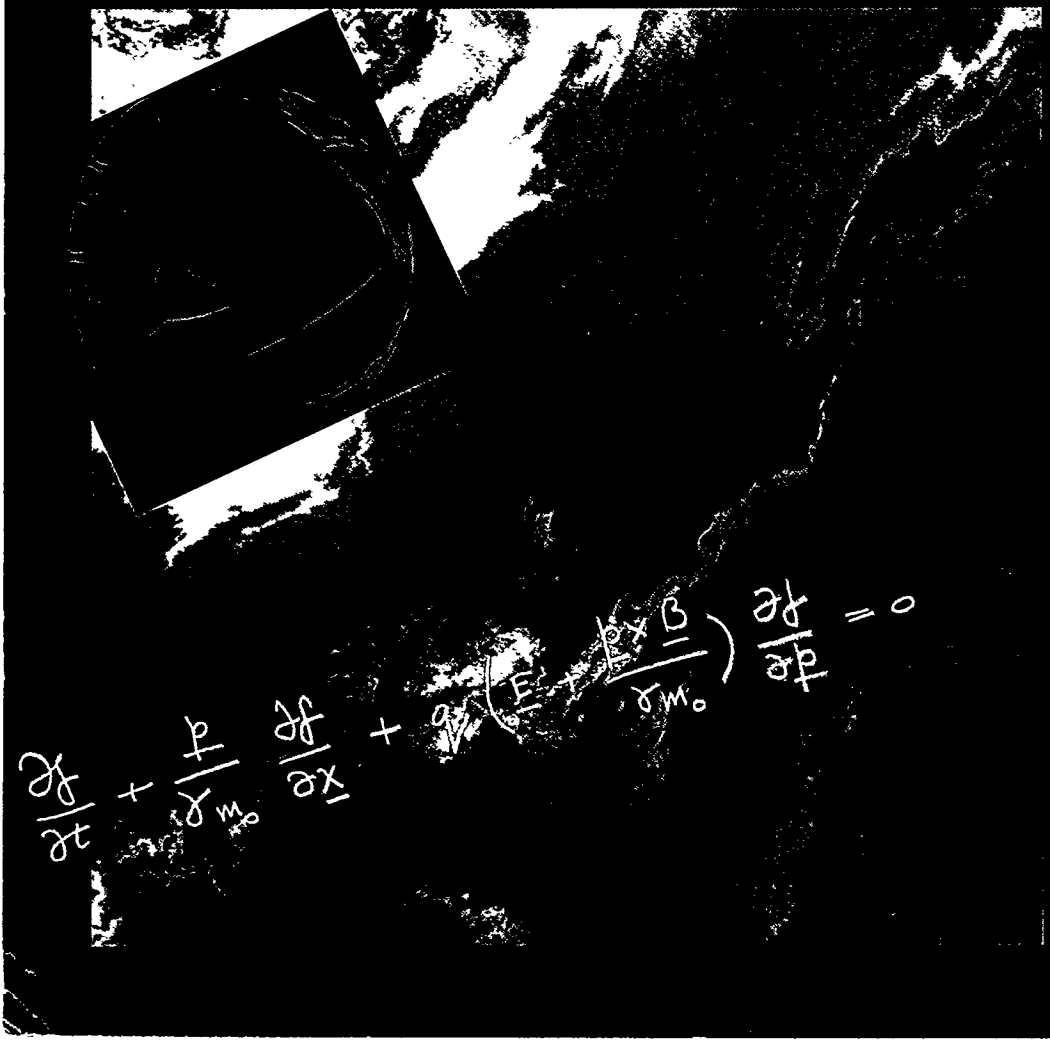
Los Alamos
NATIONAL LABORATORY

Los Alamos National Laboratory is operated by the University of California for the United States Department of Energy under contract W-7405-ENG-36.

Abstract

This report summarizes progress during FY 1995 in projects funded by the Laboratory-Directed Research and Development (LDRD) program. The report comprises an overview of the LDRD program, summaries for the 332 R&D projects undertaken during FY 1995, and an index to the projects' principal investigators. Projects are grouped by LDRD component—Individual Projects, Competency Development, and Program Development—with projects within each component being grouped according to the nine technical disciplines for LDRD research: materials science; engineering and base technologies; plasmas, fluids, and particle beams; chemistry; mathematics and computational sciences; atomic and molecular physics; geoscience, space science, and astrophysics; nuclear and particle physics; and biosciences.



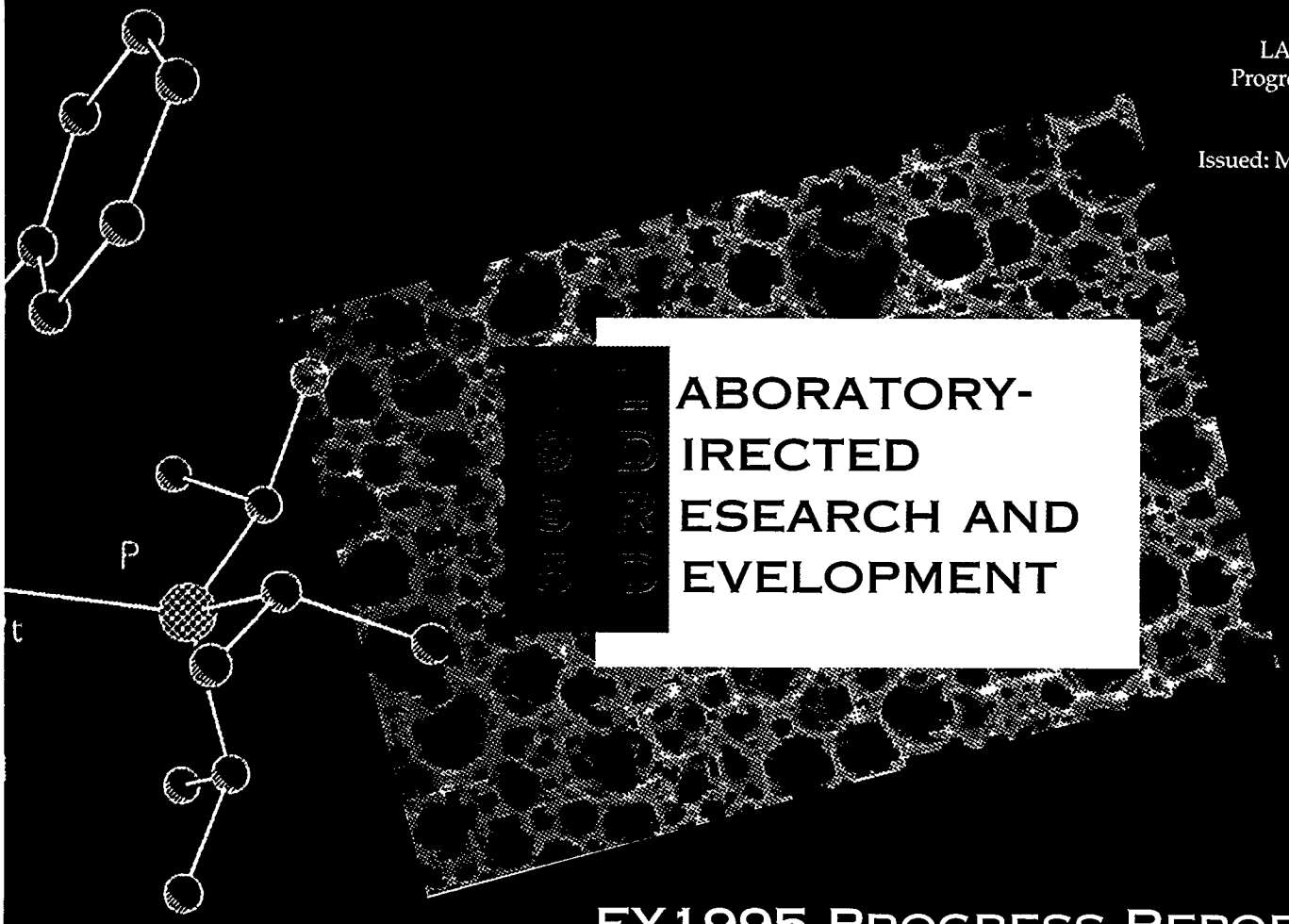


Front cover:

The background image is a two-dimensional simulation of temperature distributions due to fluid turbulence; lighter areas represent higher temperatures (S. Chen, "Studies of Structure of Turbulence by High-Resolution Simulation and Theory"). The superposed image is a three-dimensional simulation of the thermal structure of convection in the earth's mantle (G. Glatzmaier, "Modeling the Heat Flow and Resulting Dynamics in the Earth's Interior"). The Vlasov equation describes the motion of charges under the influence of self-fields and external fields.

LA-13110-PR
Progress Report

UC-900
Issued: March 1996



LABORATORY-DIRECTED RESEARCH AND DEVELOPMENT

FY1995 Progress Report

Compiled by
John Vigil and Judy Prono

Los Alamos
NATIONAL LABORATORY
Los Alamos, New Mexico 87545

PUBLISHED BY LOS ALAMOS NATIONAL LABORATORY

LABORATORY DIRECTOR: SIG HECKER

DIRECTOR FOR SCIENCE AND TECHNOLOGY BASE PROGRAMS: AL SATTLEBERGER

OFFICE LEADER FOR LABORATORY-DIRECTED RESEARCH AND DEVELOPMENT: ED HEIGHWAY

SCIENTIFIC EDITOR: JOHN VIGIL

LDRD OFFICE TEAM: AUDREY ARCHULETA, SHELLY CROSS, AND LEONARD SALAZAR

MANAGING EDITOR: JUDY PRONO (CIC-1)

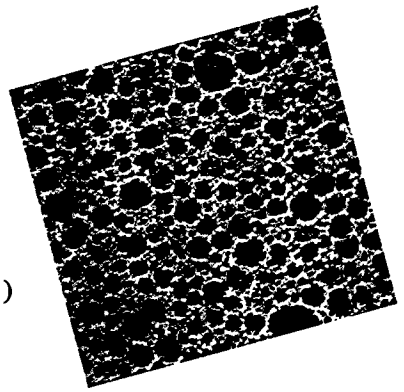
EDITORS: ILEANA BUICAN, AMY FERGUSON, BRIAN FISHBINE, TODD HEINRICHS, AMY REEVES, AND JAMES RUSSELL (CIC-1)

EDITORIAL SUPPORT: EILEEN PATTERSON (CIC-1)

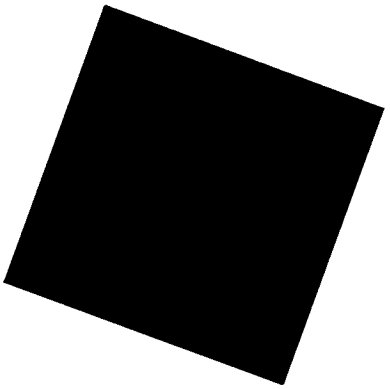
COVER DESIGN: SUSAN CARLSON (CIC-1)

LAYOUT, COMPOSITION, AND PRODUCTION: WENDY BURDITT (CIC-1)

PRINTING COORDINATION: GUADALUPE ARCHULETA (CIC-17)



THE PREVIOUS REPORTS IN THIS SERIES, UNCLASSIFIED, ARE LA-12499-PR, LA-12680-PR, AND LA-12880-PR.





This report was prepared as an account of work sponsored by an agency of the United States Government. Neither the Regents of the University of California, the United States Government nor any agency thereof, nor any of their employees, makes any warranty, express, or implied, or assumes any legal liability or responsibility for the accuracy, completeness, or usefulness of any information, apparatus, product, or process disclosed, or represents that its use would not infringe privately owned rights. Reference herein to any specific commercial product, process, or service by trade name, trademark, manufacturer, or otherwise, does not necessarily constitute or imply its endorsement, recommendation, or favoring by The Regents of the University of California, the United States Government, or any agency thereof. The Los Alamos National Laboratory strongly supports academic freedom and a researcher's right to publish; therefore, the Laboratory as an institution does not endorse the viewpoint of a publication or guarantee its technical correctness.

LA-13110-PR

CONTENTS

1 LDRD PROGRAM OVERVIEW—FY 1995

INDIVIDUAL PROJECTS

MATERIALS SCIENCE

7 Artificially Structured Nonlinear Optical and Electrooptic Materials

10 Rigid Molecular Foams

10 Monte Carlo Code for Neutron Scattering Instrument Design and Analysis

11 Dynamic Properties of Advanced Materials

14 Thermodynamic and Electrodynamic Studies of Unusual Narrow-Gap Semiconductors

14 Phase Stability of Transition Metals and Alloys

15 Chemical Vapor Deposition of Complex Oxides: Materials and Process Development

16 Characterization and Manipulation of Broken-Symmetry Materials at Phase Boundaries

16 Optical Spectroscopy of Porous Silicon

18 Ultrasensitive Ultrasonic Transducer Studies

19 Structural Phase Transitions in Nonstoichiometric Oxides and Other Materials

19 Strain Measurement in Individual Phases of Multiphase Materials During Thermomechanical Loading

22 New Deposition Processes for the Growth of Oxide and Nitride Thin Films

22 Strongly Correlated Electronic Materials

ENGINEERING AND BASE TECHNOLOGIES

25 Generation of High-Power, Subpicosecond, Submillimeter Radiation for Applications in Novel Device Development and Materials Research

28 Optical-Fiber Laser Amplifier for Ultrahigh-Speed Communications

28 Polymers for Integrated Optical Interconnects

30 High-Temperature Materials Synthesis Without Heat: Oxide Layer Growth on Electronic Materials Using High-Kinetic-Energy Atomic Oxygen

30 Large Dynamic Range, Picosecond-Resolution Radiation Detection Based on Low-Temperature-Grown Epitaxial GaAs Films

32 Instrumentation for High-Efficiency, High-Sensitivity Actinide Analysis

34 Development of Multimode Neutron-Noise Theory

34 Optical Imaging Through Turbid Media Using a Degenerate Four-Wave-Mixing Correlation Time Gate

35 New Applications for Zeeman Interferometry

DISTRIBUTION OF THIS DOCUMENT IS UNLIMITED MASTER

Individual Projects (cont.)

Engineering and Base Technologies (cont.)

35 A Comprehensive Monitoring System for Damage Identification and Location in Large Structural and Mechanical Systems

36 Gravity Gradiometry Based on High-T_c Superconducting Sensors

36 Development of New and Efficient Hard-Rock Mining Methods Using Pulsed Laser Excavation

37 Application of Intense Surface Discharge VUV Light Sources to Photoresist Ashing in Semiconductor Manufacturing

37 The Development of Fullerene-Based Hydrogen Storage Systems

38 Generation of Intense Electromagnetic Radiation with Explosively Driven Piezoelectric Material

39 Femtosecond Scanning Tunneling Microscope

40 Ultratough Ultrasonic Transducers and Robust Algorithms for Resonant Ultrasound Spectroscopy

40 Value Analysis Technology for R&D Environments

41 Materials Analysis of Deposits Made by the Directed Light Fabrication Process

42 Novel Thin-Film Electrocatalytic Sensors

42 Telemetric Heat Stress Monitor (THSM) Spin-offs

43 Bartas Iris Biometrics

43 A Gated, Integrating, Cathode-Pad Readout Chamber

44 Telepresence Control of Robots Used in Hazardous Environments

Plasmas, Fluids, and Particle Beams

45 Turbulent Scaling in Fluids

46 Dusty Plasmas

47 Developing Electron-Beam Bunching Technology at Subpicosecond Pulse Lengths for Improving Photon Sources

47 Delta-f and Hydrodynamic Methods for Semiconductor Transport

48 Plasma Immersion Ion Implantation for Semiconductor Film Growth

49 Investigation of Charge Transport and Electromagnetic Effects in Advanced Microelectronics and Optoelectronics

51 Turbulence and Turbulence Spectra in Complex Fluid Flows

52 High-Impedance Plasma Opening Switches

53 Determination of the Nuclear-Induced Electrical Conductivity of ^{3}He for Magnetohydrodynamic Energy Conversion

54 A Feasibility Study of Beam-Chopping at Low Energy for the Manuel Lujan Jr. Neutron Scattering Center

54 A Compact Compton-Backscattering X-Ray Source for Mammography and Coronary Angiography

55 Next-Generation Magnetic-Nozzle Prototype

56 High-Power, High-Frequency, Annular-Beam, Free-Electron Maser

INDIVIDUAL PROJECTS (CONT.)

CHEMISTRY

57 Technetium Chemistry

57 New Approaches for Quantum Chemical Calculations on Very Large Molecules

59 Quantum Resonance Effects in Exchange, Photodissociation, and Recombination Reactions

59 Metal Vapor Synthesis in Organometallic Chemistry

60 Separations Chemistry of Toxic Metals

61 New Catalytic Processes for the Production of Specialty Polyolefins

62 Multifunctional Self-Assembled Monolayers

63 Temperatures and Vibrational Frequencies of Liquid N_2/O_2 and CO/O_2 Mixtures Shock Compressed to 100 kbar and 2000 K

64 Metal-Ligand "Multiple" Bonding: Revelations in the Electronic Structure of Complexes of High-Valent f-Elements

65 Chemistry and Catalysis in Supercritical Media

66 Binding of Hydrocarbons and Other Extremely Weak Ligands to Transition Metal Complexes that Coordinate Hydrogen: Investigation of *cis*-Interactions and Delocalized Bonding Involving σ-Bonds

68 Ionically Conducting Polymers for High-Energy-Density Batteries

69 Photoredox Reactions: Energy Storage and Halocarbon Degradation

69 Decay of Surface Nanostructures via Long-Time-Scale Dynamics

70 Molecular-Level Assemblies on Metal Oxide Surfaces

71 Asymmetric Catalysis in Organic Synthesis

72 New Fullerene-Based Mixed Materials: Synthesis and Characterization

73 Self-Assembled Thin-Film Chemical Sensors

MATHEMATICS AND COMPUTATIONAL SCIENCES

75 Dispersive Internal Long-Wave Models

76 Multidimensional Methods for Hyperbolic Problems

76 Algorithms for Adaptive, Composite, Overlapping Meshes Used on Message-Passing Architectures

77 Theoretical Design Tools for Advanced Semiconducting Devices

77 Development of the Applied Mathematics Originating from the Group Theory of Physical and Mathematical Problems

78 New Class of Random Number Generators Required for Advanced Computer Architectures

79 Hard Chaos, Quantum Billiards, and Quantum-Dot Computers

80 Applied Mathematics of Chaotic Systems

81 Modeling Mesoscopic Phenomena in Extended Dynamical Systems

82 Studies of Structure of Turbulence by High-Resolution Simulation and Theory

83 Industrial Processing of Complex Fluids: Formulation, Modeling, and Algorithms

84 Wavelet Theory and Its Applications

84 Solution-Adaptive Methods for Low-Speed Flows and All-Speed Flows

Individual Projects (cont.)

Mathematics and Computational Sciences (cont.)

85 Parallel Three-Dimensional Spherical-Harmonics Transport Methods

85 Geometry in the Large and Hyperbolic Chaos

86 Mimetic Difference Approximations of Partial Differential Equations

86 Data Embedding Research

87 Dispersive Water Waves in One and Two Dimensions

88 Developing the R&D 100 Award– Winning Lattice Boltzmann Permeameter Toward a Marketable Product

88 Combinatorics, Geometry, and Mathematical Physics

89 Wavelet Transforms as Solutions of Partial Differential Equations

90 The Fundamental Role of Solitons in Nonlinear Partial Differential Equations

Atomic and Molecular Physics

91 Multiphoton Processes for Atoms in Intense Electromagnetic Fields

93 Final-State Effects and Correlation in Atomic Systems

93 Determination of Interionic Potentials in Molecules

94 Nonlinear Interactions of X-Rays with Atoms

96 Calculation of Satellite Line Structures in Highly Stripped Plasmas

98 Nucleation and Condensation Science

99 State-to-State Photodetachment in the Two-Electron Hydrogen Ion

99 Dynamics of Quantum Wave Packets

Geoscience, Space Science, and Astrophysics

101 A Study by Computer Simulation of the Generation and Evolution of the Earth's Magnetic Field

103 Cosmological Gamma-Ray Bursts

103 Magmatic Tritium

104 Lead Immobilization in Thermally Remediated Soils and Igneous Rocks

104 Spacetime Geodesy

106 The Galactic/Globular Cluster Pulsar Content and the 2.1-ms Pulsar Candidate in Supernova 1987A

108 Mineralogical and Geochemical Aspects of Mineral-Induced Disease

108 Using Microspheres as Tracers for Flow in Geologic Media

109 Magnetic Reconnection in Space Plasmas

110 A Coupled Regional Climate-Biosphere Model for Climate Studies

112 New Mechanism for Lightning Initiation

114 Macroscopic Time and Altitude Distribution of Plasma Turbulence Induced in Ionospheric Modification Experiments

Individual Projects (cont.)

Geoscience, Space Science, and Astrophysics (cont.)

114 Experimental Studies of Auroral-Arc Generators

115 Heterogeneous Processing of Bromine Compounds by Atmospheric Aerosols: Relation to the Ozone Budget

116 Atmospheric Aerosol Chemistry Analyzer: Demonstration of Feasibility

118 Measuring the Magnetic Connectivity of the Geosynchronous Region of the Magnetosphere

118 Integrating Chemistry into Three-Dimensional Climate Models: Detailed Kinetics in the Troposphere and Stratosphere of a Global Climate Model

120 Particle Acceleration from Reconnection in the Geomagnetic Tail

121 Stochastic Imaging of Oil and Gas Reservoirs

121 Flare Star Monitoring with a New Single-Photon-Counting Imaging Detector

122 Minerals of the Earth's Deep Interior

122 Deriving the Structure of Presupernovae and δ-Scuti Stars Using Nonradial Oscillations

123 Remote Sensing of Thundercloud Electric-Field Airglow

124 The Powering of Black Hole Objects by Accretion

125 Plasmasphere Refilling: New Numerical and Computational Tools

126 Experimental Cosmology: The Early Universe after Cosmic Microwave Background Explorer

128 The Detectability of Asteroids and Comets before Earth Impact

Nuclear and Particle Physics

129 Neutrino Properties and Fundamental Symmetries

130 Development of Radioactive Beams at the LANSCE Linear Accelerator for a High-Precision Test of the Standard Model

132 Nonperturbative Estimates of the Standard Model Parameters

132 A Continuous Watch of the Northern Sky Above 40 TeV with the CYGNUS Array

133 L3 Physics at the Z Resonance and a Search for the Higgs Particle

133 Research in Baryon Number Violation at Supercollider Energies

134 Exploring and Testing the Standard Model and Beyond

135 Determination and Study of Cosmic-Ray Composition Above 100 TeV

135 Nonequilibrium Dynamics of the Quark-Gluon Plasma in Heavy-Ion Collisions

136 Antiquark Distributions In The Proton

136 Design of a Neutrino Oscillation Experiment

137 Time-Reversal Tests in Polarized Neutron Reactions

137 Theoretical Research Relevant to Medium Energy Upgrades and Experiments

Individual Projects (cont.)

Biosciences

139 Theoretical Studies of the Interaction of Water with DNA Oligomers and Proteins

140 Structural Determination of Larger Proteins Using Stable Isotope Labeling and NMR Spectroscopy

140 Positional Cloning of Disease Genes on Chromosome 16

141 Sum-Frequency Generation Studies of Membrane Transport Phenomena

142 Predicting B-DNA Structure from Sequence

144 Directly Labeled Fluorescent DNA Probes for Chromosome Mapping

145 Fast Events in Protein Folding

146 Measurement of Photodynamic Therapy Drug Concentrations in a Tissue Phantom

147 Ultrasensitive Nucleic Acid Sequence Detection by Single-Molecule Electrophoresis

147 Optimal Screening Designs For Biomedical Technology

148 Optimization and Monitoring of Hollow-Fiber Bioreactors

149 The Preparation and Utilization of ^{13}C- and ^{15}N-Labeled DNAs for the Determination of Unusual DNA Structures Relevant to the Human Genome Project by Nuclear Magnetic Resonance Spectroscopy

149 Applications of Strand-Specific In Situ Hybridization

150 Determining the Role of the Telomere on the Severity of Birth Defects

152 Engineering Sequence-Specific RNA and Single-Stranded-DNA Binding Proteins

152 Development of an Ultrasensitive and Rapid DNA Repair Assay

153 Structure and Thermodynamics of Surface Recognition

153 Computer Simulation of Protein Solvation, Hydrophobic Mapping, and the Oxygen Effect in Radiation Biology

Competency Development Projects

Materials Science

159 Bulk and Surface Electronic Structure of Actinide, Rare Earth, and Transition Metal Elements and Compounds

160 Diffuse Transport in Modern Polymeric Materials

160 Advanced Deformation Process Modeling

161 Orientation Distribution Function Determination by Rietveld Refinement

162 Implications of Diffraction In Situ Loading Macrostrain Measurements in Composites and Finite Element Interpretations

163 Characterization of Advanced Electronic Materials

164 Design and Implementation of an X-Ray Strain Measurement Capability Using a Rotating Anode Machine

Competency Development Projects (cont.)

Materials Science (cont.)

166 Lattice Coupling to Electronic and Magnetic Instabilities in High Magnetic Fields

167 Development of Pair Distribution Function Analysis

168 Measurement by Neutron Diffraction of Strains in Advanced Engineering Structural Materials Including AlSiC and AlTiC

170 Chemical and Physicochemical Properties of Submicron Aerosol Agglomerates

171 Bulk Amorphous Materials

171 Fabrication of Boron-Phosphide Neutron Detectors

172 Polymers for Nuclear Materials Processing

173 Advanced Biomolecular Materials Based on Membrane-Protein/Polymer Complexation

174 Nanometer-Scale Materials: Semiconductors to Fullerenes

174 Analysis of Structure and Orientation of Adsorbed Polymers in Solution Subject to a Dynamic Shear Stress

177 Heavy Fermions in High Magnetic Fields

177 Science and Technology of Reduced-Dimensional Magnetic Materials

178 Nonlinearity in Structural and Electronic Materials

179 Neutron Scattering as a Probe of Liquid-Crystal-Polymer-Reinforced Composite Materials

182 Formation of Drug-Bearing Vesicles in Mixed Colloids of Bile Salts and Phosphatidylcholine

182 Characterization of Bioactive Materials Using Neutron Reflectivity and Atomic Force Microscopy

183 Characterization of Active Sites in Zeolite Catalysts

183 Alloy Design and Phase Stability of the Ternary Alloy Titanium-Aluminum-Niobium

184 Structural and Magnetic Characterization of Actinide Materials

185 A Thermodynamically Consistent, Damage-Dependent Interface Debonding Model for Composites

186 Production of High Specific Activity Si-32

186 Equation of State (EOS), Thermodynamic, and Structural-Mechanical Properties of Intermetallic Compounds

187 Correlated Electron Theory Project

188 Physical Properties and Mantle Dynamics

190 Scanning Probe Microscopy Competency Development

191 High Resolution Electron Microscopy of Materials

Competency Development Projects (cont.)

Engineering and Base Technologies

195 Radiation Hardness Measurements of New Permanent Magnet Materials for High-Intensity Linac Applications

195 Laser-Sheet Imaging of High-Explosive-Driven Interfaces

196 Short-Pulse, Electric-Discharge Degradation of Toxic and Sludge Wastes

197 Ultrasensitive Sensors for Weak Electromagnetic Fields Using HTS SQUIDs for Biomagnetism, NDE, and Corrosion Currents

197 Development of Inexpensive Continuous Emission Monitors

Plasmas, Fluids, and Particle Beams

199 Generation and Compression of a Target Plasma for Magnetized Target Fusion

199 Development of Ion-Beam Techniques for the Study of Special-Nuclear-Materials-Related Problems

200 Advanced Modeling of High-Intensity Accelerators

Chemistry

201 Binding Carbon Dioxide in Mineral Form: A Critical Step Toward a Zero-Emission Coal Power Plant

201 Foreign Nuclear Test Radiochemical Diagnostics

202 The Characterization of Atmospheric Aerosols: Applications to Heterogeneous Gas-Particle Reactions

203 Detection of Arsenic by Resonance Ionization Mass Spectrometry

204 Kinetic Studies of Competitive Adsorption Processes Related to Automobile Catalytic Converters

205 Investigations of Biomimetic Light-Energy-Harvesting Pigments

Mathematics and Computational Sciences

207 The Continued Benchmarking of Ocean Circulation Models

207 Applications of Mathematical Analysis of Nonlinear Physical Systems

208 Mesoscale Ocean Dynamics Modelling

210 Lie Group Applications to the Solution of Differential Equations

COMPETENCY DEVELOPMENT PROJECTS (CONT.)

MATHEMATICS AND COMPUTATIONAL SCIENCES (CONT.)

211 Adaptive Mesh Refinement Algorithm Development and Dissemination

212 A Neural-Network-Based System for Damage Identification and Location in Structural and Mechanical Systems

213 Simulation Methods for Advanced Scientific Computing

214 Neutron Star Evolution and Emission

214 Modeling Complex Phenomena: Multiple Length and Time Scales in Extended Dynamical Systems

216 Modeling the Heat Flow and Resulting Dynamics in the Earth's Interior

217 Numerical Methods Based on Nonlinear Dynamics for Modeling the Global Ocean

218 Advanced Three-Dimensional Eulerian Hydrodynamic Algorithm Development

218 Studies of Dynamical Processes Affecting Global Climate

220 Application of Discrete Mathematics

220 Lattice Boltzmann Research

221 Phase Transitions, Nonequilibrium Dynamics, and Critical Behavior of Strongly Interacting Systems

222 Numerical Simulations of Disordered Superconductors

222 Geometrically Compatible 3-D Monte Carlo and Discrete-Ordinates Methods

223 Transactional Memories: A New Abstraction for Parallel Programming

223 Computational Modeling of Materials Processing and Processes

224 Development of the First Nonhydrostatic, Nested-Grid, Grid-Point Global Atmospheric Modeling System on Massively Parallel Machines

226 Similarity Landscapes: An Improved Method for Scientific Visualization of Information from Protein and DNA Database Searches

226 Lithospheric Processes

227 Nonlinear Analysis of Biological Sequences

227 High-Performance Computations of Electron Microstructures

228 Complex Systems—Prediction and Characterization

230 Covariation of Mutations: A Computational Approach for Determining Function and Structure from Sequence

230 Development of an Integrated System for Estimating Human Error Probabilities

231 Development of an Automated Core Model for Nuclear Reactors

231 Transport Processes in Space Plasmas

GEOSCIENCE, SPACE SCIENCE, AND ASTROPHYSICS

235 Analysis and Visualization of Global Magnetospheric Processes

235 Subsurface Noble Gas Transport at the Nevada Test Site

236 The Microbial Dissolution of Iron from Iron-Bearing Minerals

236 Remote Sensing Science—New Concepts and Applications

Competency Development Projects (cont.)

Biosciences

237 Molecular Characterization of Flow-Sorted Mammalian Centromeres

237 Competency Development in Antibody Production for Cancer Cell Biology

238 Applications of Optical Trapping to Single-Molecule DNA Sequencing

238 Development of Biosensors/Probes Based on Spectroscopic Monitoring of Enzymes and Other Proteins Encapsulated in Sol-Gel Glasses

239 Structure, Dynamics, and Function of Biomolecules

240 The Solution Structure of the cAMP-Dependent Protein Kinase

242 Advanced NMR Technology for Bioscience and Biotechnology

Program Development Projects

Materials Science

247 Development of High-Temperature Superconducting Thick Films

247 Surface Polymerization Agents

248 Characterizing and Reducing AC and DC Losses in High-Temperature Superconducting Conductors and Cables

250 Electronic Devices Based on High-Temperature Superconducting Thin Films

250 Advancing the Technology Base for High-Temperature Membranes

251 Giant Magnetoresistance Materials for Magnetic Recording Technology

252 Subsurface Characterization and Three-Dimensional Profiling of Semiconductors by Magnetic Resonance Force Microscopy

254 Artificially Structured Electronic and Biomimetic Materials by Molecular Self-Assembly

254 Electronic Diamond: Fabrication Processes and Electron Emission Performance

255 Neutral Stream Processing of Semiconductor Materials

256 Ion Flooding to Precharge Insulating Materials

257 Microcellular Ceramic Foams for Radar-Absorbing Structures

257 Development of High Magnetic Fields for Energy Research

258 Technical Evaluation of Russian Aircraft Stealth Coating and Structural Materials

258 Development of Transparent Conducting Films for Flat-Panel Displays

259 Development of Structural Materials Exhibiting Dielectric and Magnetic Loss at Radio Frequencies

260 Structure Versus Properties in High-Temperature Superconductors

Program Development Projects (cont.)

Engineering and Base Technologies

263 Detection of Underground Structures and Tunnels

264 Accelerator-Driven Transmutation of High-Level Waste from the Defense and Commercial Sectors

265 Feasibility of Microwave Interferometry and Fourier Transform Infrared (FTIR) Spectrometry for High-Spectral-Resolution Sensing

265 Performance Monitoring for Plume Remediation and Containment Actions

266 Megagauss Technology and Pulsed-Power Applications

268 Advanced Satellite Sensors: Low-Energy Neutral Atom (LENA) Imager

269 Thermoacoustic Natural Gas Liquefier

269 A Predictive Ocean Oil Spill Model

270 Advanced Tunable Laser Source for DoD Applications

271 Establishing the Operational Durability of Polymer Light-Emitting Diodes

271 Development of a High-Count-Rate Neutron Detector with Position Sensitivity and High Efficiency

272 Development of a Low-Level In-Line Alpha Counter (LLILAC)

274 In Situ Microwave-Energy-Based Soil Remediation

275 Russian Collaborations on Lasers and Advanced Optics

275 Directed Light Fabrication—A Laser Metal-Deposition Process for Fabrication of Near-Net-Shape Components

276 Development of a High-Gradient Magnetic Separator Using High-Temperature Superconductors

277 Active Vibration Control of Civil Structures

278 Hydrogen Fueling Station Development and Demonstration

279 Night Vision Device Technology Development

279 The Application of Microrobotics in Warfare

280 Electromagnetic Targeting of Guns

281 Remote Moving Target Indication Assessment

282 Autonomous Biomorphic Robots as Platforms for Sensors

Plasmas, Fluids, and Particle Beams

283 Contamination and Uniformity Control in Plasma Processing Tools

284 Advanced Technology for Nitrogen Oxide (NO_x) Abatement in Flue Gas Using Microwave Irradiation of Coal Char

285 Waste Minimization in Chrome Plating

286 Plasma Source Ion Implantation for Advanced Manufacturing

287 Advanced Ignition of Jet Turbine Engines

Program Development Projects (cont.)

Chemistry

289 Integrated Treatment for Mixed/Legacy Wastes Containing Metals and Organic Compounds

290 Separations Technology Development for Accelerator Transmutation Technology Concepts

291 Decontamination of Radioactive Liquids by Freeze Concentration and Fractional Precipitation

292 Radionuclide Separations Using Pillared Layered Materials

293 Chemical Conversions in Supercritical Media: Environmentally Sound Approaches to Processes and Materials

293 Catalysis for the Utilization of Carbon Dioxide as an Alternative Chemical Feedstock

294 Chelating Water-Soluble Polymers for Waste Minimization

Mathematics and Computational Science

295 Global Nuclear Material Flow Model

296 Intelligent Controllers for Battlefield Simulations

296 Process Simulation, Control, and Optimization for Industrial Energy Efficiency

297 Nonproliferation/Counter-proliferation Synthetic Wargaming Environment

298 A Systems Framework for Defining Nonproliferation Program Technology Requirements

298 Modeling and Simulation for the Semiconductor and Optoelectronic Industries

299 Visualization Capability for Nonproliferation and Emergency Training: A "Poor Man's" Virtual Reality System

300 Image Processing Technology

300 Nanoscience and Technology: Self-Assembling Nanoscale Quantum Devices

302 High-Performance Computing for Simulation of Domestic Petroleum Reservoirs

302 Prototype Demonstration of Radiation Therapy Planning Code System

304 Industrial Applications for the Los Alamos Materials Modeling Platform

306 Low-Speed Flow Hydrodynamics

306 National Information Infrastructure Applications

Atomic and Molecular Physics

307 Measurement Criteria Analysis for Krypton, Xenon, and Hydrogen (Hydrogen/Deuterium/Tritium) Isotopes and Concentration Variability at Distance

Program Development Projects (cont.)

Geoscience, Space Science, and Astrophysics

309 Advanced Laser Remote Sensing

310 Prestack Migration of Three-Dimensional Seismic Data

311 Coupled Transport and Chemical Interactions in Petroleum Reservoirs: Multicomponent-Tracer Large-Scale Application Demonstration

312 Hyperspectral Scanner Design and Analysis

Nuclear and Particle Physics

313 Development of the Accelerator-Driven Energy Production Concept

314 A High-Power Accelerator Driver System for Spallation Neutron Sources

315 Disposition of Weapons Plutonium as Nonfertile Fuel for Light-Water Reactors

316 Spallation Source Neutron Target Systems

318 An Ultracold Neutron Facility at LANSCE

Biosciences

319 A Consortium for Biomedical Applications of Single Molecule Detection

320 Cancer Risk Assessment

321 Molecular Medicine for the 21st Century: A Computational Basis for Design and Critique of Vaccines and Therapeutics

321 Safe Extension of Red Blood Cell Storage Life at 4°C

322 Human Brain Mapping: Experimental and Computational Approaches

323 Deformable Human Body Model Development

324 Development of Experimental Techniques to Study Protein and Nucleic Acid Structures

326 Development and Testing of Biosensors that Quantitatively and Specifically Detect Organic Contaminants

327 Neutron Scattering and Nuclear Magnetic Resonance (NMR) Spectroscopy Structural Studies of Protein-DNA Complexes

328 Computational and Theoretical Aspects of Biomolecular Structure and Dynamics

335 Index of Principal Investigators

LDRD PROGRAM OVERVIEW—FY 1995

Ed Heighway

The Laboratory-Directed Research and Development (LDRD) Program is authorized by Congress as a means for the Laboratory to invest in innovative research that will extend our science and technology capabilities in support of Laboratory missions. This extension may come through exploring fundamentally new areas of science, through publishing results of quality research and thus attracting and retaining the best personnel, or through developing new approaches or improved techniques to solve existing scientific problems.

All LDRD projects must be relevant to the Laboratory's missions. The LDRD program invests in projects across the full spectrum of competencies and disciplines underlying these missions. The majority of projects are also dual-use in nature—that is, they benefit both the civilian and national security missions of the Laboratory. To place the LDRD investment in context, a breakdown of the FY 1995 funding for major programs at the Laboratory is shown in Fig. 1.

LDRD Program Structure

The LDRD program at Los Alamos has three components—Individual Projects (IP), Competency Development (CD), and Program Development (PD). All components are competed, and proposals are reviewed by Laboratory managers or through peer review before being funded. In FY 1995, the program funded 332 projects for a total expenditure of $61.6 million; Fig. 2 shows funding distribution among the three components. Progress summaries for these projects are given in this report.

Individual Projects. This component funds basic and innovative research whose potential is high but whose payoff may be distant. These projects are more exploratory in nature—mapping uncharted territory—than those of the other two components. Proposals are evaluated and ranked by technical peer-review teams (one team for each of nine technical disciplines), and the highest ranked and most relevant ones are selected for funding by the director of the Laboratory's Science and Technology Base Program. These projects are generally three years in duration. In FY 1995, 157 IPs were funded at an average cost of $170,000.

Competency Development. This component funds the Laboratory's key science and technology competencies that underlie our ability to execute our missions and be responsive to new Department of Energy (DOE) and national issues. CD projects are intended to be cross-cutting: that is, they draw on the resources of several Laboratory divisions and have clear institutional value beyond the strategic interest of any single division. CD projects are proposed by the scientific staff through their technical division and program offices, reviewed both for technical content and strategic value, and ultimately selected by the Laboratory Director.

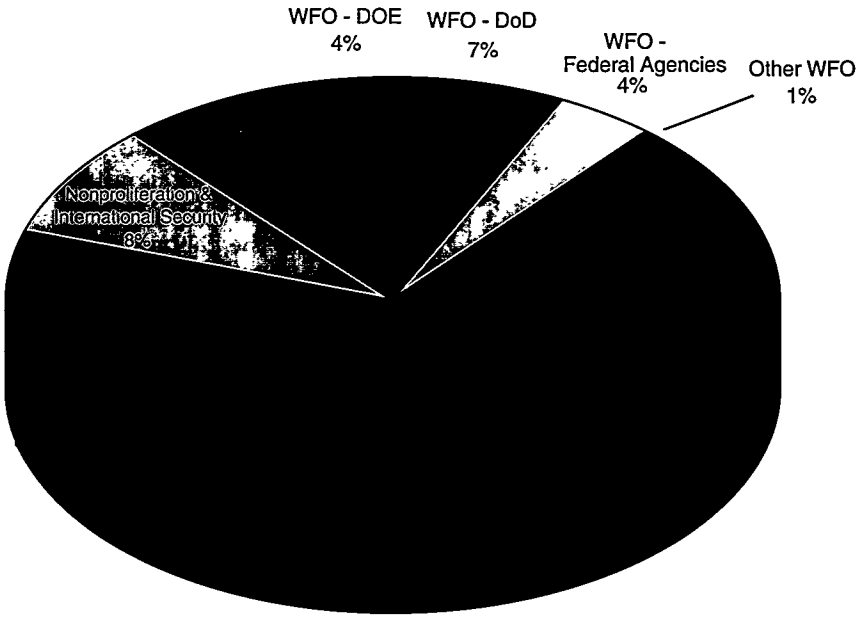


Fig. 1. Proportional funding for major programs at the Laboratory.

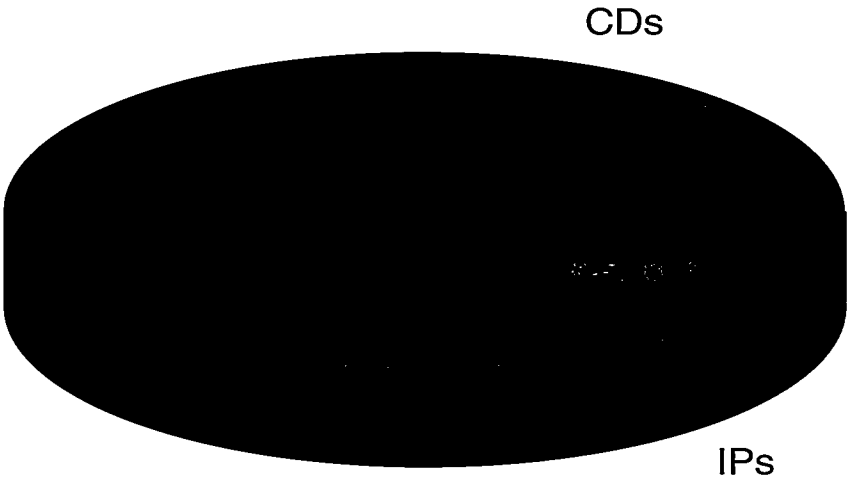


Fig. 2. FY 1995 LDRD research investment by program component.

There were 88 CD projects funded in FY 1995 at an average cost of $145,000. Duration of CD projects is generally three years. The Laboratory's core competencies are as follows:

Nuclear Weapons Science and Technology

Complex Experimentation and Measurement

Nuclear and Advanced Materials

Theory, Modeling, and High-Performance Computing

Nuclear Science, Plasmas, and Beams

Analysis and Assessment

Earth and Environmental Systems

Bioscience and Biotechnology

Program Development. This component funds innovative R&D that allows the Laboratory to examine ways of meeting extended or future needs of program sponsors. The research is exploratory or demonstrational, assessing the feasibility of new scientific approaches or technologies and establishing a technical path to advanced solutions of existing problems. PD projects are generally of shorter duration than those in the other two components, typically being funded for only one or two years. In FY 1995, 87 PD projects were funded at an average cost of $275,000. Proposals are solicited, reviewed, and ultimately selected by scientific managers and technical staff within the Laboratory's eight program offices.

The high quality of science supported by all components of the LDRD program is attested by the number of related scientific publications, patents, and awards. Over the ten year period from 1985 to 1994, LDRD projects generated 53% of the Laboratory's refereed publications, 40% of our patent awards, and 60% of our R&D 100 awards. In addition, the LDRD program is a significant testing ground for the talent attracted to the Laboratory through our postdoctoral program. Almost 50% of postdoctoral staff members participate in LDRD projects. Of these, some 20% go on to become permanent Laboratory employees and contribute to our core scientific missions.

LDRD Research Highlights

Advanced research projects are by their very nature explorations at the edge of scientific understanding. Most LDRD projects are multipurpose in that they generally support more than one Laboratory competency, involve more than one scientific discipline, and have potential applications to both the civilian and defense sectors. While the R&D investment may be made with a particular goal in mind, the actual return is often realized in a broad increase in capability or understanding that can be widely applied.

In this progress report, a number of projects have been highlighted with longer summaries that provide more insight into the projects' scope and accomplishments. These highlighted projects were selected across the spectrum of LDRD research to reflect the diversity of the program's portfolio.

Projects highlighted in the field of nuclear materials and processes are the work of Wills on predicting the properties of actinide alloys under pressure, Jarvinen's study of the use of polymers in processing nuclear materials separations, Lindemuth's collaborative research with the Russians on extreme matter conditions, and Olivares' new instrumentation to rapidly measure actinide abundance and composition.

Conventional (nonnuclear) materials projects that have been highlighted are Maley's studies of high-temperature superconducting materials that achieved record high-current densities in tape conductors, Thompson's use of high magnetic fields to study the electronic, magnetic, and structural correlations of high-temperature superconductors, Gray's study of high-strength, high-stiffness composites for use at high temperature, Donohoe's work evaluating the properties of high-performance nonlinear optical materials, Bedell's development of a theoretical understanding of strongly correlated electron materials, and Kwan's

micromodeling to simulate potential electronic device performance.

Earth and environmental science projects highlighted describe the work of Glatzmaier in modeling Earth's magnetic field and successfully showing field reversal, Roussel-Dupré's study of the role of runaway air breakdown in explaining transionospheric pulse pairs, Holm's development of tools to model and understand nonlinear behavior in mesoscale ocean dynamics, Paul Smith's design of ligands to separate toxic materials with high selectivity, and Gregory Smith's study of the effects of solvents and stress on the effectiveness of polymer-based separation.

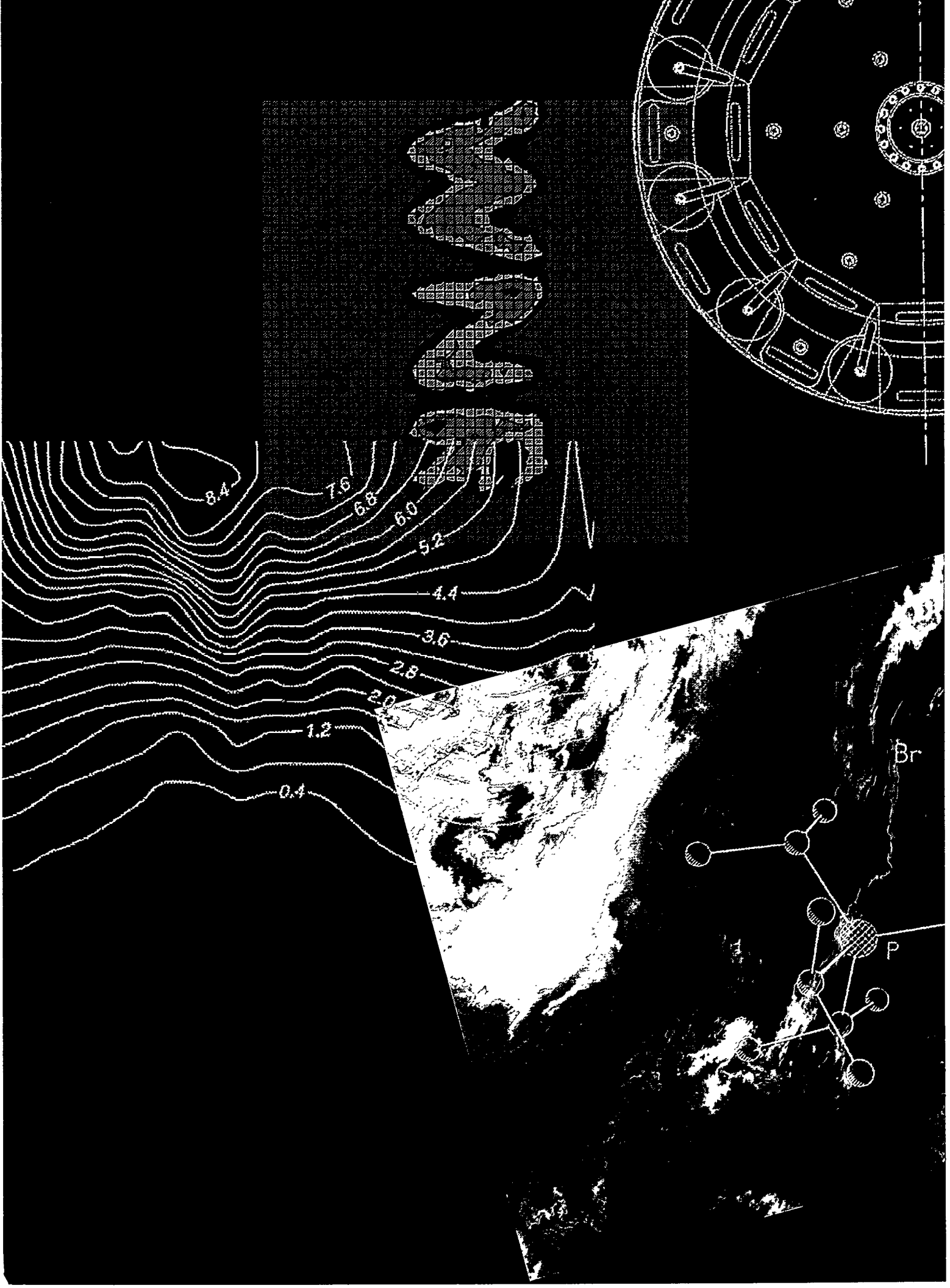
In mathematics and computation, the projects highlighted are the work of Mainieri in his search for low-dimensional ways to capture the dynamics and patterns of complex problems, Jen's work to allow analytical and computational description of chaotic systems, and Garcia's modeling of the complex dynamics and nonlinear motion of biomolecules.

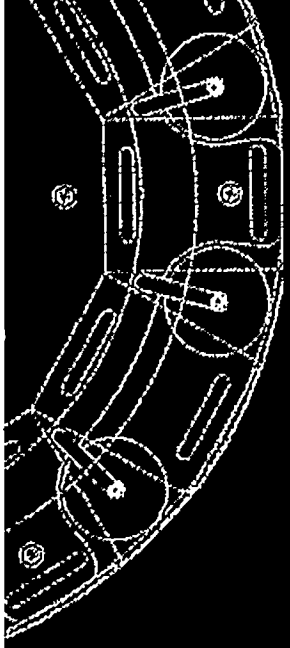
Highlighted projects focused on developing applications of radiation in different forms are Hjelm's study of neutron scattering as a means to measure nanoscale organization in composite materials, Tuszewski's use of plasma immersion ion implantation to grow thin films, Fazio's production of intense radiation from piezoelectric materials for defense applications, Taylor's development of terahertz radiation, and Schultz's study of laser radar as a means to measure aerosol drift and the presence of airborne particulates.

Finally, the most fundamental projects highlighted are Bowles' development of an ultra-low-background helium-3 detector to measure solar neutrino fluxes, Collins' study of multiphoton atomic processes in laser-generated intense electric fields, Kyrala's study of nonlinear effects of x-rays such as two-photon ionization of atoms, Marrone's development of DNA probes for chromosome mapping, and Trewhella's use of neutron and x-ray scattering to study proteins and nucleic acid.

This report is divided into three sections that describe the projects in each LDRD program component. Within each section, project summaries have been further subdivided into nine technical disciplines that reflect the spectrum of R&D activities at Los Alamos:

- Materials Science
- Engineering and Base Technologies
- Plasmas, Fluids, and Particle Beams
- Chemistry
- Mathematics and Computational Sciences
- Atomic and Molecular Physics
- Geoscience, Space Science, and Astrophysics
- Nuclear and Particle Physics
- Biosciences

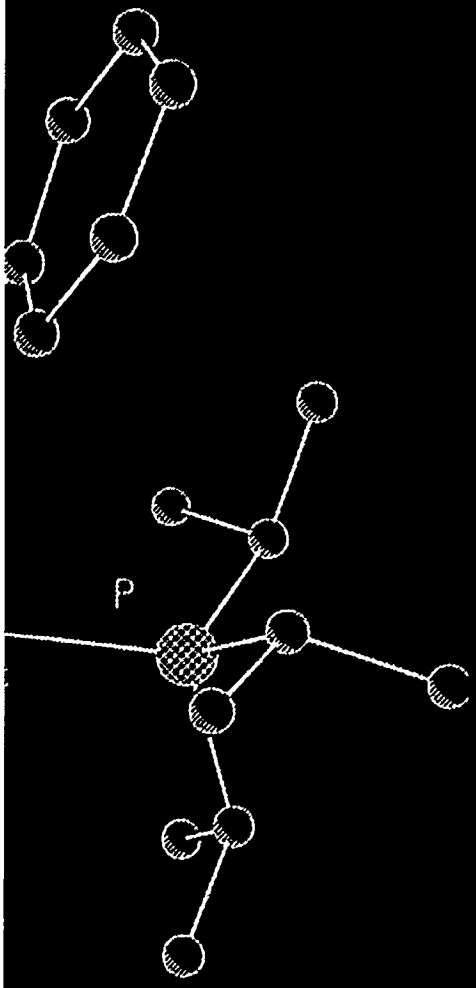

8.4
7.6
6.8
6.0
5.2
4.4
3.6
2.8
2.0
1.2
0.4
Br
P



1

Individual Projects

Individual Projects (IPs) are staff-initiated R&D geared to strengthening the Laboratory's science and technology base and fostering a stimulating research environment. These projects accounted for 41% of this year's LDRD funding and almost half of its numbers, with their subjects ranging from transducers and robotics to quark-gluon plasmas and DNA. They also varied in their scope of work, with some occupying only a fraction of a single staff member's time and others involving small teams of investigators.



IPs supported research in all nine LDRD disciplinary categories, reflecting their alignment both with the Laboratory's primary mission of reducing the nuclear threat and with our extensive involvement in R&D related to nonnuclear defense, energy, environment, space, health, and transportation initiatives. IPs play a key role in maintaining the expertise and state-of-the-art technologies that underpin the Laboratory's scientific and engineering excellence.

ARTIFICIALLY STRUCTURED NONLINEAR OPTICAL AND ELECTROOPTIC MATERIALS

Robert Donohoe

Emerging electrooptic technologies—optical signal processing, switching, and data manipulation—will require high-performance nonlinear optical (NLO) and electrooptical (EO) materials that can be made into useful devices. The goal of this project is to combine physical characterization and materials modeling to guide the rational synthesis of artificially structured materials optimized for NLO and EO applications.

In this project we have produced new chromophoric materials which contain donor and acceptor chemical groups that have been optimized for the red and near-infrared spectral regions. We attached the chromophores directly to optical substrates using covalent bonding of self-assembled mono- and multilayers. We then measured the NLO response of these new materials.

We also measured the coverage and molecular orientation of other self-assembled monolayers (SAMs). We determined that ordering in these materials arises from the competition of bonding to the surface and mutual steric effects which force alignment of the dipolar chromophores.

Developing New Self-Assembled NLO Chromophores

Organic NLO chromophores are typically π-conjugated molecules with a D-π-A structure, where D and A are, respectively, electron donor and acceptor portions of the molecule and π is a π-conjugated segment or sensitizer. This structure has been widely used to attain large values of the molecular second-order nonlinear susceptibility β. For these experiments we used the chromophore calixarene.

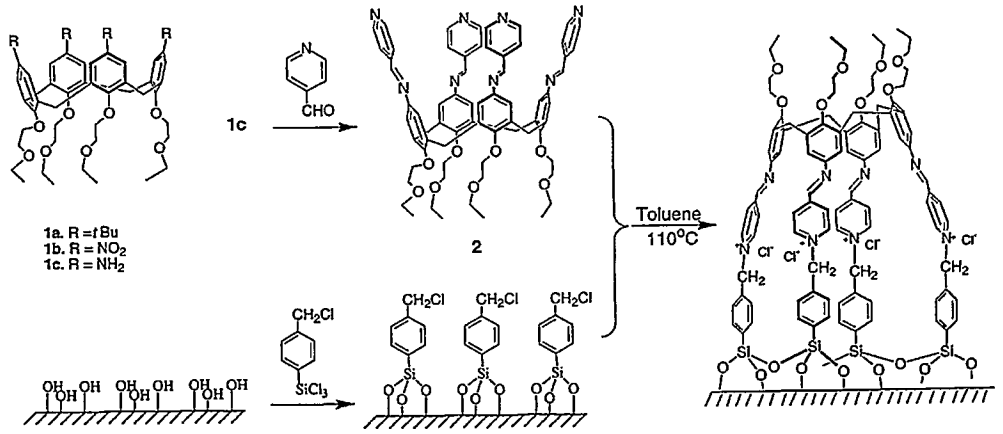
We tethered D-π-A molecules together with methylene bridges to build a chromophoric pyramid, as shown in the first figure. To obtain maximum molecular β, the orientations of the D-π-A units should be more or less parallel. We achieved this condition by synthesizing calix[4]arene into a frozen "cone" by substituting ethoxyethyl groups at the lower rim of the calixarene. We functionalized the upper rim of the calixarene to incorporate pyridyl units. We then constructed the covalently bonded SAMs of the pyramid-like imine derivative of calix[4]stilbazole using the methodologies reported by Li et al. A space-filling model on the surface of the pyramid is shown in the first figure.

Using ^{1}H nuclear magnetic resonance and Fourier transform infrared spectroscopy, we showed that the resulting calixarene precursor has a rigid structure and fixed dipole orientation. SAMs of this compound should show higher alignment and better thermal and structural stability than SAMs with a single chromophoric unit.

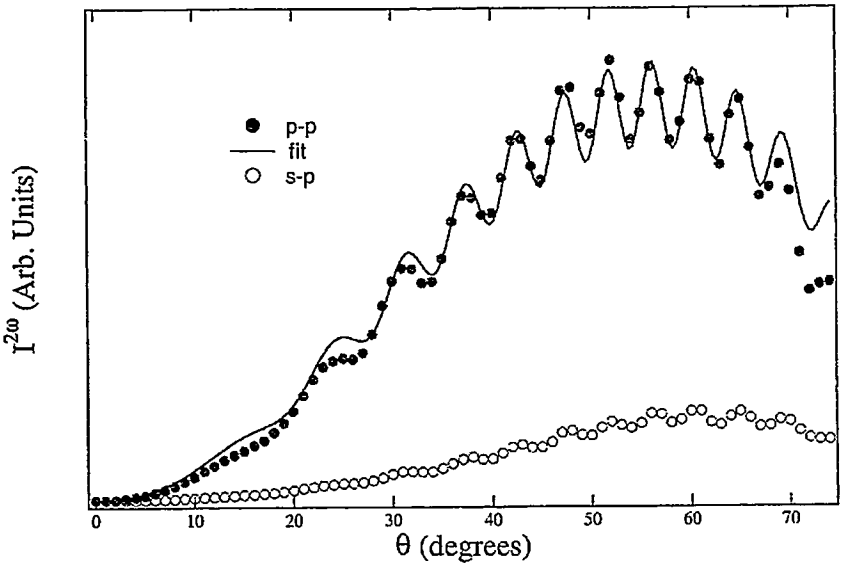
In order to study the molecular orientation and the NLO response of this monolayer, we measured its second-harmonic generation (SHG). Using femtosecond pulses with a fundamental wavelength of 862 nm, we observed *p*-polarized SHG from both *p*- and *s*-polarized fundamentals and measured the angular dependence of the SHG, as shown in the second figure. We deduced an average molecular orientation of $\psi \sim 37 \pm 3^\circ$ by modeling the angular-dependent SHG response (assuming the thin-film index of refraction to be 1.7). By calibrating to reference *y*-cut quartz, we also deduced an absolute magnitude for d_{33}, the second-order nonlinear susceptibility, of ~60 pm/V—an exceptionally large value.

The solid lines in the second figure are best fits to an expression which has the same physical origin and angular dependence as the well-known Maker fringes seen in bulk samples. The wavelength dependence (fundamental λ = 890–750 nm, harmonic λ = 445–375 nm) indicates a gradual increase of d_{33} as the fundamental moves to shorter wavelengths. This behavior is consistent with normal refractive-index dispersion in this spectral region as the charge-transfer resonance at 390 nm is approached. The longest wavelength (890 nm) is far from the charge-transfer resonance; the value quoted for d_{33} (60 pm/V) is largely nonresonant. We find a value for d_{33} of ~90 pm/V at λ = 750 nm, indicating a slight two-photon enhancement at shorter wavelengths.

We have concluded that this technique produces monolayers with exceptionally large d_{33} values and robust molecular-dipole alignment. We expect that multilayer films fabricated from "pyramid"-like molecules will have similarly attractive properties.



Synthesis of surface building blocks—calix[4]arene-based molecular pyramids and strategy for the construction of self-assembled monolayer architectures.



Femtosecond SHG signal vs. incident angle for p-polarized SHG from both p- (solid circles) and s-polarized (open circles) fundamental at a wavelength of 862 nm, plotted together with best theoretical fit (solid line).

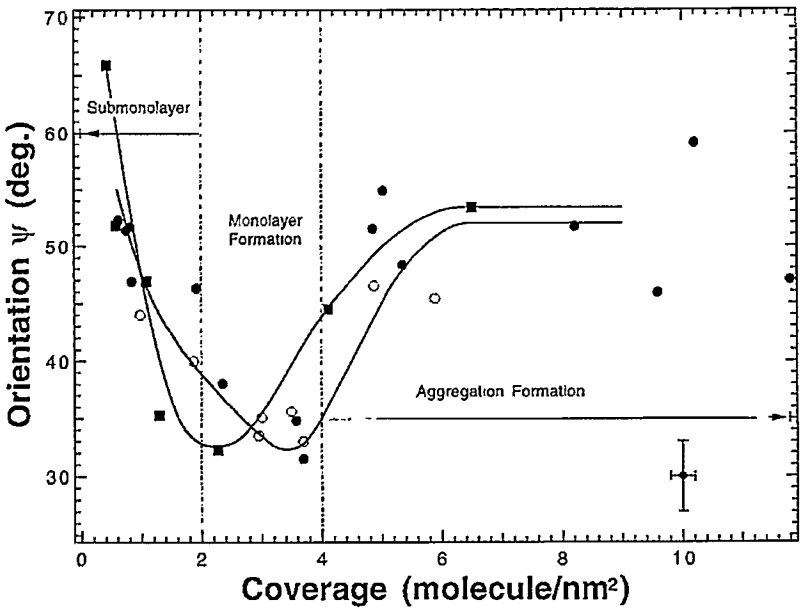
Understanding Ordering and Coverage in Polar SAMs

Most current self-assembly (SA) strategies are ad hoc, with little understanding of structure-function relationship and mesoscale ordering. The key SA issues are the following: (1) How does the surface coverage of monolayers compare with the surface coverage of aggregates? (2) At the mesoscale level is the SA structure random or ordered? (3) What is the intrinsic relationship between molecular orientation and surface coverage? We performed some experiments to resolve these questions.

In these experiments we used a zirconium-sulphonate linkage which allows convenient quantitative exchange with phosphate salts upon exposure to phosphate buffer. We "developed" the zirconated surfaces by anchoring various sulfonate chromophores to silica substrates. Most of these chromophores can be considered as rigid-rod-like sensitizers with a charge-transfer state in the blue-to-red region of the optical spectrum. We can derive the average angle $\langle\psi\rangle$ of the transition moments with respect to the surface normal by comparing the thin-film absorbance of light polarized parallel to the surface with that for the same number of identical species in solution.

The third figure shows that SAM formation can be divided into three categories: partially ordered submonolayers, well-ordered monolayers, and randomized aggregates. When surface coverage is low, submonolayers form, with some net alignment. As surface coverage increases, highly ordered mesoscale structures start to organize. The optimized alignment, $\langle\psi\rangle = 32\pm3^{\circ}$, was achieved when the surface coverage approached a close-packed state of ~2.0–4.0 molecules per nm^2. Aggregation forms on surfaces when the surface coverage is thicker than that of a monolayer and the orientation is random.

This result shows that the average molecular orientation is a complex function of the surface coverage and the resulting steric interactions of adjacent rod-like molecules. The optimum surface coverage (minimum points in the



Plot of molecular orientation (optical transition moment) with respect to the surface normal vs. chromophoric monolayer coverage, in units of molecules per nm² for AABDS (solid circles), Sulfarsazene (open circles), and Orange I (solid squares). The solid lines serve as a visual aid only.

third figure) is governed by the cross-sectional area of the molecule on surfaces. For example, the optimum coverage of 4-amino-1,1'-azobenzene-3,4'-disulfonic acid sodium salt (AABDS) and Sulfarsazene is approximately 1.6 times that of Orange I (3.7 molecules/nm^2 vs. 2.3 molecules/nm^2). This result is consistent with the molecular cross-section ratio of 1.5 because of the bulky naphthanyl group and its steric hindrance effect. We performed SHG measurements on these SAMs to verify the chromophoric alignment. We obtained the following values of d_{33} relative to crystalline quartz for SAMs of Orange I, AABDS, Tropaeolin, and Sulfarsazene: 6.56, 3.88, 6.04, and 1.17 pm/V, respectively. The values obtained for $\langle\psi\rangle$ from these measurements were similar for all of the compounds, within the experimental resolution: $\langle\psi\rangle = 35° \pm 5°$. These results support the conclusion that we indeed formed oriented, polar monolayer films.

Modeling

We used a combination of many-body techniques, including high-performance computing and analytical methods, to perform the following studies:

1. We estimated hyperpolarizability factors for a sequence of organic molecules. Within modified neglect diatomic overlap accuracy, we identified polarizable regions and sensitivities to side groups. These estimates can be incorporated into models by including anisotropic polarizability in the self-assembly and macroscopic nonlinear-optics coefficients.

2. We calculated electroabsorption spectra and the two susceptibility coefficients $\chi^{(2)}$ and $\chi^{(3)}$ in extended conjugated organic systems using exciton theory, including the effect of lattice relaxation in the photoexcited states. We also used configuration-interaction, coupled-exciton-phonon (Condon-Herzberg-Teller), and sum-over-states techniques to study the geometries of 1Bu and mAg1 states. We determined the dependence of spectra and Huang-Rhys factors on the strength of electron-electron and electron-lattice coupling.

3. We used fully nonadiabatic numerical quantum-mechanical methods to explore "breather" excitations in nonlinear, coupled electron-phonon lattices. These bound multiphonon states and their associated electronic properties will be fundamental to the interpretation of time-resolved spectroscopy being developed at Los Alamos.

Publications

Buscher, C.T., D. McBranch, and D. Li, "Understanding the Relationship Between Surface Coverage and Molecular Orientation in Polar Self-Assembled Monolayers" (to be published in *J. Am. Chem. Soc.*).

Yang, X., D. McBranch, B. Swanson, et al., "Design, Construction, and Architecture of Covalently Bound, Polar Self-Assemblies of Molecular Pyramids on Oxide Surfaces" (to be published in *Angewandte Chemie*).

Rigid Molecular Foams

Michael Mitchell

Porous materials are widely used in government and industry for chemical separation, processing, environmental cleanup and remediation, energy efficiency, and conservation. Porous materials used in these applications include foams, filters, membranes, absorbents, ion-exchange resins, molecular sieves, zeolites, catalyst supports, sensors, and electrodes. Rigid molecular foams have ideal nanostructure for use as absorbents and chromatographic media, molecular filters and sieves, catalyst supports, and organic zeolites. The purpose of this project is to thoroughly evaluate this new class of materials as media for chemical separations and processing.

We are currently producing hyper-cross-linked materials which have very small pore sizes (less than 10 Å) and very large surface areas (100 to 1200 m^2/g). By using special supercritical-fluid processing techniques, we have isolated monolithic articles that may be suitable as membranes and/or catalyst supports. The isolation of an article (as opposed to a powder) is highly significant and represents a first in this field of study.

The hyper-cross-linked materials are produced by polycondensation with a Friedel-Crafts alkylation reaction using aryl dialkylchlorides and aromatic compounds. This method of polymerization is very useful because of the large variety of inexpensive monomers available. Also, the polymerization is very robust—trace impurities do not hamper the polymerization.

When polycondensation is complete, the material has formed a continuous gel. If dried by normal techniques, the gel would be reduced to a powder because of high internal stresses that develop during polymerization. Therefore, we carefully dry the gel using a critical-point drying technique. In this process we remove the gelation solvent by extraction with liquid carbon dioxide. We then remove the carbon dioxide by increasing temperature and pressure above carbon dioxide's critical point. The carbon dioxide is then safely vented without destruction of the hyper-cross-linked foam.

Monte Carlo Code for Neutron Scattering Instrument Design and Analysis

Luke Daemen

The demand for neutrons in physics, chemistry, materials science, and biology is increasing rapidly. Indeed, neutron scattering was recently recognized as an essential tool for the study of materials in the nuclear stockpile. Because of this increased demand, researchers at the Laboratory are studying a new, accelerator-driven, 1-MW long-pulse spallation source (LPSS) and are upgrading the existing neutron source at the Manuel Lujan Jr. Neutron Scattering Center (MLNSC).

Our main objective for this project is to develop a Monte Carlo computer code that will allow the design, optimization, and analysis of instruments for neutron scattering. The code will be used with complex models of neutron sources to explore the dependence of the performance of neutron- scattering instruments on different sources. Besides helping with the optimization of instrument performance, the code will provide guidance on numerous parameters of the target stations, such as repetition rate, pulse length, moderator characteristics, and chopper requirements.

The code originates from a library of subroutines for neutron optics written at the Rutherford-Appleton Laboratory in 1982. In order to simulate the instruments considered for the MLNSC upgrade and LPSS projects, we had to restructure and expand this code. To date, we have produced computer models for several types of small-angle neutron-scattering diffractometers and neutron reflectometers, a powder diffractometer, a triple-axis spectrometer, and a time-of-flight multichopper spectrometer. We compared the performance of these instruments at several types of sources (continuous and pulsed). The usefulness of the code to optimize instrument performance was demonstrated for small-angle neutron scattering and reflectometry.

To make the code usable by a wider audience, we developed a user-friendly, window-based, mouse-driven interface that will assist in the definition of arbitrarily complex instrument geometries from basic building blocks such as moderators, choppers, apertures, guides, samples, shielding blocks, monochromators, detectors, and others. A first version of the interface has been unofficially released. A second version will be released before the end of the year.

Dynamic Properties of Advanced Materials

George Gray III

Composites (metallic, ceramic matrix, or polymer matrix) are receiving increased attention because of their high specific strengths and stiffnesses and their high-temperature properties. Composites also possess unique dynamical properties, in contrast to common single-phase materials.

Fiber reinforcement produces mechanical anisotropy and internal interfaces that cause wave interactions on the spatial scale of 10–100 μm. Impacting a composite can produce low-amplitude elastic waves; if the internal interfaces are perfectly periodic and ideally bonded, the composite acts as a band-pass filter.

In modern practical applications, however, wave amplitudes can be large enough to drive composite materials beyond the elastic limit, internal interface locations may not be perfectly periodic, and tension can separate interfaces. In this case the individual structural components can undergo rate-dependent plastic deformation in the presence of second-phase components that can strongly influence microstructural response.

To use these materials under dynamic loading conditions and to develop models which predict their behavior, we must understand their high-rate/shock-wave response. The objective of this project is to provide high-quality experimental measurements on composites and to develop computational models which describe the deformation response of composite materials.

In our dynamic loading experiments, we found that the stress/strain response of a 3M-fiber 6061-T6 aluminum/alumina continuous-reinforced composite varied with fiber orientation, strain rate, and temperature. We measured the composite yield strength parallel to the fibers to be ~4 times that of quasi-static measurements made orthogonal to the fibers at 298 K. This finding is consistent with the idea that high-strength alumina carries the bulk of the stress when loading is parallel to the fibers.

We also measured the rate sensitivity of the 3M-fiber composite at 298 K as a function of fiber orientation; we found the composite response parallel to the fibers to be low, consistent with the documented weak rate dependence of monolithic alumina. Composite samples tested in this orientation failed by buckling or "brooming" of the alumina fibers. We found significant strain-rate and temperature dependence of the composite when loaded orthogonal to the fibers. We believe that this temperature dependence reflects the rate and temperature behavior of the high-density dislocation substructure in the aluminum matrix formed during fabrication.

We compared preliminary wave-profile data for the continuous-fiber-reinforced Al/Al_2O_3 composite measured across the fibers with data obtained under similar loading conditions for a particle-reinforced Al/Al_2O_3 composite. In both cases we used *z*-cut quartz impactors with projectile velocities close to 0.5 mm/ms.

In spite of similar impact conditions, the final particle velocities are quite different for the two materials. The elastic precursors are also different: the fiber material showed a well defined, low-amplitude elastic wave; the particle-material composite showed wave dispersion. Shock rise times were similar for the two data sets, but the fiber material exhibited what looked like a multiple wave structure. This is possibly an experimental artifact caused by impedance mismatch at the sample/LiF window interface. We need data with a higher-impedance window to determine the origin of this feature. The bulk part of the release paths agreed well. However, the final particle velocity for the fiber material was lower than that for the particle material. This difference results from using a glass-reinforced-foam backing on the quartz impactor for the fiber experiment; we used polymethyl methacrylate (PMMA) for the particle-MMC (metal-matrix composite) experiment.

Another interesting feature is separation of the elastic precursor from the plastic wave in the continuous-reinforced-composite material. This separation was not seen in material with discontinuous reinforcement. The behavior of the uniaxial-fiber-reinforced material may be caused by unique plasticity properties and material anisotropy which result in enhanced separation between elastic and plastic waves and a distinct particle-velocity overshoot in the precursor; the latter is reminiscent of an upper/lower yield point and rapid dislocation multiplication at the elastic wave front. This response is uncharacteristic of monolithic 6061-T6 aluminum alloy. The difference in behavior between the continuous (fiber) reinforcement and that of the matrix material alone (as well as that of aluminum/alumina composites at low-volume fractions of discontinuous reinforcement) is dramatic in this regard.

We also conducted spallation experiments for various particulate alumina composites and compared our experimental results to model simulations. The pull-back signals in the free-surface velocities contain information on the spall strength at depth for the three composite materials—(a) 20 vol % mullite particles, (b) 8 vol %

alumina, and (c) 17 vol % alumina—all with a 6061-T6 aluminum matrix. The spall strengths in these three cases were measured to be (a) 1.9 GPa, (b) 2.0 GPa, and (c) 1.1 GPa. These measured values are considerably less than the 2.8 GPa spall strength of the metal matrix. We also saw sluggish spallation in these composite materials. Time-dependent effects in composite spallation remain to be investigated; the data measured in this project contain considerable information of this type.

New modeling work for the continuous-reinforced composite focused on the response of materials constructed with significant periodicity. To model these materials we used the method of cells (pioneered by Jacob Aboudi), in which we describe high-frequency motion in terms of microstructural spatial variables expanded to various orders ($n = 1$ contains the quasi-static, long-wavelength response, as well as dynamical effects related to dispersion; $n = 2$ gives a better approximation to the dynamical effects). Our approach has been to write these dynamical equations in finite-difference form and attempt to solve for transient effects in composites in the same way that is done for homogeneous, monolithic materials. Our initial efforts have been unsuccessful; the transition from discrete components to the continuum involves subtle effects required to preserve microscale stress and displacement continuity. We continue efforts in this area because it is at the forefront of composites research and, if successful, could have high payoff.

The work performed in this project has application to the mechanical properties and materials testing of a broad range of advanced materials and composites.

Publications

Albert, D.E., and G.T. Gray III, "Dislocation Reactions Responsible for the Formation of a Twin in the Ordered Intermetallic Alloy Ni-20Al-30Fe," *Philos. Mag. A* **71**, 473 (1995).

Blumenthal, W.R., G.T. Gray III, and T.N. Claytor, "Response of Aluminum-Infiltrated Boron Carbide Cermets to Shock-Wave Loading," *J. Mater. Sci.* **29**, 4567 (1994).

Gray III, G.T., "Influence of Shock-Loading on the Structure/Property Response of Ti-48Al-2Cr-2Nb," *J. Phys. IV* **4**, 373 (1994).

Gray III, G.T., "Influence of Strain Rate and Temperature on the Mechanical Behavior of Iron-Aluminide-Based Alloys," in *Plasticity '95*, S. Tanimura and A.S. Khan, Eds. (Gordon and Breech, Japan, 1995), p. 527.

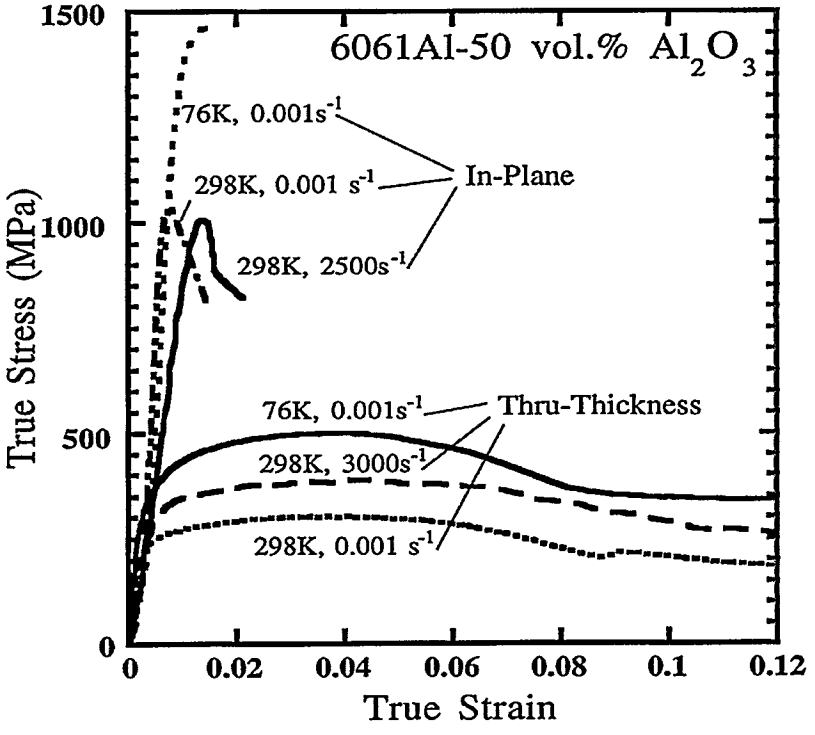
Gray III, G.T., and K.S. Vecchio, "Influence of Peak Pressure and Temperature on the Structure/Property Response of Shock-Loaded Ta and Ta-10W" (to be published in *Metallurgical Mater. Trans. A*).

Hong, S.I., and G.T. Gray III, "Dynamic Mechanical Response of a 1060-Al/Alumina Composite," *J. Mater. Sci.* **29**, 2987 (1994).

Johnson, J.N., R.S. Hixson, and G.T. Gray III, "Impact Loading of an Aluminum/Alumina Composite," *J. Phys. IV* **4**, 325 (1994).

Johnson, J.N., R.S. Hixson, and G.T. Gray III, "Shock-Wave Compression and Release of Aluminum/Ceramic Composites," *J. Appl. Phys.* **76**, 5706 (1994).

Maloy, S.A., and G.T. Gray III, "High-Strain Rate Deformation of NiAl," *Mater. Sci. Engin.* **A192**, 249 (1995).



Stress/strain response of 6061 Al/Al_2O_3 MMC in the in-plane and through-thickness directions as functions of rate and temperature.

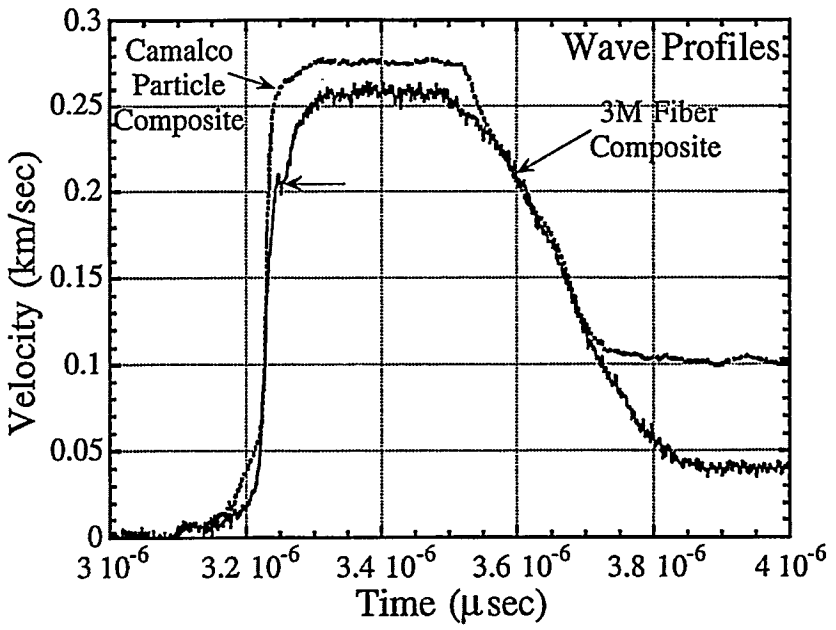
Maloy, S.A., and G.T. Gray III, "High Strain Rate Deformation of Ti-48Al-2Cr-2Nb" (to be published in *Acta Metall. et Materialia*).

Song, S.G., and G.T. Gray III, "Double Dislocation Pole Model for Deformation Twinning in FCC Lattices," *Philos. Mag. A* **71**, 661 (1995).

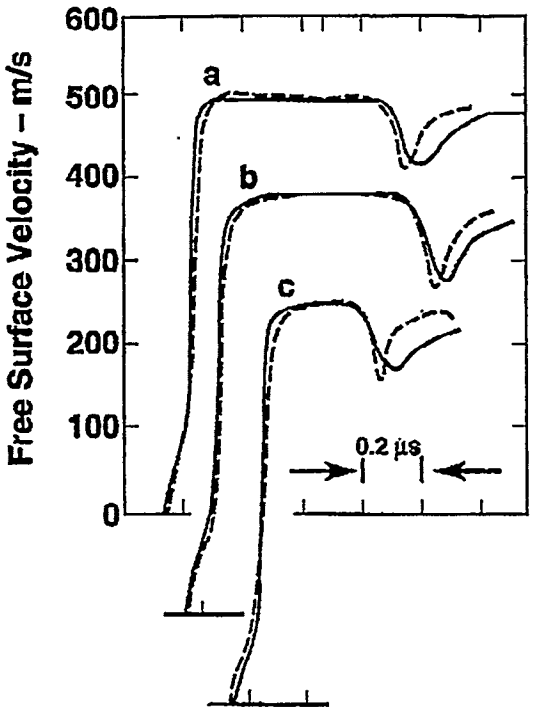
Song, S.G., and G.T. Gray III, "Influence of Temperature and Strain Rate on Slip and Twinning Hardening Behavior of Zr" (to be published in *Metall. Mater. Trans. A*).

Song, S.G., and G.T. Gray III, "TEM Examination and Analysis of a New Type of Stacking Fault in HCP Metals," *Philos. Mag. A* **71**, 263 (1995).

Tonks, D.L., R.S. Hixson, J.N. Johnson, et al., "Shock Wave Plasticity in Tantalum and Tantalum Alloys," in *Tungsten and Refractory Metals*, A. Bose & R.J. Dowding, Eds. (Metal Powder Ind. Fed., Princeton, New Jersey, 1994), p. 481.



Wave profiles for spherical particulate and 3M-fiber MMCs.



Spall traces and model simulations of the spallation response of three different particle-reinforced 6061-T6 aluminum-matrix composites—(a) 20 vol % mullite particles, (b) 8 vol % alumina, and (c) 17 vol % alumina.

Thermodynamic and Electrodynamic Studies of Unusual Narrow-Gap Semiconductors

Albert Migliori

Cryogenic solid-state refrigerators based on the Ettingshausen effect (that is, heat transport by carriers in a magnetic field) can provide vastly superior performance to Peltier devices, thereby opening up new markets in electronics, superconductor, and medical applications. Surprisingly, this most effective of solid-state cooling processes is not being studied at present anywhere else although it is much less restrictive in the possible materials that can be used, is simpler to implement (even noting that a small permanent magnet must produce a field at the device), and has already achieved lower temperatures than Peltier coolers, the only devices presently under investigation.

Recent discoveries of new hybridization-gap semiconductors and semimetals and the commercially available high-strength $Nd_2Fe_{14}B$ permanent magnets open the way for development of new ultrahigh-performance solid-state Ettingshausen refrigerators. As part of our project, we will develop and study the transport and thermodynamic properties of new materials appropriate for such devices. This project has applications to military and commercial refrigeration, solid-state cooling of high-speed electronics and low-noise electronics, and spot cooling for medical uses.

We measured thermopower, resistivity, thermal expansion, and elastic moduli of FeSi, $YbAgCu_4$, single-crystal graphite, and other novel narrow-gap semiconductors. We also constructed probes to measure the Nernst coefficient (thermopower in a magnetic field perpendicular to the heat flux) and thermal conductivity. We developed new theoretical approaches to guide materials searches and have used them to begin development of appropriate materials, especially Bi-based compounds, of which we have grown several single crystals.

Publications

Chu, F., M. Lei, S.A. Maloy, T.E. Mitchell, et al., "Single Crystal Elastic Constants of C40 NbSi(2)" (to be published in *J. Mater. Res.*).

Mandrus, D., A. Eklund, A. Migliori, et al., "Electronic Transport in the Heavy Fermion Semiconductor FeSi" (submitted to *Phys. Rev. B*).

Mandrus, D., J.L. Sarrao, A. Migliori, et al. "Thermal Expansion Study of Fe(1-x)Co(x)Si," *Physica B* **199**, 471 (1994).

Mandrus, D., J.L. Sarrao, A. Migliori, et al., "Thermodynamics of FeSi," *Phys. Rev. B* **51**, 4763 (1995).

Park, C-H., Z.-H. Shen, A.G. Loeser, et al., "Direct Observation of a Narrow Band Near the Gap Edge of FeSi" (submitted to *Phys. Rev. Lett.*).

Sarrao, J.L., D. Mandrus, A. Migliori, et al., "Complete Elastic Moduli of La(2-x)Sr(x)CuO(4) (x=0.00 and x=0.14) Near the Tetragonal- Orthorhombic Structural Phase Transition" (to be published in *Phys. Rev. B*).

Sarrao, J.L., D. Mandrus, A. Migliori, et al., "Elastic Constants of FeSi," *Physica B* **199**, 478 (1994).

Phase Stability of Transition Metals and Alloys

Robert Hixson

Unresolved differences exist between the theoretically predicted and experimentally measured phase stability of elements from both group IV-B (titanium) and group VI-B (molybdenum). If the compelling theoretical arguments that link phase stability for these metals to D-band occupancy number are correct, then phase-transition pressures in these metals will change by alloying with D-electron donor metals. Temperature should also have a significant effect on transition pressures.

We are performing a series of well-characterized experiments to study these effects for both group IV-B and group VI-B metals and the appropriate alloys. Diamond-anvil cell (DAC) x-ray diffraction experiments will allow us to unambiguously determine crystalline phases and transition pressures. Our unique DAC techniques are able to cover a wide range of pressures and temperatures.

Theoretical techniques will use the results of these experiments as benchmarks to develop predictive capabilities for phase stability for transition-metal alloys. This work has many potential benefits besides addressing the fundamental issues described above. These issues

include increasing our understanding of the connection between structure and material properties, increasing our basic understanding of the metallurgy of the chosen binary alloys, and developing an ability to predict the phase stability of alloys.

This year we have concentrated our theoretical work on developing a method that allows electronic-structure calculations on alloys where the solute and base metal are in different rows on the periodic chart. With this tool completed, we have calculated the structures of titanium-tantalum and molybdenum-rhenium alloys. We have also completed new structure calculations on titanium and hafnium using an improved exchange or correlation potential.

Three series of alloys were produced in the foundry for use in the DAC. These were

- zirconium-vanadium(0.5%) and zirconium-vanadium(1%);
- zirconium-tantalum(0.5%), zirconium-tantalum(1%), and zirconium-tantalum(1.5%); and
- hafnium-niobium(2%) and hafnium-niobium(3%).

We formed cast buttons of each alloy. We rolled these buttons to 60% reduction to achieve a fine grain size. We then heat treated and recrystallized them to produce fine-grained samples for the DAC.

The most important experimental result for this year was the development of a new, accurate technique for locating phase boundaries. This technique consists of pressurizing the DAC with silicone fluid up to a high enough pressure to observe the ω phase. The silicone fluid can support shear stress for a few hours but will eventually relax to a hydrostatic state. We then reduce the pressure a step and allow the anvil to sit for several days to undergo diurnal heating and cooling. We reduce pressure in steps until single-crystal diffraction patterns are observed. This means that the phase boundary has been crossed. When we used this technique on titanium the ω phase was observed to revert to the α phase at 6 GPa, and for the titanium-tantalum(4%) alloy the transition was observed at 8 GPa.

Chemical Vapor Deposition of Complex Oxides: Materials and Process Development

Ross Muenchausen

The demand for higher performance and lower cost in electronics is driving the need for advanced materials and consequent process integration with current manufacturing methods. Ceramic thin-film technology is becoming more important in the manufacture of microelectronic devices, photovoltaics, sensors, microwave and radio-frequency communication devices, and high-temperature superconducting tapes. Current thin-film deposition technologies based on physical vapor deposition are limited in scale-up potential and in their control of processing parameters. Our project investigated chemical vapor deposition (CVD) and alternative processes for commercial-scale manufacturing of electronic materials.

We began by investigating CVD approaches to the production of decoupling capacitors and thin-film resistor-capacitor (RC) networks currently manufactured by AVX Corp. For these applications, 2-μm-thick films must be produced. Conventional tape casting cannot consistently produce films less than 4 μm thick. Optimized sol-gel processing has difficulty producing films greater than 1 μm thick. The prime driver in our study was cost. Unfortunately, the need for vacuum processing and organometallic precursors for high-throughput production of such relatively thick films kept the CVD process from being cost-competitive.

We then investigated alternatives to CVD processing. The most promising approach we identified was aerosol-source plasma vapor deposition. Compared with CVD, plasma vapor deposition does not require high vacuum and can use much cheaper water-soluble salts, oxalates, or citrates as precursors. In addition, since only polycrystalline films are required for capacitors and RC networks, careful control of the surface-chemistry-regulated film growth in a CVD process is not required either.

Characterization and Manipulation of Broken-Symmetry Materials at Phase Boundaries

Robert Donohoe

Our primary motivation in this project is to understand the magnetic properties of low-dimensional materials. Exchange energies, exchange anisotropies, g factors, and other measurable magnetic parameters can play an important role in determining both the ground and defect-state properties and the photodynamics of solid-state materials. These measurements are of interest because they will reveal important physical properties that we can relate to the chemical composition of materials and thereby permit enhanced control of a material's electronic and photophysical properties.

We have chosen the low-dimensional materials, including the halogen-bridged platinum group metal linear-chain complexes (the MX materials), for characterization because the linear, anisotropic nature of these materials simplifies characterization, both experimentally and theoretically, by limiting the scope of magnetic interactions to one dimension. In addition, the MX materials are known to have widely variable electronic and magnetic properties as a function of the choice of metal (platinum, palladium, or nickel), halogen (chlorine, bromine, or iodine), and other ancillary components such as counterions and equatorial (perpendicular to the chain axis) ligands. We will use this known capability to tune chemical compounds to enhance our ability to manipulate the magnetic properties of synthesized materials. Such a control of materials properties could eventually be of value in the development of practical solid-state devices such as diode lasers, superconductors, and detectors.

During the past year, we have developed the instrumentation to examine the inelastic scattering of weak charge density wave (CDW) materials (electronic semiconductors) of the PtI MX class under applied magnetic fields at the National High Magnetic Field Laboratory at Los Alamos. In some instances, these materials are known to undergo phase transitions under field, although this property has not been systematically measured. We have also characterized the magnetic-defect states in strong CDW MX chains such as PtCl by electron paramagnetic resonance (EPR) using isotopically pure platinum and chlorine to simplify the spectrum. The EPR of MX chains such as PtCl and PtI shows the progressive lengthening of the magnetic-defect states as the CDW is weakened, further demonstrating the variability of the magnetic interactions as a function of chemical composition.

Optical Spectroscopy of Porous Silicon

D. Wayne Cooke

Light-emitting porous silicon (LEPSi) emits visible luminescence at room temperature and has significant potential optoelectronics applications. An important unresolved issue regarding LEPSi is the origin of the luminescence. There is general agreement that it is due either to quantum confinement of electrons in nanoscale silicon particles or to molecular species residing on the surface of nanoscale silicon particles.

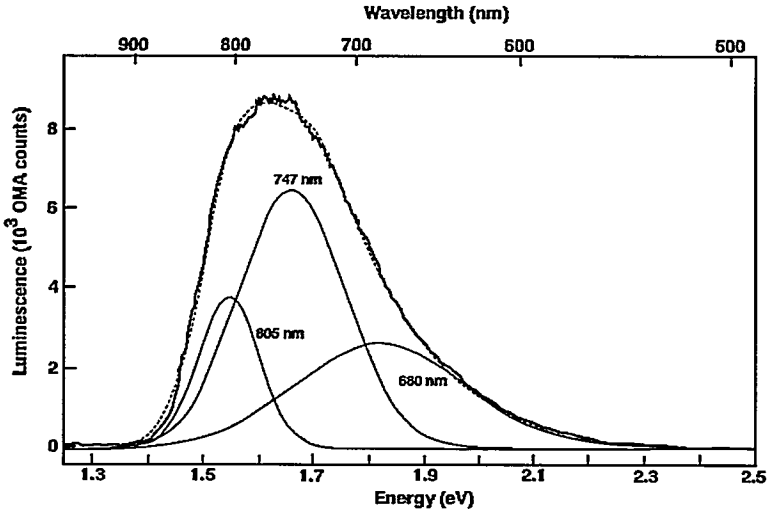
The objective of our work was to use optical and surface science techniques to investigate the origin of luminescence. Our scientific approach was to systematically remove hydrogen from the surface of LEPSi by annealing the silicon at various temperatures; measure the surface hydrogen content by forward recoil spectrometry; record the luminescence spectrum; and correlate the results. The accompanying figures provide data related to our work.

Major findings were the following: (1) LEPSi luminescence intensity as a function of annealing temperature is directly related to surface hydrogen content. The hydrogen is presumably contained within SiO_x surface layers, and its role is to establish luminescence centers; (2) spectral emission consists of three peaks, which are similar to those found in amorphous SiO_2; and (3) the LEPSi surface is composed of nanoscale silicon particles covered with a thin layer of SiO_x. We conclude that LEPSi luminescence is attributable to electron-hole formation in nanoscale silicon, with subsequent tunneling and recombination in SiO_x surface layers. Therefore, *both* quantum confinement *and* surface molecular species are necessary for the luminescence.

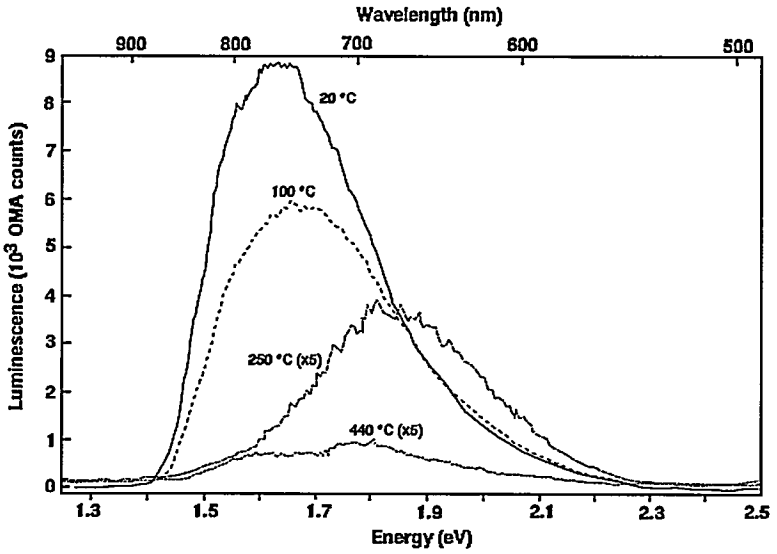
Publications

Cooke, W., B. Bennett, E. Farnum, et al., "Hydrogen Effusion in Light-Emitting Porous Silicon" (submitted to *Mater. Res. Soc. Proc.*).

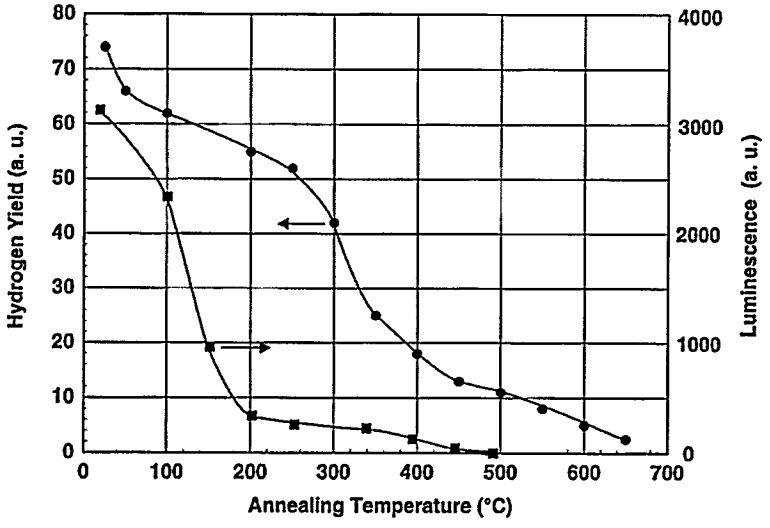
Cooke, W., B. Bennett, E. Farnum, et al., "Hydrogen Loss and Luminescence in Light-Emitting Porous Silicon: Support for the Quantum Confinement/ Luminescence Center Model" (submitted to *App. Phys. Lett.*).



Deconvolution of typical LEPSi luminescence. The thin solid lines represent Gaussian waveforms; the dashed line is a composite of the three Gaussian bands; and the bold solid line is experimental data.



Representative luminescence from thermally annealed LEPSi. Temperatures indicate the annealing temperatures; all measurements were done at 20°C.



Dependence of LEPSi luminescence and hydrogen surface content on annealing temperature. The right and left ordinates refer to luminescence and hydrogen content, respectively. The dashed line is a guide to the eye, and the solid line is fit to an equation that describes the effusion of hydrogen from SiO_x.

Ultrasensitive Ultrasonic Transducer Studies

Raymond Dixon

This project involves research and development of ultrasensitive ultrasonic transducers that have a smooth response across a broad frequency range and are well suited to a variety of ultrasonic testing techniques. The research and development consists of refining bonding techniques for the metal-to-metal and ceramic-to-metal joints that are needed and producing testing apparatus and techniques to evaluate the transducers.

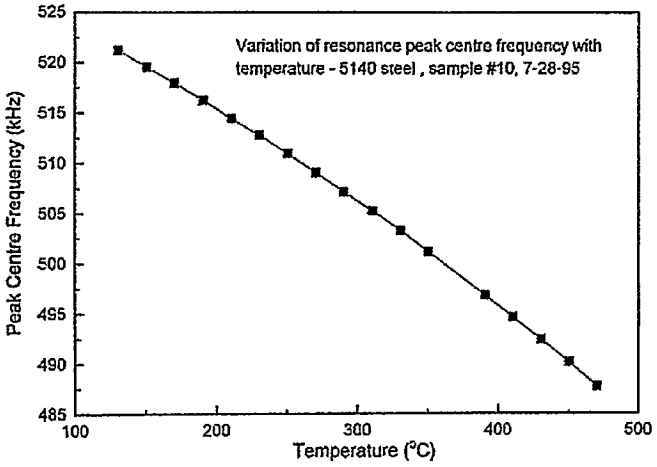
We make bonds by the process of metal diffusion bonding, using silver as our primary bonding metal. We have explored deposition methods of the silver films—and the parameters used in making the bonds—to optimize the performance of the transducers. We have evaluated the results by measuring the electrical impedance of the transducer unit and its mechanical ringdown. Additionally, we have built an apparatus to make calibration measurements with a reciprocity technique using multiple transducers. We have successfully constructed and measured various sizes of transducers made only of stainless steel, silver, and piezoelectric crystals, with either a diamond or alumina backload. Data verify the improved electrical characteristics and the much-improved durability of the transducers.

The figures compare the electrical impedance response of a commercially available transducer and a metal-diffusion-bonded unit made at Los Alamos and show the behavior of the elastic response of a heat-treatable steel measured with the new transducers at up to 500°C.

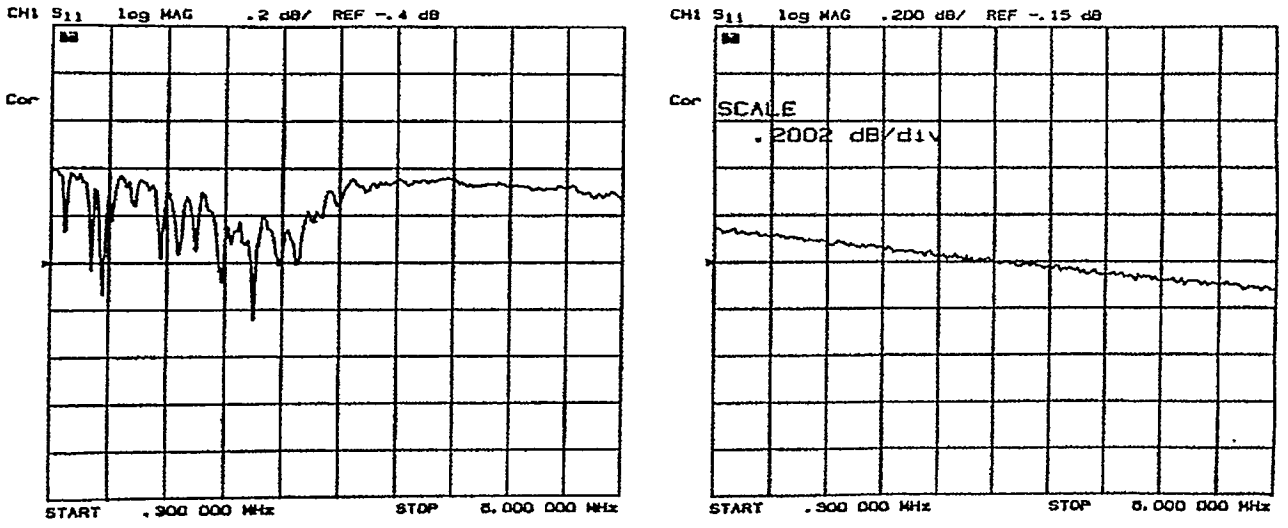
We are continuing reciprocity measurements. The work performed in this project has application to industrial nondestructive testing and basic materials science.

Publications

Dixon, R.D., and A. Migliori, "Fabrication and Performance of Ultrasensitive Ultrasonic Transducers" (submitted to *Rev. Sci. Instrum.*).



The variation of an elastic mode of a steel cube at temperatures up to 500°C, made by resonant ultrasound spectroscopy techniques using metal-bonded transducers.



(a) (b)

Comparison of (a) the electrical frequency response of a commercial transducer and (b) a Los Alamos metal-bonded transducer.

Structural Phase Transitions in Nonstoichiometric Oxides and Other Materials

Albert Migliori

Structural phase transitions (SPTs) have profound effects on the mechanical, magnetic, and electronic properties of materials. In some stoichiometric compounds, SPTs are well understood; they produce the types of magnetism in ferrites and ferroelectricity in piezoelectric oxides that make these materials so important. However, for nonstoichiometric compounds and for stoichiometric compounds in which thermally induced fluctuations produce effects analogous to those arising from impurities and dopants, SPTs are very far from clear.

The purpose of our research is to provide precise elasticity and thermal expansion data, which are important to developing good theories of SPTs in heavily doped or fluctuating crystals and are crucial for a broad spectrum of applications that our research is relevant to—from thermoelectric converters, ceramics, and semiconductors to materials testing and the physics of condensed matter.

We studied order parameters and coupling of electronic and structural contributions to the free energy of nonstoichiometric and stoichiometric systems—such as FeSi, YUPd3, $La_{2-x}Sr_xCuO_4$, $SrTiO_3$, $CeRu_2$, and other materials—by making detailed quantitative resonant ultrasound spectroscopy (RUS) and thermal-expansion measurements and obtaining full elastic constant data where good single crystals were available. We also studied the perovskite phase transitions by constructing Monte Carlo models that, though phenomenological, began to reproduce some of the more-complex features of the RUS data.

Publications

Chu, F., M. Lei, S.A. Maloy, et al., "Single Crystal Elastic Constants of C40 NbSi(2)" (to be published in *J. Mater. Res.*).

Fisk, Z., J.L. Sarrao, J.D. Thompson, et al., "Kondo Insulators" (to be published in *Physica B).*

He, Y., R.B. Schwartz, and A. Migliori, "Elastic Constants of Single Crystal y-TiAl" (to be published in *J. Mater. Res.*).

Mandrus, D., and A. Migliori, "Simple Small-Sample Capacitance Dilatometer" (to be published in *Rev. Sci. Instrum.*).

Mandrus, D., J.L. Sarrao, A. Lacerda, et al., "Low Temperature Thermal Expansion of SmB(6): Evidence for a Single Energy Scale in the Thermodynamics of Kondo Insulators," *Phys. Rev. B, Rapid Communications* **49**, 16809 (1994).

Mandrus, D., A. Migliori, M.F. Hundley, et al., "Electronic Transport in Lightly Doped CoSb(3)" (to be published in *Phys. Rev. B*).

Mandrus, D., J.L. Sarrao, A. Migliori, et al., "Thermodynamics of FeSi" (to be published in *Phys. Rev. B*).

Park, C-H., Z.-X. Shen, A.G. Loeser, et al., "Direct Observation of a Narrow Band Near the Gap Edge of FeSi" (submitted to *Phys. Rev. Lett.*).

Sarrao, J.L., D. Mandrus, A. Migliori, et al., "Complete Elastic Moduli of La(2-x)Sr(x)CuO(4) (x=0.00 and x=0.14) Near the Tetragonal-Orthorhombic Structural Phase Transition," *Phys. Rev. B* **50**, 13125 (1994).

Strain Measurement in Individual Phases of Multiphase Materials During Thermomechanical Loading

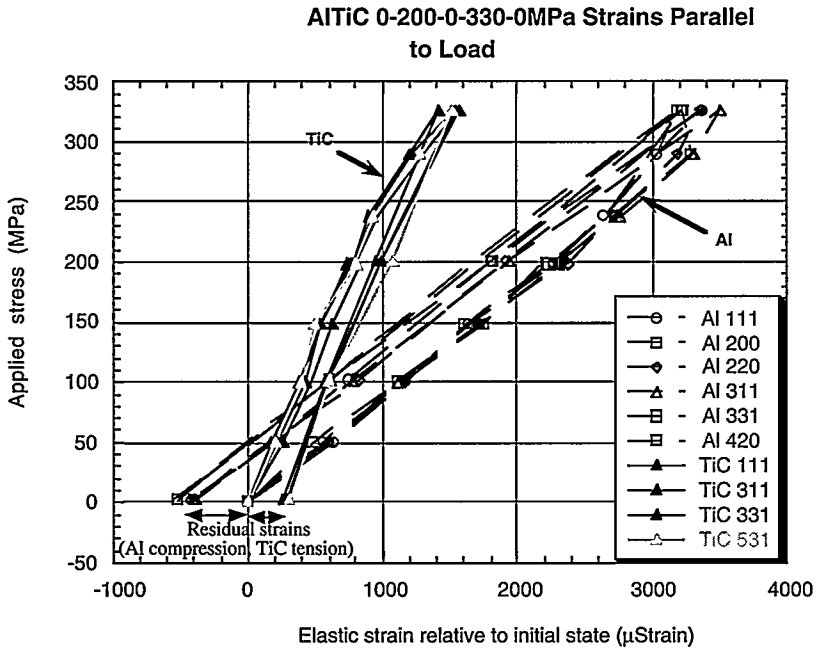
Joyce A. Goldstone

Understanding the deformation of grains in strongly anisotropic or heterogeneous polycrystalline materials is of paramount importance in predicting their mechanical characteristics. Neutron diffraction has already played a critical role in investigating residual strains in structural systems, but we have developed a powerful complementary capability—the ability to measure mean phase elastic strains during applied loading in specific crystalline directions. Initially, we designed and built a customized frame capable of loading specimens into the spectrometer of the neutron powder diffractometer at LANSCE (the Los Alamos Neutron Science Center). More recently, we added a furnace to the frame to enable measurements up to 1000°C, opening new testing regimes for simulation of service conditions.

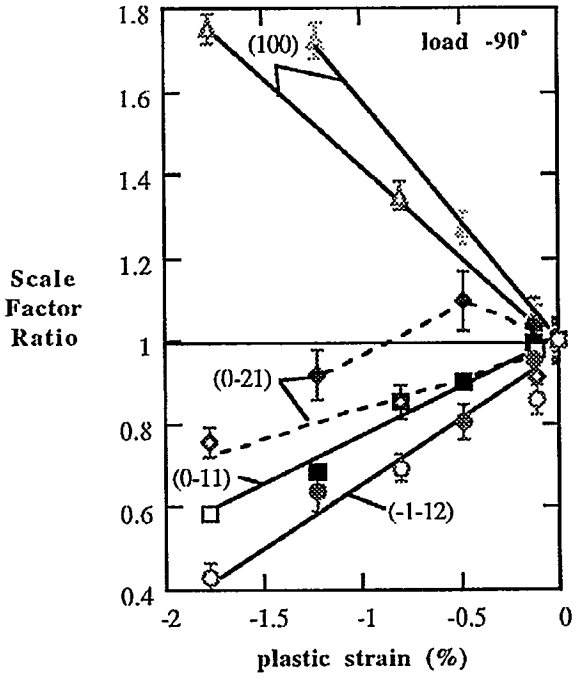
The load frame has been used to investigate a wide range of material systems including metal matrix composites (AlSiC and AlTiC), codeformable composites (CuNb and CuAg), low-symmetry intermetallics (Al_3Ti), and shape-memory alloy composites (NiTiTiC). The results have been used to investigate evolving crystallography during deformation and to validate numerical codes. Collaborators have included engineers from the Ford

Motor Company and researchers from the Massachusetts Institute of Technology. Two principal suites of experiments were performed on AlSiC and NiTiTiC.

In the first suite of experiments, we measured mean elastic phase strain in the metal and ceramic phases of Al/SiC and Al/TiC composites at a variety of temperatures. The results offered insights concerning strain relaxation and plasticity. In the second suite, we investigated the behavior of a shape-memory alloy, NiTi, both with and without TiC reinforcement. The changes in preferred orientation that occur during during deformation by martensitic twinning were related to the total amount of plastic deformation. The accompanying figures show data from these experiments. In the final month of this project, we will measure the elastic properties and load-sharing capabilities of a direct-quenched steel containing both austenite and martensite.



Elastic strain (relative to the unloaded state) measured by neutron diffraction for an Al/TiC composite in the direction parallel to the load for several Al and TiC reflections.



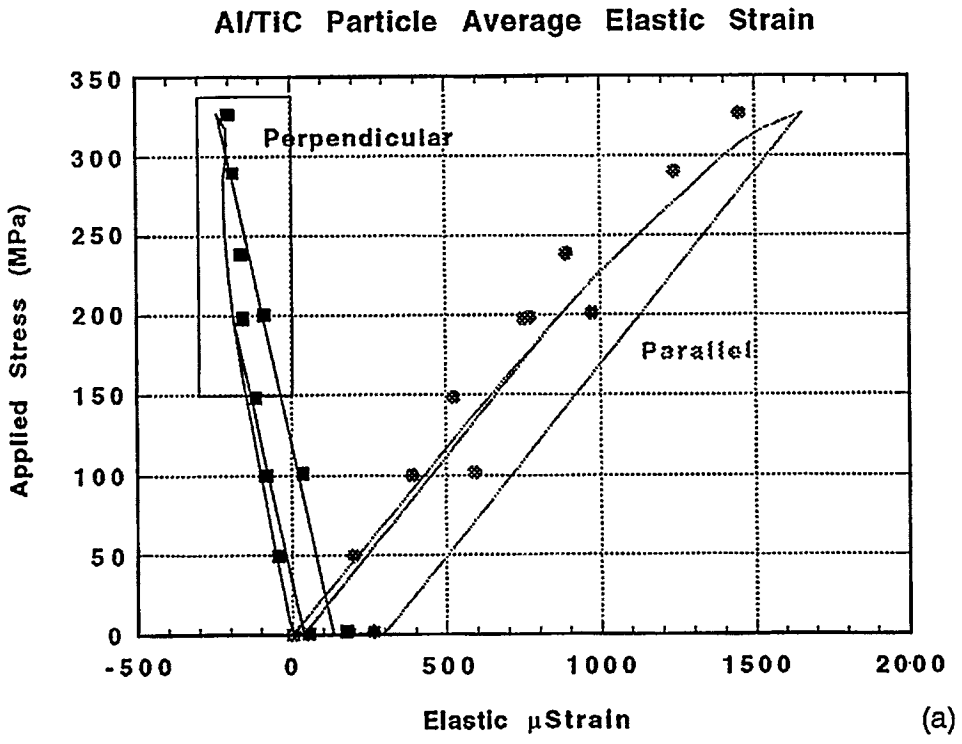
Normalized scale factor upon mechanical loading as a function of plastic strain for NiTi (solid symbols) and NiTi-20% TiC (open symbols) for planes perpendicular to the applied stress. Parenthetical numbers are the Miller indices for the crystal planes.

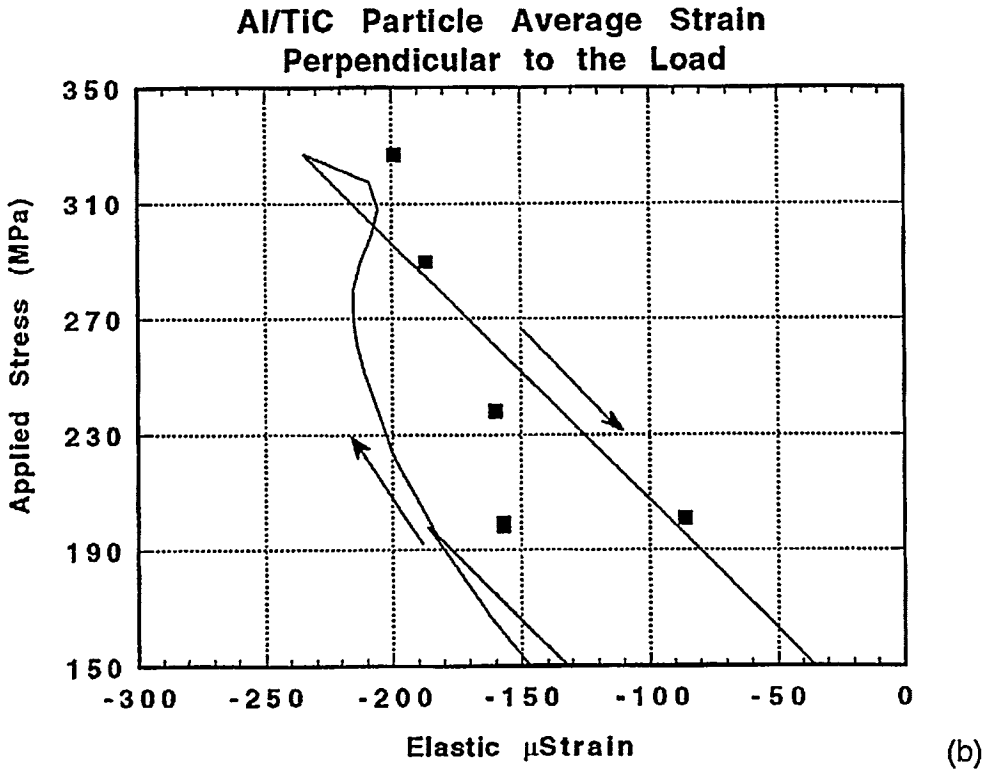
Publications

Bourke, M.A.M., J.A. Goldstone, and R.A. Robinson, "Strain Measurement by Diffraction at LANSCE," *J. Phys. B* **213 & 214**, 806 (1995).

Dunand, D.C., D. Man, M.A.M. Bourke, et al., "Neutron Diffraction Study of NiTi During Compressive Deformation and After Shape-Memory Recovery" (submitted to *Metall. Mater. Trans. A*).

Shi, N., M.A.M. Bourke, J.A. Goldstone, et al., "Influence of Thermal Residual Stresses on the Development of the Average Lattice Elastic Strain During External Loading in the Al/TiC Composites" (submitted to *Metall. Trans. A*).





(a) Particle elastic strain data (points) and finite element method calculations (solid lines) for the average particle strain in Al/TiC. (b) Particle elastic strain in the region of "zigzag" behavior [more detailed view of boxed area in (a)]. We are the first to observe and measure this zigzag behavior.

New Deposition Processes for the Growth of Oxide and Nitride Thin Films

David Smith

The general goal of our effort is to understand the details of the chemistry involved in the deposition process of oxides and nitrides from homoleptic metal amido precursors (in which all ligands are the same). This understanding will lead to new synthetic routes for high quality metal oxides and nitrides.

Organometallic chemical vapor deposition (CVD) has been slow in gaining acceptance in coatings applications despite its potentially significant advantages over metal-halide-based CVD processes. The major underlying limitation is the lack of understanding of the chemistry important to the deposition process. Control of the fundamental chemistry of the deposition process is the key to the advancement of the organometallic CVD process.

Recently, we have used the efficient transamination of homoleptic metal amides [$M(NR_2)_x$] with ammonia to yield highly reactive metal-amido or metal-imido intermediates to develop low-temperature, high growth-rate processes for the deposition of high-purity metal nitrides. We have extended our work to the low-temperature (100°C to 400°C) deposition of high-purity metal oxides. We have deposited SnO_2 and SiO_2 from the corresponding homoleptic amido complexes and O_2. The key to the deposition processes appears to be a reactive metal-nitrogen bond.

Strongly Correlated Electronic Materials

Kevin Bedell

In this project we have developed many-body theories that apply to several new electronic materials: colossal magnetoresistive (CMR) materials that will have an enormous impact on the recording industry; heavy-fermion materials, in particular, Kondo insulators, which have possible applications in thermoelectric coolers; and high-temperature superconductors (HTS), which, with the recent breakthrough at Los Alamos in HTS-tape fabrication, are on the verge of major applications. The new theoretical techniques that we have developed and applied to these materials provide a fundamental understanding of correlated-electron theory and will help to characterize and design new electronic devices.

Our work provided theoretical support for experimental activities at Los Alamos in HTS materials; heavy-fermion materials (with emphasis on the Kondo insulators); and perovskites, including CMR materials. We also addressed several issues common to these broad classes of materials: how these materials behave in magnetic fields, the field-induced metal-insulator (M-I) transition, colossal magnetoresistivity, spin-gap phenomena in HTS, the quantum Hall effect, and related issues. We also studied the properties of unconventional superconductors and impurity bound states and how the M-I transition relates to the metallic nature of low-dimensional, strongly correlated electronic materials.

The M-I transition produced by electron correlations is a fundamental problem in many-body theory. Renewed interest in this problem has been driven in part by the many materials that undergo M-I transition: HTS materials, perovskites, and vanadium oxides, to name a few. Also, large changes in the resistivity of CMR materials occur close to the M-I transition. We studied the approach to this transition from the metallic side using several techniques: we developed the local theory of a Fermi liquid to account for the approach to M-I transition in $SrLaTiO_3$; we also explored the M-I transition in the 1- and 2-D Hubbard model and studied this transition in heavy-fermion insulators in a magnetic field. These studies gave us new insights into such diverse phenomena as the field-induced M-I transition, spin-gap phenomena in underdoped HTS materials, and the ground and excited states of the CMR material $LaCaMnO_3$.

The research activities discussed so far concern physics at the atomic scale. However, the metallurgical and solid-state communities have long recognized that "texture" is often seen at larger length scales in these materials and is important to understanding them. Texture is seen on many scales in perovskites: precursor structure in ferroelectrics or martensites, antiphase boundaries, intrinsic clusters and central peaks, and tweed. Studies of HTS oxides have shown intrinsic local structural variations down to a

few bond-length scales; how bond-length scales affect macroscopic properties; and the intimate coupling of lattice, electronic, and magnetic degrees of freedom. These systematic local structures must be contrasted with average global symmetries probed by conventional techniques (e.g., Rietvelt refinement). We have developed microscopic many-body models and solution techniques which couple the relevant degrees of freedom and have allowed us to analyze and correlate recent experimental probes of local behavior. We have found that in many respects the driving force for intrinsic local structure is local, directional polarizability of electronically complex unit-cell structures such as those found in the perovskites. Polarizability can manifest itself as charge-transfer fluctuations, ferroelectric fluctuations, charged phonons, polarons, etc. We have applied these techniques to a variety of perovskite-like materials to gain new insights into the role that structure plays in determining the unique characteristics of these materials.

The research activities in this project have provided better understanding of how microscopic interactions are related to the novel characteristics of various new electronic materials. This in turn has brought us a step closer to controlling these unique properties for use in future electronic devices.

Publications

Abrahams, E., A.V. Balatsky, D.J. Scalapino, et al., "Properties of Odd Gap Superconductors," *Phys. Rev. B* **52**, 1271 (1995).

Balatsky, A.V., "Impurities and Conductivity in a D-Wave Superconductor," in *Strongly Correlated Electronic Materials: The Los Alamos Symposium 1993*, K.S. Bedell, et al., Eds. (Addison-Wesley, Reading, MA, 1994), p. 551.

Balatsky, A.V., and E. Abrahams, "Odd Time Magnetic Correlations and Chiral Spin Nematic," *Phys. Rev. Lett.* **74**, 1004 (1995).

Balatsky, A.V., and S. Matveenko, "Dynamical Properties of Quantum Hall States," *Phys. Rev. B* **52**, R8676 (1995).

Balatsky, A.V., and M. Salkola, "Impurity Induced States and Absence of Quasiparticle Localization in Disordered D-Wave Superconductors" (submitted to *Phys. Rev. Lett.*).

Balatsky, A.V., D. Pines, and P. Monthous, "Influence of Imperfections on the Low Temperature Properties of a D-wave Superconductor," *Phys. Rev. B* **50**, 582 (1994).

Balatsky, A.V., A. Rosengren, and B.L. Altshuler, "Impurities and Quasi-One Dimensional Transport in a D-Wave Superconductor," *Phys. Rev. Lett.* **73**, 720 (1994).

Balatsky, A.V., M.I. Salkola, and A. Rosengren, "Impurity Induced Bound States in D-Wave Superconductors," *Phys. Rev. B* **51**, 15547 (1995).

Bedell, K.S., "Lectures on Fermi Liquid Theory," in *The Canberra Summer School on "Modern Perspectives in Many-Body Physics,"* M.P. Das and J. Mahanty, Eds. (World Scientific, Singapore, 1994), p. 119.

Bedell, K.S., and P.F. Farinas, "Kohn's Theorem and Correlation Functions for a Fermi Liquid," *Phys. Rev. Lett.* **74**, 4285 (1995).

Bishop, A.R., "Lattice and Multiband Electronic Effects in High-Temperature Superconductors," in *Strongly Correlated Electronic Materials: The Los Alamos Symposium 1993*, K.S. Bedell, et al., Eds. (Addison-Wesley, Reading, MA, 1994), p. 374.

Bonca, J., and A.V. Balatsky, "Composite Operators for BCS Pairing," *JETP Lett.* **59**, 202 (1994).

Bonca, J., and J.E. Gubernatis, "Quantum Simulations of the Degenerate Single-Impurity Anderson Model," in *High Performance Computing and Its Application in the Physical Sciences*, D.A. Browne, J. Callaway, J.P. Dracyer, et al., Eds. (World Scientific, Singapore, 1994), p. 60.

Bonca, J., and J.E. Gubernatis, "Real-Time Dynamics from Imaginary-Time Quantum Monte Carlo Simulations: Tests on Oscillator Chains," *Phys. Rev. B* **50**, 10547 (1994).

Bonca, J., and J. Jaklic, "Spin diffusion of the t-J model," *Phys. Rev. B* **51**, 16083 (1995).

Bonca, J., and S.A. Trugman, "Effect of Inelastic Processes on Tunneling," *Phys. Rev. Lett.* **75**, 2566 (1995).

Davids, P.S., L. Wang, A.R. Bishop, et al., "Collective Level Crossings on Microtubules," *Phys. Rev. B* **49**, 5682 (1994).

Doniach, S., C. Fu, and S.A. Trugman, "Kondo Insulators: Are Simple Theories Good Enough?" *Physica B* **199**, 450 (1994).

Engelbrecht, J., and K.S. Bedell, "Robustness of a Local Fermi Liquid against Ferromagnetism and Phase Separation," *Phys. Rev. Lett.* **74**, 4265 (1995).

Gulacsi, M., and K.S. Bedell, "Spectral Function of the 1D Hubbard Model," *Physica B* **199**, 492 (1994).

Gulacsi, M., and K.S. Bedell, "Theory of the Metal-Insulator Transition in Strongly Correlated Electron Systems," *Integrated Ferroelectrics* **6**, 265 (1995).

Inui, M., S.A. Trugman, and E. Abrahams, "Unusual Properties of Mid-Band States in Systems with Off-Diagonal Disorder," *Phys. Rev. B* **49**, 3190 (1994).

Matveenko, S., A. Bishop, and A.V. Balatsky, "Superconductivity Fluctuations in 1-D 2 Band Electron-Phonon Model" (submitted to *Phys. Rev. B*)

Migliori, A., J.L. Sarrao, D. Mandrus, et al., "Ultrasound Studies of U_2Zn_{17} and UCu_5," *Physica B* **199**, 36 (1994).

Mustre de Leon, J., I. Batistic, A.R. Bishop, et al., "Reply to Comment on 'Polaron Origin for Anharmonicity of the Axial Oxygen in $YBa_2Cu_3O_7$,'" *Phys. Rev. Lett.* **75**, 584 (1995).

Rabson, D.A., and S.A. Trugman, "A Spin Model for Investigating Chirality" (to be published in *J. Physics: Condensed Matter*).

Roder H., J. Zang, and A.R. Bishop, "Lattice Effects in the CMR Manganites" (submitted to *Phys. Rev. Lett.*).

Rodriguez, J.P., J. Bonca, and J. Ferrer, "Random frustration in a two-dimensional spin-1/2 Heisenberg antiferromagnet," *Phys. Rev. B* **51**, 3616 (1995).

Roobol, L.P., G. Frossati, K.S. Bedell, et al., "Solubility of Spin-Polarized ^{3}He-^{4}He Mixtures" (to be published in *J. Low Temp. Phys.*).

Salkola, M.I., and A.V. Balatsky, "Superconducting Fluctuations in Multi-Band 1D Hubbard Model," *Phys. Rev. B* **51**, 15267 (1995).

Salkola, M.I., A.R. Bishop, V.M. Kenkre, et al., "Coupled Quasiparticle-Boson Systems: The Semiclassical Approximation and Discrete Nonlinear Schrodinger Equation," *Phys. Rev. B* **52**, R3824 (1995).

Salkola, M.I., A.R. Bishop, J. Mustre de Leon, et al., "Dynamic Polaron Tunneling in $YBa_2Cu_3O_7$ Optical Response and Inelastic Neutron Scattering," *Phys. Rev. B* **49**, 3671 (1994).

Salkola, M.I., A.R. Bishop, S.A. Trugman, et al., "Correlation-Function Analysis of Nonadiabatic and Nonlinear Systems: Polaron Tunneling," *Phys. Rev. B* **51**, 8878 (1995).

Sanchez-Castro, C., B. Cooper, and K.S. Bedell, "Consequences of Competing Hybridization for Magnetic Ordering in Correlated-Electron Lattices," *J. Appl. Phys.* **76**, 6130 (1994).

Schmeltzer, D., and A.R. Bishop, "Bosonization in Two Dimensions—A Space-Time Tunneling Approach," *Phys. Rev. B* **50**, 12733 (1994).

Silver, R.N., "Ordering of Polarons in the Holstein t-J Model: An Application to $La_{2-x}Sr_xNiO_{4+y}$," *Europhys. Lett.* **28**, 257 (1994).

Silver, R.N., and H. Roeder, "Densities of States of Mega-Dimensional Hamiltonian Matrices," *Intl. J. Mod. Phys.* **5**, 735 (1994).

Silver, R.N., H. Roder, A.F. Voter, et al., "Kernal Polynomial Approximations for Densities of States and Spectral Functions" (to be published in *J. Comp. Phys.*).

Silver, R.N., A.F. Voter, and J.D. Kress, "Linear Scaling Tight Binding from a Truncated Moments Approach" (submitted to *Phys, Rev. B*).

Spicci, M., M.I. Salkola, A.R. Bishop, "Coherence and Dynamics of Polarons in the Presence of Disorder," *J. Phys. C* **6**, 361 (1994).

Wang, L., and A.R. Bishop, "Charge Density Wave of a Multiband Fermi Liquid on a Graphitic Nanotubule," *Phys. Rev. B* **51**, 7407 (1995).

Wang, W.-Z., A.R. Bishop, and Y. Lu, "Dynamic Jahn-Teller-Induced Infrared Absorption in a Charged C_{60} Molecule," *Phys. Rev. B* **R50**, 5016 (1994).

Zang, W.-Z., "Dynamic Jahn-Teller Effect in Fullerene C_{60}" (to be published in *Phys. Rev. B*).

Zang, J., A.R. Bishop, and D. Schmeltzer, "Frustrated Spin-Peierls Chains," *Phys. Rev. B* **52**, 6723 (1995).

Engineering and Base Technologies

Generation of High-Power, Subpicosecond, Submillimeter Radiation for Applications in Novel Device Development and Materials Research

Antoinette Taylor

Single-cycle, terahertz-bandwidth electromagnetic radiation can be generated by the rapidly changing photocurrent produced when the voltage across a photoconductor is shorted by an ultrashort light pulse with photon energies greater than the bandgap energy. These terahertz pulses are directional and can be focused. Previous work in this area by others produced only small radiated fields because only low optical powers were available. The purpose of our project is to scale terahertz technology to high field strengths by using intense femtosecond-pulse lasers and to understand and minimize the mechanisms which limit scaling.

Applications of high-power terahertz sources include satellite communications, ultrafast optoelectronics, electronic sensor negation, particle acceleration, materials characterization, nondestructive inspection, and chemical imaging. Other applications will develop as this technology matures and becomes more widely known.

Our accomplishments over the duration of the project are as follows: (1) We have studied terahertz radiation emitted from biased photoconductors over a large range of optical fluences and bias fields. (2) We have observed saturation behavior at high fluences which we have shown to result from screening of the applied bias field by the generated terahertz radiation and space charge of the photocurrent. (3) We have generated high-power terahertz radiation using the electro-optic effect in unbiased nonlinear materials for which screening does not occur. (4) We have identified and characterized an efficient electro-optic emitter material, the organic material DAST. (5) In collaboration with an industrial partner, we have invented an efficient large-aperture terahertz emitter using a DAST mosaic. We have characterized the temporal and spatial profile and output energy of the radiation emitted by this mosaic and have found the mosaic to be an attractive way to generate high-power terahertz radiation.

Photoconductor Terahertz Pulse Studies

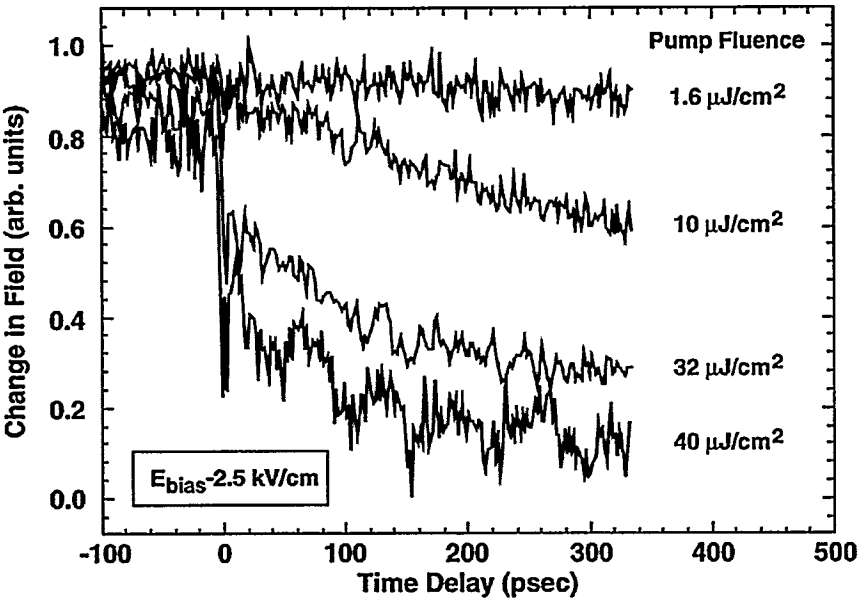
We measured the terahertz radiation emitted from the photoconductors GaAs and InP over a large range of optical fluences, bias fields, and crystal orientations. We also studied saturation behavior, which must be known in order to design efficient emitters, and related it to carrier mobility in the material. We observed no crystal orientation effects, which validates the current-surge model for biased emitters.

Far-Field Radiation Model. We have developed a theoretical model of the far-field radiation emitted by biased large-aperture photoconductors. Previous models described only the near-field radiation and did not reproduce—even qualitatively—experimental waveforms. (A far-field model is required because the distance from the emitter to the radiation detector is much larger than the wavelength of the emitted radiation.) We have calculated the time-dependence and intensity of the radiated fields as functions of optical excitation energy, bias field, and fluence. We have also included in our model transient velocity effects, such as velocity overshoot, and the effects of electron-hole and electron-phonon scattering. Agreement between the model and experiment is good.

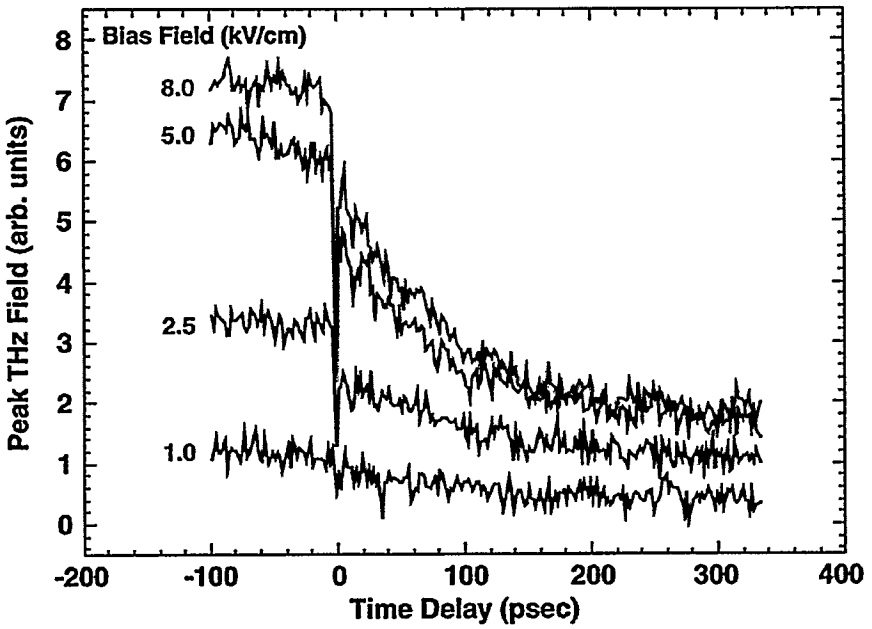
Saturation Studies. Saturation limits the terahertz output of a large-aperture, biased photoconductor at high optical fluences. Previous investigators explained saturation in terms of the screening of the applied electric field by the terahertz radiation. Space-charge screening of the applied bias field induced by separating carriers should also contribute to saturation. To elucidate the roles of these two saturation mechanisms, we performed pump-probe measurements on large-aperture, biased photoconductors. We measured the peak radiated terahertz output from the probe versus pump-probe delay for various bias voltages and probe fluences well below saturation and varied the

pump fluence to control the photoexcited carrier density. For sufficiently low carrier densities, the decrease in terahertz radiation from the probe is small near zero delay, implying that space-charge screening does not significantly affect the terahertz output in this regime. For carrier densities larger than 10^{18} cm^{-3}, the decrease in terahertz radiation near zero delay is significant, implying that space-charge screening does affect terahertz output in this range of bias fields (see first figure). For bias fields above 2.5 kV/cm, the proportional decrease in terahertz radiation at zero delay is roughly independent of bias, implying that over that range of bias fields space-charge screening does not depend on bias field (see second figure).

Screening Model. We have also modeled the effects of carrier screening at high excitation densities. To model these effects we had to solve a system of nonlinearly coupled partial differential equations. One component of the system consisted of the continuity equations for the electron density and hole density. We used current transport equations to account for the drift of electrons and holes and Poisson's equation to determine the effect of charge separation on the electric field. This model agrees with both the experimentally measured saturation curves and the pump-probe space-charge screening measurements.



Terahertz field-screening dependence on pump fluence or carrier density. (Probe pulse not in saturation.)



Effect of bias field on terahertz field screening. (Probe pulse not in saturation.)

Electro-Optic Crystal Terahertz Pulse Studies

Optical rectification of femtosecond pulses in electro-optic crystals also produces terahertz radiation. Such radiation should be linearly scalable with excitation fluence until higher-order nonlinear effects become important. We have compared the terahertz

emitter performance of three electro-optic crystals—$LiNbO_3$, $LiTaO_3$, and the organic salt dimethyl amino 4-N-methylstilbazolium tosylate (DAST). Our results extend previous studies by increasing the optical excitation energies by 6 orders of magnitude. The generated peak electric field radiated by $LiNbO_3$ and $LiTaO_3$ emitters increases linearly with increasing optical fluence for fluences up to 60 mJ/cm^2. For DAST emitters the peak field begins to saturate at fluences greater than 20 mJ/cm^2. At excitation fluences below 20 mJ/cm^2, DAST generates terahertz radiation roughly 14 times more efficiently than $LiNbO_3$. At a fluence of 60 mJ/cm^2, DAST is only 9 times more efficient (see third figure). This decrease in efficiency for DAST was accompanied by strong fluorescence, suggesting that two-photon absorption may have occurred.

Large-aperture emitters must be used in order to avoid saturation in DAST while still generating high-energy terahertz radiation. The problem with this approach is that large high-optical-quality crystals cannot be easily grown. Our solution is to use a multicrystal DAST mosaic as a terahertz emitter. To investigate this concept we fabricated a 1-cm^2 mosaic consisting of four identically oriented DAST crystals. We characterized this crystal in terms of terahertz output, beam quality, and temporal waveform and found no degradation in performance when compared with that of a single crystal. Therefore, for a given optical energy, an optimum-size emitter may be chosen to maximize terahertz output. We have applied for a patent on this mosaic emitter.

Publications

Benicewicz, P.K., J.P. Roberts, and A.J. Taylor, "Scaling of Terahertz Radiation from Large-Aperture Photoconductors," *J. Opt. Soc. Am. B* **11**, 2533 (1994).

Carrig, T.J., G. Rodriguez, T.S. Clement, et al., "Generation of Terahertz Radiation Using Electro-Optic Crystal Mosaics," *Appl. Phys. Lett.* **66**, 10 (1995).

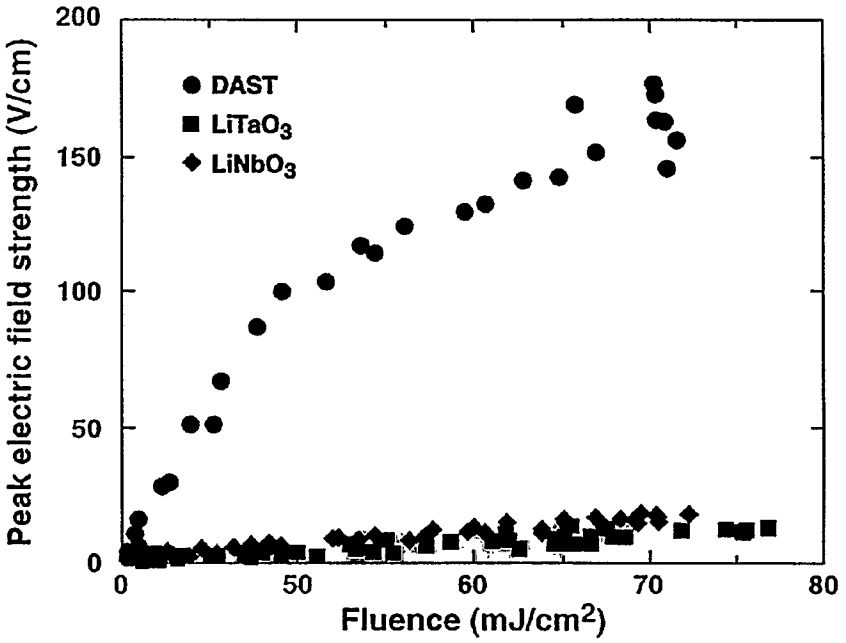
Carrig, T.J., G. Rodriguez, T.S. Clement, et al., "Scaling of Terahertz Radiation via Optical Rectification in Electro-Optic Crystals," *Appl. Phys. Lett.* **66**, 121 (1995).

Clement, T.S., G. Rodriguez, T.J. Carrig, et al., "Scaling Issues in Terahertz Radiation" (to be published in *J. Opt. Soc. Am. B.*).

Rodriguez, G., S.R. Caceres, and A.J. Taylor, "Modeling of Terahertz Radiation from Biased Photoconductors: Transient Velocity Effects," *Opt. Lett.* **19**, 1993 (1994).

Rodriguez, G., and A.J. Taylor, "The Effect of Screening of the Applied Bias Field in Terahertz Generation from Large Aperture Photoconductors" (to be published in *Opt. Lett.*).

Rodriguez, G., and A.J. Taylor, "Ultrafast Field Dynamics in Large Aperture Terahertz Emitters" (to be published in *Appl. Phys. Lett.*).



Peak terahertz field versus excitation fluence for electro-optic terahertz emitters.

Optical-Fiber Laser Amplifier for Ultrahigh-Speed Communications

Timothy R. Gosnell

Our project goal was to develop a praseodymium-based fiber amplifier for the 1.31-μm fiber-optic communications window that would be optically pumped with off-the-shelf semiconductor diode lasers operating at a wavelength of 980 nm. The 1.31-μm wavelength is commonly used in Great Britain and the United States for optical communications and could potentially support a higher rate of data transmission than any other wavelength. Development of a commercially viable optical amplifier for it—one analogous to the 1.55-μm erbium amplifier now in widespead use—would enable existing 1.31-μm communcations networks to be inexpensively upgraded to the multigigabit rates enjoyed by 1.55-μm networks.

The approach we adopted was to abandon direct optical pumping of the praseodymium ion (Pr^{3+}) in favor of an indirect pumping scheme involving radiationless energy transfer from optically excited ytterbium ions (Yb^{3+}) codoped with Pr^{3+} into the amplifying medium. This approach avoids the need for 1.017-μm diode pump lasers only now becoming commercially available in favor of more time-tested laser diodes whose output matches the 980-nm absorption band of Yb^{3+}. Because ytterbium is much more strongly absorbing than praseodymium, the use of this indirect pumping scheme could also yield a higher-gain and more compact device.

During the project, we first optimized the concentrations of Pr^{3+} and Yb^{3+} ions doped into bulk samples and then measured the gain of a fiber doped with the two ions at the optimum concentrations. We observed a gain of only 10 for a 1-m fiber length, a figure too low to be of commercial significance. (Total gains of ~1000 are required for in-line amplifiers operating in wide-area networks.) The cause for the shortfall in performance is still unknown; possibilities include improper fiber geometry and high ground-state absorption at 1.31 μm. Further work should resolve these open questions.

Publications

Epstein, R.I., M.I. Buchwald, B.C. Bradley, et al., "Observations of Laser-Induced Fluorescent Cooling of a Solid" (to be published in *Nature*).

Ping, X., and T.R. Gosnell, "Efficient Sensitization of Praseodymium 1.31-μm Fluorescence by Optically Pumped Ytterbium Ions in ZBLAN Glass," *Electron. Lett.* **31,** 191 (1995).

Ping, X, and T.R. Gosnell, "Room-Temperature Upconversion Fiber Laser Tunable in the Red, Orange, Green, and Blue Spectral Regions," *Opt. Lett.* **20,** 1014 (1995).

Polymers for Integrated Optical Interconnects

Bernhard Laurich

The discovery of electroluminescent polymers has made possible the development of optical interconnects for conventional silicon integrated circuits. The critical element of polymer-based integrated-optical interconnect technology is polymer light-emitting diodes (PLEDs).

The primary objectives of this project are to understand the light-emission mechanism of electroluminescent polymers and to use this knowledge to improve the efficiency and lifetime of the PLEDs. Our specific goals are to characterize the charge transport and radiative emission processes that occur in electroluminescent polymers; to determine the mechanisms that limit radiative efficiency and device lifetime; and to develop, test, and improve diode structures.

We have made devices from poly(*p*-phenylene vinylene) [PPV], MEH derivatives, and blends of PPV-like oligomers by a spin-on process onto an indium-tin oxide or metal-coated glass substrate, and we have demonstrated their electroluminescence. In addition, we used internal photoemission and electroabsorption measurements to determine the electronic excitation energies in the polymer; used photothermal deflection spectroscopy and photoluminescence to determine the degradation effect caused by photo-oxidation; and studied the dependence of photoluminescence intensity and decay time on temperature, using this information to determine the quantum efficiency of the polymer, oligomers, and blends (see accompanying figures).

Our device model has successfully explained electroabsorption, capacitance, and internal photoemission measurements, and we have obtained consistent values for polaron binding energies and trap densities.

Publications

Bronold, F.X., A. Saxena, A.R. Bishop, "Radiative Decay of Polaron-Excitons in Poly(Phenylene Vinylene)," *Phys. Rev. B* **48**, 13612 (1994).

Bronold, F.X., A. Saxena, A.R. Bishop, "Radiative Processes in Poly(Phenylene Vinylene)," *J. Lumin.* **60/61**, 849 (1994).

Campbell, I.H., D.L Smith, J.P. Ferraris, "Electrical Impedance Measurements of Polymer Light-Emitting Diodes," *Appl. Phys. Lett.* **66**, 3030 (1995).

Campbell, I.H., D.L Smith, J.P. Ferraris, et al., "Direct Measurements of Conjugated Polymer Electronic Excitation Energies Using Metal-Polymer-Metal Structures" (submitted to *Phys. Rev. B*).

Davids, P.S., A. Saxena, D.L. Smith, "Bipolaron Lattice Formation at Metal-Polymer Interfaces" (submitted to *Phys. Rev. B*).

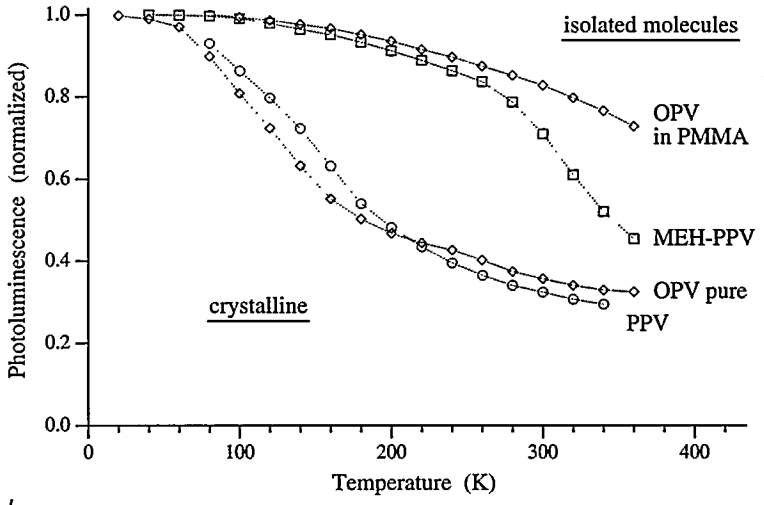
Davids, P.S., D.L. Smith, A. Saxena, "Nondegenerate Continuum Model for Polymer Light-Emitting Diodes" (to be published in *J. Appl. Phys.*).

Heller, C.M., I.H. Campbell, B.K. Laurich, et al., "Solid-State Concentration Dependence of the Optical Absorption and Emission of PPV-based Materials" (submitted to *Phys. Rev. B*).

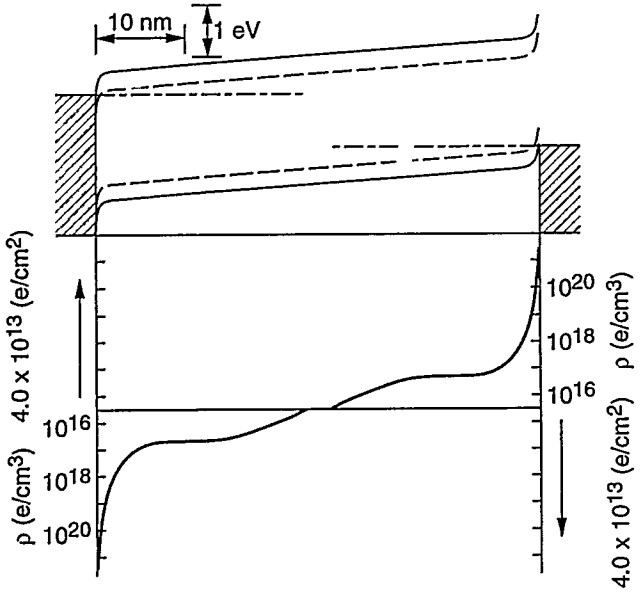
Laurich, B.K., I.H. Campbell, C.M. Heller, et al., "Photothermal Deflection Spectroscopy of Poly(para Phenylene Vinylene) Derivatives," *Bull. Am. Phys. Soc.* **40**, 107 (1995).

McBranch, D., I.H. Campbell, D.L. Smith, et al., "Optical Determination of Chain Orientation in Electroluminescent Polymer Films," *Appl. Phys. Lett.* **66**, 1175 (1995).

Wang, W.Z., A. Saxena, A.R. Bishop, "A Systematic Study of the Vibrational Properties of Poly(Phenylene Vinylene) and Related Oligomers," *Phys. Rev. B* **50**, 6068 (1994).



Integrated photoluminescence intensity vs temperature for oligomer blend, MEH-PPV, pure oligomer, and PPV. The intensities are normalized to the estimated value at 0 K.



Energy diagram (upper panel) and charge density (lower panel) at a forward bias of 1.0 V, with the chemical potential of the left (right) contact of 1.2 V (-1.2 V). A uniform density of 5 $\times 10^{16}$-cm^{-3} traps of each charge sign is included. The negative (positive) trap energy is 0.6 eV (-0.6 eV).

High-Temperature Materials Synthesis Without Heat: Oxide Layer Growth on Electronic Materials Using High-Kinetic-Energy Atomic Oxygen

Mark Hoffbauer

Our objective is to examine thin-film materials synthesis in which chemical reactions are initiated using high-kinetic-energy neutral atomic species instead of high temperatures. A key to improved material processing is the proven concept that growth temperatures can be dramatically lowered when materials chemistry is activated by the kinetic energy of one or more key species. Thus, hyperthermal atoms serve as tools for revolutionary nonthermal thin-film materials chemistry.

We have focused on the direct growth of oxide and nitride insulating layers on compound semiconductor materials, such as gallium arsenide, used in manufacturing electronic devices. Almost two decades of intensive effort with a wide variety of approaches has failed to overcome the inherent difficulties in forming useful insulating and passivating oxide layers on gallium arsenide. Our research was aimed at producing device-quality insulating oxide layers on semiconductor materials. We have formed thick, uniform, and fully oxidized insulating layers of unprecedented quality on gallium arsenide by exposing wafer substrates to a high-kinetic-energy (~3 eV) beam of neutral atomic oxygen. The nonthermal oxidation process does not disrupt the crystalline order of the substrate, and no detectable elemental arsenic is produced at the oxide/gallium arsenide interface.

This new materials synthesis process may have profound technological and economic implications when it can be used to fabricate electronic devices. Our work demonstrates the value of using novel high-energy interactions of neutral beams with advanced materials to understand the chemical and physical properties of these materials.

Publications

Cook, S.R., J.B. Cross, and M.A. Hoffbauer, "Accommodation Measurements Involving Hypersonic Gas-Surface Interactions," *Rarefied Gas Dynamics* **19**, 967 (1995).

Cook, S.R., J.B. Cross, and M.A. Hoffbauer, "Hypersonic Gas-Surface Energy Accommodation Test Facility" (to be published in *AIAA J.*).

Erkkila, V.J., M.A. Hoffbauer, and J.M. White, "Photochemistry of O_2 on Ag(110) Using Picosecond UV Laser Pulses" (submitted to *J. Vac. Sci. Technol.*).

Gregory, J.C., M.A. Hoffbauer, J.B. Cross, et al., "Surface Processing of Semiconductor Materials with Fast Oxygen," *Materials for Processing and Applications in Space* **77**, 325 (1995).

Large Dynamic Range, Picosecond-Resolution Radiation Detection Based on Low-Temperature-Grown Epitaxial GaAs Films

David Watkins

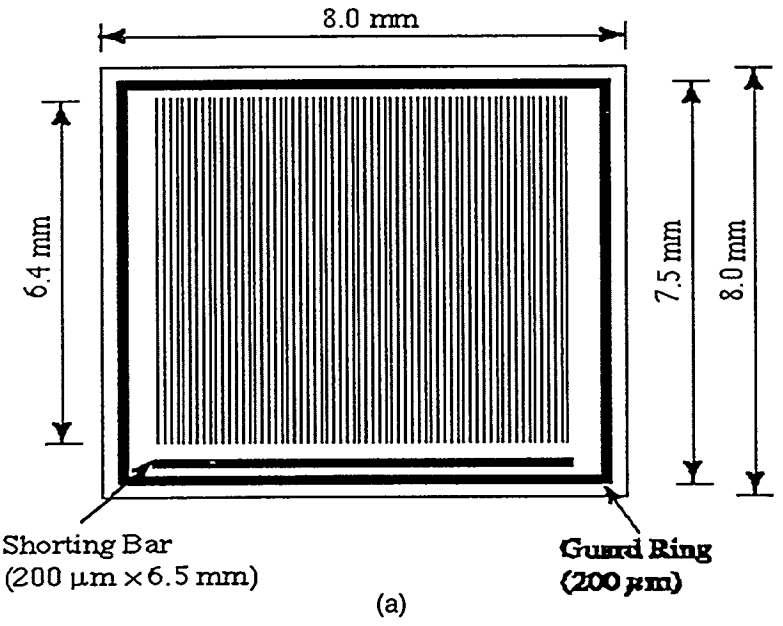
The goal of this project was to develop ultrafast radiation detectors based on GaAs epilayers grown by molecular beam epitaxy at substrate temperatures of 200°C–300°C. GaAs produced in this way is called low-temperature (LT) GaAs. LT-GaAs is known to have subpicosecond charge carrier lifetimes; therefore, detectors based on this material should have response times of the order of 1 ps, more than an order of magnitude faster than existing high-energy radiation detectors.

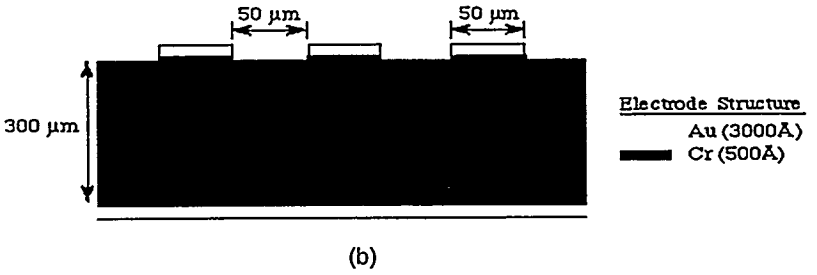
During the first year of the project, we fabricated penetrating radiation detectors of several different designs using LT-GaAs. The detectors that were tested showed faster response time than any previous penetrating radiation detector. The biggest problem with the LT-GaAs detectors was significant signal decay tailing caused by the device substrate interacting with the active layer.

We spent the second year trying to eliminate the tailing problem. We began by fabricating radiation detectors based on LT-GaAs epilayers grown on conducting n^+ GaAs substrates. We found that to eliminate the substrate contribution to the detector signal, we had to electrically isolate the substrate from the epilayer by incorporating a p-n junction barrier against carrier diffusion. We finally realized that this structure also produced a tailing contribution. Near the end of the second year, we tried to separate the LT-GaAs epilayer from the substrate by selective etching, but we found

this to be far more difficult than expected.

As various problems with adequate material structure for LT-GaAs became apparent, we changed the course of our work to develop polycrystalline CVD diamond for radiation detectors. As a result we were able to demonstrate—for the first time—the feasibility of diamond microstrip detectors for radiation detection in high-luminosity particle colliders. While developing the diamond microstrip detectors, we were also able to advance the state-of-the-art in diamond film quality.



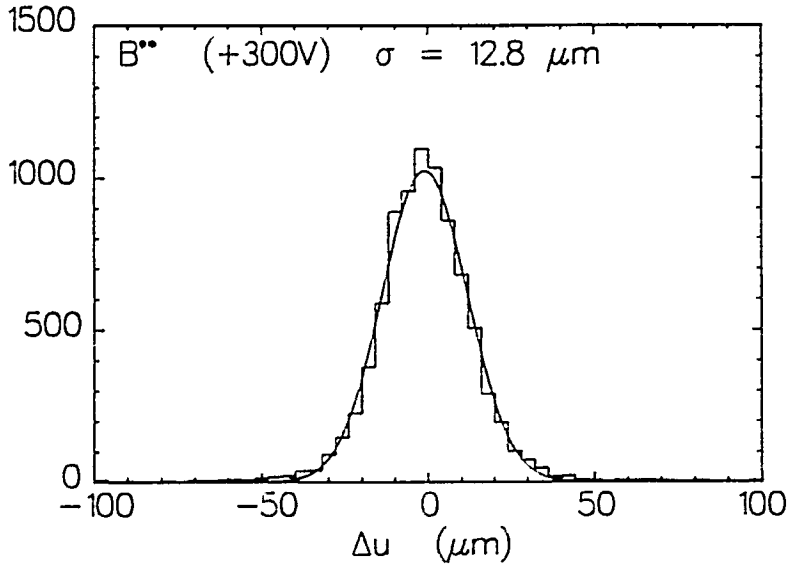


(a) Schematic diagram of periodic array of interdigital electrodes of alternating polarity to be used for current collection in LT-GaAs-based radiation detectors. (b) Schematic diagram of a diamond-based microstrip detector to demonstrate the feasibility of its use in high-luminosity colliders.

Publications

Bauer, C., I. Baumann, C. Colledani, et al., "Radiation Hardness Studies of CVD Diamond Detectors" (to be published in *Nucl. Instrum. Methods A.*).

Bauer, C., I. Baumann, C. Colledani, et al., "Recent Results from Diamond Microstrip Detectors" (to be published in *Nucl. Instrum. Methods A.*).



Position resolution of a diamond microstrip detector.

Instrumentation for High-Efficiency, High-Sensitivity Actinide Analysis

Jose Olivares

Thermal ionization mass spectrometry (TIMS) is an analytical tool used extensively to determine both the absolute abundance and the isotopic composition of elements in all types of samples. TIMS is applied to research and diagnostics in such fields as nuclear chemistry, radiochemistry, geological science, environmental analysis, and medical research. Although TIMS is a very sensitive analytical technique, the sample utilization efficiency is below 0.5% for actinides. We have developed a high-efficiency thermal ionization cavity ion source that provides one to two orders of magnitude improvement in sample utilization efficiency in comparison with the conventional ribbon-type ion source currently used in TIMS. This improved sample utilization efficiency results in a proportional increase in sample throughput and a proportional decrease in analysis time.

In conventional thermal ionization sources, the sample to be analyzed is placed on a thin, flat ribbon (rhenium, tungsten, or other high-resistance metal) filament, which is heated by passing a current through the filament much like the filament in a light bulb. The filament is heated to temperatures of up to 2,500°C, and sample atoms are evaporated from the surface of the filament. Ionization occurs as a result of the interaction between a gaseous sample atom and the filament surface in which an electron from the sample atom is passed onto the hot metal surface (which has a high potential for attracting free electrons) to produce a positive ion of the sample. Because the filament must be placed in a high vacuum (for both filament and ion survival), the atoms evaporated from the filament have limited contact with the filament surface; in fact, once the atoms leave the immediate region near the filament surface, they are not likely to interact with the filament surface again. The ionization efficiency (that is, the number of neutral atoms converted to ions) for the ribbon-type source is very low.

In our thermal ionization source, a sample is placed deep in a miniature cavity inside a small tungsten or rhenium tube (crucible). The crucible is heated by bombardment from electrons emitted by a metal filament located near and around the crucible. The heating power deposited on the crucible can be very high. For example, if the electron emission current is only 40 mA, the crucible will receive 120 W of heating power. With this much energy, the temperature of the thermal ionization cavity can reach up to 3,000°C. The crucible easily survives these higher temperatures because of its thickness (about 0.062 in.). As the sample atoms are evaporated inside the crucible cavity, the local pressure inside the crucible increases, and the gaseous atoms interact with the crucible surface to produce positive ions of the sample. Because of the small enclosed space inside the cavity, many atom-to-surface interactions occur, which (along with the high temperature) accounts for the high efficiency of the ion source. The accompanying figures show (1) the thermal ionization cavity ion source and (2) how the cavity ion source works.

The thermal ionization cavity for mass spectrometry is a miniaturized version of an existing room-sized model used in our isotope separators for producing milligram quantities of various isotopes. Because of its miniature design, our cavity ion source can be used on any small thermal ionization mass spectrometers, such as quadrupole-based mass spectrometers. Mass spectrometers that use our cavity ion source will have efficiencies one to two orders of magnitude higher than mass spectrometers that use the conventional ribbon-type ion source.

Our cavity ion source greatly improves the efficiency of thermal ionization mass spectrometers. There are two reasons for the higher efficiency of our ion source, compared with ribbon-type ion sources. First, more surface-to-atom interactions occur in the small cavity of our ion source than in the high vacuum required by conventional ion sources. Second, a higher operational temperature can be attained (about 500°C higher than the temperature reached by conventional sources). The thickness of the crucible allows it to easily survive temperatures of up to 3,000°C. The thin ribbon-type filament (about 0.004 in.) of conventional ion sources burns out at temperatures beyond 2,500°C.

For these reasons, the ionization efficiency of the cavity ion source is 10 to 100 times greater than conventional technology. Easily ionized elements (for example, alkali and alkaline elements) can reach ionization efficiencies of 50%–90%, and actinides can reach efficiencies of 1%–10%. Conventional ion sources are based on the ribbon-type thermal ionization source, which cannot reach as high a temperature and allows fewer atom-to-surface interactions. The ionization efficiency of conventional ion sources may be, at best, 10% for easily ionized

elements and 0.01%–0.5% for actinides.

The lower ionization efficiency achieved by conventional ion sources means that analysts must load 10 to 100 times more sample or must acquire 10 to 100 times more data in order to achieve results similar to those obtained with our ion source. For example, if an analyst needs 1 pg of plutonium sample to determine its radioisotope concentration, then 100 g of soil would need to be processed. In contrast, for a mass spectrometer using our ion source, only 10 g of soil would need to be processed since only 0.1 pg of sample would be required. In addition, because sample throughput, analysis time, and chemistry time are proportional to the size of the sample, our ion source increases sample throughput and lowers analysis time.

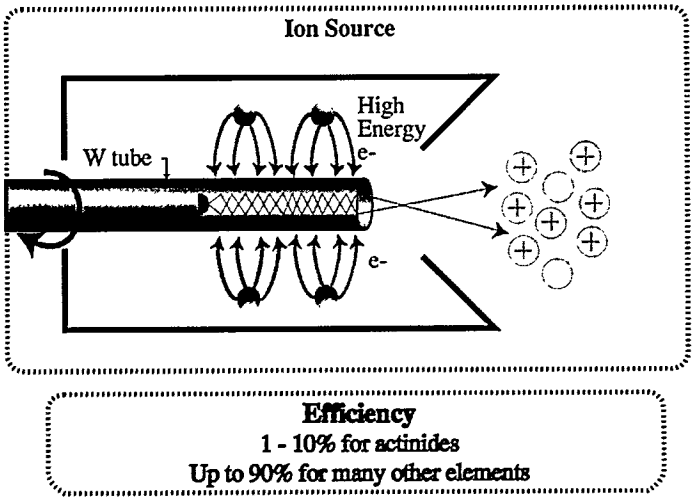
The thermal ionization cavity ion source opens up the possibility of making thermal ionization available in small, rugged, and portable mass spectrometers. The efficiency of small mass spectrometers used with our cavity ion source will be similar to or better than the efficiency of large, more-expensive magnetic sector-based mass spectrometers. These portable, more-efficient mass spectrometers would improve the field analysis of samples. As part of the project to develop the cavity ion source, we constructed and successfully tested a new high-performance, quadrupole-based thermal ionization cavity mass spectrometer.

Our new ion source also opens up the possibility of equipping (or retrofitting) existing mass spectrometers with our ion source to increase their efficiency. At present, there are at least 1,000 small, low-efficiency mass spectrometers in existence.

During the past year, we further designed the ion optical-transfer system so that this ion source can be used with large magnetic-sector-based mass spectrometers. When built, this instrument will increase the current performance of these instruments from a detection limit of 10^6 atoms to an impressive 10^4 (low attogram quantities of sample material).



In this close view of the thermal ionization cavity ion source, the tube-like crucible can be seen in the center. Samples are placed in a cavity deep within the crucible. The high efficiency of the cavity ion source is primarily the result of the small enclosed space inside the cavity, which allows many interactions between the gaseous atoms of a sample and the surface of the crucible.



In the thermal ionization source, a sample is placed deep in a miniature cavity inside a small tungsten or rhenium tube (crucible). The crucible is heated by bombardment from electrons emitted by a metal filament located near and around the crucible. The crucible can be heated to temperatures as high as 3,000°C. The small enclosed space inside the cavity allows for many atom-to-surface interactions, thus increasing the probability of ionization.

Development of Multimode Neutron-Noise Theory

Gregory Spriggs

During the summer of 1993, an international research team representing six countries (France, Russia, Italy, Belgium, Japan, and the United States) participated in a series of benchmark reactor-physics experiments on several prototypical fast reactors. During the measurements, the team observed multiple-decay modes in a series of neutron-noise measurements using two techniques that were presumed to be unrelated to each other. This was a completely unexpected result that raised several questions concerning the validity of any results that might be obtained using simple models to describe the integral systems.

The purpose of our project was to develop, if possible, a unifying theory that can explain the data observed using the two techniques.

We have developed a two-region kinetic model for reflected reactors as a first step to explaining neutron-noise measurements in more complex multiplying systems. We successfully tested the model against experimental data obtained from the University of New Mexico's AGN-201 reactor. The successful development and testing of the reflected-core model are important accomplishments. The test demonstrated that neutron-noise measurements in more complex multiplying systems can be analyzed using relatively simple models. This will become particularly important when trying to reverse-engineer neutron-noise signatures obtained from nuclear-weapon components, an approach currently being proposed in the international nonproliferation and safeguards arena. Furthermore, we expect the two-region model to be useful in providing benchmark numerical solutions to verify and validate time-dependent, multidimensional, deterministic transport solutions under the accelerated strategic computing initiative.

Publications

Spriggs, G.D., R.D. Busch, and J.G. Williams, "Two-Region Kinetic Model for Reflected Reactors" (submitted to *Nucl. Sci. Eng.*).

Optical Imaging Through Turbid Media Using a Degenerate Four-Wave-Mixing Correlation Time Gate

Nicholas Nogar

In the past several years, much effort has been applied toward developing optical tomography for applications such as mammography and brain imaging. The objective is to eliminate ionizing radiation as a means of imaging human tissues. Because of its nondamaging nature, an optical diagnostic could safely be used more frequently than current x-ray sources, thus leading to a higher probability of successful intervention. Resonant, degenerate four-wave mixing (DFWM) is a coherent, nonlinear-optical phenomenon that permits the use of correlation time-gating to reduce detected scattered light and improve image quality for objects in scattering media.

The primary goal of this research is the demonstration of a system that can image an object in an optical surrogate for human breast tissue. Ideally, the object would have properties similar to those of breast tumor and be a few millimeters in diameter. This system should eventually have demonstrable resolution for imaging blood clots and tumors in the brain. It can also be applied to the study of radiation effects on man, atomic and molecular physics, and the interaction of atoms and molecules with photons.

Our initial work has targeted breast tissue diagnostics. Specific activities initiated so far include an extensive literature survey of past efforts in imaging scattering media and a review of nonlinear optics and development of a model for DFWM. In addition, we have developed a DFWM apparatus based on a Nd^{+3}:YAG laser, performed preliminary experiments with alternate-phase conjugate materials, primarily $BaTiO_3$, and developed and characterized a breast tissue phantom (that is, a model or surrogate that can be used instead of real tissue for laboratory experiments).

New Applications for Zeeman Interferometry

Roger Johnston

The Zeeman Refractive Index Detector received an R&D 100 Award in 1992. We are exploring and developing new applications and instrumental approaches for this technology, including pollution and process monitoring, chromatography detection, ultrasensitive spectrophotometry, and real-time gel-electrophoresis detection.

During the past review period, we made major advances in reducing the instrument's size (by 60%), cost (by nearly 400%), and complexity. The instrument is now more robust and easier to use.

We also showed that two new approaches—membrane-sample introduction (demonstrated experimentally) and waveguide-assisted refractometry (demonstrated theoretically)—have good potential to further improve the instrument's performance and usefulness. In particular, both approaches offer the possibility of greatly improved specificity to detect trace contaminants during pollution and process monitoring: there would be less interference from chemical species that are not of interest, and sample size would be greatly reduced. Work to date has led to two cooperative research and development agreements (CRADAs) to explore the commercialization potential of the instrument.

Publications

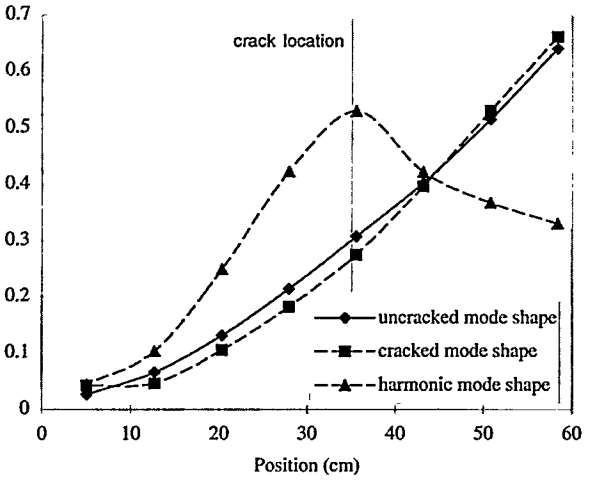
Johnston, R., S.D. Schroder, and A. Mallawaaratchy, "Statistical Artifacts in the Ratio of Discrete Quantities," *Am. Statistician* **49**, 285 (1995).

A Comprehensive Monitoring System for Damage Identification and Location in Large Structural and Mechanical Systems

Charles Farrar

There are many large structures and mechanical systems for which it would be desirable to monitor the "health" of the system and to identify damage at the earliest possible stage. This research effort combines expertise from diverse disciplines to develop a comprehensive damage detection system. Our first year's efforts have been extremely successful. We used a finite element model of nonlinear damage to identify likely damage detection parameters. Initial experimental tests have shown some of these parameters to be superior to those in the technical literature. The figure shows experimental results comparing a "harmonic mode shape," which was developed in this project, with a cracked mode shape, which is a conventional damage detection parameter. As evidenced by the hump near the crack location, the harmonic mode shape is superior for locating damage.

To prepare for the second-year goals, we have purchased aluminum I-beams as test specimens; the beams are being fatigue loaded to induce cracks. In preparing for the third-year goals of our work, we identified an actual highway bridge near Truth or Consequences, New Mexico, and obtained tentative approval to instrument the bridge and test it in both undamaged and damaged states. We performed preliminary tests on the undamaged bridge to allow knowledgeable planning for future tests. Most likely, we will take data on the damaged bridge before the end of the project's second year.



Superiority of harmonic mode shape for damage detection. The peak near 35 cm indicates the location of the crack.

Gravity Gradiometry Based on High-T_c Superconducting Sensors

Robert Kraus

The gravitational field of the earth has minuscule local variations that, though universal, are difficult to observe with any but the most sensitive instruments. Local variations in the density of the earth's crust, such as voids or concentrations of high-density material, cause these variations in the gravitational field. Such anomalies can be observed directly by mapping the magnitude of the gravitational field (gravimetry) or by measuring the gradient of the gravitational field (gradiometry).

We believe gradiometry is potentially superior to gravimetry because the measurement and interpretation of the results are generally simpler, and gradiometry is less susceptible to masking by other effects (such as accelerations). Gradiometry also is a completely passive measurement, introducing absolutely no energy or radiation into the region of interest. Furthermore, we believe that we can adapt this method to moving platforms. Finally, the capability to take real-time data over large areas is certainly feasible. The purpose of our project is to examine the feasibility and performance of a gradiometer that uses high-T_c (critical temperature—temperature at which the superconducting transition occurs) materials and is capable of being deployed in the field (a device that can be transported by hand, ground vehicle, and/or aircraft).

The focus of our project during the review period was to complete an extensive literature search of the current state-of-the-art for gravity gradiometry and to investigate the specific technical challenges associated with the design and fabrication of a superconducting gravity gradiometer that is both simple and capable of determining the existence of and characterizing underground anomolies such as voids. Simple detection will be our first goal. These voids in the earth cause a local perturbation to the gravitational field which shows up as a varying gradient. Consequently, by measuring the gravitational gradient, we should be able to deduce what is under the surface. Our second goal is to quanitify the nature of the anomaly—for example, to be able to assess the size, depth, and extent of underground voids that might be tunnels or rooms.

The technical challenges we addressed in our effort were the conceptual design of

- a 4-component (dGx/dx, dGx/dy, dGy/dx, dGy/dy; only three of which are unique) superconducting gravity gradiometer and
- a controllable high-T_c persistent-current circuit,

and the conceptual design and modeling of a vibration-damping scheme for a superconducting gravity gradiometer.

Development of New and Efficient Hard-Rock Mining Methods Using Pulsed Laser Excavation

David A. Cremers

Our objective in this project is to develop a laser-based method for fracturing hard rock (e.g., granite and basalt) into small particles to increase the efficiency, safety, and cost effectiveness of industrial mining. The approach is based on the use of pulsed Nd:YAG lasers having 2 to 40 J/pulse and pulse widths from 10 to 40 nanoseconds. Using large laser systems, we are conducting experiments at Los Alamos and Battelle Institute. Our accomplishments during the past year included (1) scaling up experiments (to lasers with 10 and 40 J/pulse); (2) demonstrating the effectiveness of water to enhance rock fracture; (3) demonstrating the importance of focal-spot size on rock fracture; and (4) demonstrating the importance of maintaining optimum focus on the rock sample.

Our experiments showed that a 10-J laser pulse with a large spot size (i.e., 3 to 5 mm in diam) does not transfer energy efficiently into the rock samples. In contrast, we found that a 1-J laser pulse that was tightly focused generated much larger stresses in hard rock. The larger spot size did not generate a strong pressure wave in the rock. In addition, proper focusing is critical to producing maximum coupling between the rock face and the laser pulse because of the air plasma formed above the rock face that decouples the laser pulse from the surface. Therefore, the air plasma must be minimized through proper focusing to achieve maximum energy coupling.

In ongoing work, we will continue to determine the optimum laser parameters (using minimum laser energy) for rock fragmentation. With our industrial collaborator, we will also direct our work toward specifying a proof-of-principle laser machine for mining hard rock.

Application of Intense Surface Discharge VUV Light Sources to Photoresist Ashing in Semiconductor Manufacturing

Robert Sze

In this project we use intense surface-discharge vacuum-ultraviolet (VUV) light sources to ash the photoresist used in semiconductor manufacturing. We generate the light source by initiating an arc discharge on a dielectric surface to produce a high-temperature plasma which strongly emits in the VUV. Photodissociation of molecular oxygen is most efficient in this spectral region. The atomic oxygen produced by the photoflash oxidizes the polymer photoresist into gaseous products. Surface discharges ash photoresist much faster than existing techniques and without contamination of, or damage to, the underlying surface.

In the past year we have optimized a very-large-surface-area, intense VUV light source for semiconductor and flat-panel-display device processing. We constructed the source with materials containing no hydrocarbon compounds that could contaminate the substrate to be processed. The source can deliver a surface energy density in the ultraviolet wavelengths of >2 J/cm^2 per pulse of light, with uniformity of >5% over the entire area of the source. The discharge occurs at atmospheric pressure and is far removed from the material to be processed, thus providing a particulate- and ion-free processing environment.

There are many potential processing applications for this source because it is particulate- and ion-free and because of its extremely high luminous intensity. For example, the 15- × 15-cm prototype currently operating in our laboratory produces >450 J of uniform ultraviolet emission; the device can easily be scaled to much larger dimensions. Other potential applications for this source are flash annealing of amorphous silicon to polysilicon devices, activation of electroluminescent phosphors, and light-assisted, low-temperature CVD-deposition processes.

The Development of Fullerene-Based Hydrogen Storage Systems

Shimshon Gottesfeld

The goal of this project is to determine the feasibility of hydrogen storage systems based on fullerenes. We would like to store hydrogen reversibly in solid-state form at levels exceeding 3% hydrogen by weight. This is an important technical challenge for fuel-cell-powered electric vehicles, which require an effective and safe mode of hydrogen storage. We have evaluated recent data on hydrogen uptake by fullerenes and designed and assembled an experimental system for precise measurements of hydrogen uptake/release by fullerenes.

First we evaluated the options of using fullerenes as media for physisorption of hydrogen at low temperatures/pressures or as media for chemisorption of hydrogen at high temperatures/pressures. Based on comparisons with other hydrogen storage modes, we concluded that chemisorption is the only technologically viable option. Thus we designed the experimental system to accommodate temperatures exceeding 500°C and pressures up to 3000 psi.

We have just finished construction of a computer-controlled system to measure gas uptake and release at the required temperatures and pressures. The same experimental system will allow us to perform surface area measurements under cryogenic (Brunauer-Emmett-Teller) conditions before performing hydrogenation/dehydrogenation cycles.

We evaluate hydrogen uptake and release of the fullerene sample by measuring gas pressure as a function of time. We observe changes in gas pressure after a change in hydrogen pressure or in temperature. Computer-aided analysis of this data provides heats of adsorption and activation energies for both adsorption and desorption. We have just started hydrogenation/dehydrogenation measurements. Activities planned for the near future include collecting basic data on the hydrogen/fullerene system and studying the effects of metal catalysts and chemical modifications of fullerenes.

Generation of Intense Electromagnetic Radiation with Explosively Driven Piezoelectric Material

Michael Fazio

This project focuses on developing explosively driven piezoelectric sources of electromagnetic radiation. These sources include sinusoidal radio frequency (rf), wideband microwave, and high-voltage, high-current pulsed-power devices. Piezoelectric material produces electrical charges when it is mechanically deformed. It also changes dimensions when placed in an electric field. Using explosives to compress piezoelectric material can produce large amounts of electrical energy in short time periods. The goal of this effort is to produce very simple and compact piezoelectric devices able to generate enough electromagnetic energy to damage significant military targets.

Conventional pulsed-power sources have energy densities $<0.5\ J/cm^3$. The theoretical energy-density limit for explosively driven piezoelectric sources is tens of J/cm^3. Thus, devices as small as a 40-mm round could deliver enough energy to produce substantial effects on targets. In addition to possessing high energy density, piezoelectric sources can be made very rugged and can be easily configured to produce a wide variety of frequency outputs for direct connection to targets or to antennas.

Traditionally, piezoelectric materials have been used in sonar transducers and in shock sensors. In these applications high energy and high energy density were not critical parameters. We have conducted experiments and modeling that have produced sinusoidal rf; wideband microwave radiation; and high-voltage, high-current pulses using piezoelectric material—compressed by a high-explosive-generated shock wave—with significant energy and energy density.

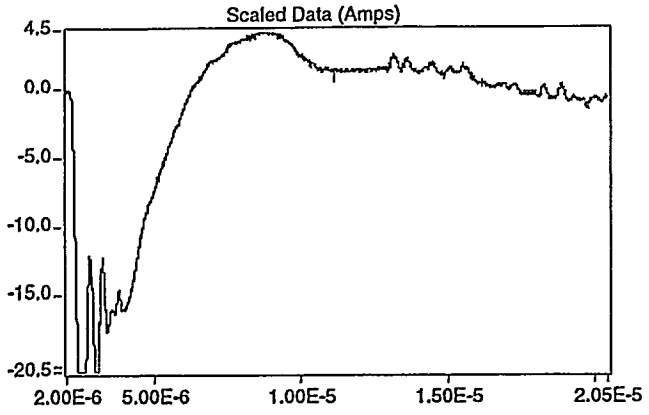
Over the past three years we have studied several different piezoelectric materials, including lead zirconate titanate. However, a recently developed organic polymer—polarized polyvinylidine fluoride (PVDF)—has far greater piezoactivity that any other synthetic or natural material. PVDF is a flexible clear plastic film that can be readily cut, shaped, and metallized. PVDF has several properties which make it ideally suited for use in electromagnetic sources: a very large pressure range (μtorr to Mbar), high-voltage output, high dielectric strength (75 V/μm), and high mechanical strength. We have conducted explosive experiments with PVDF which have produced high-voltage pulses with extracted energy densities $>1\ J/cm^3$.

In the third year of this project, we have concentrated on improving our understanding of the relevant physics, scaling the devices to higher energies, testing devices as sources for driving magnetic-flux compressors, and developing copolymer technology in order to make large amounts of piezoelectric material inexpensively. Using hydrodynamic codes and explosive experiments has allowed us to develop a detailed understanding of the physics of piezoelectric electromagnetic sources.

For piezoelectric devices to be practical, not only does the energy density have to be high, but large amounts of energy must be obtained (tens to hundreds of joules). We have explored two geometries to scale piezoelectric sources to high energies: a planar stack of piezoelectric films (see first figure) and the cylindrical "pipe bomb" geometry. Both techniques have been successful. However, our most recent work has concentrated on the planar geometry because the computer modeling and the behavior of the shock waves are much simpler for this geometry. This past year we fired devices containing up to



A large-area planar piezoelectric experiment.



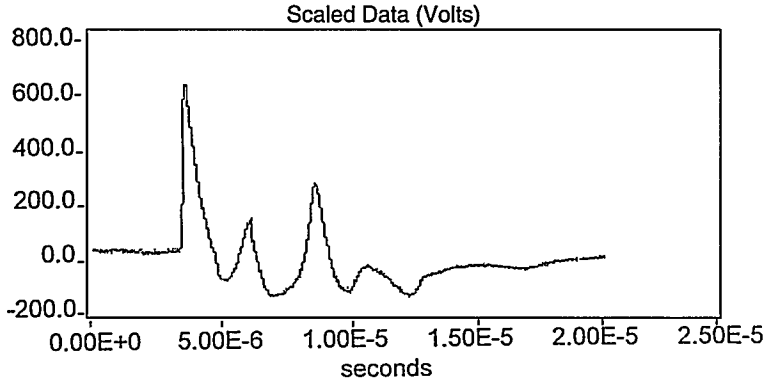
Piezoelectric output into an inductive load typical of a magnetic-flux compressor.

10 cm^3 of PVDF, an increase of over three orders of magnitude over what has traditionally been used in shock-sensor applications.

One near-term application of piezoelectric generators is to provide "seed" energy for large magnetic-flux-compressor generators. Traditionally, large capacitor banks have been used to provide seed energy. However, these banks have low energy densities and are hard to make rugged enough for military weapons. This year we conducted a set of experiments to determine if piezoelectric generators could drive the inductive load typically found in magnetic-flux compressors (see second figure). The near-term use of piezoelectric technology in this application could greatly reduce the size of electromagnetic weapons.

Finally, we have studied ways to produce polarized PVDF in optimum geometries and in significant quantities. This year we performed studies on a castable form of PVDF known as PVDF copolymer. This inexpensive powder can be readily cast into a variety of shapes and has the added advantage that it is somewhat self-polarizing, which reduces the laborious and expensive step of electrically polarizing large areas of PVDF film. Initial lab and explosive tests of these samples show promise (see third figure).

Our three years of work with piezoelectric sources have shown that explosively driven piezoelectric sources can produce the outputs required for practical devices.



Output waveform from a large-volume copolymer piezoelectric source.

Femtosecond Scanning Tunneling Microscope

Antoinette Taylor

By applying ultrafast optical techniques to the scanning tunneling microscope (STM), we are developing a tool to probe phenomena on atomic time scales as well as on atomic length scales. Our goal is to build the first STM with temporal resolution of 100 fs or less. The temporal resolution of this STM will exploit tip/sample nonlinearity induced noninvasively either with femtosecond optical pulses or optically generated femtosecond terahertz pulses. Potential applications of this device include characterizing the performance of submicron devices, studies of single-electron tunneling in nanostructures, and studies of carrier transport at interfaces.

We have assembled an experimental capability for testing the concept of optical rectification at a tunneling junction by integrating a commercial STM head and base with electronics and software developed in our lab. We have also implemented the functions of bringing the tip to the sample and stabilizing it against thermal drift and mechanical vibrations.

The optical setup splits a beam of femtosecond pulses into two trains with a variable time delay between them. The pulses spatially overlap at the tunneling junction; we measure the tunneling current as a function of the delay between the pulses. If the optical rectification process is sufficiently nonlinear, we should observe a change in the tunneling current when the pulses temporally coincide at the junction. We have found that thermal expansion of the tip caused by the incident light contributes significantly to the tunneling current.

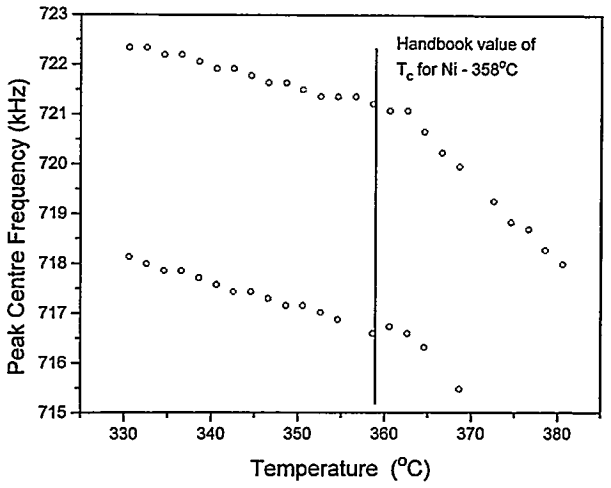
Ultratough Ultrasonic Transducers and Robust Algorithms for Resonant Ultrasound Spectroscopy

Timothy Darling

To make ultrasonic transducers optimally effective for resonant ultrasound spectroscopy (RUS), we need to optimize signals, minimize the effects on objects under test, and deal with odd shapes, limited access, and different environments. Epoxy and plastic layers in a transducer degrade performance by permitting unwanted modes of vibration. Resonances from the transducer are difficult for computer programs (not to mention experienced operators) to distinguish from resonances of the object under test. Metal diffusion bonding has been used to make transducers that produce fewer spurious peaks.

Through experiments, we have determined the optimal parameters to make good bonds with various sizes of transducers. Using silver films of 2000 to 5000 Å thick and bonding them at 250°C for 20 minutes while applying a pressure of about 2000 psi, we can reproducibly make transducer units with superior properties that are comparable in size to epoxied units. Experiments verify the removal of unwanted low-frequency modes from the transducer, which may also be used at high temperatures. The accompanying figure shows the magnetic transition of nickel at 360°C, measured with metal-bonded transducers.

The noise figures of these transducers and the removal of unwanted peaks allow certain computational processes to be more robust. In particular, algorithms developed to recognize peaks and determine center frequencies become more reliable because unwanted peaks and their effects are absent.



Variation of mode frequency with temperature for a sample of nickel, showing a change at the ferromagnetic Curie temperature.

Value Analysis Technology for R&D Environments

Anne Henriksen

The goal of this project was to develop a methodology that will assist LDRD decision makers in creating a balanced portfolio of projects and in performing a value analysis of proposed and current projects. The new methodology will also transform value analysis into an assessment of project impact.

The first part of the study consisted of developing a unified framework for evaluating the success of R&D projects, such as LDRD. To accomplish that, we presented the R&D project lifecycle model that organizes an R&D project into five distinct stages: project conception/planning, project duration, the immediate post-project period, the near-term impact period, and the long-term impact period. We then discussed the value analysis of the R&D project within the framework of this lifecycle model and suggested evaluation techniques appropriate to the different stages. We emphasized the importance of evaluating the project selection process itself by assessing (retrospectively) the success of the R&D portfolio.

Our next step was to develop an R&D project lifecycle timeline, and we correlated it to a technological innovation timeline to illustrate the fundamental relationship between basic/applied R&D (now) and technological innovation (the future). The message that seeds of research must be planted today in order to harvest technological innovation several decades into the future was demonstrated with the two (juxtaposed) timelines.

To assess proposed and ongoing LDRD projects (project conception/planning and project duration), we constructed a questionnaire that incorporated the following four criteria to be used by peer review teams during the proposal evaluation and interim assessment processes:

- *relevance* of the project to the Laboratory mission and to the strategic objectives of the LDRD program;
- *risk* associated with the project (measured in terms of probability of success);
- *reasonableness* of the proposed scope, schedule, and resource request; and
- *return* if the project is successful.

Return in this case includes three different components: scientific return, programmatic return, and business return. The relative importance of each type of return depends on the particular category of R&D (that is, basic vs applied vs engineering). Peer review teams use the questionnaire to evaluate proposals, and the resulting responses can range from very high (score of 5) to very low (score of 1).

For the purpose of ranking project alternatives, we devised a combined additive/multiplicative algorithm that converts the question responses into a proposal figure of merit. This combined additive/multiplicative algorithm represents an improvement over traditional approaches because it explicitly incorporates tradeoffs among competing evaluation criteria. We showed that this algorithm correctly discriminates for the desired characteristics and that it ranks proposals consistent with the institution's intended emphasis. The algorithm was also constructed so that use of the appropriate question weights would inherently effect the optimal portfolio; that is, the desired composition of basic and applied research initiatives of the highest quality would be intrinsically selected.

We then combined the resulting figure of merit with a funds request scaling factor to obtain a value index for each proposed project. The value index algorithm produces a measure of project value that takes into account the fact that value is a function of both merit and cost. It is incumbent on management to structure a selection process that emphasizes the appropriate criteria. The main purpose of a formal selection process is to encourage the desired characteristics in proposed projects, that is, to promote proposals with characteristics the institution prefers to reward. It is important to keep in mind that the purpose of value analysis is not to encourage a portfolio of many small projects, but to promote cost effectiveness in R&D activities. We also stress that effective implementation of a comprehensive R&D value analysis process requires a dedicated commitment from management, researchers, and peer review evaluation teams. However, it is important to remember that a decision support tool should never become a substitute for management judgment and leadership.

Materials Analysis of Deposits Made by the Directed Light Fabrication Process

Gary K. Lewis

Invented and currently being developed at Los Alamos, Directed Light Fabrication (DLF) is a process that fuses layers of powdered materials (i.e., metals) in the focal zone of a laser. By successively building up fused layers, DLF can fabricate a free-form metal part. The DLF capability eliminates conventional metal-working processes, such as forging, stamping, casting, machining, and welding.

This past year, our goal was to apply the DLF process to as many material systems as possible for comparison with conventional methods of processing. Our past work in developing the DLF process allowed us to make reliable deposits for analysis and to extend the DLF process to additional materials. We used DLF to make plate and rod samples for microstructural analyses to study solidification and chemical segregation. We then compared these properties with conventionally processed materials to determine the advantages of DLF. We performed microstructural analyses of the following DLF deposits: silver containing 19% copper (by weight), iron containing 24.8% nickel, aluminum containing 33% copper, and 316 stainless steel.

Because the dendritic and eutectic microstructures in the DLF-processed samples display continuous morphologies, a constant solid/liquid interface is maintained. The advantage of the continuous solid/liquid interface is that it allows DLF to produce fully dense metal components with optimized mechanical properties comparable to as-cast structures.

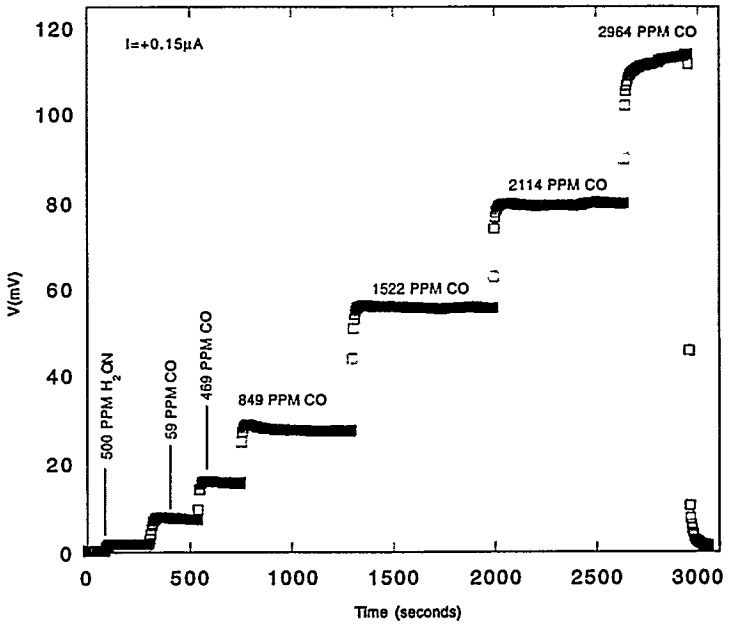
Novel Thin-Film Electrocatalytic Sensors

Fernando H. Garzon

Carbon monoxide is a colorless and odorless gas that results from incomplete combustion of typical fuels. To protect people in their workplaces and homes from this deadly gas, better sensor technologies are needed.

Our objective was to develop a simple, low-cost electrochemical sensor for detecting CO in air with tens of parts per million sensitivities, good selectivity, and fast response times. Current commercial sensor technologies cannot detect carbon monoxide below dangerous threshold levels—tens of parts per million—nor do they respond quickly at hundreds of parts per million levels.

We have developed a compact electrochemical sensor for measuring CO in air. This sensor is based on solid electrolyte technologies and does not have the associated maintenance problems that liquid-electrolyte-based sensors possess. With our sensor, carbon monoxide concentrations in air can be measured from tens of parts per million to percent levels. Our device also exhibits excellent chemical selectivity. Unlike noble metal-based carbon monoxide sensors reported in previous literature, this sensor shows little sensitivity to hydrogen. The accompanying figure illustrates the sensor's rapid response times.



Sensor response to hydrogen (interference gas) and varying concentrations of CO in air.

Telemetric Heat Stress Monitor (THSM) Spin-offs

Larry W. Berkbigler

Hazardous materials (hazmat) workers and firefighters wear clothing that protects them from external hazards, but the sealed environment of a protective suit makes its wearer susceptible to heat stress. Heat stress occurs when the body's natural cooling mechanisms fail: it can cause collapse and death. We developed the THSM to warn both workers and remote monitoring personnel of incipient heat stress by monitoring and responding to elevations in workers' skin temperatures and heart rates. The THSM won a 1994 R&D 100 Award, and there is currently a cooperative research and development agreement (CRADA) to commercialize the technology.

In this project, we began investigating spin-offs that allow the THSM to be used for other applications in addition to monitoring personnel for heat stress. We used small aerosol monitors to study the application of the THSM in monitoring hazmat workers for breaches in protective clothing suits. We also investigated the feasibility of combining other sensors with the THSM to allow remote monitoring of the environment inside and outside of the suit.

In the course of our work, we first conducted meetings with DOE, military, and industrial personnel to learn more about their needs. We then investigated other selected commercial sensors and constructed another THSM experimental device for testing. We have collected data on the sensors and are currently evaluating the information.

Bartas Iris Biometrics

Roger Johnston

In 1994 we won an R&D 100 Award for inventing the Bartas Iris Verification System. This technology can verify the identity of a person for access control, national security, law enforcement, forensics, counterterrorism, and medical, financial, or scholastic records. The technique is noninvasive, psychologically acceptable, works in real time, and obtains more biometric data than any other biometric technique except DNA analysis. The goals of this project are the following: to develop a second-generation unit that is smaller, cheaper, and faster than the original invention; to explore new applications; and to develop anti-spoofing software.

We have constructed and tested a second-generation unit that is 30% smaller, 30% cheaper, and 20% faster than the original unit. We have demonstrated this unit to Northrop Grumman's Advanced Technology Group, which is interested in putting inexpensive iris biometric units into long-haul trucks to try to reduce truck hijackings/thefts and to improve driver safety.

Publications

Johnston, R.G., "Autocorrelation Analysis of Iris Patterns and Implications for Identifying People" (submitted to *IEEE Bioengin.*).

A Gated, Integrating, Cathode-Pad Readout Chamber

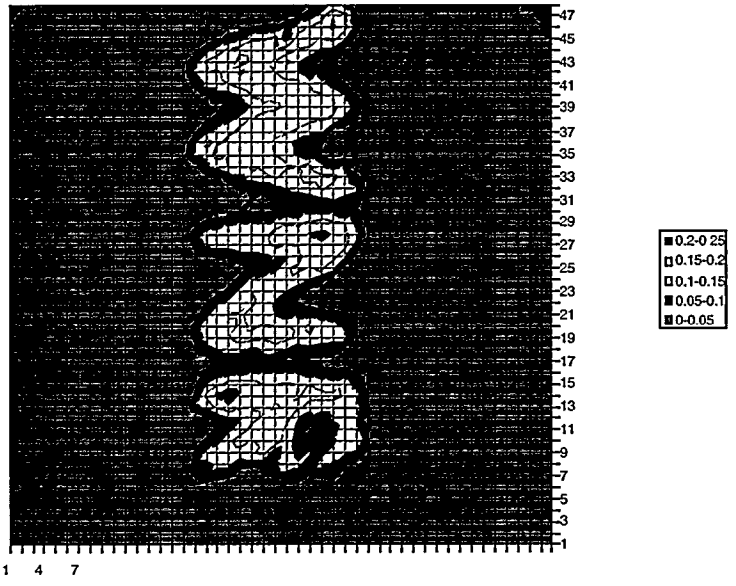
Christopher L. Morris

High-energy neutron radiography is potentially an important component of science-based stockpile stewardship. However, if neutrons are to be used as a radiography tool, the time required per exposure for a measurement must be reduced. We have developed an integrating detector—the cathode-pad readout chamber—that should allow us to significantly reduce exposure time. Because measurements are made by integrating rather than counting, minimum exposure times are limited by the neutron flux, not by the detector.

We have designed and built a complete detection system, including the multiplexer, detector, and readout chamber, and tested system performance. The detector includes either an internal or external pixel array. Each element of the pixel array is connected to a multiplexer channel through a multilayer circuit board. Charged particles, which result from neutron interactions in the converter, produce ion pairs in the wire chamber's gas volume. The charge is multiplied in the strong electric field region near the anode wires. The amplification can be varied over a range of $1–10^5$ by simply changing the voltage applied to the wires.

We measured the noise levels of the detector with x-rays. Operating the wire chamber at moderate gains, we were able to obtain quantum-limited noise levels. Electronic noise levels on the order of the amount of charge deposited by a single x-ray were obtained—it was possible to store and detect the charge deposited by a single x-ray for as long as 10 s.

The detector is now being tested in a neutron beam. The accompanying figure displays a radiograph obtained with the detector for a 2-cm-thick steel mask that has the letters WNR machined halfway through it.



Radiograph obtained with our integrating detector for a 2-cm-thick steel mask in which the letters WNR are machined halfway through on the back side. WNR refers to the weapons neutron research facility at the Los Alamos Neutron Science Center (LANSCE), where our work is done.

Telepresence Control of Robots Used in Hazardous Environments

Lawrence Bronisz and Pete Pittman

The purpose of this project was to explore teleoperation and telepresence control for robots in hazardous environments. The primary use of this technology will be in a glove box environment; it allows operators to work on hazardous materials while being completely removed from the danger of exposure. This technology is used in situations that cannot be automated because of highly unstructured environments or off-normal conditions. Our project focused on determining the most appropriate tools and methods which we can apply in the near future to design a reasonably inexpensive telepresence control system for industrial robots used in the handling of hazardous materials.

We considered a number of input devices, including position and force-reflexive devices. Although each has advantages, we had to consider the trade-offs carefully to ensure that the device will allow the user to perform all the required tasks. Much of this technology is well established, and the devices are robust and reasonably priced.

The control-system technology is largely driven by industry and very reliable but lacks the technical sophistication available in some experimental systems. As the control system will be used regularly, controller reliability will have to take precedence.

Simulation techniques are only recently at a usable stage. This is due, in part, to the increase in central processor unit power over the past few years. Several robot-simulation packages are available and being reviewed for consideration in this type of control.

Much of the work is still in the development stage, and hardware will follow; eventually our work will provide a usable tool for glove box robot control.

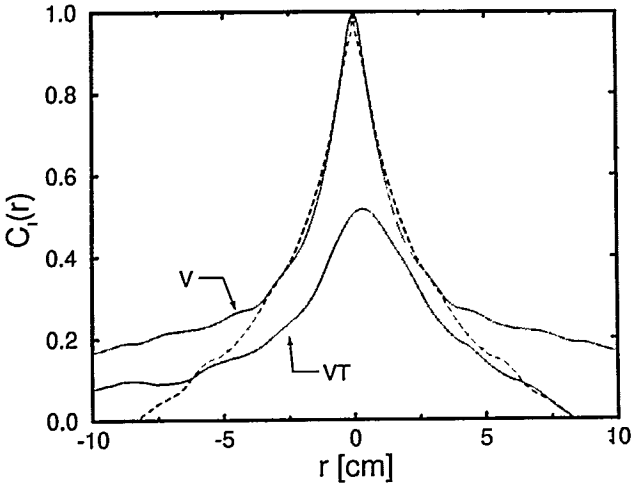
Plasmas, Fluids, and Particle Beams

Turbulent Scaling in Fluids

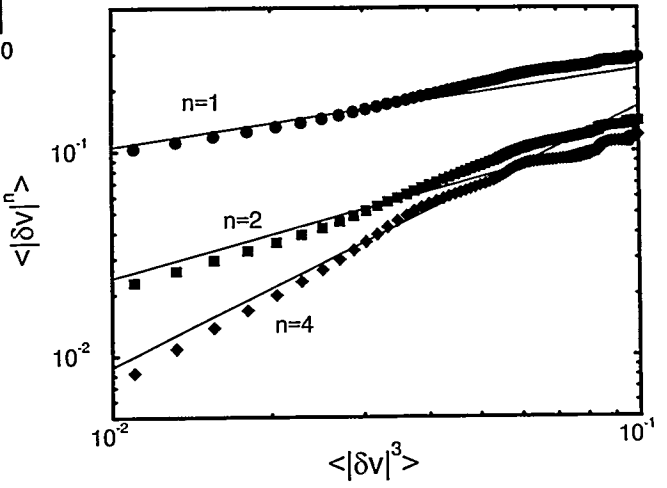
Robert Ecke

We have investigated turbulence in fluids that are subject to different body forces and external temperature gradients. Experimentally, we used (1) precision measurements (0.1%) of heat transport and local temperature, (2) flow visualization using digitally enhanced optical shadowgraph, thermochromic liquid-crystal imaging, and laser Doppler velocimetry, and (3) advanced image-processing techniques. To simulate turbulent fluid flow, we used numerical simulations to employ standard spectral and novel lattice Boltzmann algorithms implemented on parallel Connection Machine computers.

In laboratory experiments on incompressible fluids, we imposed rotational Coriolis and centrifugal forces, measured probability distribution functions and spatial correlations of temperature (T) and velocity (V) (both TT and VT correlations), and determined scaling relations for global heat transport with a Rayleigh number. We showed that a modification of Kolmogorov scaling is required above some characteristic length scale, the Bolgiano scale, and that above that length scale, temperature and velocity fluctuations are correlated (see the first accompanying figure). To show the Bolgiano scaling, we employed a novel new analysis technique called "extended self-similarity," which allows scaling to be observed through ratios of velocity correlations. The results are shown in the second figure, with the solid lines representing the predicted scalings. We also demonstrated heat-transport scaling in rotating convection, measured thermal boundary layers, and showed that rotation provides additional mixing in the turbulent state—in contradiction to expectations.



Correlation functions of temperature (dotted line), velocity (V), and temperature-velocity (VT), showing strong correlation between the two fields. This correlation demonstrates that for length scales larger than the Bolgiano length, temperature in convection is not a passive scalar field.



Single-point velocity correlation functions $<|\delta v|^n>$ vs $<|\delta v|^3>$ showing the property of "extended self similarity" in thermal convection. Solid symbols represent the data and solid lines represent the predicted scalings.

Dusty Plasmas

Michael Jones

The objective of our project is to build a Laboratory capability in the theory and modeling of dusty plasmas. We have applied these techniques to the study of charging, dynamics, and coagulation of contaminants in plasma-processing reactors for industrial etching and deposition processes and to instabilities in planetary rings and other space-plasma environments. The work we performed in this project has application to plasma kinetics, transport, and other classical elementary processes in plasmas as well as to plasma waves, oscillations, and instabilities.

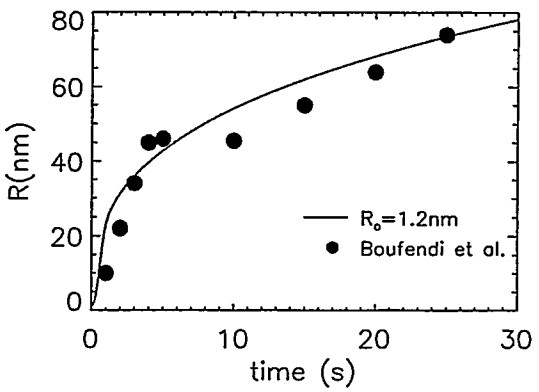
During the past year, we have constructed a model for how dust grains grow in a plasma. Our model assumes that there is a constant source of small (nanometer size) particles that coagulate into larger particles with time. The graph shows the radius of the dust grains as a function of time. The solid circles are values obtained from published experimental results. We have also used numerical simulations to study the self-consistent interaction of plasma flowing relative to charged dust grains. This interaction excites an ion acoustic instability. The three-panel figure shows the results of a simulation. It indicates the growth, in time, of the electric field fluctuations associated with the instability and the resulting effect on the plasma ions and dust grains.

Publications

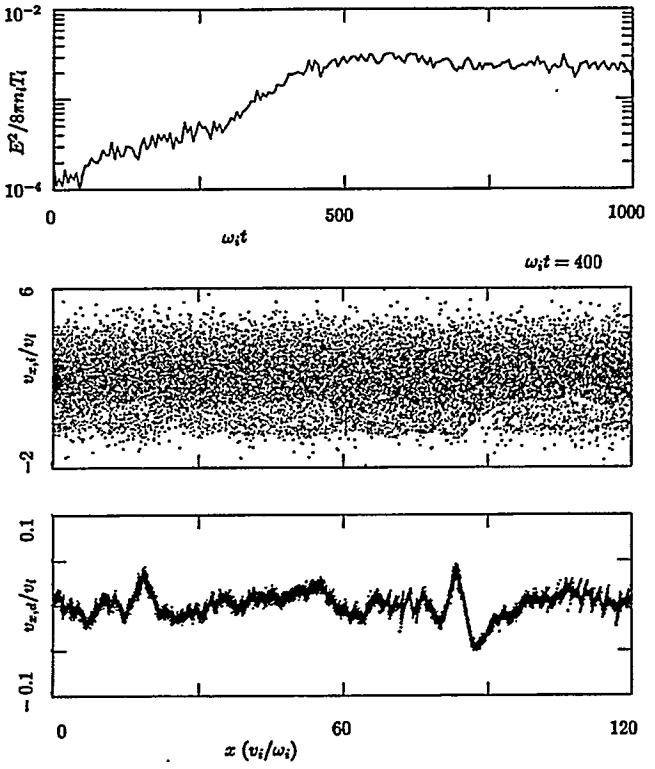
Lemons, D. S., R. K. Keinigs, M. E. Jones, et al., "Scaling Laws for Particle Growth in Plasma Reactors" (submitted to *Appl. Phys. Lett.*).

Winske, D., and M. E. Jones, "Effect of Finite Charging Time on Particulates in RF Discharges," *IEEE Trans. Plasma Sci.* **23**, 188 (1995).

Winske, D., S. P. Gary, M. E. Jones, et al., "Ion Heating in a Dusty Plasma Due to the Dust/Ion Acoustic Instability," *Geophys. Res. Lett.* **22**, 2069 (1995).



Results of calculations of our dust grain coagulation model. This graph shows particle radius R versus time; solid circles are experimental data.



Results of particle simulations of a dust/ion acoustic instability showing time history of electric field fluctuations (top panel), phase space (v-x) plots of plasma ions—some of which are trapped by the waves (middle panel)—and dust ions that are mostly modulated by the waves (bottom panel).

Developing Electron-Beam Bunching Technology at Subpicosecond Pulse Lengths for Improving Photon Sources

Bruce Carlsten

Many advanced accelerator applications and short-wavelength light sources require subpicosecond, nanocoulomb electron bunches at very low emittance. These requirements are well beyond current technology, and many advanced bunch-compression designs have been proposed to meet the requirements. Our goals for this project are

- to extend the current electron bunch-compression technology by developing a small experiment to study the essential physics associated with subpicosecond bunch compression and
- to probe the fundamental limits associated with compression.

In particular, we wish to bunch 1 nC of charge to less than 1 ps, which would represent an increase in compression of more than one order of magnitude over previous experiments.

We have been successful in analytically investigating the dominant mechanism of emittance growth. We have also built a subpicosecond compressor on a new accelerator that was constructed for a plasma light-source; the project for building the compressor was funded by a cooperative research and development agreement (CRADA) with Northrup-Grumman. Using the compressor, we demonstrated compression of 0.1 nC from 20 ps to 0.25 ps and compression of 1.1 nC from 20 ps to 0.75 ps. These levels of compression far exceed previous results and provide important guidance on advanced compressor designs. We still need to complete measurements of emittance growth from the compression, which may confirm the existence of the proposed dominant mechanism for emittance growth.

Publications

Carlsten, B., "Space-Charge-Induced Emittance Compensation in High-Brightness Photoinjectors," *Part. Accel.* **49**, 27 (1995).

Carlsten, B., "Nonlinear Subpicosecond Electron Bunch Compressor" (submitted to *Phys. Rev. E*).

Carlsten, B., and T. Raubenheimer, "Emittance Growth of Bunched Beams in Bends," *Phys. Rev. E* **51**, 1453 (1995).

Carlsten, B., and S. J. Russell, "Subpicosecond Compression of 0.1–1 nC Electron Bunches with a Magnetic Chicane at 8 MeV" (submitted to *Phys. Rev. Lett.*).

Delta-f and Hydrodynamic Methods for Semiconductor Transport

Lester E. Thode

A truly predictive device design capability is fundamental to the future success and diversity of the microelectronics industry. The most sophisticated technique for simulating semiconductor carrier transport is the Monte Carlo method. Unfortunately, the Monte Carlo method is computationally costly, which is a major practical limitation.

We propose to determine if the delta-f method, developed within the magnetic fusion community, can be applied to semiconductor transport. This new approach, which combines fluid and particle models, offers the potential to accurately treat the nonequilibrium character of the distribution function, with significantly less computation than required for a pure Monte Carlo method.

We have completed an evaluation of a number of semiconductor transport codes. None of the existing codes were deemed appropriate for the fluid part of the delta-f effort, primarily because the basic algorithms were not well-suited for parallel computation. As a result, we used our object-oriented universal-fragment toolbox to design, write, and test a new transport code. The code is multidimensional and runs efficiently, without modification, on a personal computer, a workstation, or a CRAY computer. As a spin-off, our advanced transport code approach is now being used to investigate neutron transport. In addition, we evaluated two Monte Carlo semiconductor transport codes for the particle-tracking part of the delta-f method. We selected a code designed by the University of Illinois.

Publications

Thode, L., G. Csanak, R. Hotchkiss, et al., "Two-Dimensional Model for Vertical-Cavity Surface-Emitting Lasers (VCSELs)," *Int. Soc. Opt. Eng.* **2319**, 348 (1995).

such as mobility and drain current.

We have compared the models in, and simulation results from, the bulk codes MOCABULK and SLAPSHOT. Bulk codes provide an excellent starting point for comparison since they are simpler than the device codes for which they are the basis. These particular codes are representative of full-band and analytic-band codes.

SLAPSHOT uses a sophisticated analytic fit to the band structure and density of states in its discrete-event simulation of charge carriers in bulk silicon. The analytic band and constant-gamma technique permit the analytic integration of the equations of motion between free flight times; the analytic band and density of states permit an efficient k-dependent selection of a state after a collision. SLAPSHOT categorizes the collisional phonons by their dispersion branch, and its sophisticated ionized impurity scattering model uses Brooks-Herring, Conwell-Weisskopf, and semiempirical degeneracy models. SLAPSHOT's field and doping-dependent mobilities are in excellent agreement with experimental data.

MOCABULK uses a full band and density of states in its discrete time-step simulation of charge carriers in bulk silicon. The full band and modified constant-time technique permit the discrete integration of the equations of motion; a band-structure table sorted by energy permits efficient energy-dependent selection of a state after a collision. MOCABULK's collision phonons are categorized by scattering process, and its ionized impurity scattering model uses Ridley's statistical screening model. MOCABULK's field and doping-dependent mobilities are in fair agreement with experimental data.

Both SLAPSHOT and MOCABULK represent an interesting collection of compromises between fidelity and efficiency. Design decisions made in each code inexorably limit other design choices and ultimately force the codes to take the shape they have. Such limitations make it difficult to evaluate and potentially mix models from these codes. We are working to find a way to factor out the essential, loosely coupled parts of the model.

Comparing the physics models and solution techniques used in different codes is important to understanding their effects in device simulations. Such comparisons are the first step toward developing a standard platform for Monte Carlo device simulators, which will be instrumental to developing and benchmarking a hierarchy of device simulators.

We have developed an object-oriented device code that uses models based on the models in SLAPSHOT and MOCABULK. Currently, our code solves the Boltzmann transport equation using an ensemble particle model with a modified constant-time technique for finding collision times (as in MOCABULK). We use the general field class to implement both full and analytic-fit bands, as in MOCABULK and SLAPSHOT, respectively. We are currently working on coding the scattering and final selection models in ways that are based on the energy-dependent models used in MOCABULK. When we complete the scattering and final state models, we will have a working bulk code. The modular nature of the code provides a natural development path from bulk to device codes via the addition of objects that implement boundary conditions and a field solver.

The scaling of silicon MOSFET channel lengths to increase the speed and drive current has pushed the limit of gate length toward 0.1 mm. An alternative approach to enhance drive current is by increasing the mobility of the charge in the channel. Recent reports have shown that electron and hole mobility are enhanced when they flow in strained silicon/silicon germanium channels. The mobility is enhanced because of strain-induced changes in the band structure of the material systems.

In our previous work, we simulated electron transport in strained silicon in a relaxed silicon germanium system. We have performed Monte Carlo simulations for both bulk and device cases and found that the electron mobility can be improved by a factor of 1.8 compared with the electron mobility in a silicon inversion layer with the same effective field. Our simulation results show good agreement with recent experiments. Using SLAPSHOT, we extended our work to optimize the strained silicon/silicon germanium MOSFET for best performance. In the next stage of our work, we developed a self-consistent Schrodinger and Poisson simulator to study hole transport in silicon and strained silicon germanium systems.

Because the quantum mechanical nature of two-dimensional gas in the quantum well formed by the silicon and silicon germanium heterostructure cannot be addressed by classical calculations, we calculated the sub-band energies using effective mass approximations. The effective mass of the strained silicon germanium alloy has been computed using the k•p perturbation method. Although effective mass approximation is not quite valid for hole band structure, the full-band formalism is still a formidable problem for realistic computation.

Using information on the doping concentrations, we then calculated the carrier concentrations from the subband dispersion and solved the one-dimensional

Poisson equation using the successive over-relaxation (SOR) method. The iteration between the Schrodinger and Poisson equations is continued until a convergence is achieved. Then, we compute the quantum mechanical solution at small intervals of gate bias to obtain the capacitance versus voltage characteristics for the entire range of accumulation for the inversion region.

We have found significant differences between the quantum mechanical and the classical quasi-static capacitance when the doping concentration is high and the oxide thickness is small, as is the case for a typical deep-submicron device. Because of the quantum mechanical nature of hole gas, the effective oxide thickness also increases, which results in inferior capacitance. We calculated effective hole mobility using two-dimensional scattering rates that include phonon (acoustic and optical), surface roughness, and alloy-scattering processes. Good agreement has been obtained for the effective hole mobility of the inversion layer as a function of the effective field. The mobility in the strained silicon germanium alloy increases due to strain-induced reduction of interband scattering, and the reduced effective masses though alloy scattering represents some degradation of the mobility.

Our initial results show that hole mobility in a silicon germanium system is significantly enhanced over that of conventional silicon pMOSFET. We have calculated the quantum mechanical capacitance for different strain conditions. The effective hole mobility for strained silicon germanium pMOSFET increases with increased mole fraction of germanium. However, the upper limit of the mole fraction of germanium is limited by a critical thickness, which is typically 100 Å for a mole fraction of 0.4. Using the quantum mechanical simulator, we have analyzed the structure that yields the best performance, but more experiments are required to validate our simulator's models.

Turbulence and Turbulence Spectra in Complex Fluid Flows

Timothy Clark

Fluid turbulence possesses a rich spectrum of time and length scales which defy direct computation because of the inability of current or foreseeable computers to resolve all scales. Turbulence strongly affects a flow, e.g., mixing rates of pollutants in the atmosphere, of fuel in a combustor, or of constituents in an inertial confinement fusion capsule.

We are developing theoretical statistical models of fluid turbulence in parallel with direct numerical simulations (DNS) to produce numerically tractable models of tested accuracy. These models will be used in the Laboratory's computer codes with defense and industrial applications. We begin with spectral models that describe turbulent energy and stresses over a range of length scales. By exploiting emergent self-similarities of the model predictions, we reduce these models to tractable engineering approximations.

We have (1) implemented new methods for initialization of DNS data, permitting control of isotropy and helicity, and for computing radial distributions of turbulence spectra, (2) used DNS to verify the theoretical predictions of the scaling of turbulence backscatter, (3) ported two DNS codes to the Connection Machine 5 that are now undergoing testing, (4) incorporated swirl and passive scalars into our spectra modeling and began extensions to inhomogeneous flows, (5) tested our spectral model for variable density turbulence against DNS of an accelerated stochastic density field, and (6) developed a tractable algebraic model for passive scalar flux.

We have opened several new avenues of research which we plan to pursue in the final year. The work performed in this project has application to heat transfer, fluid flow, atmospheric modeling, and statistical physics.

Publications

Clark, T., and C. Zemach, "A Spectral Model Applied to Homogeneous Anisotropic Turbulence," *Phys. Fluids* 7, 1674 (1995).

Turner, L., and T. Clark, "Descriptions of Turbulence with Helicity" (to be published in *Bull. Am. Phys. Soc.*).

Zemach, C., and T. Clark, "Exploiting a Single DNS to Estimate Ensemble Averages in Isotropic Turbulence" (to be published in *Bull. Am. Phys. Soc.*).

High-Impedance Plasma Opening Switches

Rodney Mason

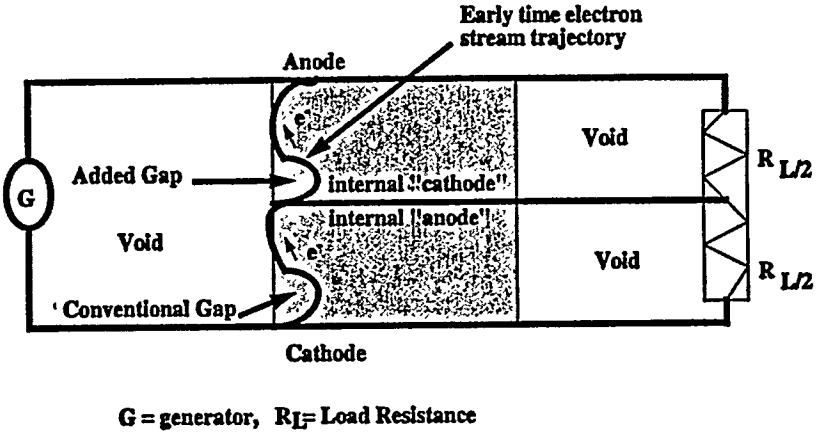
The purpose of this project is to computationally evaluate a new approach to high-voltage plasma opening switches (POSs). The conventional POS consists of a low-density plasma injected between the electrodes of a high-power transmission line. For periods up to a microsecond, the plasma short-circuits the current flow. On much shorter time scales, typically 50 to 200 nanoseconds, the plasma is disrupted so that the current can flow beyond it to a load. Successful POS designs have been limited to about a mega-amp of conduction current, opening to loads of a few ohms. At higher load impedances, switch opening has proven inefficient because of shunting of the current flow through residual plasma remaining in the transmission line.

For our new switch design, we added other internal electrodes between the anode and cathode thereby producing a multimodule POS. This has the effect of putting multiple POS plasmas in series with each other and in parallel with any load. Upon POS opening, the resultant total switch resistance erects in parallel with the load. This permits efficient energy transfer to much larger loads. Using our simulation code ANTHEM, we evaluated this new switching concept. Computationally, we demonstrated voltage doubling and tripling across two- and three-module POS designs. In addition, we characterized the required internal electrode connectivity. As a result, we devised (1) a new coaxial modular POS and (2) a prescription for the direct coupling of a multigap POS to a plasma radiation source. We publicized the new POS in the pulse-power community through talks, a paper, and the filing of a patent application.

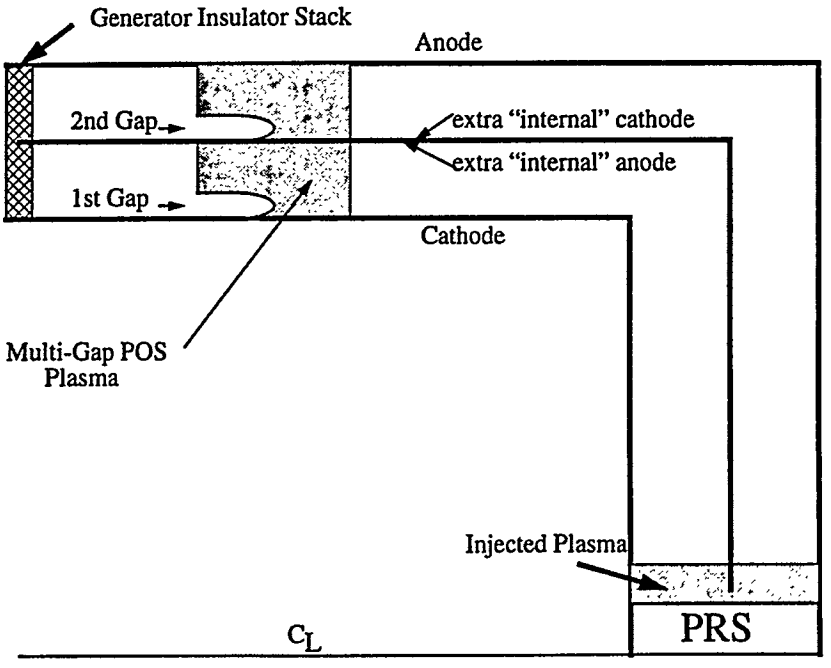
Publications

Mason, R. J., "High Impedance Multi-Gap Plasma Opening Switches," *IEEE Transactions on Plasma Science* **23**, 465 (1995).

Mason, R. J., "High Impedance Plasma Opening Switches," *Bull. Am. Phys. Soc.* **39**, 1690 (1994).



Generic multigap plasma opening switch.



Coupling of a multigap POS to a staged plasma radiation source load.

Determination of the Nuclear-Induced Electrical Conductivity of ^{3}He for Magnetohydrodynamic Energy Conversion

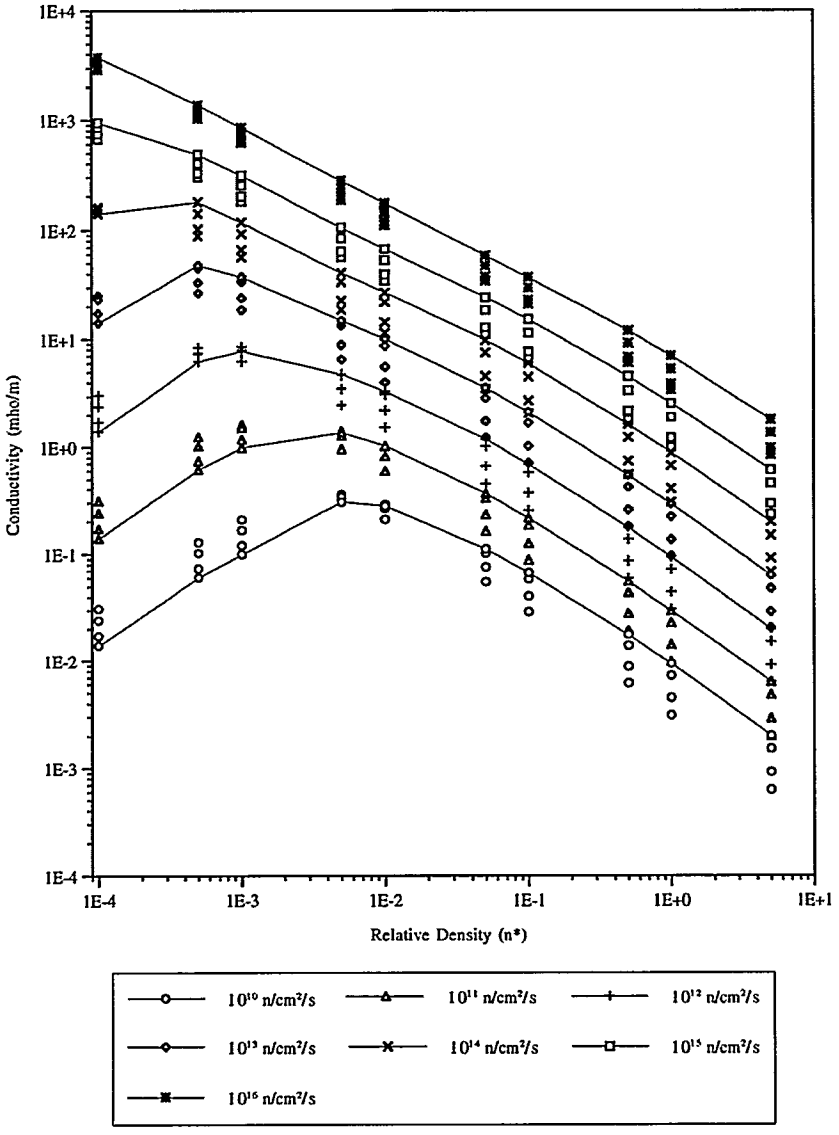
Jay Scheuer

The continual need for more efficient high-output energy conversion techniques has renewed interest in nuclear-driven magnetohydrodynamic (MHD) energy conversion. However, little data exists for use in the design of a nuclear cycle based on nuclear-driven MHD energy conversion.

The objective of our project is to provide a conclusive data set that describes the degree of nuclear-induced electrical conductivity in ^{3}He over a wide range of thermodynamic and reactor conditions including gas density from 10^{-4} to 1 standard atmospheric density, gas temperature from 300 to 1500 K, and neutron flux from 10^{10} to 10^{16} n/cm^{2}s.

We will collect this data set from a series of experiments using an experimental apparatus. The apparatus is being built and tested at Los Alamos, and the experiments will be performed at the Penn State Breazeale Reactor Facility. We will compare the collected data to the predictions of a previously developed model (see graph) and to data collected in earlier work.

The experimental apparatus, which consists of a pressure vessel, gas handling system, and instrumentation, has now been designed and built. During the testing phase, we encountered some unexpected operational problems that resulted in a delay in the experiment schedule. Some modifications of the system are currently underway to remedy these problems. These modifications should also greatly improve the quality of the data that we will collect.



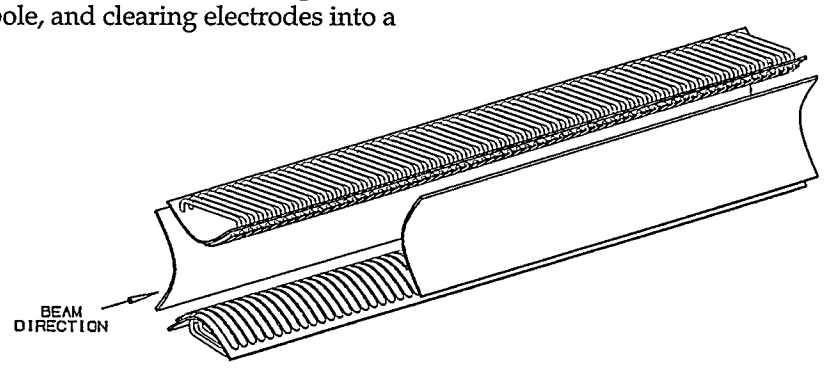
Electrical conductivity versus gas density for pure ^{3}He as a function of gas temperature and neutron flux. Data was calculated by using CSOLVE computation code to model an infinite volume.

A Feasibility Study of Beam-Chopping at Low Energy for the Manuel Lujan Jr. Neutron Scattering Center

Tai-Sen Wang

If a beam-chopping system could be developed for the low-energy beam line, there would be potential to operate the Manuel Lujan Jr. Neutron Scattering Center (MLNSC) at much higher power and duty factor and enable such operation with a radio-frequency quadrupole (RFQ) accelerator injector. This would greatly extend the capacity of the facility. However, chopping an intense H-minus beam at the energy of 100 keV or less has never been demonstrated and remains to be studied. Our goal in this project was to begin evaluating the possibility of applying the present chopping scheme at the Los Alamos Neutron Science Center (LANSCE) linear accelerator in the low-energy beam line and to look for a new design for the chopper.

We investigated the beam phase-space distortion because of plasma fluctuations caused by the sweeping chopper field. We concluded that the phase-space distortion because of the fluctuation in the background plasma could be intolerable if the conventional chopper now in the LANSCE linear accelerator were used at a lower energy (around 100 keV). We invented the quadrupole slow-wave deflector (QSWD), a design that integrates the functions of the slow-wave deflector, the electrostatic quadrupole, and clearing electrodes into a single compact device (see accompanying illustration). A QSWD operates with a constantly sustained quadrupole electric field that can sweep off the ions and electrons produced by the beam-gas scattering. Using a QSWD for beam-chopping can avoid the complicated beam-plasma effects that may occur in a neutralized beam. Utilizing the idea of QSWD, we have made a conceptual design of a low-energy H-minus beam chopper for MLNSC and the optics of the transport line from the ion source to the RFQ accelerator.



An illustration of the structure of a quadrupole slow-wave deflector (QSWD).

A Compact Compton-Backscattering X-Ray Source for Mammography and Coronary Angiography

Dinh Nguyen

We are developing a compact, tunable, monochromatic x-ray source for applications in medical imaging such as mammography and coronary angiography. Using monochromatic x-rays tunable in the range 18–25 keV improves image definition and, at the same time, reduces the x-ray dose for the patient. Our method of producing tunable, monochromatic x-rays is called Compton backscattering. In this technique, a beam of monochromatic x-rays is produced when a high-intensity laser beam scatters off a tightly focused electron beam traveling near the speed of light. The electron beams are generated from a linear accelerator that has a photocathode electron source. The laser that produces the electrons is also used in the scattering process, thereby ensuring good temporal overlap for efficient x-ray production. We have set up the tightly focused electron and laser beams at the collision point.

Our initial experiment indicates that the tightly focused electron beam produces too much background radiation, which does not come from the Compton-backscattering process but interferes with our x-ray detector. To reduce the background radiation, we have moved the collision point to a new location where the electron beam

can be focused to a small spot without scraping the wall of the beam pipe. In the new location, either the photocathode laser or the free-electron laser can be used as the scattering laser. A new x-ray detector has been tested for its ability to resolve single x-ray events. We also built improved shielding and collimators for the x-ray detector. We are ready to perform experiments to demonstrate the feasibility of producing tunable x-rays in the keV range via Compton backscattering. We estimate that collisions between a high-brightness electron beam and a high-intensity laser will produce 10^9 x-ray photons per second.

Publications

Kong, S.H., J. Kinross-Wright, D.C. Nguyen, et al., "Cesium Telluride Photocathode," *J. Appl. Phys.* 77, 6031 (1995).

Nguyen, D.C., S.M. Gierman, W. Vernon, et al., "Conceptual Design of a Compact Compton Backscatter X-ray Source Tunable From 3 to 33 keV," *Nucl. Instr. Meth. A* 358, 48 (1995).

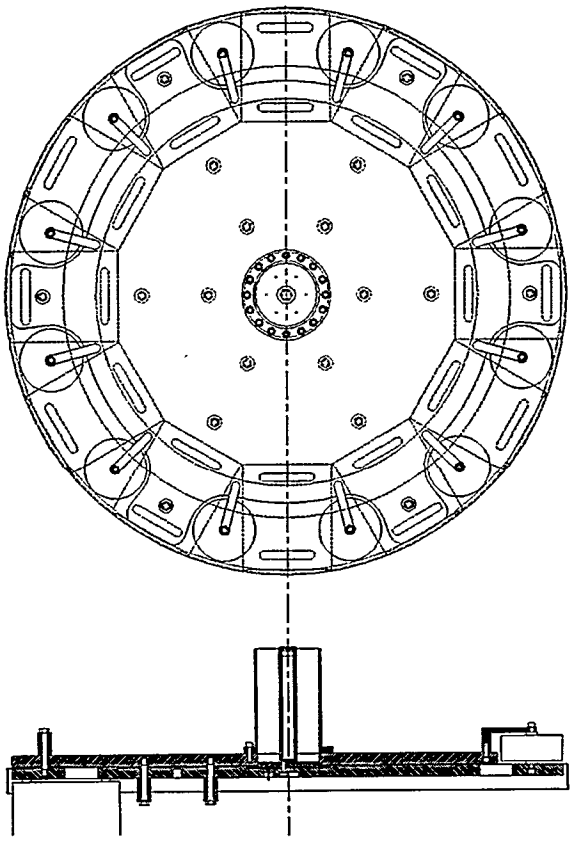
Next-Generation Magnetic-Nozzle Prototype

Henri Wagner

The simple, robust mechanical and electrical design of magnetodynamic plasma accelerators can provide US industry with low-cost and environmentally benign manufacturing and processing capabilities and thus benefit its international competitiveness. Possible applications for this inexpensive and reliable technology include pattern etching, surface engineering, and decontamination. Plasma guns also have strong relevance to Laboratory and national programs in weapons engineering, advanced material formation, magnetic-containment fusion energy, and advanced space propulsion.

The main objective of our project is to design, develop, and operate a next-generation plasma-processing tool and, with industry, identify new manufacturing applications. By using an existing quasi-analytic model that describes the functioning of a short-pulse plasma accelerator, we have determined the geometry of the gun and its operating parameters and have designed an optimized accelerator (see figure). We have expanded these modeling techniques to include the design of the magnetic nozzle that guides the plasma from the source to its target and also controls the optimal energy deposition on the target surface.

We have fabricated the parts of the plasma accelerator based on our designs. We are now in the process of assembling the plasma accelerator and installing it on a new test chamber. Once we complete the installation, our experimental work will provide data to verify the model and further optimize the accelerator.



Assembly drawing (front and side view) of our optimized plasma accelerator.

High-Power, High-Frequency, Annular-Beam, Free-Electron Maser

Michael Fazio

Free-electron masers (FEMs) operating in the microwave regime have demonstrated high beam-to-RF power-extraction efficiencies (~30%) and high output power (~gigawatts). FEMs have been identified as potential candidates to drive advanced accelerators at relatively high frequencies (>10 GHz). However, current FEM technology does not lead to adequate phase stability for this application. In addition, high output power has only been demonstrated with FEMs driven by induction accelerators at higher voltage than is practical for driving long accelerators.

The objectives of this project are the following: (1) to demonstrate 0.5-GW output power at 17 GHz by using a high-current but low-voltage electron beam and (2) to demonstrate a phase-stability scheme in which the RF phase of the output power is not affected by small fluctuations in the electron-beam voltage. In the past year we have designed a high-power FEM with which we are currently conducting cold tests (low RF power and no electron beam). We have also theoretically analyzed the phase-stability scheme. Next year we plan to verify the phase-stability scheme in the exponential growth regime of the FEM (we will keep the output power relatively low by using only a short interaction length). In the final year of the project, we plan to demonstrate high output power by extending the length of the device.

Publications

Carlsten, B., "Axial Free-Electron Laser Interaction Between an Annular Electron Beam and an Axisymmetric TM Mode," *IEEE J. Quant. Elect.* **31**, 1753 (1995).

Carlsten, B., "Enhanced Phase Stability for a Raman Free-Electron Laser Amplifier in the Exponential Growth Regime," *Phys. Plasmas* **2**, 3880 (1995).

Carlsten, B., "Stable Off-Axis Electron Orbits in a Longitudinal-Wiggler Free-Electron Laser," *J. Appl. Phys.* **78**, 2811 (1995).

Carlsten, B.E., C.M. Fortgang, J.M. Potter, et al., "Microwave Axial Free-Electron Laser with Enhanced Phase Stability" (to be published in *Nucl. Instrum. Meth. Phys. Res.*).

Carlsten, B., B. Haynes, and R. Sheffield, "Particle Acceleration by the Inverse Axial Free-Electron Laser Interaction" (to be published in *Particle Accelerators).*

theory. The conventional DFT approach, the "local density approximation," is in error by ~30 kcal/mole per bond; the gradient-corrected version of the theory leads to errors of ~10 kcal/mole

DFT and a dielectric continuum model of solvation—are compared with experimentally obtained values.

Our interest in these techniques stems from the fact that the

expect these methods, and their extensions and variants, to be the workhorses in quantum chemistry for the foreseeable future. They promise to be useful for a wide range of problems from homoge-

Quantum Resonance Effects in Exchange, Photodissociation, and Recombination Reactions

Russell T. Pack

Recent breakthroughs in accurate three-dimensional (3-D) reactive-scattering calculations have led to the discovery that a whole zoo of quantum resonance phenomena dominate most chemical reactions. Resonances are nonstationary states with prolonged lifetimes, and understanding them will be a key to laser control of reactions and to long-sought bond selective chemistry. Using our accurate 3-D quantum reactive-scattering computer codes, we are determining the contributions of resonances to measurable chemical properties by calculating, analyzing, and classifying them for exchange, photodissociation, and recombination reactions.

We have performed many calculations on both the combustion and recombination reactions of H + O_2. These included the first accurate potential energy surfaces for this reaction which properly include their conical intersections and can be used to calculate geometric phase and nonadiabatic effects, calculations of resonance lifetimes, and studies of resonances which contribute to recombination to form HO_2. We found the first clear evidence that pure three-body collisions contribute significantly to recombination reactions, which implies that their kinetics are not treated correctly by the models currently in use.

We also performed the first calculations that rigorously include the geometric phase (due to a conical intersection of potential energy surfaces) for the case in which atoms are different species. We find that the geometric phase drastically changes the spectrum of resonances and high-lying bound-vibrational states and that the states have a strange symmetry not previously discussed. The work is exciting and great progress is being made. This work has applications to collision phenomena, atomic and molecular physics, classical and quantum mechanics, chemical and physicochemical properties, and the combustion of all hydrocarbons.

Publications

Barclay, V.J., C.E. Dateo, I.P. Hamilton, et al., "Anomalous Symmetries of the Rovibrational States of HO_2: Consequences of a Conical Intersection," *J. Chem. Phys.* **103**, 3864 (1995).

Kendrick, B.K., and R.T Pack, "Recombination Resonances in Thermal H + O_2 Scattering," *Chem. Phys. Lett.* **235**, 291 (1995).

Pack, R. T, E.A. Butcher, and G.A. Parker, "Accurate Three-Dimensional Quantum Probabilities and Collision Lifetimes of the H + O_2 Combustion Reaction," *J. Chem. Phys.* **102**, 5998 (1995).

Parker, G. A., A. Lagana, S. Crocchianti, et al., "A Detailed 3D Quantum Study of the Li + FH Reaction," *J. Chem. Phys.* **102**, 1238 (1995).

Metal Vapor Synthesis in Organometallic Chemistry

John Watkin

Our research is aimed at exploring the inorganic and organometallic chemistry of transition-metal complexes uniquely accessible through the technique of metal vapor synthesis. Complexes prepared with this technique are often extremely reactive and can provide new insight into the modes of interaction and reaction of metal complexes with relatively inert substrates.

We have investigated the condensation of metal atoms into a frozen matrix of acetylene as a possible route to obtaining new metal-carbide, or "met-car," phases. The products isolated from these reactions are currently under investigation. We have also examined the possibility of using metal vapor synthesis to prepare transition-metal complexes containing perfluorinated phosphine ligands. Thus, we condensed molybdenum metal atoms with $(F_3C)_2PCF_2CF_2P(CF_3)_2$ to yield a complex mixture of products that are awaiting full characterization.

We completed construction of a parylene generator that will allow us to condense metal atoms into a matrix of parylene monomer in order to generate metal-doped parylene films. We are currently examining the reactivity of transition-metal complexes to cluster ions of the type K_3E_7 (E = P, As, Sb) as a potential synthetic route to obtaining new binary phases.

Separations Chemistry of Toxic Metals

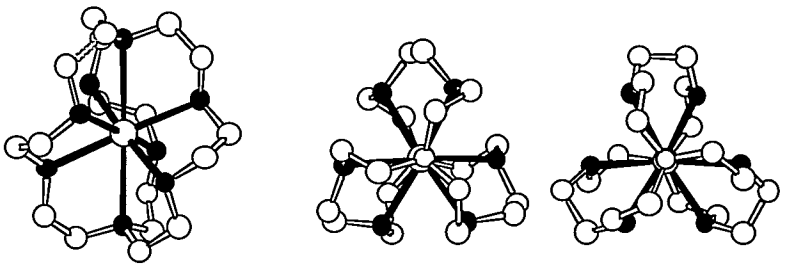
Paul Smith

Sequestering and removing toxic metal ions from their surroundings is an increasingly active area of research and is gaining importance considering current environmental-contamination problems both within the DOE complex and externally. One method of separating metal ions is to complex them to a molecule (a ligand or chelator) that exhibits a specific binding affinity for a toxic metal even in the presence of other, more benign metals. This approach makes use of the sometimes subtle differences between toxic and non-toxic metals that result from variations in size, charge, and/or shape. For example, toxic metals such as chromium, arsenic, and technetium exist in the environment as oxyanions, negatively charged species with a characteristic tetrahedral shape. Other toxic metals such as actinides and heavy metals are positively charged spheres with specific affinities for particular donor atoms such as oxygen (for actinides) and nitrogen (for heavy metals). In most cases the toxic metals are found in the presence of much larger quantities of less toxic metals such as sodium, calcium, and iron. The selectivity of the chelators is critical to the goal of removing the toxic metals from their less toxic counterparts.

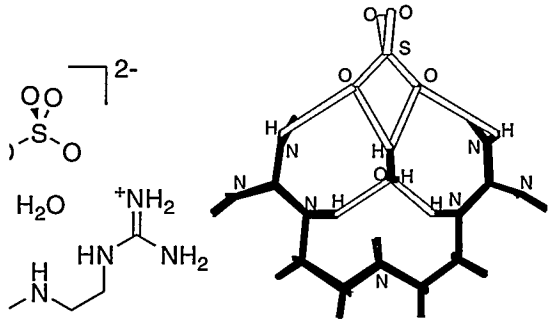
Our approach is to build a ligand framework that complements the unique characteristics of the toxic metal (size, charge, and shape) while minimizing interactions with non-toxic metals. We have designed ligands exhibiting specificity for the target metals; we have synthesized, characterized, and tested these ligands; and we have shown that they exhibit the proposed selectivity and cooperative binding effects. Each illustration and its accompanying text highlights a specific aspect of our research.

Publications

Johnson, C.P., J.W. Steed, C.L. Barnes, et al., "Supramolecular Chemistry of Calix[5]arenesulfonate: A Water Soluble, Bowl-Shaped Host with a Large Molecular Cavity," *J. Am. Chem. Soc.* **117**, 46 (1995).



The octaazacryptand L, where L = $N(CH_2CH_2NHCH_2CH_2NHCH_2CH_2)_3N$, exhibits a high affinity for cadmium, log βML = 18.3(1). Calculation of pM values (pM = -log[M]) show that L has the highest reported binding affinity for cadmium relative to other [2.2.2] cadmium polyoxa-polyaza cryptates. In the solid-state the cryptand ligand is capable of adopting two conformations, parallel or oblique, with negligible influence upon the cadmium coordination sphere. Nuclear-magnetic-resonance experiments indicate the parallel conformation is favored in solution.

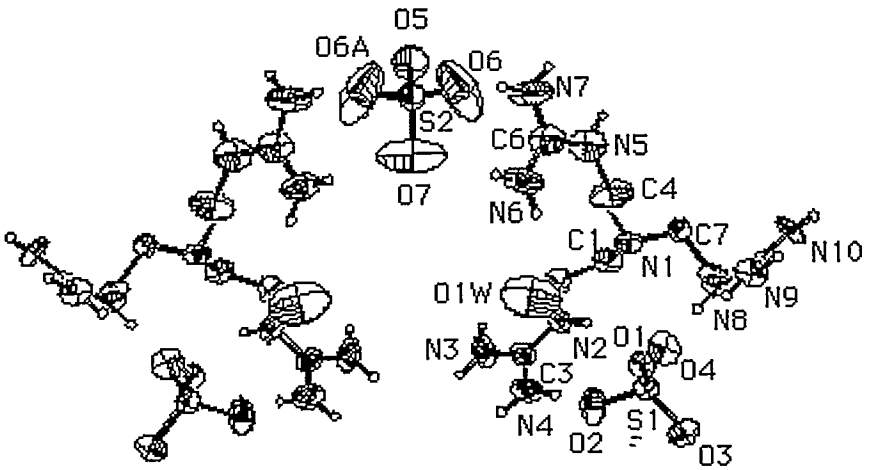


Chemical and structural diagrams that illustrate the capacity of bis(2-guanininoethyl)amine sulfate (Dieng) to act both as a chelator for sulfate anion and as a cooperative binding system for sulfate and water. We have discovered a system which demonstrates cooperative binding. In this case water is bound inside the cavity apparently assisting in the preorganization of the guanidinium units to chelate the sulfate. Therefore, it appears that cooperative binding is necessary in this complex if chelation of oxyanions is to occur. The crystal structure of this supramolecular complex is illustrated above.

Reilly, S.D., G.R.K. Khalsa, D.K. Ford, et al., "Octaaza Cryptand Complexation of Fluoride Ion," *Inorg. Chem.* 34, 569 (1995).

Sabel, D.M., J.A. Thompson, R.J. Butcher, et al., "2-Carboxyl-9-Diol-1,10-Phenanthroline Complexes of Co and Cu" (to be published in *Acta Cryst. Sect. C.*).

Thompson, J.A., M.E. Barr, D.K. Ford, et al., "Solution and Solid State Characterization of a Cadmium Octaazacryptand Complex" (to be published in *Inorg. Chem.*).



N1-C1	1.448 Å	N2-O1	2.843 Å
N1-C4	1.518 Å	N4-O2	2.942 Å
N1-C7	1.429 Å	N6-O7	3.140 Å

We have synthesized and structurally characterized 1,2-diguanidinoethane sulfate (Eng), bis(2-guanininoethyl)amine sulfate (Dieng), tris(2-guanidinoethyl)amine sulfate (Treg) (shown above), and m-xylylene diguanidium sulfate that represent a series designed to systematically vary the number of atoms in the chain connecting the two gaunidinium units. We are using sulfate in the initial studies due to its similarity in size and shape to chromate ion and to its lower reactivity and toxicity. We have shown that a five-atom bridge between guanidinium units is preferable to a two-atom bridge because it allows both guanidinium units to bind a single sulfate ion. In the 1,2-diguanidinoethane structure, no preorganization occurs and the two arms are associated with two different sulfate ions.

New Catalytic Processes for the Production of Specialty Polyolefins

John Watkin

High-T_g (glass-transition temperature) polymeric materials are becoming increasingly important in producing materials for the boards on which microprocessors are placed in electronic devices and in producing new optical materials for flat panel displays. Indeed, it has been estimated that the market for polymers to be used in such applications will quadruple in the next five years. Present-generation high-T_g polymers, including materials such as polysulfone and polyetherimide, have one significant drawback: they are produced from relatively expensive monomers. Unfortunately, inexpensive polymeric materials, such as polyethylene and polypropylene, distort at extremely low temperatures—approximately 70°C–110°C. Therefore, the production of a high-T_g polymeric material based on cheap, readily available olefin monomers would represent a significant advance.

Our principal objective is to develop novel Ziegler-type catalyst systems containing a transition-metal center that will catalyze the copolymerization of specific olefins (both cyclic and linear) to produce polymeric materials with mechanical and thermal properties that would make these materials commercially attractive. Such properties include $T_g > 150$°C, high impact strength, low dielectric constant, and low moisture absorption.

We have prepared transition-metal complexes containing a variety of supporting ligands, including substituted cyclopentadienyl, alkoxide, alkyl, and carboxylate. We have screened these complexes for suitability to the catalytic polymerization of olefins and examined the physical properties of the resulting polymers. The results obtained have provided new insight into the synthesis of olefin copolymers.

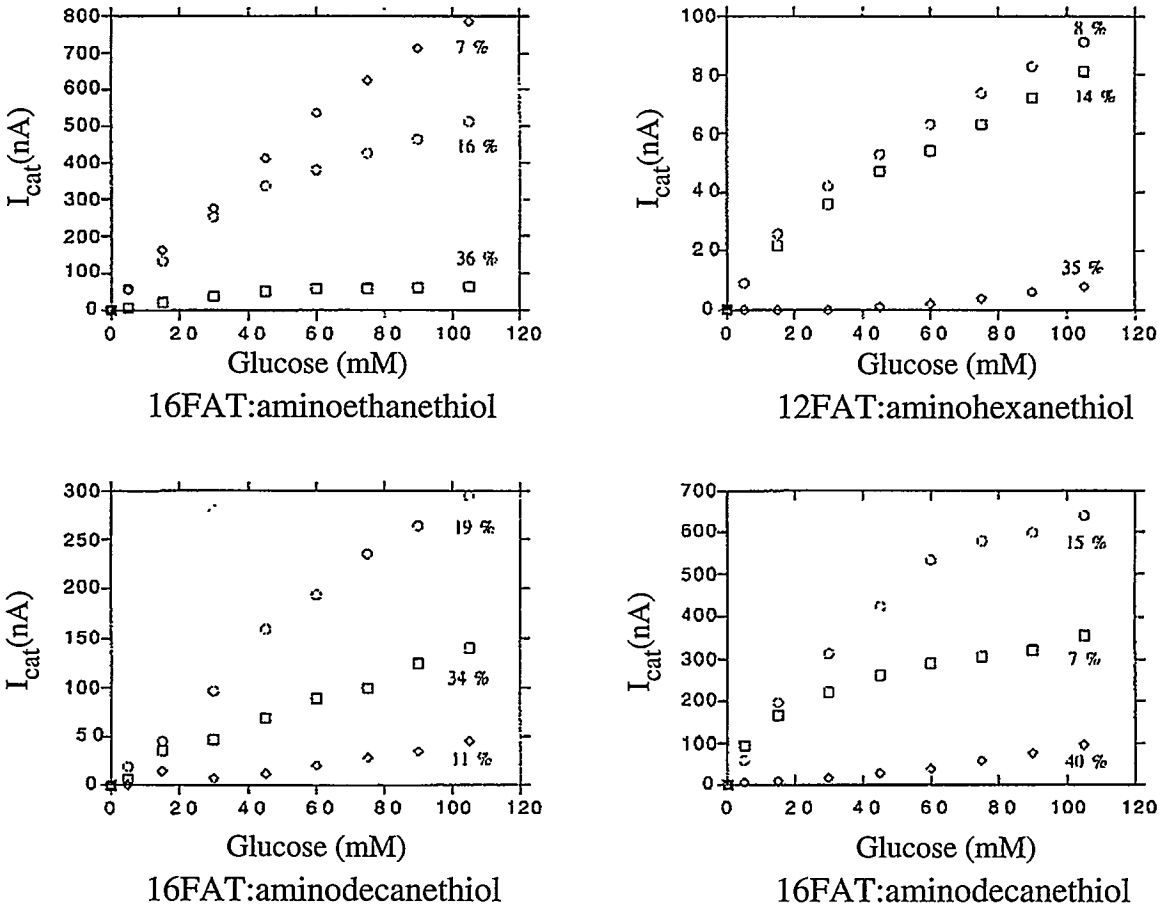
Multifunctional Self-Assembled Monolayers

Thomas Zawodzinski

The objective of our project is to establish self-assembled monolayers (SAMs) as a tool for controlling enzymatic electrochemical reactions. The capability to tailor a surface for specific electrochemical reactions is a potentially important element in molecular electronics and could have a strong impact on the development of sensors for a variety of substances.

The overall goals of our project are to develop methods of juxtaposing, in self-assembled layers, redox-active enzymes and other complexes and to study their interactions with each other. This is a specific example of a multistep, electron-transfer catalytic complex on an electrode surface with lateral electron transfers between adjacent elements introduced into the SAM as the key feature. The tasks can be divided into the following:

- synthesis and self-assembly of the desired functionalized alkanethiol molecules;
- characterization of the properties of each of the individual components, particularly the electron-transfer properties;
- attachment of enzymes to functionalized alkanethiol-modified surfaces;
- characterization of mixed monolayers of various components;
- demonstration of interaction amongst all components; and
- understanding of the role of monolayer structure in the functioning of such systems. Each can lead to applications of the chemistry in such areas as electrochemical-enzyme sensors.



The amperometric response of the different systems towards different concentrations of glucose: 16FAT (ferrocenyl alkanethiol):aminoethanethiol modified by GOx (glucose oxidase), 12FAT:aminohexanethiol modified by GOx, 8FAT:aminodecanethiol modified by GOx, and 6FAT:aminodecanethiol modified by GOx.

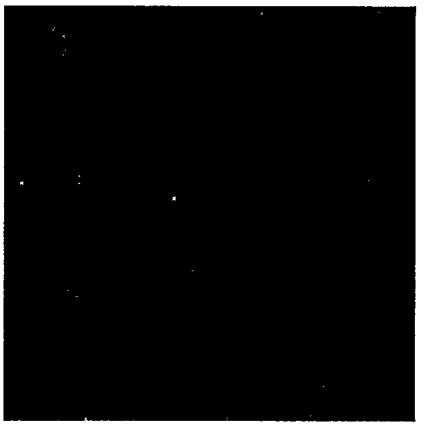
We have used SAMs consisting of multiple functionalized components to prepare novel multistep electrocatalytic systems. We have prepared working enzyme and mediator complexes on electrode surfaces and probed the factors influencing their efficiency. Natural self-assembly of multiple components leads to component domains on the surface.

We have prepared patterned self-assembled structures on surfaces and have extensively characterized these structures—most notably by scanning-force microscopy. These self-assembled structures are excellent model systems for understanding the factors providing contrast in lateral-force microscopy (LFM). We have developed novel schemes for preparing monolayers of immobilized colloids. These will lead to high-surface-area electrode structures with immobilized SAMs.

We have probed several additional applications of SAMs, including modification of electronic properties of metals and electrochemical and optical structures capable of being read, written on, and erased. The capability developed here consists of a "molecular toolkit" that provides the potential for a wide range of surface modifications. The figures show project results.

Publications

G. Bar, S. Rubin, R. Cutts, et al., "Correlation Between Microstructure and Optical Properties of Self-assembled Gold and Silver Colloid Monolayers on Dendrimer-Modified Silicon Oxide Surfaces" (submitted to *Langmuir).*



LFM image of stamped pattern. Inside the 5-micron disks is 12FAT. Outside is 16AT.

Rubin, S., J.T. Chow, J.P. Ferraris, et al., "Electrical Communication Between Components of Self-Assembled Monolayers" (to be published in *Langmuir).*

Temperatures and Vibrational Frequencies of Liquid N_2/O_2 and CO/O_2 Mixtures Shock Compressed to 100 kbar and 2000 K

Stephen Schmidt

The purpose of our project is to experimentally determine the temperatures and vibrational frequencies of N_2/O_2 and CO/O_2 mixtures that we have shock-compressed to pressures of ~100 kbar and temperatures of 1000–2000 K. We will use the measured temperatures in conjunction with existing shock- and particle-velocity data to calculate an equation of state that describes mixtures at conditions characteristic of the expansion of explosive products. We will then use the molecular vibrational frequencies to help develop molecular-potential functions that will allow us to the calculate the thermodynamic equations of state from first principles.

Previous shock-compression experiments have been used to obtain coherent anti-Stokes Raman spectra (CARS) of the nitrogen, oxygen, and carbon monoxide vibrational frequencies in mixtures of $N2/O_2$ and CO/O_2 at high pressures and temperatures. We analyzed these data using computer-based spectral-fitting techniques. This year, we made two improvements to the computer codes we used to analyze the spectral data. First, we incorporated a graphics package directly into the FORTRAN coding that we are using on the Macintosh PowerPC. Direct plotting from the codes is considerably more efficient than the previous method of using a separate graphics application to prepare plots using numerical files produced by the spectral fitting codes. Second, we installed a new, more user-friendly mathematics library, that the producers of the FORTRAN compiler distribute, in the Macintosh Programmer's Workshop we use to run the FORTRAN programs on the Macintosh PowerPC.

We have started work to verify the calibrations of the CARS data for the shock-compressed N_2/O_2 mixtures.

Metal-Ligand "Multiple" Bonding: Revelations in the Electronic Structure of Complexes of High-Valent f-Elements

Carol Burns

The goal of this project is to develop an understanding of the nature of chemical bonding between f-metals (lanthanides and actinides) and main-group elements and to examine the factors affecting the stability of oxidation states of the f-elements. Understanding the electronic structure of these complexes has far-reaching effects on evaluating and predicting interactions between f-metals and chalcogenide and pnictide elements and on predicting the physical and chemical behavior of radioactive materials, such as the actinide elements. In particular, our investigation of higher-valent complexes is providing dramatic evidence for the involvement of metal valence orbitals (nf and (n+1)d) in metal-ligand multiple bonds. This involvement helps to explain the stability of such fundamentally important species as the actinyl ions and other prevalent chemical forms of these elements under conditions relevant to environmental and process systems.

During the past year, we have uncovered an exciting and very general new route for preparing hexavalent uranium bis(imido) complexes, which are isoelectronic with the more-common uranyl species (see figure). Our method results in new and more-reactive actinide complexes and, particularly when coupled with novel activations of dihydrogen and silanes, provides us access to useful chemical transformations. We have also demonstrated a surprisingly large dependence of the redox chemistry of organoactinide complexes on the nature of ligands attached to the metal, which demonstrates an unexpected degree of covalency in the bonding of these species.

Publications

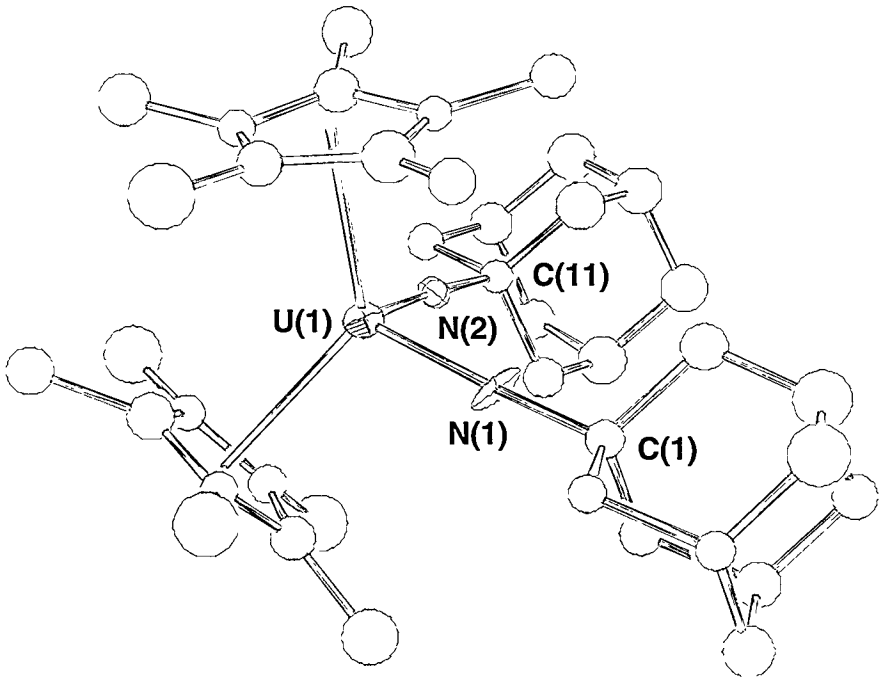
Arney, D.S.J., and C.J. Burns, "Synthesis and Properties of High-Valent Organouranium Complexes Containing Terminal Organoimido and Oxo Functional Groups. A New Class of Organo-f-Element Complexes," *J. Am. Chem. Soc.* **117**, 9448 (1995).

Avens, L.R., D.M. Barnhart, C.J. Burns, et al., "Oxidation Chemistry of a Uranium(III) Aryloxide," *Inorg. Chem.* 33, 4245 (1994).

Avens, L.R., D.M. Barnhart, C.J. Burns, et al., "Uranium-Mediated Ring-Opening of Tetrahydrofuran. Crystal Structure of $UI_2(OCH_2CH_2$-$CH_2CH_2I)_2(Ph_3P{=}O)_2$" (to be published in *Inorg. Chem.*).

England, A.F., C.J. Burns, and S.L. Buchwald, "New Syntheses of $Cp^*_2Th(Ph)_2$ and $Cp^*_2Th(Me)(Ar)$ Derivatives," *Organometallics* **13**, 3491 (1994).

Watkin, J.G., N.N. Sauer, and C.J. Burns, "Synthesis of Neutral and Anionic Uranyl Aryloxide Complex from Uranyl Amide Precursors," *Inorg. Chem.* 34, 4079 (1994).



Molecular structure of $(Me_5C_5)_2U(NR)_2$. (R = adamantyl)

Chemistry and Catalysis in Supercritical Media

William Tumas

We are exploring the potential of supercritical carbon dioxide as a reaction medium with the objective of developing new or improved processes that consume less energy and generate minimum waste and exploiting the properties of supercritical fluids to control chemical selectivity and/or reactivity. The attraction of supercritical fluids lies in their unique solvating capabilities and in their environmentally benign nature. Our approach offers the possibility of opening up new chemical pathways, increasing selectivity and rates, facilitating separations, and minimizing the need for hazardous solvents.

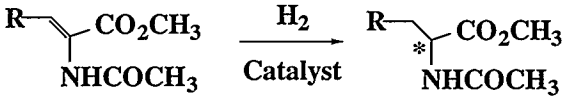
We have found CO_2 to be an effective solvent for titanium-catalyzed asymmetric oxidations of allylic alcohols, Friedel-Crafts acylations and alkylations; and an effective solvent and reagent in the synthesis of isocyanates (where it replaces phosgene). We have demonstrated improved selectivity of the acylation of naphthalene with acetyl chloride by reducing the pressure from 5000 to 2000 psi and thereby tuning the α/β substitution ratio from 60% to 70%. We have discovered other routes to reactivity control—particularly the ability to use pressure to tune solvent cage strength. We devised this technique from studies of the photolysis of α,α-dimethylbutyrophenone in supercritical CO_2. We have also demonstrated that asymmetric catalytic hydrogenation and hydrogen transfer reduction of enamide esters work as well or better in CO_2 than in conventional solvents (Scheme I). The reaction shows substantial temperature, density, hydrogen pressure, and solvent effects on enantioselectivity. We have observed higher enantioselectivities at lower temperatures and higher densities. Our work has applications to clean manufacturing, waste minimization, energy efficiency, economic competitiveness, and sustainable technology.

Publications

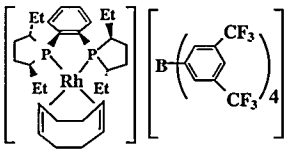
Burk, M.J, S.G. Feng, M.F. Gross, and W. Tumas, "Catalytic Asymmetric Hydrogenation in Supercritical Carbon Dioxide," *J. Am. Chem. Soc.* **117**, 8277 (1995).

Morgenstern, D.A., W. Tumas, et. al., "Supercritical Carbon Dioxide as a Substitute Solvent for Synthesis and Catalysis" (submitted to *ACS Symp. Series, "Practical Pollution Prevention"*).

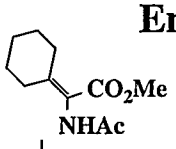
Scheme I. Asymmetric Catalytic Hydrogenation



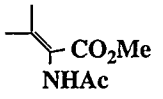
Substrate	% ee in MeOH	% ee in Hexane	% ee in SC CO_2
R = H	98.7	96.2	99.5
R = Et	98.7	96.8	98.8
R = Ph	97.5	98.3	99.2
R = 3,5-CF_3Ph	93.2	96.6	91.9



Enhanced Enantioselectivity in SC CO_2



81.8 76.2 **96.8**



62.6 69.5 **84.7**

Highest ee's for hydrogenation of β,β-disubstituted enamides

Ionically Conducting Polymers for High-Energy-Density Batteries

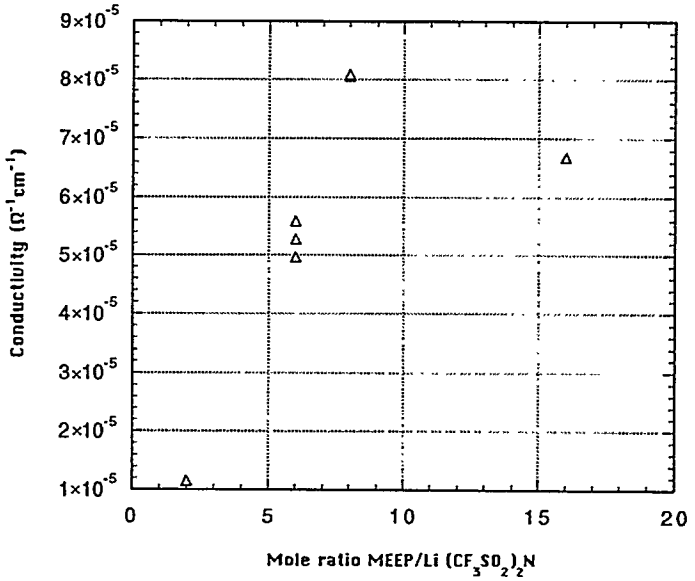
Robert E. Hermes

Rechargeable batteries using lithium-based electrodes and lithium-salt-loaded electrolytes have the highest theoretical specific energy densities of any battery system. Polyelectrolytes are used as the active separator between the electrodes for "shuttle-cock" operation of the lithium ion charge-carrier during charge and discharge cycles.

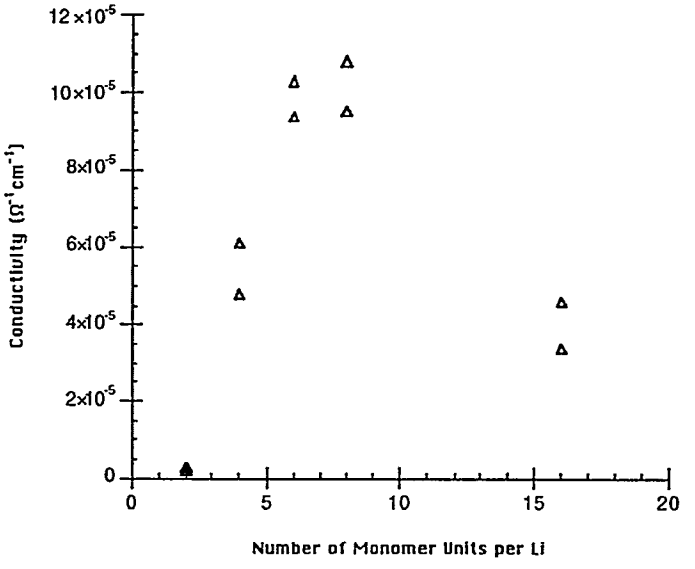
Our objective in this project is to develop and understand the transport chemistry of the polyelectrolyte component for solid-state lithium batteries. This research will provide insight into the chemical interactions involved in lithium ion transport through the polyelectrolyte. We have combined macromolecular synthesis capabilities with electrochemical characterization expertise to prepare new polyelectrolytes containing modified side chains which facilitate the movement of the lithium ion.

We have made significant progress in synthesizing polyelectrolytes and characterizing their electrochemical performance using the techniques developed earlier in the project. This included preparing lithium-salt-loaded films of modified polyphosphazenes (PPN) and characterizing the polyelectrolytes so formed using ^{7}Li nuclear magnetic resonance spectroscopy, Raman infrared spectroscopy, differential scanning calorimetry, and electrochemical analysis (conductivity). Our lithium salt-loaded 2-PPN and another specially modified PPN have room-temperature electrical conductivities of 8×10^{-5} S/cm and 1.0×10^{-4} S/cm, respectively. To our knowledge, these conductivities are the highest ever achieved for a solvent-free, lithium-salt-loaded solid polyelectrolyte (see our accompanying figures).

These results have partially validated our hypothesis and approach for obtaining improved conductivity in solid polyelectrolytes. Using the 2-PPN in a battery configuration, we were able to demonstrate that the polyelectrolyte performs according to our expectations and will have applications in both the private and government sectors.



Electrical conductivity of the lithium imide salt-loaded 2-PPN (methoxy ethoxy ethoxy phosphazene [MEEP]).



Electrical conductivity of the lithium imide salt-loaded, specially modified MEEP (two samples).

Photoredox Reactions: Energy Storage and Halocarbon Degradation

William Woodruff

We have studied the photoredox reactions of dimeric transition-metal complexes of the platinum group. Two features of this photochemistry interest us: the potential of photoinitiated electron-transfer reactions to effect the practical conversion of light into chemical energy and reactions whereby halocarbons in the environment may be photocatalytically degraded to less hazardous substances. We approached both issues by establishing the time evolution of the changes in molecular and electronic structure that occur during the photoredox processes.

In the case of energy conversion by photoinitiated electron transfer, we have studied the intramolecular electron-transfer reactions of these complexes. Our results test modern theories of electron transfer and provide an experimental basis for the rational design of energy-harvesting molecular systems. In the case of the halocarbon photodegradation reactions, we provide the first experimental study of the evolution of structure during the early events in "strongly adiabatic" redox reactions, which are poorly understood both experimentally and theoretically. Our work provides the basis for rational approaches to the molecular design of desired reactivity. Also, we have searched for reductive chemistry that will convert the photo-oxidative addition of the halocarbons into a photocatalytic cycle that results in net halocarbon degradation without consumption of the metal complex.

Publications

James, C., D. Morris, K. Dunbar, et al., "Photochemistry of $[Rh_2(CH_3CN)_{10}]^{2+}$" (to be published in *Inorganica Chimica Acta*).

Decay of Surface Nanostructures via Long-Time-Scale Dynamics

Arthur Voter

Our goals in this program are to (1) characterize the novel dynamics of metallic surface nanostructures, which decay on picosecond time scales; (2) develop improved saddle-point search methods for finding all low-lying escape routes bounding a minimum; and (3) most importantly, develop a dynamical method (hyper-MD) that can evolve an atomistic system through numerous local minima over time scales inaccessible to direct molecular dynamics (MD).

We have programmed the chain-of-states (COS) method, a state-of-the-art approach for finding complicated saddle points, into a simulation code. For surface nanostructures, some transition states are so complex that the COS method must be augmented with methods making use of the Hessian matrix and are so large that a Newton-Raphson approach is prohibitively expensive. We have implemented an N-scaling Lanczos approach that finds the few lowest Hessian eigenvectors, allowing uphill subspace searches.

Using sequential snapshots from the temperature-programmed MD runs to initialize the COS search, we have determined the saddle points for the silver nanostructure decay process. The multisaddle decay process is often initiated at the cube corners, involving dislocations on the fcc(111) planes; we are applying the method of Hoagland and Hirth to quantify the dislocation position through successive stages of formation, slip, and ejection.

We have made significant progress on the development of a hyper-MD method. Although more development will be necessary, we have achieved orders-of-magnitude speedup with a proof-of-principle simulation of surface self-diffusion of Ag on Ag(100) at a temperature of 500 K (with no specific knowledge about the nature of the transition states).

Molecular-Level Assemblies on Metal Oxide Surfaces

Jon Schoonover

At the forefront of basic and applied research today is the design of photo-driven molecular devices. Molecular devices can be designed to mimic parts of natural processes, such as photosynthesis. We are pursuing the design of artificial photonic devices, which consist of molecular-level assemblies based on polypyridyl transition-metal complexes attached to semiconductor surfaces. The potential applications include energy conversion, photoremediation of hazardous waste, and optical information storage and computing.

The rational design of photonic devices has recently become possible through synthetic strategies for the construction of molecular assemblies on semiconductor surfaces and through the continuing development of ultrafast vibrational spectroscopies to characterize these new materials. The rich chemistry of these complexes can be utilized to prepare molecular assemblies with well-defined redox or excited-state properties that can be finely tuned to produce desired materials properties.

In order to drive photonic processes, two criteria must be fulfilled: (1) efficient charge separation must occur and (2) the excited electron must be trapped, which produces a strongly oxidizing center (see figure). We have shown that sensitized titanium dioxide surfaces provide efficient charge separation following the absorption of a photon by an attached molecular assembly (sensitizer).

A fundamental understanding of the properties of the surface-attached assemblies is an essential prerequisite to the molecular design of materials and devices. Ultrafast vibrational spectroscopies have been used to characterize these materials, representing an important and new approach in this area of research. We use advanced laser techniques to elucidate the fundamental factors that determine the photochemistry and photophysics of a series of photoactive assemblies in solution and on semiconductor surfaces. This information is part of a molecular engineering approach to fabricating devices.

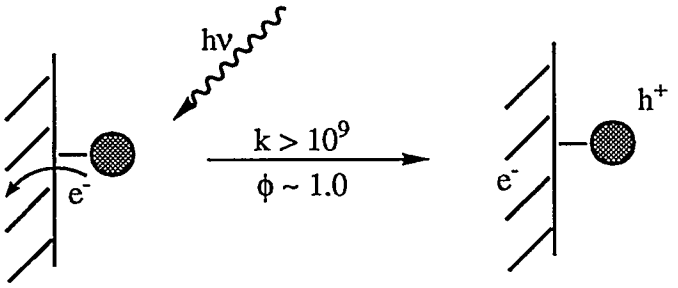
Publications

Bates, W.D., C.A. Bignozzi, P. Chen, et al., "Resonance Raman Spectroscopy or Ru(II) and Os(II) Polypyridyl Complexes Containing N-Methyl-4,4'Bipyridinium Radical (MQ) as a Ligand: Evidence for a Metal-to-Ligand Charge Transfer Transition" (to be published in *Inorg. Chem.*).

Bignozzi, C.A., J.R. Schoonover, F. Scandola, "A Supramolecular Approach to Light Harvesting and Sensitization of Wide Bandgap Semiconductors: Antenna Effects and Charge Separation" (to be published in *Prog. Inorg. Chem.*).

Schoonover, J.R., W.D. Bates, T.J. Meyer, "Application of Resonance Raman Spectroscopy to Metal Complex Excited States: Excited-State Ordering and Ligand Delocalization in Dipyrido[3,2-a:2',3'-c]phenazine (dppz) Complexes of Re(I) and Ru(II)" (to be published in *Inorg. Chem.*).

Schoonover, J.R., R.B. Dyer, W.D. Bates, et al., "Application of Time-Resolved, Step-Scan Fourier Transform Infrared Spectroscopy to Excited-State Electronic Structure in Polypyridyl Complexes of Re(I)" (to be published in *Inorg. Chem.*).



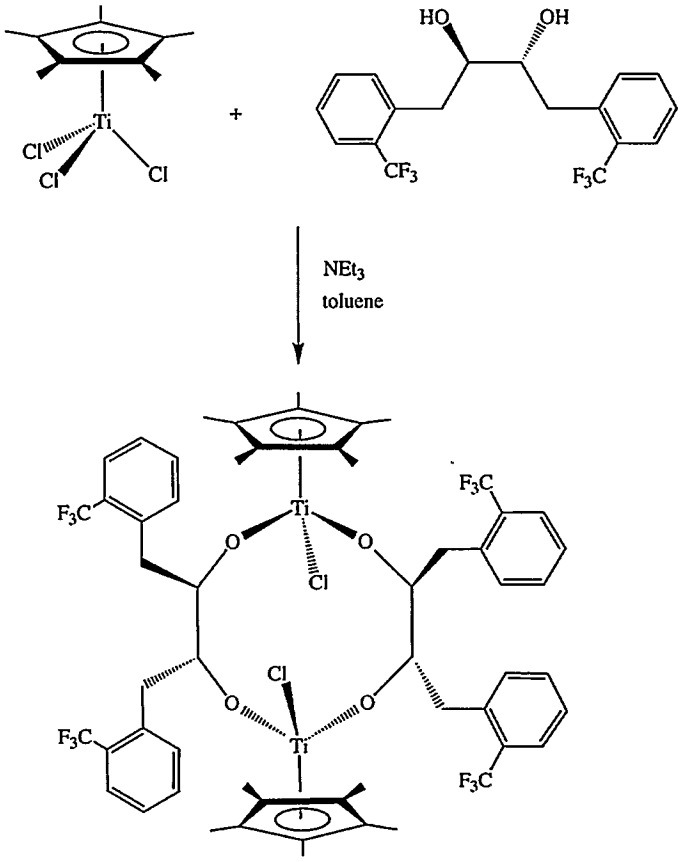
The n-type semiconductor serves as a sink for the excited electron with very rapid charge injection into the conduction band, leaving an oxidized metal center at the surface. The electron can be utilized to do work, or the hole can be used to perform oxidative chemistry.

Asymmetric Catalysis in Organic Synthesis

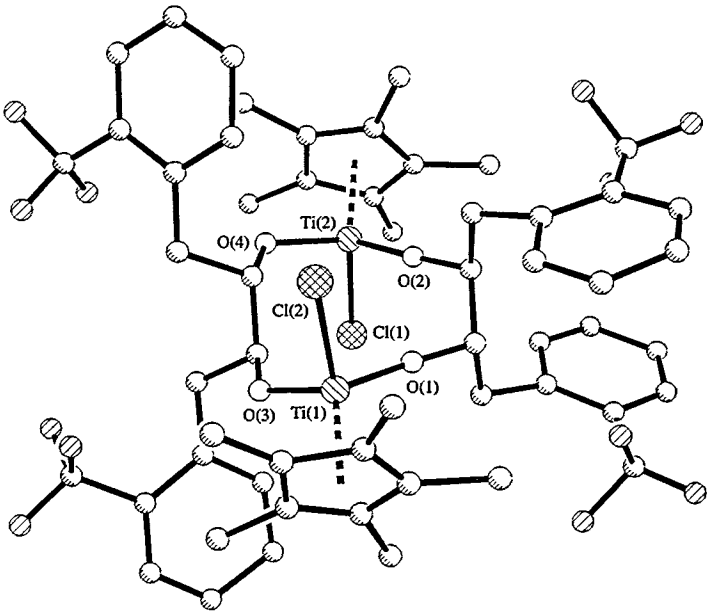
John Watkin

This research program is aimed at developing new catalysts for the formation of organic molecules by an enantioselective reaction. Such organic molecules are relevant to the pharmaceutical and agrochemical industries. Our primary goal is the development of Lewis-acidic catalytic species that feature lanthanide- or Group IV-metal centers supported by chiral alkoxide ligands. These compounds are known to be effective catalysts for processes in which carbon-carbon bonds are formed, such as aldol, Michael, Diels-Alder, and trimethylsilylcyanation reactions.

We have isolated optically pure diolate ligands containing substituted arene moieties. By following the synthetic route (see first figure), we have prepared pentamethylcyclopentadienyl titanium derivatives that contain chiral diolate ligands. Recently, we have determined the x-ray crystal structure of a dimeric titanium complex containing trifluoromethylphenyl-substituted diolate ligands (a ball-and-stick view of this diolate complex is shown in the second figure). In the future, we will investigate the possibility of using this catalyst in asymmetric Diels-Alder reactions. The chloride ligand is expected to be readily replaceable by an alkyl or amido functionality, thus providing a catalyst that is expected to be active in asymmetric Michael reactions. We are also using chiral diolate ligands as synthetic precursors in order to develop new 'ansa'-metallocene catalysts for use in asymmetric hydrogenation and amination processes.



Synthetic route to obtaining pentamethylcyclopentadienyl titanium derivatives that contain chiral diolate ligands.



Ball-and-stick view of the molecular structure of the dimeric titanium diolate complex $\{(\eta\text{-}C_5Me_5)TiCl[\mu\text{-}OCH(CH_2R)CH(CH_2R)O]\}_2$ *(R = 2-*$CF_3C_6H_4$*).*

New Fullerene-Based Mixed Materials: Synthesis and Characterization

Duncan McBranch

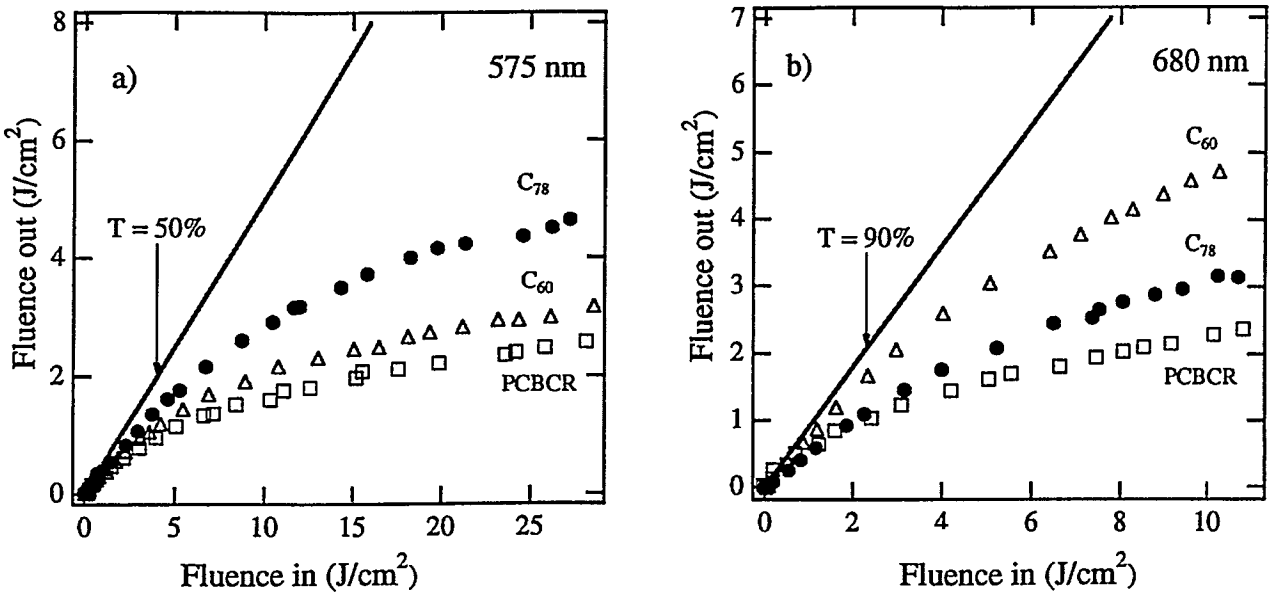
The research objectives of our project are to

- develop new synthetic routes for chemically modified fullerenes and for fullerenes combined with optical glasses and conjugated polymers to control the optical, electrical, and mechanical properties of the resulting composites;
- build upon existing collaborations and experimental capabilities to contribute to the understanding of fundamental nonlinear-optical and photoinduced charge-transfer effects in these new composites;
- exploit subpicosecond optical probes to provide guidance for further synthetic refinement of these composites; and
- identify and develop materials properties which will enhance the technological potential of these new materials.

Desirable properties which will be targeted include subpicosecond response times, large photoinduced changes in refractive index or photoinduced charge separation, high optical-damage threshold, mechanical strength, environmental and thermal stability, and chemically tunable dielectric properties and color.

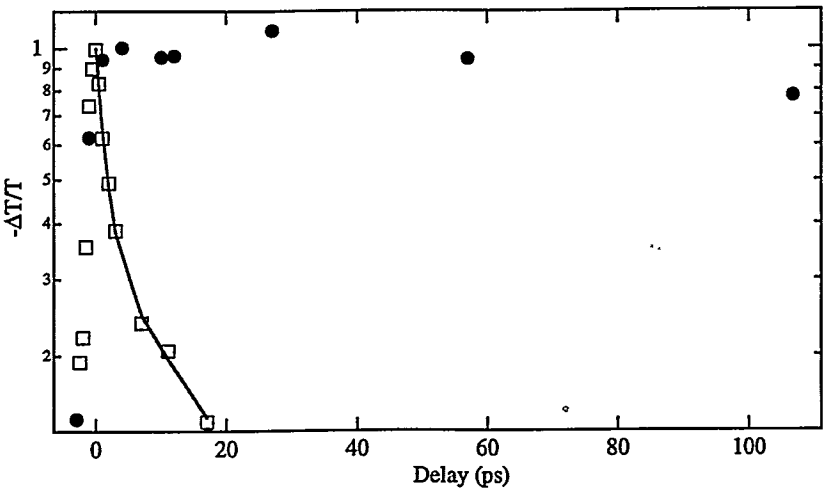
Previous studies of optical limiting in fullerenes have been performed in a limited selection of fullerenes (C_{60} and C_{70}) and only at the 532 nm wavelength. We have surveyed the optical-limiting performance for several substituted derivatives of C_{60}—C_{60}-C_2H_5N, $2[(\eta_2\text{-}C_p)_2Fe]C_{60}$, and phenyl-$C_{61}$-butyric acid cholestryl ester (PCBCR)—and higher fullerenes (C_{70}, C_{78}, and C_{84}) in a toluene solution when exposed to light between 500–1000 nm wavelengths. We measured excited-state absorption spectra with picosecond resolution using time-resolved pump-probe absorption. Our technique allowed broadband predictions of the optical limiting performance. We then tested these predictions at selected wavelengths from 532–700 nm by measuring intensity-dependent transmission (see first figure). C_{60} and its derivatives display optical limiting at wavelengths from 532–700 nm, with the limiting performance increasing to the infrared, constrained by the vanishing ground-state absorption below the 700 nm wavelength. Notably, PCBCR shows both improved solubility and enhanced limiting relative to C_{60} (again, see first figure). Higher fullerenes show potential for limiting out to the 1000 nm wavelength.

Comparisons of optical limiting and excited-state absorption in solid C_{60} (thin films and doped porous glasses) show that much-faster relaxation dynamics in the



Intensity-dependent transmission for C_{60} (open triangles), C_{78} (solid circles), and PCBCR (open squares) at both 575 nm (a) and 680 nm (b). The low fluence transmittances (corrected for reflection) for C_{60}, C_{78}, and PCBCR, respectively, are 50%, 44%, and 57% at 575 nm; and 91%, 67%, and 87% at 680 nm.

solid reduce the limiting effectiveness for nanosecond pulses (see the second figure). Hence, optimal use of fullerenes for optical limiting in a solid form will require that the fullerenes be microscopically dispersed in a solid host matrix. We have developed a procedure for producing such a material in the form of a fullerene/silicon dioxide sol-gel glass and have demonstrated optical limiting in this glass matrix.



Dynamics of the integrated transient absorption for C_{60} thin film (open squares) and toluene solution (solid circles). The solid line is a fit to a double exponential, with time constants $\tau_1 = 1.5$ ps and $\tau_2 = 20$ ps.

Publications

McBranch, D.M., B.R. Mattes, A. Koskelo, et al., "C_{60}-Doped Silicon Dioxide Sonogels for Optical Limiting," *SPIE Fullerenes and Photonics* **2284**, 15 (1995).

McBranch, D.M., L. Smilowitz, V. Klimov, et al., "Optical Limiting in Fullerene Solutions and Doped Glasses" (submitted to *SPIE Fullerenes and Photonics II*).

Self-Assembled Thin-Film Chemical Sensors

Basil Swanson

Our objective is to employ self-assembly techniques to covalently bond species-selective reagents directly to the surface of a transducer so that analyte/reagent chemistry occurs at the interface between the transducer and the media to be monitored. The use of self-assembly mono- and multilayer techniques results in stable sensing elements with optimal specificity built in through the use of reagents that have been designed for molecular recognition. Moreover, self-assembly chemistry applied to oxide surfaces allows flexible means of transduction, spanning optical, electrochemical, mass-loading, and conduction methods.

The use of self-assembly techniques represents a new paradigm for the design and fabrication of chemical sensors and offers an opportunity to develop a new generation of highly stable and sensitive real-time sensors capable of identifying multiple species in complex mixtures. While this approach is completely general and can be applied to a wide range of potential species (e.g., trace metals, organics, inorganics, biological and chemical warfare agents, and pesticides), this project focuses on demonstrating the methodology of the techniques and on applying them to selected organic vapors (i.e., aromatics and halogenated hydrocarbons).

Because the porosity of these cyclodextrin-based thin films is a key factor in the sensor performance, we have designed, in the past year, a new method for measuring the extremely small molecular pore size. This innovative technique utilizes the novel inclusion properties of cyclodextrins, i.e., their ability to accommodate "guest" contaminants. By measuring the guest concentration, we can evaluate the accessible molecular cavity in the thin film and, hence, predict its sensory property.

MATHEMATICS AND COMPUTATIONAL SCIENCES

DISPERSIVE INTERNAL LONG-WAVE MODELS

Roberto A. Camassa

Our work is a joint analytical and numerical study of internal dispersive water-wave propagation in a stratified two-layer fluid, a problem that has important geophysical fluid dynamics applications. Two-layer models can capture the main baroclinic (density-dependent) effects because they can support the observed large-amplitude internal wave motion at the interface between layers, as well as large shear velocities, which cannot be described by the simpler barotropic (vertically integrated) models. We are deriving (1) new model equations using the approach of classical asymptotics and (2) a new method that reconstitutes the Hamiltonian structure according to the original structure of Euler equations. We are studying these new model equations numerically and analytically in the presence of (1) bottom topography and (2) forcing from moving pressure distributions.

We have derived model equations for two-layer stratified fluid in the small-wave amplitude/weakly nonlinear regimes for finite depth of the lower layer. We have shown that our model equations include all known cases for these regimes as special limits (see table). We have implemented the finite difference and pseudo-spectral codes for solving numerically the one-dimensional version of the model, and we have carried out the simulations.

Publications

Camassa, R., "Comment on 'Do Resonantly Forced Internal Solitary Waves Protect the Fuel of Hurricanes?'" *Phys. Rev. Lett.* **72,** 2668 (1994).

Choi, W., "Nonlinear Evolution Equations for Two-Dimensional Surface Waves in a Fluid of Finite Depth," *J. Fluid Mech.* **295,** 381 (1995).

Choi, W., and R. Camassa, "Weakly Nonlinear Internal Waves in a Two-Fluid System" (submitted to *J. Fluid Mech.*).

Dispersive Internal Long Wave Models				
Relative layer depths		$h_1 = O(h_2)$	$h_1 \ll h_2$ (finite)	$h_2 \longrightarrow \infty$
Fully Nonlinear		Coupled Green-Naghdi System *(New)*	*New*	*New*
Weakly Nonlinear	uni-dir. (1-D)	KdV, KP Equations uni-GN Eq. *(New)*	Intermediate-Long-Wave (ILW) Equation	Benjamin-Ono Equation
	bi-dir. (2-D)	Boussinesq System	*Completed*	*Completed*
	forced	*Yes* (KdV, KP,B) *No* (uni-GN)	*Completed* (1-D) *No* (2-D)	*Yes* (1-D) *No* (2-D)

The various levels of approximation for stratified two-layer fluid models. In the table, (1) h_1 and h_2 refer to the thickness at rest of the top and bottom layer, respectively; (2) KdV and KP stand for Korteweg-de Vries and Kadomtsev-Petviashvili equations, respectively; (3) "New" refers to models we have or will derive and that, to the best of our knowledge, have not been reported in the literature before; (4) "Completed" indicates that we have successfully carried out the derivation of a model in this regime during the previous year; and (5) "Yes" indicates that some information exists on the behavior of solutions in the presence of external forcing; "No" indicates the opposite.

Multidimensional Methods for Hyperbolic Problems

James Hyman

The numerical solution of multidimensional wave-propagation problems is considerably more complex than solutions for one-dimensional problems, but improving a method's accuracy produces more significant increases in efficiency. This is particularly true for first-order accurate methods. Higher-order methods, which are already comparatively efficient, are especially difficult to construct on irregular meshes. The passive-scalar advection equation provides an ideal vehicle for investigating the relationships between accuracy, efficiency, and physical acceptability for a variety of finite-difference schemes. Development and analysis of methods for this equation provide insight into solving more complicated problems involving material and/or neutron transport.

We found that three approaches to two-dimensional upwind differencing led to schemes equivalent to the dimensionally split Lax-Wendroff method. Assuming stability, we were able to prove that both the split-Lax-Wendroff and a new two-dimensional, predictor-corrector scheme yielded second-order convergence on nonuniform tensor-product grids, despite first-order discretization errors for such grids. We were able to prove that in some cases, Roe's upwinding for triangulations (which is locally inconsistent) converges with first-order accuracy.

The sensitivity of fourth-order accurate, conservative, mimetic methods to the roughness of nonuniform grid-spacing was explored analytically and numerically in one-dimension, and for logically-rectangular two-dimensional grids. We also considered the application of a novel set of unknowns (parameters) towards conservative second-order methods on irregular polyhedral grids.

Queried, we noted that convergent, stable split schemes for ill-posed problems could not exist. This prompted us to reconsider (for hyperbolic operators whose sum is hyperbolic) conditions implying that splitting is stable for the differential operators and for related difference methods.

Publications

Castillo, J.E., J.M. Hyman, M. Shashkov, et al., "The Sensitivity and Accuracy of Fourth Order Finite-Difference Schemes on Nonuniform Grids in One Dimension," *Computers and Mathematics with Applications* **30**, 41 (1995).

Wendroff, B., "An Analysis of Front Tracking for Chromatography," *Acta Applicandae Mathematica* **30**, 265 (1993).

Algorithms for Adaptive, Composite, Overlapping Meshes Used on Message-Passing Architectures

David Brown

We have been developing computational methods and programming environments for adaptive, composite, overlapping meshes used on serial and parallel computers. This research was prompted by the need for high-level tools to aid in the modeling of large-scale, complex, physical processes described in complex geometries by fluid-flow equations. Parallel tools are based on object-oriented message-passing techniques. We used an object-oriented approach based on the C++ language to create a programming environment in which relatively high-level computational objects may be assembled into solvers for partial differential equations (PDEs). With this programming environment, users will be able to create solvers that are portable across a wide variety of computer architectures and seamlessly incorporate software that uses adaptive, composite, overlapping meshes.

To date, we have developed C++ class libraries, called A++ and P++, that handle basic array operations required in scientific codes. Parallel infrastructures are hidden from the user of these libraries. We have also developed class libraries that handle composite, overlapping meshes and arrays defined on those meshes. For help in creating solvers, we have developed class libraries for difference operators. We have also developed example PDE codes for compressible and incompressible flow problems, as well as an "all-speed" flow solver designed to handle flows with a range of Mach numbers from near zero to Mach 1. We are currently developing a C++ class library, called AMR++, for handling general adaptive mesh refinement within this programming environment.

Theoretical Design Tools for Advanced Semiconducting Devices

Patrick Hagan

Future generations of very large scale integration circuits require semiconducting devices that are an order of magnitude faster and smaller than current devices. To design these devices effectively, we need to be able to predict the electronic properties of ultrasmall, ultrafast semiconducting devices on a routine basis. We are investigating the physical and mathematical nature of these ultrasmall, ultrafast devices with the objective of developing the theoretical models and numerical software needed to design future generations of advanced devices.

Electronic properties of semiconductors can be predicted accurately from the Boltzmann equations which express how the electron density evolves in phase space. However, using Monte Carlo methods to directly solve the Boltzmann equation has proven to be exceedingly slow because of its high dimensionality (time, three space, and three wave-number dimensions). State-of-the-art Monte Carlo programs are usually limited to steady-state simulations in two space dimensions; even so, a supercomputer may take hours to simulate a single device. Yet, as devices become smaller and faster, three-dimensional and transient effects become critical to predicting device performance.

In this project we (1) re-analyze the basic physics of semiconductors in the regime corresponding to ultrasmall ultrafast devices, (2) use singular perturbation techniques to derive reduced-dimensionality equations that accurately describe the semiconductor's electronic properties in these regimes, and (3) validate the resulting theoretical models against Monte Carlo simulations and experimental data. From this project, we hope to gain the capability of simulating the time-dependent operation of ultrasmall, ultrafast devices in three spatial dimensions. The capability of accurately predicting the performance of such devices on a day-to-day basis will transform the design of new devices.

We have developed new reduced dimensionality models for simulating these effects. In addition, fast algorithms were integrated into a full-band Monte Carlo code to be used as a benchmark to test reduced dimensionality models.

Publications

Sobehart, J. R., and P.S. Hagan, "Determination of Current Distribution in Semiconductor Devices via Half-Range Resolution of the Boundary Layer" (submitted to *ZAMM Zeitschrift fuer Angewandte Mathematik und Mechanik*).

Sobehart, J. R., P.S. Hagan, "The High Field Semiconductor Equations" (submitted to *ZAMM Zeitschrift fuer Angewandte Mathematik und Mechanik*).

Development of the Applied Mathematics Originating from the Group Theory of Physical and Mathematical Problems

James Hyman

Group theoretical methods are powerful tools in mathematics and physics. The broad goal of this research is to use these methods to develop the implications of group (symmetry) structures underlying models of physical systems and to increase our understanding of simple models of chaotic systems.

In the context of physics, our main thrust is to further develop the complex mathematics that enters into many-particle quantum systems, with special emphasis on the new directions in applied mathematics that have emerged and continue to surface in these studies. In this area, we have shown that the structure of the group representations themselves is the origin of the unexpected occurrence of SU(2) 3nj-coefficients in SU(3) theory. We have used the discovery of the combinatorial structure of these representation functions to bring understanding to these complex objects, thus extending the combinatoric techniques used in the study of generalized Schur functions discovered earlier in this project.

In the context of chaos, the study of maps of the interval and the associated theory of words led to the complete solution of the Galois group of iterated quadratic maps, to the classification of fixed points, and to the solution of a problem in the classification of DNA sequences.

Publications

Beyer, W.A., and L. Holm, "Number of Left-Product Coefficients in a Mendelian Stochastic Algebra" (to be published in *The Ulam Quarterly*).

Beyer, W.A., and J.D. Louck, "Galois Groups for Polynomials

Related to Quadratic Map Iterates," *The Ulam Quarterly* 2, 1 (1994).

Beyer, W.A., J.D. Louck, and D. Zeilberger, "Generalization of a Cosine Product" (to be published in *Mathematics Magazine*).

Beyer, W.A., and W.W. Wood, "Corrigenda: On a Paper of Beyer, Roof, and Williamson" (to be published in *Math. Comp.*).

Chen, W.Y.C., and J.D. Louck, "The Combinatorial Power of the Companion Matrix" (to be published in *Linear Algebra and its Applications*).

Chen, W.Y.C., and J.D. Louck, "Interpolation for Symmetric Functions" (to be published in *Adv. Math.*).

Louck, J.D., "Angular Momentum Theory," in *Atomic, Molecular, and Optical Physics Reference Book*, G.W. Drake, Ed., (American Physical Society, Woodbury, New York, in press)

Louck, J.D., "MacMahon's Master Theorem, Double Tableau Polynomials, and Groups" (to be published in *Adv. Appl. Math.*).

Louck, J.D., L.C. Biedenharn, W.Y.C. Chen, et al., "The Role of SU(2) 3n-j Coefficients in SU(3)," in *Symmetry and Structural Properties of Condensed Matter*, T. Lulek, W. Florek, and S. Watcerz, Eds. (World Scientific, Singapore, 1995), page 150.

Zhong, R., and L. Wang, "Two Open Problems Associated with Monotone Sequences" (to be published in *Acta Applicandia Mathematica*).

New Class of Random Number Generators Required for Advanced Computer Architectures

Tony Warnock

The Monte Carlo method is used extensively at Los Alamos for simulations having a random component, such as particle transport codes, statistical mechanics computations, computer performance simulations, and economic modeling. The reliability of Monte Carlo methods ultimately rests upon the quality of the "random" numbers used in a computation. Random number generators (RNGs) can only produce a finite number of terms before repeating themselves. Advanced computer architectures and fast scientific workstations are capable of exhausting the entire sequence of presently used generators in a single computation. A new class of RNGs is required or else these new computing capabilities will be of limited value for complex Monte Carlo simulations. Using a poor RNG can give erroneous results with no indication that a problem has occurred. The purpose of this project is to extend current RNGs to much greater cycle lengths, to develop other types of generators, and to develop tests of the usefulness of RNGs.

We have developed methods for generating multipliers for congruential RNGs that should have good properties. We have produced a set of 6139 multiplier candidates by assembling small partial quotients (1,2,3) into fractions with denominators of 2^{64}. These multipliers were further screened by computing a Minkowski reduced basis for each multiplier in dimensions 2 through 20. The bases are computed both for the mathematically usual method of computing $\langle x(1),x(2),x(3)\rangle$ for the first point and then shifting to $\langle x(2),x(3),x(4)\rangle$, etc. for the rest of the points and for the normal computational practice of shifting to $\langle x(4),x(5),x(6)\rangle$, etc., for succeeding points. The Minkowski bases for the resulting lattices are different. There were 39 multipliers that had Beyer ratios of less than 2 in all dimensions from 2 to 20 and from both lattices and sublattices. The Beyer ratio is the ratio of the longest basis vector to the shortest. A multiplier having a large Beyer ratio will generate random numbers that tend to fall into low-dimensional hyperplanes.

We discovered that the Minkowski reduced basis of a lattice is not unique. Thus there may be more than one Beyer ratio for a given RNG. This fact is surprising in that Beyer ratios have been used for more than twenty years in evaluating RNGs.

Hard Chaos, Quantum Billiards, and Quantum-Dot Computers

Ronnie Mainieri

There is a limit on how small you can make a transistor in an electronic chip. Once it becomes too small, the electrons in it no longer behave as a fluid; it has become a quantum device. The quantum dot is one of the many small devices that are being investigated for use in future chips. Each dot can hold up to a few electrons. One can think of the electrons as bits in a computer memory cell. If these electrons could be manipulated as bits, then one would have a computer. Manipulating electrons is moving them from one quantum dot to another.

But at those small scales an electron moves, through wires and dots, as a ball in a billiard. The billiards I mention are the dynamic systems called billiards that are inspired by billiard tables. The model consists of point particles moving in a limited region of space (the billiard table). They are just like billiards except in two respects: there is no friction or inelastic effects, so the ball keeps bouncing forever, and the shape of the table can be any closed piecewise smooth curve. If the shape of the table is not a circle or a figure that can tile the plane, then the billiard will have chaotic regions. A square with the circle in the middle removed (the ball bounces off it) is the classical example in the mathematical literature for a chaotic billiard. An understanding of the dynamics of electrons requires an understanding of their chaotic dynamics. Therefore, a better understanding of chaotic dynamics is necessary for the reliable computation of physical quantities. Using the method of cycle expansions for chaotic systems, one needs only 1161 periodic trajectories to compute a quantity that 10 billion Monte Carlo iterations fail to compute (see figure).

In my project I concentrated on understanding the effects of noise in chaotic dynamic systems and in the classification of all trajectories. By using the equivalence between dissipation and noise, it is possible to model electron-electron collisions, impurities, inelastic scattering, and other real-life effects on the dynamics of the electrons. I did this by choosing the correct noise distribution to add to the dynamics. Every noise source is characterized by its own unique sound distribution which leads to different types of noise. I was able to replace some of the dissipative effects in the electron dynamics by the appropriate noise distribution. The remarkable result is that arbitrary noise distributions can be modeled as corrections to the action of each periodic trajectory of the system.

In classifying all trajectories for complicated dynamic systems (not just those equivalent to a finite shift), one discovers a phenomenon similar to phase transitions. Singularities develop in the computation of physically relevant averages.

Publications

Bauer, O., and R. Mainieri, "The Convergence of Chaotic Integrals" (submitted to *Chaos*).

Mainieri, R., "Cycle Expansion Solution to the Fisher Droplet Model" (submitted to *Chaos*).

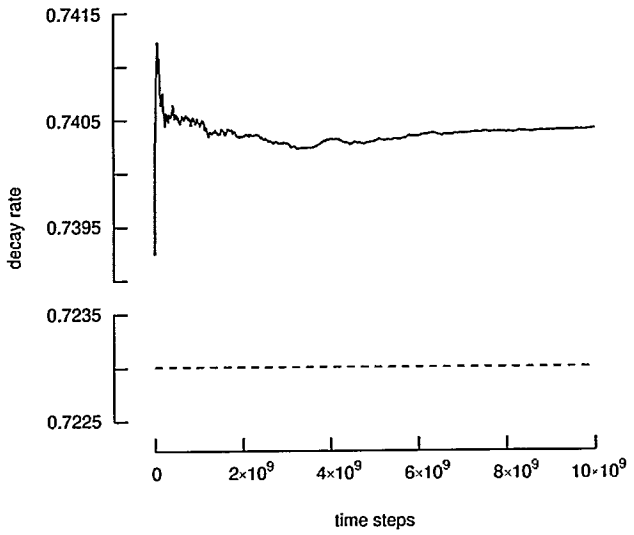
Mainieri, R., "Cycle Expansions with Pruned Orbits Have Branch Points," *Physica D* **83,** 206 (1995).

Mainieri, R., "Fourier Transforms for Periodic Orbits" (submitted to *Phys. Lett. A).*

Mainieri, R., "Geometrization of Spin Systems Using Chaotic Cycle Expansions" (submitted to *Phys. Rev. Lett.*).

Mainieri, R., and R. Ecke, "Phase Shift in Experimental Trajectory Scaling Functions," *Phys. Lett. A* **176,** 3580 (1993).

Mineev, M., and R. Mainieri, "Observation of Conservation Laws in Diffusion Limited Aggregation," *Phys. Rev. Lett.* **72,** 880 (1994).



Monte Carlo simulation (solid line) compared to a cycle expansion (dashed line) of the rate of escape in chaotic scattering. The Monte Carlo has yet to converge to the correct value of 0.7230, as the cycle expansion has.

Applied Mathematics of Chaotic Systems

Erica Jen

The objectives of this project were to develop new mathematical techniques to describe chaotic systems in order to express those systems in forms that can be solved analytically and computationally. The focus of our work has been on (1) global bifurcation analysis of finite-dimensional Hamiltonian systems and (2) an analytical technique for the exact solution of nonlinear cellular automata.

Global Bifurcation Theory of Low-Dimensional Systems

We have analyzed the hyperbolic structures for the dynamics of a class of triaxial ellipsoidal bodies which we call Kirchhoff and C. Neumann tops. Using multidimensional-Melnikov-function analysis and global-bifurcation analysis, we have identified the bifurcation parameters and sets of initial conditions that lead to qualitative descriptions of particular chaotic dynamics situations.

There are two additional main results of our study. First, by examining the transverse intersections of stable and unstable manifolds from a global point of view, we have shown that, remarkably, not all of the intersections are responsible for nonintegrability by generating chaotic motion. Second, this global point of view has provided an explicit example (and closed-form solutions) for geometric singular-perturbation theory.

The study of trajectories for the C. Neumann top has led to an interesting connection with completely integrable partial differential equations (PDEs). Specifically, orbits of the C. Neumann top correspond to new soliton-like objects which are solutions of a newly discovered integrable equation in the Dym hierarchy. Physically, the new equation is a simple model for the motion of fronts in nematic crystals. The soliton-like solutions can be viewed as geodesic motion on certain surfaces which are isomorphic to quadrics. For the case where the quadric surface is an ellipsoid, geodesic orbits can be mapped into orbits of the C. Neumann top. We are currently studying whether we can obtain new solutions of the PDEs in this class using the orbits we have examined for the C. Neumann case and if we can ascertain whether the perturbed C. Neumann orbits correspond to solutions of (perturbed versions of) the integrable PDE.

The need to analyze orbits in the neighborhood of a saddle-center fixed point in the C. Neumann problem has led us to introduce a new technique to find homoclinic orbits which experience many excursions before settling down to a fixed point or periodic orbit. This technique, which extends the celebrated Melnikov method for single-pulse orbits, contains as special cases all the previous methods for detecting multipulse orbits in Hamiltonian systems with one hyperbolic degree of freedom. Techniques of this type are becoming more and more important in studies of chaotic motion in near-integrable PDEs.

Exact Solution of Cellular Automata

Under the evolution of certain nonlinear automata, typically termed "chaotic," we have found that the lattice of processors which make up an automaton typically "organizes" itself into multiple contiguous domains within which behavior is ordered and highly correlated. The domains are separated by domain walls which may be interpreted physically as dislocations or, equivalently, as propagators of information.

The analysis of domain structure and dislocation behavior has led us to develop a solution method for a wide class of nonlinear automata. The method maps the nonlinear data onto an exactly solvable linear "template" automaton with a closely related evolution function.

A critical component of the mapping between nonlinear and linear systems is to characterize the behavior of the dislocation processors. For the prototypical cellular-automaton Rule 18 studied in the first stage of this project, we showed that the dislocations are analogous to classical, annihilating diffusive particles. The propagation of these particles leads to quasi-periodicity in these discrete dynamical systems.

Using the solution method developed for cellular-automaton Rule 18, we have obtained results for the expected number of dislocations in an arbitrary finite lattice, the expected transience time for dislocations to collide and annihilate, and maximum bounds on transience time for this cellular automaton. The results represent one of the very few analytical characterizations of nonequilibrium behavior for nonlinear, spatially extended dynamical systems.

In addition, we have developed a technique to characterize the "grammar" that generates the set of spatial sequences that appear in domain structures stable under evolution of Rule 54. We have also shown that all sequences recognized by this grammar are attracted to limit cycles of identical period. A corollary of the result provides a proof of the fact that

the rule acts upon a certain well-defined subset of spatial sequences to induce a spatial reflection of those sequences. The result represents the first demonstration of a global reflection operator induced by a local interaction rule.

Publications

Alber, M., R. Camassa, D. Holm, et al., "The Geometry of Peaked Solitons and Billiard Solutions of a Class of Integrable PDEs," *Lett. Math. Phys.* **32**, 137 (1994).

Camassa, R., "On the Geometry of an Atmospheric Slow Manifold," *Physica D* **84**, 357 (1995).

Camassa, R., M. Alber, D. Holm, et al., "On the Link Between Umbilic Geodesics and Soliton Solutions of Nonlinear PDE's," *Proc. R. Soc. London, Ser. A* **450**, 677 (1995).

Camassa, R., G. Kovacic, and S.-K. Tin, "A Melnikov Method for Homoclinic Orbits with Many Pulses" (submitted to *Arch. Rat. Mech. Anal.*).

Jen, E., and J.P. Crutchfield, "Particles and Backgrounds in Cellular Automata" (submitted to *Commun. Math. Phys.*).

Modeling Mesoscopic Phenomena in Extended Dynamical Systems

Alan Bishop

In this project, we develop appropriate analytical and numerical techniques to describe the formation and dynamics of collective, coherent structures in extended dynamical systems and their role in macroscopic space-time complexity. The influence of nonlinearity, classical and quantum stochasticity, and lattice discreteness is taken into account and is analyzed and classified.

We have completed a collective coordinate analysis of phase-locking and discrete nonlinear resonances, rf-driven and damped Josephson transmission lines, and nonlinear Schroedinger equations. We have also developed extensions of collective, coordinate mode reductions for vortex dynamics in two-dimensional Landau-Liftshitz spin systems to accurately include effects of image potentials. We have developed an efficient algorithm to simulate long-range interactions arising in many physical circumstances. We have demonstrated the phenomena of Boch oscillations and dynamic localization in discrete nonlinear Schroedinger equations. Additionally, we have established validity regimes for adiabatic and antiadiabatic slaving in quantum self-focusing models. In all of this work, we aim to test predictions of reduced nonlinear models against large-scale (including massively parallel) simulations and then extend predictions of reduced models to macroscopic scales of structure and dynamics.

Publications

Blackburn, J.A., and N. Gronbech-Jensen, "Phase Diffusion in a Chaotic Pendulum" (submitted to *Phys. Rev. E*).

Cai, D., A.R. Bishop, and N. Gronbech-Jensen, "Discrete Lattice Effects on Breathers in a Spatially Linear Potential" (to be published in *Phys. Rev. E*).

Cai, D., A.R. Bishop, and N. Gronbech-Jensen, "Perturbation Theories for Perturbed Ablowitz-Ladik Nonlinear Schrodinger Systems" (to be published in *Phys. Rev. B*).

Cai, D., A.R. Bishop, and N. Gronbech-Jensen, "Spatially Localized, Temporally Quasi-Periodic, Discrete Nonlinear Excitations" (to be published in *Phys. Rev. E*).

Cirillo, M., G. Rotoli, A.R. Bishop, et al., "High-Frequency Pumping of Josephson Soliton Oscillators," *Phys Rev. B* **52**, 506 (1995).

Dandoloff, R., et al., "Violation of Self-Duality for Topological Solitons Due to Soliton-Soliton Interaction on a Cylindrical Geometry," *Phys. Rev. Lett.* **74**, 813 (1995).

Gronbech-Jensen, N., P.S. Lomdahl, and M. Cirillo, "Uniform Coupling of Microwaves to Nonlinear Resonant Modes in Josephson Junctions," *Phys. Rev. B* **51**, 11690 (1995).

Kenkre, V., et al., "Memory-Function Approach to Interacting Quasiparticle-Boson Systems" (to be published in *Phys. Rev. B*).

Raghavan, S., V. Kenkre, and A.R. Bishop, "Phase-Nonlinearity Interplay in Small Quantum Systems" (to be printed in *Phys. Rev. B*).

Salkola, M., et al., "Coupled Quasiparticle-Boson Systems: The Semiclassical Approximation and the Discrete Nonlinear Schroedinger Equatio," *Phys. Rev. B*, **52**, R3824 (1995).

Villain-Guillot, S., et al., "Topological Solitons and Geometrical Frustration" (to be printed in *Phys. Rev. A*).

Studies of Structure of Turbulence by High-Resolution Simulation and Theory

Shiyi Chen

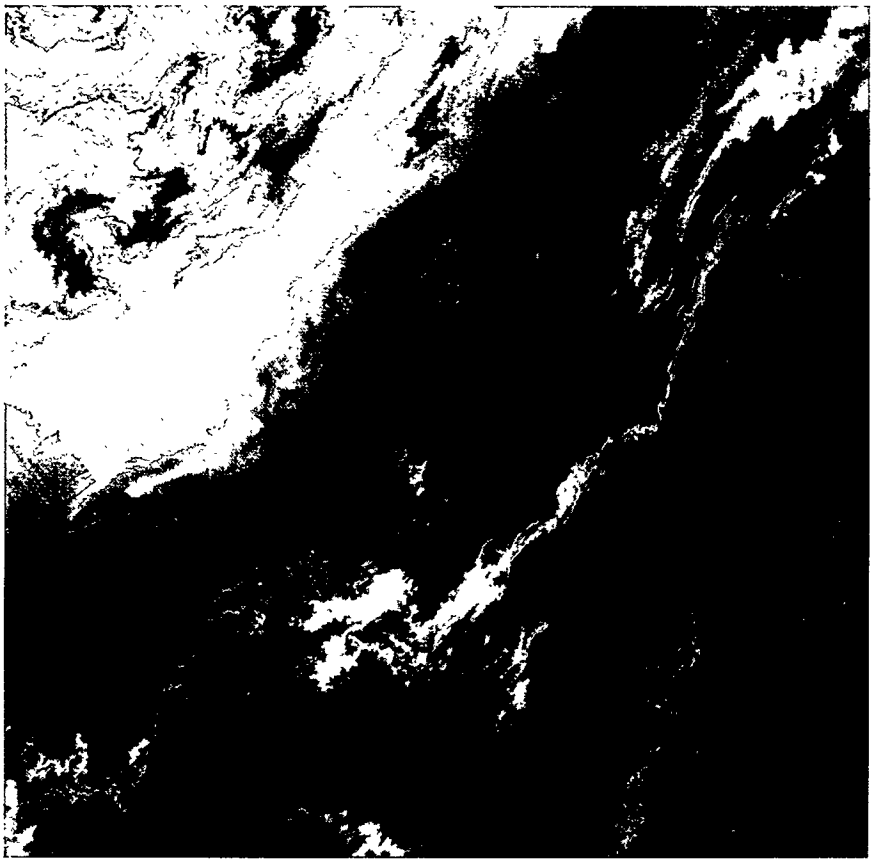
This project consists of two interlocking parts. First, we use high-resolution computer simulations to study turbulence structures with particular emphasis on large-scale coherence and intermittency phenomena. An important part of this work is the development of powerful interactive visualization techniques to exhibit the topology, geometry, and life history of the flow structures. Second, we carry out theoretical research using newly developed methods that are nonperturbative. These contrast the perturbative (low order closure) techniques that have dominated turbulence theory in the past. Particular objectives of the theoretical work are the elucidation of the relative roles of local-strain and long-range-pressure forces on flow probability distribution functions and prediction of the statistics of nonlinear chemical reactions that take place in the presence of turbulent convection and molecular diffusion.

In this year, we have made significant advances in the study of fundamental fluid turbulence through numerical and theoretical work. For the first time, we analytically predicted the anomalous scaling exponents for a passive scalar (temperature field or particle transport) advected by fluid turbulence. The predicted exponents agreed with results from large-scale simulation (8192×8192 grid points). This research has attracted great attention from the whole turbulence community.

We predicted a saturation of scaling exponents of velocity structure functions. We observed the scaling exponents to approach a fixed limit as the Reynolds number becomes very large. The results are supported by the latest experimental work in France using He^{+4} at very-high Reynolds numbers.

We developed a hyperviscosity concept for doing direct numerical simulation in fluid turbulence. The numerical scheme is used for studying the measurement of anomalous scaling of fluid turbulence and suspension dynamics in fluid turbulence occurring in the chemical-production process.

For the first time, we successfully confirmed the theoretical predictions of a long-standing theory by completing a two-dimensional 16384×16384 mesh turbulence simulation. The results confirm the 25-year-old theory of Kraichnan that in two-dimensional fluid turbulence, such as occurs in atmospheric turbulence, the entropy flux is constant. Also, the measurement of scaling exponent in the Fourier space shows a logarithmic correction, in agreement with the theory.



Two-dimensional temperature distribution advected by fluid turbulence. The simulation has been carried out using 8192×8192 mesh resolution on the CM-5 at the Advanced Computing Laboratory at Los Alamos National Laboratory. The plot shown here is only 1024×1024, which is $1/64^{th}$ of the whole simulation. The lighter areas indicate high temperature; the darker areas indicate low temperature.

Publications

Chen, S. and N. Cao, "A Note on Inertial Range Scaling in Turbulence" (submitted to *Phys. Rev. E*).

Cao, N., S. Chen, G.D. Doolen, et al., "Statistics and Structures of Pressure in Isotropic Turbulence" (submitted to *Phys. Fluids*).

Cao, N., S. Chen, and Z. She, "Scalings and Relative-Scalings in the Navier-Stokes Turbulence" (submitted to *Phys. Rev. Lett.*).

Kraichnan, R.H., V. Yakhot, and S. Chen, "Scaling Relations for a Randomly Advected Passive Scalar Field," *Phys. Rev. Lett.* **75**, 240 (1995).

Martinez, D.O., S. Chen, and G.D. Doolen, "Energy Spectrum in the Dissipation Range of Fluid Turbulence" (submitted to *Phys. Fluids*).

Industrial Processing of Complex Fluids: Formulation, Modeling, and Algorithms

James Scovel

The production of many important commercial materials involves the evolution of a complex fluid through a cooling phase into a hardened product. Textile fibers, high-strength fibers such as KEVLAR and VECTRAN, plastics, chopped-fiber compounds, and fiber optical cable are but a few examples of such materials.

Industry contacts for each of these materials are keenly aware of the physics and chemistry that dominate their manufacturing processes and desire to replace experiments with on-line, real-time models of these processes. The lead scientists are equally aware of a humbling fact: solutions to their problems are not only a matter of technology transfer but also require a fundamental description and simulation of their processes that lies just beyond the current state of science.

The goals of our project are to develop models that can be used to optimize macroscopic properties of the solid product, to identify sources of undesirable defects, and to seek boundary-temperature, flow, and material controls to optimize desired properties.

We have searched for and found a finite-element fluid code called FIDAP that can handle phase changes and non-Newtonian fluids. We have successfully implemented this code in simple two-dimensional geometry for a quasi-steady-state solidification problem. We have been, as yet, unsuccessful in applications to fully transient effects because of our current inability to accurately track the solidification front. We have begun deriving equations coupling the orientation effects based on Ericksen's liquid-crystal models. These equations can be reduced to standard simplifications and at the same time give qualitative theoretical characterizations of observed physical phenomena.

Presently, we seek a multiscale representation based upon Kalman filter methodology. We have begun by ignoring orientation effects and concentrating on the simple fluid. This technique involves representation of the fluid on separate scales; we will begin with medium and fine scales. The equations of motion of the fine scale are understood but the system is too large and nonlinear to simulate effectively. Therefore we couple the medium and fine scales through the aggregation that relates them. If we could simulate the medium-scale representation by itself, and if the equations for the fine scale were linear, we could use the Kalman filter to disaggregrate and thus obtain the fine-scale variable evolution. We have developed an algorithm to this effect based on the expectation-maximization technique of Dempster and are in the process of testing. However, in the case where the equations of motion for the fine scale are nonlinear, we are investigating whether we can efficiently simulate the Kalman filter solution for the evolution of the fine scale as we simulate the medium-scale phenomena. In the real problem, we will couple the medium-scale solution to the fine scale both ways and we will have to use a fully coupled simulation representation of a solution to the Kalman filter representation.

Wavelet Theory and Its Applications

Vance Faber

The theory of wavelet transforms is a recent development that draws from a number of different fields, including harmonic analysis, digital signal processing, approximation theory, and numerical analysis. A discrete-time version exists for sampled data, and it is known as the discrete wavelet transform (DWT).

By studying the related issues of computational complexity and filter bank design, we have developed two factorization theories for filter banks, reduced the computational complexity of the software, and provided a new framework for future filter designs. We are also making progress in classifying multichannel, multirate filter banks. In related research supported by this project, we have obtained new theoretical results that characterize rational transfer matrices with polynomial finite-impulse-response (FIR) inverses. These results are very general theorems about abstract multi-input/multi-output linear systems, and they both generalize and simplify results known previously only for polynomial transfer matrices.

We have studied multichannel FIR filter banks with filters satisfying various symmetry conditions. This work has led to a complete classification of all multichannel FIR filter banks. We have characterized the fundamental building blocks that can be used to construct filter banks. These building blocks are essential for efficiently exploring filter design space in order to construct filter banks that are optimized for certain physical properties. We have also developed computer software to decompose filter banks with symmetries into their fundamental building blocks; such work can be used in designing efficient chips and in accelerating software.

Currently, we are helping the FBI develop a nationwide standard for DWT-based compression of digitized fingerprint images as the FBI converts its fingerprint database into a digital format. The standard incorporates theoretical results obtained from our work on this project. By using object-oriented software developed at Los Alamos, we are providing data compression and analysis capabilities for the Laboratory's High-Performance Data System.

We have also applied our theoretical work to image transmission for projects that use the national information infrastructure to exchange large data sets.

Publications

Bradley, J., and C. Brislawn, "Vector Quantization of Discrete Wavelet Transform Coefficients," *CNLS Newsletter* 84, 1 (1992).

Brislawn, C., "Classification of Nonexpansive Symmetric Extension Transforms for Multirate Filter Banks" (submitted to *Appl. Comput. Harmonic Anal.*).

Brislawn, C., "Preservation of Subband Symmetry in Multirate Signal Coding" (to be published in *IEEE Trans. Signal Processing*).

Solution-Adaptive Methods for Low-Speed Flows and All-Speed Flows

Jeffrey Saltzman

We are developing "solution-adaptive" methods for efficiently computing fluid problems that involve low-speed flows or a mixture of low- and high-speed flows. A solution-adaptive method uses different algorithms in different parts of the domain. In regions where the flow is slightly compressible (low-speed), we use a scheme that is based on efficient and accurate methods recently developed for incompressible flows. In regions of the domain where the flow is compressible, we will switch to a high-quality shock-capturing method. If there are regions where only sound waves are present, we will use a method that is optimized for the wave equation of acoustics.

We have developed an "all-speed" flow solver that is based on the Godunov-Projection algorithm method for incompressible flows. Versions of this solver have been written for both rectangular and overlapping grids, enabling us to simulate problems in complex geometries. Significant supporting work has been done on the C++ object-oriented environment for writing partial differential equation solvers. Classes for grids and grid-functions have been devised and implemented. Operator classes that implement differentiation, interpolation, projections, and boundary conditions are being worked on. This work will allow us to implement sophisticated solution-adaptive methods on complicated geometries using adaptive and moving grids. Using these grids, we are developing a Navier-Stokes solver class that can solve both compressible and incompressible equations on overlapping grids.

Parallel Three-Dimensional Spherical-Harmonics Transport Methods

Jim Morel

Solution of the Boltzmann transport equation is essential in modelling a wide variety of physical phenomena. Monte Carlo methods can suffer from persistent statistical errors, while deterministic discrete-ordinates, or S_n methods, can produce nonphysical solutions, commonly known as ray effects, that result from a lack of rotational invariance. Spherical-harmonics, or P_n methods, are the only deterministic methods that preserve the rotational invariance of the analytic transport operator. Such invariance is critically important in a wide variety of applications. Unfortunately, production computer codes for solving the multidimensional P_n equations do not currently exist.

Our project will provide the theoretical and algorithmic bases to fill this technology need. Specifically, our project will proceed in three phases. In the first phase, we will develop a massively parallel algorithm for solving the three-dimensional (3-D), neutral-particle P_n equations on unstructured tetrahedral meshes using standard node-based, spatial finite-element discretization schemes in conjunction with a parallel conjugate-gradient solution technique. In the second phase, we will extend our first algorithm to use hybrid finite-element meshes composed of hexahedra, wedges, and tetrahedra. In the third phase, we will solve the P_n equations in the primal first-order form in order to model problems with void regions. Standard second-order formulations of the P_n equations become singular as the total material cross section approaches zero. The coefficient matrices associated with our third scheme will be asymmetric and thus cannot be solved with conjugate-gradient techniques. We will solve these equations using parallel implementations of Krylov-space schemes such as the biconjugate-gradient-squared and quasi-minimum-residual methods.

During the past year we developed a parallel solution algorithm and associated code on the Connection Machine 5 to solve the 3-D, even-parity P_n equations using node-based, finite-element spatial discretizations on unstructured hybrid meshes composed of hexahedra, wedges, and tetrahedra. This algorithm has proven to be accurate, efficient, and highly parallel. We also developed a novel self-adjoint formulation of the transport equation that offers many advantages relative to the classical even- and odd-parity formulations.

Geometry in the Large and Hyperbolic Chaos

Brosl Hasslacher

In the study of strongly chaotic systems, global geometrical information from the original dynamical system gets entangled in an unknown way throughout the usual one-dimensional shift map projection. Calculating observables by using orbit expansions is blocked by the lack of a workable orbit classification for strongly chaotic systems. Our research uses geometrical methods from modern mathematics and recent connections between global geometry and quantum field theory (QFT) to study hyperbolic manifolds, which are the natural geometrical objects belonging to hard chaos.

Working with mathematicians from other research institutes, we first tried to dimensionally lift strong chaotic systems by exploiting their connection to knot theory; the complement of a knot is a hyperbolic space. This work led to the study of the monodromy groups of representations for knot polynomials in a multipunctured plane. There was an insurmountable problem in passing to the infinitely punctured case: a functional equation—the so-called pruning front equation—exists that is encoding all information on missing orbits. We could not find this equation explicitly from a direct lift approach.

Our goal is to now descend upon the problem from the infinite degree of freedom case, using flavors of topological QFTs whose classical limit are strongly chaotic systems. Because our initial approach will be a metric-free one, we will deal with chaotic geometries described by such QFTs. These QFTs appear to be exactly integrable in the sense of Duestermat-Heckman functional integrals over equivariant cohomologies. We will study such models and expect to find, in a cleaner form, the functional relation for the pruning front system appearing in the topological QFT.

Mimetic Difference Approximations of Partial Differential Equations

James Hyman

When computing numerical solutions to partial differential equations (PDEs), difference operators that mimic the crucial properties of the differential operators are usually more accurate than those that do not. Properties such as symmetry, conservation, stability, and the identities between the gradient, curl, and divergence operators are all important. The goal of this research is to derive local, accurate, and efficient difference methods that mimic these properties on nonuniform grids. We will target methods for the numerical solution of complicated systems of nonlinear PDEs arising in fluid dynamics, combustion, and nonlinear optics. Our primary goal is to strengthen and expand the capabilities of our large-scale simulations by developing better algorithms, analysis tools, and software techniques.

This past year, we developed a new class of mimetic difference approximations for both space and time operators that arise in solving PDEs. The spatial operators were derived using theoretical and numerical research based on finite volume methods. We also used the homogenization theory to derive better difference approximations for equations where the subgrid scale effects must be included to accurately approximate the solution.

We constructed local fourth-order finite-difference approximations of first and second derivatives on nonuniform grids in one dimension. The approximations satisfy the symmetry relationships that come from the analogous higher-dimensional fundamental operators: the divergence, the gradient, and the Laplacian. For example, we require that the discrete divergence and gradient be negative adjoints of each other, DIV* = - GRAD, and the discrete Laplacian is defined as LAP = DIV · GRAD. The adjointness requirement on the divergence and gradient guarantees that the Laplacian is a symmetric negative operator. The discrete approximations we derive are fourth-order on smooth grids, but the approach can be extended to create approximations of arbitrarily high order. We also analyzed the loss of accuracy in the approximations when the grid is not smooth and verified the analysis through numerical examples demonstrating the effectiveness of the higher order methods on nonuniform grids.

Publications

Shashkov, M., and S. Steinberg, "Support-Operator Finite-Difference Algorithms for General Elliptic Problems," *J. Comput. Phys.* **118**, 131 (1995).

Data Embedding Research

Maxwell Sandford

Data embedding is a method for combining digital data streams. The stochastic noise component of a host data set is used as a carrier for a separate bit-stream. Embedding data into a host, or carrier, data set does not increase the size of the host.

Data embedding works by replacing the stochastic, or random, noise present in the original host data set with pseudorandom, or generated, noise that carries separate information. Thus, embedded data are part of the host and is carried along with the host data during digital transmissions. The presence of embedded information is believed to be undetectable if the original data set is not available for comparison. Moreover, the embedded data are secure from unauthorized extraction.

The embedding method works for any data generated by a measurement process because noise is always present in data created by digital sampling. Examples are medical data (EEGs, EKGs, and MRI images), forensic data (photographs and fingerprints), maps and aerial photography, and digital images created by film or video cameras.

The purpose of this project is to demonstrate proof-of-principle of the data embedding method in several applications and to determine the vulnerability of the method. In addition to national security applications, such as nonproliferation data collection, the new technique has considerable commercial potential for applications including high-definition television and most data communication systems.

We have written software for the IBM-ThinkPad laptop computer that demonstrates data embedding with facsimile data and have transmitted facsimile information containing embedded data through AT&T long-distance lines

within the continental U.S. In addition, we began analyzing the security of the data embedding process. Security of the embedded data is reduced by features we intentionally included in the demonstration program. However, we have still not found a simple, automated method for extracting embedded information without knowledge of the key pairs.

Finally, we have adapted data embedding to the formalism of transform, "lossy" compression methods by exploiting the uncertainty in the integer representation of the transform coefficients. Compression embedding is being used to authenticate the digital images transmitted from cameras used for on-site inspection of nuclear materials.

Dispersive Water Waves in One and Two Dimensions

Darryl D. Holm

With applications in mind for geophysical ocean dynamics, we are using multiple-time-scale perturbation theory to derive new equations in one and two dimensions for the long-time asymptotic behavior of dispersive shallow water flow in a thin domain over a varying bottom. The method we use guarantees that the resulting equations are Hamiltonian and preserves the symmetry of the Hamiltonian equations under particle-relabeling transformations. The Hamiltonian property and the infinity of conservation laws associated with this symmetry play a crucial role in solving these equations.

In one dimension, these equations are unique among their family in being bi-Hamiltonian and completely integrable by a linear isospectral transform method. In two dimensions, our new shallow water equations will allow us to derive analytical estimates of the long-time asymptotic effects of bottom topography and hydrostatic pressure imbalance on the vertically averaged horizontal velocity. This is of fundamental importance for addressing the issue of predictability in geophysical ocean dynamics.

We derived new dispersive shallow water equations in one and two dimensions by using multiple-time-scale asymptotic expansions on Euler's equations. We have studied the solutions to these equations in one dimension analytically and numerically to assess the remarkable phenomena they describe. These phenomena include development of weak solutions with shock formation in finite time, followed by emission of solitary waves with discontinuous velocity derivatives at their peaks; the waves then interact as solitons. The work performed in this project has applications to applied mathematics and to dynamical system and pattern formation theory.

Publications

Alber, M., R. Camassa, D. Holm, et al., "On the Link Between Umbilic Geodesics and Soliton Solutions of Nonlinear PDE's," *Proc. R. Soc. London* **450**, 677 (1995).

Alber, M., R. Camassa, D. Holm, et al., "The Geometry of Peaked Solitons and Billiard Solutions of a Class of Integrable PDE's," *Lett. Math. Phys.* **32**, 137 (1994).

Camassa, R., D. Holm, and M. Hyman, "A New Integrable Shallow Water Equation," *Adv. App. Mech.* **31**, 33 (1994).

Camassa, R., D.D. Holm, and C.D. Levermore, "Long-Time Dispersive Equations for Shallow Water with a Varying Bottom" (submitted to *Physica D*).

Developing the R&D 100 Award–Winning Lattice Boltzmann Permeameter Toward a Marketable Product

Wendy Soll

Computational models of oil, gas, and water flow through porous reservoir rock are used in reservoir management to decide whether or not, and how, to develop and produce hydrocarbon reserves. Because these flow models have major impact on these decisions, their accuracy, cost, and speed are important. Groundwater remediation and site assessment are described by the same set of equations as oil and gas production and are subject to the same challenges in understanding the system. The accuracy of field-scale flow models is strongly dependent on the accuracy of the physical characterization of the reservoir rock's pore-fluid system. In the past year, we completed precision studies, through the use of three-dimensional tomographic data of oil-bearing rocks, on the dependence of pore-scale flow on several parameters , and we expanded the functionality of the model to increase accessibility to a wider range of users.

We benchmarked the permeameter software, which won an R&D 100 Award in 1995, by testing the code on a large variety of multiphase flow problems. We held semi-weekly meetings to promote interactions between code users and code developers. We identified and corrected all known problems, most of which pertained to using the code in regions of parameter space for which it was not originally intended. The software was improved to provide higher order accuracy than originally provided. In addition, we automated volume averaging of quantities, improved the speed and efficiency of the lattice Boltzmann permeameter, and initiated work on improving the visualization and user interfaces for the permeameter. We received 37 inquiries into the relevance of the lattice Boltzmann permeameter; most of them were from oil companies and companies interested in modeling porous media flows.

Publications

He, X., and Q. Zuo, "Analysis and Boundary Condition of the Lattice Boltzmann BGK Model with Two Velocity Components" (submitted to *Phys. Rev. E*).

Hou, S., Q. Zou, S. Chen, et al., "Simulation of Cavity Flow by the Lattice Boltzmann Method," *J. Comput. Phys.* **118** (2), 329 (1995).

Shan, X., and H. Chen, "Simulation of Nonideal Gases and Liquid-Gas Phase Transitions by the Lattice Boltzmann Equation," *Phys. Rev. E* **49** (4), 2941 (1994).

Zou, Q., S. Hou, S. Chen, et al., "An Improved Incompressible Lattice Boltzmann Model for Steady Flow," *J. Stat. Phys* **81** (1/2), 35 (1995).

Combinatorics, Geometry, and Mathematical Physics

William Chen

Combinatorics and geometry are among the most active areas of mathematics. These areas of mathematics will continue to be important for the next several decades because of the power they bring both in new techniques and the linkages that have emerged between them and several established fields. In the work done in our project, we extend this linkage to an area of mathematical physics dealing with symmetry and the quantum description of many-particle systems. As a result, we have identified a specific area of applied mathematics with applications to physics, chemistry, and perhaps biology.

During the first year of our project, we have advanced our goal of bringing combinatorics to bear on physical problems by the publication of four papers dealing respectively with

- a general treatment of the companion matrix using combinatorial methods that unifies several families of mathematical functions arising in physical theory,
- a formulation of the generating functions for 3n-j coefficients (physical quantities) as functions defined on cubic graphs (combinatorial objects),
- the discovery of the relationship of group representations (physical theory) to the famous MacMahon's Master Theorem (combinatorics), and
- the discovery of a generalization of the Lagrange interpolation formula to symmetric functions (combinatorics) with attendant important applications to the unitary functions of physics.

Each of these results opens further avenues of exploration in our goal of establishing connections between combinatorics, geometry, and physics.

Publications

Chen, W.Y.C., and J.D. Louck, "The Combinatorial Power of the Companion Matrix" (to be published in *Linear Algebra Appl.*).

Chen, W.Y.C., and J.D. Louck, "Symmetric Function Generalization of Lagrange Interpolation" (to be published in *Adv. Math.*).

Chen, W.Y.C., L.C. Biedenharn, M.A. Lohe, et al., *Role of SU(2) 3n-j Coefficients in SU(3), in Symmetry and Structural Properties of Condensed Matter*, T. Lulek, W. Florek, and S. Watcerz, Eds. (World Scientific Publishing, Singapore, 1995), p. 150.

Chen, W.Y.C., K.W. Lih, and Y.N. Yeh, "Cyclical Tableaux and Symmetric Functions," *Stud. Appl. Math.* 94, 327 (1995).

Louck, J.D., "MacMahon's Master Theorem, Double Tableau Polynomials, and Representations" (to be published in *Adv. Math.*).

Wavelet Transforms as Solutions of Partial Differential Equations

George Zweig

A significant recent development in applied mathematics is the study of continuous and discrete wavelet transforms. Like Fourier transforms, wavelet transforms express functions in terms of simple building blocks; in particular, wavelet transforms decompose functions into components with respect to a set of expansion functions that are dilations and translations of a single function called the "parent wavelet." Of greatest interest are parent wavelets confined in both time and frequency. Such wavelet transforms are useful in representing "transients" whose time and frequency structure reflect the dynamics of an underlying physical system. Speech sound, pressure in turbulent fluid flow, or engine sound in automobiles are excellent candidates for wavelet analysis.

Two outstanding problems relating to wavelet transforms are the primary focus of this project:

- choosing the parent wavelet for a continuous wavelet transform in pattern-recognition applications and
- speeding up the computation of continuous wavelet transforms by understanding the relationship between discrete wavelet transforms and discretized, continuous wavelet transforms.

We demonstrated that certain continuous wavelet transforms can be computed most efficiently by interpreting them as solutions to generalized wave equations and computing the solutions to those equations numerically. The continuous wavelet transform that emulates the hydromechanical processing of sound by the inner ear is an example of such a transform. We have started to develop numerical algorithms of wavelet transforms to solve the generalized wave equation. These algorithms are based on the "nonstandard form" of the derivative operator.

Publications

Zweig, G., and C. Shera, "The Origin of Periodicity in the Spectrum of Evoked Otoacoustic Emissions," *J. Acoust. Soc. Am.* 98, 2018-2047 (1995).

The Fundamental Role of Solitons in Nonlinear Partial Differential Equations

James Hyman

Numerical simulations and mathematical analysis have proved crucial to understanding the fundamental role of solitons in the evolution of general initial data for quasilinear dispersive partial differential equations (PDEs), such as the Korteweg-de Vries, nonlinear Schrödinger, and the Kadomtsev-Petviashvili equations. These equations have linear dispersion and the solitons have infinite support. Recently, we discovered a new class of solitons with compact support for similar equations with nonlinear dispersion. These "compactons" display the same modal decompositions and structural stability observed in earlier integrable PDEs. They form from arbitrary initial data, are nonlinearly self stabilizing, and maintain their coherence after multiple collisions, even though the equations are not integrable. This research is the opening for a far-reaching and new understanding of the central role of solitons in nonlinear dispersion.

We have made the remarkable discovery that a similar nonlinear dispersive equation can be described by the evolution of solitons with a peaked solution. We analyzed the initial value problem and soliton solutions for our newly discovered, completely integrable, dispersive shallow-water equation. This equation is biHamiltonian, so it possesses an infinite number of conservation laws in involution. Also, it may be recast into a compatibility condition for a linear isospectral problem, so its initial value problem may be solved by the inverse-scattering-transform method. The equation is derived by using a small-amplitude asymptotic expansion directly in the Hamiltonian for the vertically-averaged Euler's equations for an incompressible fluid with a free surface, after substituting a solution Ansatz of columnar fluid motion and restricting to a unidirectional invariant manifold. Numerical studies with this equation demonstrate that a typical localized initial condition breaks up into a train of solitons. Each of these solitons vanishes at infinity and has a limiting form that has a discontinuity in the first derivative at its peak. We also analyzed the elastic collision properties of the N-soliton solution.

Publications

Camassa, R., D. Holm, J. Hyman, "A New Integrable Shallow Water Equation," *Adv. Appl. Mech.* **30**, 1 (1994).

Atomic and Molecular Physics

Multiphoton Processes for Atoms in Intense Electromagnetic Fields

Lee A. Collins

With the advent of new laser technology capable of producing tightly focused, short-duration (ps to fs) pulses, electromagnetic fields on the order of 10^{14} to 10^{21} W/cm^2 can be generated. At these intensities, the laser and atomic fields become comparable in strength, and we enter a new realm of atomic physics. Since standard perturbative treatments for multiphoton processes may no longer be practical because of the large number of terms required, we must develop new techniques to probe this high-intensity regime. Unique features of this new realm include phenomena such as large-scale multiple ionizations and above-threshold ionization (ATI) in which series of peaks separated by the photon energy are observed in the electron energy distribution.

As electromagnetic field intensities are increased, we expect that features such as relativistic effects may become important. In addition, as the pulse lengths become shorter (a few fs) and approach the order of a few cycles of the electromagnetic field, we anticipate that transient effects will play a major role in the interpretation of the observations. For this case, standard steady-state models will eventually fail, and we shall have to develop fully time-dependent formulations to probe this regime. All of these processes may have additional applications to laser technologies and plasma modeling, particularly in the development of ultrafast x-ray sources through the use of short-pulse (subpicosecond) laser-produced plasmas.

Our objective is to perform a theoretical study of the interaction of matter with intense electromagnetic radiation in which the energy in the field is comparable to that of the bound atomic electrons. Our principal endeavor centers on a basic understanding of multiphoton ionization of atoms by direct and indirect radiation from the new lasers, which use short pulses to produce very intense fields in confined areas.

This scientific area is quite young, and therefore the full ramifications are still unclear. However, such intense matter-radiation interactions are known to be important in the design of short-wavelength lasers, in material damage, and in plasma modeling. Such mechanisms as coherent control of the interaction process can be accomplished through shaping of the short pulse. In addition, we have a collaboration with other experimental teams at the Laboratory and at the University of New Mexico who plan to study multiphoton processes in H^- at the Los Alamos Neutron Science Center (LANSCE) linear accelerator.

In close support of the Los Alamos laser experiments, we have calculated two-photon excitation and ionization cross sections from atomic species, such as chlorine, in the x-ray regime. Because the x-rays will be produced from a secondary source, the intensity range, although high, will still permit a perturbative formulation. We employed standard second-order, time-dependent perturbation theory to determine the basic cross sections and transition rates. The bound-bound and bound-free matrix elements are generated using the Los Alamos atomic structure programs, CATS and GIPPER. These programs allow the matrix elements to be treated at various levels of sophistication, including Hartree-Fock and configuration interaction. The sum over bound and continuum states is performed using the Dalgarno-Lewis technique, which converts the summation to the solution of a second-order inhomogeneous differential equation.

We have demonstrated that these sophisticated calculations predict ionization rates substantially larger than simple theories based on hydrogenic scaling. The higher rates bode well for the first experimental measurement of this multiphoton event. Such experiments are currently underway using the Trident Laser at Los Alamos. These detailed calculations will also greatly assist in the analysis of the experimental data as well as suggest other systems that would merit investigation. The calculations will also greatly refine the region in which the search must be mounted for the Auger signature by which the two-photon process will be detected. The observation of multiphoton processes in the x-ray region would be a first.

The basic interaction of an atom with an intense electromagnetic field lies at the heart of any

analysis of microscopic and macroscopic processes stimulated by the irradiation of matter (whether gas, solid, or plasma) using high-intensity, short-pulse lasers. Therefore, gaining an intricate understanding of this basic process is essential to modeling more complex systems such as deposition and transport in high-energy, high-density plasmas. In addition, the intense field regime places extreme demands on theory because standard perturbative approaches no longer apply. To this end, we have solved the time-dependent Schroedinger equation, which describes the quantum mechanical interaction of an atom with an electromagnetic wave, by converting it to a time-independent prescription using Floquet theory in the Kramers-Henneberger gauge. The resulting coupled equations bear a striking similarity to those for electron-molecule scattering, and we have applied the formidable techniques developed for molecular systems to this case. The classical displacement, proportional to the electric field strength over the square of the frequency, serves an analogous role to the internuclear distance of a molecule. We have expanded the molecular linear algebraic method to encompass this wider domain of displacements.

We have employed the technique to calculate collisional parameters for electron-atom scattering in an intense field as well as multiphoton ionization rates for atoms and ions. The scattering calculations were the first using a linearly polarized field for laser-assisted electron collisions with protons. The calculations revealed capture-escape resonances resulting from trapping in the bound states of hydrogen. The field-free electron-proton collisional process exhibits no resonance structure. However, the inclusion of the laser field allows the emission of photons to drop the electron temporarily into a bound state of the compound hydrogen system. Absorbing photons from the field promotes the electron back into the continuum and gives rise to a distinct structure in the cross section. We have obtained angular distributions and partial cross sections for various multiphoton events for the scattered electrons from the rare gases (i.e., helium and neon) and compared our results with recent experiments by Wallbank and coworkers. Our results resolved several discrepancies between simpler theories and the experiments.

We have also calculated detachment rates for the negative ion of hydrogen H^- in regimes being explored by a joint University of New Mexico and Los Alamos experiment mounted at the LANSCE ground test accelerator. The importance of this system stems from its simplicity: it has only two electrons. Therefore, very sophisticated theoretical techniques can be brought to bear. In addition, the experimental results have a straightforward interpretation. We predicted that the two-photon process would yield an observable signal; this prediction was verified by the experiments. This marks the first observation of multiphoton detachment in H^-. In detachment in weak fields, only electrons with an energy equal to the difference of the photon and binding energies are observed. However, in the intense fields of the short-pulse lasers, a second set of electrons appear at an energy of one photon above the first set. This second peak in the continuum distribution from the absorption of two photons marks an important new detachment mechanism. We accomplished this demonstration by extending our analysis procedures to encompass branching ratios or partial rates. We verified that the time-dependent and time-independent formulations gave results in very good agreement.

Publications

Abdallah, J., L. Collins, G. Csanak, et al., "Two-Photon Ionization of an Inner Shell of the Cl Atom" (to be published in *Zeit. f Phys.*).

Collins, L.A., and B.I. Schneider, "Linear Algebraic Methods," in *Computational Methods for Electron Molecule Collisions*, W.M. Huo and F.A. Gianturco, Eds. (Plenum, New York, 1995), p. 45.

Collins, L., B. Schneider, D. Lynch, et al., "Electron Scattering from the Hydrogen Molecular Ion," *Phys. Rev. A* **52**, 1310 (1995).

Wallbank, B., and J.K. Holmes, "Laser-Assisted Elastic Electron-Atom Collisions," *J. Phys. B* **27**, 1221 (1994).

Final-State Effects and Correlation in Atomic Systems

Roger J. Bartlett

The one-electron model has found widespread use in many areas of physics because of its calculational simplicity. However, the model does not faithfully reproduce phenomena such as multiple ionization from electron-electron interactions. To determine the limits of the model and the strength of the electron-electron interactions, we studied phenomena that are caused by electron correlation and many-body processes. To test recent theories that incorporate the electron-electron interactions, we measured the double ionization of helium at photon energies well above its ionization threshold (K-edge) and the multiple ionization of argon and neon near their K-edges using the Los Alamos synchrotron radiation source for soft x-rays and a time-of-flight ion-state spectrometer.

Upon completion of the experimental measurements, the project focused on analysis and publication of technical papers. These focused on single-photon multiple ionization of argon and neon in their K-edge regions, the effect of Compton scattering on the double-to-single photoionization ratio in helium, and measurement of the double-to-single photoionization ratio in Compton scattering from helium for $h\nu$ = 12 keV.

Publications

Morgan, D.V., R.J. Bartlett, and M. Sagurton, "Single-Photon Multiple Ionization of Argon in the K-Edge Region," *Phys. Rev. A* **51**, 2939 (1995).

Sagurton, M., R.J. Bartlett, D.V. Morgan, et al., "The Effect of Compton Scattering on the Double to Single Photoionization Ratio in Helium," *Phys. Rev. A* **52**, 2829 (1995).

Sagurton, M., D.V. Morgan, and R.J. Bartlett, "Measurement of the Double to Single Photoionization Ratio in Compton Scattering from Helium for $h\nu$ = 12 keV" (submitted to *Phys. Rev. A*).

Determination of Interionic Potentials in Molecules

Steven Conradson

The objective of this project is to demonstrate a method of direct, experimental determination of ion-ion potentials. These potentials will be of use in the calculation of initial- and final-state overlap and the resulting paths and probabilities of state-to-state transformations in molecules and can ultimately result in the development of a rational approach to the accurate prediction of molecular reactivities and relaxation mechanisms. We have focused our efforts on

- measurement and analysis of some pure metals;
- determination of the best analytical model for potential;
- calculation of thermodynamic and vibronic parameters and comparison with known data;
- comparison of two-body with many-body potential; and
- determination of the range of validity of the temperature-independent, effective pair-potential approximation.

We have established a collaboration with Professor Frank Bridges of the University of California at Santa Cruz to perform analyses of the interatomic potentials in metals. It has long been recognized that a Morse pair-potential can be used to satisfactorily predict the macroscopic properties, such as energy of vaporization and compressibility, of simple body-centered and face-centered cubic metals. This provides a bridge between microstructure and bulk properties.

We have, however, found significant discrepancies between such Morse potentials calculated from high-temperature x-ray absorption fine structure (XAFS) data and the temperature dependence of pair-distribution functions in certain metals. There are two possible origins of this problem. The first is that the existing analytical forms for pair potentials are inadequate and that their successful application has depended on restricting their use to situations dependent on the potential depth and the slope of the potential on the small-distance side. The second is that the potential itself exhibits significant temperature dependence. We are completing an analysis of the temperature-dependent XAFS of copper, silver, and gold and performing molecular-dynamics calculations to determine the accuracy of the current analytical forms and the range of validity of the temperature-independent, effective pair-potential approximation.

Nonlinear Interactions of X-Rays with Atoms

George A. Kyrala

The interaction of radiation with matter has been of great interest since the beginning of atomic theory. Before the invention of lasers, studies concentrated on the linear interactions of radiation with matter. Since the advent of lasers, intense visible-wavelength radiation has become available, allowing the study of nonlinear interactions. Among other possibilities, these interactions have allowed the generation of harmonics of the incident radiation at much shorter frequencies. Using nonlinear interaction to generate novel sources of tunable radiation has caused an explosion in the knowledge of atomic- and molecular-physics spectroscopy and led to a number of novel techniques now used routinely in biological, forensic, and analytic applications. An extension of these techniques to the x-ray region would lead to similar tools that could be widely applied. However, a basic knowledge of the relevant efficiencies of the properties of the materials under these unusual conditions is required to build such tools. The focus of our work was to perform the first experiments on nonlinear interactions using x-rays in the kilovolt energy range.

Our objective was to measure the simplest nonlinear process, two-photon ionization of chlorine, using kiloelectronvolt x-rays generated from an aluminum target irradiated with an intense laser. Initial estimates showed that a measurable signal should be obtained using the aluminum L_α line from the Los Alamos Bright Source (LABS) laser. Theoretically, the problem is interesting because the closest intermediate states are not vacant, in contrast to hydrogenic calculations. Thus, a measurement would be one of the first tests of this new approach to two-photon ionization.

Scientific Approach

There are two ways to observe the nonlinear interaction: production of x-rays from the target ions and production of Auger electrons. Initial studies indicated a preference for observing the Auger spectrum because it has a higher detectivity and a higher sensitivity to the effect. We have since determined, however, that we have a much better chance to see the effect using x-rays than electrons mainly because we could not detect all the electrons and because there is a large hot-electron background.

The cross sections for these processes were calculated, and we used them to make a first design of the target. We also designed a target that would, theoretically, withstand the initial shock due to the preheat from the amplified spontaneous irradiation that would precede the main laser irradiation. The setup consists of a three-layer foil target placed at the focus of LABS. X-rays from the first layer of the target, the converter layer, propagate through the target and through its middle layer, which acts as a high-pass filter. The last layer then emits fluorescent x-rays or Auger electrons. Our first design used a 5-μm-thick aluminum converter, a 10-μm silicon filter, and a 1-μm sodium chloride target.

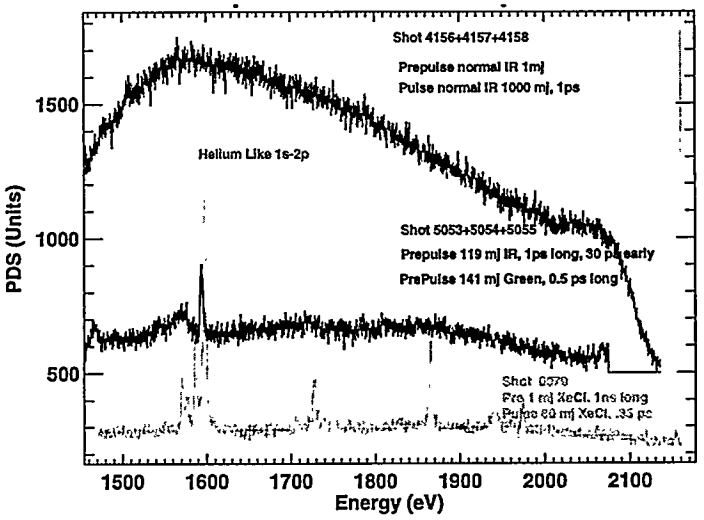
When the chlorine atoms ionize, holes in their ground state are filled, resulting in fluorescent x-rays as well as Auger electrons. An x-ray crystal spectrometer monitors the incident x-ray. The expected signals are weak fluorescent lines that sit on top of a semicontinuous background spectrum. A 256,000-element charge-coupled detector (CCD), with single x-ray-photon sensitivity, monitors the emerging x-ray flux. The output amplitude from each element depends on the x-ray photon energy and has less than 120-eV resolution. By resolving the x-ray spectra, we can distinguish between nonlinear and linear processes. Using a target with a K-edge that requires three converter photons to ionize it should give no two-photon signal but should produce a continuum background that is similar to the two-photon case. Sodium in the target acts as such a monitor.

During the first year of our work, we analyzed detection methods and started to calculate the relevant cross sections. During the second year, we started our experimental work. First, we observed the back of 10-μm-thick silicon target foils with an imaging streak camera, and we confirmed that the foil's rear surface was not damaged before the main laser pulse arrived. Second, we observed the front of the foil with an x-ray crystal spectrometer that monitored the plasma-generated x-ray flux. We found that the x-ray flux from the thin foil was much less that that from a thick target, hence the expected signals would be much less than expected. We found that one of the reasons for the low efficency was the existence of temporal structure in the laser pulse. Instead of one 270-fs pulse containing all the energy, several pulses were present, and the peak irradiance in a pulse was much lower than that necessary to perform the experiment. Because we had no alternative laser source, however, we persevered, devoting considerable effort to eliminating the multiple pulsing. Third, we used an x-ray sensitive CCD detector and calibrated it with an electron-beam x-ray source. We were able to resolve the K_α and K_β

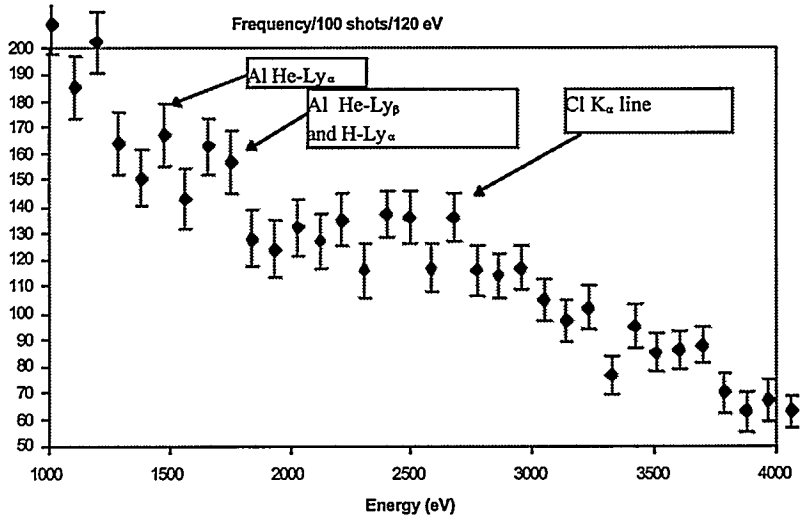
emissions from a titanium target. We used the CCD camera in place of the crystal spectrometer and tried to compare the signals from the two detectors. We also monitored the x-ray output from the back of a compound target, hoping to observe the chlorine lines even with the laser's multiple pulsing. We recorded 100 shots on the target with the CCD system.

At the beginning of our third year, the LABS laser was shutdown. Because no similar intense source of radiation exists, we had to search for an alternate x-ray source. The front end of the TRIDENT laser was capable of generating laser radiation at 1 mm with a pulse length of 500 fs and an energy of 0.7 J. However, we had to study and optimize the laser's generation of x-rays. Fifty shots were used to optimize laser focusing and to look at the effect of the laser prepulse on x-ray production. While we increased the x-ray production over that of similar lasers, the output power in the x-ray lines was significantly less, the line width of the radiation was larger, and the continuum radiation from hot electrons was much larger than with LABS.

Our attempt to use the laser prepulse to emulate the plasma conditions at LABS was not successful because we could not duplicate the laser conditions at LABS. We tried next to use two short pulses separated in time to duplicate the LABS pulses. The first low-amplitude infrared pulse created a long-scale plasma, and a second pulse at 0.5 μm interacted with the preformed plasma to generate x-rays. Twenty shots with 30-ps pulse separations were used to study x-ray generation. The presence of a controlled prepulse reduced the continuum and improved the contrast of the spectrum. However, as our first figure shows, the signal amplitude was less than that generated using the LABS XeCl system; thus



Comparison among the different spectra observed. Top curve is for the case of an unmodified TRIDENT beam, the middle curve is for adding a prepulse to the beam, and the lowest curve is from the LABS laser.



Measured x-ray spectrum from 100 laser shots using 120-eV-wide energy bins, with 1σ statistical error bars.

thousands of shots would have been needed to observe the signal.

Results

We analyzed our data on the XeCl system. The pulse-height distribution, excluding readout noise, and the background counts are shown in our second figure. The energy bins were 120 eV wide (about the resolution of the detector), as measured with an electron beam source of x-rays. The histogram shows the aluminum lines around the 1.6-keV bin and a weak signal from the chlorine K_α line at 2.672 keV. With a bin that large, we do not observe the K_α from the potassium target, indicating that the hot-electron production rate of holes was less than that from the two-photon absorption rate. The aluminum line at 1.48 keV cannot be resolved.

The amplitude of the unresolved aluminum He-Ly_α line at 1.48 keV

gives us a source strength of 10^{12} photons/shot, roughly three times the estimate from crystal spectrometry. The amplitude of the chlorine feature gives us a hole production rate of 1.1×10^6 vacancies, also three times that predicted using crystal spectrometry and the theoretical cross sections. These measurements should be viewed with caution, however, since the x-ray pulse length was not measured accurately, the laser was generating multiple x-ray pulses, and the immense attenuation of the nickel filter amplifies any attenuation cross-section measurement errors.

In summary, although our experiment proves the feasibility of measuring the two x-ray-photon absorption rate, many difficulties must be overcome before we can accurately measure cross sections.

Publications

Abdallah, J., L.A. Collins, G. Csanak, et al., (1995), "Two-Photon Ionization of an Inner Shell Electron of the Chlorine Atom" (to be published in *Zeit. Für Physik.*).

Jiang, Z., J.C. Kieffer, et al., "X-ray Spectroscopy of Hot Solid Density Plasmas Produced by Subpicosecond High Contrast Laser Pulses at 10^{18}-10^{19} W/cm^2," *Phys. Plasmas* **2**, 1702-1711 (1995).

Calculation of Satellite Line Structures in Highly Stripped Plasmas

Joseph Abdallah, Jr.

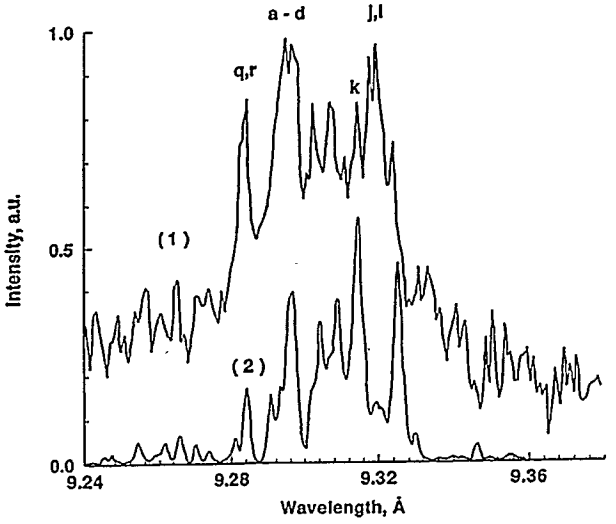
This project stems from a collaboration between Los Alamos and Russian physicists. It combines the ability of the Russians to measure highly resolved spectra from plasma sources and the Laboratory's unique capability to calculate spectral lines involving autoionizing levels (often called satellite lines). Our objective is to use these capabilities to provide temperature and density diagnostics for plasmas of various types, such as those encountered with laser interactions and pulsed-power devices. Theoretical simulations of the observed spectra are used to deduce the plasma conditions.

We published our findings on using beryllium-like satellite lines for interpreting a magnesium plasma produced by the picosecond Max-Born laser. We also identified many new spectral lines. Our first figure compares the calculated beryllium-like spectrum to an experimental spectrum.

We determined the plasma density and temperature for a silicon plasma produced at the sub-picosecond Los Alamos Bright Source laser facility. Many satellite lines near the resonance line of hydrogen-like silicon were identified. Our second figure shows a comparison of the observed and calculated spectra.

We also studied the influence of hot electrons on the spectral properties of satellite lines observed in the Cornell X-pinch pulsed-power device. A model electron-energy distribution function was developed to account for the hot electrons. Our third figure shows their effect on the calculated satellite structure.

Recent experiments by M. Wilke, A. Faenov, and T.A. Pikouz at the Trident laser facility were supported by this project. Their observations will motivate new calculations during the next year.

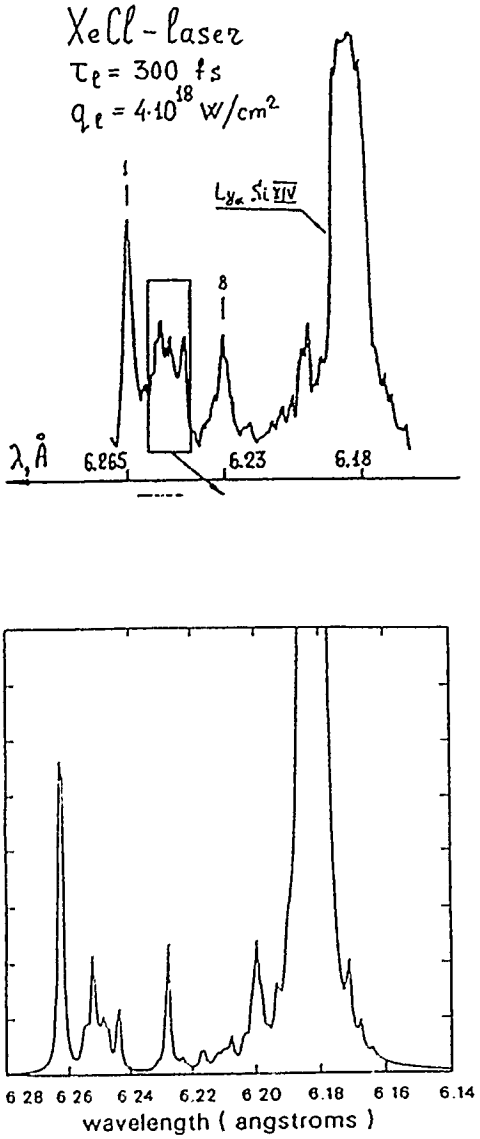


Comparison of the experimental spectrum (1) with the calculated beryllium-like spectrum (2). Note that the experimental curves also contain lines from the lithium-like ion stage.

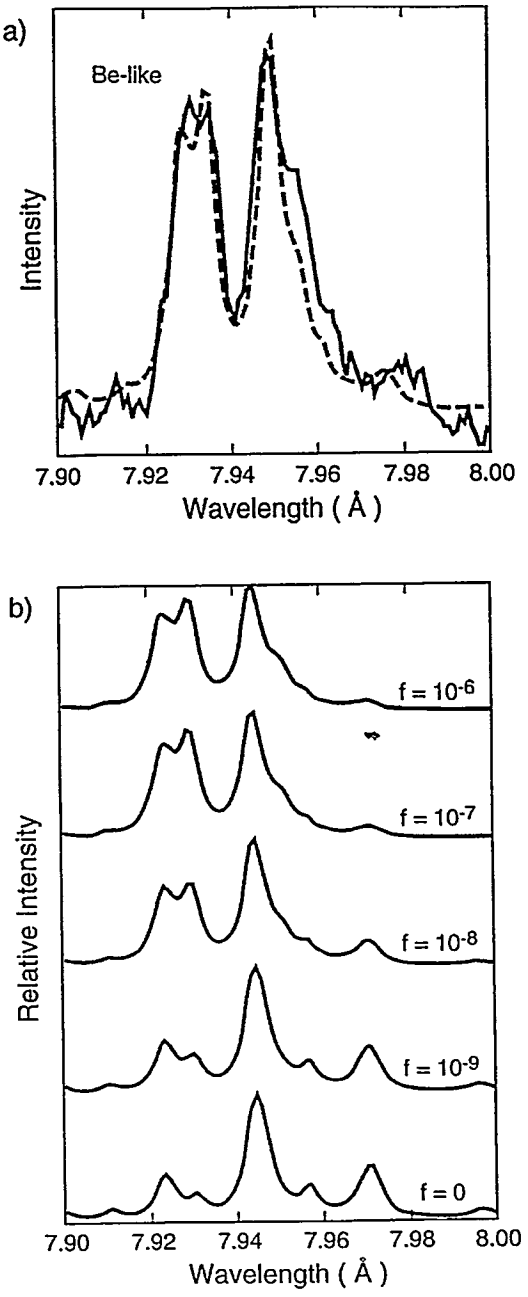
Publications

Abdallah, J., A.Y. Faenov, D. Hammer, et al., "Electron Beam Effects on the Spectroscopy of Satellite Lines in Aluminum X-Pinch Experiments" (to be published in *Physica Scripta*).

Bryunetkin, B.A., A.Y. Faenov, M. Kalashnikov, et al., "X-Ray Spectral Investigations of a High Irradiance Picosecond Laser Produced Plasma," *J. Quant. Spectros. Radiat. Transfer* 53, 45 (1995).



Comparison of experiment (top curve) with our calculations (bottom curves) for a silicon plasma produced by the Los Alamos Bright Source laser.



Top figure (a): comparison between experiment (solid line) and theory (dashed line) for the beryllium-like satellites observed in the Cornell University X-pinch. Bottom figure (b) shows the effect of increasing the hot-electron concentration on the spectrum.

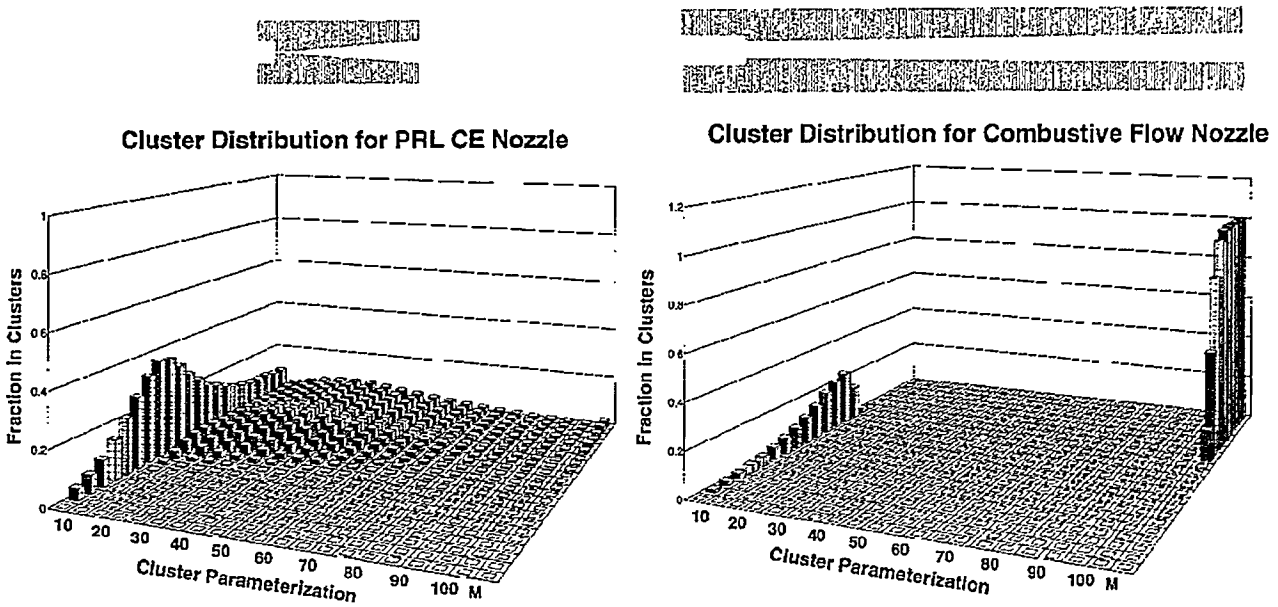
Nucleation and Condensation Science

Herbert Fry

The purpose of this project was to perform water nucleation and condensation experiments to provide data with which to compare our model of how droplets form from water vapor. Specifically, we wanted to benchmark our calculations of the formation rate for water nuclei in flowing gases, the growth rate of those nuclei, and their eventual size distribution. We performed two sets of experiments. In the first set, we adapted the Combustive Flow Facility (CFF) and the Pulsed Recirculating Loop (PRL) to achieve flow conditions in an expansion nozzle such that the static temperature decreased monotonically along the direction of the gas flow but was uniform in a plane transverse to the flow. We then measured water condensation in the nozzle by using infrared spectroscopy to monitor the disappearance of water monomers (see figure).

The second set of experiments was performed in a collaboration with the Max Planck Institute for Biophysical Chemistry, which has the best available experimental apparatus for measuring the nucleation rate by Mie scattering. We used this apparatus to measure the growth rate of water droplets under various conditions with different diluent gases. As a result of these measurements, we reached a preliminary conclusion that the process that limits droplet growth is monomer diffusion through the partially evacuated region around the droplets.

One of the key elements of our modeling efforts was the inclusion of a moment formalism that expands the range of conditions to which our chemical kinetics model applies. This model provides variables for water clusters containing 2 (a dimer) to 100 water monomer units. Under rapid expansion conditions, this range provides an adequate description since only



Nozzle design (top) and model predictions (bottom) for experiments involving constant expansion (CE) nozzles at the PRL (left) and the CCF (right). The PRL nozzle has a 4.5° expansion angle and a 3.5-mm throat height. The CFF nozzle has a 1° expansion angle and a 5-mm throat. The two nozzles provide dramatically different rates of expansion. One rate measure is the distance required to attain Mach 3: for the PRL nozzle, it is 10 cm; for the CFF nozzle, it is 50 cm. Cluster distributions from our nucleation and condensation model show the qualitative differences between the two nozzle experiments. The horizontal axis represents bins of droplets (in terms of the number of monomers in a cluster) for both the explicitly included individual droplets and those represented by the moment formalism (indicated by M). The vertical axis is the fraction of water monomers in these bins. The third axis represents distance down the nozzle: for the PRL, about 5 cm; for the CFF, about 50 cm. The time scales are 100 and 800 μs, respectively. In the PRL nozzle, the kinetics are dominated by the growth of small droplets (<100 monomer units) that are explicitly included in the model. In the CFF nozzle, the moment formalism is required for a good description.

small clusters are formed. However, at low expansion rates and low supersaturations, very large clusters (trillions of water molecules) are formed, which would require too many variables. The moment formalism allows us to describe the growth of such large clusters with only four variables. This formalism was necessary to describe the experiments performed in Germany. As shown in the accompanying figure, the CFF nozzle provides data in an intermediate regime where the moment formalism is becoming necessary.

State-to-State Photodetachment in the Two-Electron Hydrogen Ion

Charlie E. M. Strauss

We are investigating the state-to-state photodetachment of the simplest two-electron system, the negative hydrogen ion, that is most important to the development of three-body quantum mechanics. Results of our research will also be relevant to atomic and molecular physics, particle accelerators, photochemistry, biomedical sciences, and materials processing. We have completed construction of the ion source and ultraviolet laser source; we have also upgraded our modeling of the two-photon cross section.

We observed, for the first time, excess photon detachment in the negative hydrogen ion. We managed to do so in the particularly interesting regime where the strength of the optical field is comparable to the strength of the internal, atomic, electric field. We also observed a resonant multiphoton detachment. This is the first time that a multiphoton detachment resonance has been seen in any negative atomic ion. We have also observed the first nonresonant excess photon detachment in the negative hydrogen ion. Our next study requires bright, narrow linewidth, highly collimated vacuum ultraviolet (VUV) radiation to examine, as a function of VUV wavelength and electron energy distribution, the photodetachment spectrum of the Feshbach and Shape resonances in the negative hydrogen ion, near 113 nm.

Publications

Stintz, A., X.M. Zhao, C.E.M. Strauss, et al., "Resonant Two Photon Detachment Through the Lowest Singlet D State in H Minus" (to be published in *Phys. Rev. Lett.*).

Dynamics of Quantum Wave Packets

Timothy R. Gosnell

This project concerns the controlled assembly of quantum-mechanical vibrational wave packets in diatomic molecules. Of special interest is their subsequent dynamical evolution. With a femtosecond laser used as an optical pump source, we will construct vibrational quantum states of matter otherwise not found in nature and study how the details of the laser-excitation process uniquely affect the time development of the vibrational states created. Controlling chemical reactions with light has been discussed since well before the invention of the laser. Our project represents a new level of experimental sophistication applied to this elusive goal. Long-term potential applications of such control include the assembly and operation of molecular nanostructures.

Our work entails applying two new experimental methodologies in the area of ultrafast optical spectroscopy. Specifically, we will apply frequency-resolved optical gating (FROG) and Fourier spectral filtering to diagnose and control the optical pump pulses used to excite vibrational wave packets in diatomic potassium and cesium molecules.

We assembled an experimental chamber, a FROG diagnostic, and a pump-probe apparatus to investigate wave-packet dynamics in diatomic potassium. We detected oscillating vibrational wave packets, and initial results indicate that their shape is affected by changing the degree of "chirp" in the optical pump pulse (i.e., by changing the pulse's frequency over time). We tentatively conclude that diatomic potassium will prove fruitful in further studies.

GEOSCIENCE, SPACE SCIENCE, AND ASTROPHYSICS

A STUDY BY COMPUTER SIMULATION OF THE GENERATION AND EVOLUTION OF THE EARTH'S MAGNETIC FIELD

Gary A. Glatzmaier

A fundamental goal of geophysics is to develop a coherent understanding of the structure and dynamics of Earth's interior. An integral part of this understanding must be a model of Earth's magnetic field that reproduces its salient features, i.e., a field that is maintained for many magnetic diffusion times, is dominantly dipolar at the surface with a dipole axis that on the average lies close to the geographic axis of rotation, and exhibits secular variation with occasional excursions and reversals. The only plausible candidate for such a model is the geodynamo theory, which proposes that new magnetic field is continually being generated by the shearing and twisting fluid motions within Earth's liquid, electrically conducting outer core.

To gain an understanding of the geodynamo, we have produced the first fully self-consistent, three-dimensional (3-D) numerical simulation of a convective strong-field dynamo. A magnetic field is maintained for more than 40,000 years (three magnetic diffusion times) and has energy at least three orders of magnitude greater than the kinetic energy of the convection that maintains it. The exciting feature we captured is a reversal of the dipole polarity, which occurs near the end of our simulation. Because our simulation is self-consistent and maintains a field that resembles Earth's in many respects, we believe that it provides a plausible description of the geomagnetic field and the way it reverses. Our effort is internationally recognized as the leading computer modeling study of the generation of Earth's magnetic field.

Our numerical model solves the nonlinear magnetohydrodynamic equations that govern the 3-D structure and evolution of an electrically conducting fluid undergoing thermal convection in a rapidly rotating spherical shell. A specified heat flux at the shell's inner core boundary (ICB) drives thermal convection in the fluid outer core. This convection, influenced by the rotation of the core, twists and shears magnetic field, generating new magnetic field to replace that which diffuses away. The field diffuses into a solid, electrically conducting inner core that provides magnetic torque between the inner and outer cores. Magnetic torque also exists between the outer fluid core and the solid mantle above via a thin conducting layer at the core-mantle boundary (CMB). The rest of the mantle is assumed to be an insulator; thus, the field above this layer is a source-free potential field. The time-dependent rotation rates of the solid inner core and solid mantle are determined by the net torques at the ICB and CMB, respectively.

With Earth-like parameters, our simulation spans over 40,000 years, with no indication that the magnetic field will decay away, which is convincing evidence that our solution is a self-sustaining convective dynamo. After an initial period of adjustment (roughly 10,000 years) during which the dipole part of the field gradually becomes dominant, our time-dependent solution maintains its dipole polarity until near the end of the simulation when it reverses in slightly more than a thousand years; the solution then maintains the new dipole polarity for roughly the remaining 4,000 years of the simulation. The simulation required over 2 million computational time steps that took more than 2,000 computing hours on a Cray C-90.

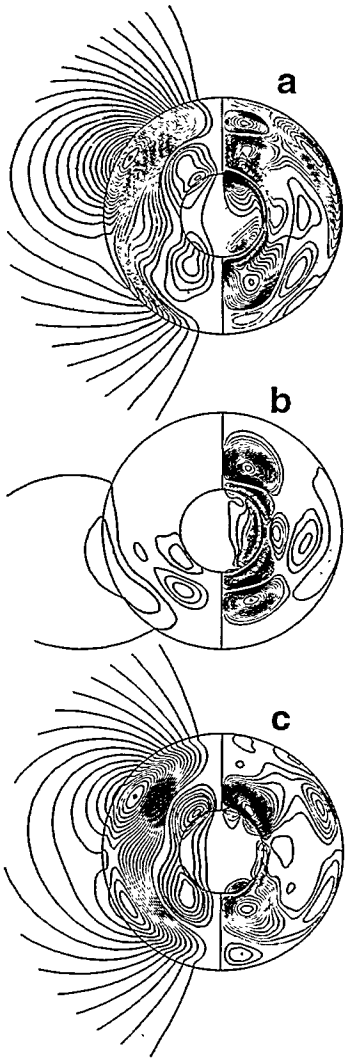
To illustrate the magnetic field reversal, we show in the figure the longitudinal average of the 3-D field (a) at 9,000 years before the end of our simulation, (b) at roughly the middle of the polarity transition as seen at the ICB (about 5,000 years before the end), and (c) at the end of our simulation. The right side of each plot shows the contours of the east-west (toroidal) part of the field; the left side shows the lines of force of the meridional (poloidal) part of the field. There are typically two main toroidal field concentrations, one in each hemisphere, in opposite directions. These concentrations are usually inside the imaginary cylinder tangent to the inner core, where large zonal flows shear poloidal field, thus generating toroidal field. Toroidal field also diffuses into the inner core from the ICB, where it is generated, when poloidal field is sheared by the inner core as it moves differentially with respect to the fluid just outside the ICB.

The longitudinally averaged poloidal field typically has two dipolar polarities: one in the outer part of the fluid core (which is also the dipole polarity observed at the surface) and the opposite polarity in the inner part of the fluid core and the inner solid core. Poloidal field is generated by helical flow that twists toroidal field; for example, in the northern hemisphere, the time-dependent helicity of the flow (i.e., the correlation between velocity and vorticity) is usually right-handed and much larger in magnitude inside the "tangent cylinder" and left-handed outside.

A movie of our simulation shows how the field in the fluid outer core is continually attempting to reverse its axial dipole polarity on a short time scale (roughly 100 years), corresponding to convective overturning. This reversal usually fails because the field in the solid inner core, which can only change on a longer diffusive time scale (about 1,600 years), usually does not have enough time to diffuse away before it is regenerated at the ICB. Once in many attempts, the 3-D configurations of the buoyancy, flow, and magnetic fields in the outer core are correct for a long enough period of time for the inner core axial dipole field to diffuse away (see part (b) of figure), thus allowing the reversed axial dipole polarity in the outer core to diffuse into the inner core. If this scenario is representative of Earth, it suggests that the strong nonlinear feedbacks in 3-D and the different time scales of the fluid and solid cores are responsible for Earth's stochastic reversal record.

During the transition, eastward and westward toroidal field are alternately generated several times in both hemispheres at the ICB before the reversed polarity finally becomes established. Notice in the figure how the toroidal field is asymmetric with respect to the equator before (see part (a) of the figure) and after (see part c) the transition but is symmetric midway through the transition (see part b). In our simulation, the toroidal field reverses first, followed by the inner poloidal field that penetrates the solid core, and finally, somewhat later, the outer poloidal field that appears at Earth's surface reverses. This entire process takes (depending on how one defines the beginning and end of the reversal) a little more than a thousand years, roughly the characteristic magnetic diffusion time scale for the inner core.

Our fields at the surface and at the CMB are qualitatively similar to Earth's present field, with multimode contributions and several flux concentrations. The maximum intensity of the radial component of our simulated field at the CMB is typically about 3.0 mT, which is a little greater than what it is for present-day Earth; however, like Earth, the dipole part of the field dominates at the surface. During the reversal, the maximum intensity of our field at the CMB drops to about 0.8 mT, with the dipole part dropping more than the other modes, as some palaeomagnetic reversal records indicate.



The longitudinal average of the 3-D magnetic field is displayed with the contours of the toroidal (east-west) part of the field plotted in the right hemispheres and the lines of force of the meridional (poloidal) part of the field plotted in the left hemispheres. Snapshots are displayed (a) before the reversal (9,000 years before the end of our simulation), (b) midway through the transition as seen at the inner core boundary (ICB), i.e., when the axial dipole part of the field at the ICB goes through zero (about 5,000 years before the end), and (c) after the reversal (at the end of our simulation). The north geographic pole is at the top of each plot. The outer circular boundary is the core-mantle boundary and the inner circular boundary is the ICB. Light contours are eastward-directed toroidal field; dark contours are westward-directed toroidal field. The dark lines of force are clockwise-directed poloidal field that are plotted out to the surface; the light lines of force are counterclockwise-directed poloidal field.

Publications

Glatzmaier, G.A., and P.H. Roberts, "A three-dimensional convective dynamo solution with rotating and finitely conducting inner core and mantle," *Phys. Earth Planet. Inter.* **91**, 63 (1995).

Glatzmaier, G.A., and P.H. Roberts, "A three-dimensional self-consistent computer simulation of a geomagnetic field reversal," *Nature* **377**, 203 (1995).

Cosmological Gamma-Ray Bursts

Edward Fenimore

Gamma-ray bursts are brief events that dominate the emission from all other gamma-ray objects in the sky; they flicker for tens of seconds and then turn off. However, their nature remains uncertain despite years of efforts to understand them. One school of thought believes that the bursts arise within our galaxy, albeit in an extended halo of neutron stars. The other school of thought uses the isotropic distribution of gamma-ray bursts to argue that such bursts come from near the edge of the universe. If gamma-ray bursts originate from cosmological distances, then the expansion of the universe should cause the dimmer (presumably farther away) bursts to last longer.

We have developed the average autocorrelation method of measuring the amount of time stretching between bright and dim gamma-ray bursts. This method uses most of the time history of the bursts rather than just the strongest peak; it is therefore more stable statistically and less susceptible to how it is implemented. We have used standard cosmology models to relate the amount of time stretching determined from the average autocorrelation to the time dilation expected because of the expansion of the universe. Such an analysis reveals the distance to the source. The distance that we found corresponds to a cosmological redshift of approximately 6. This distance is much larger than one expects from current models and from other observations. For example, we used standard cosmology models and the distribution of the intensities of gamma-ray bursts to show that such distributions are consistent with a distance that corresponds to a cosmological redshift of only 1.

Publications

Fenimore, E.E., and J.S. Bloom, "Determination of Distance from Time Dilation of Cosmological Gamma-Ray Bursts," *Astrophys. J.* 453, 25-36 (1995).

Fenimore, E.E., R.W. Klebesadel, and J.G. Laros, "The 1979, March 5 Gamma Ray Transient: Was It a Classic Gamma-Ray Burst?" (to be published in *Astrophys. J.*).

Fenimore, E.E., J. In't Zand, J.P. Norris, et al., "Gamma-Ray Burst Peak Duration as a Function of Energy," *Astrophys. J.* 448, 101 (1995).

In't Zand, J., and E.E. Fenimore, "The Autocorrelation of Gamma-Ray Burst Time Profiles" (to be published in *Astrophys. J.*).

Magmatic Tritium

Fraser Goff

Tritium (^3H) is one of the reaction products that should be produced during "cold fusion" in condensed matter. We are trying to determine whether anomalous quantities of ^3H are universally present in magmatic waters from volcanoes of different magma types and tectonic settings. Such tritium could provide independent evidence for cold fusion as a potentially viable Earth process and would require reevaluation of accepted concepts on primordial helium, mantle heat flow, and plate tectonics.

The object of our work is to collect samples of high-temperature fumarole condensates, thermal and nonthermal groundwaters, precipitation, and fresh volcanic products from one additional volcano to determine the ^3H content of its magmatic water. Our approach is unique because we analyze water of three isotopic compositions (containing deuterium, tritium, or oxygen-18) to eliminate effects of meteoric contamination and contamination by near-surface groundwaters.

We successfully sampled Sierra Negra and Alcedo volcanoes in the Galapagos Islands (Ecuador), Vulcano (Italy), and Paracutin (Mexico). We determined that neither of the Galapagos sites contained measurable magmatic water and redetermined the magmatic tritium of Mount St. Helens (^3H=0.7 tritium units [T.U.]). This value is lower that the value of 3.1 T.U. we determined on samples and analyses from 1989. We have not yet finished analyzing the samples from Italy and Mexico. For the last year of the project, we plan to collect samples from Oldoinyo Lengai, the world's only active carbonatite volcano, which is located in Tanzania.

Publications

Goff, F., "Vesicle Cylinders in Vapor-Differentiated Basalt Flows" (to be published in *J. Volcanol. Geotherm. Res.*).

Goff, F., and C. Werner, "Monitoring Active Volcanoes" (submitted to *GSA Today*).

Lead Immobilization in Thermally Remediated Soils and Igneous Rocks

Donald D. Hickmott

Cleanup of rocks, soils, and aquifers contaminated with mixtures of lead and organic or high-explosives wastes is a problem of considerable importance across the nation. This project is designed to (1) investigate the speciation of lead in soils and igneous rocks, (2) use numerical methods to investigate phases that may immobilize lead, and (3) complete laboratory-scale experiments in which lead is immobilized by thermal treatment of soil. Our project will result in a procedure for minimizing the mobility and toxicity of lead in the environment, following the thermal treatment of amended soils.

Our principal accomplishments during the review period were (1) using proton-induced x-ray emission and scanning electron microscopy to characterize lead speciation in tuffs and soils; (2) successfully using laser-induced breakdown spectroscopy and field-based x-ray fluorescence to identify lead-contaminated soils; and (3) identifying the minerals pyromorphite, alamosite, and epidote as possible lead immobilizers in thermally treated soils. Speciation studies of the Bandelier Tuff show that high lead concentrations observed in water from monitoring wells at Los Alamos National Laboratory may be the result of vapor-phase lead minerals such as cerussite interacting with groundwater. Thermodynamic modeling suggests that amending contaminated soils, before thermal treatment, with phosphate-bearing minerals such as apatite or aluminum-rich minerals such as corundum may produce a remediation byproduct in which lead is immobile.

Publications

Stimac, J., D. Hickmott, D. Broxton, et al., "Redistribution of Pb and Other Volatile Trace Metals During Eruption, Devitrification, and Vapor-Phase Crystallization of the Bandelier Tuff, New Mexico" (submitted to *J. Volcanology and Geothermal Res.*).

Spacetime Geodesy

Warner Miller

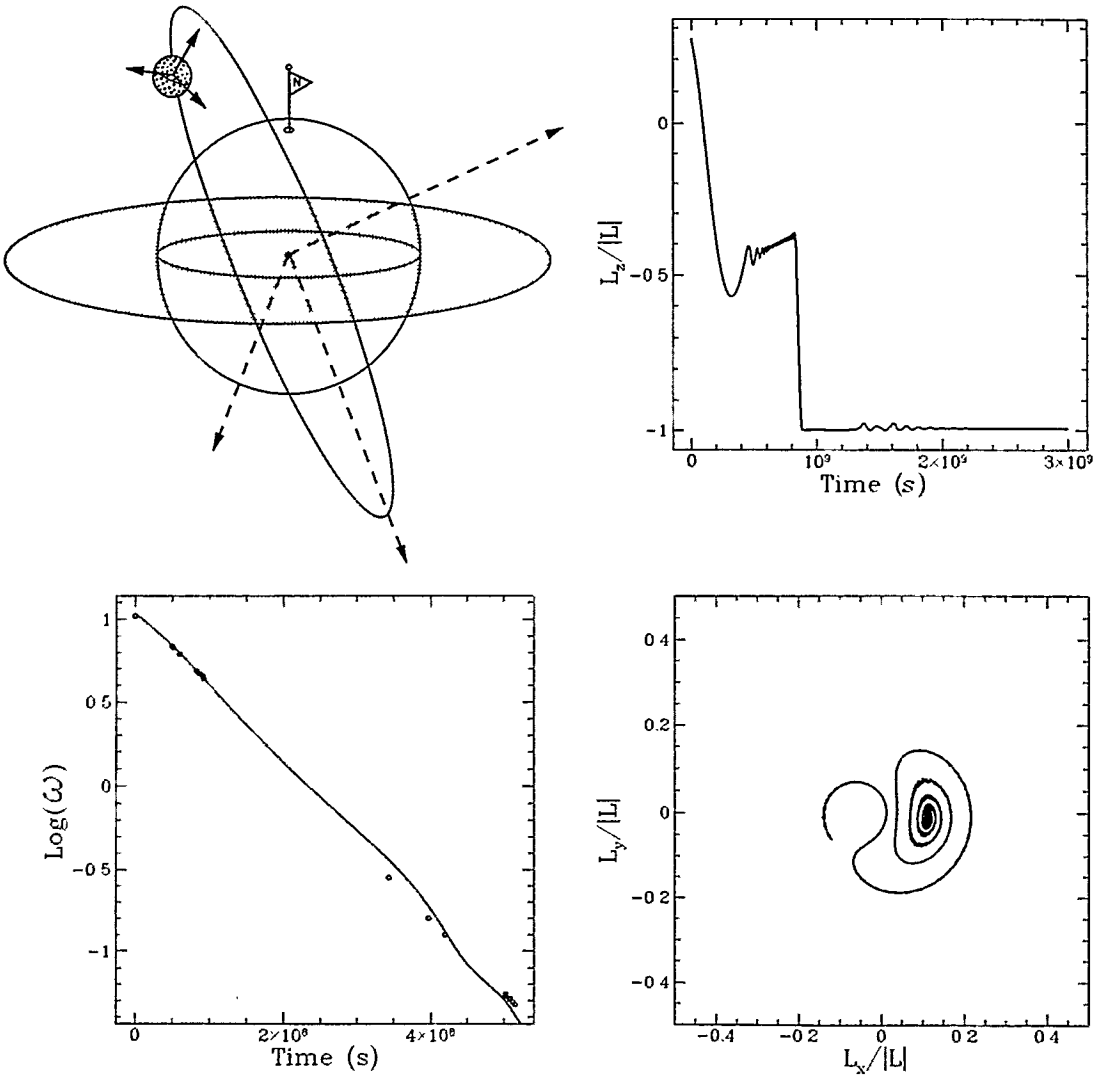
LAGEOS is an accurately-tracked, dense, spherical satellite covered with 426 retroreflectors. The tracking accuracy yields a medium-term (years to decades) inertial reference frame determined via relatively inexpensive observations and is used as an adjunct to the more difficult and more data intensive absolute frame measurements via very long baseline interferometry. There is a substantial secular precession of the satellite's line of nodes consistent with the classical, Newtonian precession due to the non-sphericity of the earth. Ciufolini has suggested the launch of an identical satellite (LAGEOS-3) into an orbit supplementary to that of LAGEOS-1; LAGEOS-3 would then experience an equal and opposite classical precession to that of LAGEOS-1.

Besides providing a more accurate real-time measurement of the earth's length of day and polar wobble, this paired-satellite experiment would provide the first direct measurement of the general relativistic frame-dragging effect. Of the five dominant error sources in this experiment, the largest one involves surface forces on the satellite and their consequent impact on the orbital nodal precession. The surface forces are a function of the spin dynamics of the satellite. Under this project we modeled the spin dynamics of a LAGEOS-type satellite and used this updated spin model to estimate the impact of the thermal rocketing effect on the LAGEOS-3 experiment (see our first accompanying figure). We have also developed a general, relativistic ray-tracing code that can model accretion around objects such as black holes. An example of its capabilities is shown in the second figure.

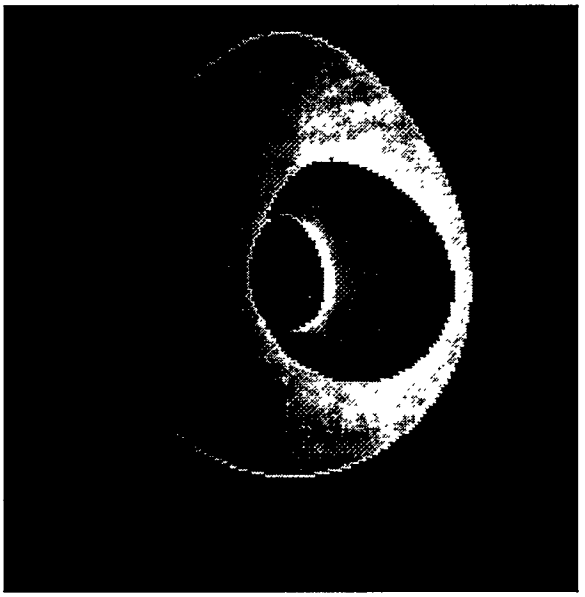
Publications

Habib, S., D. Holz, A. Kheyfets, et al., "Spin Dynamics of the LAGEOS Satellite in Support of a Measurement of the Earth's Gravito-Magnetism," *Phys. Rev. D* **50**, 6068 (1994).

Holz, D., K. Chen, and W. Miller, "Can We Measure the Angular Momentum of a Black Hole?" (submitted to *Phys. Rev. Lett.*).



Dynamics of the Euler angles. The evolution of the nutation (angle of obliquity\theta) of the model satellite (upper left). In the asymptotic limit the angular velocities of nutation and precession average to zero (upper and lower right, respectively). However, the precession rate omega\phi locks into the orbital velocity. The asymptotic limit (lower left): this plot demonstrates clearly the dynamics through the spin-orbit resonance phase.



Contour plot of a thin accretion disk about a maximally spinning black hole of mass (M) and radius (R_M). The inner radius of the disk is at $3R_M$ while the outer edge is at $20R_M$. The distortion was calculated using a general, relativistic ray-tracing code developed under this project. The inclination of the photographic plate is at 60° (the most probable viewing angle), while the distance from the black hole was $1000R_M$. The distortion of the disk is caused by the bending of the light rays by the spinning black hole. This is why the disk appears oblong in the "wrong" direction. The contours represent the observed Doppler-shifted frequencies of the iron lines.

The Galactic/Globular Cluster Pulsar Content and the 2.1-ms Pulsar Candidate in Supernova 1987A

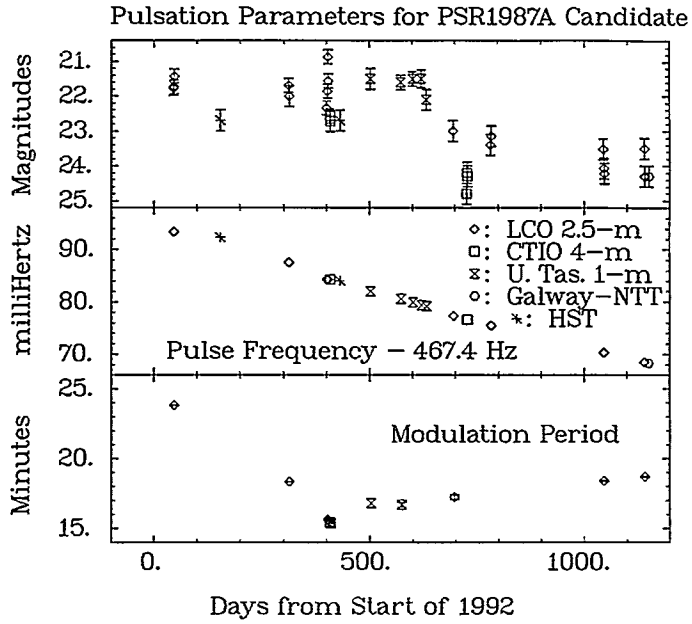
John Middleditch

We have continued to detect and measure the 2.1-ms signature that seems to be present within Supernova 1987A (SN1987A) over the last year in spite of the faintness of the signal (see first figure). We have done so by measurements taken on two telescopes. Because of the faintness of the signal, we still have no definitive, extremely significant result, but measurements taken over the past year by three telescopes—the Las Campanas Observatory (2.5 m), the European Southern Observatory (3 m) New Technology Telescope, and the University of Tasmania (1 m—which did *not* detect the too-faint source)—all remain consistent with the presence of the faint 2.1-ms source.

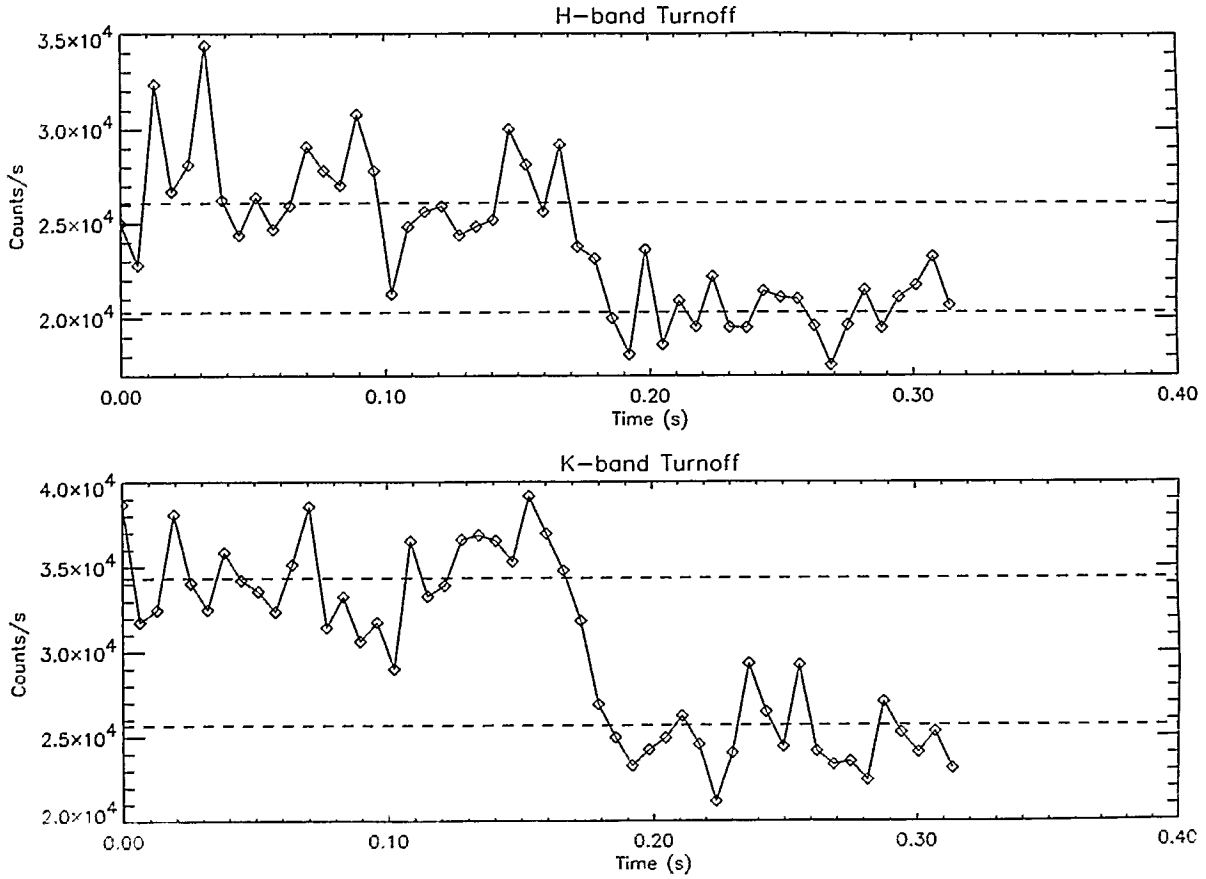
In the meantime, we have engineered improvements in the solid state photomultiplier, and, in spite of the relative insensitivity of the instrument (1% quantum efficiency), have discovered an object in the globular cluster M15 which is very difficult to explain. This object is 10,000 times as luminous as the sun in the wavelength bands near 2 microns, and suffers eclipses every 1.016696 days that happen within only 30 ms and persist for hours afterward (see eclipsar graph). We think this is a young pulsar like that in SN1987A, but we have not yet clearly established the pulse frequency. We failed to image this source during the year following these observations when the transition would have been expected to take place (see photo). Nevertheless, given the number of double-takes made, there seems to be little doubt about the reality of the source. It even showed guiding lapses characteristic of an object moving from near the center of the aperture toward the edge as the tracking error of the telescope increased in the time intervals following the offset checks. The collaborators from Harvard/Smithsonian Astrophysical Observatory, Eikenberry and Fazio, who are developing the Solid State Photomultiplier, sum it up as: "It'll happen again after we're dead."

Publications

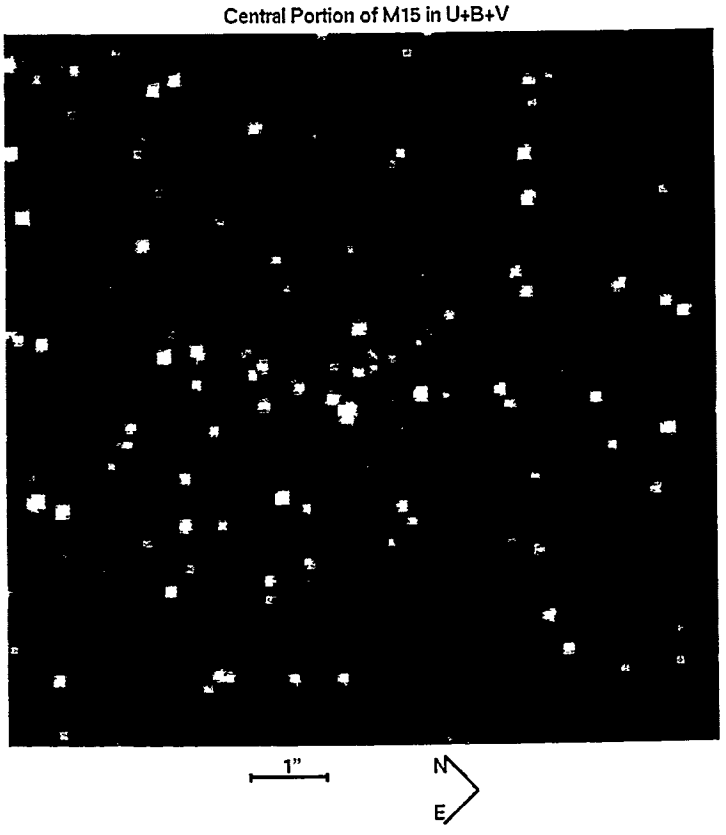
Ransom, S.M., G.G. Fazio, S.S. Eikenberry, et al., "High Time Resolution Infrared Observations of the Crab Nebula Pulsar," *Astrophys. J. Lett.* **431**, 43 (1994).



The magnitude, pulse frequency, and modulation period (probably due to neutron star precession) for the 2.1-ms candidate pulsation in SN1987A are plotted vs time since 1992. The apparent slowdown of the ~467.5 Hz pulse frequency implies a pulsar luminosity at least ten times the total luminosity of the Crab Nebula pulsar, some 99.9% of which must be due to gravitational radiation, that, in turn, results from the same oblateness (exceeding the Maclaurin value) that causes the apparent precession.



The extremely rapid onsets of the eclipses for the "eclipsar" in the globular cluster M15 are shown for the K (2.2-2.4 microns) and H (1.65 microns) wavelength bands. Such eclipses occur within 0.03 s and last for hours.



An image of the stars close to the center of the globular cluster M15, made with the Wide Field Planetary Camera (II) of the Hubble Space Telescope. The "eclipsar" very probably lurks somewhere in this field (but where?). Credits for the image go to

- *P. Guhathakurta (UCO/Lick Observatory, UC Santa Cruz),*
- *B. Yanny (Fermi National Accelerator Lab),*
- *D. Schneider (Pennsylvania State Univ),*
- *J. Bahcall (Princeton, Inst. for Advanced Study), and*
- *NASA.*

Mineralogical and Geochemical Aspects of Mineral-Induced Disease

George D. Guthrie, Jr.

Many minerals, including asbestos, silica, zeolites, and clays, are known to cause disease following inhalation. The mineralogical properties that determine toxicity are not known, hindering effective risk assessment. Consequently, many minerals that do not pose risks are highly controlled, whereas many minerals that do pose risks remain uncontrolled.

We are integrating mineralogy and biology in an interdisciplinary scientific investigation of the mechanisms of mineral-induced disease. Our biological endpoints include the formation of ferruginous bodies, chemical signaling by cells (e.g., production of cytokines or active oxygen species), and the induction of genes. Our mineralogical variables include structure, composition, and surface properties. We are also determining what information about the biological reaction is preserved in the mineral surface (i.e., can the surface tell us something about the reaction?).

Our work has focused on the synthesis of ferruginous bodies in a cell-free system and the monitoring of gene induction (c-*jun* and c-*fos*) in rat pleural mesothelial cells exposed to several samples of cation-exchanged erionite and mordenite. Our synthesis experiments are ongoing, but the results we obtained during the reporting period suggest that ferruginous bodies can be synthesized in the absence of cells. Our gene-induction experiments are also ongoing, but we have obtained the first definitive links between a mineralogical property (cation buffering) and a biological response.

The work performed in this project has application to air pollution and air quality (biological effects, policy), biomedical sciences (environmental pollutants, toxicity), health and safety in minerals industries (coal, fly ash, shale oil, petroleum, mining, ceramics), environmental legislation, public health, and radioactive waste disposal.

Publications

Guthrie, G.D., Jr., "Eat, Breathe, and Be Wary: Mineralogy in Environmental Health," *Rev. Geophys., Suppl.* 33, 117 (1995).

Guthrie, G.D., Jr., "Mineralogical Factors Affect the Biological Activity of Crystalline Silica" (to be published in *Appl. Occup. Environ. Hygiene*).

Guthrie, G.D., Jr., and P.J. Heaney, "Mineralogical Characteristics of the Silica Polymorphs in Relation to Their Biological Activities" (to be published in *Scand. J. Work, Environ., and Health*).

Werner, A.J., M.F. Hochella, Jr., G.D. Guthrie, Jr., et al., "Crocidolite Dissolution in the Presence of Fe Chelators: Implications for Mineral-Induced Disease" (to be published in *Amer. Mineral.*).

Using Microspheres as Tracers for Flow in Geologic Media

Bruce Robinson

The use of microspheres as groundwater tracers will provide researchers with an additional tool with which to investigate groundwater flow and transport systems. By comparing the results of dissolved tracers and microspheres, we will be able to determine the role of diffusion versus fracture transport in the mobility of groundwater contaminants. The goals of our project are to develop the analytical techniques for measuring microsphere concentrations in natural groundwaters and to demonstrate the usefulness of microspheres as tracers in the field.

We achieved the first goal of this project by using flow cytometry to obtain a highly sensitive technique for measuring microsphere concentrations. We demonstrated the effectiveness of our technique through extensive testing in actual groundwaters. The second goal is being demonstrated with every use of microspheres in field tests.

During the reporting period, we successfully carried out field tests in a granitic system at Raymond Quarry, California, using polystyrene microspheres of two different sizes. We have shown that the flow-cytometer analytical method is a highly sensitive technique for measuring microsphere concentrations. The use of microspheres in field tracer tests is practical, given the successful results of the field-testing program. Future analyses that compare the breakthrough curves of microspheres and dissolved tracers will yield new information on the nature of transport in fractured rocks.

Magnetic Reconnection in Space Plasmas

John Gosling

Magnetic reconnection is an important physical process in space plasmas and is thought to be important in laboratory and astrophysical contexts as well. It is the prime means by which the magnetic topology of a plasma is changed.

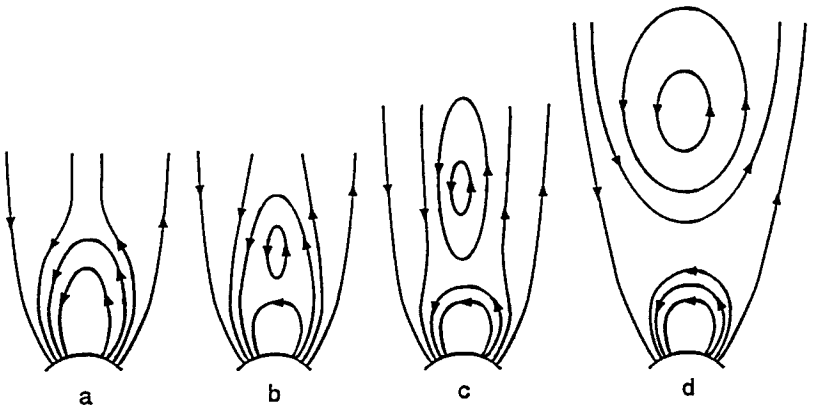
Our work has been oriented primarily toward examining three-dimensional reconnection in the solar corona and its role in determining the magnetic topology of coronal mass ejections (CMEs) in the solar wind. Our study utilized plasma and magnetic field data from the ISEE 3 spacecraft stationed in the solar wind well upstream from the earth, as well as results from numerical simulations of the reconnection process. Using charged solar wind particles as tracers of magnetic field lines, we have determined that although field lines threading CMEs in interplanetary space are usually attached to the sun at both ends, occasionally they are either attached to the sun at only one end or are completely detached from it.

We have found that the observed mixture of field topologies within CMEs finds a natural explanation in terms of sustained three-dimensional magnetic reconnection occurring close to the sun. The work performed in this project has application to treaty verification; auroral, ionospheric, and magnetospheric phenomena; and elementary and classical processes in plasmas.

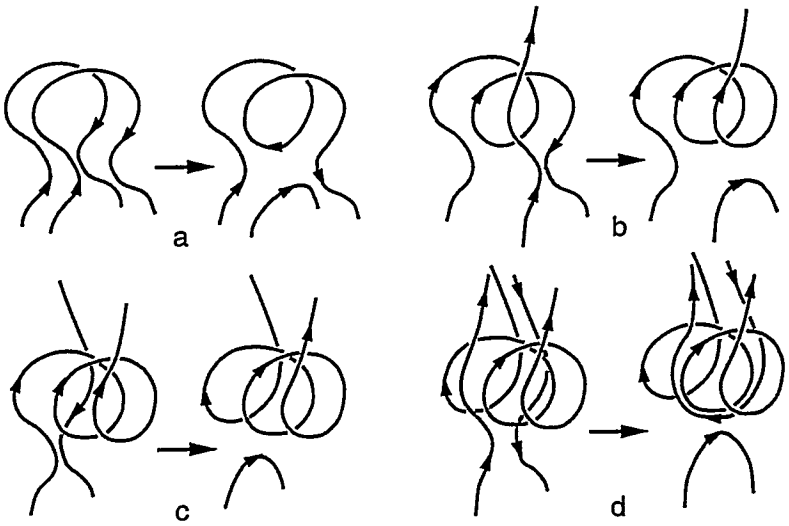
Publications

Feldman, W.C., E.W. Hones, B.L. Barraclough, et al., "Possible Conjugate Reconnection at the High-Latitude Magnetopause," *J. Geophys. Res.* **100,** 14913 (1995).

Gosling, J.T., J. Birn, and M. Hesse, "Three-Dimensional Magnetic Reconnection and the Magnetic Topology of Coronal Mass Ejection Events," *Geophys. Res. Lett.* **22,** 869 (1995).



Magnetic reconnection within rising coronal loops threading a coronal mass ejection as is commonly envisioned in two dimensions.



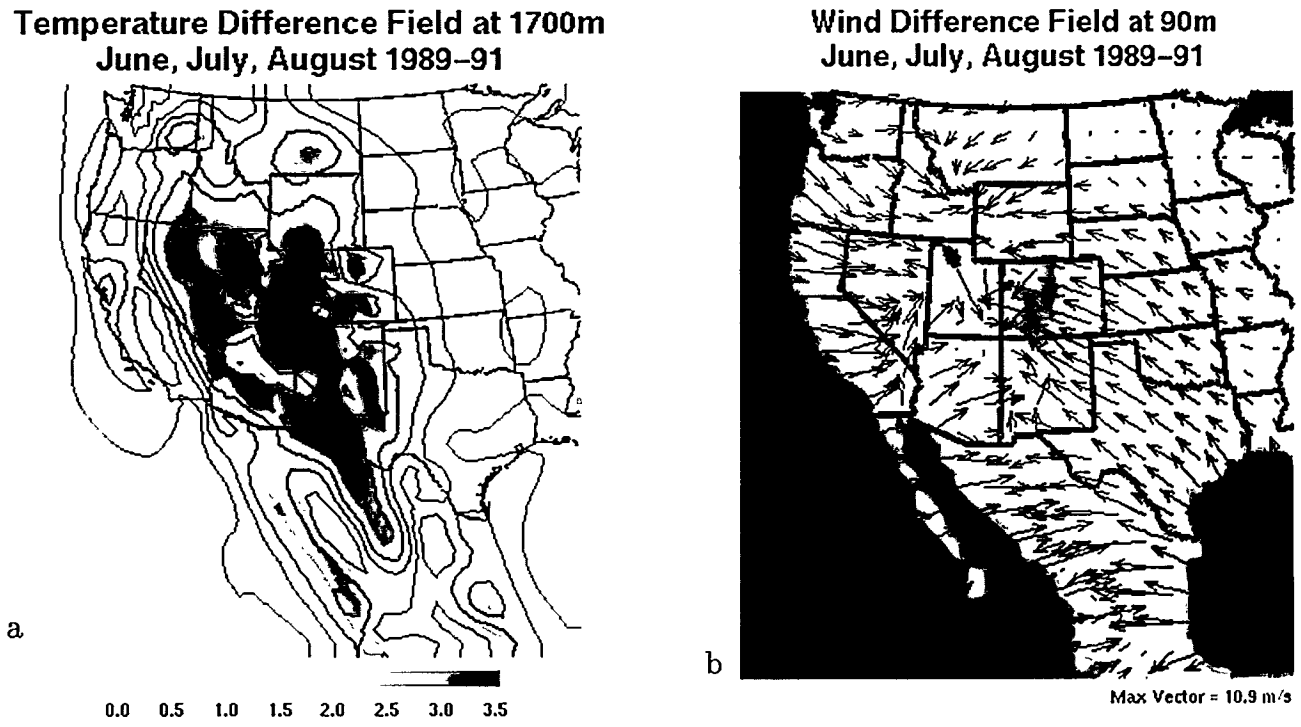
Sketches of successive steps in three-dimensional reconnection of magnetic field lines threading coronal mass ejections. The sketches are not to scale and are intended only to illustrate successive changes in magnetic topologies resulting from reconnection.

A Coupled Regional Climate-Biosphere Model for Climate Studies

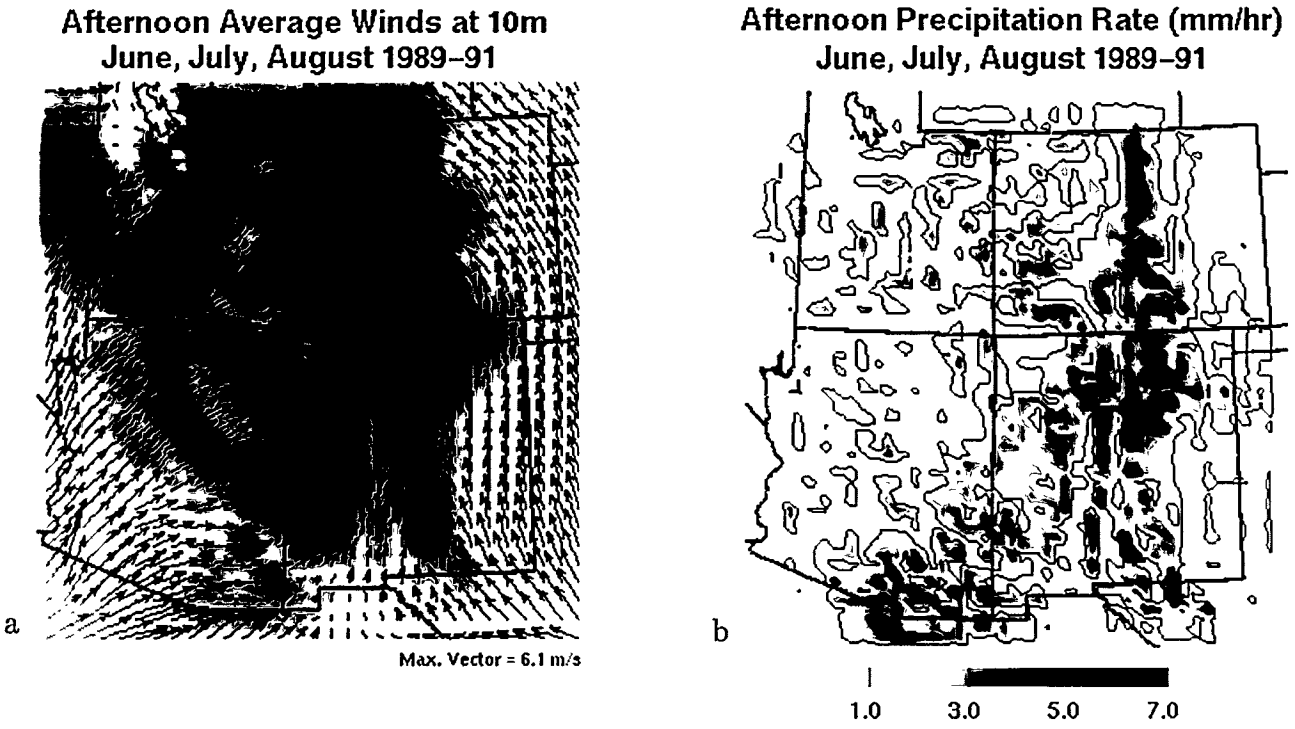
James Bossert

The objective of our project has been to develop and test a regional climate-modeling system that couples a limited-area atmospheric code to a biosphere scheme that properly represents surface processes. The development phase included investigations of the impact of variations in surface forcing parameters, meteorological-input data resolution, and model grid resolution. The testing phase included a multiyear simulation of the summer climate over the southwest United States at a higher resolution than has been attained by previous studies.

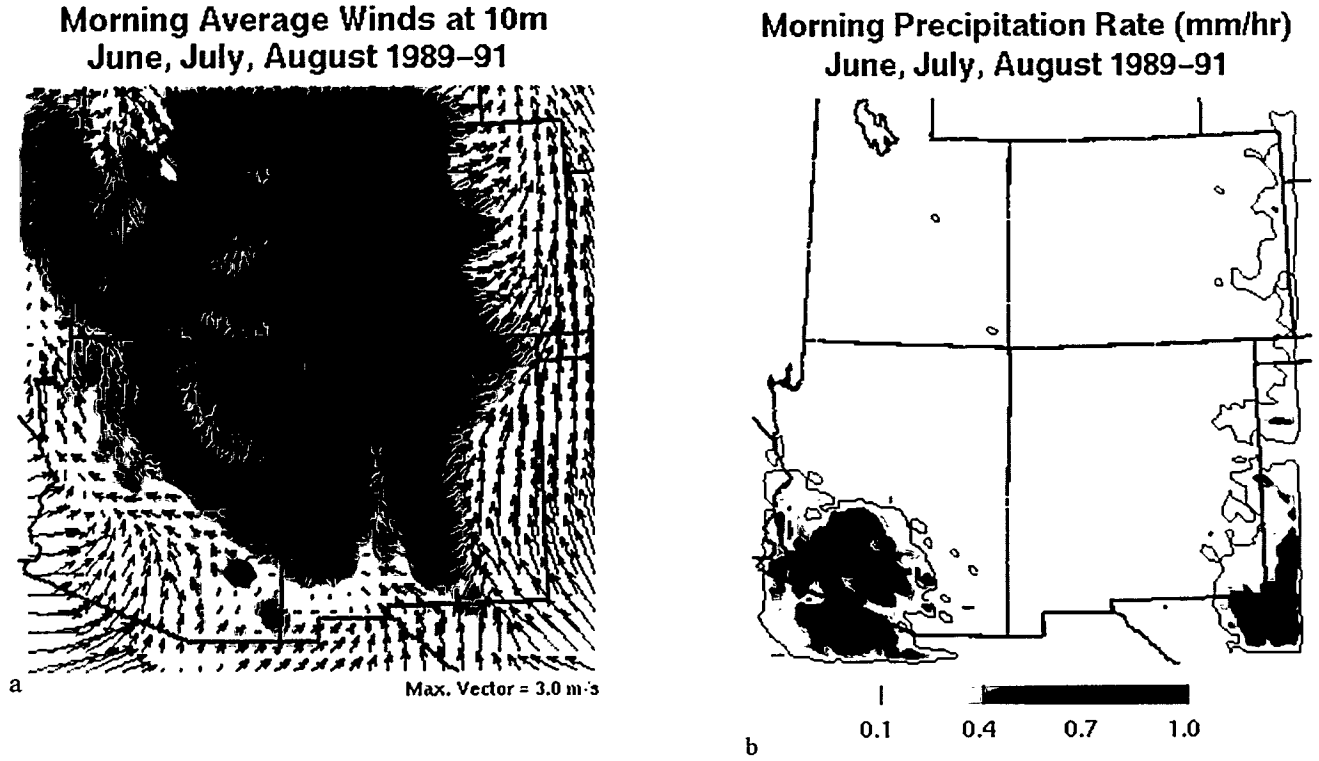
Averaged results from a nine-summer-month (June, July, and August of the years 1989–91) simulation demonstrate the capability of the regional model to produce a representative summer climate of the Southwest (see figures). The results also show the importance of strong summertime thermal forcing of the surface in defining this climate. These simulations allow us to observe the climate at much higher temporal and spatial resolutions than existing observational networks. For instance, the diurnal wind systems over complex mountain terrain shown in the regional climate model have not been previously studied in any detail, simply because of a lack of adequate data. The model also allows us to see the full three-dimensional state of the climate and thereby to deduce the dominant physical processes at any particular time. The information obtained from this regional-modeling approach can greatly enhance our understanding of climate processes and the potential impacts that may arise from variations in land use or large-scale circulation patterns due to global climate change.



A regional air-monitoring system regional climate simulation of June, July, and August 1989-91. (a) Outer grid averaged potential temperature difference field [1700–0500 local standard time (LST)] at 1700 m above ground level. Contours interval is 0.5 K. (b) Outer grid averaged wind vector difference field (1700–0500 LST) at 90 m above ground level. Maximum wind vector is equal to 10.9 m/s.



(a) Inner grid averaged wind vector field at 10 m above ground level for 1700 LST. Maximum wind vector is equal to 6.1 m/s. (b) Simulated average convective precipitation rate (mm/hr) at 1700 LST. Contour interval is 2 mm/hr.



(a) Inner grid averaged wind vector field at 10 m above ground level at 0500 LST. Maximum wind vector is equal to 3.0. (b) Simulated average convective precipitation rate (mm/hr) at 0500 LST. Contour interval is 0.3 mm/hr.

New Mechanism for Lightning Initiation

Robert A. Roussel-Dupré

To distinguish radio-frequency (RF) signals generated by lightning from the electromagnetic pulses produced by nuclear explosions, we must understand the fundamental nature of thunderstorm discharges. The current debate surrounding the origin of transionospheric pulse pairs (TIPPs) detected by the BLACKBEARD RF experiment illustrates this point. The primary goal of our project was to identify the specific role played by runaway air breakdown in terms of thunderstorm electricity and in so doing develop lightning models that predict the optical, RF, and gamma-ray emissions that are observed from space.

Mechanisms for the initiation of lightning have been proposed and studied for decades. In all cases, air breakdown is assumed to occur as a result of the acceleration of thermal seed electrons to ionizing energies by thunderstorm electric fields. Several years ago, we described a new mechanism for air breakdown—which we termed runaway breakdown—that results in an avalanche of energetic electrons, seeded by cosmic rays, and the formation of an electron beam. A significant characteristic of this mechanism is that the threshold field is calculated to be 10 times less than that needed for thermal air breakdown and 2 to 3 times less than the maximum large-scale fields measured in active thunderstorms. One of the unique signatures of runaway breakdown is the strong gamma-ray flux produced when the electron beam interacts with air.

Observational evidence for the runaway mechanism comes from measurements by others of sharp increases in the gamma-ray flux from 5 to 110 keV before lightning strokes. Even more intriguing are recent measurements of high-altitude optical flashes over the tops of thunderstorms and the satellite measurements of gamma-ray and radio flashes that appear to be associated with thunderstorms. Bursts of intense gamma-ray emission from the atmosphere were observed by the Burst and Transient Signal Experiment (BATSE) aboard the Compton Gamma-Ray Observatory (CGRO) when the CGRO was directly over large thunderstorm complexes. The association of these emissions with upward discharges follows directly from the fact that strong atmospheric absorption and scattering limit the source region to altitudes above 25 km. The BLACKBEARD experiment aboard the ALEXIS satellite has measured numerous TIPPs that consist of a time-correlated pair of VHF pulses separated by from 30 to more than 100 μs but having individual full-widths at half maximum of from 3 to 10 μs.

During the first two years of our project, we focused on developing a detailed kinetic theory for runaway breakdown and a corresponding fluid theory for lightning discharges. Two journal articles and a Los Alamos technical report were published describing our results. The mounting evidence for optical flashes over the tops of thunderstorms prompted us to apply our fluid theory to model upward discharges. For high-altitude modeling, we had to modify our existing kinetic code to include the effects of the geomagnetic field. In the second year of our project, we also initiated a series of experiments to look for gamma-ray emissions from cloud-to-ground lightning and began an analysis of satellite gamma-ray data obtained from the Army Beam Experiment (ABE).

This past year, we successfully used our fluid model of runaway breakdown to simulate upward-propagating discharges and reproduce many of the temporal and spatial characteristics of the measured optical flashes termed sprites and blue jets. In addition, we pointed out that the gamma-ray pulses recorded by the CGRO probably originate from the same phenomenon. We also developed a semiempirical model normalized to the optical observations and calculated the expected VHF radio emissions. We succeeded in reproducing many of the characteristics of TIPPs, including their double pulses, their intensity, the time separation between pulses, and the duration of each pulse. A comparison between observation and theory is shown in the accompanying figure.

Three papers describing the ABE gamma-ray measurements have been submitted for publication. CGRO-type pulses were detected, further supporting runaway breakdown as the source of upward discharges, as were frequent occurrences of Trimpi-type precipitation events. We also conducted ground-based experiments to look for gamma-ray emissions from lightning. Although the results are inconclusive, measurements recently obtained from the Ivory Coast in Africa have yielded some interesting temporal coincidences between RF and gamma-ray measurements that could confirm the presence of runaway discharges in lightning. We also participated this year in an experiment in the Ivory Coast to detect ionization from upward-propagating discharges by means of high-frequency sounding and to obtain broadband RF measurements of lightning. We succeeded in measuring echoes from ionization columns produced in the stratosphere and lower mesosphere. The measurements further confirm that runaway

breakdown is the driving mechanism for upward discharges.

In summary, we have developed new models that predict many of the observed characteristics of thunderstorm discharges relating to both the development of leader channels and the details of upward discharges. In the case of the latter, we have been able to reproduce the observed optical flashes known as sprites and to show that TIPP radio emissions and the gamma-ray bursts measured by ABE and the CGRO could originate from these discharges. The BLACKBEARD and FORTE experiments have benefited and will continue to benefit from our results. Several programs at Los Alamos—e.g., the MCG (magnetocumulative generator) Balloon project and the analysis of ABE data—are direct outgrowths of this project.

Publications

Feldman, W.C., E.M.D. Symbalisty, and R.A. Roussel-Dupré, "Association of Discrete Hard X-ray Enhancements with the Eruption of Mount Pinatubo" (to be published in *J. Geophys. Res.*).

Feldman, W.C., E.M.D. Symbalisty, and R.A. Roussel-Dupré, "Hard X-ray Survey of Energetic Electrons from Low-Earth Orbit" (to be published in *J. Geophys. Res.*).

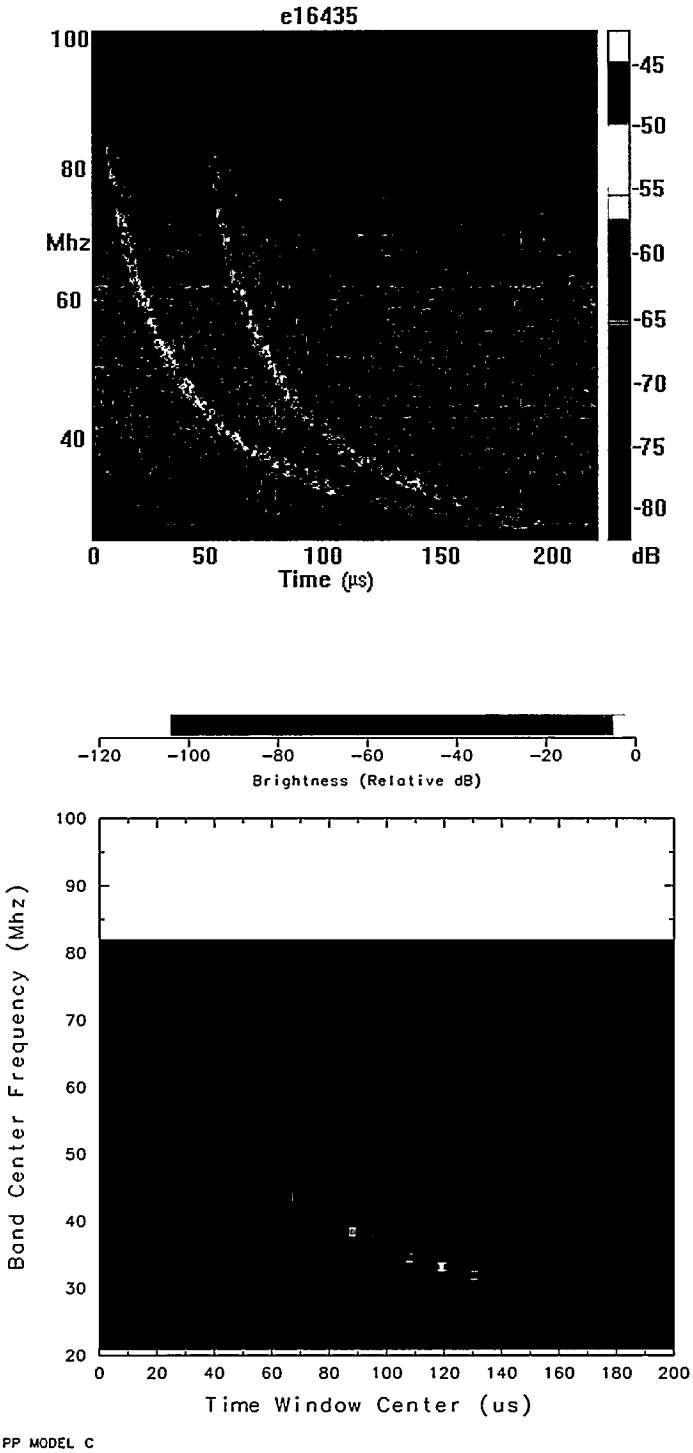
Feldman, W.C., E.M.D. Symbalisty, and R.A. Roussel-Dupré, "Survey of Discrete Hard X-ray Enhancements Observed from Low-Earth Orbit" (to be published in *J. Geophys. Res.*).

Gurevich, A.V., G.M. Milikh, and R.A. Roussel-Dupré, "Nonuniform Runaway Air Breakdown," *Phys. Lett. A* **187**, 197 (1994).

Roussel-Dupré, R.A., and A.V. Gurevich, "On Runaway Breakdown and Upward Propagating Discharges" (to be published in *J. Geophys. Res.*).

Suszcynsky, D.M., R.A. Roussel-Dupré, and G. Shaw, "Ground-based Search for X-rays Generated by Thunderstorms" (submitted to *J. Geophys. Res.*).

Taranenko, Y.N., and R.A. Roussel-Dupré, "High-Altitude Discharges and Gamma-Ray Flashes: A Manifestation of Runaway Air Breakdown" (to be published in *Geophys. Res. Lett.*).



A BLACKBEARD-recorded TIPP event is shown at the top. A sample calculation of radio emissions expected from an upward discharge is shown below. The calculated RF emissions were propagated through a nominal ionosphere with a total electron content of $1 \times 10^{18}\ m^{-2}$.

Macroscopic Time and Altitude Distribution of Plasma Turbulence Induced in Ionospheric Modification Experiments

Harvey Rose

To understand macroscopic spatial and temporal distribution of turbulence induced in the ionosphere by powerful radio waves, we investigated the stability of the observed early-time, horizontally layered turbulence and compared the results to the observed late-time breakup of the layers and the formation of geomagnetic field-aligned irregularities. We used mesoscaling methods to compute the macroscopic-layered equilibrium turbulence state and its stability.

During the final year of this project, we concentrated our research on the time dependence of the heater, induced turbulence, and electron density profiles excited in the ionosphere by a powerful radio frequency heater wave. We then used the mesocaling theory—developed earlier in this project—for these calculations. The macroscopic density is driven by the ponderomotive pressure and the density self consistently determines the heater propagation. For typical parameters of the current Arecibo heater, we found a dramatic quasiperiodic behavior. For about 50 ms after turn on of the heater wave, the turbulence (as observed) is concentrated at the first standing wave maximum of the heater near reflection altitude. From 50–100 ms the standing wave pattern drops by about 1–2 km in altitude and then quasiperiodically reappears at the higher altitudes with a period of roughly 50 ms. This behavior is due to the half-wavelength density depletion grating which is set up by the ponderomotive pressure at the maxima of the heater standing wave pattern. Once the grating is established, the heater can no longer propagate to higher altitudes. The grating is then unsupported by the heater at these altitudes and decays, allowing the heater to propagate again and initiate another cycle. For stronger heater powers corresponding to the Arecibo upgrade and the high-power active auroral research project (HAARP) heater now under construction, the effects are much more dramatic. The important lesson here is that the heater and ionospheric density profiles are not known a priori, as usually assumed, after the first cycle and must be self-consistently determined.

Publications

DuBois, D.F., D. Russell, H.A. Rose, "Reduced Descriptions of Strong Langmuir Turbulence from Kinetic Theory," *Phys. Plasmas* **2**, 76 (1995).

Experimental Studies of Auroral-Arc Generators

David Suszcynsky

One of the major mysteries of magnetospheric physics involves the origin and production of auroral arcs. A three-year study is in progress to identify the auroral-arc generator mechanism(s) using Laboratory geostationary satellite plasma and energetic-particle data and state-of-the-art low-light-level video equipment.

During the past two winters, we have fielded all-sky video cameras in the Alaskan auroral zone at the foot of the magnetic field line that passes through geostationary satellite 1989-046's position. The two campaigns produced simultaneous satellite and ground-based observations of aurorae for nearly 80 days. By comparing the ground-based auroral activity that was observed at the foot of the field line to various plasma and energetic-particle signatures in geostationary orbit, we can evaluate existing models and suggest new models for the auroral-arc generator mechanism(s).

As a first test of the capabilities of our technique, we have begun to compare satellite data with occurrences of pulsating aurorae. Through analysis of the satellite data, we have confirmed that the pulsations are associated with the electron plasma sheet and occur during the recovery phase of auroral substorms. We presented these preliminary studies at the Fall 1994 American Geophysical Union meeting and at the 1995 International Union of Geodesy and Geophysics/International Association of Geomagnetism and Aeronomy meeting and will expand on them in FY96.

Heterogeneous Processing of Bromine Compounds by Atmospheric Aerosols: Relation to the Ozone Budget

Jeanne M. Robinson

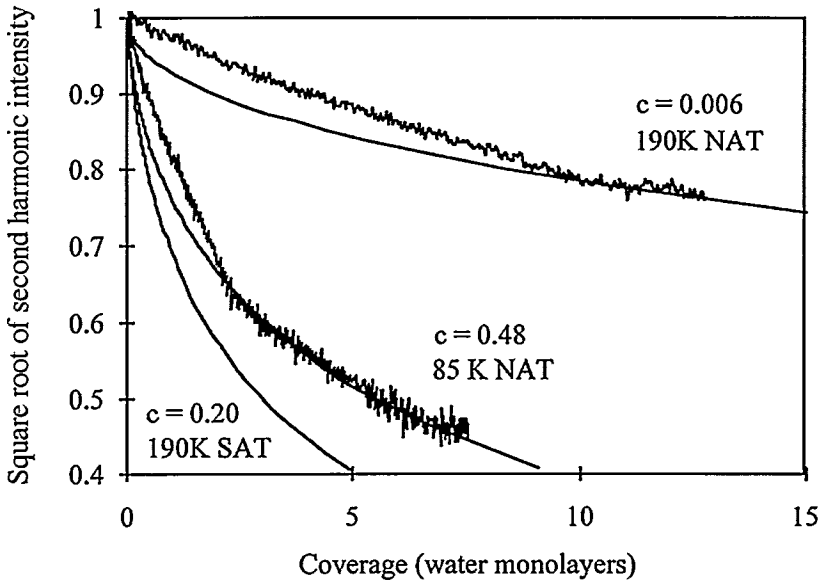
The seasonal depletion of ozone in the Antarctic has attracted considerable attention from the scientific community as well as from the popular press. Despite the progress made in understanding the heterogeneous reactions of chlorine compounds on polar stratospheric particles that dominate this phenomenon, less is known of the analogous bromine mechanisms, even though it has been recognized for two decades that catalytic destruction of ozone by bromine could be more efficient than by chlorine. Field measurements and modeling calculations suggest that these heterogeneous reactions are not restricted to the Antarctic regions but are likely global. The purpose of this project is to investigate the kinetics of the heterogeneous (gas/surface) interaction of bromine compounds on simulated stratospheric and tropospheric aerosols to help elucidate their role in catalytic ozone destruction cycles.

We have used nonlinear light scattering to monitor the evolution of a simulated Type I nitric acid trihydrate (NAT) polar stratospheric cloud particle to a Type II particle by water condensation. Our observed adsorption spectra for this system, and for many other acid/water ice and organic/water ice systems, indicate significant migration of species into our porous, laboratory-grown ices. These results are of considerable importance with respect to modeling the kinetics of surface-mediated processes on laboratory ice substrates because it is clear that reaction is not limited to the small geometric surface of these ice films.

Utilizing recent theoretical results for second harmonic generation (SHG) in scattering media, we have correlated adsorption spectra on films of differing thicknesses with scattering depths calculated using our measured pore distributions. We have formulated a model to explain annealing experiments on HNO_3 ice films based on vapor pressure and surface restructuring arguments. We have examined the photolytic reaction of methyl bromide with ice. We have also combined the published molecular theory of harmonic generation with the theory of harmonic generation in scattering media to simulate the data observed in adsorption and thermodynamics measurements. Our formalism allows the SHG efficiency from an adsorbate/ice system to be rationalized in terms of structure and adsorbate density. We have successfully incorporated a classical multilayer theory of adsorption into this model and used it to explain the adsorption of an organic compound into porous H_2O ice over a 100-K temperature range (see figure).

Publications

Henson, B.F., K.R. Wilson, and J.M. Robinson, "A Physical Adsorption Model of the Dependence of $ClONO_2$ Heterogeneous Reactions on Relative Humidity" (submitted to *Geophys. Rev. Lett.*).



The data are from two experiments in which water was introduced onto a nitric acid monohydrate (NAM) film at 85 and 190 K. The linear regime in the spectra at low coverage may be direct reaction of water with NAM to form the trihydrate, NAT. The curves are fits from the Brunauer, Emmett, and Teller (BET) theory describing the subsequent multilayer physical adsorption of water on NAT. The different c values reflect different adsorption energies on the amorphous (85 K) and crystalline (190 K) NAT. The curve shown for sulfuric acid tetrahydrate (SAT) is calculated from our physical adsorption model; we are currently performing measurements to test this prediction.

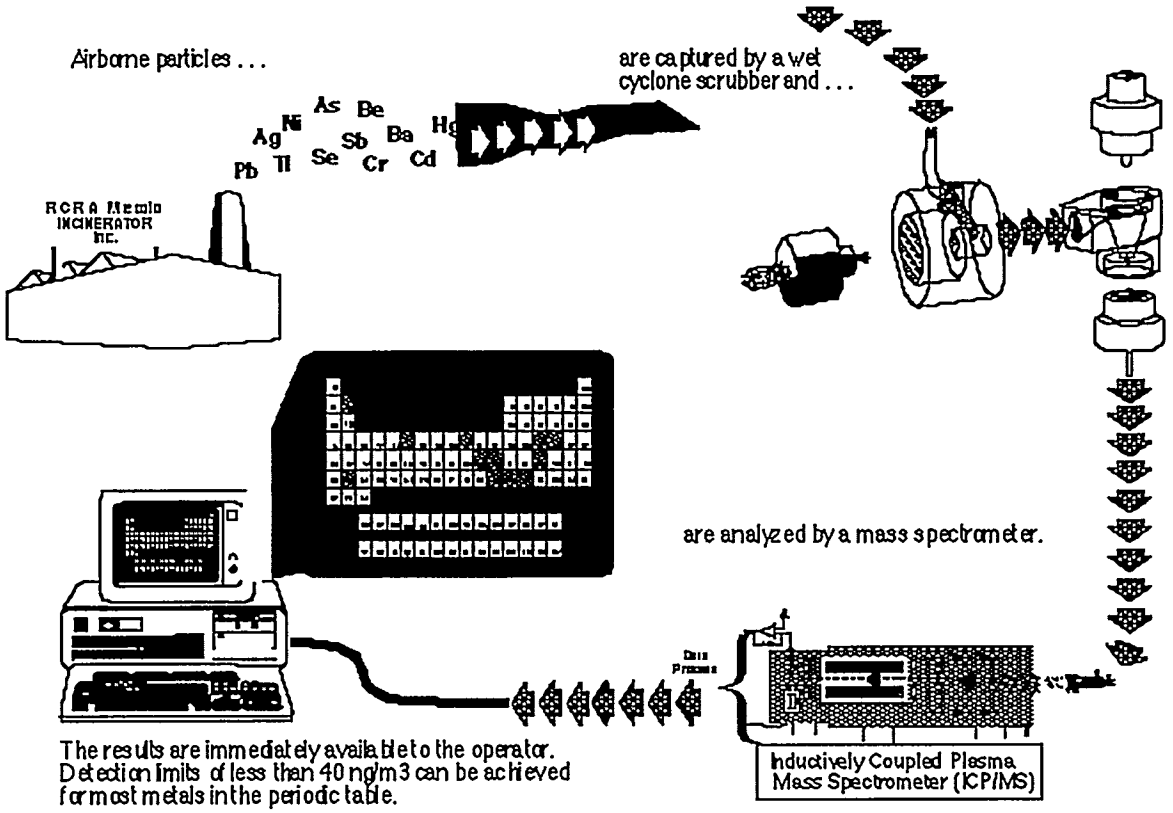
Atmospheric Aerosol Chemistry Analyzer: Demonstration of Feasibility

Eugene Mroz

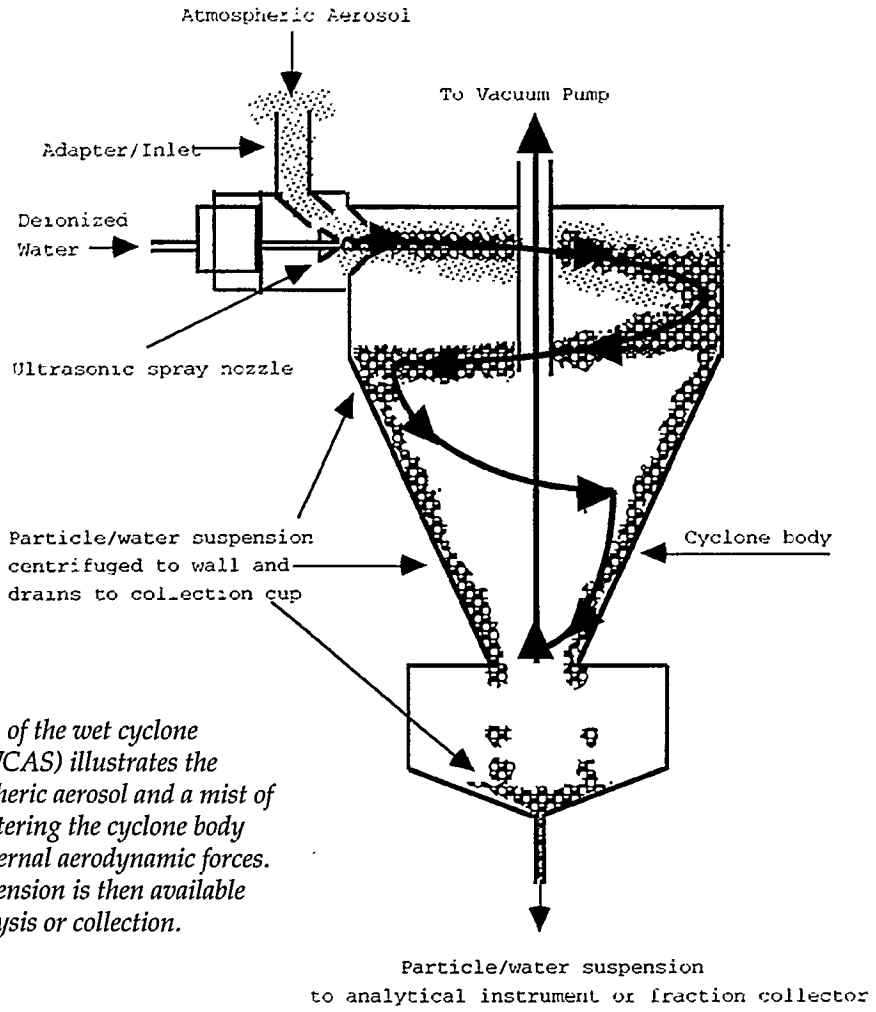
The conventional method for analyzing the chemical composition of atmospheric aerosols is a two-step process: filtration of the particles from air followed by chemical analysis in the laboratory. The utility of this approach is severely impaired because the results are not available in a timely fashion. Our objective was to demonstrate the technical feasibility of an atmospheric aerosol chemistry analyzer (AACA) that will provide a continuous, real-time analysis of major, minor and trace chemical compounds in atmospheric aerosols (see first figure).

The AACA concept is based on sampling the atmospheric aerosol through a wet-cyclone scrubber that produces an aqueous suspension of the particles (see second figure). We can then analyze this suspension for elemental composition by inductively coupled plasma mass spectroscopy or collected for subsequent analysis by other methods. The key technical challenge was to develop a wet-cyclone aerosol sampler suitable for respirable particles found in ambient aerosols. We adapted an ultrasonic nebulizer to a conventional, commercially available cyclone aerosol sampler.

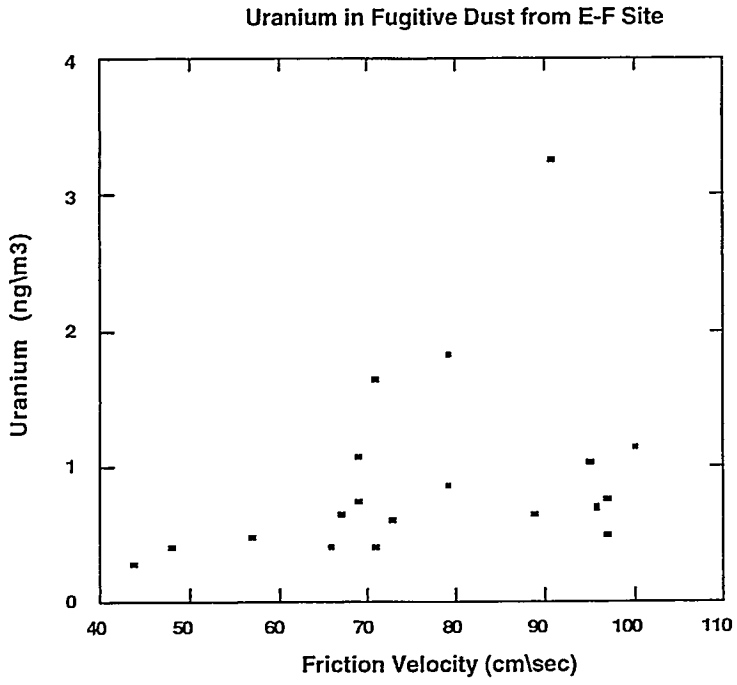
We completed collection-efficiency tests for the wet-cyclone aerosol sampler. The sampler was shown to efficiently collect particles as small as 0.2 microns. In a demonstration experiment we detected as little as 1 ng/m^3 of uranium in aerosols generated by wind erosion of a uranium-contaminated high-explosive firing site (see third figure). We have completed the necessary basic research and have demonstrated the feasibility of the AACA concept. This research has direct application to the characterization and monitoring of respirable particulates from fossil-fueled power plants, incinerators, and other sources of particulate air pollution.



Real-time elemental analysis of atmospheric aerosols.



Schematic diagram of the wet cyclone aerosol sampler (WCAS) illustrates the operation. Atmospheric aerosol and a mist of deionized water entering the cyclone body are collected by internal aerodynamic forces. The resulting suspension is then available for immediate analysis or collection.



Uranium in fugitive dust from an area contaminated with uranium as a function of friction velocity. Note the significant increase in concentration at friction velocities in excess of a threshold of about 70 cm/sec.

Measuring the Magnetic Connectivity of the Geosynchronous Region of the Magnetosphere

Michelle Thomsen

The purpose of this project is to determine the magnetic connectivity of the geosynchronous region of the magnetosphere (~40,000 km from Earth, near the equatorial plane) to the auroral zone in the polar ionosphere in order to test and refine current magnetospheric magnetic field models. We use plasma data from Los Alamos instruments on three geosynchronous satellites and from US Air Force instruments on three low-altitude, polar-orbiting, Defense Meteorological Satellite Program (DMSP) satellites. Magnetic connectivity is tested by comparing plasma energy spectra from the DMSP and geosynchronous satellites when they are in near-conjunction. The times of closest conjugacy (that is, best spectral match) are used to evaluate the field models.

Previously, we developed the tools for each step of the process and applied them to the study of a one-week test set of conjunctions. During the reporting period we automated the analysis and applied it to four months of two-satellite observations. This produced a database of approximately 130 definitive magnetic conjunctions. We compared this database with the predictions of the widely used Tsyganenko magnetic field model and showed that in most cases one of the various parameterizations of the model could reproduce the observed field line connection. Further, we explored various measurables (for example, magnetospheric activity indices or the geosynchronous field orientation) that might point to the appropriate model parameters for these conjunctions, and ultimately, for arbitrary times.

This project has application to space-based treaty verification and to auroral, ionospheric, and magnetospheric phenomena. In addition, it will help clarify the solar wind/magnetosphere interaction, such as during geomagnetic storms.

Publications

Hones, E.W., M.F. Thomsen, G.D. Reeves, et al., "Observational Determination of Magnetic Connectivity of the Geosynchronous Region of the Magnetosphere to the Auroral Oval" (to be published in *J. Geophys. Res.*).

Weiss, L.A., M.F. Thomsen, G.D. Reeves, et al., "An Examination of the Tsyganenko (T89a) Field Model Using a Database of Two-Satellite Magnetic Conjunctions" (submitted to *J. Geophys. Res.*).

Integrating Chemistry into Three-Dimensional Climate Models: Detailed Kinetics in the Troposphere and Stratosphere of a Global Climate Model

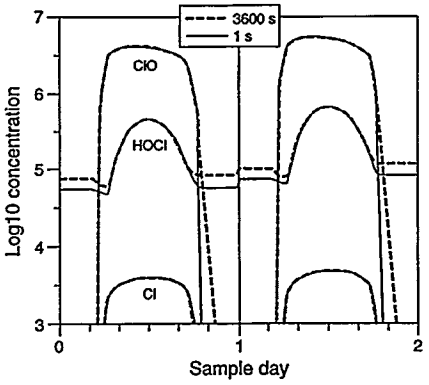
Chih-Yue J. Kao

Several atmospheric gases including ozone and methane are both radiatively and kinetically active, influencing global climate but controlled by photochemical processes. The role of such gases in the terrestrial climate system has generally been simulated either in low dimensionality or with chemistry decoupled from dynamics. Three-dimensional chemical models have been compromised by focusing on either above or below the tropopause. The goal of our project is to overcome these limitations by incorporating kinetics interactively into both the troposphere and stratosphere of a general circulation model, providing the first full simulation of global photochemistry.

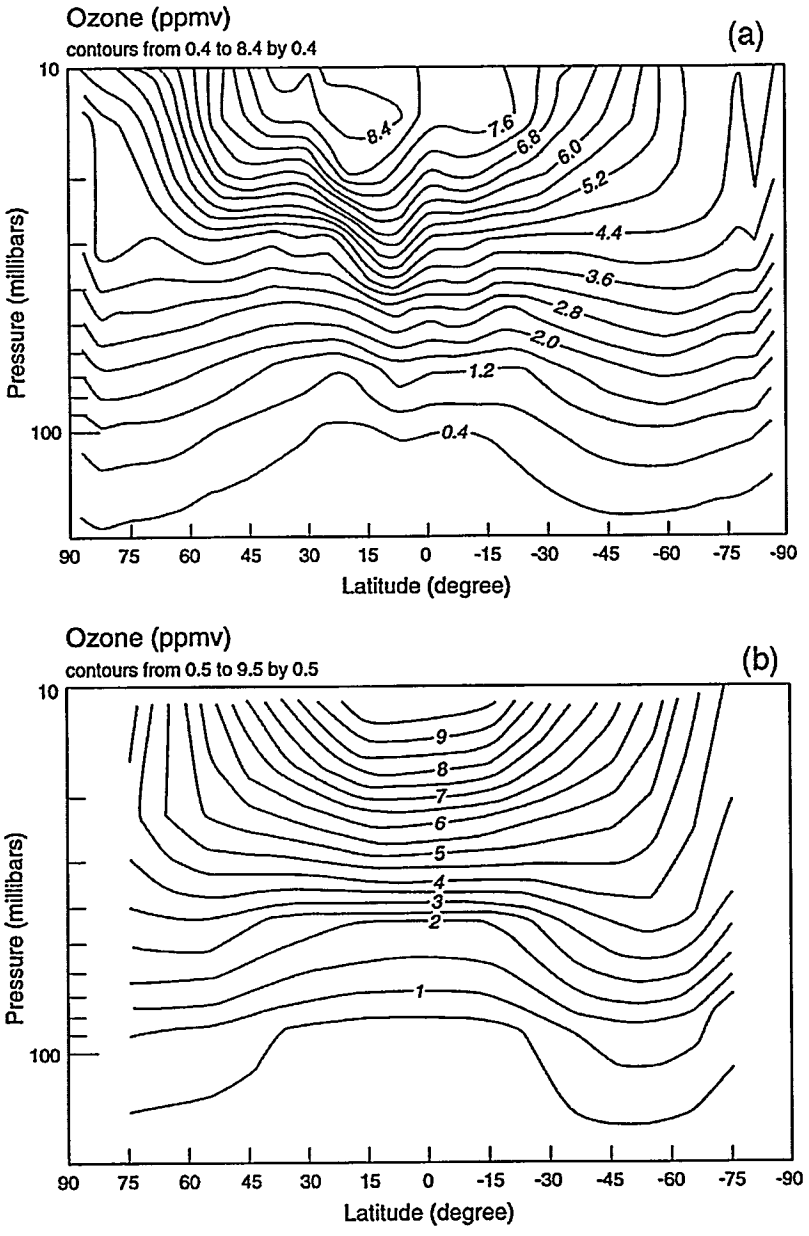
During the first two years of this project, the major problems in three-dimensional photochemistry modeling in terms of computational speed, numerical instability, and conservation of mass for chemical species have been remedied with our improved numerics and automation and with a novel chemical parameterization. Our stratospheric photochemical module includes all the required chemical families—45 species, 99 kinetic reactions, and 30 photodissociation processes. The accompanying figures demonstrate its success: our parameterized chemistry with a time step of 1 h agrees well with a fully resolved chemical scheme with a time step of 1 s, and incorporating this chemistry in the Laboratory's low-resolution climate model produces ozone distributions that agree with satellite data. In the tropospheric regime, we have utilized automated continuity equations to experiment with organic oxidation chains affecting

ozone and methane distributions. An integrator with complete hydrocarbon kinetics developed by co-workers at the University of California at Los Angeles has been successfully tested.

Our complete photochemical module is now being incorporated in the the newest version of the Community Climate Model—CCM2—from the National Center for Atmospheric Research. Recent tests at Los Alamos with a multidecade simulation of CCM2 indicate that the model is very robust, which leads us to be optimistic about its modeling capabilities once our chemistry module is fully incorporated.



Comparison of ClO_x concentrations in a 1-h time-step integration with our numerics vs a 1-s time-step integration with individual species fully resolved; concentrations are at 20 km, 45-deg N latitude from a 5-day zero-dimensional model run. The close agreement demonstrates the fidelity of our parameterized chemistry.



Monthly and zonally averaged meridional distributions of global ozone in parts per million by volume for September: (a) three-dimensional global model results, and (b) derived data from satellite measurements. Again, agreement between the simulation and data is very good.

Publications

Elliott, S., C.-Y.J. Kao, F. Gifford, et al., "Free Tropospheric Ozone Production after Deep Convection of Dispersing Tropical Urban Plumes," (submitted to *Atmos. Environ.*).

Elliott, S., M. Shen, C.-Y.J. Kao, et al., "A Streamlined Family Photochemistry Module Reproduces Major Nonlinearities in the Global Tropospheric Ozone System," (to be published in *Comput. Chem.*).

Elliott, S., P. Turco, X. Zhao, et al., "Efficient and Modular Kinetics for Global Scale Photochemical Modeling," *J. Appl. Meteorol.* 34, 694 (1994).

Kao, C.-Y.J., S. Barr, A. Quintanar, et al., "Numerical Modeling of Tracer Transport Within and Out of the Lower Tropospheric Arctic Region," *Geophys. Res. Lett.* 22, 941 (1995).

Particle Acceleration from Reconnection in the Geomagnetic Tail

Joachim Birn

One of the major consequences of the reconfiguration of the geomagnetic field (created by magnetospheric substorms and the underlying magnetic reconnection process) is the acceleration of charged particles and their injection into the near-tail region of the magnetosphere and ionosphere. The goal of our project is to investigate this acceleration process using self-consistent, three-dimensional magnetohydrodynamic (MHD) simulations and by tracing test particles in electromagnetic fields.

Previously, we were able to identify the dawn flank of the magnetotail as the major source of accelerated ions. We also discovered two different acceleration mechanisms. One is the presence of a strong cross-tail electric field in the neutral sheet of the magnetotail and in some vicinity of a near-earth magnetic neutral line. An additional mechanism is based on multiple encounters of the acceleration region with intermediate mirroring closer to the earth.

Recent observations in the earth's magnetotail have identified the importance of the formation of a thin current sheet in the transition region between the dipole field and the tail for the dynamic reconfiguration. We have therefore included this region and the current sheet formation into our recent MHD modeling in order to attain more realistic results for the associated particle acceleration. The MHD results indicate a much stronger, more rapidly rising electric field in the region earthward of the reconnection site, which has important consequences for the energy gain and the increase in particle fluxes.

Publications

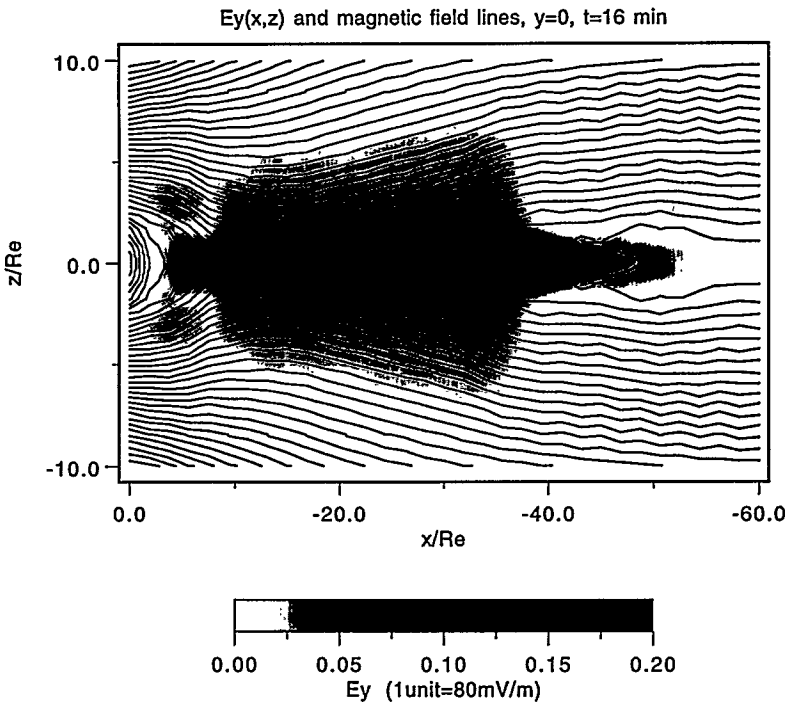
Birn, J., S.P. Gary, and M. Hesse, "Microscale Anisotropy Reduction and Macroscale Dynamics of the Magnetotail" (to be published in *J. Geophys. Res.*).

Birn, J., and M. Hesse, "Details of Current Disruption and Diversion in Simulations of Magnetotail Dynamics" (to be published in *J. Geophys. Res.*).

Birn, J., M. Hesse, and K. Schindler, "MHD Simulations of Plasmoid Formation and Current Disruption" (to be published in *J. Geophys. Res.*).

Gosling, J.T., J. Birn, and M. Hesse, "Three-Dimensional Magnetic Reconnection and the Magnetic Topology of Coronal Mass Ejection Events Isobaric Constraints," *Geophys. Res. Lett.* **22**, 869 (1995).

Moldwin, M.B., M.F. Thomsen, S.J. Bame, et al., "Flux Dropouts of Plasma and Energetic Particles at Geosynchronous Orbit During Large Geomagnetic Storms: Entry into the Lobes," *J. Geophys. Res.* **100**, 8031 (1995).



Magnetic field lines (solid contours) and cross-tail electric field intensity (grey scale) in the midnight meridian plane of the magnetotail. The figure demonstrates the reconfiguration of the tail associated with geomagnetic substorms, obtained from a magnetohydrodynamic simulation. The earth is outside the simulation domain to the left at a distance of about 5 earth radii.

Stochastic Imaging of Oil and Gas Reservoirs

Michael Fehler

In this project, we have been developing and testing methods for modeling and inverting wave propagation through complex geologic media (i.e., media that are cut by faults and that include salt layers and domes). Such modeling has applications to petroleum, natural gas, and geothermal exploration and to earthquake assessments such as predicting an area's susceptibility to seismic activity.

To date we have developed four methods of modeling wave propagation in media with both deterministic (well-defined) and stochastic components: (1) an efficient but approximate method for modeling wave propagation in complex media, (2) an exact method for modeling wave propagation in complex media using a boundary integral approach, (3) a method for determining the properties of a one-dimensional media composed of thin layers, each layer with random thickness and velocity, and (4) a method of modeling the diffraction and resonance due to a low-velocity body (i.e., a medium such as magma).

Most of our work during the past year focused on extending the approximate method to include the effects of singly reflected waves; such an extension is essential for modeling seismic data collected by the petroleum industry. In addition, we worked on quantifying the method's limitations. Although very fast, the approximate method is not always accurate. We are developing a mathematical approach to quantifying its errors such that we can determine its suitability for specific classes of models.

Publications

Wu, R.-S., "Synthetic Seismograms in Heterogeneous Media by One-Return Approximation," (submitted to *Pure Appl. Geophys.)*

Wu, R.-S., and L.J. Huang, "Reflected Wave Modeling in Heterogeneous Acoustic Media Using the De Wolf Approximation," in *Mathematical Methods in Geophysical Imaging III*, S. Hassanzadeh, Ed. (SPIE, Bellingham, Washington, 1995), pp. 176-186.

Flare Star Monitoring with a New Single-Photon-Counting Imaging Detector

Donald Casperson

Our project uses a state-of-the-art, single-photon-counting imaging detector with high spatial and temporal resolution in a ground-based astronomy experiment. The new microchannel plate with crossed delay line (MCP/CDL) detector enables us to record and characterize flares from low-luminosity red dwarf stars that deposit only a few tens of photons in our telescope-detector-readout system. This permits us to carry out a broad survey of the general galactic population of the flaring phase of red dwarf star evolution with a single-photon-counting sensitivity. This survey also provides an opportunity to search for optical transients from other, perhaps as yet undetected, phenomena.

We completed the procurement of a new custom-designed 30-cm aperture f/7 telescope for use with the MCP/CDL detector for observations in the visible and ultraviolet bands and collected some preliminary images through it. The aperture and field of view of this telescope take advantage of a higher count-rate capability in the MCP/CDL detector electronics that are currently undergoing an upgrade to a peak count rate of five million photons per second. We also received a new MCP/CDL detector with a high-quality visible photocathode during the reporting period. This new detector and new telescope will permit us to collect high-resolution data during the last year of the project. To this point we have collected our data with several smaller telescopes and with an MCP/CDL detector that had reduced quantum efficiency and reduced spatial resolution.

Our other accomplishments include modifications to an azimuth-elevation mount with star-tracking capabilities for the new telescope and the first visible-band images taken through the new telescope at a remote operations observing session in the Jemez mountains. At an International Astronomical Union Colloquium on Flares and Flashes held in Sonneberg, Germany, we presented a paper and generated interest in some alternative uses for the new detector, such as the search for optical counterparts to gamma-ray bursts. We are now awaiting completion of an upgraded set of readout electronics that will boost the photon count rate from the MCP/CDL by a factor of 10.

Minerals of the Earth's Deep Interior

David Schiferl

The mineral silicate perovskite $(Fe/Mg)SiO_3$ is believed to make up the bulk of the lower mantle and therefore to be the most abundant mineral in the earth. Determining the density and elastic modulus of this material as a function of pressure (P), temperature (T), and Fe/Mg fraction is crucial for resolving the question of whether there is layered- or whole-mantle convection. The nature of the seismic velocity and density discontinuity at the 670 km depth (the boundary between the upper and lower mantle, with T about 1900 K and P about 23 GPa) has been a major geophysical issue for over a decade. A phase change at this depth would not seriously inhibit mantle convection through the discontinuity. A density discontinuity due to a change in the composition could inhibit thermally driven convection between the upper and lower mantle. The best measurements made before this work are not even close to providing the accuracy needed to measure the densities involved.

Our principal objective is to obtain accurate measurement of densities on the candidate minerals over a considerable range of P and T to help interpret seismic data and to impose strong constraints on possible mantle compositions. In the absence of phase transitions, we can extrapolate densities and sound velocities with confidence at much higher P and T. These data should provide a major step toward resolving the decades-old controversy over whether there is whole-mantle or layered-mantle convection.

We are determining crystal structures with single-crystal x-ray diffraction using a unique high-P/high-T diamond-anvil cell (DAC) that was specially designed at the Laboratory for such measurements in conditions of up to 1000 K at 20 GPa. We measure temperatures with thermocouples and determine pressures from the lattice constants of CsCl, NaCl, or gold by using their known equations of state.

We have obtained highly accurate thermoelastic parameters (such as bulk modulus and thermal expansion) on $MgSiO_3$ in its orthoenstatite and silicate perovskite forms with our unique DACs for single-crystal x-ray diffraction at simultaneous high P and T. In the course of this work we have made a major breakthrough in high P-T x-ray-diffraction technology.

Much more data is required to draw conclusions about the earth's mantle. In the meantime, we have shown that our assembly of new techniques provides extremely good data under exceptionally well-characterized P-T conditions, and we have broken all previous records for single-crystal x-ray diffraction at high P-T.

Publications

Schiferl, D., and Y. Zhao, "High-Pressure/High-Temperature Diamond-Anvil Cell System for Single-Crystal X-Ray Diffraction up to 20 GPa at 1000 K" (to be published in *Rev. Sci. Instrum.*).

Zhao, Y., D. Schiferl, and T.J. Shankland, "A High P-T Single-Crystal X-Ray Diffraction Study of Thermoelasticity of $MgSiO_3$ Orthoenstatite" (to be published in *Phys. Chem. Miner.*).

Zhao, Y., D. Schiferl, and J.M. Zaug, "RSCU-SOS: A Rapid Searching and Centering Utility Routine for Single-Crystal X-Ray Diffraction Studies at Simultaneous High Pressures and High Temperatures" (to be published in *J. Appl. Crystallogr.*).

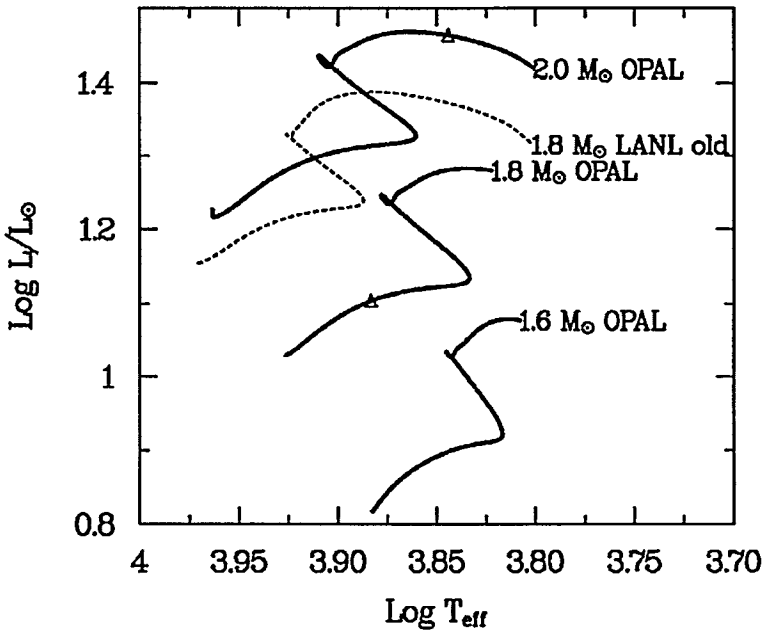
Deriving the Structure of Presupernovae and δ-Scuti Stars Using Nonradial Oscillations

Joyce Guzik

We are modeling the evolution and pulsation of luminous blue variables (LBVs) and δ-Scuti stars. LBVs are massive stars and Type II supernova progenitors, while δ-Scuti variables are slightly more massive than the sun. Both types of stars pulsate in multiple, nonradial modes with significant amplitudes throughout the interior; we can use these modes to probe stellar structure. We are improving the model physics and comparing predicted and observed pulsation properties to determine the structure of these stars. The study of stellar interiors can contribute to the understanding of fundamental physics, such as material properties of dense plasmas, energy transport, and turbulence. The work performed in this project has application to thermodynamics, nuclear and plasma physics, fusion, and computer modeling.

This year we implemented new opacities and a new equation of state in our modeling codes, and find that these changes signifi-

cantly affect the evolution and pulsation frequencies (see figure). We are attempting to match the 19 pulsation frequencies recently reported for the δ-Scuti star FG Virginis and will use the discrepancies as clues to remaining deficiencies in model physics. For LBVs we find that radial "strange modes" are unstable; these modes potentially grow to large amplitudes and may be responsible for LBV outbursts. We find that the matter temperature differs from the radiation temperature near the surface of LBVs, and we are implementing a nonequilibrium diffusion treatment that should modify our frequency predictions. We presented results at an international stellar pulsation conference in Cape Town, South Africa, in February 1995.



Evolution tracks of models in the Hertzsprung-Russell diagram (the log of the luminosity vs the log of the surface temperature) for 1.6, 1.8, and 2.0 solar-mass models. The solid lines show the evolutionary path of models with the new Lawrence Livermore National Laboratory opacity-library (OPAL) opacities, and the dashed line is the evolutionary track of a 1.8 solar-mass model using old Los Alamos National Laboratory opacities. FG Virginis is a well-studied d-Scuti star being modeled by Guzik and Bradley. It lies closer to the 1.8 solar mass OPAL evolutionary track. If the researchers had used the old Los Alamos tracks, FG Virginis would lie close to the 1.6 solar mass track in a more-advanced evolutionary state.

Publications

Rogers, F. J., F. J. Swenson, and C. A. Iglesias, "OPAL Equation of State Tables for Astrophysical Applications" (to be published in *Astrophys. J.*).

Remote Sensing of Thundercloud Electric-Field Airglow

Joseph Borovsky

The purpose of this project is to determine what information can be gathered by examining 391.4-nm emission from thunderclouds and lightning. The 391.4-nm emission from air indicates the presence of energetic electrons. For thunderclouds we expect enhanced 391.4-nm emission to occur from regions where the thundercloud electric fields are strong enough to accelerate cosmic-ray secondary electrons. For lightning the emission of 391.4-nm photons would be an indicator that energetic electrons are produced in the discharge.

The objectives of this project are the following: (1) to use photometers to experimentally confirm the electric-field enhancement of the cosmic-ray-produced airglow near thunderclouds, (2) to measure the magnitude of the emission enhancement with photometers and to compare the measurements with models, and (3) to spatially image the regions of enhanced airglow around thunderclouds.

We have collected records of diurnal and nocturnal lightning strokes in the Los Alamos area with no evidence of significant 391.4-nm emission compared with slightly off-band emission. We tested our equipment against the "Teller Light" created by an alpha-particle source in laboratory air and found the contrast between on- and off-band 391.4-nm emission to be marginal. We rehabilitated and calibrated a Cary 17 photometer that had been in storage and were surprised to find that two of its Barr interference filters had been made improperly. The errors in manufacture were enough to have allowed us to miss anomolous 391.4-nm emissions even if they had been present at significant intensity. The manufacturer has accepted responsibility for these errors, and we are prepared to begin our new campaigns with the precisely correct interference filters.

We have collected large numbers of lightning events with digital oscilloscopes that can acquire data for long time histories. We have observed both the real rise time of the optical emission as well as the pulse trains of breakdowns. The rise time we see, of course, may be dominated by continuum emission.

Publications

Borovsky, J., "Lightning Energetics: Estimates of Energy Dissipation in Channels, Channel Radii, and Channel-Heating Risetimes" (to be published in *J. Geophys. Res.*).

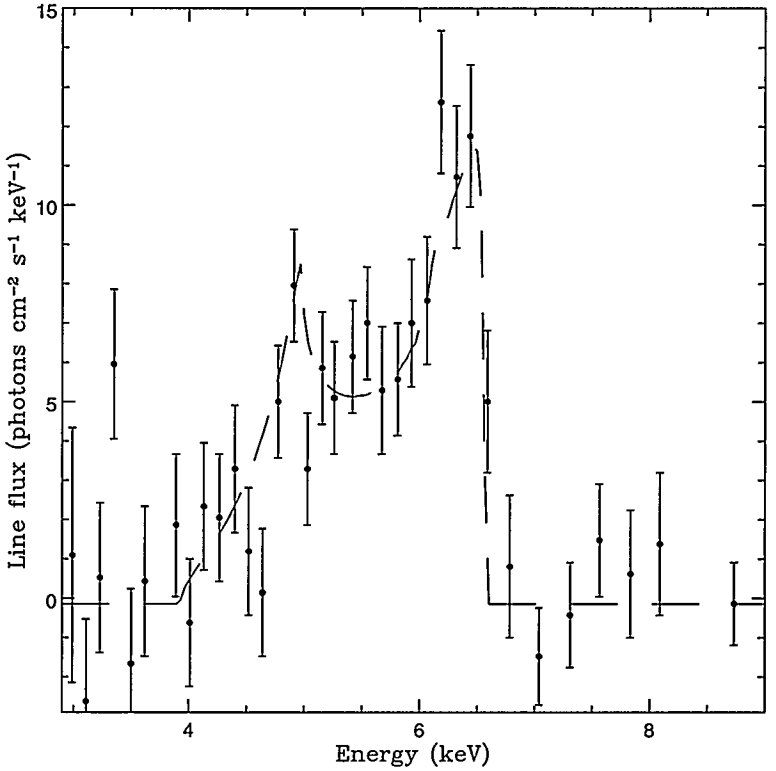
Buchwald, M.I., and J. E. Borovsky, "Time-Resolved Photometry of Lightning and Thunderclouds near 391.4 nm," *Trans. Am. Geophys. Union* 75, 99 (1994).

The Powering of Black Hole Objects by Accretion

Warner Miller

Most objects in the observable universe have a reasonable explanation in terms of physics although the details in depth may be missing or inconsistent. The outstanding few where the basic concept is still elusive are gamma-ray bursts and the combination of quasars, so called active galactic nuclei (AGN), and their associated collimated radio sources or jets. Our project is directed towards a consistent model of AGN and their jets.

We believe it to be most likely that the first objects formed in galaxies started with an accretion disk and a black hole (a quasar). Subsequently, rapid star formation occurred and, along with it, the generation of a magnetic field. This model offers a global view of our research in general relativity, star-disk collisions, star-black hole collisions, collimated radio sources, and dynamo theory. We have calculated, with K. Chen, the line shape of the iron x-ray line emission from the innermost stable orbit around a Kerr black hole. This line shape is the first direct evidence of a general relativistic effect and substantiates black holes in quasars (see graph). We proposed a theory of disk formation from the Lyman-alpha cloud. Star collisions later feed the black hole. This combination is sufficient to create a dynamo and, furthermore, sufficient to generate the galactic magnetic flux and the collimated radio sources (see Disk Dynamo illustration). In collaboration with M. Fullbright and W. Benz, we can now express with an analytical scaling law the ratio of mass accreted and the mass ejected in star-black hole encounters. This simplification of the tidal capture and loss of stars allows a direct understanding of the feeding of a black hole. We worked on Regge calculus with D. Holz and Arkady, galactic gamma bursts with P. Leonard, the ring and millisecond pulsar of Supernova (SN) 1987A with K. Chen,



The very recent detection of the broad-line profile of an x-ray iron-potassium alpha line (rest energy at 6.4 keV) from a Seyfert galaxy, MCG-6-30-15 [Y. Tanaka et al. "Gravitationally Redshifted Emission Implying an Accretion Disk and Massive Black Hole in the Active Galaxy MGC-6-30-15," Nature 375, 659 (1995).]. The broad-line profile is consistent with what might be expected from a relativistic accretion disk with size extended from 3 to 10 Schwarszchild radius ($2GM/c^2$) (dashed line).

SN1A theory with C. Fryer and K. Hand, and a neutrino rocket with M. Herant.

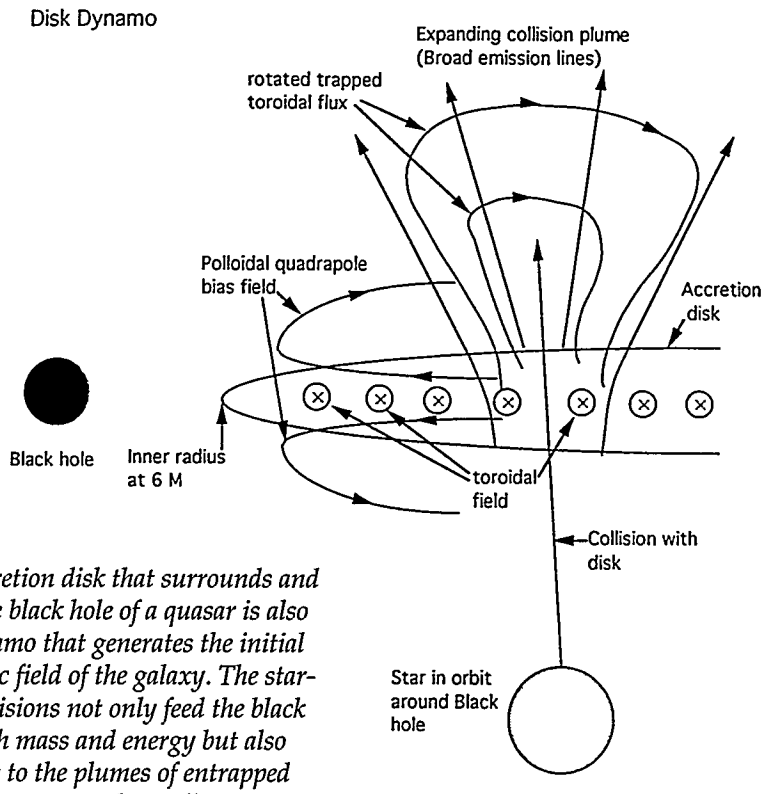
Publications

Barret, J., W.A. Miller, R. Sorkin, et al., "An Implicit Evolution Algorithm for Regge Calculus" (to be published in *Class. Quantum Grav.*).

Colgate, S. and K. Chen, "The Formation of Inner Ring Around SN 1987A and the Emergence of a MS Pulsar" (submitted to *Astrophys. J.*).

Herant, M., W. Benz., W.R. Hix, et al., "Inside a Supernova: A Powerful Convective Engine," *Astrophys. J.* 435, 339 (1994).

Kheyfets, A. and W. Miller, "The Initial-Value Problem in Tetrad Gravity" (submitted to *Int. J. Theor. Phys.*).



The accretion disk that surrounds and feeds the black hole of a quasar is also the dynamo that generates the initial magnetic field of the galaxy. The star-disk collisions not only feed the black hole with mass and energy but also give rise to the plumes of entrapped flux that generate the α effect or rotation of the flux of the dynamo.

Plasmasphere Refilling: New Numerical and Computational Tools

Dan Winske

The goal of this project is to use a newly developed Laboratory capability to model semicollisional plasmas—along with Los Alamos plasma data from satellites in geosynchronous orbit and related theoretical analysis—to construct a computer model to study the fundamental and long-standing problem of refilling the plasmasphere after a geomagnetic storm. The plasmasphere is a region of cold plasma near to and rotating with the earth.

We use the computer model to follow the initially collisional flow from the ionosphere as it becomes collisionless at higher altitudes and to study the interaction of the flows at the magnetic equator through classical and anomalous collision processes. We use satellite data to verify the computer model. During the past year the computer model has been used to study how the outward flow of plasma is enhanced by the pondermotive force resulting from Alfven waves propagating down into the ionosphere. We have also investigated the scattering of outward-flowing ions by electromagnetic instabilities produced by hot ring-current ions.

The work performed in this project can be applied to auroral, ionospheric, and magnetospheric phenomena; plasma kinetics, transport, and impurities; and plasma waves, oscillations, and instabilities.

Publications

Gary, S.P., M.B. Moldwin, M.F. Thomsen, et al., "Hot Proton Anisotropies and Cool Proton Temperatures in the Outer Magnetosphere," *J. Geophys. Res.* 99, 23603 (1994).

Gary, S.P., M.F. Thomsen, D. J. McComas, et al., "Warm Protons at Geosynchronous Orbit" (to be published in *J. Geophys. Res.*).

Gary, S.P., M.F. Thomsen, L. Yin, et al., "Electromagnetic Proton Cyclotron Instability: Interactions with Magnetospheric Protons" (to be published in *J. Geophys. Res.*).

Miller, R.H., C.E. Rasmussen, M.R. Combi, et al., "Pondermotive Acceleration in the Auroral Region: A Kinetic Simulation" (to be published in *J. Geophys. Res.*).

Experimental Cosmology: The Early Universe after Cosmic Microwave Background Explorer

Wojciech H. Zurek

The cosmic background explorer (COBE) detection of microwave background anistropies (and its more recent confirmations and refinements) has redefined the field of cosmology. COBE has provided solid evidence that—in the early universe—there existed sufficient density perturbations to act as seeds for gravitational development of the present-day structures. COBE has also normalized the power spectra of predicted density perturbations by competing theories on very-large scales.

Our objective in this project was to supply a "missing link" between cosmological models and observations by evaluating the consequences of nonlinear aspects of cosmological evolution. N-body tree code simulations on parallel supercomputers have allowed these evaluations. We have focused on scales of 100–1000 megaparsecs to directly confront cosmological models with observations.

Over the past year we have made significant progress in understanding structure formation in a cosmological context. In particular, we have performed the first N-body simulations of cluster formations of cold dark matter (CDM) cosmology. In these simulations, we have discovered that individual galaxies falling into the cluster do not "dissolve" as a consequence of the tidal forces of the cluster core. Instead, each of the galactic halos becomes gradually stripped in the course of the repeated encounters with the cluster core, but more than 95% of them survive over the lifetime of the model universe (see our first accompanying figure).

We have also investigated the velocity distribution of galactic halos. We have shown that for halos separated by a typical distance between neighboring galaxies (i.e., approximately one megaparsec), the distribution is exponential (rather than, say, Maxwellian) in the velocity difference between them. Recent observational results confirm this prediction, which has attracted a lot of attention from the cosmological-structure-formation community.

Our results indicate that much of the discrepancy between past CDM model simulations and observations is not due to a problem of the model but is a result of the poor resolution of the "old" simulations. In particular, this was the case with the indicators of power on small scales: when the galaxies are modeled as many particle halos (rather than as individual particles), the discrepancy between the CDM model and observations becomes statistically insignificant (see second figure).

Publications

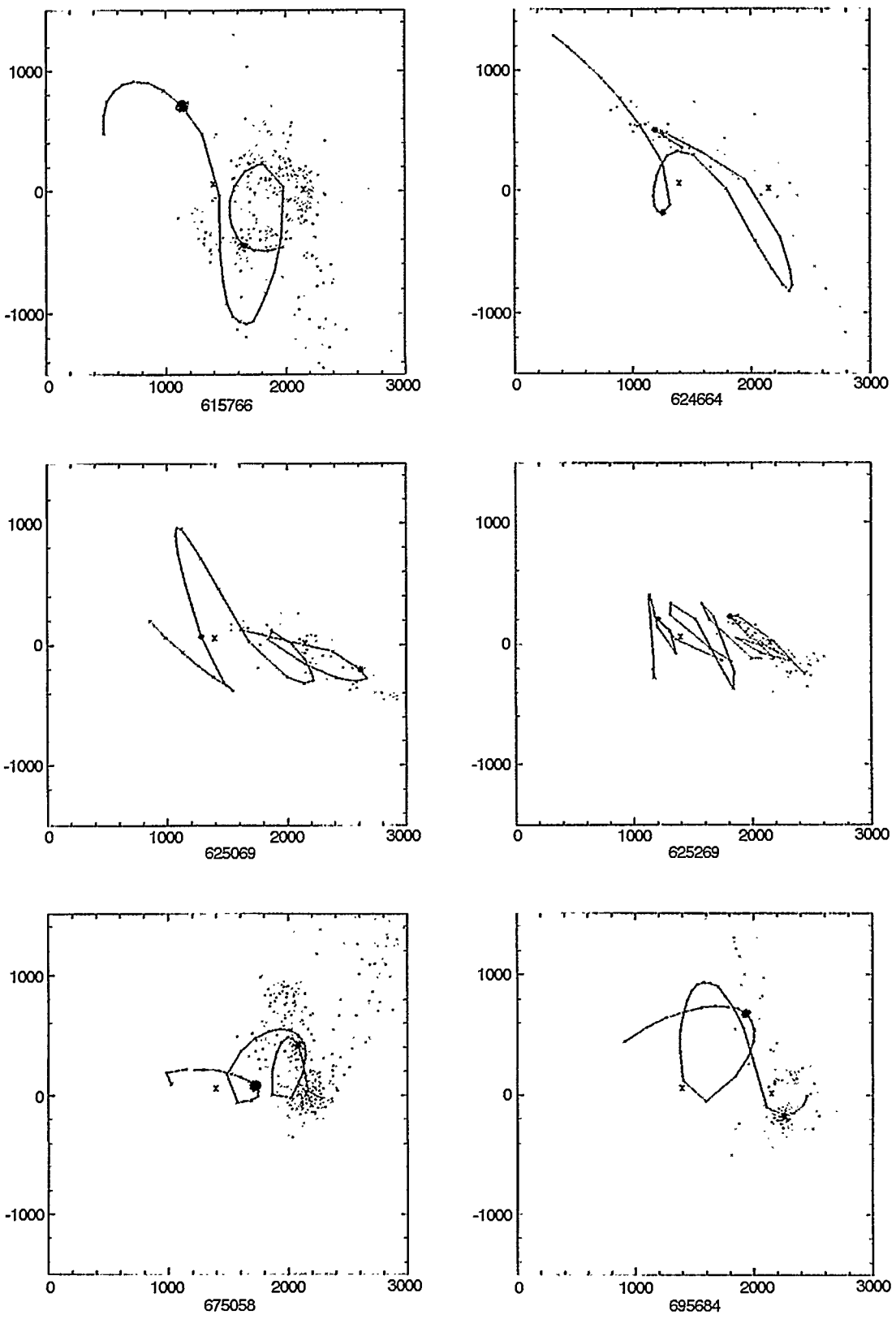
Bromley, B.C., "Finite Size Gravitational Lenses" (submitted to *Astrophys. J. Suppl. Ser.*).

Bromley, B.C., "Quasirandom Number Generators for Parallel Monte Carlo Algorithms" (to be printed in *J. of Parallel and Distributed Comput.*).

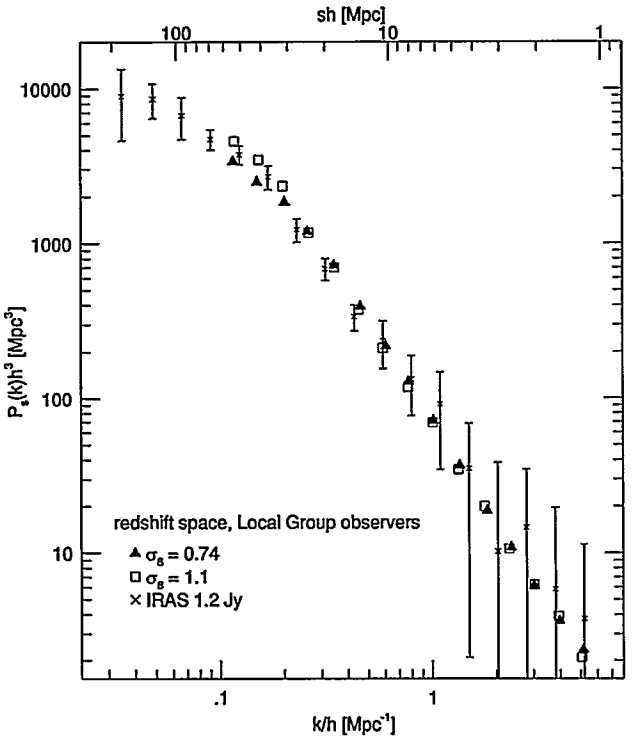
Tegmark, M. and B.C. Bromley, "Real-Space Cosmic Fields from Redshift-Space Distributions: A Green Function Approach" (submitted to *Astrophys. J.*).

Warren, M.S. and J.K. Salmon, "A Portable Parallel Particle Program," *Comput. Phys. Commun.* 87, 266 (1995).

Zurek, W.H., A. Siemiginowska, and S.A. Colgate, "Star-Disk Collision and the Origin of the Broad Lines in Quasars," *Astrophys J.* 434, (1994).



Galactic halos in the cluster. The initial position of six of the approximately 50 halos is marked early on in the evolution of the universe (i.e., at the redshift corresponding to the universe at one-third of its present age and before the collapse of the cluster) and "now." Halos are partially stripped of matter as they move in the potential of the cluster, but almost all of them survive. (The actual halo orbits are more regular—the sharp angles shown are a result of not being able to sufficiently retain many "snapshots" of the evolving model universe. Connecting the twenty or so points retained with sections of a straight line gives an idea of what the trajectory was.)



Comparison of the power spectra obtained from the cold dark matter simulations for two plausible normalizations (triangles and open squares) and observations (from the infrared IRAS satellite catalogue of galaxies).

The Detectability of Asteroids and Comets before Earth Impact

J. G. Hills

This project investigates what is required to detect asteroids and comets in the final years before they impact Earth. We shall determine the equipment and strategies needed to detect impacting asteroids and comets in all their permitted orbits. When this information is combined with the properties of possible mechanisms to divert asteroids, we will be able to determine the degree of readiness and the minimum capabilities of the deflection mechanisms required to prevent impact of these objects with Earth.

Thus far, searches for Earth-crossing asteroids (ECAs) have been concentrated near solar opposition—along a line directed from Earth to the sun. This search strategy has an inherent bias evident in a published analysis of the effectiveness of the proposed NASA Spaceguard system, which will use four to six 2-m Schmidt telescopes to search for ECAs.

Spaceguard will also concentrate its search in the solar opposition region and will detect 90% of all known ECAs but fewer than 50% of the ATENs (an ATEN is an ECA whose semimajor elliptical axis is <1 AU—the mean distance from Earth to the sun). This strongly suggests that ATENs are underrepresented among known ECAs and that the Spaceguard survey may find significantly fewer than 90% of all ECAs.

We have found that if the orbits of ECAs are completely randomized by close encounters with Earth, half of the ECAs become ATENs. We also have found that among ECAs that will hit Earth within the next 300 years, a sizeable fraction of ATENs and other ECAs with small semimajor axes will be missed by searches that are confined to the solar opposition region.

A large fraction of the asteroids that will hit Earth during the next 300 years will make close approaches to it before impact. We have found that these asteroids become bright enough to be detected with small (5- to 12-in.) telescopes at close approach, but they will often appear in directions far from solar opposition. Our analysis indicates that a potential solution to this problem might be to add a battery of small telescopes to the Spaceguard survey that would cover the entire sky (except near the sun) each night. Such a battery of telescopes would also be effective in finding asteroids as small as 100 m in diameter in the final two weeks before impact.

Publications

Hills, J.G., and P.J.T. Leonard, "Earth-Crossing Asteroids: The Last Days Before Earth Impact," *Astron. J.* **109**, 401 (1995).

Hills, J.G., and R. Carlson, "Statistics of Large Meteors Detected by Surveillance Satellites" (to be published in *Bull. Am. Astron. Soc.*).

Nuclear and Particle Physics

Neutrino Properties and Fundamental Symmetries

Thomas Bowles

A central theme of our project has been the search for the effects of a nonzero neutrino mass and tests of fundamental symmetries of nature. We have turned to solar neutrinos as a means of searching for a neutrino mass with an increased sensitivity of up to 10 orders of magnitude over that obtainable in laboratory experiments.

A "solar neutrino problem" has existed for more than twenty years in which the flux of high-energy ^{8}B neutrinos produced by fusion reactions in the Sun are observed to be a factor of more than two times lower than predicted by standard solar models. The production of ^{8}B in the Sun is preceded by the fusion of two protons to produce deuterium (the p-p process that accounts for most of the energy generation in the Sun), the production of ^{3}He and ^{4}He, and the production of ^{7}Be. The p-p and ^{7}Be processes produce lower energy neutrinos than the ^{8}B process. When we look at the combined results of a chlorine-radiochemical experiment (that is sensitive to the ^{7}Be and ^{8}B neutrinos) and the Kamiokande solar neutrino detector (a water Cherenkov detector that is sensitive only to the ^{8}B neutrinos), we see that the flux of ^{8}B neutrinos is a factor of two to three below the predicted rate and the ^{7}Be neutrinos are essentially absent.

We formed the Soviet-American Gallium Experiment (SAGE) collaboration to carry out a gallium solar-neutrino experiment that is sensitive to all of the solar neutrinos and in particular has high sensitivity to the p-p neutrinos. SAGE produced the first gallium results to verify the deficit seen in earlier experiments that studied higher-energy neutrinos from the Sun. To carry out model-independent tests of neutrino oscillations as being the source of the solar neutrino problem, we joined the Sudbury Neutrino Observatory (SNO) collaboration. Our primary interest in SNO has been in developing a means to differentiate ν_μ and ν_τ neutrinos from electron neutrinos. As the Sun cannot produce ν_μ and ν_τ neutrinos (the temperature of the Sun is too low), an observation of these neutrinos will provide a model-independent solution to the solar neutrino problem. A model-independent proof of neutrino oscillations by SNO would constitute the first observation of the long-sought new physics beyond the Standard Model and would constitute one of the most important scientific measurements of the decade.

The SNO detector consists of 1000 tonnes of 99.92% enriched heavy water surrounded by a shield of 7000 tonnes of purified light water. Solar neutrinos can interact with deuterium nuclei in either of two ways:

$$^2\mathrm{H} + \nu_e \rightarrow \mathrm{p} + \mathrm{p} + e^- - 1.44\ \mathrm{MeV}$$
[charged current (CC)]

$$^2\mathrm{H} + \nu_x \rightarrow \mathrm{p} + \mathrm{n} + \nu_x - 2.22\ \mathrm{MeV}$$
[neutral current (NC)]

Because any active flavor of neutrino induces the NC process, whereas fusion reactions in the Sun produce only ν_e, comparison of these two rates provides direct information about neutrino oscillations, independent of any solar model. SNO will also provide a direct spectrum of electron neutrinos above 6.5 MeV, to reveal possible Mikheyev-Smirnov-Wolfenstein resonant neutrino oscillations in matter which result in a distortion of the energy spectrum.

SNO is being built at a depth of 2200 m in the INCO Ltd. Creighton nickel mine in Sudbury, Ontario, by a collaboration of 12 Canadian, U.S., and U.K. institutions, including Los Alamos. We anticipate gathering initial data in late 1996. Los Alamos is responsible for a number of items in SNO because the NC reaction is of such fundamental importance. We have proposed to detect it by capturing the liberated neutron in ^{3}He proportional counters placed in the heavy water. Such a method offers event-by-event discrimination of NC and CC events, high statistical accuracy, and full-time NC sensitivity in case a supernova should occur.

We have carried out a research and development project to demonstrate the feasibility of using ultra-low background ^{3}He proportional counters to detect the existence of ν_μ and ν_t neutrinos from the Sun as part of our collaboration in SNO. Counters of this type offer unique advantages over other techniques. The primary difficulties are the requirements that the counters introduce no appreciable level of

radioactivity into the SNO detector and that they have a very low internal background and extremely low noise. As the heavy water in the SNO detector must be free of uranium and thorium at the 10^{-14} level and the expected detected neutron signal is only about 4 events per day, these requirements are obviously very stringent. We have developed a number of novel techniques to meet these requirements. This work consists of developing and testing counters made of ultrapure nickel bodies made by chemical vapor deposition along with a variety of possible means to read both position and rise-time information from the counters.

The ^{3}He counters for neutral current detection in SNO must not only have very low external and internal backgrounds, but they must also have high neutron detection efficiency, cause no substantial interference with the Cerenkov light in the SNO detector, and be able to survive immersion in the heavy water for a period of 10 years. The internal-background rates must be reduced by a factor of 100 below the best obtained by any other group. We have investigated a variety of possible solutions to these requirements and have shown that ^{3}He counters made primarily of ultrapure nickel will be satisfactory. We have identified other required components (such as feedthroughs) with acceptably low radioactivity.

We have demonstrated that we can meet the design requirements for the detectors. For most of the samples tested, uranium and thorium concentrations in the nickel are within our requirements. We have finalized mechanical designs and developed low-noise preamplifiers and the associated electronics. Data on prototype counters taken at our Waste Isolation Pilot Plant low-background counting facility has demonstrated levels of intrinsic alpha activity that are 250 times lower than achieved elsewhere. We have carried out initial studies of pulse propagation down the counters along with extensive studies of background rejection using pulse waveform information. We have essentially addressed all of the questions concerning construction, deployment, and use of the ^{3}He counters.

DOE convened a technical-feasibility review panel in March 1995. Their report was very favorable and concluded that we had demonstrated technical feasibility and that DOE should fund construction of the full NC detector array. Subsequently, DOE released $2.5 million in capital-construction funds for NC detector construction.

Publications

Bowles, T.J., "Solar Neutrino Experiments," *1994 Yearbook of Science and Technology, McGraw-Hill* 359 (1994).

Bowles, T.J., and V.N. Gavrin, "The Status of the Solar Neutrino Problem," *Annu. Rev. Nucl. Part. Sci* **43**, 117 (1993).

Hime, A., "Do Scattering Effects Resolve the 17-keV Conundrum?" *Phys. Lett. B* **299**, 165 (1993).

Wilkerson, J.F., "Neutrino," *McGraw-Hill Encyclopedia of Science and Technology, McGraw-Hill* (in press).

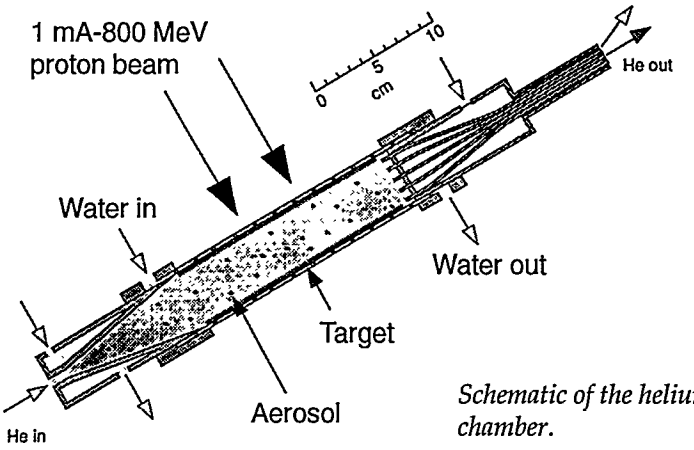
Development of Radioactive Beams at the LANSCE Linear Accelerator for a High-Precision Test of the Standard Model

David Vieira

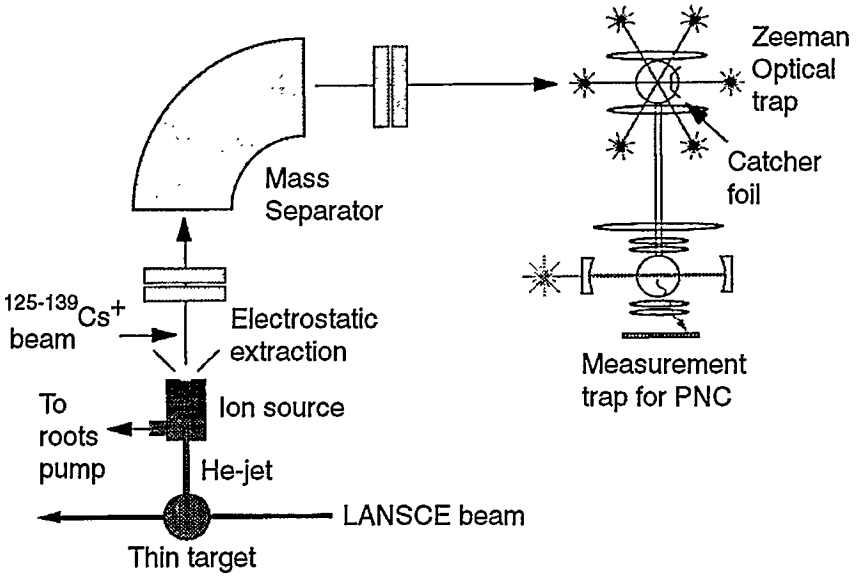
The main objective of this project is to design, fabricate, and test a thin-target, helium-jet system (see figure) at the Los Alamos Neutron Science Center (LANSCE) linear accelerator to provide high yields of radioactive cesium isotopes for an atomic parity nonconservation (PNC) experiment (see figure). In this experiment, we seek to determine the 6S-7S parity-forbidden transition rate for a series of cesium isotopes with high precision. These measurements would yield an important test of the standard model of electroweak interactions. The secondary goal of this work is to use the new system to demonstrate the high production rates for a variety of refractory species that will be used as high-intensity production sources at a future radioactive beam facility called the IsoSpin Laboratory (ISL).

We designed, installed, and tested the thin-target, helium-jet target chamber and its associated gas-handling and collection/counting system during the first two years of the project. This past year we analyzed the results and prepared them for publication. The helium-jet system proved remarkably successful, operating at beam intensities of 700 μA (which is more than 100-times higher than any other helium-jet system), with no signs of degradation. In the subsequent off-line analysis and Monte Carlo modeling, we determined the collection rates of cesium and many other refractory radioisotopes to be in the range of 10^7 to 10^8 atoms/s, with helium-jet transport efficiencies of 15% to 25%. These high

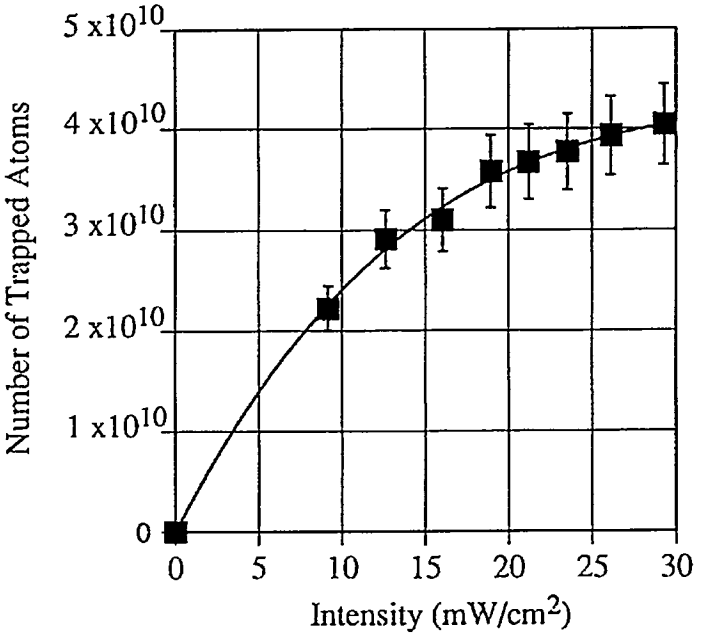
intensities are sufficient to undertake the cesium-PNC experiment, and these refractory isotopes are drawing considerable interest in the radioactive beam community as a robust production source. We also made initial steps toward concentrating the cesium atoms of interest to the PNC experiment by assembling the Laboratory's first magneto-optical trap. Using this technology, we have recently trapped more than 4×10^{10} atoms of stable cesium (see figure).



Schematic of the helium-jet target chamber.



Overview of the cesium-PNC experiment.



High-intensity trapping of stable cesium atoms with a magneto-optical trap. The number of trapped atoms is shown as a function of laser intensity using 4-cm-diam beams and a red-detuning of 20 MHz from the $6S_{1/2}$–$6P_{3/2}$ cycling transition at 852 nm.

Nonperturbative Estimates of the Standard Model Parameters

Rajan Gupta

We have presented state-of-the-art results for the hadron spectrum, meson decay constants, semileptonic form factors, form factors for the rare decay $B \rightarrow K^* \gamma$, and weak-matrix elements of 4-fermion operators using 170 quenched lattices of size $32^3 \times 64$. Results of these calculations are inputs in the analysis of experimental data and will help pin down the unknown parameters of the standard model in the next few years.

Some of the highlights of our calculations are results for the

- baryon masses and the pattern of symmetry breaking for the octet and decuplet states,
- semileptonic form factors for the decay $D \rightarrow K e \nu$ which are used to test the pole-dominance hypothesis, and
- kaon B-parameter and related B-parameters using Wilson fermions.

The key results of the study of semileptonic form factors are that

- by comparing the lattice result

of the symmetry that the laws of physics are left unchanged by a combination of the operations of charge combination (C) and space inversion (P). It has been observed in the decay of neutral K-mesons.

In addition, we have started to develop codes to include heavy quarks (charm and bottom) in our analysis using the nonrelativistic quantum chromodynamic (QCD) method. All these calculations are being done using highly efficient codes on the Thinking Machines Connection Machine 5 (CM-5) as part of the DOE High-Performance Computing and Communications Grand Challenge initiative. We have contributed significantly to helping debug the CM-5 and to making it a stable production environment.

Publications

Bhattacharya, T., R. Gupta, and S. Sharpe, "Decay Constants with Wilson Fermions" (submitted to *Phys. Rev. D*).

Bhattacharya, T., R. Gupta, and S. Sharpe, "Hadron Spectrum with Wilson Fermions" (submitted to *Phys. Rev. D*).

Gupta, R., and J. Mandula, "Matrix Elements of the Singlet Axial Current in the Proton," *Phys. Rev. D* **50**, 6931(1994)

A Continuous Watch of the Northern Sky Above 40 TeV with the CYGNUS Array

Cyrus Hoffman

The primary scientific objective of the CYGNUS air-shower array is to search for ultra-high-energy (UHE) gamma rays from the heavens. Given the sporadic

from gamma-ray bursts. For several of the stronger bursts, this implies that the spectrum is cut off at high energies. Our results were presented in several papers at the

Exploring and Testing the Standard Model and Beyond

Geoffrey West

Our research is designed to extend our knowledge of the fundamental constituents of nature. Using relativistic quantum field theory, we are attempting to elucidate the physics of the gravitational, electromagnetic, and weak and strong nuclear force interactions of the elementary particles in terms of the highly successful standard model which

this regard, we have explored the role of conformal field theory in superstring models in order to be able to incorporate quantum mechanics into Einstein's theory of relativity.

Publications

Bender, C., F. Cooper, and P. Meisenger, "Spherically Symmetric

Mottola, E., F. Cooper, Y. Kluger, et al, "Non-Equilibrium Quantum Dynamics of Disoriented Chiral Condensates," *Phys. Rev. D* **51**, 2377 (1995).

Mottola, E., S. Habib, and P. Tinyakov, "Finite Energy Instantons in the O(3) Non-Linear Sigma Model" (submitted to *Phys. Lett. B*).

Nieto, M. M., "Quantum Interference: From Kaons to Neutrinos (with Quantum Beats in Between)" (to be published in *Hyperfine Interact.*).

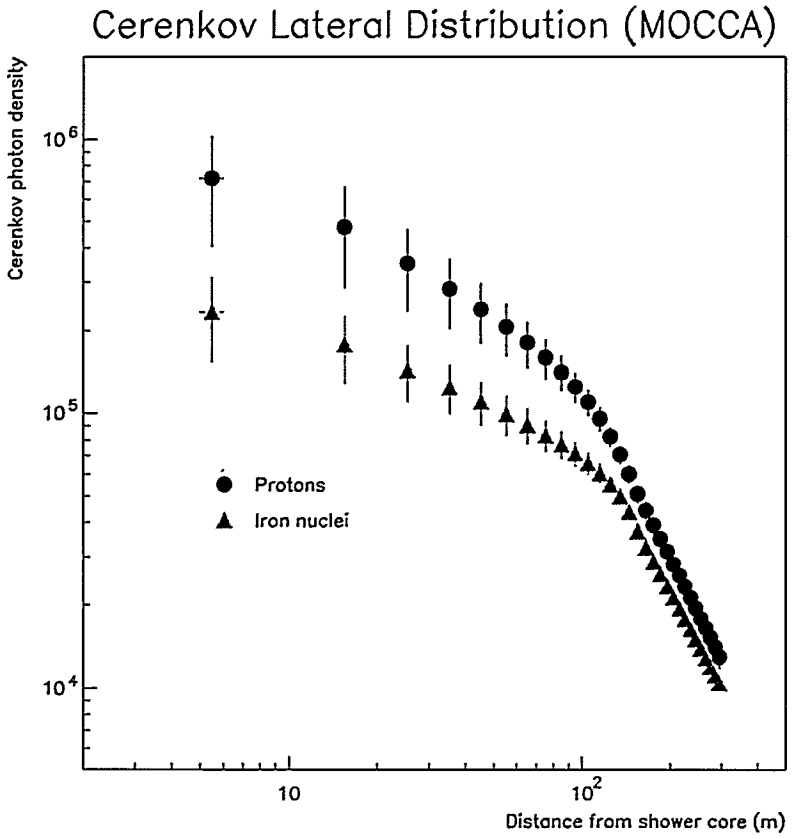
Nieto, M. M., and J. Daboul, "Exact E=0, Classical Solutions for General

Determination and Study of Cosmic-Ray Composition Above 100 TeV

Constantin Sinnis

The origin of cosmic radiation has eluded researchers for nearly a century. The composition of cosmic rays is perhaps the single most-important clue to this problem. Despite the paucity of data, a consensus is growing in the cosmic-ray community: it is thought that cosmic rays with energies less than approximately $10^{15.5}$ eV are of galactic origin, accelerated in the shock waves formed by supernovae. At this energy, there is a change in the energy spectrum of the cosmic radiation, namely, the spectral index steepens from –1.7 to –2.5. A change in composition at this energy would signal the onset of a new source of cosmic rays. If the cosmic rays are composed of protons, then they are probably extragalactic. If the cosmic rays are heavy nuclei (i.e., iron), then they are probably of galactic origin. We are employing a new technique to study the cosmic-ray composition in this energy regime.

We have constructed six air Cherenkov detectors and placed them within the CYGNUS extensive air shower (EAS) array. Monte Carlo studies indicate that the lateral distribution of Cherenkov light, used in conjunction with the information from an EAS array and muon detectors, is a sensitive probe of the composition of the incident radiation (see figure). During the past year, we have completed construction of the experiment, which ran for three months, and we have started analyzing the data obtained. At the 24th International Cosmic Ray Conference, we will present a paper detailing the results of the experiment.



Results of Monte Carlo simulations showing the difference in the lateral distribution of Cherenkov light from air showers generated by a cosmic ray.

Nonequilibrium Dynamics of the Quark-Gluon Plasma in Heavy-Ion Collisions

Emil Mottola

We are developing field theory and numerical methods for tackling time-evolution problems in quantum field theory, such as the backreaction of quantum fields on classical fields as well as the dynamics of nonequilibrium phase transitions. Our main focus is on problems related to experimental programs planned for the Relativistic Heavy-Ion Collider at Brookhaven National Laboratory and for Fermi National Accelerator Laboratory. We are studying the production of unusual muon pairs from a time-evolving quark-gluon plasma produced following a relativistic heavy-ion collision and the production of Centauro events (large regions with no neutral pions) from disoriented chiral condensates produced in the chiral, nonequilibrium phase transition expected during the time evolution of the plasma.

Having understood that a gauge-invariant approach is needed for the quark-gluon plasma, we have begun reformulating the problem in terms of

gauge-invariant quantities. We have also studied how particle production leads to the dissipation of mean fields when there are zero-mass particles. We have studied the dissipation effects in a scalar field theory and have extended our methods to the Yang-Mills theory. At the same time, we have been collaborating with experimentalists for possible applications of our code to model their planned experiments. Using the closed-time-path formalism of Schwinger, we have also made progress in formulating the rescattering corrections to the mean-field theory.

Publications

Cooper, F., J. Dawson, S. Habib, et al., "Semi-Quantum Chaos and the Large N Expansion," *Physica D* **83**, 74 (1995).

Cooper, F., S. Habib, Y. Kluger, et al., "Nonequilibrium Quantum Fields in the Large N Expansion," *Phys. Rev. D* **50**, 2848 (1994).

Cooper, F., Y. Kluger, E. Mottola, et al., "Quantum Evolution of Disoriented Chiral Condensates," *Phys. Rev. D* **51**, 2377 (1995).

Habib, S., Y. Kluger, E. Mottola, et al., "Dissipation and Decoherence in Mean Field Theory" (submitted to *Phys. Rev. Lett.*).

Antiquark Distributions In The Proton

Jen-Chieh Peng

The study of quark and antiquark distribution in nucleons has been a major endeavor in nuclear and particle physics. Results from a recent deep-inelastic scattering experiment suggest the surprising possibility that the up and down antiquark distributions in the proton are not symmetric. A sensitive and direct determination of the antiquark distributions in the proton can be made by comparing the Drell-Yan cross sections on hydrogen versus deuterium targets. We have proposed a new experiment (E866) at Fermilab to carry out such measurements.

Our proposed E866 experiment will be performed with 800-GeV proton beam together with a high-resolution, high-rate magnetic spectrometer. The expected statistical accuracy and the range of coverage in χ (the fraction of nucleon momentum carried by the antiquark) are unmatched by other experiments. E866 will have sufficient accuracy to test all theoretical models that predict asymmetric up and down antiquark distributions. E866 will also provide additional data on the production of J/psi and Υ resonances.

Preparation for E866, including upgrade of the data-acquisition system and the design of new trigger electronics, is under way. E866 is scheduled to run during 1996–1997.

Publications

Peng, J. C., and D. M. Jansen, "Probing U-Bar/D-Bar Asymmetry in the Proton via W and Z Production," *Phys. Lett. B* **354**, 460 (1995).

Peng, J. C., J. M. Jansen, and Y. Chen, "Probing U-Bar/D-Bar Asymmetry in the Proton via Quarkonium Production," *Phys. Lett. B* **344**, 1 (1995).

Design of a Neutrino Oscillation Experiment

Fred Federspiel

The purpose of our project is to lay the foundation for a major new experimental initiative in the fast-changing field of neutrino physics. We are developing the technologies needed to mount a definitive measurement of neutrino oscillations. We plan to carry out this measurement using neutrinos from the Fermi National Accelerator Laboratory booster, which will give us several advantages over our current liquid scintillator neutrino detector experiment here at the Los Alamos Neutron Science Center (LANSCE).

During the review period, we have demonstrated proof of principle of a neutrino beamline design that will produce the required purity and intensity of muon-neutrinos. We have produced an interactive Monte Carlo simulation of particle tracks in a generic detector. This allows us to develop the crucial intuitive understanding of the behavior of the higher-energy particles produced by the booster neutrinos. We are also using this simulation to study more completely the feasibility of the segmented detector—a detector based on the charge coupled device (CCD). We have also obtained first prototypes of an extruded plastic tubing that could form the basis for the optical isolators required for the CCD-based detector. We are in the process of testing these prototypes.

Time-Reversal Tests in Polarized Neutron Reactions

J. David Bowman

Previous work by our team has demonstrated the existence of large enhancements (10^6) of the effects of parity violation in the compound nucleus. Our attempts to relate the parity-violating asymmetries that we have measured to the parameters of the underlying weak nucleon-nucleon interaction give us confidence in our understanding of the physics involved. The purpose of our project is to design experiments that take advantage of these enhancements to search for a violation of time-reversal invariance. We propose to

- design and build polarized ^{3}He targets for use as neutron polarizers and analyzers,
- design and build neutron-spin transport, and
- measure the spin rotation of polarized neutrons passing through ^{139}La.

We plan to continue to search for candidate resonances in xenon and holmium that might be used for time-reversal tests.

We have done extensive preliminary work to determine the design and operating parameters of a ^{3}He system for neutron experiments using the University of Minnesota system. We have fixed design parameters for the ^{3}He system as well as determined different operating parameters such as

- laser power level,
- requirements for the power supply of the diode lasers,
- noise level in the current of the Helmholtz coils during the adiabatic fast-passage nuclear-magnetic-resonance (NMR) measurements of the ^{3}He polarization, and
- noise limit in the NMR system.

We have designed a sequence of experiments to be done at the Manuel Lujan Jr. Neutron Scattering Center (MLNSC). The MLNSC Nuclear Physics Program Advisory Committee approved our program with an A priority. We will measure the polarization of the neutron beam produced by our polarized-proton spin filter by using the polarized ^{3}He system we are developing.

Theoretical Research Relevant to Medium Energy Upgrades and Experiments

Terrence Goldman

Our research objectives are the increased understanding of and predictive capability for dynamical processes in hadron- and hyperon-scattering and related nuclear structures, and the weak interaction and symmetry violating processes (including electromagnetic and collective effects). These are important for advancing fundamental science and for making intelligent decisions on investments in future accelerator and experimental facilities, including many of specific interest to the Laboratory. Our goals include calculating scattering amplitudes for specific nuclear and hadronic reactions and spectra, and bounds on symmetry violating processes determined from extant data.

Our major results during the review period include (1) the first accurate microscopic calculations of the low-lying states in the nuclear six-body system, (2) recognition of a quantum field theory mechanism as a possible origin of gamma ray bursts, (3) completion of calculations of the euclidean response of ^{3}H and ^{3}He in scattering processes, (4) calculation of H-dibaryon cross-section tests in hyperon-deuteron breakup scattering, (5) a complete relativistic and nonrelativistic theoretical survey of all SU(3) dibaryon candidates with accurate estimate of predicted mass uncertainties, (6) new conjectures on the spatial variation of confining field strengths, (7) completion of enhanced approximations for electromagnetic corrections in heavy ion scattering, (8) more fully developed models of collective nuclear excitations, and (9) stringent bounds on branching ratios for specific rare decay processes and fundamental symmetry violations. Work performed in this project has application to fundamental science, basic research in nuclear physics, and the development of particle accelerators, nuclear energy, and energy resources.

Publications

Ahluwalia, D.V., T. Goldman, and M.B. Johnson, "Majorana-like (j,0) + (0,j) Representation Spaces: Construction and Physical Interpretation," *Mod. Phys. Lett. A* 9, 439 (1994).

Ahluwalia, D.V., T. Goldman, and M.B.Johnson, "(j,0) + (0,j) Representation Space: Majorana-like Construct," *Acta Phys. Pol. B* **25**, 1267 (1994).

Burdman, G., T. Goldman, and D. Wyler, "Radiative Leptonic Decays of Heavy Mesons," *Phys. Rev. D* **51**, 111 (1995).

Carlson, J., "Recent Progress in Path Integral Calculations of Nuclei" (to be published in *Few-Body Systems*).

Forest, J.L., V.R. Pandharipande, J. Carlson, et al., "Variational Monte Carlo Calculations of ^{3}H and ^{4}He with a Relativistic Hamiltonian-II," *Phys. Rev. C* **52**, 576 (1995).

Forest, J.L., V.R. Pandharipande, and J.L. Friar, "Relativistic Nuclear Hamiltonians," *Phys. Rev. C* **52**, 568 (1995).

Friar, J.L., "Dimensional Regularization and Nuclear Potentials" (submitted to *Phys. Rev. C*).

Friar, J.L., and S.A. Coon, "The Leading-Order Nuclear Pi-Gamma-Exchange Force" (submitted to *Phys. Rev. C*).

Friar, J.L., and G.L. Payne, "Assessment of Triton Potential Energy" (to be published in *Few-Body Systems*).

Friar, J.L., G.L. Payne, W. Glockle, et al., "Benchmark Solutions for N-D Breakup Amplitudes," *Phys. Rev. C* **51**, 2356 (1995).

Ginocchio, J.N., "The Fractional Quantum Hall Effect and the Spherical Shell Model, from Spectroscopy to Chaos," in *From Spectroscopy to Chaos*, A. Das, D.S. Koltun, Eds. (World Scientific, Singapore, 1994).

Ginocchio, J.N., and C.W. Johnson, "Hermitian Boson Mapping and Finite Truncation," *Phys. Rev. C* **50**, R571 (1994).

Ginocchio, J.N., and A. Leviatan, "Quadrupole Collectivity with Isospin," *Phys. Rev. Lett.* **73**, 1903 (1994).

Ginocchio, J.N., P. von Neumann-Cosel, and A. Richter, "Relation between the Scissors Mode and the Interacting Boson Model Deformation" (submitted to *Phys. Rev. Lett.*).

Goldhaber, A.S., and T. Goldman, "Confinement, Crossing Symmetry, and Glueballs," *Phys. Lett. B* **344**, 319 (1995).

Pudliner, B.S., V.R. Pandharipande, J. Carlson, et al., "Quantum Monte Carlo Calculations of $a \leq 6$ Nuclei," *Phys. Rev. Lett.* **74**, 4396 (1995).

Ping, J., F. Wang, and T. Goldman, "An Extension of Fractional Parentage Expansion to the Nonrelativistic and Relativistic Three Flavor Unitary Group Dibaryon Calculations," *Phys. Rev. C* **51**, 1648 (1995).

Redman, J., and R.R. Silbar, "Experimental Physics, Selecting an Operating System, Part II: NEXTSTEP," *Comput. Phys.* **9**, 261 (1995).

van Kolck, U., J.L. Friar, and T. Goldman, "Phenomenological Aspects of Isospin Violation in the Nuclear Force" (submitted to *Phys. Lett.*).

Wang, F., G.H. Wu, L.J. Teng, et al., "Quark Delocalization, Color Screening, and Nuclear Intermediate Range Attraction II," *Mod. Phys. Lett. A* **10**, 1895 (1995).

Wang, F. G.H. Wu, L.J. Teng, et al., "Quark Delocalization, Color Screening, and Dibaryons," *Phys. Rev. C* **51**, 3411 (1995).

Zhang, S., J. Carlson, and J.E. Gubernatis, "A Constrained Path Quantum Monte Carlo Method for Fermion Ground States," *Phys. Rev. Lett.* **74**, 3652 (1995).

THEORETICAL STUDIES OF THE INTERACTION OF WATER WITH DNA OLIGOMERS AND PROTEINS

Angel Garcia

The structure, dynamics, and stability of biomolecules are influenced by the strong interaction of biomolecules with solvents. These interactions are locally mediated by hydrogen bonding, the finite size of water molecules, and long-range electrostatic and multiple correlation interactions with the bulk water network. Structural and bulk water molecules play important roles in determining the structure-to-function relationship of biomolecules. The bulk properties of a solvent, such as viscosity, determine the ability of a biomolecule to undergo a transition from an equilibrium state to an active metastable state. At the same time, changes in the conformation of biomolecules are limited by the ability of bound water molecules around mobile sites to change conformations and adopt a new structural pattern or be released and form part of the bulk solvent. To understand the function of biomolecules we have to understand each of these fundamental interactions.

Given the large size of biomolecular systems and the enormous requirements for computer time and storage needed to simulate these systems, it is necessary to extract a set of general principles describing the equilibrium properties of water molecules around biomolecules. We have developed a computationally efficient method to describe the organization of water around solvated biomolecules. The method is based on a statistical-mechanical expression of the water-density distribution in terms of two- and three-particle correlation functions. We have applied the method to the analysis of the hydration of proteins and small nucleic-acid molecules in the crystal environment and have reported high-resolution x-ray crystal structures. A detailed comparison of the theoretical results and experimental data shows positional agreement for the experimentally observed water sites. Our method can be used for the refinement of the water structure in x-ray crystallography, hydration analysis of nuclear-magnetic-resonance structures, and theoretical modeling of biological macromolecules. Studies have indicated that hydration analyses of large biomolecular assemblies are unattainable by current molecular dynamics and Monte Carlo simulations. The speed of the computations achieved by our method allows hydration analyses of molecules of almost arbitrary size (for example, transfer ribonucleic acids, protein nucleic-acid complexes, and antigen-antibody complexes) in the crystal environment and in aqueous solution.

Publications

Garcia, A.E., G. Hummer, and D.M. Soumpasis, "Theoretical Description of Biomolecular Hydration—Application to A-DNA," in *Neutrons in Biology*, B.P. Schoenborn and R. Knott, Eds. (Plenum, New York, in press).

Hummer, G., and D.M. Soumpasis, "A Statistical-Mechanical Treatment of the Structural Hydration of Biological Macromolecules: Results for B-DNA," *Phys. Rev. E* **50**, 5085 (1994).

Hummer, G., A.E. Garcia, and D.M. Soumpasis, "Hydration of Nucleic-Acid Fragments: Comparison of Theory and Experiment for High-Resolution Crystal Structures of RNA, DNA, and DNA-Drug Complexes," *Biophys. J.* **68**, 1639 (1995).

Hummer, G., A.E. Garcia, and D.M. Soumpasis, "Potentials of Mean Force Description of Ionic Interactions and Structural Hydration in Biomolecular Systems," in *Non Linear Excitation in Biomolecules*, M. Peyrard Ed. (Springer/Editions de Physique, Paris, 1995), p. 83.

Hummer, G., D.M. Soumpasis, and M. Neumann, "Computer Simulation of Aqueous Na-Cl Electrolytes," *J. Phys.: Condens. Matter A* **6**, 141 (1994).

Mariapan-Santhana, S.V., A.E. Garcia, and A.E. Gupta, "Structure and Dynamics of the DNA Hairpins Formed by Tandemly Repeated CTG Triplets Associated with Myotonic Dystrophy" (to be published in *Nucleic Acids Res.*).

Structural Determination of Larger Proteins Using Stable Isotope Labeling and NMR Spectroscopy

Clifford Unkefer

Nuclear magnetic resonance (NMR) spectroscopy is an important tool for determining high-resolution structures of biological macromolecules in solution. Stable isotope labeling extends the molecular weight range of this important technology by making it possible for larger molecules or even molecular complexes to be analyzed. We are using both techniques to determine the structures of large protein complexes in solution.

We are focusing on two complexes: (1) calmodulin, with its binding domain on phosphorylase kinase, and (2) the troponin C/troponin I complex. First, we developed a bacterial expression system for labeling calmodulin, troponin C, and their target peptides, the binding domains of the molecules with which they form complexes. Our expression system uses a methylotrophic bacterium, which grows on methanol as its sole source of carbon. We can produce ^{13}C-labeled proteins by culturing the bacterium in the presence of ^{13}C-methanol and inducing the expression of relatively large quantities of proteins.

Next, we obtained two-dimensional NMR spectra of the troponin C/troponin I complex that enabled us to identify protons that are either attached to adjacent carbons or spatially proximal. These spectra allowed us to make a significant proportion of the chemical shift assignments of the bound troponin I peptide.

Finally, we observed long-range nuclear Overhauser enhancements (NOEs) from the troponin I complex, which provide the distance constraints required for determining the structure of the complex. We are currently analyzing the NMR data in terms of the structure of the troponin C/troponin I complex.

Publications

Lodwig, S.N., L.A. Silks III, and C.J. Unkefer, "Synthesis of 1-Chloro-1-[^{15}N]Nitrosocyclohexane, an Electrophilic Aminating Agent" (to be published in *J. Labelled Compds. and Radiopharm.*).

Lodwig, S.N., and C.J. Unkefer, "Stereoselective Synthesis of Stable Isotope-Labeled L-α-Amino Acids: Electrophilic Amination of Oppolzer's Acyl Sultams in the Synthesis of L-[^{15}N]Alanine, L-[^{15}N]Valine, L-[^{15}N]Leucine, L-[^{15}N]Phenylalanine, and L-[1-^{13}C,^{15}N]Valine" (to be published in *J. Labelled Compds. and Radiopharm.*).

Lodwig, S.N., and C.J. Unkefer, "Stereoselective Synthesis of Stable Isotope-Labeled L-α-Amino Acids: Enantioselective Synthesis of ^{13}C-,^{15}N-Labeled L-Proline Using Oppolzer's Glycine Template" (submitted to *J. Chem. Soc. Perkin Trans. 1*).

Olah, G.A., and J. Trewhella, "A Model Structure of Muscle Protein Complex 4Ca^{+2}-Troponin C-Troponin I Derived from Small-Angle Scattering Data: Implications for Regulation," *Biochemistry* 33, 12800–12806 (1994).

Positional Cloning of Disease Genes on Chromosome 16

Norman Doggett

This project had proposed to elucidate the molecular basis of Batten disease (a progressive neurodegenerative disease of childhood) by molecular cloning of the affected gene with the aid of chromosome 16 maps and data available from Los Alamos National Laboratory's Human Genome Program. An overlapping clone map of chromosome 16 was available [>95% of the chromosome in yeast clones (YACs) and 60% of the chromosome in fingerprinted bacterial clones (cosmids)], and these data greatly facilitated the search for the Batten disease gene.

We have worked in collaboration with the Batten Disease Consortium to identify the gene responsible for this disease. During the past and final year of this project, the ultimate goal was realized. Two candidate genes, members of the phenol sulfotransferase family, which we located in the Batten disease region last year, were excluded from consideration as the causative gene because mutations in these genes could not be found. Our collaborators isolated a novel gene from a high-resolution physical map of bacterial clones that we constructed for the Batten disease region. They found that this gene contains a 1000-base-pair deletion in most Batten disease patients. Members of the Batten Disease Consortium group found additional mutations in this gene in other patients. These results

confirm that this gene is responsible for Batten disease.

Publications

Dooley, T.P., H.M. Mitchison, P.B. Munroe, et al., "Mapping of Two Phenol Sulphotransferase Genes, STP and STM, to Chromosome 16p: Candidate Genes for Batten Disease," *Biochem. Biophys. Res. Comm.* **205,** 482 (1994).

Dooley, T.P., R.D. Obermoeller, P. Probst, et al., "Phenol Sulfotransferases: Candidate Genes for Batten Disease," *Am. J. Medical Genetics* **57,** 327 (1994).

Dooley, T.P., P. Probst, P.B. Munroe, et al., "Genomic Organization of the Human Catecholamine-Sulfating Phenol Sulfotransferase Gene (STM)," *Biochem. Biophys. Res. Comm.* **205,** 1325 (1994).

International Batten Disease Consortium, "Isolation of a Novel Gene Underlying Batten Disease (CLN3)," *Cell* **82,** 949 (1995).

Järvelä, I.E., H.M. Mitchison, D.F. Callen, et al., "Physical Map of the Region Containing the Gene for Batten Disease (CLN3)," *Am. J. Medical Genetics* **57,** 316 (1994).

Järvelä, I.E., H.M. Mitchison, A.M. O'Rawe, et al., "YAC and Cosmid Contigs Spanning the Batten Disease Region (CLN3) at 16p12.1-p11.2," *Genomics* **29,** 478 (1995).

Lerner, T.J., K.L. D'Arigo, J.L. Haines, et al., "Isolation of Genes from the Batten Candidate Region Using Exon Amplification," *Am. J. Medical Genetics* **57,** 320 (1994).

Taschner, P.E.M., N. De Vos, A.D. Thompson, et al., "Chromosome 16 Microdeletion in a Patient with Juvenile Neuronal Ceroid Lipofuscinosis (Batten Desease)," *Am. J. Human Genetics* **56,** 663 (1994).

Sum-Frequency Generation Studies of Membrane Transport Phenomena

R. Brian Dyer

We are using nonlinear vibrational spectroscopy to better understand the fundamental molecular mechanisms of biological energy transduction, ion transport, and signaling at membrane interfaces. With this goal, we are pioneering the development and application of a new technique, sum-frequency generation (SFG), for the study of the transport of protons and ions across biological membranes.

Vectorial pumping of ions, generally carried out by membrane-bound proteins, is one of the most fundamental processes in living organisms, critical for energy transduction in respiration and photosynthesis and for a wide variety of cellular signal transduction events. Because of the difficulty of obtaining structural and dynamic information about both membrane-bound proteins and membranes, a molecular-level understanding of proton and ion pumping has remained elusive.

Our studies have focused on membrane phenomena for two specific systems, bacteriorhodopsin (bR), a light-induced transmembrane proton pump, and colicin A, a water-soluble protein that can form voltage-sensitive ion channels. We have developed a nonlinear spectroscopic technique that is uniquely sensitive to interfaces and that has demonstrated structural specificity

Our technique uses a femtosecond Ti:sapphire laser to parametrically generate broadband infrared (IR) pulses, tunable throughout the mid-IR. The infrared pulses are combined in a nonlinear, SFG process at the membrane interface. Our initial studies have focused on the water/phospholipid interface of vesicles oriented randomly in solution. We expect this approach to provide unique insight into the structures and dynamics that affect transmembrane ion transport.

Publications

Dyer, R.B., K.A. Peterson, P.O. Stoutland, et al., "Picosecond Infrared Study of the Photodynamics of Carbonmonoxy Cytochrome *c* Oxidase," *Biochem.* **33,** 500 (1994).

Decatur, S.M., S. Franzen, G.D. DePillis, et al., "Trans Effects in Nitric Oxide Binding to Myoglobin Cavity Mutant H93G: A Model for Nitric Oxide Activation of Guanylate Cyclase" (submitted to *Biochem.*).

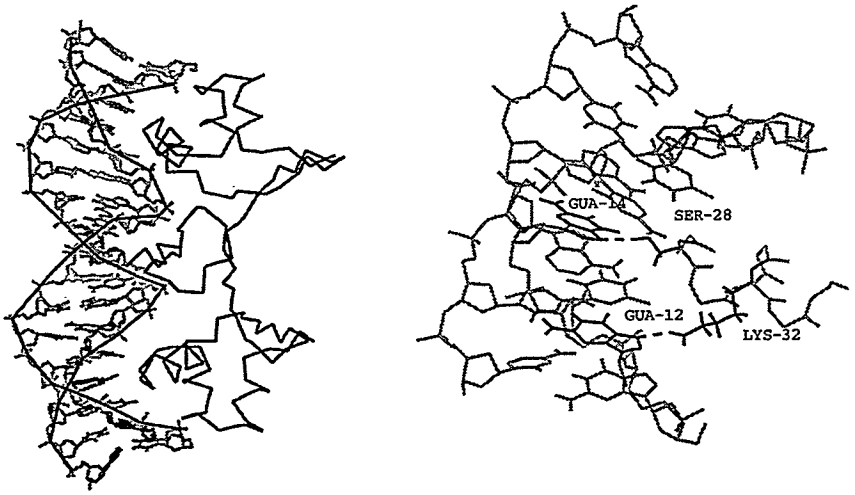
Predicting B-DNA Structure From Sequence

Chang-Shung Tung

The major goal of this project is to develop a reliable way to predict the tertiary structure of DNA duplexes from sequence information. In our prediction method, tetramers (polymers consisting of four identical monomers) are used as the basic structural unit to include the next-nearest-neighbor interactions.

We have developed a new sampling method to study the tetramer structures. Using the Latin hypercube approach, we first generate structures that cover the conformational space evenly. Then we select structures with energies below a predetermined cut-off value for Metropolis Monte Carlo equilibrations. From the Monte Carlo results we deduce the energy-weighted average structure of the tetramer. We choose boundary conditions in our simulations to reflect the fact that the tetramer is embedded in a long polymer; we treat solvent effects with the potential-of-mean-force approach, with pair correlations calculated from the hypernetted-chain approximation. The predicted twist and roll angles of a DNA dodecamer (CGCGAATTCGCG) compare favorably with those deduced from crystal data.

To show the utility of the sequence-dependent structure of DNA in biological recognition, we have also developed a method to predict the complete structure of the DNA molecule based on the structure of its phosphorus atoms. This work opens the possibility of an alternative DNA-sequencing method to determine base sequences from the structure of the phosphorus atoms. Using this method we were able to predict specific interactions between Cro protein and the DNA operator from bacteriophage lambda.



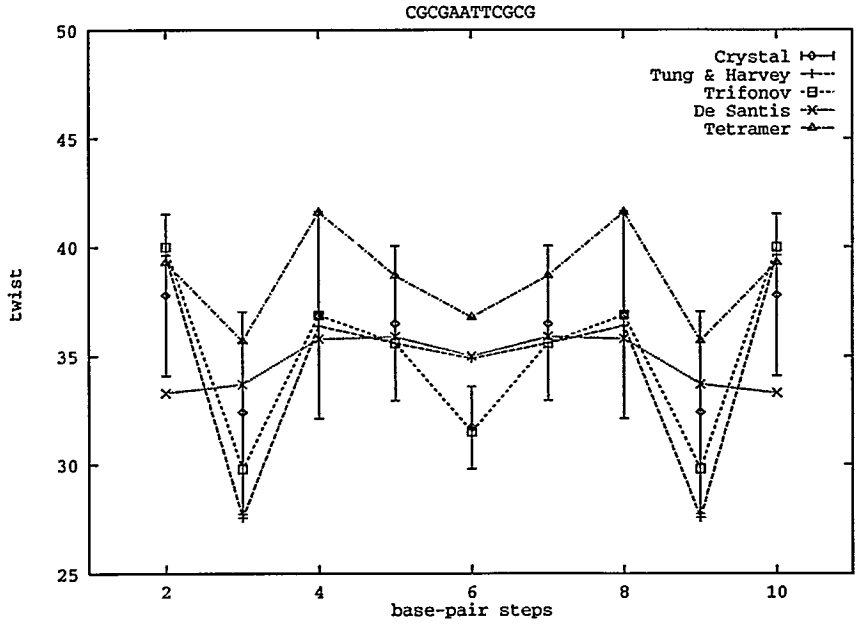
The modeled structure of the operator DNA and two side chains of the Cro protein that form specific H-bonds with the DNA. The all-atom structure of the DNA (in grey), together with the phosphorous and C-alpha atoms (in black) of the crystal structure (4Cro), is plotted on the left side of the figure. A section of the operator DNA and the alpha-3 helix of the protein are plotted on the right side of the figure. Ser-28 hydroxyl and Lys-32 amino protons form H-bonds with Gua-14 and Gua-12, respectively.

Publications

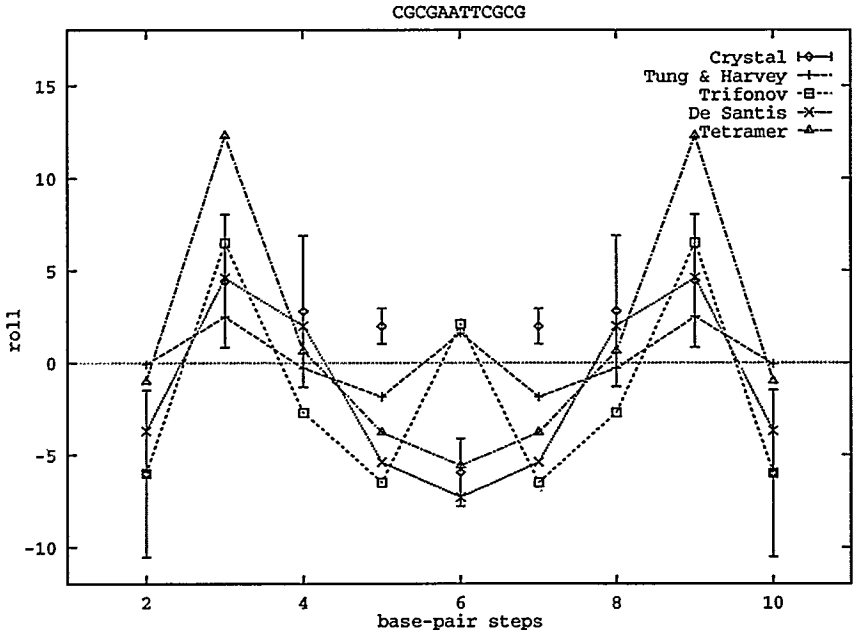
Tung, C.-S., "Structural Prediction of B-DNA Duplexes Based on Coordinates of the Phosphorus Atoms" (to be published in *Biophys. J.*).

Tung, C.-S., D.M. Soumpasis, and G. Hummer, "An Extension of the Rigorous Base-Unit Oriented Description of Nucleic Acid Structure," *J. of Biomol. Struct. Dyn.* **11,** 1327 (1994).

Edwards, C.A., J.M. Gatewood, C.-S. Tung, et al., "Binding of Cro Protein to Nitrogen-15 Labeled Operator DNA Indicates Specific Interaction of Cro with N7 of Guanosine-14" (to be published in the *J. Biol. Chem.*).



(a)



(b)

Plots of (a) twist angle and (b) roll angle of the dodecamer CGCGAATTCGCG calculated with four different prediction methods and from crystal structure. We calculated the average crystal structure of a particular base-pair step embedded in its two neighboring base pairs (a tetramer) from all the tetramers of the same sequence in a set of 58 DNA oligonucleotide structures in the Protein Data Bank.

Directly Labeled Fluorescent DNA Probes For Chromosome Mapping

Babetta Marrone

The objectives of this project are to develop and implement new strategies for chromosome mapping using fluorescently labeled nucleic acid probes and quantititive image analysis. Specifically, we are developing fluorescence in situ hybridization (FISH) probe technology to optimize regional localization of multiple DNA sequences along a single chromosome. The techniques we develop will be used to map cloned fragments of selected human chromosomes, which in turn will help researchers integrate physical and cytogenetic maps of the human genome.

Our goals are the following: (1) to develop new techniques for preparing and characterizing labeled DNA probes using fluorescently labeled nucleotides; (2) to refine cooled CCD (charge-coupled device) microscopy capabilities for quantitative, high-resolution, high-precision, multispectral analysis of FISH probes; and (3) to develop software to facilitate or even semiautomate chromosome mapping.

We are incorporating fluorescently labeled nucleotides into nucleic acid probes, which are then hybridized in situ to their target sequences on chromosomes. The location of the FISH probes on the chromosome are then mapped using digital imaging microscopy to produce a high-precision, high-resolution (within 1–2 megabases) map of selected human chromosomes.

After hybridizing the fluorescent probe to the chromosome and staining the chromosome with a general fluorescent dye, we capture one image of each chromosome of interest (such as chromosome 21) containing the fluorescent probe and draw a line with the cursor through the long axis of the chromosome. The imaging system displays the relative intensity of each pixel along this line and expresses the map position of the probe as the fractional length of the total chromosome relative to a fixed reference point. We usually analyze 20 to 30 chromosomes from each hybridization.

We have used fractional length mapping of FISH probes to map genes on a variety of chromosomes and vectors, and we have used multiple-color mapping to produce additional, higher-resolution maps. During the review period, we mapped cosmids of the region of chromosome 16 containing the gene for the inherited disease Familial Mediterranean Fever, the double-strand DNA repair gene XRCC4 on chromosome 5q13-14, the DNA repair gene FEN-1 on chromosome 11q13, and the gap regions on chromosome 16. Both single-color fractional length analysis and multiple-color mapping are now in routine use in our laboratory and will continue to be applied to future chromosome and gene mapping efforts at Los Alamos.

We have also used the primed in situ labeling technique (PRINS) to incorporate fluorescent dUTP into a trinucleotide-repeat DNA sequence. The PRINS technique is a fast (2-hour) and simple one-step procedure for sequence-specific detection of nucleic acids in situ. We are continuing to map the PRINS hybridization domains on chromosome 1. The tandem expansion of certain trinucleotide DNA sequence repeats has been implicated as a common cause of human genetic disease, a relationship supported by our preliminary results: we found a correspondence between high-density clusters of the trinucleotide repeat CAG and cytogenetic bands known to contain fragile sites where breakage may occur. We are adapting the PRINS method so that it can be applied to routine FISH analyses of monochromosomal cell hybrids and purity checks of flow-sorted chromosomes.

We have intensified efforts to develop new software to facilitate chromosome mapping. First, we further automated and refined the quantitative procedure for measuring the fractional length of FISH probes on metaphase chromosomes. In addition, we developed software methods to resolve two closely spaced or overlapping FISH signals using mathematical centroid-finding techniques and to facilitate assignment of FISH or PRINS signals to the locations of cytogenetic bands. These programs will continue to be refined as they are applied to future chromosome mapping projects.

We also expanded our application of quantitative fluorescence analyses to include mapping cell immunofluorescence from digitized images collected by confocal microscopy and our cooled CCD microscope system, and we developed software to analyze immunofluorescence in subcellular regions and to count aggregates of fluorescence signals in nuclei. Our software has been used to quantify the cellular distribution of immunofluorescence staining of the DNA repair protein XPG and its analogs and to compare the distributions in normal cells and in cells with DNA breakage from UV irradiation. Other researchers are using our techniques in their cell immunofluorescence analysis projects.

Our work on direct-labeled fluorescent probes, computer-assisted microscopy, and quantitative image analysis will contribute

to a wide range of research projects. It will

- Facilitate DNA mapping and sequencing efforts of the Human Genome Program. Direct-labeled DNA probes will reduce the time required for sample analysis since time- and reagent-consuming post-hybridization/immunological amplification steps will be eliminated. Furthermore, multispectral imaging will make it possible to obtain more information from the same sample.

- Enhance cell and radiation biology initiatives. Multicolor, direct-mode labeling techniques will greatly facilitate the simultaneous assessment of multiple gene-regulation events in single cells.

- Contribute to structural biology efforts. Direct-labeled fluorescent DNA probes will improve spatial resolution of probes located strategically on chromatin.

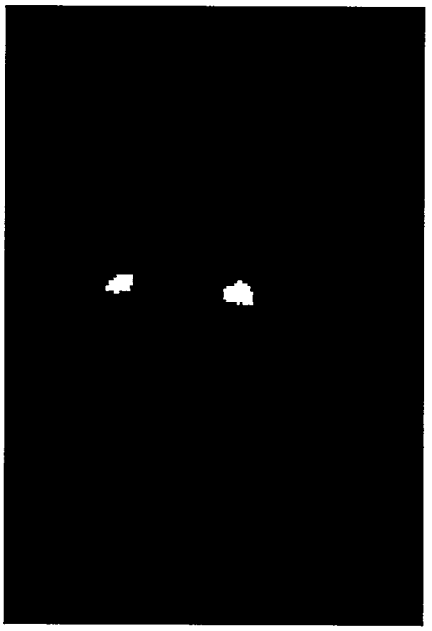
- Provide technological improvements that will enrich quantitative fluorescence microscopy capabilities and image cytometry throughout the biosciences.

Publications

Doggett, N.A., et al., "An Integrated Physical Map of Human Chromosome 16," *Nature*, Supp., 335-365 (1995).

Jarvela, I.E., et al., "YAC and Cosmid Contigs Spanning the Batten Disease (CLN3) Region at 16p12.1-p11.2" (to be published in *Genomics*).

Stackhouse, M.A., B.L. Marrone, D. Grady, et al., "Regional Assignment of the Human DNA Repair Gene (XRCC4L) to the 5q13-14 Boundary by Fluorescence In Situ Hybridization," *Genomics* **27**, 215 (1995).



Composite image of a human chromosome 11 labeled with two fluorescent DNA probes. The top set of signals is from a DNA sequence coding for a DNA repair gene, and the bottom set is from a DNA sequence in a region containing a gene for an inherited cancer. The direct-labeling techniques we are developing will be used to determine the physical relationship between the two genes.

Fast Events in Protein Folding

William Woodruff

The objective of this work is to achieve a molecular understanding of how proteins build their native three-dimensional, folded structures. Such understanding requires the identification and characterization of intermediates in the protein folding process on all relevant time scales, from picoseconds to seconds. The short-timescale events in protein folding are entirely unknown. The present state of the art in experimental approaches is limited to milliseconds or longer, by which time much of the folding process is already over. The gap between theory and experiment is enormous: current theoretical and computational methods cannot realistically model folding processes with lifetimes longer than one nanosecond.

Our unique approach is to employ laser pump-probe techniques that combine novel methods of laser reaction initiation with time-resolved vibrational spectroscopic probes of protein transients. In this scheme, we use a picosecond to nanosecond laser photolysis pulse to produce a pH or temperature jump, which initiates a protein folding or unfolding reaction. We then use structure-specific time-resolved vibrational probes to identify and characterize protein folding intermediates. This information has provided the first tests of the validity of molecular dynamics simulations on the subnanosecond time scale, as well as the first structural information of any sort from the temporal "abyss" between one nanosecond and one millisecond. Given the primary structure of a protein, we now have an important experimental basis for understanding and predicting folding pathways (dynamics), the stable native structures of proteins, and thermally and kinetically accessible conformational substates.

Publications

Williams, S., T. Causgrove, R. Gilmanshin, et al., "Fast Events in Protein Folding: Helix Melting and Formation in a Small Peptide" (to be published in *Biochemistry*).

Measurement of Photodynamic Therapy Drug Concentrations in a Tissue Phantom

Judith Mourant

The purpose of this project is to develop methods for measuring light absorption in highly scattering media. The particular application we addressed was the measurement of photosensitizers for use in photodynamic therapy (PDT), an experimental treatment for cancer that is nearing FDA approval.

For PDT, a photosensitive drug with an affinity for cancerous tissue is administered topically, orally, or intravenously. After the drug has been allowed to selectively concentrate in the tumors, it is activated with a light source of a specific wavelength. The mechanism leading to cell death is believed to involve the creation of singlet oxygen in the tumor, which is toxic to cells.

Knowledge of the concentration of the photosensitive drug present in tissue is necessary for proper light dosimetry during PDT. Presently, control of the light dosage is problematic: if too much light is applied, the tissue surrounding the tumor is also damaged; if insufficient light is applied, the targeted tumor remains viable. Ideally, implementation of PDT would use a feedback system for light delivery that incorporates the optical properties of the tissue and knowledge of the concentrations of photosensitive drugs in the tissue to be treated.

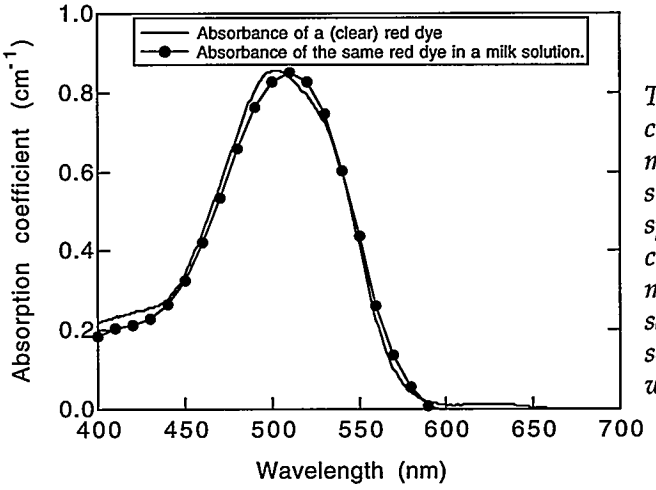
We have shown that under some circumstances white-light elastic-scatter spectroscopy can be used to measure absorption, and we have measured absorbers in relatively large (~500 mL) volumes of highly scattering media (see figure). Generalization of this technique to smaller volumes is quite difficult, however, and requires a detailed understanding of how the elastic-scatter signal is determined by scattering parameters, such as the reduced scattering coefficient and the distribution of scattering angles.

To this end, we have furthered the development of a Monte Carlo simulation for modeling the transport of photons from a source fiber to a detection fiber in close proximity (see schematic), and we have compared our code with experimental measurements of tissue phantoms. We have also obtained some interesting results regarding the role of the angular scattering distribution in determining the elastic-scatter signal.

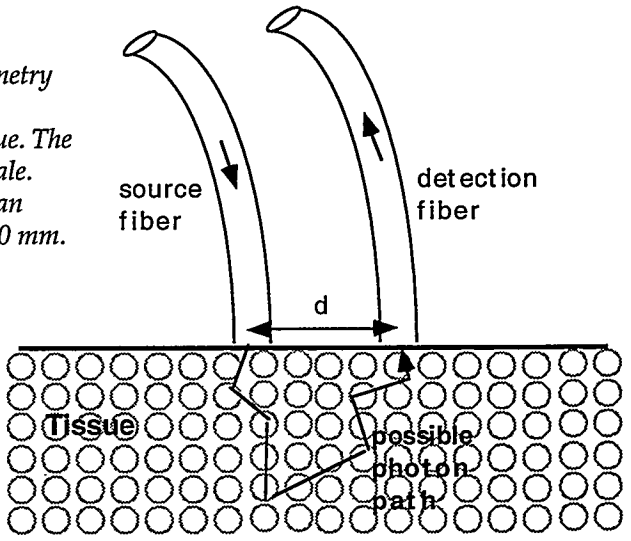
Publications

Mourant, J.R., I.J. Bigio, J. Boyer, et al., "Detection of Gastrointestinal Cancer by Elastic Light Scattering Spectroscopy" (submitted to *Biomedical Optics*).

Mourant, J.R., T.F. Fuselier, J. Boyer, et al., "Predictions and Measurements of Scattering and Absorption over Broad Wavelength Ranges in Tissue Phantoms" (submitted to *Applied Optics*).



The absorbance of a clear red dye measured in a standard spectrophotometer compared with the measurement of the same red dye in a solution of 10% whole milk.



A representative geometry for elastic scatter measurements of tissue. The schematic is not to scale. Fiber separation, d, can range from 0 to ~1500 mm. The diameter of the fibers is typically between 200 and 500 mm.

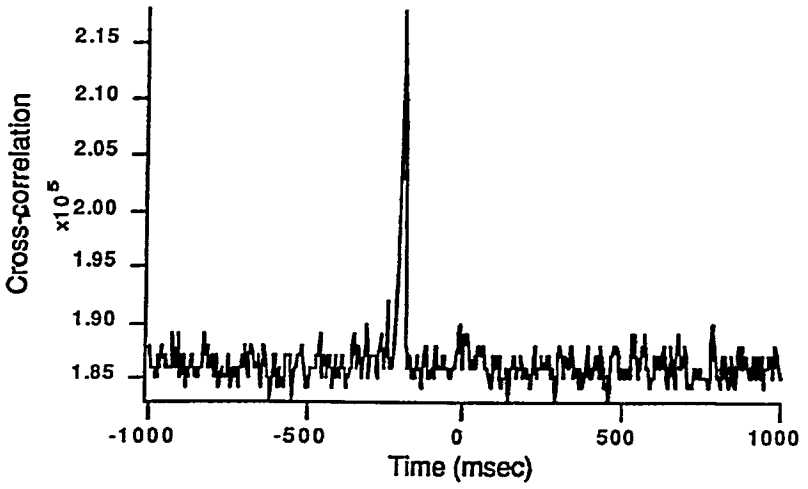
Ultrasensitive Nucleic Acid Sequence Detection by Single-Molecule Electrophoresis

Alonso Castro

The detection of specific DNA sequences with high sensitivity is of fundamental importance for diagnosing the early-stages of bacterial and viral infections, detecting genes associated with genetic disorders, and detecting the early-stages of tumor development. The most important drawback of current methods is their lack of adequate sensitivity, which makes quantitative detection difficult. In many cases, the specific sequence is present at concentrations so small that detection is impossible.

In this project, we have demonstrated the initial steps required for the development of a new method for the detection and quantification of specific DNA sequences with single-copy sensitivity. The proposed method is based on our single-molecule electrophoresis (SME) detection technique, which consists of measuring the electrophoretic velocities of individual molecules in solution under an applied voltage.

Our approach is based on monitoring for the presence of specific DNA sequences that are unique to a particular disease agent or gene. After hybridizing a fluorescent DNA probe to the target DNA, we run the sample through our SME apparatus. By performing the analysis under specific conditions, we can obtain two electrophoretic velocity distributions, corresponding to the probe-target complex and the unbound probe. If the particular DNA sequence sought is not present, no probe-target complex peak is observed.



Cross-correlation between the two detector signals for a 5-fM solution of a 33-mer oligonucleotide labeled with tetramethylrhodamine in Tris-borate-EDTA buffer and sieving medium.

In this project, we have successfully demonstrated the detection of a labeled 33-mer oligonucleotide with single-molecule sensitivity. These initial experiments show the applicability of SME to the detection of single-stranded short fragments of DNA with single-molecule sensitivity.

Publications

Castro, A., and E.B. Shera, "Single-Molecule Electrophoresis," *Anal. Chem.* **67**, 3181–3186 (1995).

Optimal Screening Designs For Biomedical Technology

David Torney

Screening many types of molecules to isolate a few types of molecules with unusual properties is an important process in biomedical technology. To efficiently isolate unusual types of molecules (p) from a collection of types of molecules (n), we employ pools containing subsets of the n types. The pool designs we will construct, such as t-designs, require a number of pool assays approximately equal to p multiplied by the logarithm (base two) of n.

Because screening technology is information-based, our results will have broad applicability. For example, we will demonstrate their use in screening individuals for a large number of genetic diseases. We will also construct pooling schemes for new developments in biotechnology, such as the current emphasis on batch screening of sequence-tagged sites (STSs) against large yeast artificial chromosome (YAC) libraries. We will program and employ commercially available robots to

implement pooling for optimally efficient STS-based screening of large YAC libraries.

We focused on two different issues. The first issue was what type of pooling should we do when we have objects which are independently positive but with different probabilities. For example, when we pool clones of different lengths, they have different prior probabilities of containing markers. We found that the number of pools these clones should occur in is only logarithmically dependent upon the prior probability.

We also continued to characterize optimal pooling designs. We considered all designs that have the same number of clones in each pool and found that designs in which every pair of clones coincides in the same number of pools are particularly well suited for our clone-library screening applications. (These new designs are different from the t-designs we initially proposed). We gave some consideration to the construction of these designs.

In addition we carried out some experiments to understand the nature of the errors present when screening pools of YAC clones. We also continued to implement our Markov-Chain Monte Carlo technique for ranking candidate positive clones in the presence of experimental errors. We collaborated with Dr. Shizuya of the California Institute of Technology to construct a pooling design for one of his clone libraries that has over 100,000 clones.

Publications

Balding, D., and D. Torney, "Optimal Pooling Designs with Error Detection" (to be published in *Combinatorial Theory A*).

Balding, D.J., W. J. Bruno, E. Knill, et al., "A Comparative Survey of Non-Adaptive Pooling Designs," in *Genetic Mapping and DNA Sequencing*, T. P. Speed and M. S. Waterman, Eds. (Springer-Verlag, New York, in press).

Bruno. W., E. Knill, D. Balding, et al., "Efficient Pooling Designs for Library Screening," *Genomics* **26**, 21(1994).

Knill, E., W. Bruno, and D. Torney, "Non-Adaptive Group Testing in the Presence of Errors" (submitted to *Discrete Appl. Math.*).

Optimization and Monitoring of Hollow-Fiber Bioreactors

James Freyer

Multicomponent fluid separation modules based on hollow-fiber polymer membranes (HFPM) can be used as bioreactors to produce very high density cultures of mammalian cells. Because HFPM bioreactors can transport metabolites and metabolic products to and from dense cultures of cells, they have many potential applications in basic research and industry. For example, they can be used to synthesize genetically engineered products, serve as artificial organs in humans, and realistically model tumors for cancer research. However, current hollow-fiber bioreactor designs are largely empirical, and the performance of such systems is far from optimal. We are developing improved bioreactors based on novel high-performance polymer membranes and new methods for assessing bioreactor performance noninvasively and in real time.

We have made progress in several areas. We constructed and tested a 5-mm-diameter hollow-fiber bioreactor for use in nuclear magnetic resonance (NMR) imaging. This reactor supports the growth of mouse mammary tumor cells. In addition, we developed a system for suspending a single fiber for NMR imaging of transport properties, and we developed NMR pulse sequences for generating high-resolution images of water transport in both of these experimental systems.

We are also developing specialized cell culture systems to take full advantage of the unique capabilities of NMR microscopy in measuring nutrient transport properties. We have tested sheets of novel membrane materials for cell attachment and growth. In addition, we have recently developed a new cell culture system for perfusing cells embedded in a matrix through a membrane sheet. This system has been optimized for NMR analysis of both membrane transport properties and transport properties within the cell mass. We have demonstrated that viable cells can be recovered from different locations within the matrix, locations that represent different microenvironments as a function of distance from the nutrient supply.

The Preparation and Utilization of ^{13}C- and ^{15}N-Labeled DNAs for the Determination of Unusual DNA Structures Relevant to the Human Genome Project by Nuclear Magnetic Resonance Spectroscopy

Louis Silks

Recent reports have highlighted the role of DNA-triplet repeats in the genome as factors in human diseases. In affected individuals, stretches of unstable, repetitive DNA-nucleotide triplets can expand into hundreds or even thousands of copies, thereby mangling gene expression. The health-related effects of this expansion ranges from myotonic dystrophy to Huntington's disease. To help understand the causal factors of these diseases, elucidation of the solution structures of these stretches of DNA is critical. The unusual DNA structures that are of immediate interest are (1) the repetitive $(TTAGGG)_n$ sequence at the human telomere, (2) the repetitive $(AATGG)_n{\cdot}(CCATT)_n$ sequence at the human centromere, and (3) the repetitive $(GGC)_n{\cdot}(GCC)_n$ sequence.

The complexity of these DNA motifs requires stable isotope labeling for structural determination by nuclear magnetic resonance (NMR) spectroscopy. We have constructed a $(C[6\text{-}^{15}N]AG)_5$ repeat. At first we experienced a few problems during the purification process because we were using a slight excess of the valuable labeled phosphoramidite but we have overcome that difficulty and we have optimized the purification using semipreparative reverse-phase (C6) high-performance liquid chromatography (HPLC). By taking the crude ammonia solutions from the automated 394 ABI synthesizer, we obtain excellent separation of the CAG repeat containing triphenylmethyl (trityl) from the truncated failure sequences. The trityl-containing $(C[6\text{-}^{15}N]AG)_5$ repeat has a retention time of 19.1 minutes, which compares favorably with that of the unlabeled trityl on DNA.

We have purified 40 micromoles of the $(C[6\text{-}^{15}N]AG)_5$ repeat and begun taking NMR measurements. Initial multidimensional NMR spectroscopy studies have unambigously correlated the hydrogens that are directly bonded to the labeled nitrogens. All five enriched nitrogens can be clearly observed from the one-dimensional ^{15}N NMR spectrum. Moreover, in variable-temperature NMR experiments, we may have discovered what appears to be the presence of a single-stranded hairpin conformation at 15°C.

Publications

Ashburn, D., J. Kelly, R. Michalczyk, et al., "An Improved Synthesis of [amino-^{15}N]Adenine and β-2'-Deoxy-[amino-^{15}N]Adenosine," *J. Labelled Compds. Radiopharm.* **36**, 631 (1994).

Orji, C., J. Kelly, D. Ashburn, et al., "The First Synthesis of β-[9-^{15}N]-2'-Deoxyadenosine" (to be published in *J. Chem. Soc. Perkin Trans. 1*).

Orji, C., and L.A. Silks "The First Synthesis of [9, amino-$^{15}N_2$]Adenine and β-2'-Deoxy-[9, amino-$^{15}N_2$]Adenosine" (submitted to *J. Labelled Compds. Radiopharm.*).

Applications of Strand-Specific In Situ Hybridization

Edwin Goodwin

Fluorescence in situ hybridization (FISH) is used to determine the location of specific DNA sequences on chromosomes. It is an effective tool in genomic mapping and is finding increasing use in medical diagnosis. We have developed a strand-specific version of FISH. The new procedure reveals not only location but also the 5'-to-3' direction of a target sequence, such as the sense strand of a gene. (On one end of a DNA strand is a 5' phosphate group, and on the other end is a 3' hydroxyl group. The locations of these groups establishes a 5'-to-3' polarity of the DNA.)

This project will expand the range of applications of strand-specific FISH. Specifically, we intend to develop methods to

- examine changes in gene expression induced by malignancy,
- investigate gene amplification, and
- facilitate genomic mapping.

We have probed by chromosome-oriented FISH (CO-FISH) several repetitive DNA sequences, including sequences informative on human, mouse, and hamster

cells. Results of this study show that almost all tandem repeats exist in a head-to-tail orientation. In contrast, the dispersed repeats show no preferential orientation. We also continued an ongoing investigation of the mechanisms of aneuploidy-inducing agents.

The source of the lateral asymmetry, that is, the asymmetrical fluorescence intensity between adjacent chromosomal regions, was investigated. We realized that CO-FISH could provide a crucial test for a twenty-year-old proposed mechanism based on differential fluorescence quenching by bromodeoxyuridine. After one cycle of growth in bromodeoxyuridine, mitotic mouse chromosomes have sister chromatids in which one centromere has incorporated twice as much bromodeoxyuridine as the other. The sister chromatid with the greater amount of bromodeoxyuridine was expected to fluoresce less brightly because of greater fluorescence quenching. This would result in lateral asymmetry. We found that the dimmer chromatid did in fact contain a greater amount of bromodeoxyuridine—a result that supports the proposed mechanism.

Publications

Goodwin, E. H., J. Meyne, S.M. Bailey, et al., "On the Origin of Lateral Asymmetry" (to be published in *Chromosoma*).

Meyne, J., and E.H. Goodwin, "Direction of DNA Sequences Within Chromatids Determined Using Strand-Specific FISH," *Chromosome Research* **103,** 375 (1995).

Meyne, J., E.H. Goodwin, and R.K. Moyzis, "Chromosome Localization and Orientation of the Simple Sequence Repeat of Human Satellite I DNA," *Chromosoma* **103,** 99 (1994).

Determining the Role of the Telomere on the Severity of Birth Defects

Michael Altherr

Many birth defects are associated with the loss of genetic material near the ends (termini) of chromosomes. At least one-third of human chromosomes can have terminal deletions that result in live births but significant clinical abnormalities. Terminal deletions can arise by a variety of mechanisms, including the clastogenic effects of ionizing radiation.

Terminal deletion syndromes in newborns are often identified by common diagnostic criteria. For example, the cat-like cry of infants with *cri-du-chat* syndrome results from the loss of the terminus of the short arm of chromosome 5. However, there is often extreme variability in other symptoms, for example, the degree of mental retardation.

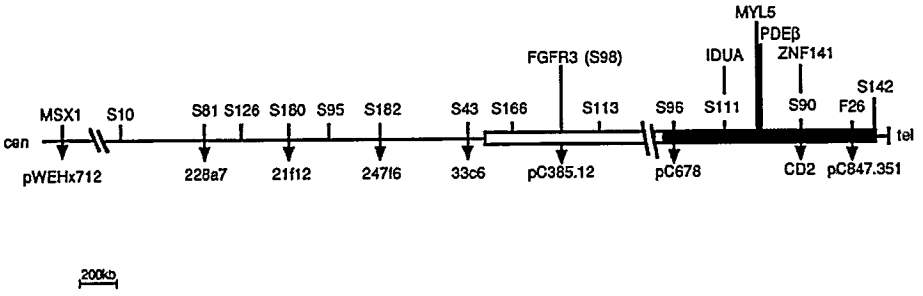
Chromosome stability is severely impaired if the terminal structure, the telomere, is missing. In fact, complete chromosomal loss has been observed in experimental organisms when the telomere is removed or disrupted. With the exception of Turner syndrome—for which only a single X chromosome is present—monosomy (having a single member of a chromosome pair) is invariably fatal in humans. Therefore, it is important to know how terminal deletions are healed to stabilize the chromosome.

The telomere is a unique chromosomal element that has been demonstrated to generate novel structures, to initiate DNA replication at the ends of chromosomes, and to affect the expression of genes in its proximity. We have assembled a collection of cosmid clones representing the terminus of chromosome 4p to use as landmarks in determining the extent of chromosome 4 deletions associated with a congenital abnormality called the Wolf-Hirschhorn syndrome (WHS). The primary-level clones are depicted in the first of the accompanying figures.

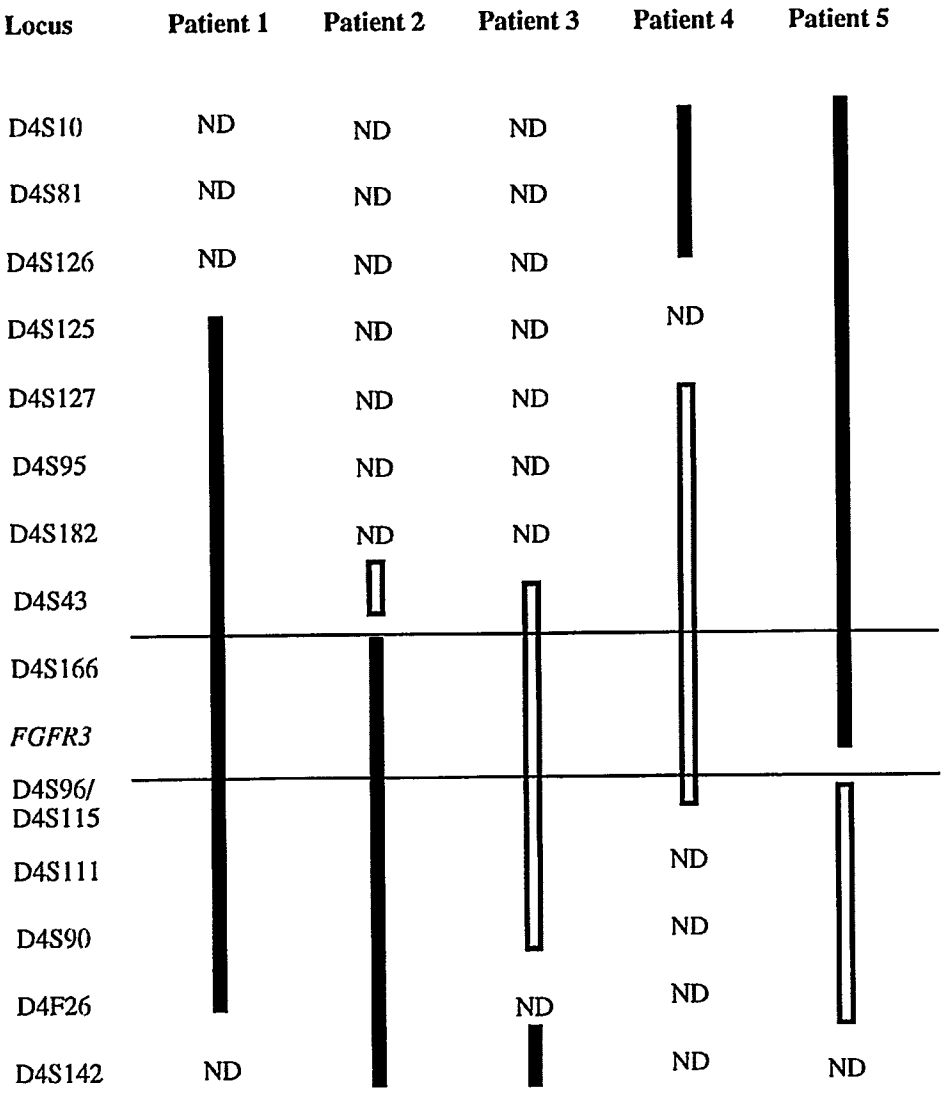
We have used cosmid clones—and additional clones comprising interval-specific subsets—to begin high-resolution analysis of a collection of cell lines derived from patients with chromosome 4 deletions. Our work has reduced—by more than 1 million base pairs—the region of chromosome 4 thought to contain genes that contribute to normal development. The second figure shows a summary of this analysis on five cell lines and the newly defined critical region for this congenital abnormality. We have also begun RNA isolation from these and other cell lines to study the effects of these deletions on the expression of a number of marker genes.

Publications

Altherr, M.R., K. Dennison, T. Wright, et al., "A Patient with the Deletion of Chromosome 4p Redefines the Wolf-Hirschhorn Syndrome Critical Region" (submitted to *Am. J. Human Genetics*).



Representation of the terminus of the short arm of human chromosome 4. We list the cosmid probe names below the horizontal line representing chromosome 4. We give locus designations above the line and use genetic designations for known genes. S-numbers represent anonymous DNA segments. The critical region thought to contain genes responsible for normal development, and missing in WHS patients, is indicated by the box on the horizontal. The open box represents the new critical region defined by our work. The solid box represents a segment of chromosome 4 not contained in cosmid clones.



Summary of analysis of five patients with symptoms of WHS. The newly defined critical region is bounded by the horizontal lines. Locus designations are the same as in our first figure; again, the open box represents the new critical region defined by our work, and the solid box represents a segment of chromosome 4 not contained in cosmid clones. ND means not determined.

Engineering Sequence-Specific RNA and Single-Stranded-DNA Binding Proteins

Thomas Terwilliger

The technology to design a protein that binds to any given RNA or single-stranded DNA sequence has many potential applications. For example, viral diseases such as AIDS could be treated by transmitting a sequence-specific engineered protein into an infected cell, where it would bind to and inactivate a key messenger RNA.

In this project we are constructing a set of protein modules that recognize specific four-nucleotide sequences of RNA or single-stranded DNA. In addition, we are developing the technology to link four or more of these modules in any order to generate proteins that bind specifically to any 16-nucleotide (or longer) sequence of RNA or single-stranded DNA.

Our protein modules are based on the gene 5 protein from bacteriophage f1. The gene 5 protein has several properties that suit it well for our application: (1) gene 5 protein naturally recognizes four nucleotides at a time, (2) the natural protein has limited specificity, recognizing either RNA or single-stranded DNA, and (3) gene 5 protein molecules bind cooperatively.

Last year we constructed a generic module that contains four binding sites, each of which binds a single-stranded sequence of four nucleotides. During the upcoming year we will modify our generic binding module through random mutagenesis and isolate modules with different sequence specificities.

Publications

Cheng, X., A.C. Harms, P.N. Goudreau, et al., "Direct Measurement of Oligonucleotide Binding Stoichiometry of Gene 5 Protein by Mass Spectrometry" (submitted to *Proc. Natl. Acad. Sci. U.S.A.*).

Sandberg, W.S., P.M. Schlunk, H.B. Zabin, et al., "Relationship between In Vivo Activity and In Vitro Measure of Function and Stability of a Protein" (to be published in *Biochem.*).

Terwilliger, T.C. and J. Berendzen, "Difference Refinement: Obtaining Differences between Related Structures" (to be published in *Acta Crystallogr.*).

Terwilliger, Thomas and Joel Berendzen, "Bayesian Weighting for Macromolecular Refinement" (submitted to *Acta Crystallogr.*).

Development of an Ultrasensitive and Rapid DNA Repair Assay

Min S. Park

We have developed a rapid, highly sensitive, and quantitative assay for DNA repair. We recognized the need for such an assay after observing that the quantity of full-size, in vitro transcripts synthesized from DNA templates decreased as a function of chemical- or radiation-induced damage to the DNA.

First, we developed a nonradioactive means of monitoring DNA repair by refining the use of chemiluminescent ribonucleotide analogs as substrates in the in vitro transcription reaction. Then we tested the functionality of the purified DNA repair protein XPG using these nonradioactive substrates. The progress to date strongly indicates that our assay provides high sensitivity, high reproducibility, and high sample throughput, while minimizing risks to users. We anticipate that our assay can be further improved as more sensitive chemiluminiscent substrates become available in future.

During the upcoming year, we will refine the assay so that it can be made more user friendly. In addition, we will use our assay to further characterize the catalytic activities of purified XPG and to monitor the repair of DNA templates containing bulky adducts to assess its value in screening for chemicals that form such adducts or DNA cross-links. We hope that our assay will eventually be used in large-scale epidemiological studies to assess skin-cancer susceptibility and to screen for new environmental mutagens. Our assay may also be used to identify cancer patients who might be highly sensitive to radiation so that their doctors can choose lower-risk alternative therapies.

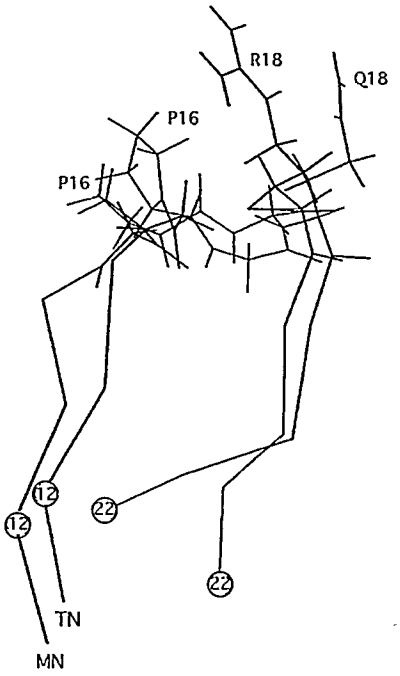
Structure and Thermodynamics of Surface Recognition

Goutam Gupta

This project combines molecular modeling, two-dimensional nuclear magnetic resonance (NMR) spectroscopy, and antibody binding experiments (both equilibrium and kinetic) to study the structural and thermodynamic aspects of HIV surface recognition. Our goal is to identify the structural features in the third variable region (V3) of the HIV surface glycoprotein gp120 and in particular the principal neutralizing determinant (PND), the structure of which remains conserved despite sequence variations.

The conserved structure of the PND is a solvent-accessible protruding knob, structurally similar to the immunodominant knobs in the tandem repeat of the human mucin 1 (MUC1) protein, a tumor antigen for breast, pancreatic, and ovarian cancer. By replacing the mucin antigenic knobs (see figure) with the PND knobs in a set of chimeric human MUC1/HIV V3 antigens, we have produced multivalent HIV antigens in which PNDs are located at regular intervals, separated by extended mucin spacers.

We have used two-dimensional NMR spectroscopy to confirm that the native structure of the PNDs is preserved in the multivalent antigens. In addition, we have used an enzyme-linked immunosorbent assay to demonstrate that the PNDs on our multivalent antigens bind to monoclonal antibodies and polyclonal antisera from HIV-infected patients.



Superimposition of the protruding motifs of two NMR structures: theV3 loop from the HIV-MN isolate (designated MN) and that from the Thailand TN243 isolate (named TN). The crests in the two sequences are oriented in the same way.

Publications

Fontenot, D.J., J. Gatewood, S.V.S. Mariappan, et al., "Human Immunodeficiency Virus (HIV) Antigens: Structure and Serology of Multivalent Human Mucin MUC1-HIV Chimeric Proteins," *Proc. Natl. Acad. Sci. U.S.A.* **92**, 315–319 (1995).

Computer Simulation of Protein Solvation, Hydrophobic Mapping, and the Oxygen Effect in Radiation Biology

Lawrence Pratt

The goal of this project is to develop the theory and computational tools required to use computer simulation data on protein solvation for identifying hydrophobic and hydrophilic regions of solvated biomolecules.

The project is based on recent discoveries in the theory of aqueous solutions that have resolved decades-old controversies over the solubility in water of simple hydrophobic species such as inert gases—argon or xenon—or oxygen. We expect that our work will provide information on stabilizing folded protein structures, binding proteins to DNA or other substrates, and binding ligands to proteins. This work can also be applied to studies of the structure and function of proteins, hormones, and nucleic acids.

In trying to apply the techniques developed for inert-gas solutes to proteins in water, we anticipate that acquiring simulation data for solvated proteins will be difficult and expensive and therefore that the resolution and statistical surety will not be as good as those obtained for the inert-gas solutes.

In the first year of the project—FY94—we carried out baseline studies of classical small-molecule hydrophobic effects, and we began to acquire simulation data on larger modelled aqueous systems. We also began to adapt and recode image restoration algorithms that should allow us to

use low-resolution, noisy primary data to construct hydrophobic maps of complex solutes in water.

During the past year we analyzed simulation results using maximum entropy models. This analysis has led us to a simple heuristic molecular model of hydrophobic interactions that accounts quantitatively for the central hydrophobic phenomena of cavity formation and the association of inert-gas solutes in water. We have submitted a paper describing this discovery to *Science* magazine.

Publications

Corcelli, S.A., J.D. Kress, L.R. Pratt, et al., "Mixed-Direct-Iterative Methods for Boundary Integral Formulations of Continuum Dielectric Solvation Models" in *Pacific Symposium on Biocomputing* (World Scientific, Teaneck, NJ, in press).

Hummer, G., L.R. Pratt, and A.E. Garcia, "On the Free Energy of Ionic Solvation In Water" (to be published in *J. Phys. Chem.*).

Hummer, G., L.R. Pratt, and A.E. Garcia, "The Hydration Free Energy of Water" (to be published in *J. Phys. Chem.*).

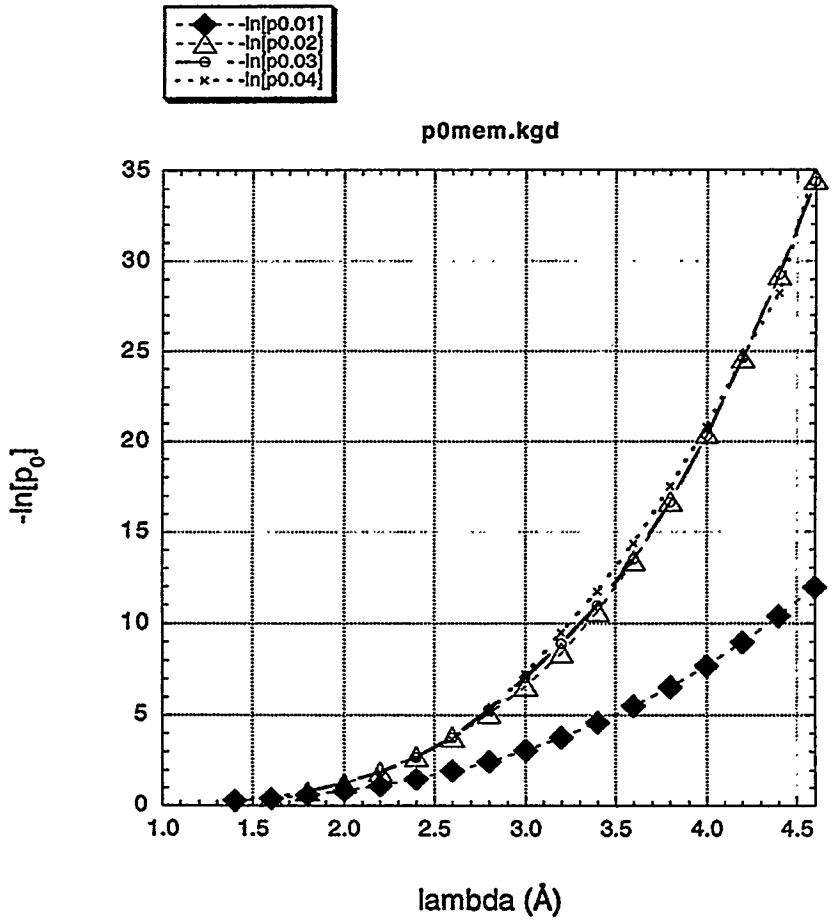
Hummer, G., S. Garde, A.E. Garcia, et al., "A Heuristic Molecular Model of Hydrophobic Interactions" (submitted to *Science*).

Pratt, L.R., G.J. Tawa, G. Hummer, et al., "Boundary Integral Methods for the Poisson Equation of Continuum Dielectric Solvation Models" (submitted to *J. Phys. Chem.*).

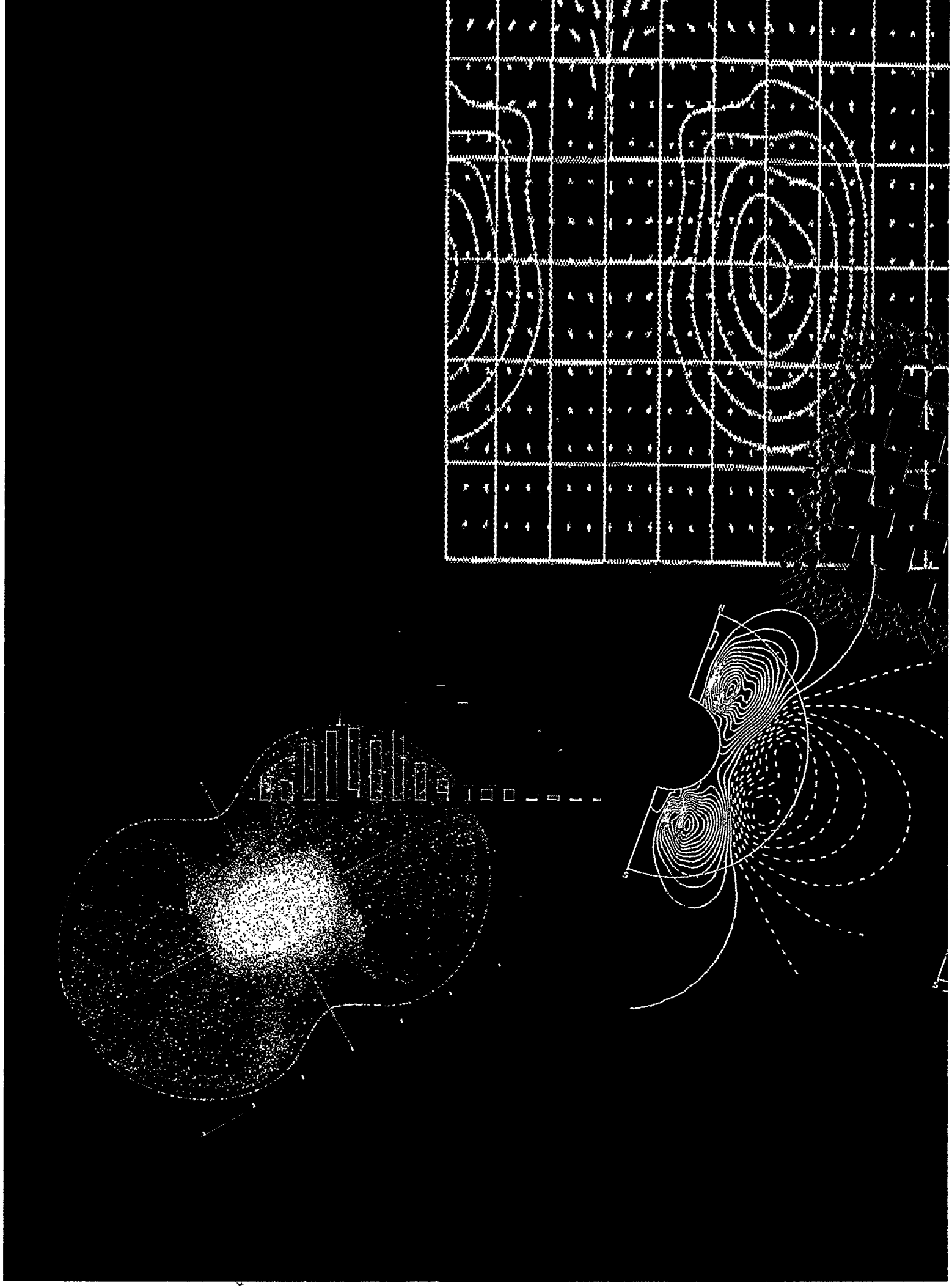
Tawa, G.J., and L.R. Pratt, "Tests of Dielectric Model Descriptions of Chemical Charge Displacements in Water," in *Structure and Reactivity in Aqueous Solutions: Characterization of Chemical and Biological Systems*, ACS Symposium Series, C. J. Cramer and D. G. Truhlar, Eds. (Americal Chemical Society, Washington, DC, 1994), Vol. 568, pp. 60–70.

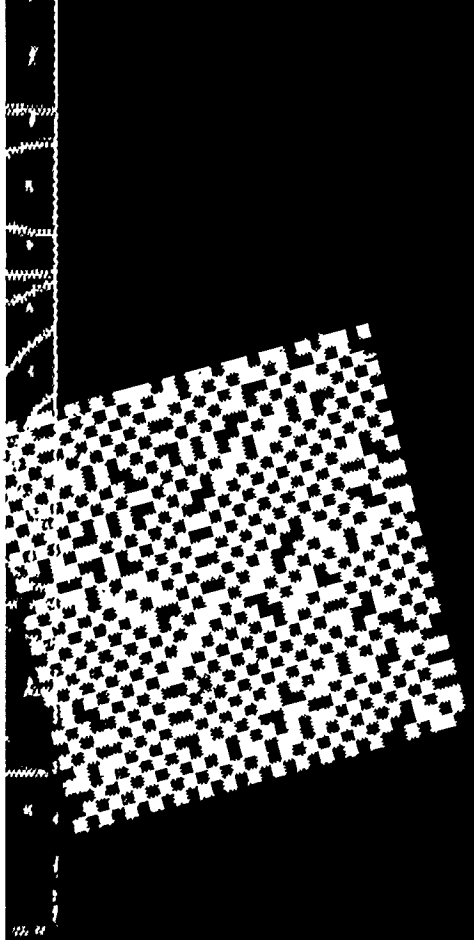
Tawa, G.J., and L.R. Pratt, "Theoretical Calculation of the Water Ion Product Kw," *J. Am. Chem. Soc.* **117**, 1625 (1994).

Tawa, G.J., R.L. Martin, L.R. Pratt, et al., "Solvation Free Energy Calculations Using a Continuum Dielectric Model for the Solvent and Gradient Corrected Density Functional Theory for the Solute" (submitted to *J. Phys. Chem.*).



Information theory predictions of free energies of solvation—in thermal energy units k_BT—for spherical solutes as a function of the distance of closest approach (λ). We obtained the solid diamond data points using only the first moment of the occupancy <j>. We obtained the other curves using the 2nd, 3rd, and 4th binomial moments.





1

Competency Development Projects

The Laboratory's core competencies grew out of our historical mission of developing and maintaining the nation's nuclear deterrent. They are not only key to fulfilling the Laboratory's central mission of reducing the global nuclear danger but also contribute to carefully selected civilian programs and industrial collaborations. The core competencies cut across the Laboratory's organizational boundaries and, hence, offer a means of coordinating and integrating our planning and more fully exploiting our multidisciplinary capabilities. The Laboratory's eight core competencies focus on nuclear weapons science and technology; complex experimentation and measurement; nuclear and advanced materials; theory, modeling, and high-performance computing; analysis and assessment; earth and environmental systems; and bioscience and biotechnology.

CD projects support management-initiated R&D in new areas that will stretch—not just maintain—the Laboratory's core competencies. Our CD projects are grouped here as they relate to seven of the nine disciplinary categories for LDRD research.

BULK AND SURFACE ELECTRONIC STRUCTURE OF ACTINIDE, RARE EARTH, AND TRANSITION METAL ELEMENTS AND COMPOUNDS

John M. Wills

Using high-precision electronic structure calculations, we studied the unusual magnetic and structural properties of rare earth, actinide, and transition metals. We studied magnetic moment anisotropies in bulk and surface systems, with an emphasis on novel surfaces with unusual magnetic properties that have possible applications in magnetic recording. We also studied the structural stability, bonding properties, and elastic response of the actinides, as well as transition and rare earth elements and compounds. Our objectives were to understand the unusual crystallographic and cohesive properties of the actinides, the importance of correlation to structural stability, the nature of the delocalization transition in these elements, and the structural stability and elastic response of transition metal elements and alloys.

A task that has run through the lifetime of this project has been the total energy calculation of magnetic anisotropy energies in elemental iron, cobalt, and nickel. This work was the first successful description of these properties in these elements. Our results elucidated the role of orbital polarization in magnetocrystalline anisotropy. A by-product of this work was a new technique for Brillouin zone integrations. We studied the magnetic structure of the surface of iron, cobalt, and nickel on copper substrates; we studied the cobalt surface in conjunction with experimental work. One significant result was finding strongly enhanced orbital moments on the surface and demonstrating that this is a systematic phenomena.

A significant result of our work on structural properties has been the demonstration that the crystal structure stabilities of both d- and f-electron materials are driven by similar mechanisms; in particular, the unusual crystal structures of the light actinides may be understood as a consequence of normal itinerant electron bonding in a regime of narrow bandwidths. This result is important in indicating that the structural properties of the actinides may be in both actinide and transition metals. We calculated elastic constants systematically for transition metal alloys with cubic symmetry and found that the tetragonal shear modulus is correlated with (cubic) structural energy differences—hence band-filling—and that the modulus of alloys can be predicted on this basis.

As part of this project, we also studied structural stability in a variety of other materials over a wide range of pressures. This included a demonstration that the high-pressure phase transition observed in samarium is a delocalization transition. With few exceptions, we found that the body-centered cubic structure is always favored at high pressures. We have demonstrated that, at least in the transition metals, this is a result of increasing hybridization between semicore p-electrons and valence d-electrons.

Publications

Eriksson, O., R. Ahuja, A. Ormeci, et al., "Bulk and Surface Magnetism and Interplanar Spacings in Gd from First-Principles Calculations" (to be published in *Phys. Rev. B*).

Hjelm, A., J. Trygg, O. Eriksson, et al., "Field Induced Magnetism in Itinerant F-Electron Systems: U, Pu, and Ce," *Phys. Rev. B* **50**, 4332 (1994).

Soderlind, P., O. Eriksson, B. Johansson, et al., "Unified Picture of the Crystal Structures of Metals," *Nature* **374**, 524 (1994).

Soderlind, P., O. Eriksson, and J.M. Wills, "Density Functional Calculations Force Metal" (to be published in *Phys. Rev. B*).

Trygg, J., J.M. Wills, M.S.S. Brooks, et al., "Calculation of Elastic Constants in UC, US, and UTe," *Phys. Rev. B* **52**, 2492 (1995).

Trygg, J., J.M. Wills, B. Johansson, et al., "Field Induced Magnetism in Uranium Compounds: UGe_3 and URh_3," *Phys. Rev. B* **50**, 9226 (1994).

Trygg, J., J.M. Wills, B. Johansson, et al., "First Principles Study of the Magnetization Density in $CeFe_2$," *Phys. Rev. B* **50**, 4200 (1994).

Diffuse Transport in Modern Polymeric Materials

Charles Doering

Polymers, composites, and synthetic modern materials are replacing traditional materials in many older scientific, engineering, commercial, and military applications. Wholly new devices, applications, and even new fields are emerging because of the existence of these new materials. New adhesives, bonding materials, and sheet-molding compounds offer both great gains in strength and flexibility and great savings in weight when used as critical materials in commercial and military vehicles and devices. "Smart" polymer gels will provide the basis for innovative and sophisticated devices for use in drug delivery, agriculture, environmental chemistry, and environmental protections and clean-up.

Our project focuses on new polymeric materials. We are deriving and analyzing models that can predict their seemingly mysterious transport properties. We shall identify the dominant physical mechanisms and the pertinent dimensionless parameters, produce viable theoretical models, and devise asymptotic and numerical methods for use in specific problems.

We have studied several new problems in the design, fabrication, and use of polymer-penetrant systems. Because of the nature of the novel phenomena involved, it was necessary to derive new models. Specifically, the problems involve diffusive transport inducing a glass-rubber phase change and strong mechanical relaxation of a viscoelastic nature in the polymer. In a series of papers over the past few years, D.S. Cohen and his students and coworkers have derived a comprehensive model based on physically reasonable partitions of the penetrant flux. A crucial step is to identify and incorporate memory phenomena, indicative of the effects of mechanical relaxation, as an explicit variation in the chemical potential (or equivalently in the appropriate free energy). This leads to difficult new nonlinear partial differential-integro equations.

Initially, several of Cohen's thesis students studied simplified problems in order to fully understand the theoretical implications, identify the important dimensionless parameters, and to obtain and fully develop useful approximate and numerical methods. We then applied the model to successfully account for and predict both the concentration profile and the motion of the interface in Case II diffusion, including the difficult problems of the motion of actual multi-dimensional glass-rubber fronts.

We have also studied diffusive transport in chemical and biological kinetics and pattern dynamics. We carried out a Monte Carlo study of the wave-front structure in a microscopic model of a diffusion-controlled reaction. As a result, we discovered an instability in the two-dimensional problem (appropriate to reactions taking place on surfaces). Our result challenges the classical mean field theory and raises questions of the influence of internal fluctuations on nonequilibrium structures. We applied the concept of fluctuation-dominated transport, where nonlinear, dynamic processes help to rectify random noise into directed motion, to develop a model of a molecular motor operating on DNA strands (a one-dimensional problem). Our study suggested experimental measurements that may be used to test the model.

Publications

Doering, C., B. Ermentrout, and G. Oster, "Rotary DNA Motors" (to be published in *Biophys. J.*).

Riordan, J., C. Doering, and D. Ben-Avraham, "Fluctuations and Stability of Fisher Waves," *Phys. Rev. Lett.* 75, 565 (1995).

Advanced Deformation Process Modeling

U. Fred Kocks

We are developing a comprehensive, coherent description of how material behaves in deformation processing. The products we are aiming for are not only rules and equations but also useful subroutines for engineering finite-element computation codes. One of our aims is to assure that these codes will be compatible with an increasing number of different computing environments. On the experimental side, we will develop both prescriptions for determining the parameters required for applications of the model and techniques for ascertaining the model's applicability in a particular case. The materials we will include in our efforts are metals and alloys of arbitrary lattice structure as well as metal-matrix composites. The aspects of behavior we will model include the kinetics of flow, of strain hardening, and of recrystallization over the widest possible regime of temperatures and strain rates; the

various anisotropies of strength and compliance; the assessment of potential instabilities; and the prediction of post-process microstructural and textural features.

Over the past year we have improved constitutive relations for large-scale plasticity, especially in the high-temperature regime and are extending them to a further class of materials, intermetallic aluminides. We have verified the LApp model and provided material constants for it through an extensive comparison of predictions and observations in the area of the dependence of texture formation on material and grain shape. Through the application of the finite-element code for macroscopic plasticity (MicMac) to the problem of local grain interactions we have also improved the prediction of stochastic and systematic spreads in strain and texture and have discovered an interesting mechanism for nucleation in recrystallization. We have customized the texture analysis program (popLA) for specific applications at the Reynolds Metals Company and the Naval Surface Weapons Laboratory.

Publications

Beaudoin, A.J., Jr., P.R. Dawson, K.K. Mathur, et al., "A Hybrid Finite Element Formulation for Polycrystal Plasticity with Consideration of Macrostructure Microstructure Linking," *Intern. J. Plasticity* **11**, 501 (1995).

Beaudoin, A.J., Jr., T. Kota, H. Uto, et al., "Simulation of Sheet Metal Forming Using Polycrystal Plasticity," in *Dynamic Plasticity and Structural Behaviors*, Tanimura and Khan, Eds. (Gordon and Breach, New York, 1995), p. 221.

Beaudoin, A.J., Jr., H. Mecking, and U.F. Kocks, "Development of Local Shear Bands and Orientation Gradients in FCC Polycrystals," in *Simulation of Materials Processing (NUMIFORM-5)*, Shen and Dawson, Eds. (Balkema, Rotterdam, 1995), p. 225.

Beaudoin, A.J., Jr., H. Mecking, and U.F. Kocks, "Development of Localized Orientation Gradients in FCC Polycrystals" (to be published in *Phil. Mag.*).

MacEwen, S.R., A. Langille, J. Savoie, et al., "Characterization, Validation, and Finite Element Modelling of Extrusion," in *Simulation of Materials Processing (NUMIFORM-5)*, Shen and Dawson, Eds. (Balkema, Rotterdam, 1995), p. 85.

Maudlin, P.J., S.I. Wright, U.F. Kocks, et al., "An Application of Multisurface Plasticity Theory: Yield Surfaces of Textured Materials" (submitted to *J. Appl. Phys.*).

Orientation Distribution Function Determination by Rietveld Refinement

Robert Von Dreele

The arrangement of crystallites, described by an orientation distribution function (ODF), within a manufactured part can have a profound effect on its strength and possible failure modes. The traditional method of determining an ODF from a small number of reflection pole figures is inefficient with time-of-flight neutron diffraction. Thus, we have proposed to produce an ODF directly from Rietveld refinement of full diffraction patterns in a limited number of orientations.

Our research objectives were to develop a simple experimental procedure and mathematical treatment to produce an ODF directly from full diffraction patterns. This full-diffraction ODF will advance the development of sophisticated materials such as high-temperature superconducting wires and high-strength composite materials. Our approach is to obtain diffraction data from "standard" texture samples and from more complex test specimens, determine their textures with our methods, and compare the results with those obtained by more traditional methods.

We have implemented the generalized spherical harmonic description of texture in our Rietveld refinement program. It has been tested with numerous neutron powder data sets collected from various test samples. The resulting pole figures calculated from the harmonic coefficients agree with those published for similarly prepared samples of these materials.

Combining ODF determination and crystallite stress/strain measurement embodied in our techniques will allow us to fully understand the relationship of these properties and the strength and failure properties of a manufactured part.

Implications of Diffraction In Situ Loading Macrostrain Measurements in Composites and Finite Element Interpretations

Ning Shi

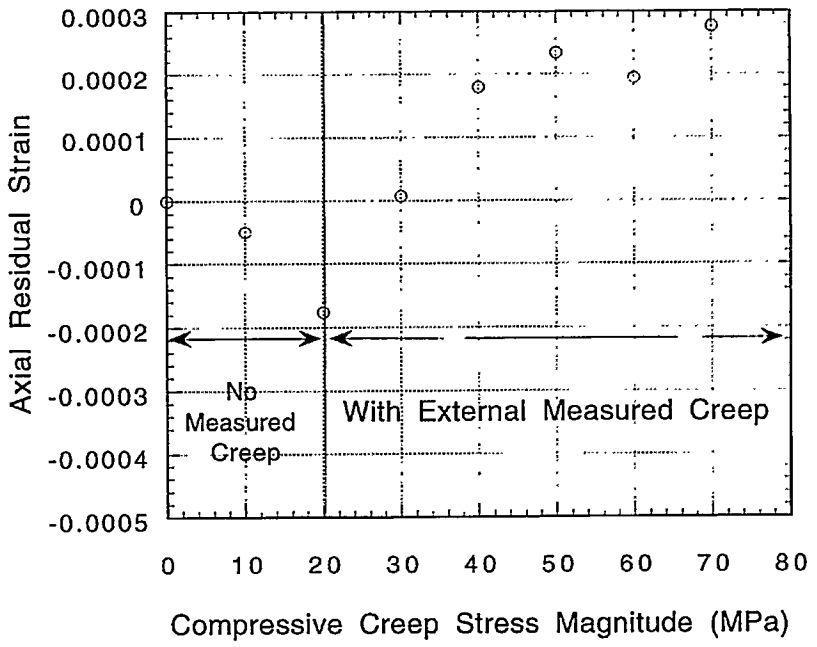
We are applying neutron diffraction and finite element modeling to study the effects of in situ matrix creep on load sharing in metal matrix composites (MMCs). Two creep mechanisms are known for MMCs. The first is power-law creep within the matrix, and the second is creep due to diffusion flow around reinforcement particles at the matrix/reinforcement interfaces. Although the two creep mechanisms have been extensively discussed on a theoretical basis, there is only limited experimental evidence supporting these discussions. In this project, we have measured the relaxation of residual elastic lattice strain in prior creep-loaded Al/SiC MMCs using a neutron diffraction technique, and we have performed finite element modeling on the creep phenomena. For the first time, we have experimental data on strain relaxation that is potentially important in understanding creep mechanisms.

The accompanying figure displays the changes of residual elastic lattice strain in the aluminum matrix along the loading direction after uniaxial compressive creep. In our work, we have observed significant initial relaxation of elastic lattice strain in the matrix when there is no measurable macroscopic creep (i.e., below the creep threshold stress value of ~30 MPa). We interpret this relaxation to be a result of enhanced local diffusion along the reinforcement/matrix interfaces. The stress-gradient-induced local mass transfer reduces the geometrical incompatibility between the matrix and its reinforcing particles and, therefore, the residual mismatch strains. With the onset of bulk matrix power-law creep ($\sigma > 30$ MPa), this incompatibility increases, resulting in an increase in residual strain.

Our work is significant in that it addresses the fundamental physics of inelastic deformation in MMCs, and it provides a practical understanding on the modification of internal stresses by high-temperature inelastic deformation. Internal stresses are important factors in affecting the performance of MMCs.

Publications

Song, G.S., N. Shi, G.T. Gray III, et al., "Particle Shape Effect on the Fracture Path and Ductility of the Discontinuously Reinforced 6061-Al Matrix Composites" (submitted to *Metall. Trans. A*).



Axial residual strain as a function of creep stress. When there is no measurable macroscopic creep, there is an initial relaxation of residual strain. At higher loads, residual strain increases with the load.

Characterization of Advanced Electronic Materials

Joe D. Thompson

The ability to measure and interpret properties of advanced electronic materials bridges the gap between materials synthesis and theoretical modeling. Our work extends the Laboratory's competency in nuclear and advanced materials by characterizing the ground states of materials whose properties are dominated by electronic correlations. Our goal is to discover new physics by understanding the complex interplay among the microscopic interactions that produce these ground states.

In the past year, we had four important accomplishments. First, we discovered pressure-induced superconductivity as antiferromagnetism (at ambient pressure) in $CeRh_2Si_2$ is suppressed. Second, we discovered an unexpected temperature dependence of the charge-excitation spectrum in a correlation-derived, small-gap semiconductor $Ce_3Bi_4Pt_3$ and found a potential link between the physics of this f-electron and related d-electron systems. Third, we discovered a phenomenological relationship between the large magnetoresistance in $La_{1-x}Ca_xMnO_3$ and its field-dependent magnetization, which together are consistent with polaron-hopping conductivity. Fourth, from very-high-pressure studies, we provided the first confirmation of a theoretical model (also applicable to $CeRh_2Si_2$) for competing electronic interactions in an ytterbium-based correlated-electron material.

Publications

Ahrens, E.T., R.H. Heffner, P.C. Hammel, et al., "(9)Be and (11)B NMR Study of Superconductivity in Boron Doped UBe(13)," *Physica B* **206-07**, 589 (1995).

Cornelius, A., J.S. Schilling, D. Mandrus, et al., "Anomalous Hydrostatic Pressure Dependence of the Curie Temperature of the Kondo-Lattice Compound YbNiSn to 38 GPa" [to be published in *Phys. Rev. B (Rapid Communication)*].

Feyerherm, R., A. Amato, C. Geibel, et al., "On the Competition between Superconductivity and Magnetism in CeCu(2)Si(2)," *Physica B* **206-07**, 596 (1995).

Fisk, Z., J.L. Sarrao, J.D. Thompson, et al., "Kondo Insulators," *Physica B* **206-07**, 798 (1995).

Heffner, R.H., and M.R. Norman, "Heavy Fermion Superconductivity" (to be published in *Comments on Condensed Matter Physics*).

Heffner, R.H., J.L. Smith, M.F. Hundley, et al., "Effects of Boron Substitution on the Superconducting State of UBe(13)," *Phys. Rev. B* **51**, 404 (1995).

Hundley, M.F., M. Hawley, R.H. Heffner, et al., "Transport-Magnetism Correlations in the Ferromagnetic Oxide La(0.7)Ca(0.3)MnO(3)" *Appl. Phys. Lett.* **67**, 860 (1995).

Mandrus, D., J.L. Sarrao, A. Migliori, et al., "Thermodynamics of FeSi," *Phys. Rev. B* **51**, 4763 (1995).

Movshovich, R., T. Graf, D. Mandrus, et al., "Response of CeRh(2)Si(2) to Pressure" (to be published in *Physica B*).

Nieuwenhuys, G.J., S.A.M. Mentink, A.A. Menovsky, et al., "μ(+)SR in Antiferromagnetic UNi(4)B," *Physica B* **206-07**, 470 (1995).

Rainford, B.D., D.T. Adroja, A. Severing, et al., "Inelastic Neutron Scattering Study of U(3)Pt(3)Sb(4)," *Physica B* **206-07**, 464 (1995).

Reyes, A.P., L.P. Le, R.H. Heffner, et al., "(209)Bi NMR in Heavy-Electron System YbBiPt," *Physica B* **206-07**, 589 (1995).

Design and Implementation of an X-Ray Strain Measurement Capability Using a Rotating Anode Machine

Joyce A. Goldstone

The need to monitor and preserve the strength of materials during manufacture and service, coupled with component designs that utilize a greater percentage of the available strength, has been a strong driving force for nondestructive testing and numerical prediction of material properties. The measurement and prediction of residual stress is one aspect that has repeatedly proven important. In crystalline materials, diffraction is the measuring technique of choice. By combining x-ray and neutron diffraction measurements, we have been examining some of the fundamental aspects of strain measurements. Our accomplishments to date are as follows (see accompanying figures):

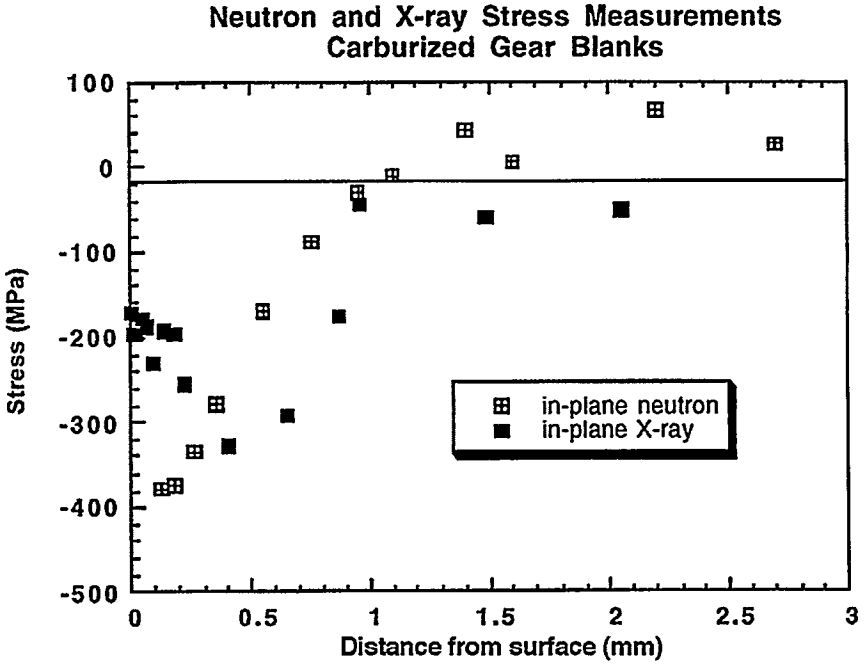
- We have produced a complete strain mapping through a carburized steel layer using neutron diffraction and depth profiling by x-ray diffraction. Our neutron stress profiles are similar to the x-ray data but with a larger peak stress.
- By analyzing complete and single-peak x-ray patterns through a carburized case, we can separate strain from microstructural effects. This separation provides an independent mechanism for determining carbon content, which is very useful in validating numerical modeling. Our measured carbon profiles and retained austenite fractions show excellent agreement with data obtained with conventional techniques.
- We completed experimental and numerical studies of residual stress and microstructure for a carburized steel specimen. Stresses measured in the austenite and martensitic phases, retained austenite fractions, and carbon profiles qualitatively agree with predictions based on numerical codes.

Publications

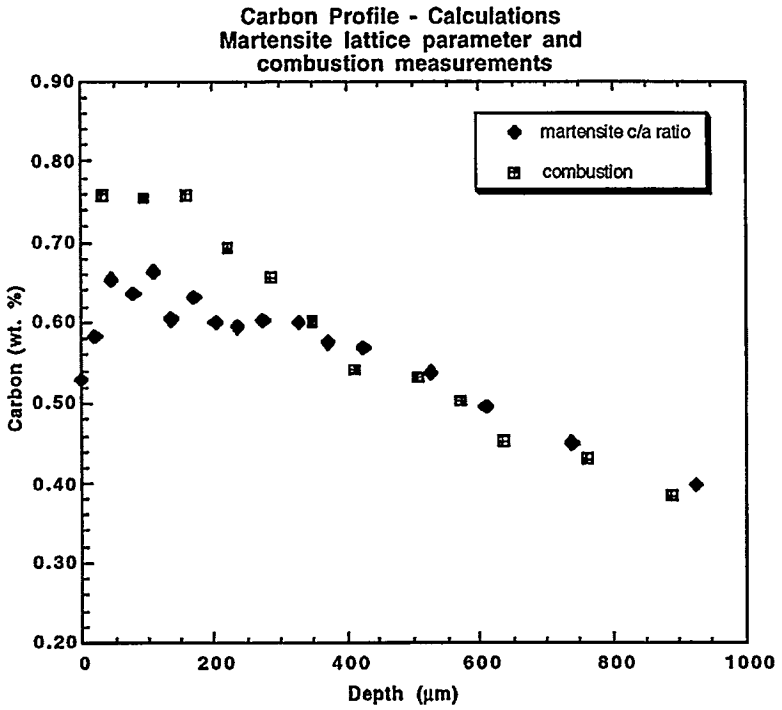
Bourke, M.A.M., P. Rangaswamy, T. Holden, et al., "Complementary Neutron and X-Ray Measurements in an Attempt to Obtain a Strain Profile Through a Carburized Layer" (submitted to *J. Neutron Res.*).

Jayaraman, N., and P. Rangaswamy, "Oxide Scale Stresses in Polycrystalline Cu/Cu_2O System" (to be published in *Adv. X-Ray Analysis*).

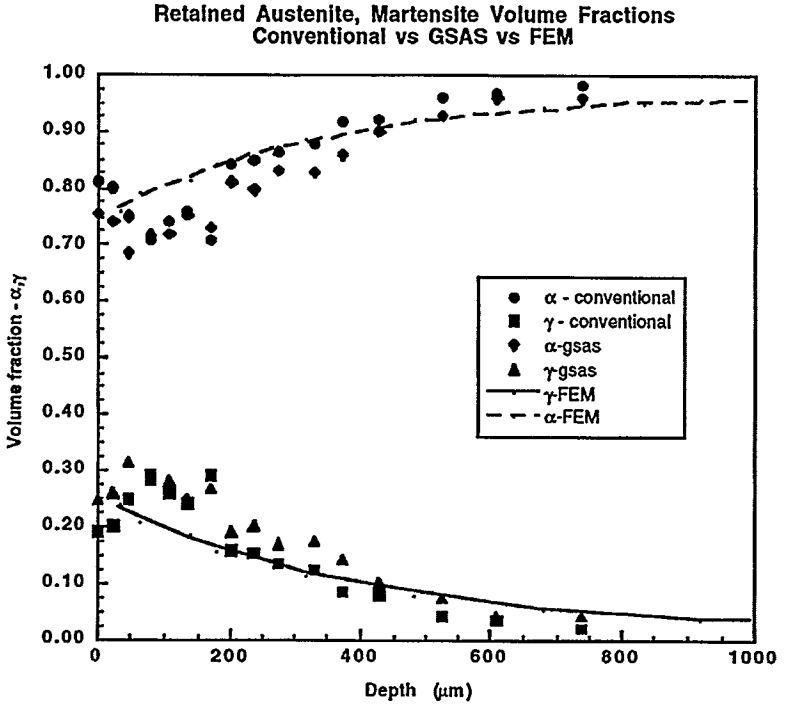
Rangaswamy, P., M.A.M. Bourke, A.C. Lawson, et al., "Residual Stress and Microstructural Characterization Using Rietveld Refinement of a Carburized Layer in a 5120 Steel" (to be published in *Adv. X-Ray Analysis*).



Stress measurements on a carburized gear blank from neutron and x-ray depth profiling.



Carbon profiles obtained using x-ray (Rietveld analysis) and combustion/ burnout techniques.



Retained austenite profiles obtained from predictions based on finite element method (FEM) techniques and by measurements both with conventional x-ray techniques and with Rietveld analysis (i.e., generalized structure analysis system, or GSAS) of the x-ray data.

Lattice Coupling to Electronic and Magnetic Instabilities in High Magnetic Fields

Joe D. Thompson

Properties of materials are determined ultimately by the configuration of their electronic states. Occasionally, this configuration leads, for example, to enhanced mechanical characteristics or corrosion resistance, which are desirable for applications. In other materials, it can produce unusual structural or electronic instabilities. Materials with these desirable or unusual properties are often labeled advanced materials, but quite frequently we do not understand fundamentally how these properties arise. It is important to provide this understanding for their desired properties to be realized fully and to guide the development of new advanced materials.

Our project focuses on understanding classes of materials with unusual structural and/or electronic (including magnetic) properties. Quite generally, the properties can be attributed to instabilities that arise from the interplay between electronic configurations and the underlying structural lattice, which allows scientifically as well as technologically important ground states, e.g., high-temperature superconductivity. In addition, this interplay is at the heart of a vast range of materials phenomena found in actinides or their compounds. Magnetic field, along with pressure and temperature, are the three fundamental thermodynamic variables that can be used both to discover these phenomena and to provide insight into their origin. Of these variables, magnetic field is, within the US, the most underutilized, but it has the potential for discovering new phenomena and for providing a fundamental understanding of advanced materials. Recently, a part of the new National High Magnetic Field Laboratory (NHMFL) was established at Los Alamos with the mission of developing a world-class facility emphasizing pulsed magnetic fields to 60 T. A mandate of the NHMFL is to establish a strong in-house research program that utilizes these high-field resources. This, combined with the importance of studying advanced materials at high magnetic fields, represents an outstanding opportunity. To realize this opportunity, we have developed and applied two particularly important experimental capabilities—high-field specific heat and thermal expansion/magnetostriction—that are related thermodynamically by the so-called Gruneisen parameter, which provides a measure of lattice coupling to electronic and magnetic interactions. This lattice coupling is poorly understood yet is fundamental to understanding strong electronic correlations that characterize broad classes of materials. Prominent among these materials are actinides, high-temperature copper-oxide superconductors, and systems that exhibit heavy-fermion behavior. Common to all of these are electronic and magnetic instabilities that are coupled to the lattice and dominate their low-temperature properties. Explaining these properties at a fundamental level poses theoretical and experimental challenges at the forefront of materials science/condensed matter physics.

In general, the interplay among structural, magnetic, and electronic interactions can lead to a modification of electronic states at the Fermi surface, through many-body (strong correlation) effects, and to an instability in the Fermi surface, as evidenced by the opening of a gap over part or all of the surface. An outstanding example of the first case is heavy-fermion compounds in which many-body interactions renormalize the Fermi energy downward by two to three orders of magnitude. In this case, the characteristic energy scale of the correlated electrons becomes small, on the order of tens of kelvin or, equivalently, tens of tesla. The second case of Fermi surface instability represents cooperative phase transitions, such as superconductivity, long-range magnetic order, metamagnetic transitions, and spin-or charge-density wave states. The energy scale in both cases is in the range of magnetic fields available at the NHMFL. By studying the response of these materials at low temperatures to fields of this order, we can probe interactions responsible for their electronic and magnetic instabilities. These effects are known to produce either a significant change in the low-temperature specific heat or a specific heat anomaly at the phase transition. From purely thermodynamic arguments, there must be a corresponding change in thermal expansion that measures the lattice coupling.

In the course of this project, we have developed a capacitance dilatometer that resolves length changes of 1 part in 10^{10} in samples 2-4 mm long and that operates from 1 to 300 K. This dilatometer has been used to make the first magnetostriction (i.e., isothermal, field-induced length change) measurements at Los Alamos. We have measured the diagonal and off-diagonal components of the magnetostriction tensor of the electronically correlated small-gap semiconductor $Ce_3Bi_4Pt_3$. Although each tensor

component is relatively large, the volume magnetostriction (a linear combination of the components) is relatively small, $\lambda_v = (V(H) - V(0))/V(0) = 2.75 \times 10^{-6}$ in 10 T at 4 K, and is comparable to that of strongly mixed valent metals, such as $CeSn_3$ and $CePd_3$. The coefficient of magnetostriction, $S_v = \partial\lambda_v/\partial H^2$, exhibits a maximum near 50 K, as does the thermal expansion and specific heat. By combining our measurements of magnetostriction, thermal expansion, specific heat, magnetic susceptibility, and pressure-dependent resistivity, we can show that the electronic-free energy obeys a single scaling relationship, but the electronic and magnetic Gruneisen parameters are inequivalent. This result supports the theoretical prediction that the charge and spin gaps in $Ce_3Bi_4Pt_3$ are inequivalent. We also find that the field-dependent volume change cannot account for the large negative magnetoresistance in this material.

An extensive set of high-field specific heat, resistivity, and magnetization measurements of the strongly correlated metal $YbAgCu_4$ has been compared with theoretical predictions of the Anderson impurity model, which is believed to describe the physics of this material. This model accounts well for the temperature and field dependence of the measured properties, but the characteristic energy scales determined from the various measurements differ by nearly a factor of two, which is not expected from the model. This discrepancy is not understood but could arise from a field-dependent 4f occupancy (valence), which is not included in the model but could be tested experimentally by field-dependent inelastic neutron-scattering experiments. Our work is the first serious test, using magnetic field as the primary variable, of the Anderson model and is the first to suggest the possibility of a field-dependent valence in electronically correlated metals.

Finally, we have used very high field magnetoresistance measurements to study properties of strontium-doped La_2CuO_4. In the case of $La_{1.99}Sr_{.01}CuO_4$, we have mapped the field-temperature phase diagram, which can be understood if there is strong coupling between doped-charge carriers and interlayer order of the out-of-plane Cu^{2+} spin component. Careful measurements of longitudinal and transverse magnetoresistance of $La_{1.925}Sr_{.075}CuO_4$ show that, contrary to previous reports, the magnetoresistance follows Kohler's rule. We explain these results as arising from eccentric hole-pockets on the Fermi surface, an interpretation that is consistent with band-structure calculations.

Publications

Graf, T., J.M. Lawrence, M.F. Hundley, et al., "Resistivity Magnetization and Specific Heat of $YbAgCu_4$ in High Magnetic Fields," *Phys. Rev. B* **51**, 15053 (1994).

Hundley, M.F., J.J. Neumeier, J.D. Thompson, et al., "Magnetostriction and Thermal Expansion of the Kondo Semiconductor $Ce_3Bi_4Pt_3$" (to be published in *Physical Phenomena in High Magnetic Fields-II*).

Lacerda, A., G. Graf, J.H. Cho, et al., "High Field Magnetoresistance of $La_{1.99}Sr_{.01}CuO_{4+d}$," *Physica C* **235-240**, 1353 (1994).

Lacerda, A., T. Graf, M.F. Hundley, et al., "High Field Magneto-transport and Specific Heat in $YbAgCu_4$," *Physica B* **206 & 207**, 358 (1995).

Lacerda, A., J.P. Rodgriguez, M.F. Hundley, et al., "Magneto-resistance in the Normal State of $La_{1.925}Sr_{.075}CuO_{4+d}$," *Phys. Rev. B* **49**, 9097 (1994).

Development of Pair Distribution Function Analysis

Robert Von Dreele

It has become increasingly evident that structural coherence in the CuO_2 planes of high-temperature superconducting (HTSC) materials over some intermediate length scale (in the nanometer range) is important to superconductivity. We propose to use the pair distribution function (PDF) analysis of powder diffraction data to extract structural information on these length scales. By PDF analysis of neutron powder diffraction data, we plan to obtain a detailed knowledge of the local and intermediate-range structure of selected HTSC materials.

We have obtained neutron scattering data for the $La_{2x}Sr_xCuO_4$ system over a large range of x = 0 to 0.3, where phonon dispersion curves indicate that the high-temperature tetragonal to low-temperature orthorhombic phase transition follows a "soft-mode" behavior. Of particular interest was the region x = 0.2 to 0.25, where the tetragonal-to-orthorhombic phase boundary appears to coincide with the superconducting/semiconducting boundary. We also obtained neutron scattering data for $YBa_2Cu_3O_7$ made with pure isotopes of ^{63}Cu and ^{65}Cu, which

have widely different neutron scattering lengths. This allowed us to obtain the copper differental PDFs, which provided much more detailed information about the copper local structure without contributions from uninteresting pair-correlations (such as the Y-O bonds) to the PDF.

This work has shown the power of the PDF technique in determining intermediate structure information which is not otherwise available. The results are also shown to be largely complementary to those obtained by the more standard method of Rietveld analysis.

Measurement by Neutron Diffraction of Strains in Advanced Engineering Structural Materials Including AlSiC and AlTiC

Mark Bourke

Many modern engineering materials consist of two or more materials combined to produce a composite with properties superior to those of the individual phases. Although composites offer economic advantages over conventional materials, their internal mechanical performance can be hard to characterize. Measurements of bulk properties such as Young's modulus, yield stress, or fracture toughness are symptomatic indicators but do not record directly how the constituents interact during loading. Neutron diffraction is the only experimental technique that can unambiguously and nondestructively measure the volume-averaged, mean-phase strains (applied or residual) in crystalline composites. By using neutron diffraction in conjunction with numerical modeling, our goal is improved understanding of the deformation, load sharing, and plasticity mechanisms that occur in polycrystalline, multiphase systems. In the course of the research, we have also developed and improved data collection and interpretation techniques that are used to measure strain with neutron diffraction.

In the past year we used neutron diffraction to measure strain in specimens removed from an extruded AlSiC plate. Despite initial complications caused by systematic effects, we determined strain variations with respect to the plate axes. Residual strains in the aluminum ranged from 300 μstrain parallel to the plate surface to 800 μstrain at 45°. The corresponding strains in the SiC were approximately -300 to -600 μstrain.

In a complementary study of the same material, we determined the relaxation free temperature explicitly by comparing the temperature dependence of the SiC in a composite with an unrestrained powder. The results suggest that above 200°C the aluminum matrix remains soft enough to accommodate the coefficient of thermal expansion mismatch between aluminum and SiC through creep but that residual stresses begin to be "locked in" between 150°C and 200°C.

In studies of NiAl-Al_2O_3, which is quite distinct from the AlSiC system, we recorded residual strains in specimens for which we varied the ratio of Al_2O_3 particle size to matrix grain size (keeping the respective volume fractions constant). Surprisingly, for constant NiAl grain size, the residual strains were largest for the smallest reinforcement particles. Clearly this cannot be predicted using continuum mechanics. The effect appears to be caused by the low symmetry of the NiAl. Accordingly, when the residual strain fields associated with the particles of Al_2O_3 extend over many NiAl grains, collaborative slip in the matrix is facilitated, which relaxes the residual strains more efficiently.

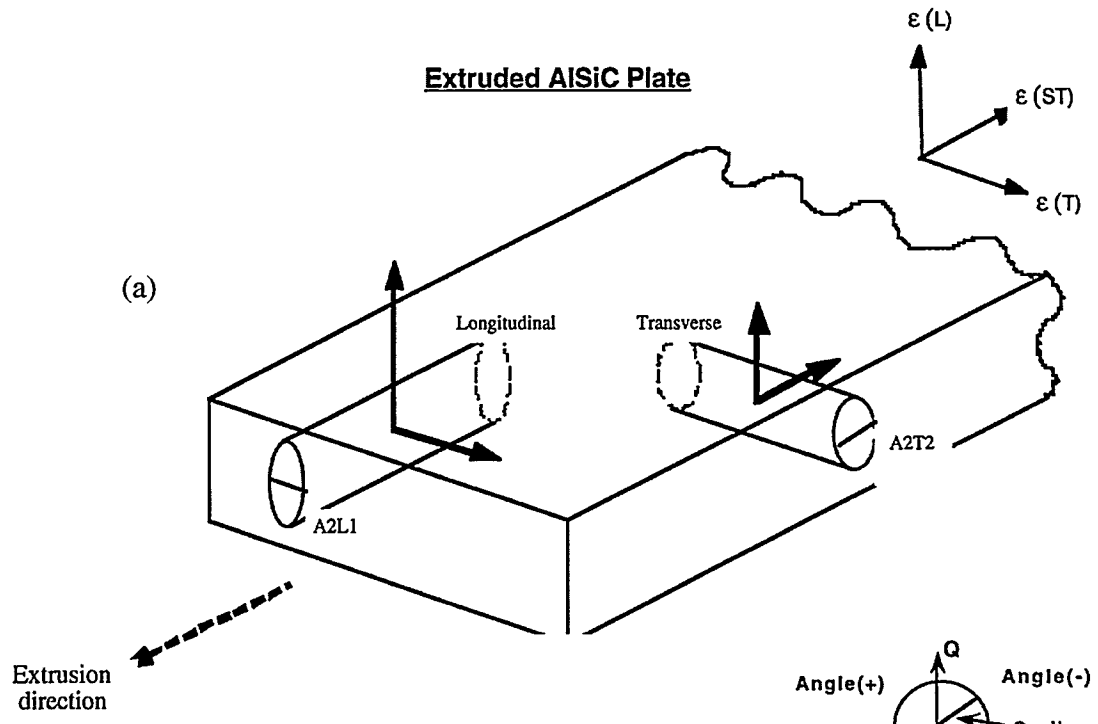
Publications

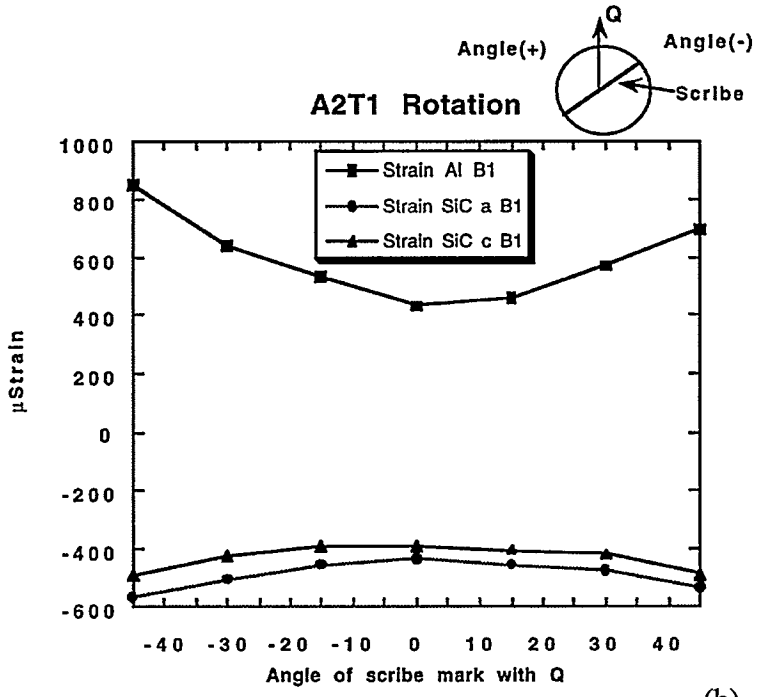
Bourke, M.A.M., J.A. Goldstone, and R. Robinson, "Strain Measurement by Diffraction at LANSCE," *Physica B* **213–214**, 806 (1995).

Goldstone, J.A., M.A.M. Bourke, and N. Shi, "Internal Strain Measurement Using Pulsed Neutron Diffraction at LANSCE," in *Neutron Scattering in Materials Science*, D.A. Neumann, T.P. Russell, and B.J. Wuensch, Eds. (Material Research Society, Pittsburgh, Pennsylvania, 1994), p. 376.

Todd, R.I., C. Borsa, B. Derby, et al., "Analysis of Neutron Diffraction Peak Broadening Caused by Internal Stresses in Composite Materials," *Nucl. Instrum. Methods Phys. Res.* **A354**, 139 (1995).

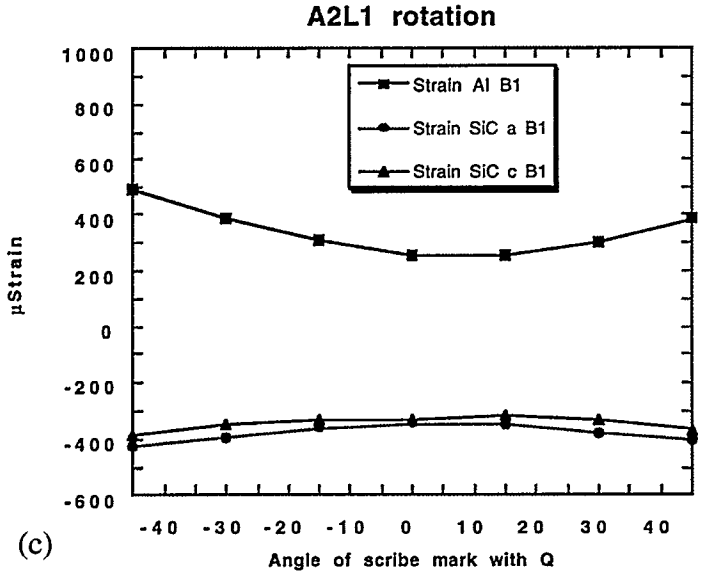
Todd, R.I., M.A.M. Bourke, C.E. Borsa, et al., "Measurement and Role of Residual Stresses in Alumina/SiC Nanocomposites," in *Euroceramics*, Vol. 4, A. Bellosi, Ed. (Gruppo Editorale Faenza Editorice, Italy, 1995), p. 217.



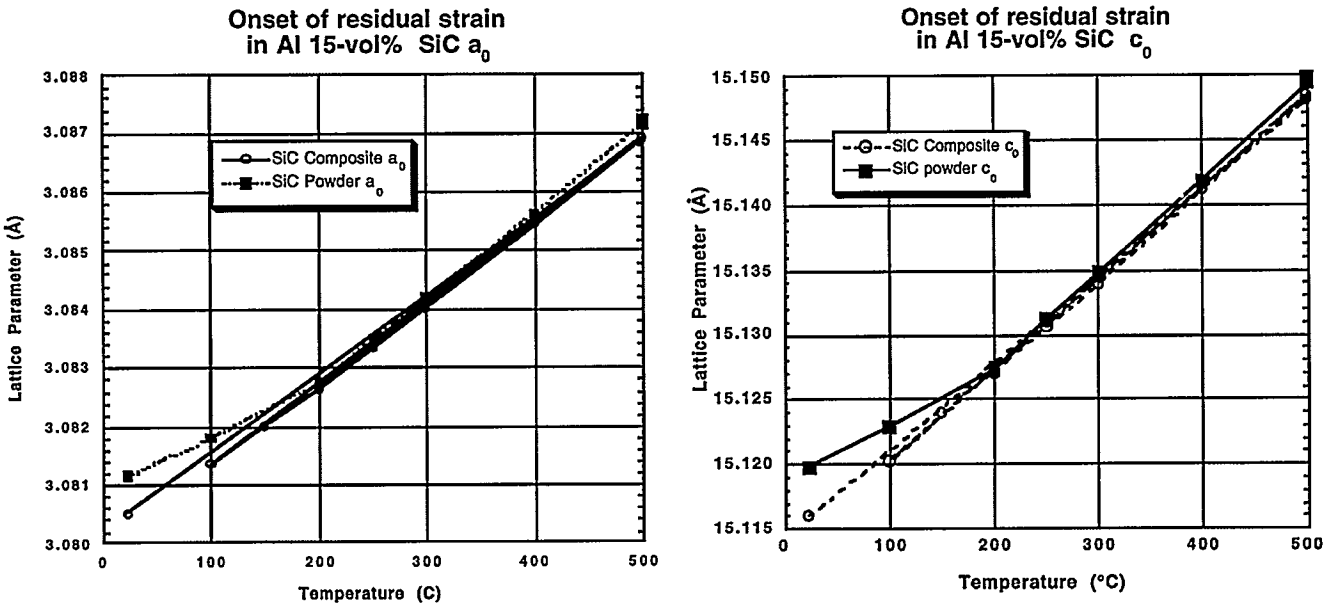


(b)

(a) Schematic of extruded plate showing orientation of the transverse and longitudinal specimens, results for which are given in (b) and (c), respectively; (b) Al and SiC residual strains in transverse specimen; and (c) Al and SiC residual strains in longitudinal specimen.



(c)



(a) Values of SiC a_0 for composite and powder, showing divergence below 200°C; (b) values of SiC c_0 for composite and powder, showing divergence below 200°C.

Chemical and Physicochemical Properties of Submicron Aerosol Agglomerates

Ronald Scripsick

Inorganic nanometer-size particles are byproducts of high-thermal-energy processes such as waste incineration, coal combustion, and explosions. They may also be intentionally generated for use in such applications as advanced ceramic materials, superconducting powders, and ultraviolet screening films. Our research project focuses on the chemical and transport properties of nanometer-size particles and their agglomerates including the

- effect of adding a second chemical species on the size distribution of agglomerates generated by gas-to-particle conversion,
- distribution of chemical species with particle size for binary aerosols,
- arrangement of individual chemical species in the aerosol agglomerates (particle-to-particle variation), and
- transport of fractal-like aerosol agglomerates.

We can gain valuable leads to multicomponent aerosol behavior by examining the simplest case—one that involves only two components (a binary aerosol).

The University of California at Los Angeles Aerosol Technology Laboratory developed flat-flame aerosol generators that provide a near one-dimensional agglomerate aerosol formation configuration. Formation studies use electron microscopy and aerosol impactors. Transport studies use electrical, scattered light, and diffusional classifications to evaluate agglomerate mobility and deposition.

In the past year, our electron micrographs of binary-aerosol samples showed chemically distinct primary particles that were coagglomerated. Differences in the chemical kinetic behavior of the precursor materials can explain this segregation in the early stages of particle growth.

Transport studies on single-component agglomerates compared electrostatic classification with scattered-light measurements. Preliminary results indicate that the effective light-scattering diameter was less than the single-charge electrical mobility diameter. We believe this result is related to both anisotropic effects on particle mobility and light-scattering dependence on agglomerate size.

Bulk Amorphous Materials

Ricardo B. Schwarz

The objective of this project it to develop the ability to synthesize bulk amorphous metallic alloys and multiphase alloys that are formed by embedding nanocrystals and fibers in an amorphous matrix. We are studying the thermal stability of these alloys and the kinetics of crystallization for the controlled production of two-phase amorphous/nanocrystalline alloys. The mechanical and transport properties are measured as a function of the degree of structural relaxation in the amorphous state and following the nucleation of crystals.

Our acccomplishments include the following:

1. We built a mold-casting apparatus for preparing bulk amorphous alloys and with it fabricated lanthanum-based amorphous alloys for corrosion studies and thermal expansion measurements.

2. We measured the thermal expansion of bulk amorphous Zr-Ti-Cu-Ni-Be from 80 to 800 K, which is above the crystallization temperature for this alloy. The data was fitted to a Debye-Gruneisen model to deduce the Debye temperature (440 K) and the Gruneisen parameter ($\gamma = 1.25$).

3. We developed a fluxing technique for preparing 1-in.-diameter rods of amorphous Ni-Pd-P alloy and supplied samples to various national laboratories.

4. We measured the palladium partial-pair correlation function in amorphous Ni-Pd-P using anomalous x-ray scattering at the the Brookhaven National Laboratory synchrotron.

5. We received approval from DOE for establishing a multilaboratory "DOE Center of Excellence for the Synthesis and Processing of Bulk Amorphous Alloys" at Los Alamos.

Publications

He, Y., R. Schwarz, et al., "Elastic Moduli, Density, and Structural Relaxation in Bulk Amorphous Zr-Ni-Cu-Ni-Be Alloy" (to be published in *J. Non-Cryst. Alloys*).

He, Y., R. Schwarz, and D. Mandrus, "Thermal Expansion of Bulk Amorphous Zr-Ti-Cu-Ni-Be Alloy" (to be published in *J. Mater. Res.*).

Nash, P., H. Choo, and R. Schwarz, "Thermodynamic Calculation of Phase Equilibria in the Ti-Co and Ni-Sn Systems" (to be published in *J. Mater. Res.*).

Schwarz, R., A. Migliori, and S.H. Whang, "Elastic Constants of Single Crystal Gamma-TiAl," *J. Mater. Res.* **10**, 1187 (1994).

Wasz, M., P. Desch, and R. Schwarz, "The Effect of Tin Alloying on the Structure of LaNi-5" (submitted to *Philos. Mag. A*).

Yvon, P., R. Schwarz, et al., "Covalent and Liquid-like Amorphous Phases in Al-Ge Alloys," *Phil. Mag. Lett.* **72**, 167 (1995).

Fabrication of Boron-Phosphide Neutron Detectors

Michael Fitzsimmons

Conventional neutron detectors tend to be slow and expensive, especially when position sensitivity is required. These deficiencies can be addressed by a new generation of semiconducting neutron detectors that use boron-phosphide (BP)—a semiconductor—as the detection and charge-collection medium. BP is grown by chemical-vapor-deposition (CVD) techniques; large-area detectors might be fabricated during a single deposition, thereby reducing costs. The objective of this project is to develop an improved BP neutron detector for use by the neutron scattering community.

Such a development is timely since new neutron sources, such as the Advanced Neutron Source or even an upgraded Los Alamos Neutron Science Center (LANSCE), will be underutilized unless faster and more efficient detectors are available. Industrial users of neutrons—as well as researchers doing basic neutron-scattering studies—may also benefit from the reduced cost of a BP detector.

During the first phase of this project, we detected thermal and cold neutrons with a BP film using the neutron-powder diffractometer and reflectometer at LANSCE. The neutron-detection efficiency of the prototype was only 0.2%. We believe that the poor efficiency of this detector resulted from structural imperfections introduced into the lattice during growth. The presence of structural imperfections might result from the large lattice mismatch—about 20%—between BP and silicon.

To address the mismatch problem we intended to grow the film on a SiC substrate whose lattice mismatch with BP is much smaller, about 4%. Devcom (a manufacturer of CVD films) delivered to us three samples believed to have BP deposited on a SiC substrate. After we examined these substrates with x-ray diffraction and Rutherford backscattering spectroscopy, we concluded that none of the substrates had BP on them. We have since decided to fabricate the films within the Laboratory.

Nanometer-Scale Materials: Semiconductors to Fullerenes

David Smith

There is growing interest in molecular-level (nanometer-scale) control of materials for a wide variety of materials-dominated applications, such as advanced computing architectures, microelectronics, and catalysis. Molecular-level control allows us to fabricate structures and nanometer-scale functional materials that will provide the impetus to develop entirely new devices and chemistries. In this project we are pursuing two areas of investigation: (1) molecularly engineered catalysts, and (2) two-dimensional (2-D) ordered materials.

In the last year we accomplished the following in the area of molecularly engineered catalysts: (1) We prepared monometallic nitrides of molybdenum and tungsten from various molybdenum and tungsten dimers. We also developed an improved $Mo_2(NMe_2)_6$ synthesis technique. (2) Using thermal analysis we studied the conversion of the amido/imido intermediates. (3) We began studying the effects of transamination reaction conditions on these intermediates; we are characterizing intermediate metal amido/imido complexes with elemental analysis, Fourier transform infrared spectroscopy, x-ray diffraction, Auger electron spectroscopy, and x-ray photoelectron spectroscopy. (4) We began, and are now finalizing, the process for a cooperative research and development agreement (CRADA) with Akzo Corporate Research America. This CRADA is for the synthesis and evaluation of new mixed-metal nitride and carbide catalysts for petroleum refining and specialty-chemical manufacturing.

We also accomplished the following in the area of 2-D ordered materials: (1) We prepared and imaged silver- and gold-colloid monolayers (particle size of 4–100 nm) on various substrates. (2) We showed that if we choose proper conditions we can manipulate particles of this size with the atomic force microscope. (3) We prepared patterned, self-assembled monolayers (SAMs) of alkanethiols terminated with different types of chemical functionality on a variety of substrates. We also probed the topographic contrast of these SAMs with different imaging techniques. (4) We discovered that lateral force microscopy shows strong contrast between regions of different chemical functionality.

Analysis of Structure and Orientation of Adsorbed Polymers in Solution Subject to a Dynamic Shear Stress

Gregory Smith

Polymer-based separation techniques rely on the accessibility of the polymer's binding region to specific molecules in solution. Consequently, the location of the binding site inside or outside the entangled polymer chains is crucial to the effectiveness of such techniques.

Polymer geometry depends on the interactions between polymer molecules, the surface of the support matrix, and the solvent—the polymer chains may be closely packed on the matrix surface, tightly intermingled, or extended into the solution. The flow of the solution around the adsorbed polymer also affects the polymer's geometry and accordingly its interactions with molecules in solution. For this reason, the details of flow-induced deformation of the polymer chains is important for such applications as exclusion chromatography, wastewater treatment, ultrafiltration, and enhanced oil recovery. Knowledge of the effects of polymer thickness, chain orientation, and different solvents and shear rates is imperative for the design of optimal systems—if the binding region of the polymer does not extend into the solution, no chemical separation can take place.

The goal of this project is to use neutron reflectometry to determine with submolecular resolution the structure and orientation of adsorbed polymers as a function of solvent power, shear rate, polymer molecular weight, polymer surface coverage, and surface heterogeneity. Because neutrons of the energies used in our studies can penetrate a single crystal of quartz (up to 70% transmission through a 3-in. block), we were able to use an enclosed shear cell that allowed us to precisely control the shear rate. We determined the average polymer thickness directly from the nuclear density profile, and we used selective isotopic substitution to provide detailed information (to 5-Å resolution) on the location of various parts of the

polymer and solvent relative to the quartz surface. Thus we can use neutron reflectometry to collect information on the packing of the polymer, solvent interactions, and the location of the interactive end groups of the polymer in and out of the polymer "brush."

Building on the design of a quartz cell developed for previous studies of polymers under static conditions, we designed a new cell consisting of a polished single-crystal quartz block sealed to a Teflon reservoir and attached to a temperature control box. The polymer solution, a polystyrene-polyethylene oxide (PS-PEO) diblock copolymer in toluene or cyclohexane, is placed in the reservoir and a monolayer of polymer is adsorbed from the solution onto the quartz surface. Because toluene and cyclohexane are extremely poor solvents for the PEO, the diblocks chemisorb strongly to the quartz, forming an "anchor." We then generate a shear flow by flowing the remaining solution past the polymer/solvent interface.

By varying the molecular weight of the PEO relative to that of the PS, we can control the effective grafting density. This in turn permits us to choose from closely spaced polymers that have an extended "brush" morphology or sparsely spaced polymers that are characterized by a depleted layer of polymer near the surface and are referred to as "mushrooms." Toluene is a good solvent and cyclohexane is a theta solvent (T_θ=33°C) for PS. (T_θ is the temperature at which the polymer segments attract each other with the same force as that with which the solvent attracts the polymer segments.) Thus, using various combinations of polymers, solvents, temperatures, and solvent flow rates, we could examine the effects of shear flow on the polymer as a function of shear rate, solvent quality, and concentration.

Our initial measurements were taken on 0.05 mg/mL PS-PEO (with molecular weights of 184,000 and 7300, respectively) diblocks in toluene. The static density profiles were well established, which gave us a known starting point. We found that at near-surface shear rates of up to 2500 s^{-1} (with an average shear rate across the cell of ~400 s^{-1}) there were no changes in the reflectivity profiles.

We then changed the solvent from toluene to cyclohexane at room temperature, which is a poor solvent. The sample was adsorbed from solution and the excess polymer left in contact with the adsorbed monolayer. The measured static density profile was consistent with a polymer mushroom (see density profile). When the shear was applied at any rate between 300 s^{-1} and 2500 s^{-1}, there was a dramatic change in the density profile, indicating an increase in the polymer's thickness. We also found that the relaxation time for the system to return to its initial profile was on the order of days, suggesting that entanglement of the PS chains is playing a role in the shear behavior. Since most theories of polymers subject to shear are for grafted polymers in a good solvent, we have modified our shear cell to reach shear rates roughly an order of magnitude higher than those previously obtained so that we can see a change in the polymers in good as well as poor solvents.

Since we saw a dramatic change in the polymer's behavior under shear as a function of solvent quality, we undertook several experiments to understand the static effects of solvent quality on the density profiles of adsorbed diblocks. In the first set of experiments, we adsorbed the polymer from cyclohexane at 45°C (above T_θ) and replaced the polymer-containing solvent with pure solvent so there would be no further adsorption. We then measured the reflectivity as a function of temperature down to 20°C (below T_θ). At room temperature, we applied a shear force to the polymer.

Our preliminary results suggest that the high-temperature profile (above T_θ, when cyclohexane changes from being a poor solvent to a good solvent) is consistent with static adsorption from toluene (also a good solvent). At low temperatures, however, the polymer collapses (as would be expected from a decrease in the radius of gyration resulting from the change from a good to a poor solvent) and changes from a brush to a mushroom. We saw little change with shear at the low temperature, which suggests that the presence of excess polymer in solution plays a key role in the shear effects we observed. Finally, when we exchanged the cyclohexane at room temperature with toluene, the reflectivity profile was consistent with an instantaneous change in the polymer profile where the profile changes from a mushroom to a brush.

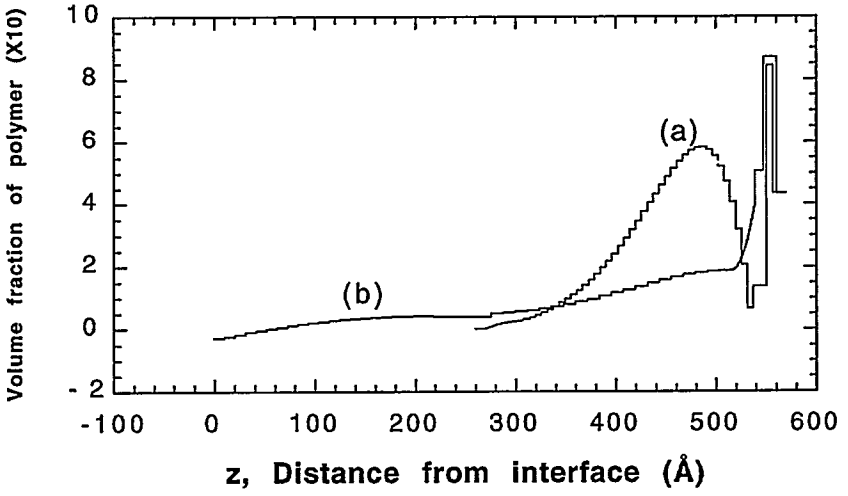
Because the polymer's shear behavior was different depending on whether pure solvent or excess polymer was next to the monolayer, we decided to study the effect of polymer concentration on the static density profile. We prepared solutions at three concentrations (0.0078 mg/mL, 0.0096 mg/mL, and 0.05 mg/mL of PS-PEO in cyclohexane) and permitted them to adsorb for several days. We then measured the density profiles. While it is not clear why the polymer concentration affects the ultimate surface coverage and profile, we do find a marked difference in the density profiles of the polymer adsorbed at different concentrations from a poor solvent (see neutron reflectivity data). We plan to

further investigate this effect using a good solvent.

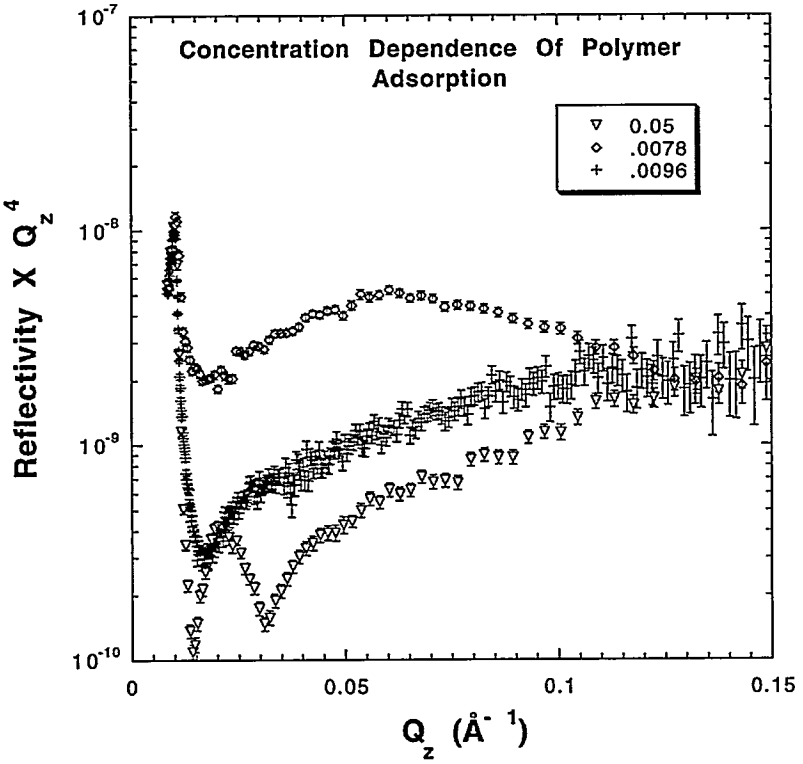
Publications

Baker, S.M., P.D. Butler, W.A. Hamilton, et al., "Shear Cell for the Study of Liquid-Solid Interfaces by Neutron Reflectometry," *Rev. Sci. Instr.* **65**, 412 (1994).

Smith, G.S., C. Toprakcioglu, S.M. Baker, et al., "Neutron Reflectivity Study of Adsorbed Diblock Copolymers," *Nuovo Cimento Della Societa Italiana Di Fisica D—Condensed Matter Atomic, Molecular, and Chemical Physics of Fluids, Plasmas, and Biophysics* **17**, 721 (1994).



The density profile of the (a) static and (b) sheared diblock copolymer in a poor solvent.



Neutron reflectivity data for three concentrations of polymer in cyclohexane. The surface coverage increases with concentration, as indicated by the increasing depth of the first minimum.

Heavy Fermions in High Magnetic Fields

Stuart Trugman

Many of the most interesting and important new materials, including heavy-fermion compounds and high-temperature superconductors, are composed of strongly interacting electrons. Our present understanding of these systems, even at a qualitative level, is primitive. The focus of this project is an investigation of heavy-fermion systems, which are perhaps the most interesting and surprising of the known, strongly interacting electron systems. We paid particular attention to the high-magnetic-field response of these systems. We also studied many-body effects on the properties of heavy-fermion materials with the objective of gaining new insights into the microscopic origins of the novel characteristics of these materials.

To study these materials, we have introduced model Hamiltonians. An example of a model Hamiltonian that contains the essential physics is the Anderson lattice model. A simpler model is the Kondo lattice Hamiltonian. We have studied the phase diagram for the Kondo lattice at half filling and zero temperature. Some aspects of the phase diagram are known, and some are speculative.

The optical properties of the heavy-fermion insulators are most unusual. From the measurements of the optical conductivity on FeSi and $Ce_3Bi_4Pt_3$, we see a loss of spectral weight, at low frequency, as we go from the metallic to the insulating phase. According to sum rules, we know this weight cannot disappear. We have worked to explore the role sum rules play in limiting how spectral weight can be shifted in the transition.

Finally, we explored the metal-insulator transition in the two-dimensional Hubbard model. This model is relevant to high-temperature superconductors because it is an antiferromagnetic insulator at half filling and it undergoes a metal-insulator transition with doping.

Publications

Bonca, J., and J.E. Gubernatis, "Degenerate Anderson Impurity Model in the Presence of Spin-Orbit and Crystal Field Splitting," *Phys. Rev. B* **50**, 10427 (1994).

Bonca, J., and J.E. Gubernatis, "Quantum Simulations of the Degenerate Single-Impurity Anderson Model," in *Quantum Monte Carlo Methods in Condensed Matter Physics*, M. Suzuki Ed. (World Scientific, Singapore, 1994), pp. 251–264.

Doniach, S., C. Fu, and S.A. Trugman, "Kondo Insulators: Are Simple Theories Good Enough?" *Physica B*, **199**, 450 (1994).

Guerrero, M., and C.C. Yu, "Kondo Insulators Modeled by the One-Dimensional Anderson Lattice: A Numerical-Renormalization-Group Study," *Phys. Rev. B* **51**, 10301 (1995).

Guerrero, M., and C.C. Yu, "Numerical Renormalization Group Study of the One-Dimensional Anderson Lattice," *Physica B* **206**, 151 (1995).

Gulacsi, M., and K.S. Bedell, "Metal-Insulator Transition in 1D Hubbard Model," *Phys. Rev. Lett.* **72**, 2765 (1994).

Gulacsi, M., and K.S. Bedell, "Spectral Function of the 1D Hubbard Model," *Physica* **199**, 492 (1994).

Gulacsi, M., and K.S. Bedell, "Theory of Metal-Insulator Transition in Strongly Correlated Electron Systems," *Integrated Ferroelectrics* **6**, 265 (1995).

Migliori, A., J.L. Sarrao, D. Mandrus, et al., "Ultrasound Studies of U_2Zn_{17} and UCu_5," *Physica B* **199**, 36 (1994).

Science and Technology of Reduced-Dimensional Magnetic Materials

Robert Heffner

Transition-metal oxide materials $(La,A)MnO_3$—where A can be calcium, strontium, or barium—order ferromagnetically, undergo a metal-to-insulator transition, and exhibit a large reduction in resistivity in a moderate magnetic field (called colossal magnetoresistance). If understood and properly tailored, these materials could find use as magnetic sensors. Our research, therefore, combines materials synthesis, physical characterization, and theoretical modeling to develop a clear microscopic understanding of the physical mechanisms governing these materials.

We have found a specific functional form for the correlation between the resistivity ρ and magnetization M $\{\rho(H,T) \propto \exp[-M(H,T)/M_0]\}$, which is consistent with the interpretation that polarons are present at all temperatures, with their

characteristic size strongly affected by the onset of ferromagnetic order. In addition, our theoretical studies indicate that a complete description could involve ferromagnetic double exchange, in combination with spin, lattice, or Jahn-Teller interactions leading to the formation of polaronic quasiparticles. Future work will entail single-crystal growth with the optical float-zone facility at Los Alamos for thermal expansion, magnetostriction, μSR, and neutron scattering experiments. Theoretical studies will involve polaron dynamics, multipolaron ordering, and interpretation of local-structure measurements.

Publications

Hundley, M.F., M. Hawley, R.H. Heffner, et al., "Transport-Magnetism Correlations in the Ferromagnetic Oxide $La_{0.7}Ca_{0.3}MnO_3$," *Appl. Phys. Lett.* 67, 860 (1995).

Neumeier, J.J., M.F. Hundley, J.D. Thompson and R. H. Heffner, "Substantial Pressure Effects on the Electrical Resistivity and Ferromagnetic Transition Temperature of $La_{1-x}Ca_xMnO_3$," *Phys. Rev. B* 52, R7006 (1995).

Roder, H., J. Zang, J., and A.R. Bishop, "Lattice Effects in the Colossal Magnetoresistance Manganate Perovskites" (submitted to *Phys. Rev. Lett.*).

Tyson, T.A., J. Mustre de Leon, S.D. Conradson, et al., "Structural Model of the Reference State in Doped $LaMnO_3$" (submitted to *Phys. Rev. Lett.*).

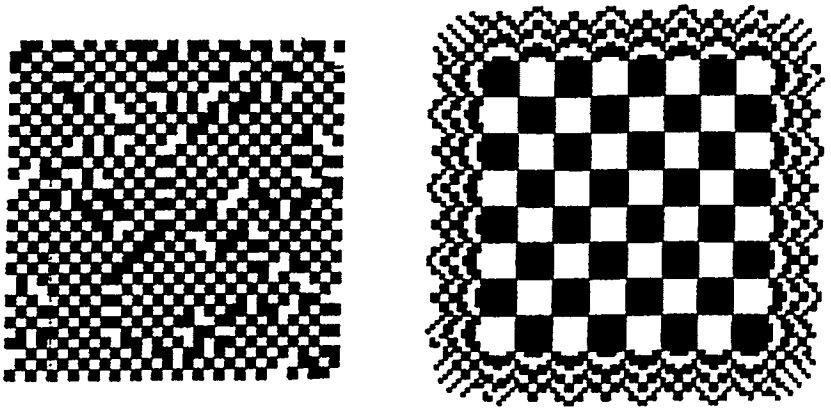
Nonlinearity in Structural and Electronic Materials

Alan Bishop

This project develops and supports a nonlinear-techniques technology base relevant to a variety of nonlinear, non-equilibrium problems arising in condensed matter and materials science. In this way, the controlled synthesis of and experimentation on novel electronic and structural materials motivates nonlinear science at Los Alamos. Reciprocally, nonlinear techniques advance our understanding of the processes controlling the structure and dynamics of complex materials facing modern technology.

Important concepts and techniques from "nonlinear science" include (i) the prevalence of coherent space-time structures in strongly nonlinear classical and quantum systems; (ii) the possibility of deterministic chaos even in low-dimensional dynamical systems; and (iii) the coexistence of (i) and (ii) leading to a rich variety of phenomena connoted by the term complexity. This project cultivates these concepts and applies them to significant problems in condensed-matter physics and materials science, as well as promoting team-building, visitors, and conferences.

We have hosted an international conference, "Fractal Material Properties," to discuss crack propagation and shape-memory alloys. We have developed a new microscopic model of shape-memory martensites, which predicts functional hierarchical texture (see accompanying figure). We have analyzed a model of fracture tips, including intrinsic oscillatory propagation. We have completed large-scale simulations and nonlinear analysis of surface growth and smoothing, and of three-dimensional anisotropic superconductors—emphasizing relevant multi-length-scale mesoscopic morphologies and topological nonlinear excitations (especially vortices and domain walls) in the presence of temperature and external fields. We have completed an analysis of unusual solutions to nonlinear equations due to discrete lattices (nonlinear Bloch oscillations), finite samples



Left panel: "Fine" tweed pattern for a square-rectangular martensitic transformation obtained by molecular dynamics simulations. Black and white areas represent regions of positive and negative strain, respectively. Right panel: "Coarse" tweed surrounded by a hierarchical strain region at the habit plane (i.e. austenite-tweed interface). The outer white region in both panels is the austenite (square) phase with zero strain.

(Josephson soliton oscillators), and curved geometries (e.g., cylindrical nanoscale structures). We have studied nonlinear, many-body electronic effects in low-dimensional materials (polymers and solids) due explicitly to coexisting electron-electron and electron-lattice interactions—especially excitonic and polaronic contributions to structural, optical, and magnetic properties.

Publications

Blumenfeld, R., "Formulating a First-Principles Statistical Theory of Growing Surfaces in Two-Dimensional Laplacian Fields," *Phys. Rev. E* **50**, 2952 (1994).

Blumenfeld, R., "A Minimal Model for Fracture Propagation in Amorphous Media: Steady State and Velocity Oscillations" (submitted to *Phys. Rev. Lett.*).

Blumenfeld, R., et al., "Exact Dynamical Multi-Twist Solutions for Isotropic Antiferromagnetic Chains and for the Belavin-Polyakov Equation" (submitted to *Phys. Rev. Lett.*).

Blumenfeld, R., et al., "Exact Multi-Twist Solutions for Heisenberg Spins on an Elastically Deformable Cylinder" (submitted to *Phys. Rev. Lett.*).

Blumenfeld, R., et al, "Fracture Surfaces: A Critical Review and a Morphological Analysis of Scanning Tunneling Microscopy Measurements," *Progress in Materials Science* **38**, 425 (1994).

Blumenfeld, R., et al., "Two Dimensional Laplacian Growth as a System of Creating and Annihilating Particles," *Phys. Rev. E* **51**, 3434 (1995).

Cai, D., et al., "Electric-Field-Driven Bloch Oscillations and Dynamic Localization," *Phys. Rev. Lett.* **74**, 1186 (1995).

Dominguez, D., et al., "Resistive Hysteresis and Nonlinear IV Characteristics at the First Order Melting of the Abrikosov Vortex Lattice" (to be published in *Phys. Rev. Lett.*).

Dominguez, D., et al., "Transformer Configurations in 3-Dimensional Josephson Lattices at Zero Magnetic Field," *Phys. Rev. Lett.* **75**, 717 (1995).

Sanchez, A., et al., "Roughening Transition of Driven Surface Growth," *Phys. Rev. B* **51**, 14664 (1995).

Sanchez, A., et al., "Simulation of Surface Smoothing" (to be published in *Phys. Rev. B*).

Saxena, A., et al., "A Model of Shape-Memory Materials with Hierarchical Twinning" (to be published in *J. de Physique-Colloque*).

Shuai, Z., et al., "Electroabsorption of Poly (paraphenylene vinylene) and PtI: Exciton vs Band Descriptions" (to be published in *Solid State Commun.*).

Zang, J., et al., "Frustrated Spin-Peierls Chains" (to be published in *Phys. Rev. B*).

Neutron Scattering as a Probe of Liquid-Crystal-Polymer-Reinforced Composite Materials

Rex Hjelm

The toughness and strength of composite materials can be improved by several orders of magnitude by designing these materials at the nanoscale to molecular level. This project has focused on obtaining nanoscale and molecular-level information about the mechanisms which can improve the mechanical properties of composites reinforced by rigid-rod liquid-crystal polymers (LCPs).

We have obtained this information with small-angle neutron scattering (SANS) measurements at the Los Alamos Neutron Science Center (LANSCE). SANS can probe the structure of composites on scales of 10–1000 Å, the most relevant scales for understanding molecular organization in these materials.

Applications for polymer composites are growing, and there is a pressing need for superior composite materials in applications such as the advanced technology fighter, stealth bombers, submarine hulls, and the suborbital supersonic transport. The light weight and potential strength of polymer composites will also make them suitable for structural components in more fuel-efficient automobiles and other types of commercial transportation applications.

LCP Development

Polymers that exhibit liquid-crystalline order in solution or in the melt show a high degree of order in the solid state as well, and several such polymers have been developed with high strength and high modulus. Some of these polymers have been used as reinforcements in coil-like polymer matrices; theory has been devised for these systems. Based on considerations that the structural strength of these materials is limited by LCP-fiber imperfections, fiber fibrillations, poor interfacial adhesion, and stress concentrations at the fiber ends,

theory predicts that mechanical enhancement can be improved by about an order of magnitude over present phase-separated systems if the reinforcing phase is homogeneously dispersed in the matrix. Producing this molecular composite has been difficult, however, and structural studies on the materials that have been made have been inconclusive; the theory has yet to be verified.

To produce molecular-reinforced LCP-matrix composites, we must disperse the LCP in the matrix material despite unfavorable free energy of mixing of the components. Complex schemes have been devised to process melts of the polymers into a "homogeneous phase" followed by a deep quench below the glass transition. However, the mixtures almost always show some phase separation which limits the theoretically achievable strength. In addition, the mixtures are thermodynamically unstable, and further phase separation results with time.

Our solution to the dispersal problem is to use a matrix which better disperses the LCP phase. We mix a liquid-crystal thermoset (LCT) with LCP in solvent, cast films from this mixture, and then raise the temperature to make an extended, cross-linked-polymer matrix.

SANS Studies of LCP/LCT Systems

We have used SANS to study the nanoscale morphology of LCP/LCT in NMP (N-methyl-2-pyrrolidinone) solvent systems and LCP/LCT systems. These studies—done along the lines of those already performed on polymer blends and block copolymers—determined the characteristic sizes of the phases, the phase morphology, and the degree of component segregation among the phases. We contrasted the organic components by labeling one of them with deuterium; substituting deuterons for protons changes the scattering-length density and hence the scattering contrast.

We analyzed the experiment by identifying signatures in the scattering curves. It is well known that microphase separation causes correlations which give characteristic scattering patterns whose exact form depends on the morphology of the phases. On the other hand, a true solution of LCP in matrix would be characterized by scattering from a concentrated solution of rod-like chains.

We have developed new analytical methods to determine the amount of segregation of components between phases based on the quadratic dependence of the scattering intensity I at zero momentum transfer Q on the amount of deuteration of one component (in this case LCP). The coefficients of this quadratic dependence are related to the difference in the volume-fraction distribution of the LCP in each phase. This difference is near unity for strong segregation and approaches zero as the segregation, hence phase distinctions, disappears.

LCP/LCT composite films have been cast from LCP/LCT solutions using nitro-substituted Kevlar—which has excellent solubility—selectively deuterated to provide the necessary contrast for this phase mapping. These experiments also test the widely cited liquid-crystal miscibility criterion that similar liquid-crystal phases should be completely miscible.

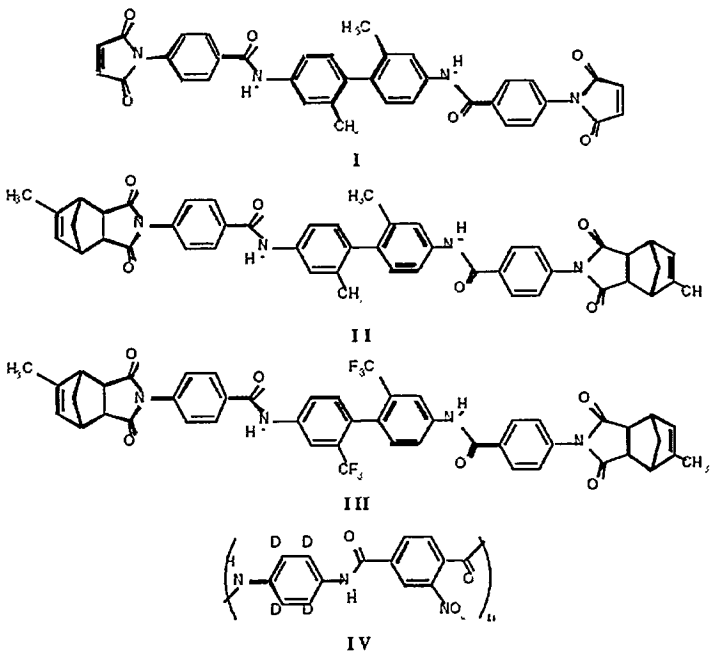
SANS studies on these materials have shown that 20 wt % loading of LCT in LCP produces microphase separation whose morphology is modeled by rod-like inclusions with a characteristic radius of 80 Å in a continuous phase. At 40 wt % loading the microphase separation persists and can be modeled as a system of randomly interpenetrating phases (the Debye-Bueche model). The characteristic length for this model is 80 Å. In both of these cases, the phases appear to be near-equilibrium structures; extensive annealing does not change the scattering measurements. We have taken a complete sequence of data, and preliminary indications are that the results can be modeled as a spinodal. We have shown in the 40 wt % loading case that there is weak segregation of the components in the two phases; we are approaching the molecular composite ideal without having optimized our system.

To understand how the films form in this system, we made LCP/LCT solutions at the required weight ratio and then heated them to the processing temperature, 100°C or 60°C. As expected, the nanoscale morphology depends on the initial state, although our analysis of this morphology is not complete and the results we have obtained are for processing from the samples dried at 100°C. Questions which arise from these results are the following: What is the initial state in solution? What are the changes that occur as the solution concentrates and reaches the gel point? What is the relation of these changes to the final state measured in the film?

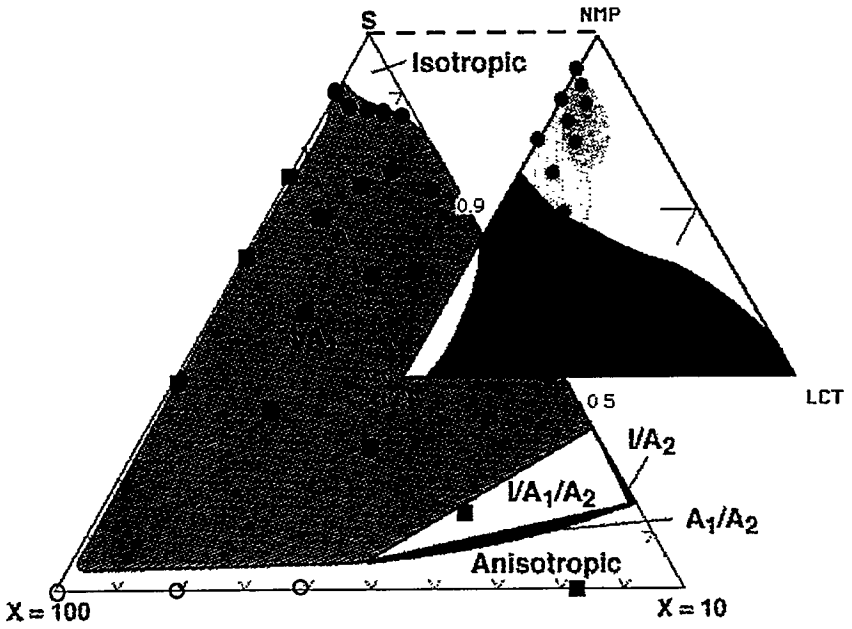
To address these questions we made SANS measurements on these solutions. The dilute solution results show that at room temperature, LCP in NMP forms large domain-like structures, as seen by the fact that $I \propto Q^{-4}$ at low Q. These structures are broken up by the addition of LCT into combinations of smaller domains and filamentous LCP/LCT structures, which is indicated by the $I \propto Q^{-1}$ dependence when the concentration is 5 wt % or less but not at 9 wt %, in which case the domain-like structure is retained.

We have determined the changes in solution structure as the gel point is approached along different LCP/LCT composition

lines. We have found that the microscopic biphase found in the dilute solution studies becomes larger and is readily apparent in the polarization light microscopy at higher concentrations. We have seen that the biphase is a mixture of an isotropic phase and a liquid crystalline phase, which is probably LCP-rich. As the solution is further concentrated toward the gel point, we observe a single liquid-crystalline phase. The neutron scattering profiles show a variety of structures that are different from the film morphologies mentioned above.



Liquid-crystal thermosets and liquid-crystal polymer used in this study. Liquid-crystal thermosets: (I), 2,2'-dimethylbiphenyl bismaleimide amide; (II) 2,2'-dimethylbiphenyl bis(methylnadimide) amide; (III), 2,2'-bis(trifluoromethyl)biphenyl bis(methylnadimide) amide. Liquid-crystal polymer: (IV), poly(p-phenylene-2-nitroterephthal amide).



Calculated phase diagram for a mixture of long (n = 100) and short (n = 10) rigid-rod polymers. I refers to isotropic phases. A1 and A2 refer to, respectively, long (X = 100) and short (X = 10) rod-rich anisotropic (nematic) phases. The solvent is represented by S. The points on the map sampled in this study are shown by solid circles for biphase samples of isotropic and liquid-crystalline phases. Open circles are films. Closed squares are samples found in the liquid-crystalline phases. On the expanded solvent corner of the map (upper right), the light and dark regions around the points correspond to domain-like and dispersed-solution structure, respectively. The axes units are volume fraction.

Publications

Douglas, E., D. Langlois, M.E. Smith, et al., "Properties of Liquid Crystal Thermosets" (to be published in *High Temp. Polymers*).

Hjelm, R., E. Douglas, and B. Benicewicz, "The Solution Structure of a Liquid Crystal Polymer with Small Liquid Crystal Thermosets," *Polymeric Mater. Sci. Eng.* **71,** 287 (1994).

Hjelm, R., E. Douglas, and B. Benicewicz, "The Solution Structure of Liquid-Crystal Polymers with Small Liquid-Crystal Thermoset Maleimides and Nadimides," *Int. J. Thermophys.* **16,** 309 (1995).

Formation of Drug-Bearing Vesicles in Mixed Colloids of Bile Salts and Phosphatidylcholine

Rex Hjelm

Liposomes have been demonstrated to be effective as intravenous delivery systems for insoluble drugs. Presently, they are produced through mechanical means. A better approach, however, would be through the development of systems that form liposomes spontaneously.

Mixed colloids of bile salt and phosphatidylcholine form liposomes spontaneously, but there is little understanding of how clinical conditions affect liposome formation. Such systems also may be useful in oral formulations where the natural action of the bile salt could serve to protect and enhance absorption of the drug. However, the lipids of the liposome are altered as a consequence of enzymatic action in the gut, and the fate of bile salt/phosphatidylcholine liposomes must be understood to further this application.

We are using small-angle neutron scattering, supplemented by light scattering, to study issues associated with such methods of forming drug-bearing liposomes. We are studying liposome stability under physiological conditions and the effects of certain classes of drugs on vesicle formation to determine the effects of enzymatic action on liposome stability.

We have continued work on understanding how enzymatic degradation of dietary triglycerides, which results in a combination of monoolein and oleic acid, affects the self-assembly and morphology in bile salt/phosphatidylcholine particles. We studied the particle morphology in mixtures of cholylglycine or chenodeoxycholylglycine with monoolein, oleic acid, or deuterated monoolein and oleic acid. Our studies show that particle morphology is not affected by inclusion of these molecules, which implies that the structure of the particles is conserved in the intestine as the components are altered by the action of enzymes. Our findings suggest that the form of the particles is important for the physiological function of bile.

We have also begun examining the effects of drugs (Taxol, cholesterol, and progesterone) on particle morphology.

Publications

Hjelm, R., C. Schteingart, A. Hofmann, et al., "Form and Structure of Self-Assembling Particles of Monoolein-Bile Salt Mixtures" *J. Phys. Chem.* **99**, 16395–16408 (1995).

Hjelm, R., P. Thiyagarajan, C. Schteingart, et al., "Probing Self-Assembly in Biological Mixed Colloids by SANS, Deuteration, and Molecular Manipulation" (to be published in *Neutrons in Biology).*

Characterization of Bioactive Materials Using Neutron Reflectivity and Atomic Force Microscopy

Gregory Smith

We are using neutron reflectivity and atomic force microscopy to characterize a new class of bioactive molecular systems composed of self-assembled membrane proteins complexed with associating and surfactant polymers. We are examining the structure, phase behavior, and shape stability of these molecules, as well as the interactions between layers and macromolecules.

First we analyzed neutron reflection data from films of stacked lipid bilayers. Our data are unique in that they contain diffuse scattering unlike that in any sample we have run in the past. Such scattering generally indicates a rough sample surface, but in this case the scattering is somewhat different from that caused by other types of rough surfaces.

To better understand the nature of this surface roughness, we examined the lipid films using atomic force microscopy. Our initial results reveal holes of varying sizes in the films. We are trying to correlate the data from our atomic force microscopy and neutron reflectivity studies to determine whether the holes are related to the ability of the lipid to wet the substrate or are structures inherent to lipid films.

Finally, we completed the design of a new humidity- and temperature-controlled oven for use in our neutron reflectivity studies.

Characterization of Active Sites in Zeolite Catalysts

Juergen Eckert

Despite the fact that zeolites have been in large-scale use as industrial catalysts for many years the molecular level details of their activity are still incompletely understood. In order to facilitate development of more effective and/or environmentally benign catalysts, a more complete understanding of the nature of the interaction of adsorbed molecules with the catalytically active sites is required.

To this end we are carrying out neutron-scattering studies combined with Quantum Monte Carlo simulations of the dynamics of small molecules inside the cavities of zeolite catalysts which are both of fundamental and practical importance. Our principal approach has been to utilize molecular hydrogen as a probe of active sites in zeolites because H_2 (1) is the smallest molecule of interest in catalysis, (2) is more mobile, (3) and can access more sites in the zeolite than other molecules. The interaction of H_2 at adsorption sites in zeolites gives rise to a barrier to rotation for the molecule which can be obtained by neutron-scattering techniques. We found this barrier to differ substantially for different sites.

Our combined neutron-scattering and theoretical studies have now enabled us to achieve a major breakthrough in the development of this technique and has resulted in a new picture of hydrogen adsorption in various ion-exchanged zeolites A. We are now able to correlate a specific rotational transition of adsorbed hydrogen with a particular active site, and have thereby demonstrated that the rotational spectrum of adsorbed hydrogen is a new, highly sensitive probe of adsorption sites in zeolites.

Publications

Eckert, J., J. Nicol, J. Howard, et al., "Adsorption of Hydrogen in Ca-Exchanged Na-A Zeolites Probed by Inelastic Neutron Scattering Spectroscopy" (to be published in *J. Phys. Chem.*).

Ong, E., J. Eckert, L. Dotson, et al., "Nature of Guest Species within Alkaline Earth -Ammonia Intercalates of Titanium Disulfide," *Chem. of Mater.* 6, 1946 (1994).

Alloy Design and Phase Stability of the Ternary Alloy Titanium-Aluminum-Niobium

Robert C. Albers

Several classes of binary intermetallic compounds, such as titanium-aluminum, have important potential application as high-temperature structural materials because of their high melting temperature, low density, and high strength. The use of these binary alloys is limited, however, by their poor low-temperature ductility and fracture toughness. Adding a third element (e.g., niobium) to these binary alloys is one possibility for improving their low-temperature properties without sacrificing, for example, the desirable high-temperature ductility.

We are using high-precision electronic structure calculations and molecular dynamics simulations to study the electronic and structural properties of selected ternary intermetallic alloy systems. The goal of our research is to understand and predict the structural stability of these ternary intermetallics and to understand the correlation between the changes in electronic properties and the improved low-temperature properties in these materials.

In the past year, we discovered the mechanism for and the role of niobium in the structural stability of the O-phase of the ternary intermetallic Ti_2AlNb. We developed and tested the capability to perform structural energy calculations with full optimization of internal degrees of freedom. In addition, we analyzed the structural stability of the Laves-phase compounds $NbCr_2$ and HfV_2 and enumerated the electronic properties associated with stability in these compounds.

Publications

Chu., F., A. Ormeci, T.E. Mitchell, et al., "Stacking Fault Energy of the $NbCr_2$ Laves Phase," *Phil. Mag. Lett.* 72, 147 (1995).

Ormeci, A., F. Chu, J.M. Wills, et al., "Total Energy Study of Electronic Structure and Mechanical Behavior of C15 Laves Phase Compounds: $NbCr_2$ and HfV_2" (submitted to *Phys. Rev. B*).

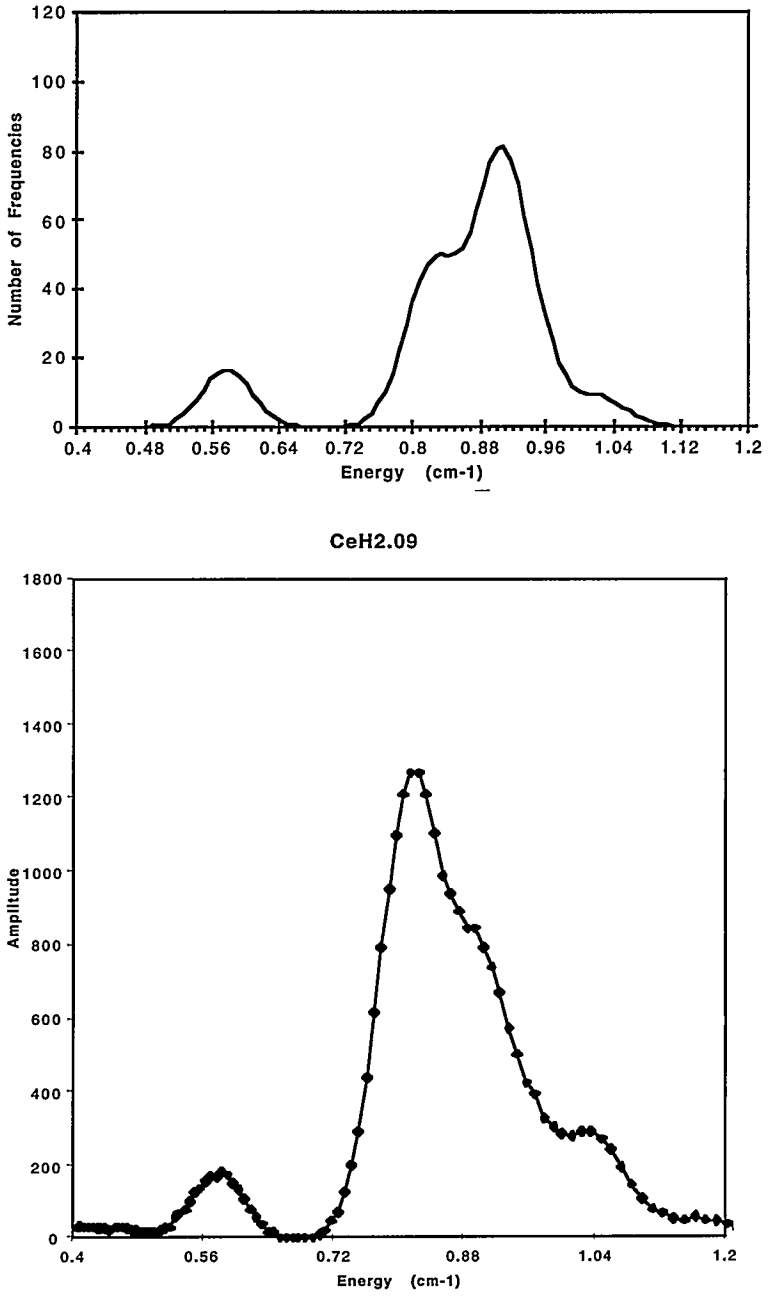
Structural and Magnetic Characterization of Actinide Materials

Barbara Cort

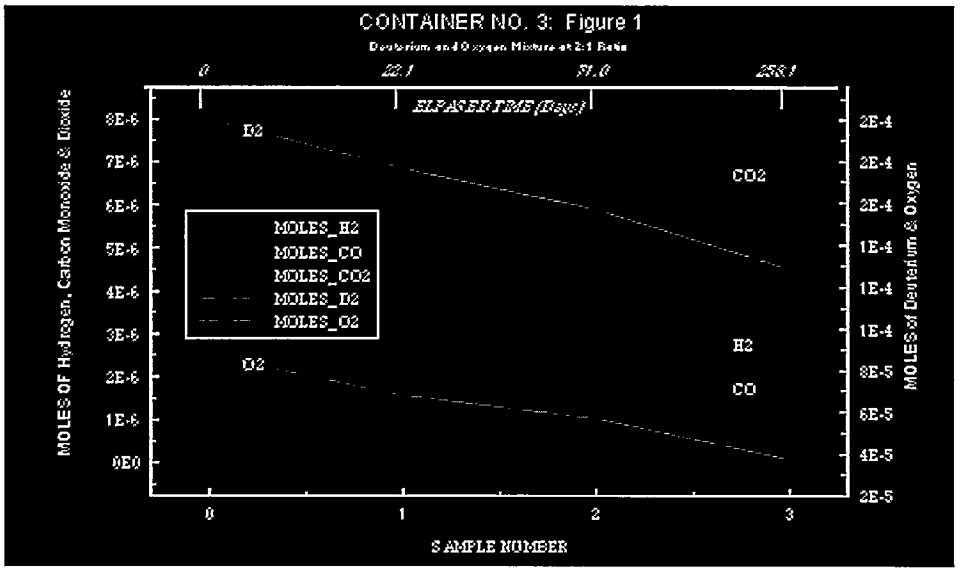
We have successfully used neutron scattering techniques to investigate physicochemical properties of elements, compounds, and alloys of the light actinides. With the end of the Cold War and concomitant cessation of both underground nuclear testing and the manufacture of new nuclear weapons, new issues vital to the Laboratory mission have arisen. Specific examples are long-term storage of nuclear materials and aging of plutonium in the nuclear stockpile.

The focus of this work is to extend our fundamental research capability and to answer questions of practical importance to stockpile integrity and long-term storage of nuclear material. Specific focus areas are (1) developing neutron diffraction techniques for smaller actinide samples, (2) modeling inelastic scattering data for actinide metal hydrides, (3) characterizing actinide oxide structures, and (4) investigating aging effects in actinides. To perform our studies, we use neutron scattering supported by resistivity, magnetic susceptibility, x-ray diffraction, and Sieverts equilibrium studies and kinetics.

Our major accomplishments include (1) the development of encapsulation cells for small actinide samples to enable neutron diffraction studies of rare or radiologically difficult actinides; (2) the refinement of a lattice dynamics model to elucidate hydrogen-hydrogen and hydrogen-metal interactions in rare-earth and actinide hydrides; (3) studies with PuO_2, indicating that the recombination reaction is faster than radiolytic decomposition of adsorbed water but a chemical reaction produces H_2; and (4) model calculations of helium ingrowth in aged plutonium, predicting bubble formation only at grain boundaries at room temperature. The accompanying figures relate to our lattice dynamics model and PuO_2 studies.



The spectra for $Ce_{2.09}$ show the quality of agreement between the experimental data (top) and the lattice dynamics model (bottom).



The data for the reaction of PuO_2 with a 2:1 ratio of deuterium and oxygen shows that the consumption of deuterium and oxygen over time forms the gaseous reaction products CO_2, H_2, and CO. The consumption resulting in gas products does not account for the total drop in oxygen pressure, which indicates that higher plutonium oxides are also formed.

A Thermodynamically Consistent, Damage-Dependent Interface Debonding Model for Composites

James N. Johnson and John B. Aidun

The ability to design composite materials and analyze processing procedures relies on the availability of constitutive models that describe the composites' dynamic response accurately. The strength, damage evolution, and failure of interfaces within composites often dominate their macroscopic performance but are not well-characterized.

We have developed a procedure to represent the average effects of interface strength and failure on an overall dynamic mechanical response of engineered composites. Our mesoscopic-scale interface behavior models are compatible with the macroscopic averaging (homogenization) procedure for selected classes of composites. Thermodynamic considerations, combined with existing measurements and observations of microstructure evolution, guide the constitutive development. Resulting models for overall response are used in continuum mechanics computer programs for simulating the average thermoelastic-plastic response to arbitrary loading.

Our specific accomplishments include combining an interface model with previous results (anisotropy, plastic deformation, and nonlinear elasticity) to average composite mechanical properties. In this interface model, the traction (force) across a pre-existing interface is given as a function of the jump in displacement. The jump in displacement field becomes large as the interface fails. The interface model provides the response of both the fiber-matrix interface (debonding) and the interface between laminae (delamination).

Computational simulations of spallation for unidirectional fiber-reinforced composites are also performed. Surface velocity histories are obtained for four cases—no damage, matrix damage, debonding, and both matrix and interface damage—for unidirectionally reinforced composites.

Publications

Aidun, J.B., and F.L. Addessio, "An Enhanced Cell Model with Nonlinear Elasticity" (submitted to *J. Composite Mater.*).

Addessio, F.L., and J.B. Aidun, "Analysis of Shock-Induced Damage in Fiber-Reinforced Composites" in *High-Pressure Shock Compression of Solids*, Vol. 3, L. W. Davison and M. Shahinpoor, Eds. (Springer-Verlag, New York, in press).

Production of High Specific Activity Si-32

Dennis Phillips

In this project, we use Los Alamos capabilities and facilities to produce the radionuclide Si-32 in unusually high specific activity and Los Alamos expertise to develop field-usable radioanalytical methods for application of the radionuclide in oceanographic research. Expertise from the University of California at Santa Barbara is used to develop and implement the biological oceanographic experiments and to reserve and coordinate the necessary time on oceanographic research vessels.

Diatoms, i.e., siliceous phytoplankton, require silicate as a nutrient to produce their opaline shell. They require other nutrients such as bicarbonate, inorganic nitrogen, and inorganic phosphorus for their life cycles. By using Si-32 to perform oceanographic, kinetic silicate-uptake studies, we provide information about the role of diatoms in the global climate; because of their sheer volume, the diatoms sequester significant amounts of atmospheric carbon dioxide. Theories indicate that silicate may be the limiting nutrient in some important ocean bodies, and data from this work can be used to test these models.

We performed our first oceanographic experiments through participation in the 1995 Coastal Ocean Processes cruise in Monterey Bay, sponsored in part by the National Science Foundation and the Monterey Bay Aquatic Research Institute. We successfully demonstrated our analytical methods and showed that the application of Si-32 in real time will greatly enhance the quality of global climate research. The remainder of this project will focus upon refinement of the radioanalytical technique and its continued application in biological oceanographic experiments.

Publications

Phillips, D.R., V.T. Hamilton, D.J. Jamriska, et al., "Application of Sephadex to Radiochemical Separations," *J. of Radioanal. Nucl. Chem. Articles* **195,** 251 (1995).

Equation of State (EOS), Thermodynamic, and Structural-Mechanical Properties of Intermetallic Compounds

John Wills

Several classes of binary intermetallic compounds have important potential application as high-temperature structural materials because of their high melting temperature, low density, and high strength. Their use is limited, however, by their poor low-temperature ductility and fracture toughness. A possibility for improving the low-temperature properties while retaining the desirable high-temperature properties is the stabilization of these alloys in new structures. The polysynthetically twinned titanium-aluminum alloy, for example, exhibits improved low-temperature ductility for unidirectional stress.

We may also be able to stabilize different structures with the addition of a tertiary component. We are studying the elastic properties and EOS of selected alloys with high-precision electronic-structure calculations and a new procedure for calculating the EOS of material, including melting, from first principles. The goal of our research is an ab-initio understanding of the elastic properties of these materials and the relation between structure, composition, and mechanical properties.

During the past year, we carried out an extensive study of binary titanium-aluminum and niobium-aluminum and ternary titanium-aluminum-niobium alloys in several different structures. Our study focused on elasticity and structural and meta-stability. Significant results included a new theory explaining body-centered cubic (bcc) instability in binary alloys, high temperature bcc stability in the ternary alloy, and the role of niobium in stabilizing the low-temperature phase of ternary titanium-aluminum-niobium alloys. We also completed calculations of the energies of idealized stacking faults and twinning in the titanium-aluminum alloy. We are presently analyzing those calculations.

Publications

Straub, G.K., J.B. Aidun, J.M. Wills, et al., "Ab-Initio Calculation of Melting and Thermodynamic Properties of Crystal and Liquid Aluminum," *Phys. Rev. B* **50,** 5055 (1994).

Correlated Electron Theory Project

Kevin Bedell

The foundations of the theory of metals and superconductors have been shaken by a number of discoveries over the last fifteen years. These discoveries include the Quantum Hall effect, heavy fermions, low-dimensional conductors, and high-temperature superconductors.

The standard theory of metals is the Landau–Fermi-liquid theory; for superconductors, it is the *s*-wave, phonon-mediated pairing theory of Bardeen, Cooper, and Schrieffer. While many of the traditional metals and superconductors can be understood in terms of these theories, many of the new materials exhibit behaviors that do not fall within these standard models.

The newer classes of materials have a number of properties that favor a much richer spectrum of ground and excited states. These properties include strong electronic and lattice correlations, reduced dimensionality, restricted geometry, disorder, and nonlinearity. The competition and interplay between these various properties lead to the rich variety of ground states observed in these strongly correlated materials. The development of microscopic theories to describe and understand the behavior of these materials is one of the biggest challenges in condensed-matter theory today. What makes this development even more exciting is that the novel characteristics of these materials will make them likely candidates for new electronic applications in the future.

In the last year we have investigated the fundamental physics of high-temperature superconductors. The critical issues studied were the properties of odd-gap superconductors and the influence of magnetic imperfections on the properties of *d*-wave superconductors. In addition we held two conferences that involved about 100 participants, 40 external and 60 internal. One conference reviewed 40 years of many-body theory, which is essential to understanding superconductivity, and the second meeting addressed current topical problems in correlated-electron physics.

Publications

Abrahams, E., A.V. Balatsky, D.J. Scalapino, et al., "Properties of Odd Gap Superconductors," *Phys. Rev. B* **52**, 1271 (1995).

Balatsky, A.V., and E. Abrahams, "Odd-Time Magnetic Correlations and Chiral Spin Nematics," *Phys. Rev. Lett.* **74**, 1004 (1995).

Balatsky, A.V., D. Pines, and P. Monthoux, "Influence of Magnetic Imperfections on the Low-Temperature Properties of D-Wave Superconductors," *Phys. Rev. B* **50**, 582 (1994).

Chen, J., Z.H. Levind, J.W. Wilkins, "Calculated Second-Harmonic Susceptibilities of BN, ALN, and GAN," *Appl. Phys. Lett.* **66**, 1129 (1995).

Noack, R., D.J. Scalapino, and S.R. White, "Ground State Properties of the Two-Chain Hubbard Ladder" (to be published in *Philos. Mag.*).

Noack, R.M., S.R. White, and D.J. Scalapino, "The Doped Two Chain Hubbard Model," *Europhys. Lett.* **30**, 163 (1995).

Smith, R.A., M.Y. Reizer, and J.W. Wilkins, "Suppression of the Order Parameter in Homogeneous Disordered Superconductors," *Phys. Rev. B* **51**, 6470 (1995).

Steiner, M.M., W. Wenzel, K.G. Wilson, K.G., et al., "The Efficient Treatment of Higher Excitations in CI Calculations—A Comparison of Exact and Approximate Results," *Chem. Phys. Lett.* **231**, 263 (1994).

Vekic, J., J.W. Cannon, D.J. Scalapino, et al., "Competition Between Antiferromagnetic Order and Spin-Liquid Behavior in the Two-Dimensional Periodic Anderson Model at Half-Filling," *Phys. Rev. Lett.* **74**, 2367 (1995).

White, S.R., R.M. Noack, and D.J. Scalapino, "Density Matrix Renormalization Group Calculations for Doped Hubbard Ladders," *J. Low Temp. Phys.* **99**, 593 (1995).

Physical Properties and Mantle Dynamics

Thomas Shankland

Understanding the physical properties of minerals and rocks reveals Earth's processes and events in its history. Because planetary interiors are difficult to access, research methods that comprise sophisticated techniques and theory are essential for interpreting field measurements on seismic activity, electromagnetism, heat flow, and geological structures in terms we need for understanding the temperature, composition, stress state, convective flow, and history of our planet. The objectives this project are to study minerals and rocks using materials science methods and to develop new laboratory methods, such as high-pressure techniques or nuclear-based analyses. We are focusing on analyzing geophysical data so that we can develop physical explanations of Earth's internal properties.

In the reporting period, we developed a transient optical-grating apparatus and used it to determine sound velocities in fluids and ice at high pressure. In addition, we developed a single-crystal x-ray diffraction apparatus that can be used to analyze minerals at extremely high pressures and temperatures (see figure showing compression data). Data from such studies can be used to determine the equation of state and significant thermoelastic parameters, enabling us to discriminate between different hypotheses about Earth's composition. And finally, we developed mass spectrometers that measure molybdenum and tungsten concentrations at levels of a few parts per billion.

Recent achievements and results include (1) better physical models of materials from Earth's crust to its core, (2) new experimental techniques for understanding materials under extreme conditions, (3) new isotopic and physical methods for understanding problems of hydrocarbon reservoirs and waste isolation in soils and rocks through knowledge of their properties (see figure showing strain vs stress), and (4) better parameters for use in computer programs that model Earth's interior for nonproliferation research.

Publications

Chai, M., J.M. Brown, and L.J. Slutsky, "Thermal Diffusivity of Mantle Silicates" (submitted to *J. Geophys. Res.*).

Guyer, R.A., K.R. McCall, and G.N. Boitnott, "Hysteresis, Discrete Memory, and Nonlinear Wave Propagation in Rock," *Phys. Rev. Lett.* **74**, 3491 (1995).

Hearn, I., et al., "Effect of Anisotropy on the Development of Oceanic Lithosphere" (submitted to *J. Geophys. Res.*).

McCall, K.R., and R.A. Guyer, "Equation of State and Wave Propagation in Hysteretic Nonlinear Elastic Materials," *J. Geophys. Res.* **99**, 23887 (1994).

McCall, K.R., and R.A. Guyer, "Hysteresis, Discrete Memory and Nonlinear Elastic Wave Propagation in Rock: A New Theoretical Paradigm" (to be published in *Nonlinear Processes in Geophys.*).

Nicol, M., H. Cynn, O.L. Anderson, et al., "Grüneisen Ratio of MgO from the Entropy Calculation," *J. Phys. Chem.* **99**, 7813 (1995).

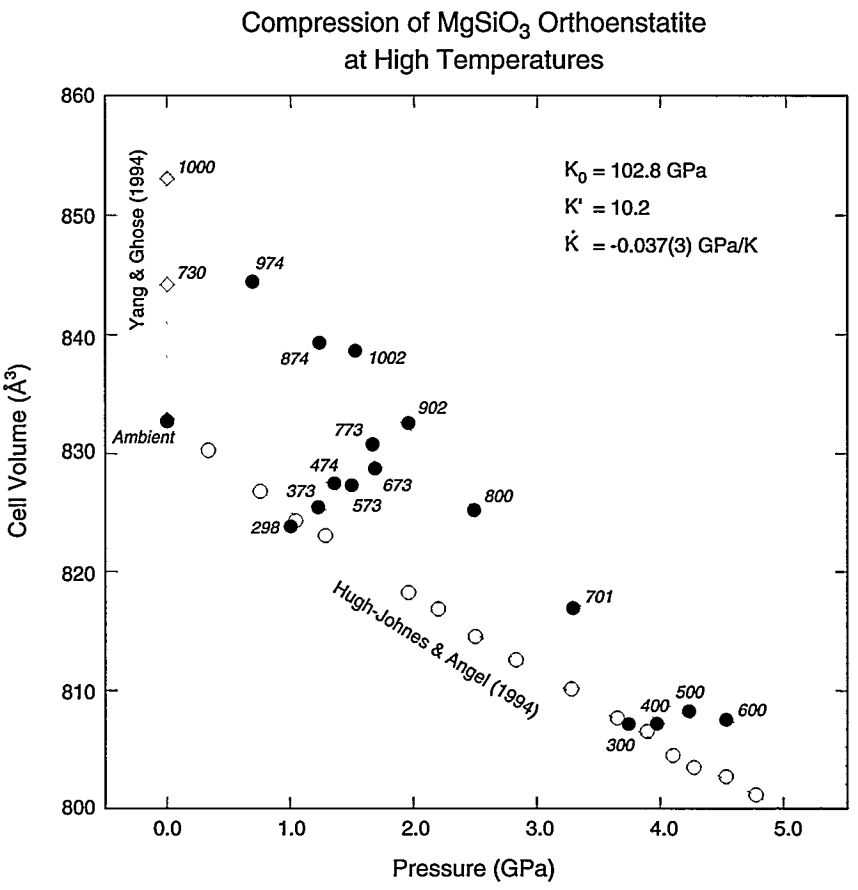
Nicol, M., S.E. Gibson, D. Reifschneider, et al., "Spectroscopic and X-Ray Studies of Materials at High Pressures: Recent Developments," in *Advanced Materials '94*, M. Kamo, H. Kanda, Y. Matsui, and T. Sekine, Eds. (International Communication Specialists, Tokyo, 1994), pp. 205–210.

Ragan, D.D., D. Schiferl, and D. Clarke, "Silicone Fluid as a Pressure Medium in Diamond-Anvil Cells" (submitted to *Rev. Sci. Instrum.*).

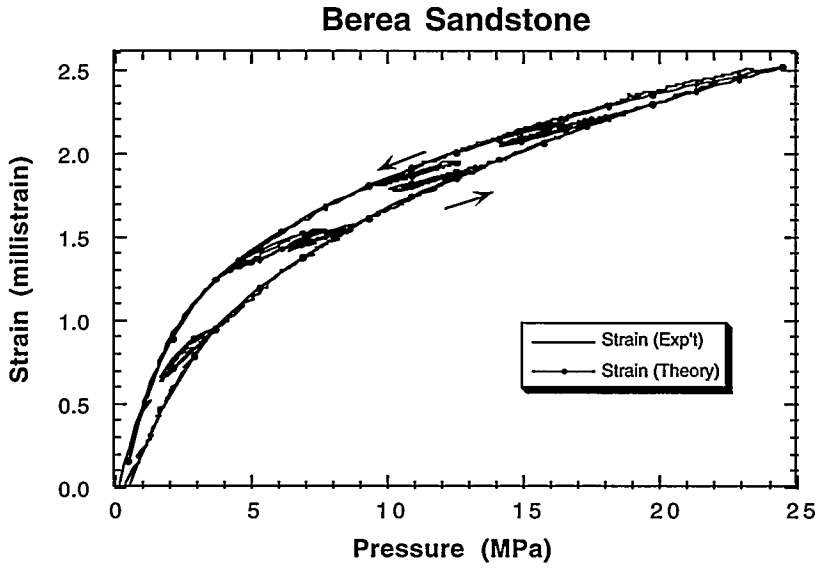
Schiferl, D., and Y. Zhao, "High-Pressure/High-Temperature Diamond-Anvil Cell System for Single-Crystal X-Ray Diffraction" (submitted to *Rev. Sci. Instrum.*).

Zhao, Y., D. Schiferl, and T.J. Shankland, "Thermoelasticity of $MgSiO_3$ Orthoenstatite, A Single-Crystal Study at Simultaneous High Pressures and Temperatures," *Phys. Chem. Minerals*, **22**, 393–398, (1995).

Zhao, Y., D. Schiferl, and J.M. Zaug, "RSCU-SOS: A Rapid Intensity Searching and Centering Routine for Single Crystal Diffraction Studies at Simultaneous High Pressures and Temperatures" (to be published in *J. Appl. Cryst.*).



Cell volume as a function of pressure at various temperatures of the mineral enstatite ($MgSiO_3$), the second most abundant mineral phase in Earth's upper mantle.



Strain vs stress cycle for a sample of Berea Sandstone. The very complex behaviors (fine lines) observed in the small inner loops were calculated (connected points) from a model of elastic hysteresis of microcracks based on data from the outer loop. Rocks from crustal reservoirs and waste isolation sites display such complexity under stress.

Scanning Probe Microscopy Competency Development

Marilyn Hawley

The primary purpose of this project is to bring an Omicron ultra-high vacuum (UHV) scanning tunneling microscope (STM) on-line and to integrate the instrument with our existing network of scanning-probe and surface technologies. The UHV STM will combine a commercially proven state-of-the-art microscope with several surface-science techniques in a dual-use configuration. The resulting capabilities will enable the Laboratory to respond to a wide variety of problems requiring localized imaging of conducting and nonconducting surfaces in liquids, air, and vacuum.

We improved the Omicron UHV STM system as follows: we upgraded the computer operating system and software program and immediately achieved atomic resolution on highly oriented pyrolytic graphite; we added new pumps capable of 10^{-11} torr vacuum and a new sample-preparation heating stage; we used a frequency analyzer to improve the signal-to-noise ratio in the imaging signals; we recently implemented ballistic electron emission microscopy capability; and we designed and ordered a new vacuum chamber and load-lock system.

We also added two new components to our air-based atomic force microscope (AFM). The first component is a phase/frequency-sensitive interface which allows us to operate in magnetic force microscope (MFM) mode. In MFM mode we can image magnetic domains in order to study the properties of the new perovskite colossal magnetoresistive (CMR) films. We also added a new AFM tip holder for conductive AFM tips which allows us to operate in electrostatic force microscope (EFM) mode. In this mode we can correlate variations in surface electrical potentials and field gradients with the structure of diamond-like carbon and high-temperature-superconductor films and devices. In MFM mode we took the first images of magnetic domains caused by strain in FeBSi tapes and of grain-dominated magnetic structure in CMR films. We also took preliminary EFM images of potential variations on a yttrium-barium-copper oxide (YBCO) film.

We have used the noncontact/tapping-mode AFM and top-view STM probe acquired last year to study the following: very thin yttrium-stabilized-zirconia growth, Yucca Mountain Project magnetite/water interface reactions, tribological wear tracks on silicon, single-crystal radiation damage of bismuth-strontium-calcium-copper oxide (BSCCO), the structure of as-deposited and annealed thin films of the CMR material $La_{0.7}Ca_{0.3}MnO_3$, the growth orientation and structure of insulating YBCO-device barrier layers made of $LaAlO_3$, the film growth and electrical band gap of thin films of the wide-band-gap material aluminum-doped GaN, the temperature-dependent growth of $SrRuO_3$ films, and the surface structure and electrical properties of carbon-coated fibers.

Publications

Arendt, P., S. Foltyn, X.D. Wu, et al., "Fabrication of Biaxially Oriented YBCO on (001) Biaxially Oriented Yttria-Stabilized-Zirconia on Polycrystalline Substrates," *Mater. Res. Soc. Symp. Proc.* **341**, 209 (1994).

Brosha, E.L., B.W. Chung, F.H. Garzon, et al., "In Situ Growth and Characterization of $La_{0.8}Sr_{0.2}CoO_3$," *J. Electrochem. Soc.* **142**, 1702 (1995).

Bryden, W.A., S.A Ecelberger, M.E. Hawley, et al. "ECR-Assisted Reactive Magnetron Sputtering of InN," *Mater. Res. Soc. Symp. Proc.* **339**, 497 (1994).

Chung, B.W., E.L. Brosha, F.H. Garzon, et al., "Growth of Atomically Flat Biaxially Oriented $La_{0.84}Sr_{0.16}MnO_3$ Perovskite Films," *J. Mater. Res.* **10**, 2518 (1995).

Hawley, M.E., "Scanning Tunneling Microscopy," in *Characterisation of High-T_c Materials and Devices by Electron Microscopy*, N.D. Browning and S.J. Pennycook, Eds. (Cambridge University Press, Cambridge, in press).

Hawley, M.E., T.J. Houlton, and F.H. Garzon, "Temperature Dependent Growth of $LaAlO_3$ Films on C-Axis Films for Multilayer Structures," *Mater. Res. Soc. Symp. Proc.* **357**, 171 (1995).

Houlton, R.J., D.W. Reagor, M.E. Hawley, et al., "Development of Materials for High Temperature Superconductor Josephson Junctions," *Trans. Appl. Supercon. Conf.*, IEEE **5**, 163 (1995).

Hundley, M., J.J. Neumeier, X.D. Wu, et al., "Transport-Magnetism Correlations in the Ferromagnetic Oxide $La_{0.7}Ca_{0.3}MnO_3$," *Appl. Phys. Lett.* **67**, 860 (1995).

Jia, Q.X., D. Reagor, S.R. Foltyn, et al., "Superconducting $YBa_2Cu_3O_{7-x}$ Based Edge Junctions with $Y_{0.7}Ca_{0.3}Cu_3O_{7-x}$ Barriers," *Physica C* **228**, 160 (1994).

Jia, Q.X., X.D. Wu, S.R. Foltyn, et al., "Fabrication and Characterization of High Temperature Superconductor Josephson Junctions with a Novel Device Design," *Trans. Appl.*

Supercon. Conf., IEEE **5**, 2103 (1995).

Kistenmacher, T.J., S.A. Ecelberger, W.A. Bryden, et al., "Structural and Electrical Properties of Thermally Annealed InN Thin Films on Native and AlN-Nucleated (00.1) Sapphire," *Mater. Res. Soc. Symp. Proc.* **317**, 461 (1994).

Kistenmacher, T.J., D.K. Wickenden, M.E. Hawley, et al., "Real and Reciprocal Space Mapping of the Mosaic Dispersion in Self-Nucleated $Al_xGa_{1-x}N$ Thin Films on (00.1) Sapphire" (to be published in *Appl. Phys. Lett.*).

Pluym, T.C., R.E. Muenchausen, P.N. Arendt, et al., "Superconducting $Tl_2Ba_2CaCu_2O_8$ Thin-Films Prepared by Postannealing in a Flow-Through Multiple-Zone Furnace," *Trans. Appl. Supercon. Conf.*, IEEE **5**, 1339 (1995).

Reagor, D., R. Houlton, K. Springer, et al., "Development of High Temperature Superconducting Josephson Junctions and SQUID's Using Low Temperature Barriers," *Appl. Phys. Lett.* **66**, 2280 (1995).

Reimanis, I.E., and M.E. Hawley, "The Fracture Characteristics of Czechrolski-Grown $Y_3Al_5O_{12}$," *J. Am. Ceram. Soc.* **78**, 2282 (1995).

High Resolution Electron Microscopy of Materials

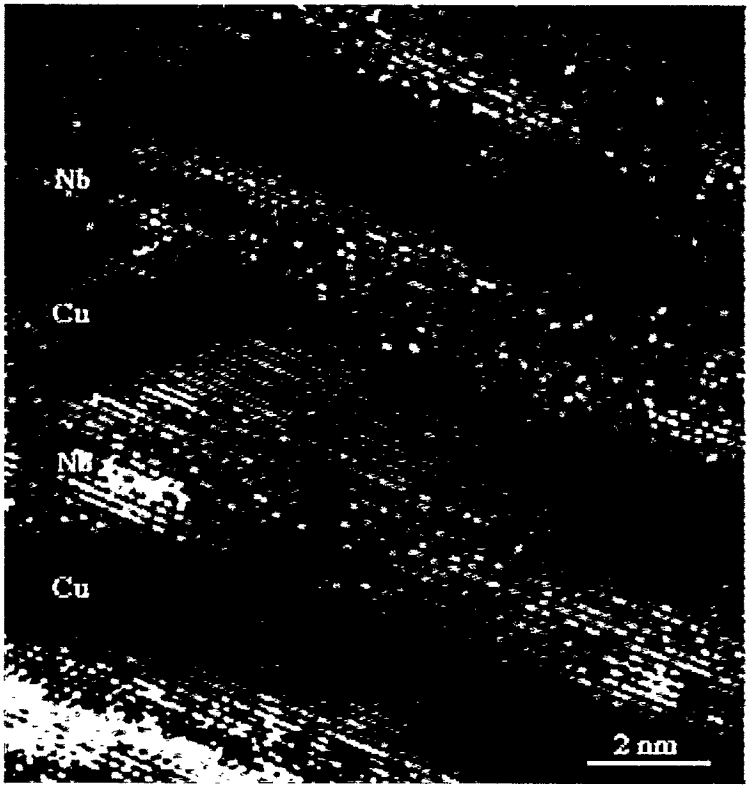
Terence Mitchell

This project supports research on the processing, microstructure, mechanical properties, radiation effects, and superconducting properties of metals and ceramics.

We recently upgraded our High Resolution Transmission Electron Microscope (HRTEM) facility by installing a field emission (FE) HRTEM—a JEOL JEM3000F with point-to-point resolution of 1.6 Å. Because of the high brightness and coherence of the FE source, the resolution can be pushed to its information limit of 1 Å by reconstructing a focal series of images by computer.

HRTEM has been used to image the atomic structure of defects such as dislocations, grain boundaries, and interfaces in a wide variety of materials, from superconductors to structural ceramics. We will use the new HRTEM to image such defects with much greater accuracy at the atomic level, making possible more accurate comparisons with modeling predictions and improved measurements of interatomic potentials.

Recent examples of applications of the new HRTEM include the following: (a) characterizing defects and interfaces in thin films of $YBa_2Cu_3O_7$ deposited on various substrates and buffer layers, (b) HRTEM analysis of interfaces in various ceramic composites, (c) analyzing the core structures of dislocations produced in ceramics and intermetallics by high-temperature deformation, and (d) analyzing nanolayered materials. Future applications will involve electron holography, x-ray energy dispersive spectroscopy, and electron energy loss spectroscopy; all of these techniques will be developed on the new microscope.



High-resolution electron micrograph showing the lattice image of a Cu/Nb-nanolayer composite with layer thickness of 2.5 nm. The interfaces are sharp and free of interfacial phase and reaction. The nanolayers exhibit superior hardness as compared with conventional large-grained materials.

Publications

Ai, R., N. Bordes, E.A. Cooper, et al., "Dislocation Loops in Spinel Crystals Irradiated Successively With Deep and Shallow Ion Implants," *Mater. Res. Soc. Symp. Proc.* **316**, 147 (1994).

Albert, D., and G.T. Gray III, "A Determination of Deformation Twinning in Dynamically Deformed and Shock-Loaded Polycrystalline Ni_3Al," *Philos. Mag. A* **70**, 145 (1994).

Albert, D.E., and G.T. Gray III, "Dislocation Reactions Responsible for the Formation of a Twin in the Ordered Intermetallic Alloy Ni-20Al-30Fe," *Philos. Mag. A* **71**, 473 (1994).

Albert, D.E., and G.T. Gray III, "Dislocation Substructures in Shock-Loaded Ni_3Al," *Mater. Res. Soc. Symp.* **364**, 725 (1995).

Albert, D.E., G.T. Gray III, and S. Guha, "Quasi-Static and Dynamic Deformation of a Ni-20Al-30Fe+90 wt.% W Composite at 77K and 300K," in *Tungsten and Refractory Metals 2*, A. Bose and R.J. Dowding, Eds. (Metal Powder Industries Federation, Princeton, New Jersey, 1995), p. 187.

Aumann, C.E., G.L. Skofronick, and J.A. Martin, "Oxidation Behavior of Aluminum Nanopowders," *J. Vac. Sci. Technol. B* **13**, 1178 (1995).

Bordes, N., L.M. Wang, R.C. Ewing, et al., "Ion-Beam Induced Disordering and Onset of Amorphization in Spinel by Defect Accumulation," *J. Mater. Res.* **10**, 981 (1995).

Butt, D.P., S.A. Maloy, H. Kung, et al., "Creep Behavior of $MoSi_2$-SiC Composites," *Mater. Res. Soc. Symp. Proc.* **322**, 197 (1994).

Carim, A.H., and T.E. Mitchell, "90° Boundaries and Associated Interfacial and Stand-Off Dislocations in $YBa_2Cu_3O_{7-d}$," *Ultramicroscopy* **51**, 228 (1994).

Chu, F., D.P. Pope, D.S. Zhou, et al., "Morphology of S3{<110>/ 70.53°} Grain Boundaries in a C15 Intermetallic Compound," in *Proceedings, 52nd Annual Meeting, Microscopy Society of America*, G.W. Bailey and A.J. Garratt-Reed, Eds. (San Francisco Press, San Francisco, California, 1994), p. 684.

Cooper, E.A., C.D. Hughes, W.L. Earl, et al., "Cation Disorder Determined by MAS 27Al NMR in High Dose Neutron Irradiated Spinel," *Mater. Res. Soc. Symp. Proc.* **373**, 413 (1995).

Cotton, J.D., J.F. Bingert, P.S. Dunn, et al., "Microstructure and Mechanical Properties of Ti-40 wt.% Ta," *Metall. Trans. A* **25**, 461 (1994).

Fernandez, T.R.C., W.E. Lee, and T.E. Mitchell, "Microstructural Aspects of the Reduction of Zimbabwe Chromite to High Carbon Ferrochromium," *Trans. Instn. Min. Metall.* **103**, 177 (1994).

Fitzsimmons, M.R., J.A. Eastman, R.A. Robinson, et al., "Magnetic Structures of Nanometer Scale Dy, Cr, and Ni," *Nanostruct. Mater.* **3**, 311 (1994).

Freim, J., J. McKittrick, J. Katz, et al., "Microwave Sintering of Nanocrystalline g-Al_2O_3," *Nanostruct. Mater.* **4**, 371 (1994).

Gray III, G.T., "Deformation Twinning: Influence of Strain Rate," in *Twinning in Advanced Materials*, M.H. Yoo and M. Wuttig, Eds. (The Minerals, Metals, and Materials Society, Warrendale, Pennsylvania, 1994), p. 337.

Gray III, G.T., "Influence of Peak Pressure and Temperature on the Shock-Loading Response of Tantalum," in *High-Pressure Science and Technology-1993*, S.C. Schmidt, J.W. Shaner, G.A. Samara, et al., Eds. (American Institute of Physics, Woodbury, New York, 1994), p. 1103.

Gray III, G.T., "Influence of Shock Loading on the Structure/ Property Response of Ti-48Al-2Cr-2Nb and Ti-24Al-11Nb," *Les Editions de Physique*, **C8**, 373 (1994).

Gray III, G.T., "Shock-Loading Response of Advanced Materials," in *High-Pressure Science and Technology-1993*, S.C. Schmidt, J.W. Shaner, G.A. Samara, et al., Eds. (American Institute of Physics, Woodbury, New York, 1994), p. 1161.

Hoke, D.A., and G.T. Gray III, "Arrangement of Dislocation Networks in Hot-Pressed Titanium Diboride," *Scripta Metall. et Materialia* **33**, 171 (1995).

Jia, Q.X., X.D. Wu, S.R. Foltyn, et al., "Fabrication and Characterization of High Temperature Superconductor Josephson Junctions with a Novel Design," *IEEE Trans. Appl. Supercond.* **5**, 2103 (1995).

Kung, H., T.R. Jervis, J.-P. Hirvonen, et al., "Characterization of Structure and Mechanical Properties of $MoSi_2$-SiC Nanolayer Composites," *Mater. Res. Soc. Symp. Proc.* **322**, 27 (1994).

Kung, H., T.R. Jervis, J.-P. Hirvonen, et al., "High Temperature Structural Stability of $MoSi_2$-Based Nanolayer Composites," *J. Vac. Sci. Tech. A* **13**, 1126 (1995).

Kung, H., T.R. Jervis, J-P Hirvonen, et al., "Phase Transformation and Layer Evolution in Molybdenum Disilicide-Silicon Carbide Nanolayered Coatings," in *Proceedings, 52nd Annual Meeting, Microscopy Society of America*, G.W. Bailey and A.J. Garratt-Reed, Eds. (San Francisco Press, San Francisco, California, 1994), p. 538.

Kung, H., T.R. Jervis, J.-P. Hirvonen, et al., "Structure and Mechanical Properties of $MoSi_2$-SiC Nanolayer Composites," *Phil. Mag. A* **71**, 759 (1995).

Lagerlof, K.P.D., A.H. Heuer, J. Castaing, et al., "Slip and Twinning in Sapphire (a-Al_2O_3)," *J. Am. Ceram. Soc.* **77**, 385 (1994).

Maloy, S.A., and G.T. Gray III, "The Temperature and Strain Rate Dependence of the Flow Stress of Single Crystal NiAl Deformed along <110>," *Mat Res. Soc. Symp. Proc.*, **364**, 549 (1995).

Maloy, S.A., G.T. Gray III, and R. Darolia, "High Strain Rate Deformation of NiAl," *Mater. Sci. and Eng.* **A192/3**, 249 (1995).

Maloy, S.A., T.E. Mitchell, and A.H. Heuer, "High Temperature Plastic Anisotropy in $MoSi_2$ Single Crystals," *Acta Met. Mater.* **43**, 657 (1995).

Maloy, S.A., T.E. Mitchell, and J.J. Petrovic, "The Temperature and Strain Rate Dependence of the Flow Stress in $MoSi_2$ Single Crystals," *Mater. Res. Soc. Symp. Proc.* **322**, 21 (1994).

Maloy, S.A., S.-Q. Xiao, A.H. Heuer, et al., "Precipitation of Mo_5Si_3 in $MoSi_2$," *J. Mater. Res.* **8**, 1079 (1994).

Mitchell, T.E., and S.A. Maloy, "Structure of Dislocations in $MoSi_2$," *Les Editions de Physique* **2A**, 89 (1994).

Mitchell, T.E., M. Nastasi, T.R. Jervis, et al., "Structure and Mechanical Properties of Nanolayered Composites of Mo, $MoSi_2$, $MoSi_2N_x$ and SiC," in *Novel Techniques in Synthesis and Processing of Advanced Materials*, J. Singh and S. Copley, Eds. (The Minerals, Metals, and Materials Society, Warrendale, Pennsylvania, 1995), p. 271.

Peachey, N.M., J.A. Samuels, B.F. Espinoza, et al., "MOCVD of Gallium and Calcium Sulfides for Improved Phosphor Processing," in *Novel Techniques in Synthesis and Processing of Advanced Materials*, J. Singh and S. Copley, Eds. (The Minerals, Metals, and Materials Society, Warrendale, Pennsylvania, 1995), p. 365.

Sickafus, K.E., A.C. Larson, N. Yu, et al., "Cation Disorder in High-Dose, Neutron-Irradiated Spinel," *J. Nucl. Mater.* **219**, 128 (1995).

Song, S.G., and G.T. Gray III, "Double Dislocation Pole Model for Deformation Twining in FCC Lattices," *Philos. Mag. A* **71**, 661 (1995).

Song, S.G., and G.T. Gray III, "Microscopic and Crystallographic Aspects of the Retained Omega Phase in Shock-Loaded Zirconium and Its Formation Mechanism," *Philos. Mag. A* **71**, 275 (1995).

Song, S.G., and G.T. Gray III, "Omega Phase Formation in Shock-Loaded Zirconium," in *High-Pressure Science and Technology-1993*, S.C. Schmidt, J.W. Shaner, G.A. Samara, et al., Eds. (American Institute of Physics, Woodbury, New York, 1994), p. 251.

Song, S.G., and G.T. Gray III, "Structural Interpretation of the Nucleation and Growth of Deformation Twins in Zr and Ti - I. Application of the Coincidence Site Lattice (CSL) Theory to Twinning Problems in hcp Structures," *Acta Metallurgica et Materialia* **43**, 2325 (1995).

Song, S.G., and G.T. Gray III, "Structural Interpretation of the Nucleation and Growth of Deformation Twins in Zr and Ti - II. TEM Study of Twin Morphology and Defect Reactions during Twinning," *Acta Metallurgica et Materialia* **43**, 2339 (1995).

Song, S.G., and G.T. Gray III, "TEM Examination and Analysis of a New Type of Stacking Fault in HCP Metals," *Philos. Mag. A* **71**, 263 (1995).

Tiwari, P., X.D. Wu, S.R. Foltyn, et al., "High-Quality Epitaxial YBCO Thin Films Directly on $LiNbO_3$," *Philos. Mag. B* **71**, 903 (1995).

Tiwari, P., X.D. Wu, S.R. Foltyn, et al., "Synthesis of Epitaxial Pt on (100)Si using TiN Buffer Layer by Pulsed Layer Deposition," *Appl. Phys. Lett.* **65**, 2693 (1994).

Tiwari, P., X.D. Wu, M.Q. Lee, et al., "Study of Low Resistivity Oxides on Pt/MgO," *Philos. Mag. B* **69**, 1101 (1994).

Unal, O., T.E. Mitchell, and A.H. Heuer, "Microstructures of Y_2O_3-Stabilized ZrO_2 Electron Beam-Physical Vapor Deposition Coatings on Ni-Base Superalloys," *J. Am. Ceram. Soc.* **77**, 984 (1994).

Vollath, D., and K.E. Sickafus, "Synthesis of Ceramic Oxide Powders by Microwave Plasma Pyrolysis," *J. Mater. Sci.* **28**, 5943 (1994).

Vollath, D., D.V. Szabo, R.D. Taylor, et al., "Synthesis and Properties of Nanocrystalline Superparamagnetic g-Fe_2O_3," *Nanostruct. Mater.* **6**, 941 (1995).

Wilson, M.S., Fernando Garzon, Kurt E. Sickafus, et al., "Surface Area Loss of Supported Platinum in Polymer Electrolyte Fuel Cells," *J. Electrochem. Soc.* **140**, 2872 (1994).

Wright, S.I., G.T. Gray III, and A.D. Rollett, "Textural and Microstructural Gradient Effects on the Mechanical Behavior of a Tantalum Plate," *Metall. & Matls. Trans. A* **25**, 1025 (1994).

Yan, M., S.P. Chen, T.E. Mitchell, et al., "Atomistic Study of Energy and Structure of Surfaces in NiO," *Philos. Mag. A* **72**, 121 (1995).

Yano, T., M. Ikari, T. Iseki, et al., "Effect of Neutron Irradiation on Knoop Hardness Anisotropy in $MgO{\cdot}3Al_2O_3$ Single Crystal," *J. Am. Ceram. Soc.* **78**, 1469 (1995).

Yu, N., K.E. Sickafus, and M. Nastasi, "First Observation of Amorphization in Single Crystal $MgAl_2O_4$ Spinel," *Philos. Mag. Lett.* 70, 235 (1994).

Yu, N., K.E. Sickafus, and M. Nastasi, "Temperature Effects on Ion Irradiation Damage in $MgAl_2O_4$ Spinel Single Crystals," *Mater. Res. Soc. Symp. Proc.* 373, 401 (1995).

Zhou, D.S., and T.E. Mitchell, "Grown-in Defects in CVD a-Si_3N_4," in *Proceedings, 52nd Annual Meeting, Microscopy Society of America*, G.W. Bailey and A.J. Garratt-Reed, Eds. (San Francisco Press, San Francisco, California, 1994), p. 640.

Engineering and Base Technologies

Radiation Hardness Measurements of New Permanent Magnet Materials for High-Intensity Linac Applications

David Barlow

The objective of this project is to measure the radiation resistance of the commercially available high-strength samarium cobalt (SmCo) permanent magnet material. SmCo is of interest in accelerator applications because of its high remanence, high coercivity, and stabile temperature. However, the magnetic strength of SmCo, as well as other rare-earth permanent magnet materials, has proven to be quite sensitive to radiation damage. The sensitivity to radiation damage has been shown to be linked to variables in the manufacturing process that cause changes in the material properties that ultimately affect the radiation resistance. Hence, as the manufacturing processes evolve, it is necessary to periodically remeasure the radiation resistance of the material. Past measurements have indicated that SmCo has about an order-of-magnitude better radiation resistance than neodymium-iron-boron, another commonly available high-strength rare-earth magnet material. For this reason, we are limiting our measurements to samples of SmCo.

During the reporting period, we sectioned samples of SmCo magnet material, which were obtained from four different vendors, into small blocks weighing about 3 g each. The blocks were encapsulated into small (nonmagnetic) stainless steel containers. We fabricated a simple measurement setup to measure, with a relative uncertainty of less than 0.5%, the magnetic moment of the encapsulated samples. We then exposed the encapsulated samples to four different neutron fluences ranging from 1×10^{16} to 1×10^{19} n/cm^2. Our next step will be to remeasure the magnetic moment for comparison with the preirradiation values.

Laser-Sheet Imaging of High-Explosive-Driven Interfaces

Robert F. Benjamin

Improved understanding of interfacial fluid instabilities is a fundamental issue in fluid dynamics and could have significant impact on science-based stockpile stewardship. Detailed experimental data provide benchmarks for testing our physical understanding and predictive capabilities. This project will supply a benchmark for the shock-driven instability of a liquid layer, which is a process of central importance to applications.

We made progress on identifying liquids with suitable fluid-mechanical and optical properties, and on developing a design for high-explosive experiments. Small-scale, detonator-driven experiments diagnosed by backlighting were used to examine fluid transparency. We observed adequate transparency under shock-loading in several materials. The goal is to find a material for the embedded layer that (1) is initially solid, (2) rapidly becomes liquid when shock-accelerated, and (3) is transparent in the liquid state. Computer simulations of the experiment show feasibility but predict flow patterns slightly different than those observed with a gaseous layer.

A diagnostic challenge is fielding a laser-sheet apparatus at an explosive firing point. We have acquired candidate lasers for multiframe viewing, developed optical systems for laser-sheet illumination, and consulted with university groups about advanced laser-sheet techniques.

Upcoming experiments will provide quantitative data on mix and fluid instabilities in a complex environment typical of real applications. Development of codes that successfully simulate these experiments will lead to validated tools that can be used with confidence for inertial confinement fusion studies, science-based stockpile analyses, and other problems involving complex fluid flows.

Short-Pulse, Electric-Discharge Degradation of Toxic and Sludge Wastes

Louis Rosocha

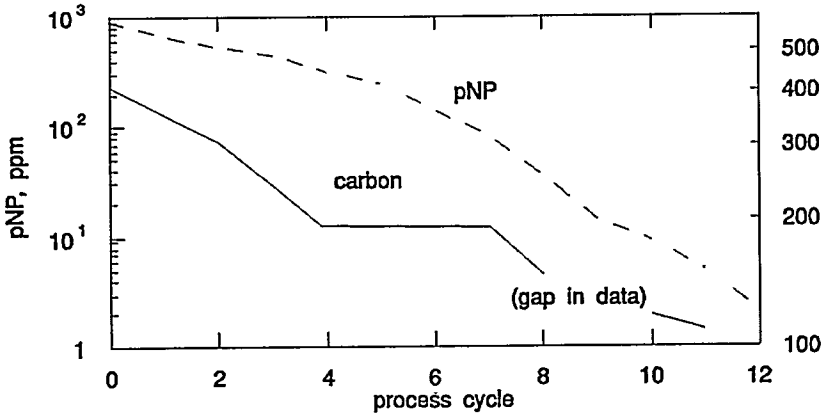
The objective of this project is to break down aqueous pollutants—particularly organics such as chlorinated solvents, bi-phenyls, etc.—to harmless levels of carbon and low-molecular-weight gases. Our approach is to ionize a highly atomized mixture of air and polluted water with a repetitive (10 Hz–1 kHz), short-pulse (10–100 ns), high-voltage (10–50 kV) electrical discharge in order to create highly reactive free radicals, ozone, and UV.

In the first year of the project, we have demonstrated the feasibility of the technique by building a small-scale, engineering-prototype reactor; characterizing reactor operating parameters; and analyzing water processed in the reactor. First-year tasks are nearly complete, and work so far has been successful.

We have determined stable operating parameters for the reactor, including pulse voltage and duration, electrode geometry, droplet size and concentration, and aerosol flow velocity. Under these stable operating conditions, we studied degradation of paranitrophenol (pNP) as a model contaminant for a broad class of industrial pollutants.

When we analyzed treated, aqueous-based pNP with a gas chromatograph/mass spectrometer, we found degradation to a few tenths of a percent of the initial concentration. We solved earlier contamination problems caused by construction materials (i.e., Lucite and polyethylene) by fitting the reactor with Teflon components. Our work so far has demonstrated relatively high efficiency and low specific-energy cost of degradation for pNP. (The specific-energy cost of degradation is the energy required to degrade a unit mass of pollutant.)

We expect subsequent work to focus on optimizing the reactor's electrical circuit efficiency, installing corrosion-resistant materials in the reactor, systematically studying the degradation of several key pollutants with different solubility properties (i.e., hydrophilic, hydrophobic, and volatile), and analyzing the major treatment byproducts.



Concentrations of pNP and carbon vs. sample reprocessing cycles.

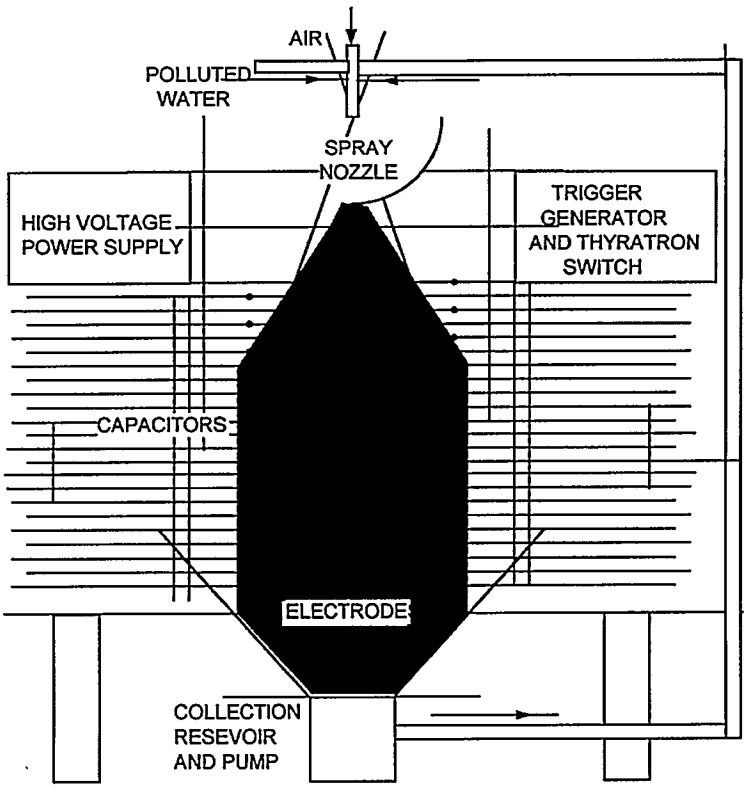


Illustration of the reactor.

Ultrasensitive Sensors for Weak Electromagnetic Fields Using HTS SQUIDs for Biomagnetism, NDE, and Corrosion Currents

Edward R. Flynn

Los Alamos has made important advances in three areas that may significantly impact the development of weak-magnetic-field sensor systems. These advances include (1) improved high-temperature superconducting (HTS) Josephson junctions used in HTS quantum interference devices (SQUIDs), (2) a new superconducting weak-field sensor concept, and (3) the use of digital signal processors (DSPs) in the SQUID control circuit. By integrating these advances into our work, we plan to develop exceptional sensors for measuring weak magnetic fields in harsh electromagnetic environments.

The HTS Josephson junctions demonstrate lower noise at liquid nitrogen temperatures than previously obtained, enabling a wider application of weak-field sensors than previously possible. SQUIDs fabricated with HTS technology are practical for use in the field, such as on-site nondestructive evaluation (NDE), magnetic anomaly detection, and underground structures characterization. DSP technology enables the development of sensor systems with much greater dynamic range, direct digital output, and reduced cost. These are necessary components for the use of SQUIDs in unshielded environments, such as those one would expect in the field.

Patented by Los Alamos, our superconducting imaging-surface sensor design allows new applications for both liquid nitrogen and liquid helium devices. We have built and are currently testing one sensor system based on this design; the system is designed for both biomedical and NDE applications. In addition, we are building a second system, which is in the final stages of fabrication, for biomedical applications. Ultimately, our work will result in the design and testing of weak-electromagnetic-field sensors for a large variety of applications, including nuclear stockpile surveillance as well as programs related to nuclear nonproliferation and detection.

Publications

Kung, P., R. Bracht, P. Lewis, et al., "DSP Control of SQUID" (accepted by *Rev. Sci. Instrum.*).

Van Hulsteyn, D., W. Overton, A. Petscheck, et al., "The Theory of Superconducting Image Surface Gradiometers," *Rev. Sci. Instrum.* 66, 3777 (1995).

Development of Inexpensive Continuous Emission Monitors

David Funk

There is little doubt that combustion is the major cause of poor urban air quality, depletes the ozone layer, and is a major source of carbon dioxide. Furthermore, there is little doubt that global combustion activity is increasing. We are addressing these concerns by researching and developing sensitive, inexpensive, continuous emission monitors based on the optical properties of the expected gas-phase hazardous materials.

To date we have worked on two specific tasks: proof-of-principle experiments for an inexpensive solid state NO_x detector, and proof-of-principle experiments of a solid state Fourier Transform Spectrometer (FTS), which has led to a disclosure and pursuit of a patent. In studying the NO_x detection system, we have designed a simple apparatus to measure combustion sensitivities using conventional laser technology. Preliminary experiments indicate high sensitivity and we are in the process of quantifying these results. Our solid-state FTS studies were conducted by (1) using a broad band light source, (2) dispersing the radiation, (3) modulating four bands of light at four different frequencies, (4) recombining the light, and (5) recording the time output in single shot mode. We then Fourier transformed the data and observed the four frequency peaks corresponding to the four bands.

We expect that these types of sensors will assist in direct feedback of turbine power systems and provide assurance to the public and the operators of facilities that their facility emissions lie within accepted bounds.

Plasmas, Fluids, and Particle Beams

Generation and Compression of a Target Plasma for Magnetized Target Fusion

Ronald Kirkpatrick

Magnetized target fusion (MTF), in which a magnetothermally insulated plasma is hydrodynamically compressed to fusion conditions, is an approach to controlled fusion which avoids the difficulties of traditional inertial or magnetic confinement. MTF may be an inexpensive and unique source of high-energy-density plasmas, which are of interest to defense-related and energy research at Los Alamos. In this project, we are designing experiments and using computer models to demonstrate the key principles of MTF to address issues of importance to science-based stockpile stewardship.

We have examined plasma configurations such as Z-pinches and spheromaks for their application to MTF and evaluated Los Alamos facilities which may be used for MTF experiments. We also began design calculations (including two-dimensional computational modeling) of a solid-deuterium-initiated Z-pinch-target-plasma experiment utilizing the Colt capacitor bank. Results to date show promise that such an experiment could produce the necessary conditions (density, temperature, and magnetic field) for an MTF target plasma.

We are continuing theoretical and computational investigations of important aspects of MTF, such as magnetically enhancing the energy deposition of alpha particles produced by deuterium-tritium (D-T) fusion, developing capabilities to simulate diagnostics for MTF experiments, and modeling the compression of target plasmas by imploding liners. We have presented our MTF studies and concepts in numerous meetings and briefings and in some publications.

Publications

Kirkpatrick, R.C., I.R. Lindemuth, and M.S. Ward, "Magnetized Target Fusion—An Overview," *Fusion Technol.* 27, 201 (1995).

Lindemuth, I.R., R.E. Reinovsky, R.E. Chrein, et al., "Target Plasma Formation for Magnetic Compression/Magnetized Target Fusion," *Phys. Rev. Lett.* 75, 1953 (1995).

Sheehey, P., "Magnetized Target Fusion," *The World & I* 10, 192 (1995).

Development of Ion-Beam Techniques for the Study of Special-Nuclear-Materials-Related Problems

Carl Maggiore

The purpose of our project is to develop the ion-beam-related techniques for characterizing the surfaces and near surfaces of special nuclear material and the materials with which they come in contact. Our project directly addresses the problems of both characterizing of actinides and their effects on other materials. We will use the alpha-particle-simulation beams at the Ion Beam Materials Laboratory (IBML) at Los Alamos to accelerate the aging of materials in contact with actinides.

We have shown that the accelerator of the IBML can simulate the energy range and dose distribution of the alpha radiation from solid actinide material in contact with another material. We have also undertaken initial experiments that demonstrate our ability to measure the radiolytic activity of plutonium by monitoring the residual gases produced during irradiation.

We have successfully transported plutonium-contaminated samples to the IBML and measured the absolute surface contamination using alpha and heavy-ion backscattering. At the extreme lower limits of measurable contamination (less than one thousandth of a monolayer), we have found that traditional alpha backscattering is not applicable to realistic substrate materials because of background effects. A real, non-ideal substrate of stainless steel contains heavy-element contamination at the several-ppm level and the resulting background limits sensitivity. We have

extended the use of heavy-ion backscattering using 5-MeV beams of ^{60}Ni to measure the surface contamination of plutonium on real stainless steel substrates at the required lower limits of contamination. In our attempts to measure the depth distribution at the lowest levels of contamination we have determined the limitations of traditional solid-state detectors for this problem.

We have also demonstrated the application of the low-energy nuclear techniques of elastic recoil detection in weapons-component hydrogen and helium isotopes. The distribution of deuterium, tritium, ^{3}He, and ^{4}He is critical to the long-term stability of weapons. Direct measurement of hydride isotope loading in critical components has the potential for enhanced scientifically based certification of replacement components.

Advanced Modeling of High-Intensity Accelerators

Robert Ryne

Accelerator-driven schemes have been proposed to solve several problems of national importance: waste transmutation, plutonium conversion, tritium production, and others. However, present computer simulations cannot accurately predict certain phenomena that occur in accelerators, such as beam halo and beam loss. Our goal is to develop simulations that can accurately model these phenomena.

We have had many successes in FY95 using new algorithms and hardware that have advanced the state-of-the-art in accelerator simulation. For example, we have developed two-dimensional (2-D) particle simulations on the CM-5 massively parallel computer and routinely run them with 1 million to 10 million particles. Previous simulations were typically run with 10 thousand particles; we have increased the number of simulated particles by 2–3 orders of magnitude.

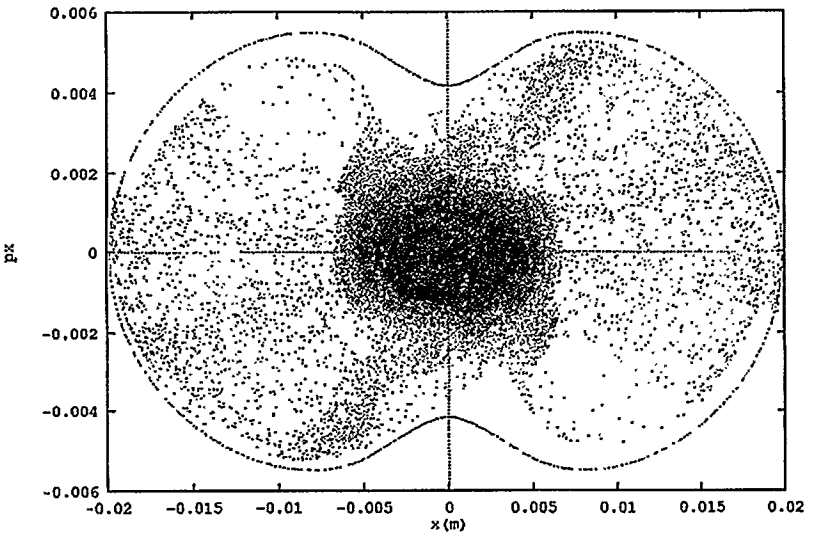
One of our major accomplishments was to test the validity of the widely used particle-core model. Our simulations showed that this model accurately predicts the maximum halo radius in constant focusing channels. Also, we settled the controversial issue of whether or not beam-envelope oscillations in matched beams in quadrupole channels can cause significant halo formation: Using analysis and numerical modeling, we showed that, in the physics regime of the above-mentioned projects, envelope oscillations in matched beams do not cause halo formation.

We also studied the importance of chaos in the particle-core model, and we developed a completely new way to compute the Lyapunov exponents in the Hamiltonian systems that we applied to this model. Finally, we have developed a preliminary version of a three-dimensional code for simulation studies on the CM-5, and we are starting to study the effects of noise using a 2-D Langevin code. In summary, we are developing advanced mathematical and computer models to simulate beam-dynamics and space-charge effects in accelerators and storage rings.

Publications

Habib, S., and R. Ryne, "Symplectic Calculation of Lyapunov Exponents," *Phys. Rev. Lett.* **74**, 70 (1995).

Ryne, R., and T. Wangler, "Recent Results in Analysis and Simulation of Beam Halo," in *AIP Conference Proceedings 346, International Conference on Accelerator-Driven Transmutation Technologies and Applications, Las Vegas, Nevada*, E. Authur, A. Rodriguez, and S. Schriber, Eds. (American Institute of Physics, Woodbury, New York, 1994), p. 383.



Beam phase space from a simulation with two million particles performed on the CM-5 massively parallel computer. The outer peanut-shaped set of points; obtained independently using the particle-core model, shows that the maximum halo extent predicted by the model is in excellent agreement with high-resolution numerical simulations.

BINDING CARBON DIOXIDE IN MINERAL FORM: A CRITICAL STEP TOWARD A ZERO-EMISSION COAL POWER PLANT

Klaus Lackner

Fossil fuels are a large and well-established energy resource—coal reserves will last for centuries. However, if fossil fuels are to remain in use as an important energy source, the effects of their CO_2 emissions on the climate must be eliminated. Our goal is to develop an economical process that binds CO_2 into environmentally safe, solid waste products. Such a process would remove the most difficult obstacle on the path to reduced CO_2 emissions—clean power generation from coal—and would reduce the greenhouse effect.

We are developing chemical technology to bind carbon dioxide to calcium- and magnesium-bearing minerals. We demonstrated the necessary fundamental processes experimentally and showed that the required minerals are available. We also developed and tested a first processing chain to form carbonates from readily available mineral rock. An important step in this process is direct carbonation of magnesium hydroxide at high temperature; this has been done only at Los Alamos. We have concluded from comparisons with industrial practices that this first process is economically viable.

From the standpoints of a national energy strategy, the preservation of the global environment, and national security, the long-term benefit of a zero-emission power plant is clear: the United States will be assured of energy self-sufficiency for centuries without the danger of global warming. When we consider the large coal reserves in developing countries, notably in China, this technology will also improve America's competitive position in a growing international energy market without introducing the dangers of nuclear proliferation.

Publications

Butt, D.P., K.S. Lackner, C.H. Wendt, et al., "Kinetics of Thermal Dehydroxylation and Carbonation of Magnesium Hydroxide" (submitted to *J. Am. Ceram. Soc.*).

Lackner, K.S., C.H. Wendt, D.P. Butt, et al., "Carbon Dioxide Disposal in Carbonate Minerals," *Energy—Int. J.* **20**, 1153 (1995).

FOREIGN NUCLEAR TEST RADIOCHEMICAL DIAGNOSTICS

Michael Macinnes

During the time of atmospheric nuclear testing, the United States maintained the capability to analyze materials released by the detonation of nuclear devices. As a result of the lack of recent atmospheric testing, new personnel have not been trained in the interpretive skills necessary for evaluating nuclear technology. The objective of this project is to train individuals and document our analytical methods before such capabilities are lost.

Expertise in the evaluation of atmospheric nuclear test data is best gained through manipulations of actual radiochemical data. We are focusing our efforts this year on a survey of early tests of nuclear weapons states.

During the reporting period, we brought two computer codes used to evaluate atmospheric tests back on-line, and we trained three analysts to use these and other evaluation tools on several nuclear tests. In the process, we uncovered significant findings that we will present at an upcoming laboratory conference.

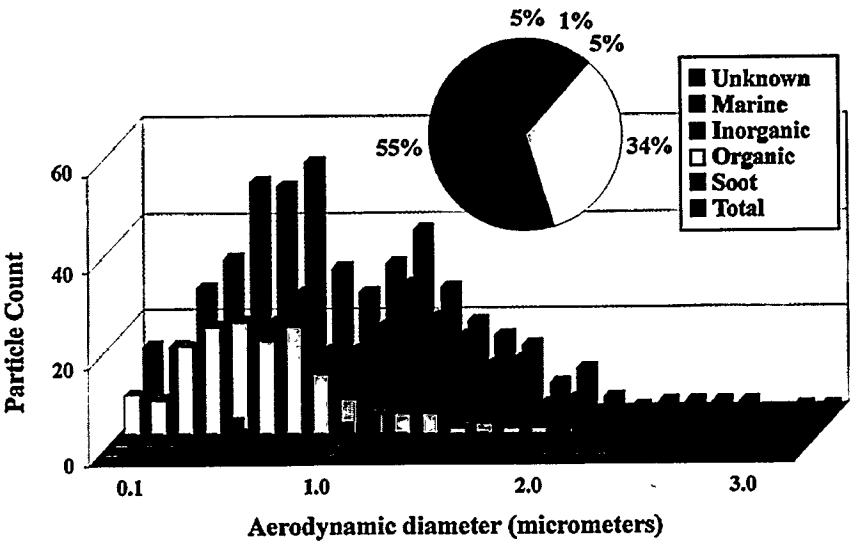
Maintaining this analytical capability is paramount to national security interests and will prove invaluable in times of crisis, such as that which may exist following the detonation of a terrorist or proliferant nuclear device.

The Characterization of Atmospheric Aerosols: Applications to Heterogeneous Gas-Particle Reactions

Jeanne M. Robinson, Los Alamos National Laboratory
Kimberly A. Prather, Univ. of California, Riverside

To identify the emission sources of atmospheric aerosol pollutants requires measurement of the aerosols' size and chemical composition. During the past year, we used the aerosol time-of-flight mass spectrometry technique developed at the University of California, Riverside, to monitor atmospheric aerosol particles in real time. We obtained size and composition profiles that show distinct correlations between particle size and composition, enabling us to distinguish between types of aerosols. Data from a typical sampling are shown in the accompanying bar graph.

We also investigated the thermodynamics of model polar stratospheric aerosols. We measured the adsorption of HCl onto water ice films in the laboratory under conditions simulating those of the stratosphere. We measured the partial pressure of HCl vapor with mass spectrometry, and we measured surface coverage during the quantitative introduction of HCl onto the ice surface with nonlinear light scattering. By simultaneously observing the total amount of HCl on the surface and the surface coverage, we obtained constants which parameterize HCl adsorption as a function of temperature and pressure via the Langmuir and the Brunauer, Emmett, and Teller (BET) theories. These constants agree with values in the literature. The accompanying adsorption spectra for HCl on ice show inflections that correlate with changes in the phase of the HCL/water ice interface.

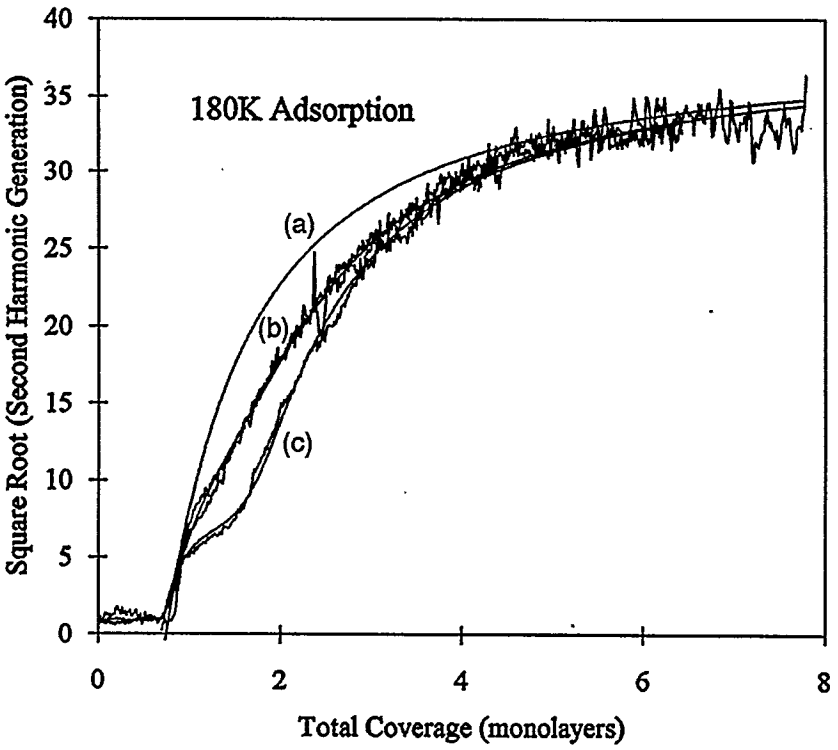


Particle size distribution as a function of composition sampled from 7:45 a.m. through 10:15 a.m. on May 1, 1995. These data are typical of aerosol emissions at Riverside during the morning hours.

Publications

Salt, K., C. Noble, and K.A. Prather, "Aerodynamic Particle Sizing Versus Light Scattering Intensity Measurement as Methods for Particle Sizing Coupled with a TOF Mass Spectrometer" (to be published in *Anal. Chem.*).

Noble, C. and K.A. Prather, "Real Time Size and Composition Profiles of Ambient Aerosol Particle Samples in Riverside, CA, in Spring 1995" (submitted to *Environ. Sci. Tech.*).



Adsorption spectra for HCl on H_2O ice. Three identical spectra are shown for adsorption at 180 K monitored by second harmonic generation. Curve (a) is a model calculation based on multilayer adsorption governed by the BET theory. Curve (b) is a model calculation based on a modification of the BET theory including molecular interaction between adsorbate molecules governed by the Bragg-Williams theory; the curve is a fit to two superimposed spectra. Curve (c) is the same model calculation fit to one spectrum. The differences in the data of (b) and (c) may result from ice substrate heterogeneity modifying the number of average neighbors next to an adsorbed molecule. The region of no signal up to 0.7 monolayers may reflect the adsorption of a liquid phase into small pores in the ice substrate. The adsorption energies determined from the spectra are consistent with literature values.

Detection of Arsenic by Resonance Ionization Mass Spectrometry

Nicholas Nogar

Development of sensitive analytical techniques for environmental analysis is of immediate interest to both Los Alamos and DOE. Waste residues containing heavy metals such as chromium, lead, and arsenic are particular problems because of their widespread presence and sometimes incomplete recovery or inadequate storage. The objective of this project is to apply resonant laser ablation (RLA) to detect trace levels of arsenic. Detection of arsenic in environmental matrices is important because of the toxicity of arsenic compounds and their widespread presence in all phases of the ecosystem—soil, water, and air. Commercial production and use of inorganic and organic arsenic compounds have raised local concentrations of this element well above natural backgrounds levels, particularly in soil and ground water.

Common methods for detecting arsenic generally require extensive extraction, separation, derivatization, and preconcentration steps before actual analysis. RLA offers the possibility of reducing sample pretreatment because of its selectivity and sensitivity. It is also particularly well-suited to the analysis of heavy metals in a variety of samples. The use of selective laser ionization greatly reduces background or interfering signals and allows more accurate measurement with minimal sample preparation. Our major research effort is directed towards demonstration of RLA for heavy-metal analysis. Further work will determine the technique's sensitivity and applicability to environmental samples.

We initially implemented RLA for detecting arsenic in multilayer GaAs/AlGaAs samples. Arsenic could easily be detected in this work but was difficult to quantify. To better quantify and understand the process, we explored a simpler system: single-crystal silicon wafers overcoated with 20 Å of copper. We had previously demonstrated the facile detection of copper via a "2+1" (photons to resonance plus photons to ionize) resonance ionization process. Initial results showed the detection of both silicon and copper when the sample was irradiated with low-energy laser pulses tuned to the two-photon copper resonance at 465 nm. We observed both the resonant copper transition as well as nonresonant contributions from silicon, sodium, and potassium.

Publications

Eiden, G.C., and N.S. Nogar, "The Two-Photon Spectrum of Iron and Silicon Detected by Resonant Laser Ablation," *Chem. Phys. Lett.* **226**, 509 (1994).

Eiden, G.C., J.E. Anderson, and N.S. Nogar, "Resonant Laser Ablation: Semiquantitative Aspects and Threshold Effects," *Microchem. J.* **50**, 289 (1994).

Allen, T.M., P.B. Kelly, J.E. Anderson, et al., "Depth Profiling of Copper Thin Films Resonant Laser Ablation," *Appl. Phys. A* **61**, 221 (1995).

Allen, T.M., C.H. Smith, P.B. Kelly, et al., "Analysis of Surfaces, Films and Multilayers by Resonant Laser Ablation," *Proc. SPIE LASE '95, Advanced Optical Methods for Ultrasensitive Detection* **2385**, 39 (1995).

Kinetic Studies of Competitive Adsorption Processes Related to Automobile Catalytic Converters

Mark Paffett

To design better catalytic converters for automobiles, we are determining sticking coefficients and reaction probabilities for CO, NO, and O_2 on platinum, palladium, and rhodium surfaces as a function of surface coverages under conditions resembling those encountered in real catalytic systems. Unique to our research is the fact that we measure sticking coefficients in situations emulating competitive adsorption, either by studying the adsorption of a given gas on a surface partially or totally covered with another type of molecule or by performing reaction probability experiments with mixtures of two or more gases. These measurements are of interest because they will provide important values for systems that closely mimic catalytic converters under operational conditions.

We have examined the effect of local surface arrangements on the reactivity of adsorbed species for the oxidation of carbon monoxide on Pt(111) surfaces. We measured the kinetics of that reaction by using a dynamic method originally devised at Oxford University, and we characterized the adsorption geometry of the reactant by reflection-absorption infrared spectroscopy. Our findings showed that the presence of preadsorbed atomic oxygen on the surface does not significantly affect the initial sticking coefficient of CO, but that it does reduce the saturation coverage of that coefficient by preferentially blocking the bridge sites.

No reaction takes place below 300 K, but above 400 K, CO_2 desorption from oxygen-precovered surfaces is controlled by the impinging frequency of the incoming CO. On clean surfaces, the oxidation rate is equally determined by the CO incoming flux as long as the $CO:O_2$ ratio in the $CO+O_2$ mixed beams is low. For high $CO:O_2$ ratios, however, the CO steady-state coverage increases, poisoning the adsorption of oxygen and slowing down the overall CO_2 production. However, the most interesting temperature range is from 300 to 400 K, where the rate of surface recombination of CO with oxygen competes with that of CO adsorption; under those conditions, not all the surface oxygen is reactive, and the overall dynamic behavior becomes fairly complex. The behavior observed in that regime suggests that the reactivity of the adsorbed oxygen depends on the local coverage of neighboring sites. We believe that such local arrangements modify the adsorption energy for atomic oxygen and that the modification of adsorption energy, in turn, changes the activation energy for the oxidation reaction.

Publications

Liu, J. , M. Xu, T. Nordmeyer, et al., "Sticking Probabilities for CO Adsorption on Pt(111) Surfaces Revisited," *J. Phys. Chem.* **99**, 6167 (1995).

Investigations of Biomimetic Light-Energy-Harvesting Pigments

Robert Donohoe, Los Alamos National Laboratory
David F. Bocian, Univ. of California, Riverside

Natural light-harvesting proteins include numerous chromophores, such as chlorophyll, that absorb and transduce solar energy. The purpose of our research is to identify the critical structural features that control the energy and electron transfer processes in synthetic light-harvesting pigments. The systems we are investigating, which we refer to as arrays due to the numerous chromophores that can be linked together, incorporate ethyne-modified phenyl bridging groups between multiple porphyrin chromophores. The porphyrins serve as synthetic analogues of the chlorophyll pigments found in plants and bacteria. This structure permits indirect electronic pathways for energy and electron transfer between the chromophores. (Direct, through-space, communication between the pigments is known to be limited.) The phenyl bridging groups can be modified to include substituents that influence the degree of communication between the bridge and the porphyrins and, hence, between the individual porphyrins.

We are focusing on the influences of these structural alterations on the electrochemistry, vibrational spectroscopy, and electron paramagnetic resonance (EPR) of the neutral and oxidized arrays. These measurements reveal the driving force for electron or hole transfer (from the reduction/oxidation potentials from the electrochemistry), the influence of changes in the bridge structure on the electronic and nuclear structure of the porphyrins (from the energies and intensities of the vibrational peaks), and the rates of hole or electron hopping between chromophores (from linewidth studies of the EPR spectra), respectively. In general, these methods will teach us how structural changes in the arrays influence the degree of communication between the porphyrin chromophores in the arrays.

We have conducted systematic studies of a variety of arrays, including the examination of data derived from five-, three-, and two-pigment arrays. We used both zinc and free-base porphyrins to vary the electronic structure of the arrays, and we sterically substituted bridging groups that hindered the communication between the porphyrins and bridging groups. Our data reveal that the ground- and excited-state structures of these arrays are strongly influenced by the presence of steric substituents. By examining the temperature dependence of the EPR linewidths, we observed the rates of hole hopping between pigments and determined that this process takes place with a rate of roughly 10^7 Hz. We also examined the effects of creating linear and right-angle arrays on the hole hopping process.

Mathematics and Computational Sciences

The Continued Benchmarking of Ocean Circulation Models

David Poling

The earth's oceans are the driving forces of its atmosphere and shape the global climate. Before we can answer any questions about change to the environment, we must have a better understanding of the oceans. Since the early 1950s, we have understood the mechanisms that form the prevalent ocean surface currents. However, we are only beginning to understand the deep ocean currents—either experimentally or theoretically. Simple analytic models are very limited in their applicability to deep oceans because of the profound effects of seafloor topology. In the early 1960s, to overcome this deficit, researchers began to develop numerical simulation codes to model global ocean circulation.

The objectives of our project are to perform a series of numerical experiments using the existing ocean circulation models, benchmark those models against empirical data and analytical solutions which are now available, and use the results of these experiments to improve the numerical treatment of ocean dynamics. We intend to become proficient at both developing ocean- and climate-related simulation codes and analyzing the simulation results. We intend to use this proficiency to follow the migration of simulation to massively parallel simulation machines.

We completed a 100-year simulation that used an unforced, coupled ocean and atmosphere model. In the implementation plan for the upcoming Baltic Sea experiment this simulation was referred to as representative of the state of the art. We have amassed a huge amount of data from this simulation and are now in the process of analyzing it. We are examining the data to see if it confirms the two theories proposed during the central equitorial Pacific experiment—the thermostat hypothesis and the super-greenhouse effect.

We are also in the process of running a set of shorter simulations with slightly varying initial conditions. This has not been done before and should provide valuable information about the ability of this type of simulation to predict accurate results. The work performed on this project has applications to basic geological or soil studies, basic atmospheric studies, and basic studies of aquatic systems.

Applications of Mathematical Analysis of Nonlinear Physical Systems

Hans Frauenfelder

This project supported a wide variety of activities related to developing and applying mathematical methods for nonlinear physical systems.

In particular, we developed new techniques to analyze heat transport in turbulent fluid flows by formulating a variational principle which determines limits on heat transport. We derived this variational principle from the fundamental equations of motion without introducing any further assumptions; this principle produces bounds that are free from the kind of uncontrolled approximations so often implemented in turbulence modeling.

A major focus of this project was to organize a workshop on Mathematical Problems in Industry which brought students, postdocs, and researchers together with industrial representatives who presented real challenges to the applied and computational mathematics communities. Specific problems presented and studied in the workshop included optics (determining the index of refraction from refracted or diffracted rays), fluid and solid mechanics (cleaning filters with gas jets, gas release from waste tanks, cracks in welds), and applied mathematics (Monte Carlo analysis of oil-well data, uncertainty analysis of flow models for porous media).

Publications

Blumenfeld, R., "Morphology of Laplacian Growth Processes and Statistics of Equivalent Many-Body Systems," in *Nonlinear Evolution Equations & Dynamical Systems*, V. Makhankov, A. Bishop, and D. Holm, Eds. (World Scientific, River Edge, New Jersey, 1995), p. 266.

Blumenfeld, R., "Voids-Limited Propagation of Fracture: Steady State and Velocity Oscillations" (submitted to *Phys. Rev. Lett.*).

Bulsara, A., T.C. Elston, C.R. Doering, et al., "Cooperative Behavior in Periodically Driven Noisy Integrate-Fire Models of Neuronal Dynamics" (submitted to *J. Comp. Neuroscience*).

Christian, E., A. Hagberg, and E. Meron, "Dynamic Front Transitions and Spiral-Vortex Nucleation," *Phys. Rev. E.* **51**, 3052 (1995).

Doering, C.R., and P. Constantin, "Variational Bounds on Energy Dissipation in Incompressible Flows: III. Convection" (submitted to *Phys. Rev. E*).

Farengo, R., and J.R. Sobehart, "Self-Consistent Minimum Dissipation States in Magnetized Plasmas" (submitted to *Phys. Rev. Lett*).

Gabitov, I., D.D. Holm, B. Luce, et al., "Recovery of Solitons with Nonlinear Amplifying Loop Mirrors in High Dispersion Fiber Transmission Systems" (submitted to *Opt. Lett.*).

Gabitov, I., F. Kuppers, A. Mattheus, et al., "Average Pulse Dynamics in Cascaded Passive Fiber Compensated Transmission System" (submitted to *Opt. Lett.*).

Gjaja, I., "Computation of Lie Transformations from a Power Series: Bounds and Optimum Truncation" (submitted to *J. Math. Phys.*).

Millonas, M.M., and C. Ray, "Relaxation Kinetics of Nonlinear Systems Coupled to a Nonequilibrium Bath," *Phys. Rev. Lett.* **75**, 1110 (1995).

Montgomery, D., and X. Shan, "Microscopic Origins and Macroscopic Uses of Plasma Rotation" (to be published in *J. Plasma Phys.*).

Sobehart, J., "Modeling the Laser Ablation of Multilayer Polymer Films for Advanced Manufacturing Applications" (to be published in *Jpn. J. Appl. Phys.*).

Zhang, S., J. Carlson, and J. Gubernatis, "A Constrained Path Quantum Monte Carlo Method for Fermion Ground States," *Phys. Rev. Lett.* **74**, 3652 (1995).

Mesoscale Ocean Dynamics Modelling

Darryl Holm

The purpose of this project has been to coordinate, strengthen, and focus the efforts of applied mathematicians, computer scientists, computational physicists, and engineers at Los Alamos and a consortium of universities in a joint effort in mesoscale ocean dynamics by enabling research in this subject for visitors, graduate students, postdoctoral fellows, and workshops. This project has combined the core competencies of high-performance computing and complex-systems theory in a new way that has significant potential for improving ocean models now running on the CM-200, CM-5, and Cray T3D in Los Alamos' Advanced Computing Laboratory.

The ocean responds to forcing agents on a much longer time scale than the atmosphere does (essentially because of the much higher density and specific heat of water relative to air). Consequently, ocean dynamics is responsible for much of the long-time driving of the atmosphere. The importance of the ocean in climate is already evident at relatively short time scales, such as occur in El Nino, a well-known oceanic event which produces strong climate effects over large areas of the Western Hemisphere. Thus, a thorough understanding of ocean dynamics is crucial for investigating long-term climate phenomena like global warming.

The ocean is a very complex nonlinear system that is turbulent on essentially all scales, exhibits multiple equilibria, and has intrinsic variability on time scales ranging from years to thousands of years. The ocean exhibits a correspondingly wide range of spatial scales; many of these are unresolved in global modeling of ocean dynamics with supercomputers. Measurements show that much of the ocean's kinetic energy resides in scales of 20 km or less, in mesoscale eddies at a scale referred to by ocean modelers as the "Rossby deformation radius." The current state of supercomputer speeds and memories at Los Alamos allow us to compute global circulation of the ocean on meshes with horizontal dimensions of about 15 km over time intervals of about 30 simulated years. However, integrations for much longer climatic times—a millienium, say—will require much coarser spatial resolution. Thus, in com-

putational ocean modeling relevant to climatic timescales the effects of the ocean's energy at smaller scales on its dynamics at mesoscales and larger must be parameterized, say by using multiscale analysis. It is difficult to foresee all the relevant phenomena that can occur in mesoscale ocean dynamics, much less to understand their relative importance, without a solid mathematical analysis of the underlying equations. The objective of the analysis is to obtain a full understanding of the nonlinear phenomena contained in the ocean-dynamics equations at the most fundamental mathematical level consistent with the numerical modeling. We can then use this understanding to spark new approaches to solving practical engineering and scientific problems, design more effective computer simulations, and suggest new directions for experimental investigations and measurements.

The overall rationale of this project is to help develop effective mathematical and computational tools for analyzing the nonlinear behavior that appears in mesoscale ocean dynamics within the framework of the Laboratory's unique and special connections with the world community in nonlinear science. The primary emphasis of our project is on the development of a combined analytical and numerical understanding that complements and supports the development and interpretation of ongoing experimental and computational efforts both at the Laboratory and in the academic community. Thus, our rationale is to help coordinate a nonlinear-science framework for investigating mesoscale ocean-dynamic flows in strong scientific collaboration with the external nonlinear-science and oceanographic community.

This research combines two core competencies in a new way. These are high-performance computing and complex-systems theory. The combined effects of nonlinearity, stratification, dispersion, rotation, topographical and boundary forcing, and turbulence determine the ocean's dynamics. This is a major open problem with many potentially important applications and potential implications for national and global needs. Our approach established a framework for investigating ocean-dynamic flows from the viewpoint of nonlinear science and dynamic-systems methods and an external collaboration network for developing the applications of this understanding further. Moreover, we are working within the computational-science environment of the Laboratory as well as attracting collaborators from the national ocean-modeling community.

An important component of this project was a regular series of workshops on topics related to computational issues and dynamic theories of mesoscale ocean modeling. The principal purpose of these workshops was to assemble teams of researchers for extended periods to work on the Global Ocean Modeling project. This is necessary because some of the researchers on this project, while close together on scientific issues, are widely scattered geographically. Over its three-year duration, this project held three workshops each year, one on the subject of predictability in ocean modeling, one on asymptotic behavior of nonlinear shallow-water equations and one on modeling turbulent flows. In addition, we had an active visitor program that brought scores of researchers to Los Alamos for intensive, focused discussions of nonlinear science in ocean modeling. The workshops included specialized lectures and seminars given by guest scientists from the ocean modeling, climate modeling and weather prediction communities. Specific topics for the workshops included

- "Foundations of Balanced Dynamics for Mesoscale Ocean Modeling,"
- "Geostrophic Turbulence,"
- "Approximate Inertial Manifolds for Finite Difference Methods," and
- "Applications of Proper Orthogonal Decomposition."

As for research contributions, we have derived new equations describing the time-asymptotic effects of the nonlinear dispersion present due to hydrostatic pressure imbalance in the vertically averaged Euler equations for shallow, free-surface, incompressible hydrodynamics. For this, we used multiple-time-scale asymptotic expansions that included full topography and boundary information. During this work we developed a new method of "Hamiltonian asymptotics." This new method produces approximate descriptions of fluid dynamics that retain the Hamiltonian properties of the exact original system at each order in the asymptotic expansion. (This implies that the approximate equations conserve energy and potential vorticity at each order.) We also have obtained approximate descriptions of fluid dynamics at two successive orders in an asymptotic expansion in the small-aspect ratio of the flow that retain the Hamiltonian properties of the original system at both levels of approximation. The conservation laws implied by the Hamiltonian nature of these equations at each order in the expansion led to an analytical estimate of the rate at which the solution at higher order diverges from the leading-order solution due to nonlinear dispersion, thus

establishing the relative accuracy of the lower-order solution. Application of the method of Hamiltonian asymptotics continued to produce new scientific results as we derived new Hamiltonian balance equations and new equations for wave, mean flow interaction dynamics between internal waves, and mean ocean currents.

In summary, the ocean's dynamics are determined by the combined effects of nonlinearity, stratification, dispersion, rotation, topographical and boundary forcing, and turbulence. This is a major open problem, with many potentially important applications and potential implications for national and global needs. Our approach established a framework for investigating ocean-dynamic flows from the viewpoint of nonlinear science and dynamic-systems methods and an external collaboration network for developing the applications of this understanding further. We are working within the computational-science environment of the Laboratory as well as attracting collaborators from the national ocean-modeling community.

Publications

Alber, M., R. Camassa, D. Holm, et al., "The Geometry of Peaked Solitons and Billiard Solutions of a Class of Integrable PDE's," *Lett. Math. Phys.* **32,** 137 (1994).

Alber, M., R. Camassa, D. Holm, et al., "On the link between Umbilic Geodesics and Soliton Solutions of Nonlinear PDEs," *Proc. Roy. Soc.* **450,** 677 (1995).

Allen, J.S., and D. Holm, "Hamilton's Principle for Shallow Water Models with Height as the Independent Variable" (submitted to *Physica D*).

Camassa, R., D. Holm, and D. Levermore, "Long-Time Dispersive Equations for Shallow Water with a Varying Bottom" (submitted to *Physica D*).

Choi, W.Y., "Nonlinear Evolution Equations for Two-Dimensional Surface Waves in a Fluid of Finite Depth," *J. Fluid Mech.* **295,** 381 (1995).

Choi, W.Y., and Camassa, R., "Weakly Nonlinear Internal Waves in a Two-Fluid System" (submitted to *J. Fluid Mech.*)

Gjaja, I., and D. Holm, "Self-Consistent Wave-Mean Flow Interaction Dynamics and Its Hamiltonian Formulation for a Rotating Statified Incompressible Fluid" (submitted to *Physica D*).

Holm, D., "Hamiltonian Balance Equations" (submitted to *Physica D*).

Holm, D., "The Ideal Craik-Leibovich Equations" (submitted to *Physica D*).

Holm, D., B. Nadiga, and L. Margolin, "Nonhydrostatic Effects in Long Term Shallow Fluid Flow" (submitted to *Physica D*).

Jones, D., and E. Titi, "Approximations of Inertial Manifolds for Dissipative Nonlinear Equations" (to be published in J. *Differential Equations*).

Jones, D., A. Poje, and L. Margolin, "Enslaved Finite Difference Schemes for Nonlinear Dissipative" (to be published in *Numerical Methods for PDE's*).

Jones, D., E. Titi, and B. Cockburn, "Determining Degrees of Freedom for Nonlinear Dissipative Equations," *C. R. Acad. Sci.* **321,** 563 (1995).

Jones, D., E. Titi, and B. Cockburn, "Estimating the Number of Asymptotic Degrees of Freedom for Noninear Dissipative Systems" (submitted to *Math. Comput.*).

Nadiga, B., "An Adaptive Discrete Velocity Model for the Shallow Water Equations," *J. Comput. Phys.* **121,** 271 (1995).

Nadiga, B., L. Margolin, and P. Smolarkiewicz, "Different Approximations of the Shallow Fluid Flow over an Obstacle" (submitted to *Phys. Fluids.*).

Nadiga, B., L. Margolin, and P. Smolarkiewicz, "Semi-Lagrangian Shallow Water Modeling on the CM-5" (submitted to *J. Ocean and Atmos. Tech.*).

Lie Group Applications to the Solution of Differential Equations

Charles Cranfill

This project deals with finding solutions to partial differential equations describing physical systems important to the Laboratory's scientific mission. There are two basic approaches: analytic and numerical. The first approach looks for special analytic or semi-analytic solutions by reducing the partial differential equations (PDEs) to ordinary differential equations (ODEs). These ODEs are much easier to solve and can often be solved completely analytically. The resulting solutions can then be transformed back to the original space to obtain special solutions to the original PDEs. These particular solutions can then be used for (1) numerical benchmarks, (2) the basis for physical models, and (3) special solutions for particular initial/boundary conditions.

The second use of this technique is the construction of "better"

finite-difference numerical algorithms for PDEs. Differential equations of mathematical physics have certain symmetry properties (such as rotation, translation, scale invariance, etc.). Generally, the associated finite-difference algorithms do not possess the same symmetries as the original PDEs and errors are therefore more pronounced. We are attempting to systematically construct difference schemes that possess the same symmetries as the original PDEs, and preliminary results show that this technique is useful for reducing numerical error.

During the past year we focused on (1) group-invariant solutions to the PDEs describing the interpenetration of two fluids and (2) group-invariant finite-difference representations of the PDEs describing fluid dynamics. We analyzed ODEs derived from applying a self-similar transformation to the PDEs that describe a simple two-fluid system. Numerical integration of the ODEs showed that the solutions are extremely sensitive to small changes in initial conditions. Further study led to the realization that the original PDEs are ill-posed and unstable, so research is now centered on adding appropriate dissipation terms to stabilize the PDEs. The Lie Group analysis will then be repeated to produce a new set of ODEs whose solutions should be sufficiently well-behaved to serve as important benchmarks for numerical mix models used in Laboratory computer programs.

We also continued analyzing several finite-difference representations of the one-dimensional advection equation constructed to possess a subset of the group-invariances exhibited by the continuous PDE. We developed an apparently new technique for reversing this procedure to determine the group-invariance properties of finite-difference equations directly. This technique may prove useful for analyzing the advection algorithms in Laboratory computer codes.

Publications

Coggeshall, S.V., "Group-Invariant Solutions of Hydrodynamics," in *Computational Fluid Dynamics*, D. Luetloff and R.C. Srivastava, Eds. (Springer-Verlag, Berlin, Germany, 1995), p. 71–102.

Adaptive Mesh Refinement Algorithm Development and Dissemination

Jeffrey Saltzman

We are developing and disseminating adaptive mesh refinement (AMR) algorithms for structured meshes. AMR is a process in which refined mesh patches are added or deleted in a hierarchical fashion to more efficiently resolve finite-difference approximations. Application of AMR to uniform computations results in great savings in processing time and memory. Our development of AMR algorithms is proceeding in several directions, including algorithms for parallel architectures, techniques for the solution of partial differential equations on adaptive meshes, mesh generation, and algorithms for nontraditional or generic applications of AMR.

Dissemination of AMR algorithms to computational scientists currently using finite-difference or finite-volume methods on logically rectangular grids is also a goal of our work. AMR algorithms are perceived as difficult to meld to current algorithms. Through our development of easy-to-use interfaces to AMR algorithms, we hope to change this perception.

Our research into the application of the AMR technology on parallel architectures is of particular significance because it leads to one of the most important problems in parallel computing on mesh-based algorithms. This problem can be described as load balancing versus interprocessor communication for dynamic mesh algorithms. For structured meshes, this problem is particularly severe because the introduction of AMR implies having to minimize these two competing effects.

During the past year, we continued to work on optimizing the three-dimensional (3-D) AMR code running on the Thinking Machines CM-5. With the current status of Thinking Machines in some doubt, we have begun working in two new directions. The first direction is to move the 3-D code into a more portable environment. The second direction is to intensify our efforts using C++ parallel array class libraries for parallel AMR.

A Neural-Network-Based System for Damage Identification and Location in Structural and Mechanical Systems

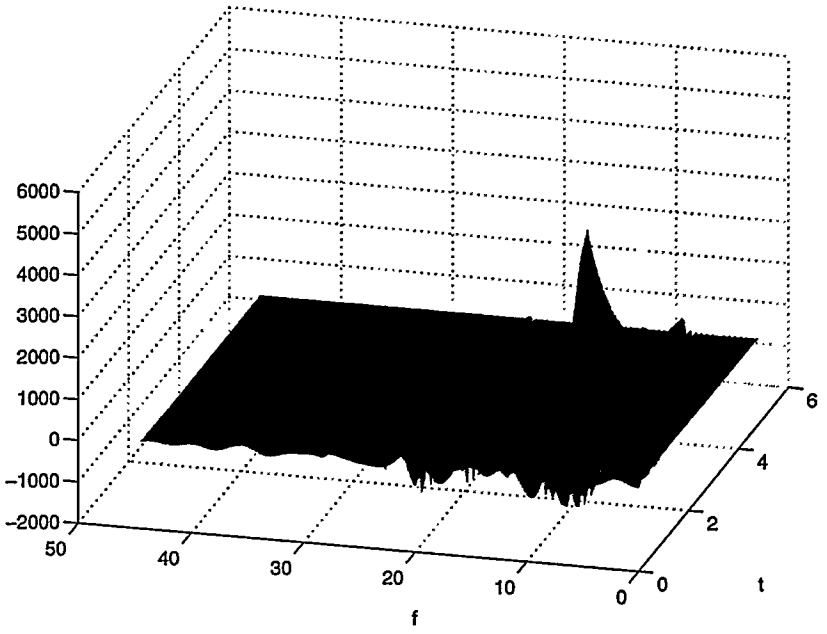
Charles Farrar

Our objective for this project is to develop and demonstrate an "intelligent system" for continuous structural monitoring and damage detection and location. The system will use coherence functions and changes in the curvature of mode shapes, which are inspected on-line by neural-network-based pattern recognition algorithms, as a damage identifier and locator. This damage detection method will be benchmarked against experimental data already acquired during an interstate highway bridge study in which tests were run with the bridge in both an undamaged and damaged state.

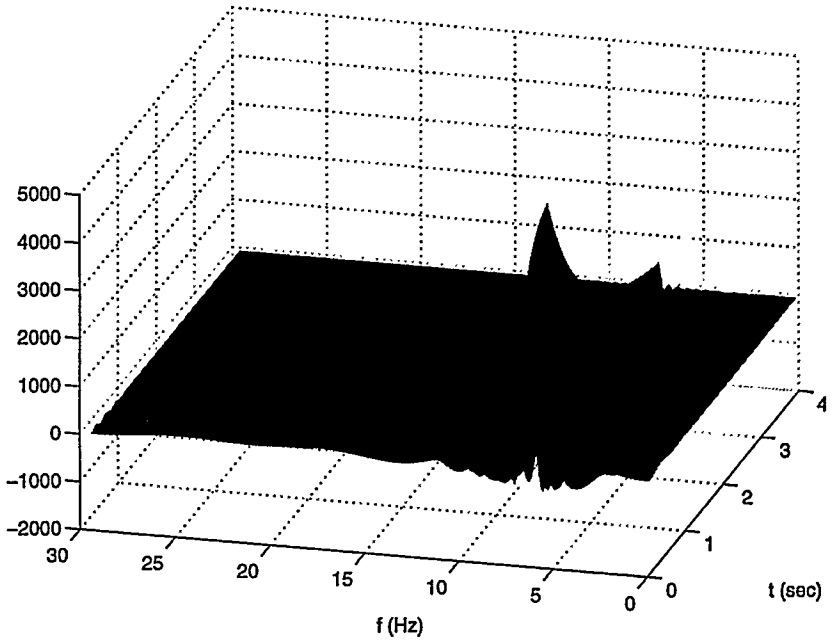
To quantify damage, we have applied nonlinear adaptive methods to a beam with a fatigue crack. In most of the existing literature, linear damage models are assumed. To determine damage, we used the nonlinear behavior of a crack opening and closing. We applied several different methods of nonlinear adaptive computation to a beam with an opening and closing crack. The first method involved using a neural network to predict crack size from vibration time-history data. A finite-element model produced data used to train the neural network. Specifically, we used power spectral densities as the input to a neural network that predicted crack length. The network performed quite well: it predicted crack length to within the resolution of the finite-element model.

A second nonlinear adaptive computational method we applied to the data was time frequency analysis. This method is designed to characterize nonstationary processes such as a crack opening and closing. We used the Wigner-Ville transform to see if a crack opening and closing could be detected and found that the higher harmonic content and ripples are clear indicators of the opening and closing crack.

Finally, we hosted a workshop on damage identification. Held at Los Alamos, the workshop attracted leading experts in the field from both federal agencies and private industry.



Wigner-Ville transform of a vibrating beam that has a crack.



Wigner-Ville transform of a vibrating beam that has no crack.

Simulation Methods for Advanced Scientific Computing

James Gubernatis

The rapid increase in raw computational power has created exciting opportunities for scientific computation. The complexity and realism of the problems that can be simulated promise to greatly advance numerous scientific and technological fields. Accordingly, scientific computing is enjoying considerable worldwide popularity. Yet many challenging scientific problems remain unsolved because of inadequate algorithms, especially algorithms that are suitable for massively parallel architectures. Our objective in this project is to create effective new algorithms for solving these problems, giving the Laboratory the initiative in key technical areas by combining the talents and efforts of our physical scientists and applied mathematicians.

In the wake of a three-day workshop on numerical algorithms for N-body simulations, research activities and collaborations produced landmark developments of simulation algorithms for quantum Monte Carlo simulations and new methods for simulating stochastic differential equations. In the quantum simulations, for example, we developed a new method for simulating systems of electrons that eliminated the fermion sign problems. This method was applied to the two-dimensional Hubbard and is permitting proper finite-sized scaling in order to assess whether the model exhibits superconductivity.

Publications

Baker, G., and N. Kawashima, "A Monte Carlo Calculation of the Renormalized Coupling Constant for the Three-Dimensional Ising Model Using Improved Estimators" in *Computer Simulation Studies in Condensed-Matter Physics VIII* (Springer Verlag, Heidelberg, Germany, in press).

Baker, G., and N. Kawashima, "Renormalized Coupling Constant for the Three-Dimensional Ising Model," *Phys. Rev. Lett.* **75**, 994 (1994).

Elston, T., and C. Doering, "Numerical and Analytic Studies of Nonequilibrium Fluctuation Induced Transport Processes" (to be published in *J. Stat. Phys.*).

Kawashima, N., "Cluster Algorithms for Anisotropic Quantum Spin Models" (to be published in *J. Stat. Phys.*).

Kawashima, N., and J. Gubernatis, "Dual Monte Carlo and Cluster Algorithms," *Phys. Rev. E* **51**, 1547 (1994).

Kawashima, N., and J. Gubernatis, "Generalization of the Fortuin-Kastelyn Transformation and Its Application to Quantum Spin Systems," *J. Stat. Phys.* **80**, 165 (1995).

Kawashima, N., and J. Gubernatis, "Loop Algorithms for Monte Carlo Simulations of Quantum Spin Systems," *Phys. Rev. Lett.* **73**, 1295 (1994).

Khamayseh, A., "Computational Conformal Mapping for Surface Grid Generation" (to be published in *J. Comput. Phys.*).

Manteuffel, T., and O. James, "On the Uniform Consistency of an Exponentially Upwinded Discretization for Singular Perturbation Problems" (to be published in *SIAM—Numerical Analysis*).

Robidoux, N., "Computer Algebra and Interpolation: A Lesson Plan" (to be published in *J. Symbolic Computation*).

Zhang, S., J. Carlson, and J. Gubernatis, "A Constrained Path Quantum Monte Carlo for Fermion Ground States," *Phys. Rev. Lett.* **74**, 3652 (1995).

Zhang, S., N. Kawashima, J. Carlson, et al., "Quantum Simulations of the Superfluid-Insulator Transition for Two-Dimensional Hard-Core Bosons," *Phys. Rev. Lett.* **74**, 1500 (1994).

Neutron Star Evolution and Emission

Richard Epstein

This project has focused on deducing the physical properties of neutron stars from their observable radiation. This effort has both observational and theoretical components.

Our air-shower measurements have set strenuous limits on the ultrahigh-energy photon emissions from pulsars and gamma-ray bursts. We performed a detailed study of the coupling of the stellar liquid core with the crust of a neutron star and found that composition stratification in the core prevents it from coupling to the crust through Ekman pumping; instead, magnetic coupling must be dominant. Comparison of our models of the coupling processes with observations of the spin-rate fluctuations of the Vela pulsar indicates that the internal magnetic field of this neutron star is nearly as strong as its surface field.

We have completed a study of the cooling and heating process in young neutron stars. Differential rotation between the neutron star crust and a more rapidly rotating superfluid interior produces frictional heating, and neutrino emission cools the star. By comparing our results with data on the surface temperature of neutron stars, we found that stars with soft equations of state and modest frictional heating are in closest agreement with the data.

Publications

Alexandreas, D.E., et al., "Point-Source Search Techniques in Ultra-High-Energy Gamma Ray Astronomy," *Nucl. Instrum. Methods A* **328**, 570 (1994).

Alexandreas, D.E., et al., "Search for Ultra-High-Energy Emission from Gamma-Ray Bursts," *Astrophys. J. Lett.* **426**, 1 (1994).

Alexandreas, D.E., et al., "Search for Ultra-High-Energy Point-Source Emission over Various Timescales," *Astrophys. J* **423**, 714 (1994).

Lattimer, J.M., et al., "Rapid Cooling and the Structure of Neutron Stars," *Astrophys. J.* **425**, 802 (1994).

Van Riper, K.A., B. Link, and R.I. Epstein, "Frictional Heating and Neutron Star Thermal Evolution," *Astrophys. J* **448**, 294 (1995).

Modeling Complex Phenomena: Multiple Length and Time Scales in Extended Dynamical Systems

Peter Lomdahl

Our research combines competencies in high-performance computing, theory of complex systems, and materials science in a new way that has great potential for applications to multiple length- and time-scale phenomena in condensed matter and materials science. We develop and apply massively parallel simulation techniques and analytical techniques from nonequilibrium and nonlinear science to the study of mesoscopic textures and their associated dynamics for a number of topical problems in condensed matter.

We have used our experience in modeling complex systems to explain the so-called transformer effect, experimentally observed in layered superconductors with and without external magnetic field. The figure illustrates the vortex configurations with no external magnetic field in the model at intermediate temperature (upper figure) and at the critical temperature (lower figure). Only at the critical temperature do the vortex lines percolate the system, which explains the no-field transformer effect.

We have also implemented a molecular dynamics algorithm with long-range interactions for studying vortex dynamics in two-dimensional disordered systems. This approach has led to new interpretations of experimental data obtained at Stanford University. We have developed a solid-on-solid model of surface dynamics and have identified several growth and smoothing regimes in surface growth arising from the multiple space- and time-scale structures. The consequences of mesoscopic textures and patterns for macroscopic strength and response properties of the above-mentioned systems remain the important target of our study.

Publications

Dominguez, D., N. Gronbech-Jensen, and A.R. Bishop, "Resistive Hysteresis and Nonlinear IV Characteristics at the First-Order Melting of the Abrikosov Vortex Lattice" (to be published in *Phys. Rev. Lett.*).

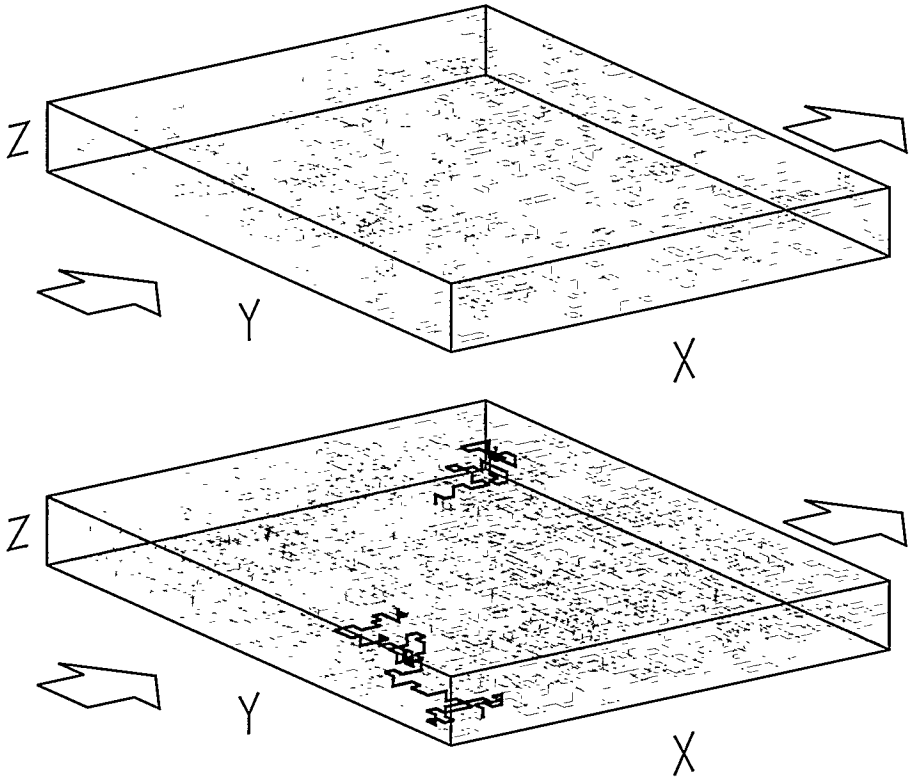
Dominguez, D., N. Gronbech-Jensen, A.R. Bishop, et al., "Transformer Configuration in Three-Dimensional Josephson Lattices at Zero Magnetic Field," *Phys. Rev. Lett.* **74**, 717 (1995).

Gronbech-Jensen, N., and M.R. Samuelsen, "Long-Range Magnetic Interaction Between Josephson Junctions," *Phys. Rev. Lett.* **74**, 170 (1995).

Gronbech-Jensen, N., and M.R. Samuelsen, "Phase-Locking of an Overdamped Pendulum," *Phys. Lett. A* **191**, 57 (1994).

Sanchez, A., A.R. Bishop, D. Cai, et al., "Smoothing of Rough Surfaces," *Phys. Rev. B* **52**, 5433 (1995).

Sanchez, A., D. Cai, N. Gronbech-Jensen, et al., "Roughening Transitions of Driven Surface Growth," *Phys. Rev. B* **51**, 14664 (1995).



The figure shows the vortex configuration in an anisotropic three-dimensional Josephson lattice driven by an external current (arrows) through the lower plane. At intermediate temperatures (upper figure), vortex loops are spontaneously generated with sizes smaller than the vertical distance. Thus, no resistive coupling can be detected from the bottom to the top of the system. Near the critical temperature, the melting temperature (lower figure), the vortex loops percolate the system (highlighted in solid), and resistive coupling is detected and identified with the experimentally observed transformer effect. This is an excellent example of topological excitations in a three-dimensional system.

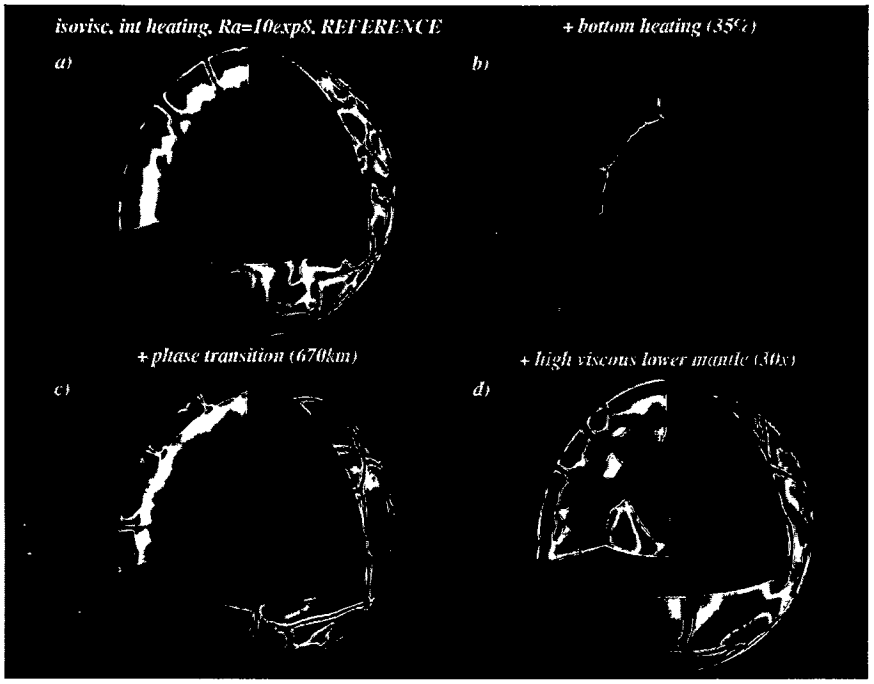
Modeling the Heat Flow and Resulting Dynamics in the Earth's Interior

Gary A. Glatzmaier

We are studying the dynamics of Earth's mantle and core that are driven by the heat flow out of Earth. By comparing fluid dynamic model predictions with laboratory experiments and with field and seismic observations, we are accomplishing our study of systems deep within Earth.

Our computer models of multiphase flow have demonstrated that, in simulations of magma chambers in cold country rock, thermal convection with temperature-dependent viscosity dies out much more quickly than thermal convection with constant viscosity. Our three-dimensional (3-D) model of thermal plumes in the mantle helped explain the formation of islands and midocean-floor spreading. Our 3-D spherical model of mantle convection demonstrated how the structure of thermal convection in the mantle depends significantly on how much viscosity increases with depth. We used another 3-D spherical mantle convection model to validate global seismic tomography inversion techniques.

Lastly, our 3-D model of magnetoconvection in Earth's liquid outer core demonstrated how (1) a strong magnetic field in Earth's core can force most of the thermal convection to occur in the polar regions instead of the equatorial region and (2) a heterogeneous heat flux boundary condition at the core-mantle boundary (because of large variations in the temperature of the lower mantle) can significantly affect the structure of convection in the liquid outer core. The accompanying figures show some of our modeling results.



Four snapshots of the 3-D thermal structure of simulated mantle convection. The figures show (a) the reference case that has constant viscosity and is heated only internally, (b) the effects of 35% of the heat coming from the core below, (c) the effects of an endothermic phase transition at 670 km below the surface, and (d) the effects of viscosity thirty times greater in the lower part of the mantle.

Publications

Bunge, P., and J.R. Baumgardner, "Mantle Convection Modeling on Parallel Virtual Machines," *Comput. Phys.* **9**, 207 (1995).

Bunge, P., M.A. Richards, and J.R. Baumgardner, "The Effect of Depth-Dependent Viscosity on Mantle Convection" (submitted to *Nature*).

Jarvis, G.T., G.A. Glatzmaier, and V.I. Vangelov, "Effects of Curvature, Aspect Ratio and Planform in Two- and Three-Dimensional Spherical Models of Thermal Convection" (to be published in *Geophys. Astrophys. Fluid Dyn.*).

Kincaid, C.G., G. Ito, and C. Gable, "Laboratory Investigation of the Interaction of Off-Axis Mantle Plumes and Spreading Centers" (to be published in *Nature*).

Kincaid, C., J.-G. Schilling, and C.W. Gable, "The Dynamics of Off-Axis Plume-Ridge Interaction in the Uppermost Mantle" (to be published in *Earth Planet. Sci. Lett*).

Koch, D.M., and M. Manga, "Neutrally Buoyant Diapirs: A Model for Coronae Topography on Venus" (to be published in *Geophys. Res. Lett.*).

Manga, M., "Dynamics of Drops in Branched Tubes" (to be published in *J. Fluid Mech.*).

Manga, M., "Mixing of Chemical Heterogeneities in the Mantle: Effect of Viscosity Differences" (submitted to *Geophys. Res. Lett.*).

Manga, M., and R.J. O'Connell, "The Tectosphere and Postglacial Rebound," *Geophys. Res Lett.* **22,** 1949 (1995).

Manga, M., and H.A. Stone, "Collective Hydrodynamics of Deformable Drops and Bubbles in Dilute Suspensions at Low Reynolds Numbers," *J. Fluid Mech.* **300,** 231 (1995).

Manga, M., and H.A. Stone, "Interactions between Bubbles in Magmas and Lavas: Effects of Deformation," *J. Volcan. Geotherm. Res.* **63,** 269 (1994).

Manga, M., and H.A. Stone, "Low Reynolds Number Motion of Drops and Bubbles through Fluid-Fluid Interfaces," *J. Fluid Mech.* **256,** 647 (1995).

Masters, G, S. Johnson, G. Laske, et al., "A Shear Velocity Model of the Mantle" (to be published in *Philos. Trans. R. Soc. London*).

Olson, P., and G.A. Glatzmaier, "Magnetoconvection and Thermal Coupling of Earth's Core and Mantle" (to be published in *Philos. Trans. R. Soc. London*).

Olson, P., and G.A. Glatzmaier, "Magnetoconvection in a Rotating Spherical Shell: Structure of Flow in the Outer Core" (to be published in *Phys. Earth Plant. Interiors*).

Sun, Z.-P., G. Schubert, and G.A. Glatzmaier, "Numerical Simulations of Thermal Convection in a Rapidly Rotating Spherical Shell Cooled Inhomogeneously from Above," *Geophys. Astrophys. Fluid Dyn.* **75,** 199 (1994).

Tackley, P.J., D.J. Stevenson, G.A. Glatzmaier, et al., "Effects of Multiple Phase Transitions in a Three-Dimensional Spherical Model of Convection in the Earth's Mantle," *J. Geophys. Res.* **99,** 15877 (1994).

Numerical Methods Based on Nonlinear Dynamics for Modeling the Global Ocean

Len Margolin

We are developing new techniques for the numerical simulation of long-term ocean dynamics. These techniques are based on nonlinear dynamic theory and, in particular, on preserving the asymptotic balances appropriate to dissipative flow regimes. During the past year, we have extended our theory from dissipative partial differential equations to more general equations that are balanced but where dissipation is not part of the principal balance of terms. In particular, we have modified a 1.5 layer model of the Atlantic Ocean basin based on the preservation of a quasi-geostrophic balance. We have used the model to study the wind-driven double-gyre flow. We have developed diagnostics for this stochastic flow to demonstrate that the new model reproduces the accuracy of the original model on a twice-finer mesh and yet runs at the timestep of the coarser mesh. Important new features of this theory include the treatment of systems of equations discretized on a staggered mesh and the use of three-time-level integration schemes that are typical of those used in global models of the ocean.

In parallel work, we have extended a two-dimensional model from a simple, shallow-fluid approximation to include the nonlinear, dispersive terms representing the vertically-averaged effects of nonhydrostaticity (the Green-Naghdi equations). These additional terms are found by asymptotic expansion of the scaled equations. We have used the new model to study the meso-scale problem of flow past a mountain. The study shows that the dispersive terms produce qualitative changes in the flow in a variety of realistic parameter regimes. We have verified that the dispersive shallow-water equations are more accurate than the traditional shallow-water equations by comparing them with fully three-dimensional Euler simulations.

Publications

Jones, D.A., L.G. Margolin, and A.C. Poje, "Enslaved Finite Difference Schemes for Nonlinear Dissipative PDEs" (to be published in *Numerical Methods for PDEs*).

Nadiga, B.T., L.G. Margolin, and P.K. Smolarkiewicz, "Various Approximations of the Shallow Fluid Flow over an Obstacle" (submitted to *Phys. Fluids*).

Advanced Three-Dimensional Eulerian Hydrodynamic Algorithm Development

Thomas Adams

Three-dimensional Eulerian hydrodynamic codes (hydrocodes) have important applications to nuclear weapons technology, conventional defense, and industrial process simulation. Our objective is to improve the fidelity of hydrocodes through better algorithms and increased use of parallel computers.

We are particularly interested in improving volume-tracking methods, adaptive mesh-refinement techniques, portability and performance, and problem setup tools. Technical achievements include an unsplit piecewise linear interface calculation (PLIC) based on the Youngs algorithm, a new interface-tracking method of marker particles, improved incorporation of interface dynamics, and more efficient and robust solution of systems of linear equations.

The unsplit PLIC method removes directional bias from the standard implementation of a volume of fluid algorithm due to Youngs. The improvement in the algorithm is twofold: the method is now truly multidimensional in every phase, and it preserves natural symmetries in a solution. These characteristics are vital components to improving the fidelity of hydrocodes for many applications.

Our new marker particle method is an alternative to the volume of fluid method. The new method is characterized by a lower numerical error than the volume of fluid method, but it bears an increased cost in computer time and memory. Nevertheless, for a certain class of problems with vigorous mixing it provides us with greater fidelity. Further research is needed to determine its applicability to a wider range of hydrodynamic situations. In conjunction with the interface tracking, we have improved the incorporation of interface physics in hydrodynamic calculations. The model we are using is the continuum surface force model. We have improved the fidelity of this model in practical calculations involving surface tension and phase change.

We have also introduced a set of more stringent criteria for judging and developing interface-tracking methods. We have applied each of these methods to the physics of low-speed hydrodynamics to demonstrate their capabilities. In working out the equations of low-speed hydrodynamics for large density changes (such as air-water flows), it becomes quite challenging to efficiently solve the system of linear equations. We have tackled this problem by coupling two modern methods: multigrid and conjugate gradient. In our approach, we use the multigrid iteration to precondition the conjugate gradient method. This results in an algorithm that shares the strengths of both methods and, as such, is more efficient and robust than if either were used in isolation.

These methods and algorithms will improve the fidelity of existing and new three-dimensional hydrocodes. The work performed in this project has application to a number of manufacturing processes (such as extrusion, forging, and molding), nuclear explosives design and safety, and commercial technologies such as ink-jet printing. Additionally, the methods can improve the ability of researchers to computationally investigate the fundamental behavior of fluids.

Studies of Dynamical Processes Affecting Global Climate

Charles Keller

The objective of this project is to study the interactions between the earth's atmosphere and its oceans. We are focusing on improving models of processes in three main areas: chemistry, water vapor, and ocean/atmosphere interactions. Our main objective is to develop improved models of dynamic processes in the oceans and atmosphere and to incorporate them into large climate codes.

We are incorporating observational data and theoretical models into existing global ocean and atmospheric general circulation models (GCMs) and studying their effects on these codes.

We are using both the National Center for Atmospheric Research (NCAR) climate code CCM2 and the Los Alamos climate code in our studies. (Although older, the Los Alamos code has several capabilities not available in the NCAR code.)

First, we have added new cloud-physics packages to the NCAR code so that it better simulates important details of climate in the northeast Pacific. Then, using numerical tracer particles to mimic release of aerosol particles over the Arctic Ocean, we have simulated the isentropic potential vorticity field resulting in Rossby wave breaking and chaotic advection in the troposphere, a result thought to require much higher resolution simulations.

Analysis of coupled ocean/atmosphere simulations of the northern Pacific showed periodic 20-yr climatic oscillations similar to those that affect western North America. Similar long-term simulations showed details of low-frequency variability in climate that had not been observed before.

We are making substantial improvements in mathematical models for existing ocean and atmospheric GCMs on supercomputers for forecasting climate variability and for determining changes in the atmospheric chemical environment, such as those caused by pollutants.

Publications

Chen, F., and M. Ghil, "Interdecadal Variability in a Hybrid Coupled Ocean-Atmosphere Model" (submitted to *J. Phys. Oceanography*).

Chen, F., and M. Ghil, "Interdecadal Variability of the Thermohaline Circulation and High-Latitude Surface Fluxes" (to be published in *J. Phys. Oceanography*).

Cockburn, D., D. Jones, and E.S. Titi, "Estimating the Number of Asymptotic Degrees of Freedom for Nonlinear Dissipative Systems" (submitted to *Mathematics of Computation*).

Fuehrer, P.L., and C.A. Friehe, "A Structural Model for Turbulence in the Atmospheric Boundary Layer" (submitted to *Phys. Fluids*).

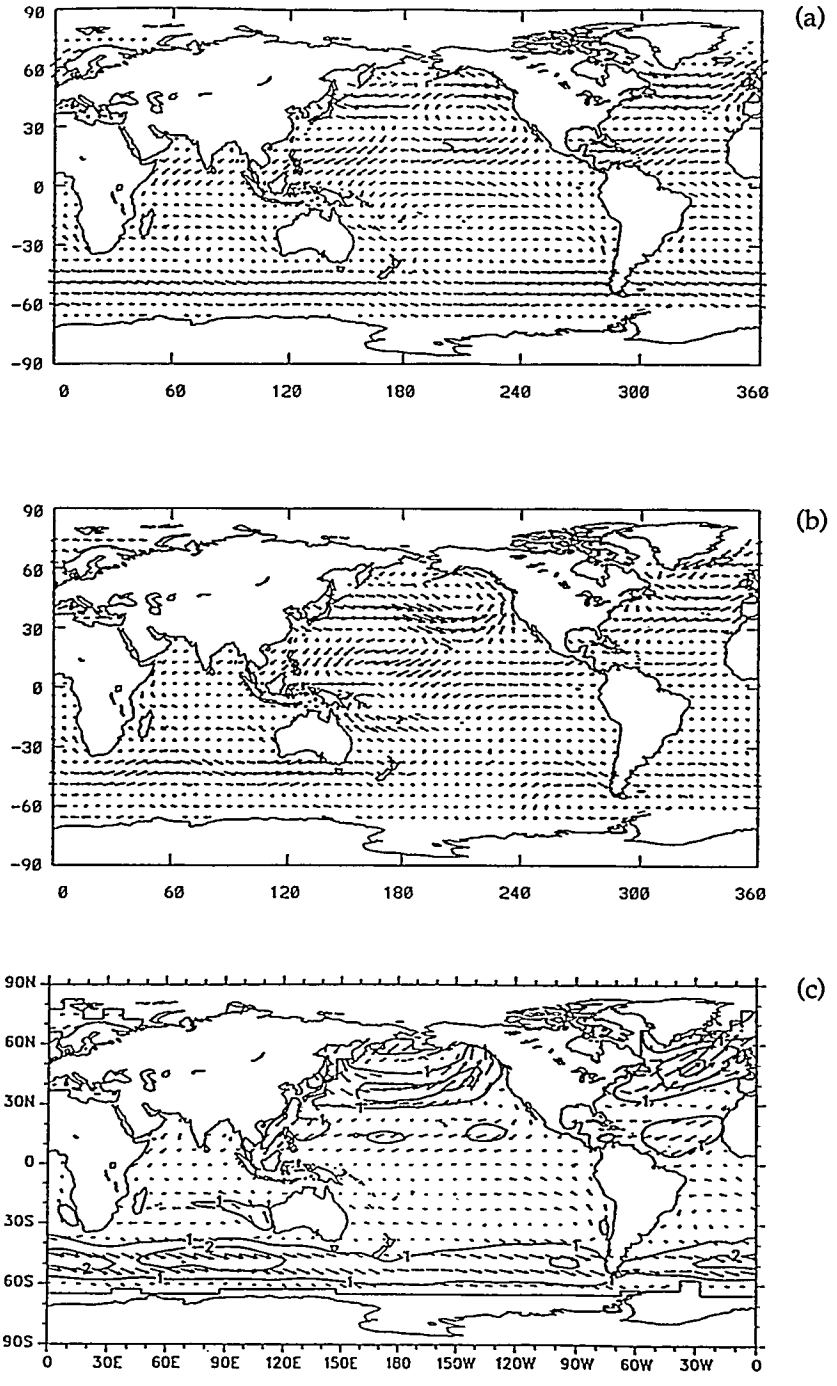
Jones, D., and E.S. Titi, "C1 Approximating Inertial Manifolds for the Dissipative Nonlinear Equations" (to be published in *J. Diff. Eqns.*).

Kao, C.-Y.J., A. Quintanar, M.J. Newman, et al., "Climate Simulations with NCAR CCM2 Forced by Global Sea Surface Temperature in 1950-1989" (submitted to *J. Climate*).

Robertson, A.W., "Interdecadal Variability over the North Pacific in a Multi-century Climate Simulation" (to be published in *Climate Dynamics*).

Smith, W.S., and C.-Y.J. Kao, "Numerical Simulations of Arctic Stratus Clouds Using a Second Order Turbulence Closure Model" (to be published in *J. Appl. Meteorol.*).

Smith, W.S., and C.-Y.J. Kao, "Using a Turbulence Radiative-Conservative Model to Study the Cloud/Radiation Interaction with the FIRE Data" (to be published in *Monthly Weather Review*).



(a) Simulated surface winds for January with the original cloud parameterization in CCM2, (b) same as (a) except with the new cloud parameterization, and (c) observed winds.

Application of Discrete Mathematics

Vance Faber

In combinatorial analysis one studies and quantifies the properties of discrete objects and their operations. The knowledge gained finds wide application in all areas of science and engineering. The goal of this project is to apply combinatorial methods to help in solving a wide variety of problems. Since this project was conceived, we have used the methods of combinatorics to solve problems in numerical analysis, computer networks, cluster analysis, learning theory, DNA mapping, group testing for biology, evolutionary trees, quantum physics, and wavelet analysis. Our basic approach in this project is to gain a deep understanding of such problems and to use our skills in combinatorial methods to solve them.

Our main accomplishments this past year are as follows:

- In the area of DNA mapping and experimental design in biology, we applied information theory methods to prove an interesting relationship between designs that arise in group testing and error-correcting designs. We also worked on protocols in quantum cryptography and on algorithms for quantum computing.
- We applied our knowledge of computational geometry to geographical information systems. In particular, we demonstrated that an algorithm developed for Delauney triangulation can speed up triangulation of meshes in existing software at the Laboratory by orders of magnitude.
- We continued work on optimal Cayley graphs in Abelian groups, obtaining several new results.
- We obtained a bijective solution to Schroeder's fourth problem in combinatorics.

We have had considerable success in developing and applying combinatorial methods to diverse problems. The work performed in this project draws heavily on our expertise in discrete algorithms, combinatorics, complexity theory, and algebra and has applications to a broad range of scientific and engineering problems.

Lattice Boltzmann Research

Gary Doolen

The lattice Boltzmann method, which grew out of the lattice gas research started at Los Alamos, is a computational approach for studying all fluid flows. This method differs from traditional numerical schemes in two significant ways: it deals with fluid properties at a microkinetic level, and it can efficiently model complicated boundary conditions. The research conducted as part of this project is applied to numerical methods, flows through porous media, enhanced oil recovery, and flowing chemical reactions.

We significantly added to previous research by extending the method to simulate biological flows, such as blood flow; conducting research on pattern formation in chemically reacting flows; developing the subgrid scaling models, thermohydrodynamic capabilities, and stability analyses necessary to simulate high-velocity turbulent flows; and developing a Mathematica program that would allow the user to input detailed microscopic rules and rapidly determine which partial differential equations are being approximated by the rules.

We successfully benchmarked lattice Boltzmann calculations for three-dimensional flows driven at a uniform velocity at the top of a closed box, and we developed boundary conditions whose accuracy is higher. At the same time, we created and successfully tested a new and more accurate method for solving incompressible flows, we developed lattice Boltzmann models to model shock fronts, and we acquired a new understanding of the time evolution of phase transitions by using lattice Boltzmann methods. Finally, we published a review of the procedure for modeling chemical reactions in fluid flows.

Publications

Chen, S., S.P. Dawson, G. Doolen, et al., "Lattice Methods and their Applications to Reacting Systems," *Comput. and Chem. Eng.* **19,** 617 (1995).

Chen, S., G. Doolen, and K. Eggert, "Lattice Boltzmann Fluid Dynamics," *Los Alamos Science* **22,** 98 (1995).

Chen, S., and T. Lookman, "Growth Kinetics in Multicomponent Fluids," *J. Stat. Phys.* **1/2,** 223 (1995).

He, X., and Q. Zou, "Analysis and Boundary Condition of the Lattice

Boltzmann BGK Model" (to be published in *Phys. Fluids*).

He, X., and Q. Zou, "Analysis and Boundary Condition of the Lattice-Boltzmann BGK Model With Two Velocity Components" (submitted to *Phys. Rev. Lett.*).

Hou, S., Q. Zou, S. Chen, et al., "Simulation of Cavity Flow by the Lattice Boltzmann Method" (to be published in *Phys. Rev. E*).

Luo, L., H. Chen, S. Chen, et al., "H-Theorems for Discrete Velocity BGK Equations" (to be published in *J. Stat. Phys.*).

Nadiga, B., and D. Pullin, "A Method for Near-Equilibrium Discrete-Velocity Gas Flows," *J. Comput. Phys.* **112,** 162 (1994).

Nadiga, B., and B. Sturtevant, "Shock Structure in a Nine-Velocity Gas," *Physica D* **73,** 205 (1994).

Nobel, D., S. Chen, J. Georgiadis, et al., "A Rigorous Hydrodynamic Boundary Condition for the Lattice Boltzmann Method," *Phys. Fluids* **7,** 203 (1995).

Shan, X., and H. Chen, "Simulation of Nonideal Gases and Liquid-Gas Phase Transitions by the Lattice Boltzmann Equation," *Phys. Rev. E* **49A,** 2941 (1994).

Wu, Y., F. Alexander, T. Lookman, et al., "Effects of Hydrodynamics on Phase Transition Kinetics in Two-Dimensional Binary Fluids," *Phys. Rev. Lett.* **74,** 3852 (1995).

Zou, Q., and X. He, "On Pressure and Velocity Flow Boundary Conditions for the Lattice Boltzmann BGK Model" (to be published in *Physica D*).

Zou, Q., and S. Hou, "Analytical Solutions of the Lattice Boltzmann Model with BGK Collision Operator" (submitted to *Phys. Fluids*).

Zou, Q., S. Hou, S. Chen, et al., "An Improved Incompressible Lattice Boltzmann Model for Steady Flow" (to be published in *J. Stat. Phys.*).

Zou, Q., S. Hou, S. Chen, et al., "Simulation of Incompressible Navier-Stokes Fluid Flows by the Lattice Boltzmann Method," *J. Stat. Phys.* **118,** 329 (1994).

Phase Transitions, Nonequilibrium Dynamics, and Critical Behavior of Strongly Interacting Systems

Emil Mottola

We are carrying out a comprehensive study using large-scale simulations of strongly interacting systems. We are exploring a variety of approaches to the nonequilibrium dynamics of phase transitions and critical behavior in strongly interacting systems. Phase transitions are the classic example of a multiple-length and time-scale problem and occur in diverse physical situations. Specifically, our project focuses on the

- finite-temperature quantum chromodynamics (QCD) phase transition and nonequilibrium dynamics of a new phase of matter (the quark-gluon plasma) above the critical temperature;
- electroweak phase transition which may account for the asymmetry between matter and anti-matter in the universe; and
- spinodal decomposition and structural phase transitions in a variety of materials and systems such as spin chains, shape-memory alloys, and amorphous metals.

It is remarkable that the same analytic and computational techniques can be applied to all of these apparently disparate examples. All of these problems require a large-scale computational effort that would not have been feasible without the advent of massively parallel computers and the capabilities provided by Los Alamos National Laboratory's Advanced Computing Laboratory.

During the past year, we investigated a number of statistical mechanical models. Simulations of the three-dimensional Ising model confirm that hyperscaling holds for this model. We developed a new method to study a candidate model describing shape-memory alloys. Lastly, we made significant progress in understanding the dynamics of disoriented chiral condensates and understanding its implications for the QCD finite-temperature transition.

Publications

Bhattacharya, T., R. Gupta, and S. Sharpe, "Decay Constants with Wilson Fermions" (submitted to *Phys. Rev. D*).

Cooper, F., S. Habib, Y. Kluger, et al., "Non-Equilibrium Quantum Fields in the Large-N Expansion," *Phys. Rev. D* **50,** 2848 (1994).

Numerical Simulations of Disordered Superconductors

Kevin Bedell

This project involves quantum Monte Carlo investigations of interacting and disordered boson systems and the related topic of how flux lines behave in superconducting materials. To study dynamic properties we apply molecular dynamics (MD) approaches to these problems as well. A crucial ingredient in this work is the development of efficient algorithms to implement our simulations on parallel computers and workstation clusters. In addition to advancing the use of these computational methods, we hope to gain new insights into the properties of dirty superconductors and transport in high magnetic fields.

We carried out Monte Carlo studies of the critical behavior of superfluid ^{4}He in aerogel. We modeled aerogel as an incipient percolating cluster and weakened the bonds at the fractal sites. Our two-dimensions (*xy*) model simulations show an increase in the superfluid-density exponent in the presence of fractal disorder, provided that the helium correlation length does not exceed the fractal correlation length. This value of the superfluid-density exponent appears to be roughly consistent with the experimental results.

We also studied how flux lines are localized by splayed columnar pins. This new type of correlated disorder enhances the critical current by orders of magnitude, but there is reason to believe it may reduce the critical temperature T_c. To test this possibility we used a sine-Gordon-type renormalization-group study to obtain an analytic form for T_c. In an independent investigation we determined T_c from the current-voltage characteristics using an MD code. The results obtained in these two ways coincide.

Finally, work is in progress to study the effects of strong interactions on the shape of the Fermi surface. In a variational approach we found that increasing interactions tend to flatten out the Fermi surface, increasing its nesting. This leads to linear temperature dependence of resistivity, in accordance with experimental findings on high-temperature superconductors.

Publications

Moon, K., and S. Girvin, "Critical Behavior of Superfluid ^{4}He in Aerogel," *Phys. Rev. Lett.* 75, 1328 (1995).

Devereaux, T.P., T. Scalettar, G.T. Zimanyi, et al., "Phase Diagram for Splay Glass Superconductivity" (to be published in *Phys. Rev. Lett.*).

Geometrically Compatible 3-D Monte Carlo and Discrete-Ordinates Methods

Jim Morel

The goal of this project is to develop massively parallel, high-order-accurate deterministic methods for performing particle transport calculations on three-dimensional (3-D), unstructured, tetrahedral spatial meshes and to modify the Monte Carlo Neutron and Photon (MCNP) transport code to perform calculations on such meshes using variance-reduction parameters defined with deterministic adjoint calculations. The tetrahedral meshes will be generated with the National Grid Project code being developed at Mississippi State University in collaboration with a consortium of industrial and government institutions that include Los Alamos. Our work will provide three important new capabilities: (1) massively parallel, high-order-accurate, deterministic transport methods capable of modeling complex 3-D geometries; (2) a truly automatic, 3-D Monte Carlo variance-reduction algorithm; and (3) a complex 3-D geometric representation common to both our deterministic and Monte Carlo codes.

During the last year we interfaced an existing deterministic neutron transport code for solving the 3-D simplified spherical-harmonics (SP_n) equations on unstructured tetrahedral meshes with the MCNP code. Biasing information provided with this SP_n code was found to dramatically increase the efficiency of MCNP for certain difficult problems. We also completed development of a deterministic code for solving the 3-D discrete-ordinates (S_n) equations on unstructured tetrahedral meshes. This code uses a third-order-accurate, linear-discontinuous, finite-element spatial discretization scheme and is much more accurate than the SP_n code.

Publications

Van Riper, K., T. Urbatsch, P. Soran, et al., "Generation of a Monte Carlo Variance Reduction Map from a Determinstic Transport Calculation" (submitted to *Nucl. Sci. Engin.*).

Transactional Memories: A New Abstraction for Parallel Programming

Joseph Fasel, Los Alamos National Laboratory
Divyakant Agrawal, Univ. of California, Santa Barbara

Multiprocessor computer systems with distributed memory make the development of parallel programs difficult. From a programmer's perspective, it would be most desirable if the underlying hardware and software could provide the programming abstraction commonly referred to as sequential consistency—a single address space and multiple threads. However, ensuring sequential consistency limits opportunities for optimizing the performance of architectural and operating systems, and it can therefore lead to poor performance.

Transactional memory is a new abstraction for parallel computing. The programming model is shared memory with multiple threads of control. However, to obtain data consistency in their applications of transactional memory, our collaborators at the University of California, Santa Barbara, use transactions rather than mutual exclusion based on locking. The transaction approach permits the underlying system to exploit the potential parallelism in transaction processing. As part of our collaborative research, we have been exploring the possibility of designing parallel programs using the transaction paradigm for data consistency and barrier thread synchronization.

So far, we have been exploring lock-free implementations of transactional memory and developing parallel applications using the transactional memory abstraction; we have thoroughly evaluated different implementations of transactional memory with respect to other notions of distributed shared memory, namely, sequential consistency, causal memory, and parallel random-access memory; and we have implemented our findings on a cluster of workstations that have an asynchronous transfer mode switch.

We have implemented transactional memory on Maya, a platform we have developed that is capable of simulating the execution of various distributed- and shared-memory protocols by using the parallel discrete-event simulation technique. Maya is also capable of executing the distributed- and shared-memory protocols directly on our network of Sun workstations.

Computational Modeling of Materials Processing and Processes

Terry Lowe

Our research objective is to develop ways to predict how low-symmetry materials deform and to provide design tools for materials processing. Our research during the past year has continued to focus on computational modeling of materials processing, particularly for low-symmetry materials. The severe internal constraints under which these materials deform produce intense internal stresses that control both the constitutive response and failure behavior. The research undertaken in this project has potential benefits to several experimental programs currently underway at Los Alamos. Most recently we have used our computational modeling to interpret the results of neutron-scattering experiments performed at the Los Alamos Neutron Science Center (LANSCE).

Our major achievement during the past year was to develop a theory for low-symmetry intermetallics based on titanium and aluminum compounds. We have used aggregate theories and detailed computational micromechanics simulations to predict how these materials deform, and we have compared these predictions to experiments on Ti_3Al/TiAl alloys.

Our research provides new tools for process modeling for several advanced materials systems, for example, high-temperature superconducting oxides; our results are being used to help design new processing methods for these superconducting materials. Our newer work on layered intermetallic compounds is also intended to provide a quantitative tool for process design.

Publications

Kad, B., M. Dao, and R. Asaro, "Numerical Simulations of Plastic Deformation and Fracture Effects in Two Phase Gamma-TiAl and α_2-Ti_3Al Lamellar Microstructures," *Philos. Mag. A* **71**, 567 (1995).

Schoenfeld, S. S. Ahzi, R. Asaro, et al., "The Bulk Processing of 2223 BSCCO Powders; Part I Densification and Mechanical Response" (submitted to *Philos. Mag. A*).

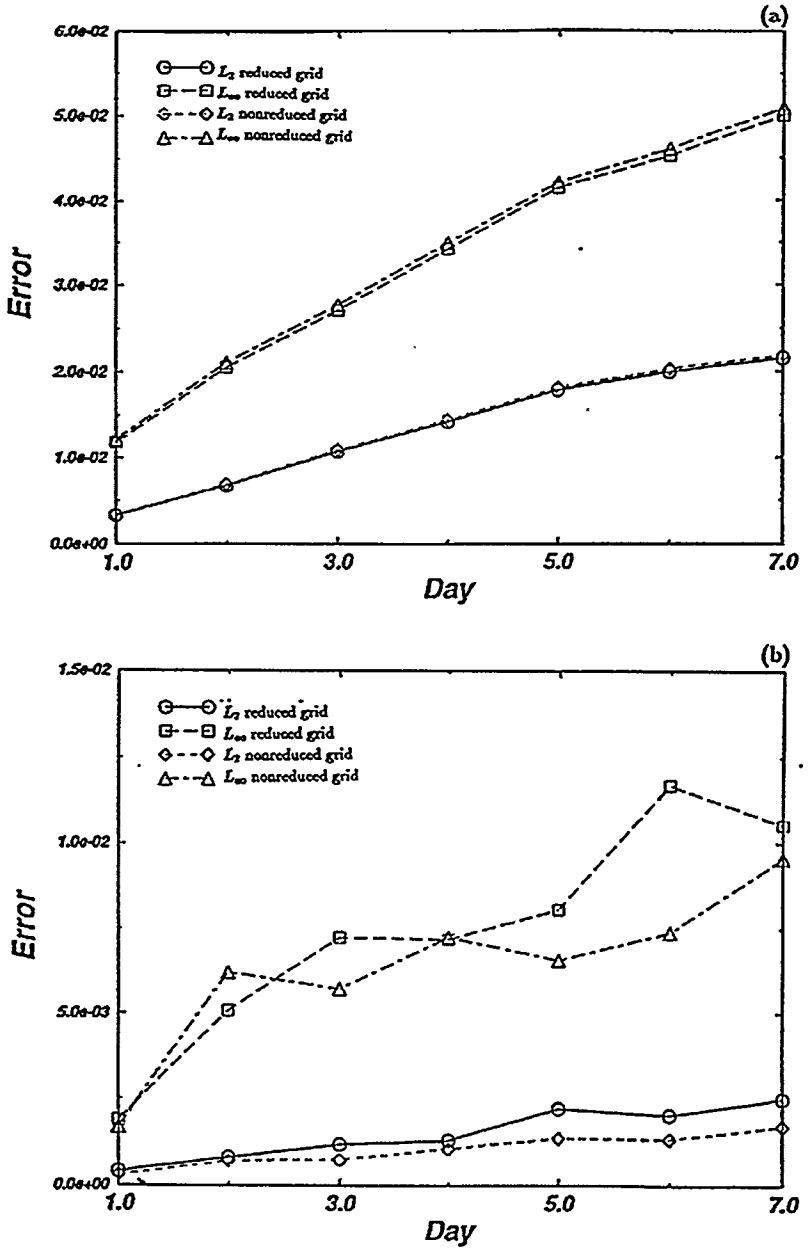
Development of the First Nonhydrostatic, Nested-Grid, Grid-Point Global Atmospheric Modeling System on Massively Parallel Machines

Chih-Yue J. Kao

Today's global atmospheric models suffer from one or more of the following shortcomings: (1) they lack an interactive nested-grid capability that would allow higher-resolution modeling over regional areas; (2) they use a spherical spectral representation of model variables (as opposed to a grid-point finite-difference representation), which hinders their performance on parallel machines; and (3) they use the hydrostatic approximation, which potentially makes them mathematically ill-posed. As a result, no atmospheric model is capable of simulating the full range of spatial scales for atmospheric circulations, such as from complex-terrain wind patterns to planetary wave disturbances.

The goal of our project is to develop a highly modularized, nested-grid, self-calibrating global atmospheric modeling system with accurate physics and chemistry. With such a system, we will be able to study a suite of atmospheric problems, ranging from local characterization to climate modeling, from thunderstorms to global phenomena such as cloud-radiative forcing, and from urban pollution to global greenhouse effects. It will also provide a unique testbed for high-performance computing architecture.

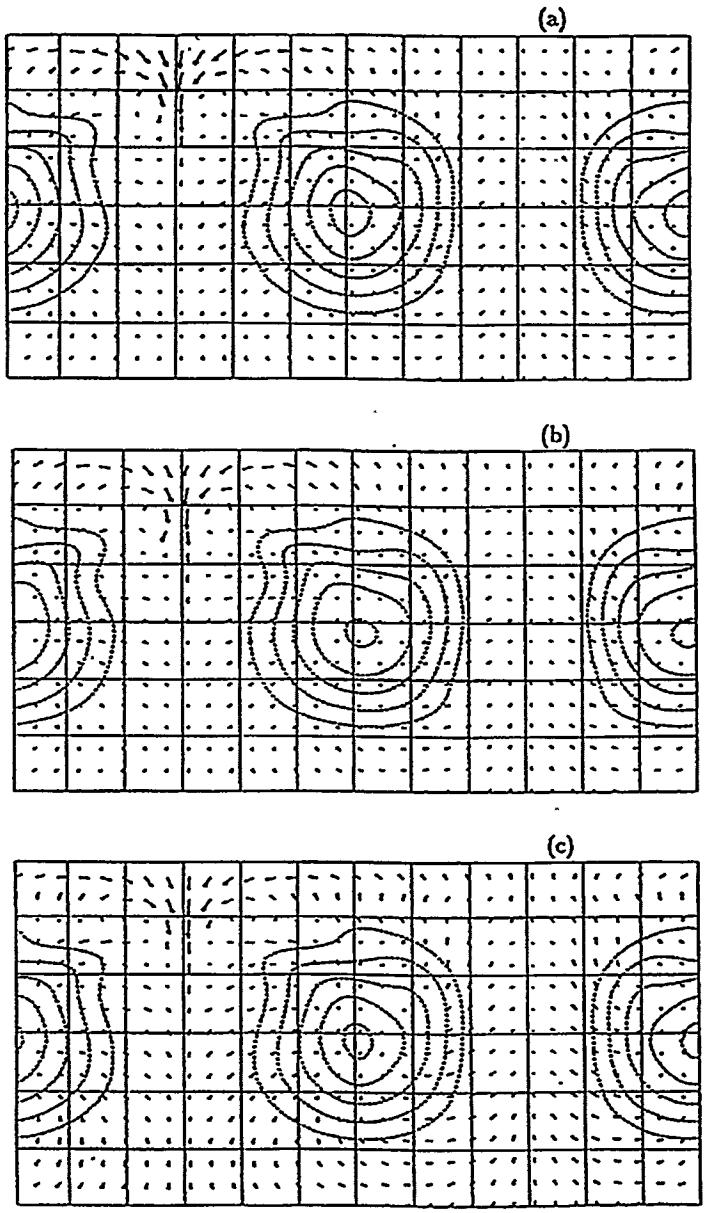
Our approach has been to modify a regional atmospheric modeling system—a nonhydrostatic mesoscale model—into a global configuration. Our work has focused on improving the model's physics and modifying its numerics. For the physics, we have concentrated



Time evolution of the error measures for a model configuration with 2.8-deg resolution for (a) the Rossby-Haurwitz wave and (b) zonal flow. In both sets of curves, the reduced-grid calculations have similar or lower error measures than the nonreduced-grid calculations.

on parameterizing cloud/radiation interaction and cumulus convection. We have also started implementing some basic NO_X and ozone chemistry into the model. For numerics, we have been experimenting with a novel approach to handling numerical problems near the poles that result from the singularities of a spherical coordinate system. Our approach is to use fewer grid points near the geographical poles; this reduced-grid system increases the allowable time step of model integration based on stability requirements.

We have tested our reduced-grid system for two global flows—the Rossby-Haurwitz wave and a zonal flow perturbed by a mountain near the north pole—on the massively parallel Connection Machine 5 at Los Alamos. Our simulations show that the reduced-grid system not only improves computational efficiency but also minimizes errors (see accompanying figures).



Geopotential perturbation and flow vectors for a global nonlinear zonal test problem involving a mountain at the north pole: (a) reduced-grid solution; (b) nonreduced-grid solution; and (c) analytical solution. The similarity of all three solutions supports the validity of our reduced-grid system.

Publications

Kao, C.-Y.J., A. Quintanar, M.J. Newman, et al., "Climate Simulations with NCAR CCM2 Forced by Global Sea Surface Temperature in 1950-1989" (submitted to *J. Climate*).

Reisner, J., L.G. Margolin, and P.K. Smolarkiewicz, "A Reduced Grid Model for Shallow Flow on the Sphere" in *Parallel Computing* (Elsevier Science Publisher, Amsterdam, The Netherlands, in press).

Smith, W.S., and C.-Y.J. Kao, "Numerical Simulations of Arctic Stratus Clouds Using a Second-Order Turbulence Closure Model" (to be published in *J. Appl. Meteorol.*).

Smith, W.S., and C.-Y.J. Kao, "Using a Turbulence Radiative-Convective Model to Study the Cloud/Radiation with the FIRE Data" (to be published in *Monthly Weather Rev.*).

Similarity Landscapes: An Improved Method for Scientific Visualization of Information from Protein and DNA Database Searches

Norman Doggett, Los Alamos National Laboratory
Christopher Wills, Univ. of California, San Diego

We are working on a new method for gathering information from large DNA and protein data bases. Our method compares information obtained from multiple data base searches and edits the findings to remove the bulk of the comparisons (90%–95%) that contain little or no phylogenetic information. The information is then ordered in such a way as to build "similarity landscapes," which permit even very slight similarities in distantly related sequences to be detected.

Our similarity landscapes enable us to thoroughly examine the ever-increasing amounts of DNA-sequence data generated by the Human Genome Project, and they can be used to detect regions of functional interest in newly sequenced genes that might go unnoticed by less global searches.

We are currently examining the evolution of genes and DNA sequences over both long and short time spans. During the past year we found that AIDS viruses are subjected to strong and conflicting selection pressures, which helps to explain how they have adapted to their human hosts. We have also found that a recently discovered class of DNA sequences is more common in our genes that had previously been suspected. These sequences, called microsatellites, are associated with cancer and other diseases.

We are also developing ways to distinguish two kinds of evolution—divergent, from a common ancestor, and convergent, from two different ancestors. Determining evolutionary directions from molecular clues will tell us a great deal about our molecular ancestry.

Publications

Field, D. and C. Wills, "Purifying and Directional Selection Have Acted Simultaneously on the Genes of the Mammalian Mitochondrial Genome" (submitted to *Science*).

Wills, C., "Improving the Analysis of Phylogenetic Data" (to be published in *Comput. Chem.*).

Wills, C., "Topiary Pruning and Weighting Reinforce an African Origin for the Human Mitochondrial Tree" (to be published in *Evolution*).

Wills, C., "Topiary Pruning of the HIV and SIV Phylogenetic Tree" (to be published in *AIDS Research and Human Retroviruses*).

Wills, C., "When Did Eve Live? — An Evolutionary Detective Story" (to be published in *Evolution*).

Lithospheric Processes

W. Scott Baldridge

Our project addresses fundamental studies of the lithosphere, the earth's solid outer shell. Our technical goals are to develop better conceptual models of processes by which the lithosphere is formed and evolves. Oceanic and continental lithosphere is a boundary layer that rests on the deep, convecting mantle. Continental lithosphere preserves a geological record of crustal and upper mantle processes over the last several billion years. Our programmatic goals are to build on and broaden existing Laboratory expertise, to forge cooperative links with educational and corporate institutions, and to develop appropriate programmatic opportunities.

Our approach combines field geological, geochemical, and geophysical studies with laboratory analysis and numerical modeling. We use seismic waves from earthquakes to image the base of the crust and intracrustal fault zones, state-of-the-art mass spectrometers to measure sensitive isotopic ratios in magmatic rocks to quantify mantle melting processes, and the unique Los Alamos proton microprobe to quantify fluid-flow processes.

Our accomplishments include the first-ever trace-element microanalyses of individual mineral grains altered by extensive fluid flow in the middle crust. These data clarify chemical and physical parameters that control element mobility within the earth and will speed up the development of improved numerical models of fluid-flow processes. We also mapped a strike-slip fault in the upper crust in New Mexico, studied eruption mechanisms in a large magma chamber, and constructed a chronostratigraphic framework for volcanic rocks in the Ethiopian rift. Our work relates to verification, seismic techniques for reservoir characterization, geothermal energy exploration, mitigation of volcanic hazards, and fluid flow.

Nonlinear Analysis of Biological Sequences

David Torney

Predictions of the structures and functions of biological sequences are becoming increasingly important to science, medicine, and technology. The purpose of this project is to develop effective new computational and mathematical techniques that can be applied to analyzing biological sequences. We are developing detailed models for the evolution of biological sequences and techniques for using contact potentials to design new protein sequences.

We have used neural networks to characterize interacting amino acid residues in proteins, rederiving contact potentials. Much of the mathematical and computational work of this project is aimed at identifying features of biological sequences. We are developing new approaches to determining the secondary structure of RNA, and we are examining ways to efficiently use existing datasets of DNA sequences to predict whether or not a sequence codes for proteins. Our more-general approach appears to make more-accurate predictions than other existing methods, which could aid scientists in their search for genes. Our improvements might also lead to new techniques for identifying features of sequences that are less obvious but just as important, such as sequences that play a structural rather than coding role.

Publications

He, X., and M. Dembo, "Modeling Chemoattractant-Elicited Relocalization of Myosin Filaments in Dictyostelium" (to be published in *J. Biochem. Cell Biol.*).

Martijn, H, P. Stadler, and W. Fontana, "Smoothness within Ruggedness: The Role of Neutrality in Adaptation" (to be published in *Proc. Natl. Acad. Sci. U.S.A.*).

High-Performance Computations of Electron Microstructures

Alan Bishop

The purpose of this project is to model the novel quantum properties of semiconductor nanostructures fabricated and measured at UCSB by using dedicated molecular beam epitaxy and free-electron laser facilities. A new time-dependent density-functional approach has been developed which can systematically handle all the relevant physical interactions including external drive fields.

We have begun parallelization of the time-dependent density functional code on a Meiko CS-2 machine in preparation for its CM-5 implementation. We have applied the technique to model nonlinear driven quantum wells and identified harmonic generation and amplitude-dependent depolarization effects. We have also developed a Floquet state basis suitable for describing transitions between Landau levels in strong driving fields. This project is a paradigm for Los Alamos' core competency in theory, modeling, and high-performance computing and will impact programs in nanotechnology, semiconductor modeling, and mesoscale complexity. It takes advantage of an excellent complementarity of UCSB and Los Alamos skills and facilities.

Publications

Bewley, W.W., C.L. Felix, J.J. Plombon, et al., "Far-Infrared Second-Harmonic Generation in GaAs/AlGaAs Heterostructures: Perturbative and Nonperturbative Response" (to be published in *Phys. Rev. B*).

Galdrikian, B., B. Birnir, and M. Sherwin, "Nonlinear Multiphoton Resonances in Quantum Wells" (to be published in *Phys. Lett. A*).

Galdrikian, B., B. Birnir, and M. Sherwin, "Self-Consistent Floquet States for Periodically-Driven Quantum Wells" (to be published in *Phys. Rev. B*).

Salkola, M.I., A.R. Bishop, V.M. Kenkre, et al., "Coupled Quasiparticle-Boson Systems: The Semiclassical Approximation and Discrete Nonlinear Schrödinger Equation," *Phys. Rev. B* 52, 3824 (1995).

Wang, L., and A.R. Bishop, "Theory of Quantized Dynamic Capacitance Charging Spectroscopy in Nanostructures," *Phys. Rev. Lett.* 74, 4710 (1995).

Complex Systems—Prediction and Characterization

Ronnie Mainieri

In a complex system many parts interact to produce an overall behavior that appears to be simple. All the parts evolve in time forming a chaotic dynamic system. It is the chaotic nature of the dynamics that makes it difficult to study and simulate complex systems. Chaos means that small errors in setting up a complex system will lead to very different outcomes. This forces the conclusion that the individual time-evolution of a complex system is not very significant. Instead, complex systems, like other chaotic systems, are studied statistically. A special quantity, thought to be important in the dynamics of the system, is chosen (an observable) and its statistical properties computed from theory and determined from experiment. Because of the fundamental use of statistical quantities in the study of complex systems, probability distributions play a central role. Many of the areas of complex systems can be understood as the study of dynamic systems and their invariant probability distributions. Time-series analysis determines the dynamic system that generated a signal. To make predictions from the time series, the invariant measure of that dynamic system must be determined. The goal of studies of pattern formation in fluids is to describe the observed patterns in a simple manner (as a low-dimensional dynamic system) and how the observed features correlate to the behavior of parameters.

Research in complex dynamic systems has great development potential. Physical problems, just like problems in computer science, can be divided into two large groups: those that require a polynomial time to solve and those that require an exponential time. For example, if we wanted to know all the words of 6 letters that one can make out of the 26 letters of the alphabet, then the program has to at least make the list of $308915776 = 26 \times 26 \times 26 \times 26 \times 26 \times 26$ combinations, regardless of what method is used to generate the different combinations. The program that generates all the words is exponential because the number of possibilities grows geometrically with the length of the letters used in the word. If n letters are used, then one has to multiply 26 with itself n times. This quantity grows so fast, that no computer in the universe could ever generate all the words of length 56.

The word generation problem is very different from polynomial algorithms. Suppose we had two groups of words. Ten words in bag A and ten words in bag B. If we wanted to know all the combinations of two words, taking one word from bag A and one word from bag B, then it would be easy to generate the 100 possibilities ($100 = 10 \times 10$). Even if we had all one hundred thousand words normally found in an English dictionary, it would only produce a list with $10000000000 = 10^{10}$ = ten thousand million words. Easy for today's computers. For a list with n words, the final list is of length $n \times n$, or n^2. So in practice we have hopes of solving polynomial problems on a computer but no hope of solving exponential problems. The difficulty is that most problems we want to solve are exponential.

Complex-dynamic-systems research deals with the problems that require an exponential amount of work to solve. Just as there are no general algorithms to deal with nonpolynomial problems in computer science, we do not expect general methods for dealing with complex dynamic systems. What we do expect are efficient algorithms that solve the problem for all practical purposes. This analogy also explains the interdisciplinary nature of the research. Just as in computer science, the investigator can gain insight by posing the problem in different forms and areas. The exponential character of the problems in complex dynamic systems implies that they are close to impossible to solve with a computer if naive methods are used. Taming the exponential behavior may lead to great advances, and that is why researchers persist on working on this difficult problem. It may be possible to design complex molecules in a computer, to develop efficient methods to study fluid flow, and to simulate biological systems.

Many of the systems studied in physics are chaotic systems in disguise. The chaos manifests itself in the slow convergence of physical quantities. Disordered systems and localization, classical spin systems, transport in mesoscopic systems, and the electronic configuration of molecules are all examples of chaotic systems. The common thread among these systems is their description in terms of a transfer operator (transfer matrix, Perron-Frobenius operator, trace of a Green's function). These systems are chaotic and dense with periodic orbits, and the invariant measure of the operator can be understood in terms of these orbits. This leads to a cycle expansion, a rapidly converging series.

Using periodic orbits, even if they are unstable, can improve the accuracy of simulations and lead to a better understanding of the resulting dynamics. In one example, Bauer and Mainieri

demonstrated that Monte Carlo simulations can be very misleading. In a simple model, we used the Monte Carlo method to compute the same quantity being computed with periodic orbits. Even though the Monte Carlo method had converged to an answer by all practical criteria, it converged to the wrong answer. If the more accurate periodic-orbit calculation had not been available, we would have never been able to detect this subtle failure of the Monte Carlo method. This observation has led us to re-examine other Monte Carlo procedures.

The prime example of a complex physical system is a turbulent fluid. To study the patterns formed in fluid motion one should, in principle, understand the high-dimensional fluid flow. This is not practical because the system is chaotic (in most cases—turbulent). This is also counter-intuitive, as after observing the fluid-flow experiments one can see that certain simple features dominate the dynamics. The problem in pattern formation has been in finding a precise description of these simple features. Phrased differently: Is there an effective low-dimensional dynamic-system model that captures most of the dynamics of the fluid flow and its patterns? The study of pattern formation is a concrete problem that offers a test bed for the problems of characterizing high-dimensional dynamic systems and the measures they generate. It is also an open problem in physics. Patterns affect the transport properties in many physical systems and they must be accounted for. This is not possible unless there are simple (low-dimensional) dynamics. Examples where patterns affect the physical properties of a system are weather and both diffusion and conductivity properties in fluids.

In a breakthrough, we described a turbulent-fluid system with coherent structures by a simple statistical model. The model approximates the motion of Earth's atmosphere and the formation of tornadoes. A simple lattice model with groups of sites with the same value representing tornadoes accurately described the number and size of these tornadoes. This is the first time that a simple model has been constructed to describe a complex-fluid system.

Fluid models, such as the one producing the tornadoes, cannot be accurately simulated on a computer because the computer needs to use a very large grid or a large number of Fourier components to complete the job properly. In our program we have developed a rigorous estimate on how many modes the computer must use to obtain accurate simulations of the Navier-Stokes equation.

Under this project we have also established that soliton-like solutions exist even for two-dimensional dissipative systems. We explained how they are formed and how these solitons interact. Our research sheds light on the poor performance of platinum catalytic converters used in cars. We also studied a different type of pattern-formation system. We demonstrated an Ising-Bloch transition to be the mechanism for the formation of spiral waves and propagating fronts in a reaction diffusion system. These systems occur in biological systems and in industrial chemical processes.

Publications

Bauer, O., and R. Mainieri, "The Convergence of Chaotic Integrals" (submitted to *Chaos*).

Brand, H., and R. Deissler, "Stable Spatially Localized Solutions and Holes in Optical Bistability," *Physica A* **216,** 288 (1995).

Brown, R., N. Rulkov, and N. Tufillaro, "Synchronization of Chaotic Systems: The Effects of Additive Noise and Drift in the Dynamics of the Driving," *Phys. Rev. E* **50,** 4488 (1994).

Deissler, R., and H. Brand, "Interaction of Breathing Localized Solutions for Subcritical Bifurcations," *Phys. Rev. Lett.* **74,** 4847 (1995).

Deissler, R., and H. Brand, "Two-Dimensional Localized Solutions for Subcritical Bifurcations in Systems with Broken Rotational Symmetry," *Phys. Rev. E* **51,** R852 (1995).

Doering, C., and E. Titi, "Exponential Decay Rate of the Power Spectrum for Solutions of the Navier-Stokes Equations," *Phys. Fluids* **7,** 1384 (1995).

Ecke, R., Y. Hu, R. Mainieri, et al., "Excitation of Spirals and Chiral Symmetry Breaking in Rayleigh-Benard Convection," *Science* **270,** 1704 (1995).

Elphick, C., A. Hagberg, and E. Meron, "Dynamic Front Transitions and Spiral-Vortex Nucleation," *Phys. Rev. E* **51,** 3052 (1995).

Gjaja, I., "Closed-Form Expressions for the Noncompact part of SP(2n), Comments" (submitted to *Phys. Rev. Lett.*).

Millonas, M., and C. Ray, "Relaxation Kinetics of Nonlinear-Systems Coupled to a Nonequilibrium Bath," *Phys. Rev. Lett.* **75,** 1110 (1995).

N. Tufillaro, P. Wyckoff, R. Brown, et al., "Topological Time-Series Analysis of a String Experiment and Its Synchronized Model," *Phys. Rev. E* **51,** 164 (1995).

Covariation of Mutations: A Computational Approach for Determining Function and Structure from Sequence

Alan Lapedes

Solving the problem of inverse protein folding is not an easy task. The protein database currently lists over forty attributes per amino acid for each protein. For the most part, the impact of each attribute is not well understood. Not only must the important attributes be identified, but the relationship between attributes and structure must be analyzed. We have approached this problem with neural nets as a research tool: given a set of inputs and some output function, a neural net can select which inputs are important and can model the relationship between the inputs and the target outputs.

A vital constituent part of inverse protein folding is to model the probability of each of the twenty amino acids in particular positions in a protein sequence, based on the geometric features of that position within the structure of the protein. To this end, we have experimented with most of the geometric feature sets used by the major groups studying inverse folding. For two amino acids in a contact pair, these feature sets describe the geometry and environment of the pair such as C-b distance between the amino acids and the solvent exposure of the individual amino acids. Determining the geometric features that allow amino acid usage is a key to developing more accurate inverse folding potentials. Such accurate potentials can be used in homology modeling of proteins to determine the structure of sequences for which x-ray crystallographic data are unavailable.

Development of an Integrated System for Estimating Human Error Probabilities

Heidi A. Hahn

Human Reliability Analysis (HRA) is a collection of methodologies to probabilistically evaluate human performance in systems. Using information about operational parameters and operator characteristics, an analyst selects a human error probability (HEP) estimate from an available source based on his or her assessment of "best match." Various methods produce estimates that are a better or worse match to the situation of interest. Sometimes there is no "best match," leaving the analyst the confusing task of integrating multiple estimates. Poor selection or integration produces invalid estimates and may underestimate risk.

This project focuses on the design of an expert system that will remedy this problem by (1) allowing input of situation-specific information, (2) comparing the situation to the methodological approaches and identifying "matches," (3) providing valid estimates based on selected matches, and (4) providing a weighted average estimate.

Our approach involves producing a HEP database, including information about underlying assumptions, developing an expert system having the above capabilities, and creating modeling techniques to explore alternative scenarios where system behavior depends upon human performance.

We have identified all major HRA data sources, designed a database and entered data sources, databased additional reference literature, and incorporated mechanisms to operate on the HEP data to account for performance-shaping factors. We also began evaluating the major human performance modeling simulation packages that are commercially available and evaluating expert system software. Rule generation for the expert system is in the conceptual design phase.

Development of an Automated Core Model for Nuclear Reactors

Russell Mosteller

This project is aimed at developing an automated package of codes that can model the steady-state behavior of various nuclear-reactor cores at any point during the reactors' operating lifetimes. As an added benefit, the data produced by the steady-state analysis can also be used as input to the transient-analysis code for subsequent safety analysis of the reactor analyzed at a specific point in its operating lifetime.

The basic capability to perform steady-state reactor-core analysis already exists in the combination of the HELIOS lattice-physics code and NESTLE core-simulation code. The purpose of our project is to complete the automated package by obtaining a cross-section library for HELIOS, developing a linkage code to transform HELIOS output into NESTLE input, developing additional steady-state thermal-hydraulics modules for NESTLE, and benchmarking HELIOS and NESTLE both separately and in combination.

We have successfully benchmarked NESTLE against several widely accepted benchmark problems and against operating data from four pressurized water reactors. In addition, we leased a cross-section library from Scandpower, Inc. (the developers of HELIOS) and began the benchmarking of HELIOS by comparing results from it with those produced by the MCNP Monte Carlo code.

Publications

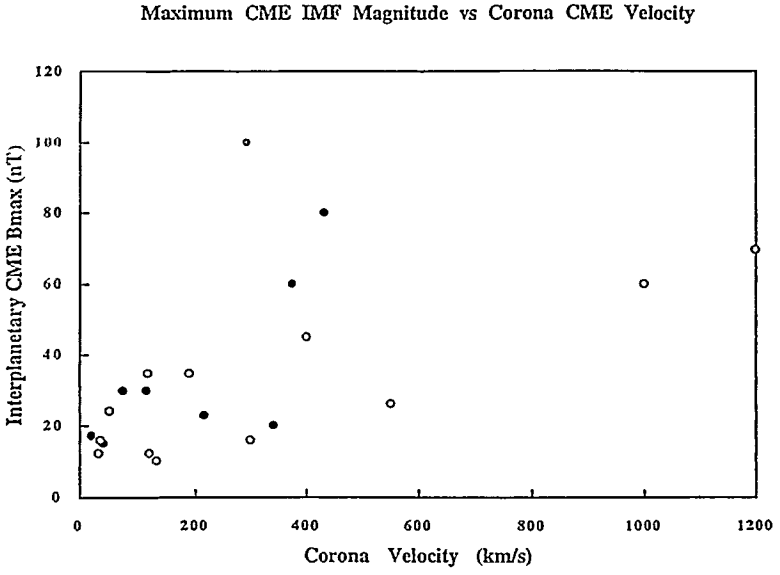
Mosteller, R.D., "Benchmarking of NESTLE Against Measured PWR Data at Beginning of Life," *Trans. Am. Nucl. Soc.* 73, 369 (1995).

Transport Processes in Space Plasmas

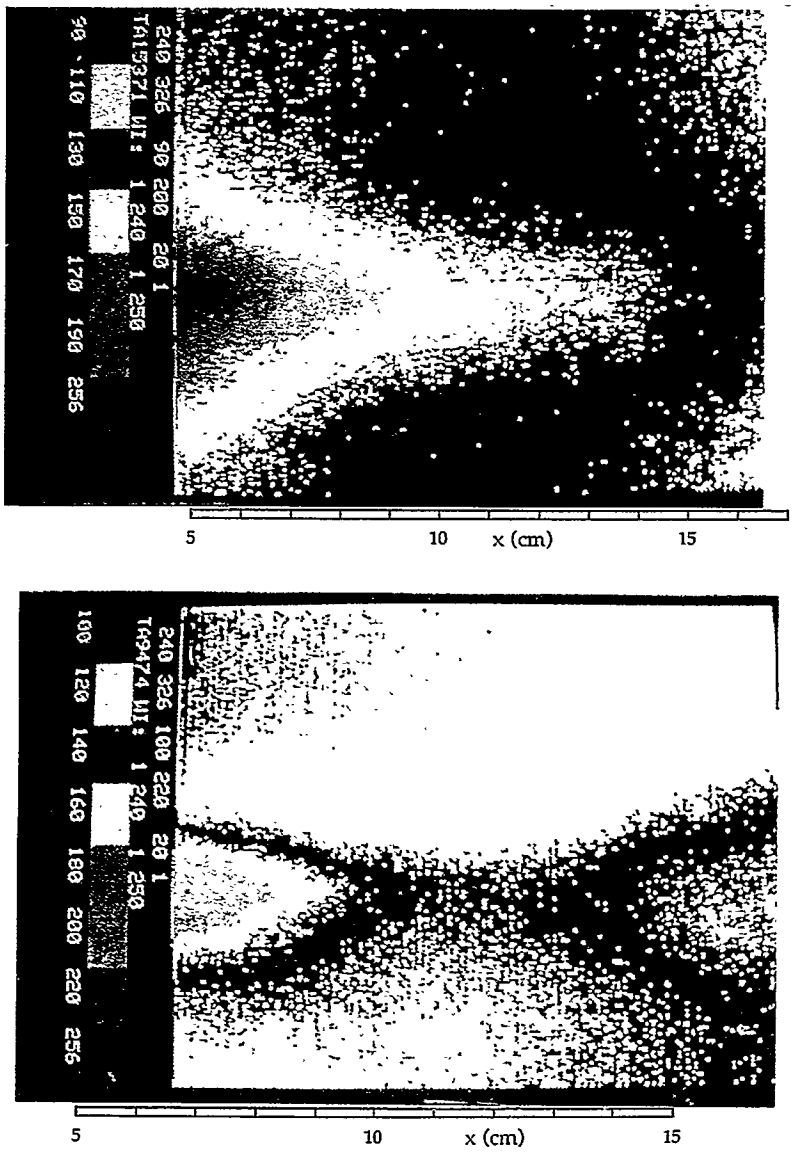
Joachim Birn

By combining efforts in space data analysis with theory and with laboratory and computer simulations, this project intends to advance our understanding of solar-terrestrial interaction through space-plasma processes. A study of coronal mass ejections established a close relation between their speed and interplanetary magnetic field enhancement, as shown in the first accompanying figure. This is highly relevant for predicting geomagnetic storms, which represent the primary solar impact on the earth's magnetosphere. A laboratory simulation of solar wind/magnetosphere interaction revealed characteristically different magnetotail structures for northward and southward interplanetary magnetic fields (see second figure).

Local simulations of the magnetopause (the solar wind/magnetosphere interface) concentrated on the role of surface waves on diffusion at this boundary and showed that they do not lead to significant transport of space plasma. These studies have also shed more light on the nature of MIAOW waves (so-called waves that have dispersion properties between mirror and slow modes). These waves are useful in diagnosing the rate of plasma transport across the magnetopause. Using linear Vlasov theory and hybrid computer simulations, we investigated the consequences of the electromagnetic proton anisotropy instability inside the terrestrial magnetosphere. We were able to obtain closed-form



Maximum magnetic field amplitude of coronal mass ejections as a function of their coronal velocity. Open data points represent cases with high confidence levels, and closed data points represent cases with moderate confidence levels.



Characteristic tail structures of magnetospheres simulated in laboratory experiments, as seen by digitized photographs obtained with a fast-gated optical imager. The top panel shows a y-type structure associated with northward interplanetary magnetic field; the bottom panel shows an x-type structure associated with southward IMF.

expressions, which are quite consistent with observations, for the instability threshold and the effects on the cool proton temperature.

Theoretical investigations of dust-plasma interactions in various space environments focused on collective processes (waves and instabilities). We were then able to explain the increase of ion temperature with radius in Saturn's inner magnetosphere by ion heating resulting from the nonlinear development of a dust-acoustic instability in the E-ring.

Publications

Chow, V.W., and M. Rosenberg, "Electrostatic Ion Cyclotron Instability in Dusty Plasmas," *Planet. Space Sci.* 43, 889 (1995).

Chow, V.W., and M. Rosenberg, "Electrostatic Ion Cyclotron Instabilities in Negative Ion Plasmas" (submitted to *Phys. Plasmas*).

Elphic, R.C., "Observations of Flux Transfer Events; A Review," in *Physics of the Magnetopause, Geophys. Monogr. Ser.* (Amer. Geophys. Union, Washington D.C., 1995), p. 225.

Gary, S.P., M.F. Thomsen, L. Yin, et al., "Electromagnetic Proton Cyclotron Instability: Interactions with Magnetospheric Protons" (to be published in *J. Geophys. Res.*).

Gary, S.P., L. Yin, and D. Winske, "Electromagnetic Proton Cyclotron Instability: Heating of Cool Magnetospheric Helium Ions" (submitted to *Annales Geophysicae*).

Kuo, H., C.T. Russell, and G. Le, "Statistical Studies of Flux Transfer Events" (submitted to *J. Geophys. Res.*).

Le, G., C.T. Russell, and J.T. Gosling, "Structure of the Magnetopause for Low Mach Number and Strongly Northward Interplanetary Magnetic Field," *J. Geophys. Res.* **99**, 23723 (1994).

Lindsay, G.M., J.G. Luhmann, C.T. Russell, et al., "CME Characteristics in the Inner Heliosphere: Relationship to Corona Velocity" (submitted to *J. Geophys. Res.*).

Maravilla, D., K.A. Flammer, and D.A. Mendis, "On the Injection of Fine Dust from the Jovian Magnetosphere," *Astrophys. J.* 438, 968 (1995).

Maravilla, D., K.R. Flammer, and D.A. Mendis, "The Nature of the Orbits of Charged Dust Injected into the Jovian Magnetosphere During the Tidal Break-Up of Comet Shoemaker-Levy 9" (to be published in *Astrophys. Space Sci.*).

McKean, M.E., N. Omidi, and D. Krauss-Varban, "Wave and Ion Evolution Downstream of Quasi-Perpendicular Bow Shocks," *J. Geophys. Res.* **100**, 3427 (1995).

Omidi, N., and Winske, D., "Diffusion at the Magnetopause: Hybrid Simulations," *J. Geophys. Res.* **100**, 11923 (1995).

Omidi, N., and D. Winske, "Kinetic Structure of the Magnetopause as Inferred from 1-D Hybrid Simulations," *J. Geophys. Res.* **100**, 11935 (1995).

Rosenberg, M., and N.A. Krall, "Low-Frequency Drift Instabilities in a Dusty Plasma" (submitted to *Phys. Plasmas*).

Rosenberg, M., and N.A. Krall, "Modified Two-Stream Instabilities in Dusty Plasmas," *Planet. Space Sci.* **43**, 619 (1995).

Rosenberg, M., and D.A. Mendis, "UV-Induced Coulomb Crystallization in a Dusty Gas," *IEEE Trans. Plasma Sci.* **23**, 177 (1995).

Scurry, L., C.T. Russell, and J.T. Gosling, "A Statistical Study of Accelerated Flow at the Dayside Magnetopause," *J. Geophys. Res.* **99**, 14815 (1994).

Walthour, D.W., B.U.O. Sonnerup, R. C. Elphic, et al., "Double Vision: Remote Sensing of a Flux Transfer Event with ISEE 1 and 2," *J. Geophys. Res.* **99**, 8555 (1994).

Winske, D., S.P. Gary, M.E. Jones, et al., "Ion Heating in a Dusty Plasma Due to the Dust/Ion Acoustic Instability," *Geophys. Res. Lett.* **21**, 2069 (1995).

Winske, D., V.A. Thomas, N. Omidi, "Diffusion at the Magnetopause: A Theoretical Perspective," in *Physics of the Magnetopause, Geophys. Monogr. Ser.* (Amer. Geophys. Union, Washington D.C., 1995), p. 321.

Yur, G., H.U. Rahman, J. Birn, et al., "An Improved Simulation Facility for Magnetospheric Modelling" (to be published in *J. Geophys. Res.*).

Yur, G., H.U. Rahman, J. Birn, et al., "Magnetotail Structures in a Simulated Earth's Magnetosphere" (to be published in *J. Geophys. Res.*).

Geoscience, Space Science, and Astrophysics

Analysis and Visualization of Global Magnetospheric Processes

Dan Winske

The purpose of our project is to demonstrate the use of coupled, large parallel computers with graphical interfaces to visualize spacecraft data with real-time processing. We use the CM-5 to calculate the global features of particle distributions (velocity and position) as a function of time and then transfer the data, via a high-speed network, to high-end workstations where it is analyzed. The resulting visualization of the data allows us to construct a global picture of particle fluxes in the magnetosphere based on a very small number of satellite measurements that will serve as boundary conditions. We have used this method to study effects on ions in the magnetotail due to packets of low-frequency waves.

In the context of first applications of our new computational tool, we used the existing code to analyze the changes in the distribution function due to a major electromagnetic shock wave as measured onboard a moving satellite. On March 24, 1991, the Combined Release and Radiation Effects Satellite observed an example of one such event. The resulting modification of the magnetosphere caused a strong bunching and energization of a subset of particles, that happened to be at the right magnetic longitude and that the satellite observed as drift echoes.

Our simulated time-dependent fluxes and the energy spectra are in good agreement with the available particle data. This event will serve as a prototype for future analysis of strong magnetospheric perturbations and their effects on populations of charged, energetic particles. We started to prepare the Advanced Visualization System computer program for incorporation in our simulation code. Our project has application to auroral, ionospheric, and magnetospheric phenomena; elementary and classical processes in plasmas; and plasma kinetics, transport, and impurities.

Subsurface Noble Gas Transport at the Nevada Test Site

Joseph Thompson

Numerous sites in the DOE complex are contaminated as a result of weapons testing and old waste disposal practices. Studies of contaminant transport modeling at the Nevada Test Site have recently focused on long-term ground water contamination.

The purpose of this project is to assess the transport of tritiated water and krypton-85 through ground water, soil, and the atmosphere. We are applying a series of analytical models of increasing complexity to identify the dominant transport processes.

We have data on levels of tritium and krypton-85 eluted with ground water from a pumped well adjacent to an underground nuclear test. Collected from 1974 to 1991, these data were gathered as part of a field experiment to track ground water and radionuclide migration from a nuclear detonation cavity. Our analysis involves formulating a hypothesis about the immediate post-shot effects at the site and then developing mathematical models that correspond to the hypothesis and observed data.

We believe that detonation of the device produced a large volume of carbon dioxide gas that transported krypton-85 upward during the chimney collapse. The krypton-85 was thus deposited throughout the chimney and perhaps even above the water table. We are now predicting how this krypton-85 would elute when pumping began at the auxiliary well. We have evaluated the use of a radially converging flow model for the pumped water (the Sauty model), but believe that the water probably had an initial vertical movement toward a hydrologically conductive zone before it radially converged.

Our next effort will be to apply the Los Alamos TRACR3D code to model the elution data using the same hypothesized initial distribution. The application of this code to the data, if successful, may prove its utility in interpreting underground movement of other radionuclides in different locations.

The Microbial Dissolution of Iron from Iron-Bearing Minerals

Larry Hersman

All life forms require iron—the fourth most abundant element in the geosphere. However, iron is virtually insoluble at physiological pH in oxidizing environments and exists in the geosphere mainly in the form of highly insoluble oxides and hydroxides: it is not known how organisms make iron soluble for biological use.

To study this question we have observed the metabolic and physiological responses of microbes to mineral-iron supplements. We have also studied structural changes on mineral surfaces caused by microbially mediated dissolution. Our results have provided a better understanding of iron uptake by microorganisms and the role it plays in mineral-surface weathering.

We have determined that the *Pseudomonas* sp., a strict aerobe, can extract iron from hematite and that the siderophore (a peptide with a molecular weight of ~500 daltons) produced by this microorganism plays a large role in dissolving hematite. We also learned that one or more extracellular compounds produced by the *Pseudomonas* sp. can reduce the iron in hematite and that these reducing compounds—with molecular weights between 500 and 3000 daltons—are relatively heat stable.

We also found that the metabolic response of *Pseudomonas* sp. depends on the source of the iron. The bacterial response to hematite was particularly noteworthy: hematite appeared to induce several metabolites (substances involved in metabolic processes), including siderophores. We used inductively coupled plasma atomic absorption to determine that most of the iron was not concentrated in the siderophores. We confirmed this result with high-performance liquid chromatography (HPLC), which showed peaks at 37 and 55 minutes; iron was eluted from the siderophore at 90 minutes.

Of the mineral-surface particles that we examined with the atomic force microscope (AFM), few showed dissolution features; those that did had large surface disturbances. We learned in our AFM studies that sample preparation—choosing the proper starting materials and minimizing contaminants on examined surfaces—is important. Using many control samples is also important, and the procedures used to prepare experimental samples must also be used to prepare control samples—artifacts can be introduced at any point during specimen preparation. Because of possible artifacts and the similarities of surface structure, composition, microtopography, and reactivity of various samples, we found that we obtained meaningful results only when we imaged each sample at many sites and under many conditions.

Publications

Hersman, L., T. Lloyd, and G. Sposito, "Siderophore-Promoted Dissolution of Hematite" (to be published in *Geochim. Cosmochim. Acta*).

Hersman, L., P. Maurice, and G. Sposito, "Iron Acquisition from Hydrous Fe(III) Oxides by an Aerobic *Pseudomonas* Sp." (to be published in *Chem. Geol.*).

Maurice, P., J. Forsythe, L. Hersman, et al., "Applications of Atomic Force Microscopy to Studies of Organic and Microbial Interactions with Hydrous Fe(III) Oxides" (to be published in *Chem. Geol.*).

Remote Sensing Science—New Concepts and Applications

Siegfried Gerstl

This six-month feasibility study was started and completed within FY 1995. Our main objective was to evaluate emerging new technologies and concepts in remote sensing science and to identify possible new applications of innovative approaches. Our work supports the Laboratory's expanding competencies in nonproliferation, environmental monitoring, and nuclear waste identification and processing.

We carried out a comprehensive scientific review to assess the state-of-the-art technologies and concepts in satellite remote sensing science, as it may be applied to the above-mentioned competencies. We have evaluated and studied active (e.g., lidar) and passive remote sensing techniques, including modeling, in the context of a feasibility analysis.

The main result from this project was the identification of the three most-promising emerging scientific subfields in remote sensing: (1) hyperspectral remote sensing science, (2) laser-assisted remote sensing of atmospheric transport parameters, and (3) new remote sensing concepts. We expect that the initiation of a strategic scientific thrust encompassing these technical components will provide an optimal science and technology base leading to expansion of the Laboratory's competencies in nonproliferation and environmental monitoring in support of the Laboratory's core mission to reduce the nuclear danger.

MOLECULAR CHARACTERIZATION OF FLOW-SORTED MAMMALIAN CENTROMERES

L. Scott Cram, Los Alamos National Laboratory
Barbara Hamkalo, Univ. of California, Irvine

We are characterizing the proteins from the centromere region of mammalian chromosomes to better understand the fundamental mechanisms underlying cellular processes, such as regulation of gene expression, differential condensation, and chromosome segregation.

Our experiments involve the use of minichromosomes, which contain functional centromeres and telomeres but little other chromosomal material, as an enriched source of centromeric proteins. The information we are obtaining will be useful for defining the molecular basis of hereditary defects that are characterized by aberrant centromere structure and/or function. Such information also brings us closer to our eventual goal of constructing an artificial mammalian chromosome for use in basic research or for adaptation as a vector for gene therapy.

We have detected polypeptides that are one-twentieth as abundant as the histone proteins in our samples, suggesting that we may eventually be able to identify the less-common, as well as the more-abundant, proteins in a sample. Our data also suggest that flow cytometric analysis may cause some proteins to cross-link to DNA, an observation that will be reported in the literature. We are currently evaluating other techniques for confirming this finding.

COMPETENCY DEVELOPMENT IN ANTIBODY PRODUCTION FOR CANCER CELL BIOLOGY

Min S. Park

Investigating the roles proteins play in complex biological processes requires the use of antibodies against specific cellular proteins. The objective of this project is to develop the technical capabilities, including the use of recombinant technology, for producing high-quality antibodies that we can use in our research on cancer development.

Our work includes both conventional and recombinant antibody-production techniques. The conventional method involves purifying cellular proteins, or antigens, and injecting them into an animal, which in turn produces antibodies to the antigen. The recombinant techniques involve isolating the genes that code for the desired antigen or antibody and inserting the genes into an expression vector. Recombinant technology enables us to make relatively large amounts of very pure antigen and antibody.

In the past year, we began to produce antigens and antibodies that are critical to identifying and monitoring the expression of crucial proteins involved in cell cycle checkpoints, the regulation of cell division, and the rate-limiting steps of DNA repair. Specifically, we produced five antigens using recombinant technology and three antibodies using conventional approaches and are working to further refine our recombinant antibody production.

Publications

Cloud, K.G, B. Shen, G.F. Strniste, et al., "XPG Protein Has a Structure-Specific Endonuclease Activity," *Mutat. Res.* 347, 55–60 (1995).

Knauf, J.A., S.H. Pendergrass, B.L. Marrone, et al., "Multiple Nuclear Localization Signals in XPG Nucleus" (to be published in *Mutat. Res.*).

Park, M.S., "Expression of Human RAD52 Confers Resistance to Ionizing Radiation in Mammalian Cells," *J. Biol. Chem.* 270, 15467–15470 (1995).

Park, M.S, J.A. Knauf, S.H. Pendergrass, et al., "UV-Induced Movement of the Human DNA Repair Protein XPG in the Nucleus"

(to be published in *Proc. Natl. Acad. Sci. U.S.A.*).

Shen, Z., K.G. Cloud, D.J. Chen, et al., "Specific Interactions Between the Human RAD51 and RAD52 Proteins" (submitted to *J. Biol. Chem.*).

Shen, Z., S.R. Peterson, M.S. Park, et al., "Self-Association of Human RAD52" (to be published in *J. Biol. Chem.*).

Applications of Optical Trapping to Single-Molecule DNA Sequencing

Richard Keller, Los Alamos National Laboratory
Greg Sonek, Univ. of California, Irvine

The goal of this project is to investigate the use of optical trapping techniques for DNA sequencing. We will also combine optical trapping techniques with fluorescence microscopy to investigate the structure of the DNA, determine its strength in a flowing stream, and collect other basic biophysical data.

A trap fluorescence-detection system in a flow geometry will contribute not only to DNA sequencing but to all other systems that require rapid fluorescence detection, scattering, sizing, and refractive index data on large numbers of samples. Such optical trapping techniques also set the stage for new studies of cells and chromosomes, such as looking for photochemical changes within cells and determining how life cycle functions are altered by external radiation sources or trapped radiation. It also provides a means for identifying and sorting specific antibody-tagged beads, cells, and molecules.

We have successfully demonstrated optical trapping in laminar flow streams and have characterized the trapping process as a function of fluid flow velocity, chamber dimension, trapping depth, incident laser power, and fluorescence measurement geometry. In particular, we integrated an optical laser trap with fluorescence excitation/emission capabilities with a flow cytometer for the study of microparticle confinement and off-axis fluorescence detection. At the trapping wavelength of 1064 nm, we can simultaneously trap and displace 2-μm-diameter fluorescent latex microspheres by up to ±20 μm by scanning the trapping beam in directions parallel and perpendicular to the flow stream while measuring particle fluorescence.

With fluorescence signal-to-noise ratios in excess of 30 dB, we can trap and measure particles in flow streams with velocities of up to 12 mm/s. We have also shown that we can noninvasively position samples upstream or downstream of the detection probe volume, a feature integral to the implementation of single-molecule detection techniques. Our current efforts are directed toward trapping, cleavage, and fluorescence measurements of DNA fragments attached to microspheres in rapid flow streams.

Publications

Wang W., Y. Liu, G.J. Sonek, et al., "Optical Trapping and Fluorescence Detection in Laminar Flow Streams," *Appl. Phys. Lett.* **67**, 1057 (1995).

Development of Biosensors/Probes Based on Spectroscopic Monitoring of Enzymes and Other Proteins Encapsulated in Sol-Gel Glasses

William Woodruff

This project involves the exploration and development of a new type of biosensors and bioprobes. Our goal is to apply advanced spectroscopic methods to the development of biosensors and bioprobes whose sensing elements consist of enzymes and other proteins encapsulated in optically transparent sol-gel glasses. Biosensors detect and measure analytes using encapsulated biomolecules, while bioprobes examine the encapsulated biomolecules to elucidate their physiological or biochemical functions or structures.

Our specific objectives are (1) to use advanced spectroscopic methods to characterize encapsulated biomolecules and their interaction with the porous glass matrix and to monitor the effect of different processing conditions; (2) to characterize similarly the interactions of the encapsulated biomolecules with potential substrates or ligands; and (3) to incorporate the above information into the development of sensing elements for use in biosensors and bioprobes.

We have demonstrated the usefulness of sol-gel-glass-

encapsulated myoglobin (Mb) as a biosensor and a bioprobe. First, we determined the linear relationship between dissolved oxygen in water and the rate of change of the absorbance of the encapsulated Mb. Second, we identified what appears to be unique transport behavior of dioxygen in Mb-containing sol-gel monoliths. And third, we developed a new experimental system based on sol-gel technology that can be used to study the fundamental mechanism of auto-oxidation of Mb and to test the possibility that a unique intermediate is involved.

Structure, Dynamics, and Function of Biomolecules

Hans Frauenfelder

This project enhances Los Alamos' core competency in bioscience and biotechnology by building on our present strengths in experimental techniques, theory, high-performance computing, modeling, and simulation as applied to biomolecular structure, dynamics, and function. Specifically, we propose to strengthen neutron/x-ray scattering, x-ray crystallography, nuclear magnetic resonance (NMR), laser, and optical spectroscopies.

In our first year we have (1) made significant advances in neutron-scattering instrument development; (2) upgraded a Monte Carlo–based computer code to determine the feasibility and parameter performance of various neutron spectrometers to be used on a long-pulse neutron spallation source; and (3) initiated scattering applications to receptor/ligand interactions focusing initially on the human serum transferrin protein, its receptor, and complexes of the two. Results from our neutron spectrometer simulations were presented at the Workshop on Neutron Instrumentation for a Long Pulse Spallation Source held at Lawrence Berkeley Laboratory, April 18-21, 1995.

To foster interactions between theory and experiment and between the biological and physical sciences, we have also organized two lecture series: (1) "Biology for Physicists" (Los Alamos lecturers) and (2) "Issues in Modern Biology" (distinguished external lecturers). Fifteen distinguished lecturers have been recruited, five of whom are Nobel Prize winners.

Publications

Chu, K., R.M. Ernst, H. Frauenfelder, et al., "Light-Induced and Thermal Relaxation in a Protein," *Phys. Rev. Lett.* **74**, 2607 (1995).

Frauenfelder, H., "Complexity in Proteins," *Nature Structural Biology* **2**, 821 (1995).

Frauenfelder, H., "From Symmetry to Complexity," *Chinese J. Phys.* **32**, 1045 (1994).

Frauenfelder, H., "The Mössbauer Effect and Biological Physics," *Hyperfine Interactions* **90**, 21 (1994).

Frauenfelder, H., "Proteins—Paradigms of Complex Systems," *Experientia* **51**, 200 (1995).

Frauenfelder, H., and H.C. Berg, "Physics and Biology," *Phys. Today* **47**, 20 (1994).

Frauenfelder, H., and P.G. Wolynes, "Biomolecules: Where the Physics of Complexity and Simplicity Meet," *Phys. Today* **47**, 58 (1994).

Frauenfelder, H., G.U. Nienhaus, and R.D. Young, "Relaxation and Disorder in Proteins," in *Disorder Effects in Relaxational Processes*, A. Richert and A. Blumen, Eds. (Springer, Berlin, 1994), p. 591.

Johnson, J.B., D.C. Lamb, H. Frauenfelder, et al., "Ligand Binding to Heme Proteins: VI. Interconversion of Taxonomic Substates in Carbonmonoxy Myoglobin" (submitted to *Biophys. J.*).

Mitchell, R.D., G.A. Olah, J. Corbin, et al., "The Effect of cGMP on the Solution Structure of Type Ia cGMP-Dependent Protein Kinase (PKG)," *Biophys. J.* **68**, 448 (1995).

Nienhaus, G.U., J.R. Mourant, K. Chu, et al., "Ligand Binding to Heme Proteins: The Effect of Light on Ligand Binding in Myoglobin," *Biochem.* **33**, 13413 (1994).

Olah, G.A., D.M. Gray, C. Gray, et al., "Structures of fd Gene 5 Protein/Nucleic Acid Complexes: A Combined Solution Scattering Electron Microscopy Study," *J. Mol. Bio.* **249**, 5760 (1995).

Olah, G., and J. Trewhella, "A Model Structure of the Muscle Protein Complex 4Ca2+.Troponin C.Troponin I Derived from Small-Angle Scattering Data," *Biochem.* **33**, 12800 (1994).

Sunnerhagen, M., G.A. Olah, J. Stenflo, et al., "Calcium Binding to the EGF Domain in Gla-EGF Module Pair of Coagulation Factor X Induces Domain Interactions," *Biophys. J.* **68**, 187 (1994).

THE SOLUTION STRUCTURE OF THE cAMP-DEPENDENT PROTEIN KINASE

Jill Trewhella

Understanding the molecular basis for biochemical regulation is a fundamental problem in human medicine. Unregulated or uncoordinated activities generally lead to pathological conditions and, if not corrected, to uncontrolled proliferation or cell death. Our project addresses this fundamental question with studies of the cAMP-dependent protein kinase, which serves as a central model for modulation of cell function by protein phosphorylation, one of the most important mechanisms of cell regulation. Our objective is to determine the molecular mechanism of the catalytic function of the kinase and its regulation by cAMP.

Protein kinase is a dimer of dimers (R_2C_2), where C and R designate the catalytic and regulatory sunbunits, respectively. Free C is fully competent to catalyze the phosphorylation of proteins. The catalytically inactive holoenzyme is activated when cAMP binds to R, which exposes the catalytic site on C, allowing access to protein substrates. We used small-angle scattering data in combination with crystal-structure data to solve the solution structure of C in the presence and absence of pseudosubstrate.

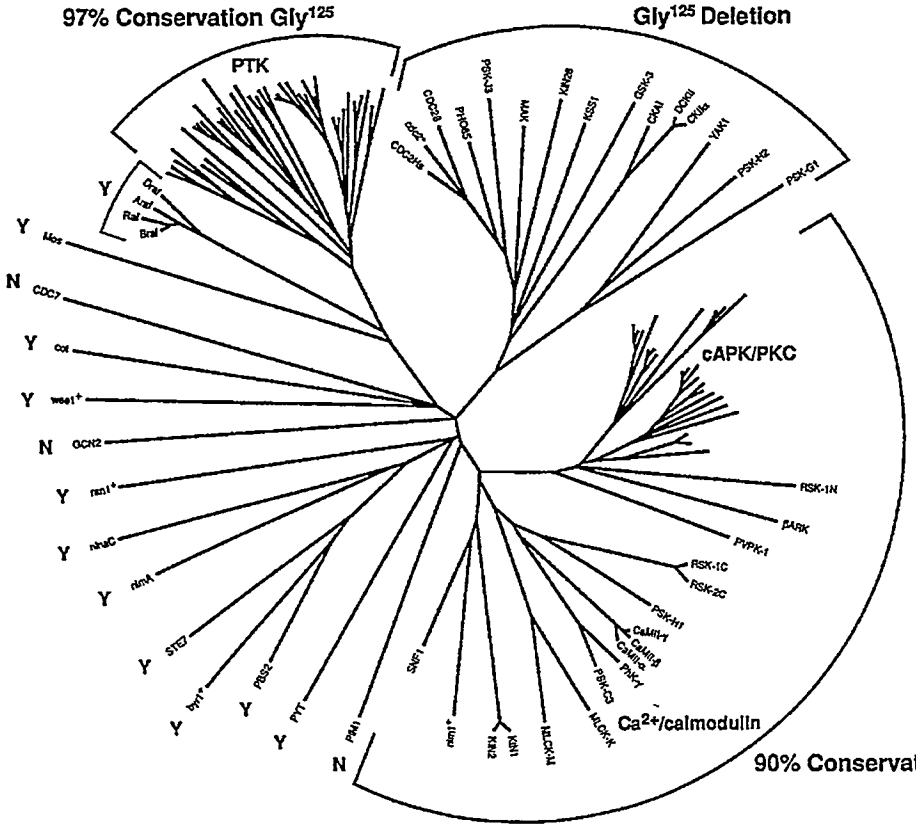
The catalytic subunit features upper and lower domains that move relative to each other upon substrate binding, bringing the key elements of the active site of the protein into contact with each other and the substrate. This movement is made possible by a pair of glycine residues that form a flexible hinge structure (at positions 125 and 126 in the amino acid sequence) and are positioned in the region of the polymer chain that connects the large and small domains.

Publications

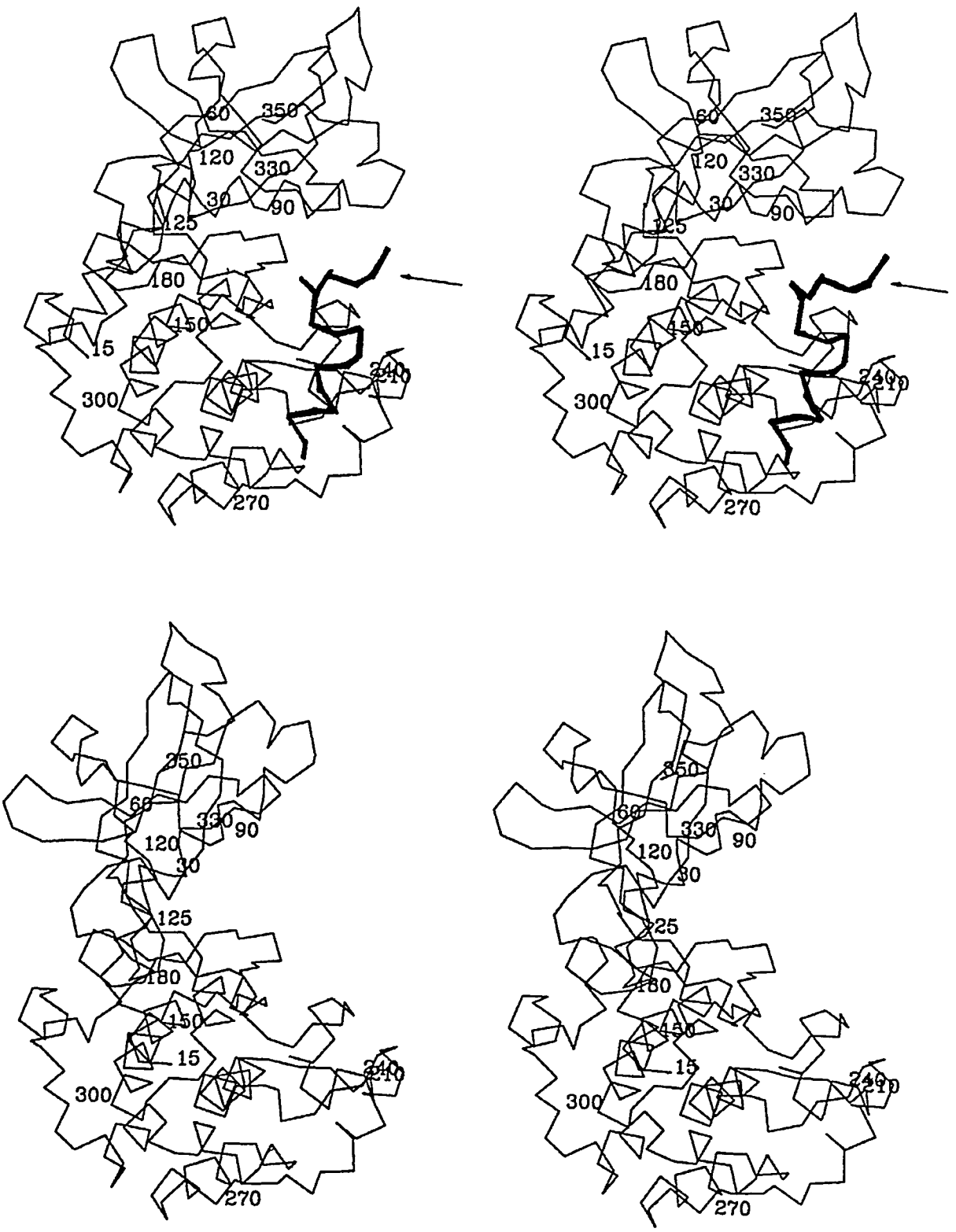
Glass, D.B., J. Trewhella, R.D. Mitchell, et al., "Conformationally Constrained Analogs of Protein Kinase Inhibitor (6-22)amide: Effect of Turn Structures in the Center of the Peptide on Inhibition of cAMP-Dependent Protein Kinase," *Protein Sci.* 4, 405 (1995).

Olah, G.A., R.D. Mitchell, T.R. Sosnick, et al., "The Solution Structure of the cAMP-Dependent Protein Kinase Catalytic Subunit and Its Contraction upon Binding the Protein Kinase Inhibitor Peptide," *Biochem.* **32**, 3649 (1994).

The Phylogenetic Conservation of Gly^{125}



Phylogenetic tree showing the evolutionary relationship between families of kinase proteins and the conservation of glycine residues 125 and 126, which play a key role in forming the flexible hinge between the two domains of the protein. The use of glycine to form a flexible hinge structure in these proteins is a common feature.



Stereo drawings of the catalytic subunit of protein kinase showing the opening and closing of the hinge that moves the small upper domain with respect to the lower domain. The protein is represented in each case by a trace of the backbone of the polymer chain. The heavier black trace represents bound pseudosubstrate. The upper pair shows the "closed" conformation induced by pseudosubstrate binding, and the lower pair shows the "open" conformation of the protein without pseudosubstrate.

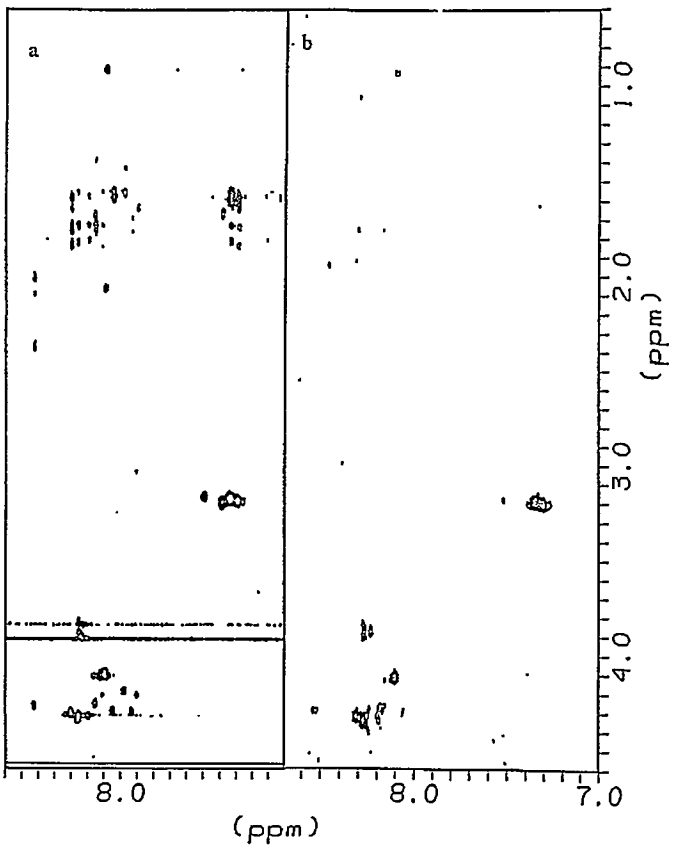
Advanced NMR Technology for Bioscience and Biotechnology

Jill Trewhella

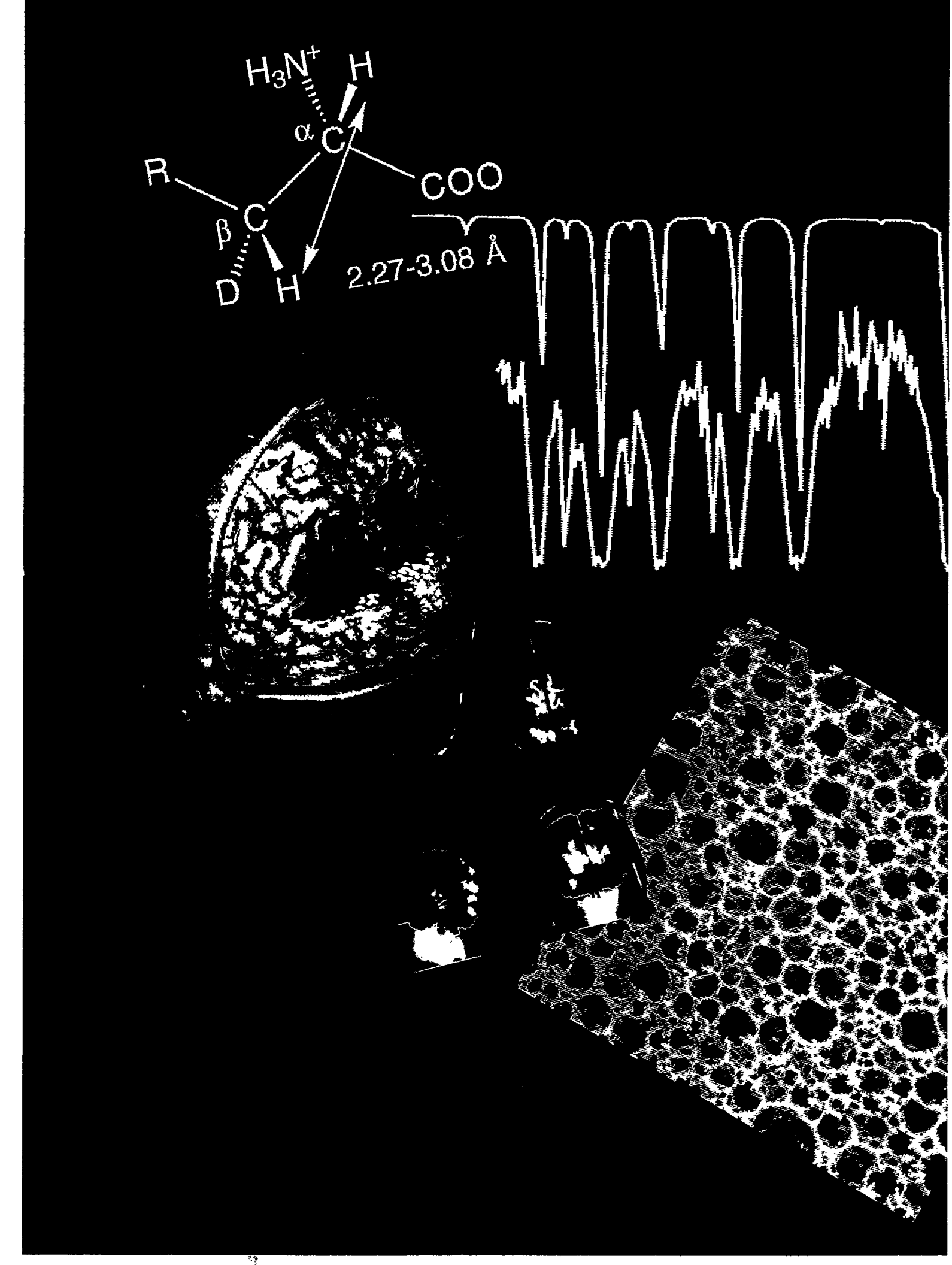
Nuclear magnetic resonance (NMR) technologies play critical roles in bioscience and biotechnology in both imaging and determining molecular structure. The major issues limiting the application of NMR to many important problems in bioscience are the inherent low sensitivity of the NMR experiment and the demands for spectral resolution required to study biological macromolecules. This project addresses both of these issues.

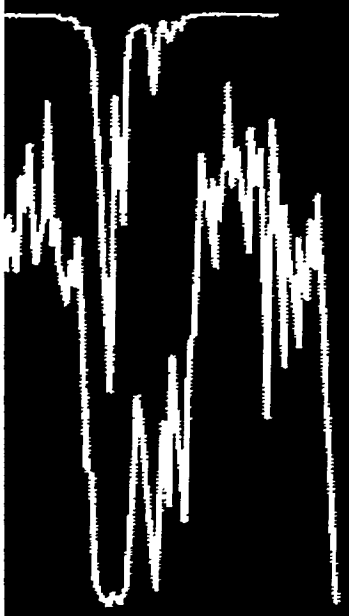
In the area of high-resolution structure determination of biomolecules in solution, high-field NMR in combination with stable-isotope labeling has seen dramatic advances in the past five years. These advances have resulted in a growing data base of three-dimensional biomolecular structures from solution studies that are of the same quality as those obtained with conventional x-ray crystallography methods. NMR methods also now offer the potential for highly sensitive, chemically specific imaging of biological systems at high resolution using force-microscopy detection.

This project focuses on developing enhanced capabilities for NMR technologies at Los Alamos, including very-high field for very-high-resolution applications to determine molecular structure and NMR force microscopy for very-high-sensitivity detection. We will use these capabilities to push the limits of size and complexity of systems that can be studied by solution techniques, e.g., protein/DNA complexes, and to evaluate the potential for imaging single-copy molecules on cell surfaces, e.g., receptor molecules that are key players in drug design.



Shown in the figure are proton-NMR spectra recorded from the protein complex that controls the muscle contraction/relaxation cycle. The complex is formed from two proteins called troponin C (TnC) and troponin I (TnI). When calcium ions bind to TnC, the contractile event is switched on through an interaction with TnI. Neutron scattering has revealed the low-resolution structure of the complex defining the molecular boundaries of the two components. We use NMR spectroscopy to define the high-resolution atomic structure within those boundaries in order to understand the molecular basis for the calcium-sensitive regulation of the contraction. These systems are not very soluble, hence sensitivity is a problem, and they also give rise to many peaks in the proton-NMR spectrum, requiring the highest-possible resolution. High-field-NMR technology helps us overcome these two problems. The figure shows total-correlation-spectroscopy (TOCSY) NMR spectra of deuterated TnC complexed with a fragment of TnI (residues 96–115) at 500 MHz (right) and at 750 MHz (left). The significantly increased resolution and sensitivity are evident in the 750-MHz spectrum. We recorded spectra for samples having the following parameters: 0.7 mM protein, a temperature of 308 K, a pH of 6.0, a mixing time of 50 ms, and a solution of 90% H_2O and 10% D_2O. The 750-MHz spectrum was collected using a Varian spectrometer at Pacific Northwest Laboratory, with 64 scans per t1 increment. The 500-MHz spectrum was collected on a Bruker instrument at Los Alamos, with 128 scans per t1 increment. These experiments are among the first to utilize what is currently the highest-available NMR field (750 MHz) for studying a biological macromolecular complex.


H3N+
H
α C
R
COO
β C
D
H
2.27-3.08 Å



Program Development Projects

The Program Development (PD) component of LDRD research supports R&D aligned with future programmatic opportunities at the Laboratory. PD projects explore and develop the technical resources needed to match Laboratory capabilities to emerging mission objectives and national research needs. With their broad and often cross-disciplinary scope of work, these projects usually involve somewhat larger technical teams and budgets. In FY 1995, they accounted for a quarter of the LDRD projects but more than a third of its funding.



Initiated by Laboratory program directors and guided by the Laboratory's strategic planning process, PD projects are conducted within eight program areas. These areas focus on technologies involving nuclear weapons, nuclear materials and stockpile management, nonproliferation and international security, conventional defense (DoD), environmental management, industrial partnerships, and energy. Our PD projects are grouped here as they relate to the nine disciplinary categories for LDRD research.

DEVELOPMENT OF HIGH-TEMPERATURE SUPERCONDUCTING THICK FILMS

Stephen Foltyn

Thick-film technology offers a new way to make long, high-temperature superconductors (HTSs) which can be used in numerous applications operating at liquid-nitrogen temperature and in high magnetic fields. These applications include supermagnets, magnetic-energy-storage systems, accelerators, transmission lines, fault current limiters, motors, generators, and magnetic resonance imaging. These devices offer opportunities to improve energy efficiency, reduce size, and increase performance and reliability while reducing environmental pollution. The objective of this project was to develop processes to achieve the best HTS thick films possible.

During the three years of this project, we developed an approach based on vapor-deposition technologies to make yttrium barium copper oxide (YBCO) thick films on nickel or nickel-based alloys. In this approach a highly textured yttria-stabilized-zirconia (YSZ) layer is deposited by an ion-beam-assisted deposition (IBAD) process so that the YSZ layer serves as a template on which to grow textured YBCO thick films. (We also deposit a thin layer of CeO_2 on YSZ for a better lattice match with YBCO.) The resulting films exhibit very-high critical current densities (over a million amperes per square centimeter) at liquid nitrogen temperature and in high magnetic fields. Currently, we have only produced short samples, although continuous processes have been developed that will allow us to make long conductors.

To demonstrate that the YBCO thick films can be used as practical conductors, we performed bending tests by either fastening the samples to a series of cylindrical mandrels or by a continuous tensile-test system. The results of these tests clearly showed that YBCO thick films on metallic substrates are highly flexible. The thinnest substrates used in our experiments were 130-μm thick; however, we feel confident that substrates with a thickness less than 25 μm should present no problems. We base this conclusion on previous work at Los Alamos on chemical-vapor-deposited Nb_3Ge thick films on 25-μm-thick copper substrates (nickel has nearly three times the yield strength of copper).

In summary, we have shown that YBCO thick films on nickel alloys with a textured YSZ buffer layer created by an IBAD process have excellent superconducting and mechanical properties. The next major challenge is to speed up the processes to demonstrate that vapor deposition can be used to make long YBCO tapes. Increasing the deposition rate and reducing the thickness for YSZ will be one of the major challenges. Finding an optimized deposition method for coating YBCO over large areas or with high deposition rates will also be necessary.

Publications

Wu, X.D., S.R. Foltyn, P.N. Arendt, et al., "Properties of $YBa_2Cu_3O_7$ Thick Films on Flexible Buffered Metallic Substrates," *Appl. Phys. Lett.* 67, 2397 (1995).

SURFACE POLYMERIZATION AGENTS

Craig Taylor

Surface polymerization agents (SPAs) are materials that can be used to block the flow of air through particulate filter systems. The SPA technology is primarily applied to the disablement of engines, but it could also be applied to command/control centers and computer facilities. It is thus relevant to both conventional defense and civilian law enforcement. Our main objective is to demonstrate the use of an unmanned vehicle or missile as a delivery platform for SPAs through a joint technical demonstration with the U.S. Army Missile Command.

During the reporting period, we performed experiments to investigate the properties of SPAs containing various molecular weights and/or mixes of molecular weights of polymers. The technical demonstration has been delayed until next year, but SPA mixtures will be ready for testing when needed.

Characterizing and Reducing AC and DC Losses in High-Temperature Superconducting Conductors and Cables

Martin Maley

High-temperature superconductivity (HTS) offers the promise of liquid-nitrogen operating temperatures for superconducting devices, but only if high current densities can be sustained at these temperatures in magnetic fields (H) of several tesla. At present there is only one group of HTS compounds, the bismuth-strontium-calcium-copper-oxide (BSCCO) system, that has been successfully made into long, continuous lengths of wires and tapes that carry high current density. Several groups have reported achieving critical current-density (J_c) values greater than 10^5 A/cm^2 at 4.2 K in fields up to 25 T in tape conductors based on the $(Bi,Pb)_2Sr_2Ca_2Cu_3O_y$ compound (Bi-2223) and prepared by the oxide-powder-in-tube (OPIT) process. Unfortunately, thermally activated motion of magnetic flux lines away from pinning centers provided by microscopic defects severely limits this system of compounds. This activated flux motion (flux creep) generates ohmic dissipation and limits operation of BSCCO-based conductors to below ~35 K. To stabilize currents with low dissipation at higher temperatures will require defect structures with much higher pinning strength.

Recent success with columnar defects produced by heavy-ion irradiation at high energy has shown that linear tracks with well-defined radii of 5–7 nm are the most effective in pinning flux lines. Unfortunately, heavy ions have a short range in solids thus making the technique impractical for application to OPIT tapes. It was recently demonstrated that randomly oriented columnar tracks can be created in situ throughout the bulk of a thick Bi-2212 film by heavy-fission fragments that result when 0.8-GeV protons collide with bismuth nuclei. Both the large range of these high-energy protons (~0.5 m) and the large cross section for fission of high-Z nuclei make it possible to generate dense arrays of columnar tracks throughout the interior of bulk conductors and even large-scale devices such as solenoids. We undertook the present investigation to test the effect of 0.8-GeV proton irradiation on transport current densities measured on standard OPIT Bi-2223/Ag tape conductors.

Below we present our results on both a monofilament and an 85-filament Bi-2223/Ag tape sample manufactured by American Superconductor Corporation (ASC). The tapes were prepared by a standard OPIT process. We used the Weapons Neutron Research Facility of the Los Alamos Neutron Science Center (LANSCE) to irradiate the samples with 0.8-GeV protons. We gave approximately equal doses to each sample. We determined the doses received by each sample from studies of the ^{22}Na activation levels on aluminum foils placed immediately behind the samples. The average proton fluences received by three sectors of the monocore tape were 1.6, 2.9, and 7.6×10^{16} protons/cm^2. For the multifilamentary tape, we measured only the sector that received the highest fluence, estimated to be 7.6×10^{16} protons/cm^2. We estimated the number of fissions produced per proton from known cross sections. Assuming an average track length of 6 μm for each fission, the areal density of tracks is then ~1.1, 2.0, and 5.2×10^{10} tracks/cm^2. If we multiply the track density by the flux quantum ϕ_o (= 2.07×10^{-11} T·cm^2), we can convert it to an equivalent magnetic field B_ϕ, at which the vortex density equals the track density. The concentrations of fission tracks per unit area therefore correspond to matching fields B_ϕ of 0.2, 0.4, and 1.1 T.

Figures (a) and (b), respectively, show the results of critical-current measurements on multi- and monofilamentary tapes. Both tapes show a remarkable improvement of the transport of J_c after irradiation. This effect is more notable at the higher fields. For example, at 1 T, figure (a) shows that for the multifilamentary tape J_c has increased from an immeasurably low value to ~5×10^3 A/cm^2 at 75 K. Also shown in Figure (a) is the magnetic-field dependence of J_c on the irradiated multifilamentary tape at 64 K. Clearly, the fall off in J_c shifts to higher fields at the lower temperature. Furthermore, the 64 K curve of $J_c(H)$ is flatter below the knee—less dependent on H—suggesting that the pinning activation energy increases at lower temperature. Figure (b) shows the transport J_c normalized to its value at zero field (J_{co}) for two different sectors of the irradiated monocore tape and for an unirradiated ASC monocore tape at 75 K. Clearly evident is the progressive improvement with radiation fluence of the field dependence of J_c, with the functional form of $J_c(H)$ at the highest fluence matching that of the multifilamentary tape.

In summary, we have shown that by means of 0.8-GeV proton irradiation it is possible to greatly improve the transport critical current at high temperatures of industrial state-of-the-art, bulk high-T_c superconductors in the

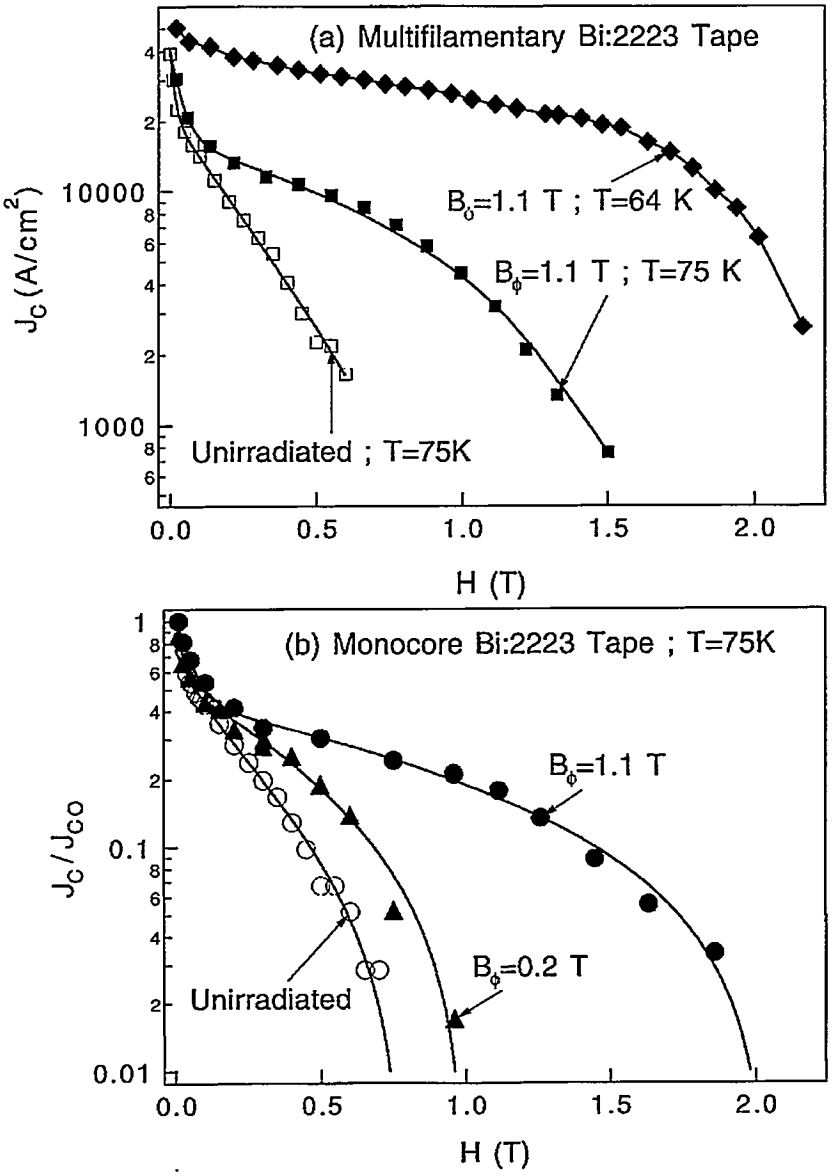
form of multi- and monofilamentary tapes. We found that the transport J_cs are homogeneously improved throughout the *H-T* plane. Thus high-energy proton irradiation appears to be an effective technique for enhancing the operating temperature of devices made with BSCCO conductors.

Publications

Bulaevskii, L., A. Larkin, M. Maley, et al., "Quantum Depinning in Layered Superconductors with Defects Produced by Irradiation," *Phys. Rev. B* **52**, 9205 (1995).

Maley, M., J. Willis, L. Bulaevskii, et al., "Effects of Splayed Columnar Defects Produced by Heavy Fission Fragments on Vortex Dynamics in BSCCO Conductors," in *Physical Phenomena at High Magnetic Fields-II*, L. Gorkov et al., Eds. (World Scientific Publishing, Singapore, in press).

Safar, H., J. Cho, S. Fleshler, et al., "Enhancement of Transport Critical Current Densities at 75 K in Bi-2223/Ag Tapes by Means of Fission Tracks from Irradiation by 0.8 GeV Protons," *Appl. Phys. Lett.* **67**, 130 (1995).



(a) Critical current density versus magnetic field for the multifilamentary Bi-2223 tape at 75 K in the unirradiated state and after irradiation with 0.8-GeV protons to a fluence corresponding to an estimated matching field of 1.1 T. Data for the irradiated tape is also shown for 64 K. (b) Normalized critical current density (J_c/J_{co}) versus magnetic field at T = 75 K for the monocore Bi-2223 tape in the unirradiated state and after irradiation with 0.8-GeV protons at two fluences at different sections of the same piece of tape.

Electronic Devices Based on High-Temperature Superconducting Thin Films

Xin Di Wu

Our objective is to optimize high-temperature superconducting (HTS) thin films of $YBa_2Cu_3O_{7-x}$ (Y-123) and $Tl_2Ba_2CaCu_2O_8$ (Tl-2212) deposited on novel substrates that will be used in the development of advanced electronic devices. We will use intermediate buffer layers (ceria and yttria) to improve lattice matching and compatibility between the HTS film and substrates. Specific goals include

- investigating Y-123 thin films deposited on zirconia, alumina, and magnesia substrates by ion sputtering and laser ablation,
- studying graded metallic and insulating thin films for use in HTS Josephson junctions,
- building and testing magnetic field sensors based on the units that have Josephson junctions to maximize signal-to-noise levels, and
- forming thin films of Tl-2212 on large-area substrates (lanthanum aluminate) for use in developing microwave cavities. Upon optimizing film processing, the resulting Tl-2212 films will be placed in a novel microwave cavity design and tested for surface resistance and quality of measurements.

Y-123 and insulating thin films were deposited by pulsed laser deposition and off-axis sputtering. Tl-1223 precursor films were deposited by sputtering and were thalliated by exposure to Tl_2O (g) to form the desired Tl-2212 superconducting thin films. We used these HTS films to develop Josephson junctions and microwave devices. We have made the best Y-123 superconducting quantum interference devices, known as SQUIDs, based on Josephson junctions with a superconductor/normal-metal/superconductor edge. We have also demonstrated tunable microwave devices based on Y-123 thin films deposited on dielectric thin films of $SrTiO_3$. Finally, we characterized Tl-2212 thin films at microwave frequency for a new application of our microwave cavity design.

Publications

Findikoglu. A., Q.X. Jia, D.W. Reagor, et al., "Electrical Characteristics of Coplanar Waveguide Devices Incorporating Nonlinear Dielectric Thin Films of $SrTiO_3$ and $Sr_{0.5}Ba_{0.5}TiO_3$," *Microwave and Opt. Tech. Lett.* **9,** 3066 (1995).

Jia, Q.X., X.D. Wu, S.R. Foltyn, et al., "Structural and Electrical Properties of $Sr_{0.5}Ba_{0.5}TiO_3$ Thin Films With Conductive $SrRuO_3$ Bottom Electrodes," *Appl. Phys. Lett.* **66,** 2197 (1995).

Jia, Q.X., X.D. Wu, D.W. Reagor, et al., "Superconducting $GaBa_2Cu_3O_{7-x}$ Edge Junctions with Lattice Matched $Y_{0.6}Pr_{0.4}Ba_2Cu_3O_{7-x}$ Barriers," *J. Appl. Phys.* **78,** 2871 (1994).

Pluym, T.C., R.E. Muenchausen, P. Arendt, et al., "Superconducting $Tl_2Ba_2CaCu_2O_8$ Thin Films Prepared by Post-Annealing in a Flow-Through Multiple-Zone Furnace," *IEEE Trans. Appl. Super.* **5,** 1339 (1995).

Advancing the Technology Base for High-Temperature Membranes

Robert Dye

This project addresses the major issues preventing the application of high-temperature membranes to separations and catalysis. We are investigating high-temperature membrane systems that can have a large impact for the Department of Energy and be industrially relevant. A major obstacle to increased use of membranes is that most applications require the membrane material to withstand temperatures above those acceptable for polymer-based systems. Advances made by this project are expected to help industry and the Department of Energy move toward high-temperature membrane applications that will improve overall energy efficiency.

Hydrogen separation membranes constructed by depositing palladium on tantalum foils show hydrogen fluxes that are better than those reported in the literature and are up to 15 times the fluxes of current commercial membranes. The zeolitic membrane deposition process was also developed at the Laboratory. Patents have been filed for both membrane technologies. Films have been deposited using both mordenite and faujasite targets that have a pore size of 8 to 12 Å.

Gas uptake measurements demonstrated that the films discriminated between 1- and 2-propanol, as well as 1- and 2-butanol. Permeation experiments showed that the separation ratio of hydrogen to argon was 5.3 and the flow rates were limited by the porous substrate.

We conducted methanol steam reforming experiments in a palladium membrane reactor with a commercially available palladium membrane. We developed and used a mathematical model of the reforming process to analyze the data, as well as to parametrically explore the potential of membrane reactors for this reaction. A membrane testing facility was assembled and is able to operate from room temperature to 1200°C and at pressures from 0.01 to 1000 torr. Currently, we can handle flat membranes of up to 2-in. diameters and can measure separation factors, diffusion coefficients, and flow rates.

Publications

Peachey, N.M., R.C. Snow, R.C. Dye, "Composite Pd/Ta Metal Membranes for Hydrogen Separation" (to be published in *J. Membrane Sci.*).

Peachey, N.M., R.C. Dye, P.D. Ries, et al., "Pulsed Laser Deposition of Zeolitic Thin Films: Novel Structures for Molecular Recognition" (submitted to *J. Porous Materials*).

Giant Magnetoresistance Materials for Magnetic Recording Technology

Robert Heffner

This project focuses on a class of transition-metal-oxide materials ($LaMnO_3$ doped with calcium, barium, or strontium) which exhibits a very large change in resistance (R) with applied magnetic field ($\Delta R/R \cong -90\%$) near a ferromagnetic phase transition. These materials may have important uses as magnetic sensors in applications ranging from automobiles to read heads for magnetic storage. For this reason, we have established strong industrial collaborations in the data-storage industry. The principal obstacle for data-storage use is the high magnetic fields (several Tesla) currently required to obtain a significant DR/R. Achieving the necessary field sensitivity requires a two-fold approach: (1) understanding in detail the underlying physics, and (2) learning to tailor the compositional, geometrical, and microstructural properties of thin-film materials to achieve the desired magneto-electrical properties.

To date we have synthesized 1000Å thick films on $LaAlO_3$ substrates at temperatures (T_S) between 500–900°C using pulsed-laser deposition, and we have characterized their resistivity, magnetization, structure/microstructure (using x-rays, transmission electron microscopy, and scanning tunneling microscopy) and composition (using Rutherford backscattering). We find that, for the same nominal composition (e.g., $La_{0.67}Ca_{0.33}MnO_3$), both the magnitude of the resistivity and the ferromagnetic transition temperature (T_c) change systematically with the deposition temperature T_S. For example, T_c decreases monotonically as T_S varies between 500 and 900°C. We believe this behavior is due to the combined effects of changes in microstructure and oxygen stoichiometry as T_S is varied.

Future work will investigate the effects of different oxygen anneals and of chemical substitutions on the sensitivity to magnetic field of $\Delta R/R$.

Publications

Hundley, M.F., M. Hawley, R.H. Heffner, et al., "Transport-Magnetism Correlations in the Ferromagnetic Oxide $La_{0.7}Ca_{0.3}MnO_3$," *Appl. Phys. Lett.* 67, 860 (1995).

Hundley, M.F., J.J. Neumeier, R.H. Heffner, et al., "Transport and Magnetism Correlations in Thin Film Ferromagnetic Oxides" (to be printed in *J. Appl. Phys.*).

Tyson, T.A., J. Mustre de Leon, S.D. Conradson, et al., "Evidence for a Local Lattice Distortion in Ca-Doped $LaMnO_3$" (submitted to *Phys. Rev. Lett.*).

Subsurface Characterization and Three-Dimensional Profiling of Semiconductors by Magnetic Resonance Force Microscopy

P. Chris Hammel

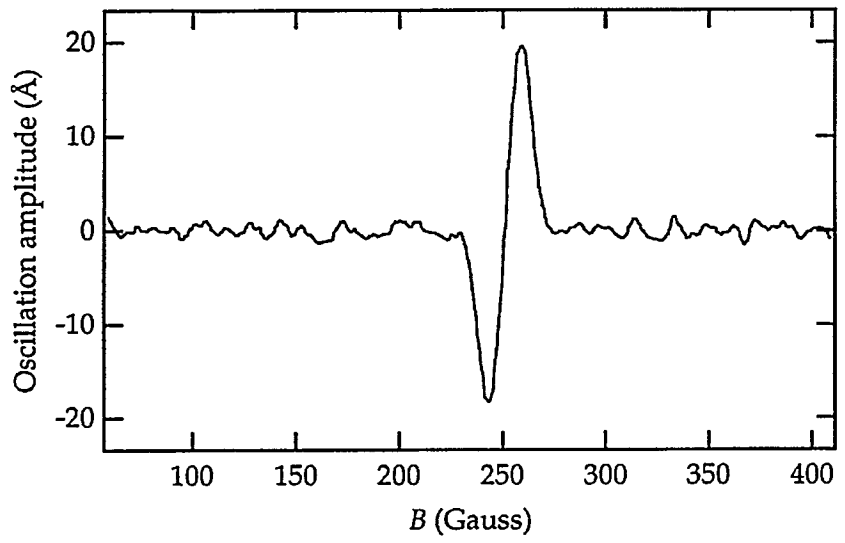
The magnetic resonance force microscope (MRFM) is based on mechanical detection of magnetic resonance signals. The force between the field gradient created by a small permanent magnet and the spin magnetization in the sample is used to drive the oscillation of a high-Q, low-spring-constant micromechanical resonator (e.g., an atomic-force-microscope cantilever). This same field gradient also permits microscopic magnetic resonance imaging.

The characteristics and capabilities of the electron spin MRFM we have fabricated are as follows: Our MRFM has a sensitivity of 3×10^{11} electron spins at room temperature in an applied field of 253 G. The vertical resolution of our MRFM is ~1 μm. We have performed one- and two-dimensional scans of a particle beneath the silicon cantilever which demonstrate the subsurface spatial imaging capabilities of the instrument. We have also made recent advances in miniaturizing two crucial MRFM components: the micromechanical resonator and the micromagnetic tip (see figures).

The work performed in this project has applications to a broad range of problems in which microscopic, three-dimensional (3-D) imaging of structure is needed, including structure of biological and structural materials. An application of particular importance is to measure dopant profiles in semiconductor devices. These measurements will permit improvements in semiconductor processing and in understanding relationships between dopant profiles and device performance. This work also has applications to the development of a commercially important instrument: a novel, high-spatial-resolution, scanning-probe microscope having 3-D, subsurface sensitivity.

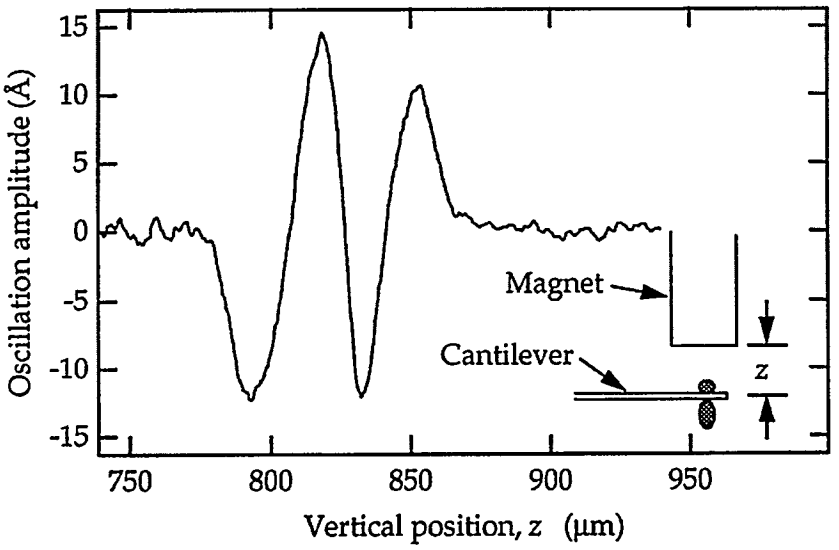
Publications

Hammel, P.C., Z. Zhang, G.J. Moore, et al., "Sub-Surface Imaging with the Magnetic Resonance Force Microscope," *J. Low Temp. Phys.* **101**, 59 (1995).

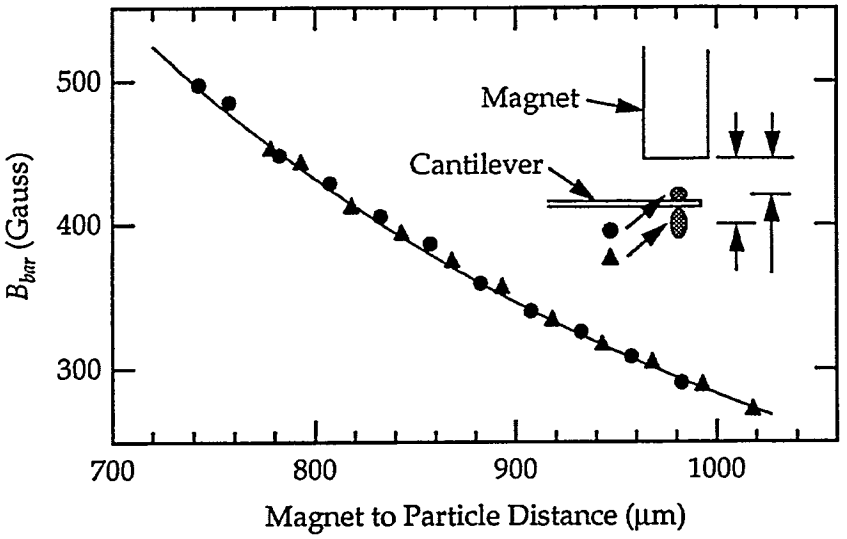


Single-shot MRFM signal from a ~18-μm-diameter (5 ng) particle of diphenyl picryl hydrazil (DPPH), an organic molecule having a single free electron spin. The amplitude of the cantilever oscillation is shown as a function of the applied homogeneous field $B = B_{bar} + B_0$, *where* B_{bar} *is the field of the bar magnet and* B_0 *is the background magnetic field. The RF frequency* f_{RF} *is 709 MHz; at resonance the total field is 253 G.*

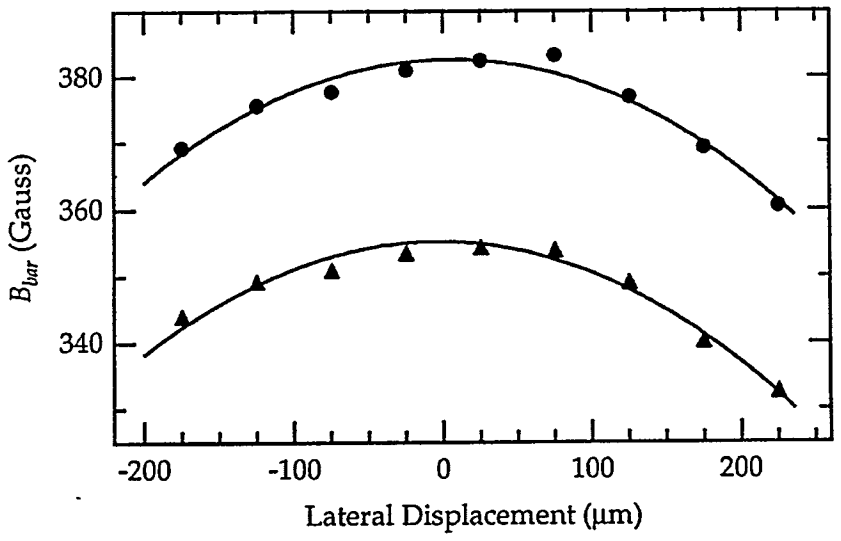
The swept-field MRFM signal from two particles of DPPH, one mounted above (~7 ng) and one below (~3 ng) the cantilever. Signal intensity is shown as a function of distance z from the end of the bar magnet to the cantilever. The signal was obtained at f_{RF} = 828 MHz. The distance z is deduced from knowledge of B_0, B_{bar}, and B_{Larmor}. A schematic (not-to-scale) representation of the geometry is shown in the inset.



The magnitude of the field of the bar magnet ($B_{bar} = B_{Larmor} - B_0$) at the center of each of the two particles (upper particle, solid circles; lower particle, solid triangles) is shown as a function of the distance between the end of the magnet and the center of the particles. The solid line is a fit to the expected dependence of field on distance from the end of a cylindrical magnet along its axis. From this fit the separation between the centers of the two particles is found to be 35.4 (±1) μm.



Variation of the magnetic field of the bar magnet at the center of the DPPH particle as its position relative to the bar magnet is varied in a direction perpendicular to the bar axis.



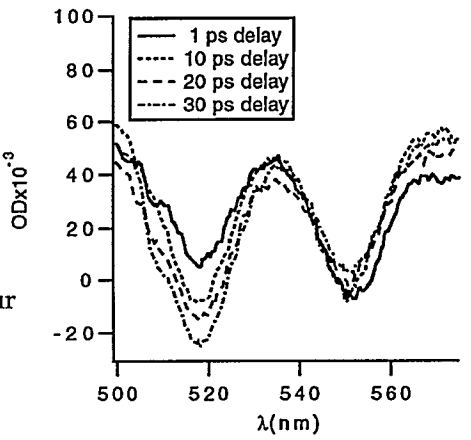
Artificially Structured Electronic and Biomimetic Materials by Molecular Self-Assembly

Duncan McBranch

The objective of this project is to create new electro-optic and photorefractive materials by engineering rationally designed, nonlinear molecular building blocks into multilayer thin films using self-assembly techniques. We are developing stable electro-optic and photorefractive materials that address shortcomings of existing materials for industrial applications. Specifically we are focusing our efforts on designing, at the molecular level, such light-controlled materials as electroluminescent polymers and oligomeric porphyrins.

We have designed several candidate molecular systems, tested the transient optical properties of these molecules, and designed self-assembly routes to thin-film formation. In addition, we have implemented transient absorption experiments that can probe subpicosecond charge and energy transfer and transient holography experiments to measure changes in polarizability following photoexcitation. And, finally, we have modeled oligomers, conjugated polymers similar to poly(*p*-phenylene vinylene) [PPV], and C_{60} molecules to attain a quantitative understanding of the electronic structure of their ground and excited states (including polarons and excitons) using a tight-binding formalism. Currently, we are combining these models to study the charge-transfer complex of a conjugated chromophore and C_{60}.

Our investigation of biomimetic light-harvesting pigments has led to a collaboration with the National Renewable Energy Laboratory and Lawrence Berkeley National Laboratory. Our strengths complement the strengths of these other institutions. We have measured the energy-transfer rates of soluble oligomers of porphyrin and polypyridyl inorganic charge-transfer complexes using transient absorption spectroscopy. The accompanying figure shows the transient bleaching of a zinc porphyrin pigment at short times (1 ps) near 550 nm that evolves into a transient bleaching near 520 nm associated with a covalently attached free base porphyrin. The energy transfer in this "dimer" takes 20 ps, indicating a through-bond mechanism even though there is little electronic coupling of the two associated pigments when they are in their ground states.



Evolution of transient absorption showing signature of a zinc porphyrin at short time (1 ps, 550 nm) with energy transfer to a free base porphyrin (20 ps, 520 nm).

Electronic Diamond: Fabrication Processes and Electron Emission Performance

Marion Scott

This project was instituted to perform R&D in the area of electron emissive materials and their applications. We originally pursued flat-panel-display applications, but our primary aim became the development of a new fluorescent light bulb, which has since resulted in a joint-patent application with DuPont.

The new light bulb eliminates the need for any gases in the fluorescent bulb and, instead, utilizes direct electron impact on the phosphor to produce visible light. This new light bulb utilizes electron emissive material for its operation instead of requiring the use of "environmentally unfriendly" mercury vapor, as is typical of more conventional fluorescent bulbs. The absence of a gas and the resulting plasma in the bulb should increase the lifetime considerably, and the number of "on-off" cycles will no longer be a factor in determining the bulb lifetime because ionic bombardment of the cathode will not occur.

We have concluded that the fluorescent light bulb will ultimately be the most successful application of the electron emissive materials investigated in this project. In the past year, we have constructed and successfully operated a laboratory proof-of-principle model of the light bulb.

Neutral Stream Processing of Semiconductor Materials

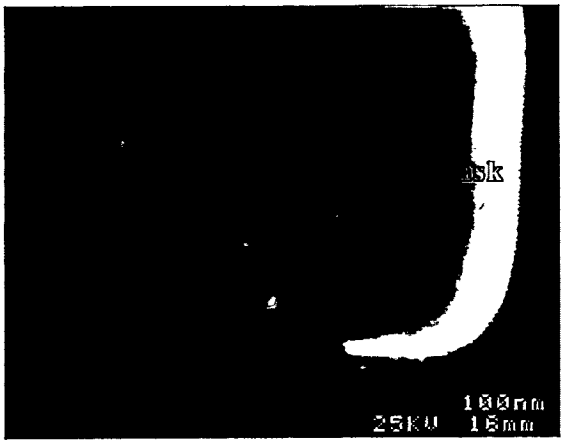
Jon Cross

The use of high-energy, neutral particles for processing electronic materials at low temperatures has been identified by the microelectronics industry and SEMATECH (Semiconductor Manufacturing Technology consortium) as a new technology that will play a critical role in manufacturing electronic devices well into the next century. With its extremely low residual damage, such processing can provide a means to manufacture ultrahigh-density computer memory chips that cannot be produced using present manufacturing methods. Los Alamos is in a unique position to address the challenge of developing such a process because of its laser-sustained, discharge beam source that produces an intense, continuous flux of high-energy neutral gas species such as atomic oxygen, nitrogen, chlorine, and fluorine.

We have demonstrated that energetic oxygen atoms produce high-resolution anisotropic etching of photoresist polymers that is far superior to that produced by plasma etching techniques (see first figure), that halogen atoms produce low-damage anisotropic etching of silicon without damaging thin gate oxides (see second figure), and that thin gate oxides can be grown at low substrate temperatures (25°C–150°C). In addition, we have proposed that these noninvasive etching techniques hold promise for reducing or eliminating dust production, substrate and chamber sputtering, liquid waste streams, and personnel radiation exposure in weapons manufacturing. These etching techniques are directly applicable to weapons cleaning and manufacturing processes as well as to industrial chip manufacturing and are thus of great importance to the Laboratory's science and technology base.



Scanning electron microscope photograph of atomic oxygen etching of photoresist polymer. Feature size is 0.3 microns.



Chlorine etching of poly-silicon after pretreatment with XeF_2 to remove native oxide.

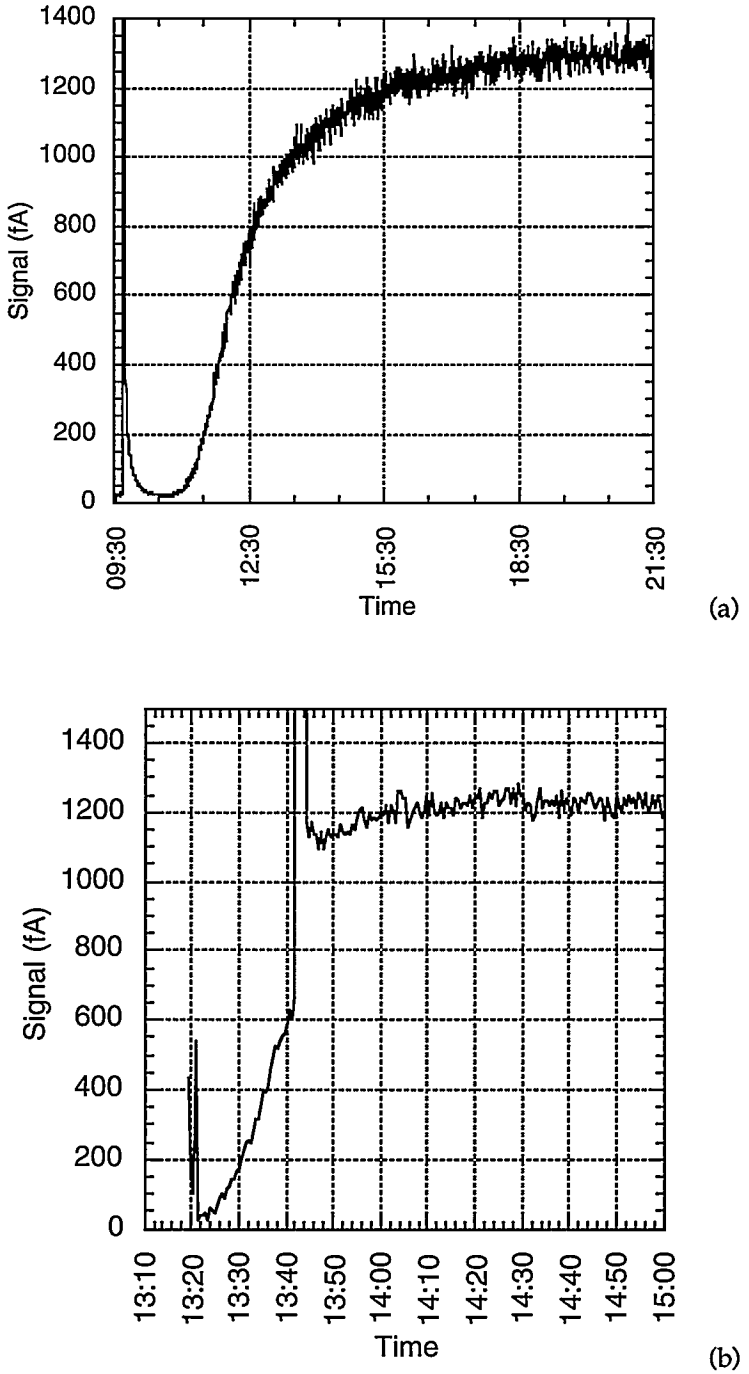
Ion Flooding to Precharge Insulating Materials

Duncan MacArthur

Detectors based on long range alpha detection (LRAD) technology are adversely influenced by the excess electric charge that can build up on insulating materials. Electric fields caused by the excess charge compete with the detector's ion-collecting mechanism, dramatically reducing detector efficiency.

One application for which LRAD technology is especially well suited is seriously affected by the problems associated with insulating materials. Tools, electronics modules, laboratory apparatuses, etc. are difficult to monitor by conventional methods but lend themselves quite well to monitoring by LRAD-based object monitors. Such monitors have been developed at Los Alamos, and commercial models have been built by Eberline Instrument Corp. However, use of these monitors will be restricted to metallic objects unless we find a solution to the problems posed by insulators.

Our project explores one possible solution to these problems: neutralizing the charge on the insulator by flooding the surrounding air with ions before taking a measurement. We have performed tests to better understand the influence of this charge and to test the efficacy of ion flooding. Although these tests are not complete, our data is encouraging, suggesting that by incorporating an ion-flooding mechanism, object monitors can be designed that will be suitable for monitoring contamination on insulating materials (see figure).



Effect of ion flooding on the response of an LRAD object monitor: (a) Response of the monitor to 11,500 dpm of plutonium-239 in the presence of a charged swatch of poly/cotton insulating material. Initially, the charge carried by the material suppresses the detector's response. The source is revealed slowly as the charge decays; 90% of peak value comes after almost six hours of exposure. (b) Effect of one minute of ion flooding begun at about 13:42; 90% of peak value is reached immediately after the flooding.

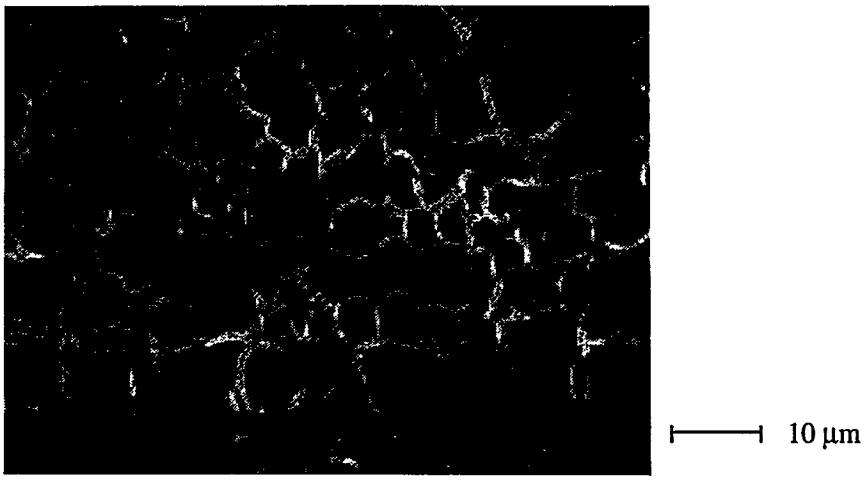
Microcellular Ceramic Foams for Radar-Absorbing Structures

Jeffrey Huling

The exhaust systems of military jet engines must be constructed using radar-absorbing ceramic materials that can withstand harsh thermal, chemical, and mechanical environments. Currently, these exhaust-system structures are heavy (and consequently compromise overall airframe design) and provide inadequate control over both radar and infrared signatures. The short service lifetime of these structures has prompted interest in designs that improve durability and contain fewer parts. The goal of our project is to develop robust, radar-absorbing structures for aircraft exhaust systems by using an existing, novel microcellular ceramic-foam technology. By reducing radar and infrared signatures, our research will help increase aircraft survivability while improving exhaust-structure durability and reducing maintenance costs.

A viable approach for reducing exhaust-system weight and radar cross section is to replace the current dense ceramic structures with a continuous layer of a lightweight, semi-structural, radar-absorbing ceramic foam. We have developed and demonstrated a novel sol-gel emulsion process for preparing microcellular ceramic foams that have highly refined cell structures (currently ~10 microns) and thin, dense cell walls (see figure). We predict the foams' microcellular structure will maximize strength-to-weight ratio and minimize thermal conductivity.

We have extended our process to include preparing crystalline mullite ($3Al_2O_3 \cdot 2SiO_2$) microcellular foams (maximum-use temperature 2800°F–3000°F), from initial work that used vitreous silica (maximum-use temperature 1400°F–1600°F). We are currently investigating the scale-up of the process. We expect a funds-in agreement with a major defense aerospace contractor to provide follow-on funding.



Los Alamos microcellular mullite foam.

Development of High Magnetic Fields for Energy Research

Joe D. Thompson

Investigating the properties of materials subject to very high magnetic fields is required for energy-related science and technologies important to the DOE mission. Prestigious panels have identified such research as a high national science priority. The National Science Foundation has taken the lead by establishing a new National High Magnetic Field Laboratory whose very high pulsed-field part is located at Los Alamos.

Because of unique power-generating capabilities present at Los Alamos, the Laboratory has the opportunity to produce a revolutionary advance in generating very high (100 T) nondestructive magnetic fields that could be used for the first time to study metallic materials at very low temperatures. These developments open the way for unprecedented capabilities for materials studies at very high fields. Our goals are to demonstrate the feasibility of constructing a novel 100-T magnet and to enable the establishment of a forefront high-field research program. Reaching these goals should result in the construction of a 100-T magnet and ultimately in the formation of a principal research team for high-field research led by Los Alamos.

A workshop was held at Los Alamos which was attended by leading scientists from national laboratories, universities, and DOE/Office of Basic Energy Sciences/Division of Materials Science, evaluated the feasibility of building a 100-T magnet and the opportunities such a magnet would afford. The materials physics community strongly

endorsed our objectives and approach. We have also developed high-field Hall-bar and cantilever magnetometers with sensitivities comparable to radio-frequency SQUIDS. Such developments open entirely new possibilities for high-field investigations of the magnetic properties of small single crystals. Finally, we have discovered a field-induced transition in Y-doped $YbInCu_4$ that is related to the valence transition in the compound. This highly unusual relationship is being pursued experimentally and theoretically.

Publications

Sarrao, J.L., C.L. Benton, Z. Fisk, et al., "YbIn(1-x)Ag(x)Cu(4): Crossover from First-Order Valence Transition to Heavy Fermion Behavior" (to be published in *Physica B*).

Technical Evaluation of Russian Aircraft Stealth Coating and Structural Materials

Frank Gac

Treating aircraft, missiles, and ships with materials that absorb electromagnetic energy continues to be an important technique for reducing a vehicle's radar cross section (RCS). A former Soviet center for the development of these electromagnetic-energy-absorbing materials technologies was at the Institute for High Temperatures of the Russian Academy of Sciences in Moscow. The Institute, now known as the Russian Scientific Center for Applied Problems in Electrodynamics (SCAPE), had the direct responsibility for the development of RCS materials since 1987. The SCAPE technology is based on at least thirty years of Soviet theoretical work on the interaction of electromagnetic radiation with materials, commonly known as percolation theory.

The primary purpose of our program is to establish a research subcontract with SCAPE and analyze the radio-frequency-absorbing coatings. We will pay particular attention to percolation-system designs. An additional objective of this collaboration is to apply SCAPE's percolation methodology toward a variety of civilian applications by transferring this technology to U.S. industry.

Progress reports from SCAPE coupled with a visit by a contingent of the U.S. Team—comprised of scientists from Los Alamos National Laboratory, the Georgia Tech Research Institute, and the University of California, Los Angeles—suggest that there is technical merit in the SCAPE approach. However, we cannot draw concrete conclusions until we receive and carefully characterize the first series of SCAPE samples.

Development of Transparent Conducting Films for Flat-Panel Displays

Joysree Aubrey

This project involves an experimental/theoretical approach to developing superior thin films (such as transparent conducting oxides, phosphors, and polysilicon) for applications to flat-panel displays. Goals of the project are the following: (a) to improve the quality of thin-film layers by using state-of-the-art deposition techniques and intelligent process-control methods, (b) to use plasma-process modeling to simulate and improve the performance of the ion-beam source, (c) to use experimental data to extend materials- and device-modeling capabilities now under development, and (d) to actively participate with academic and industrial partners to improve the products of the research.

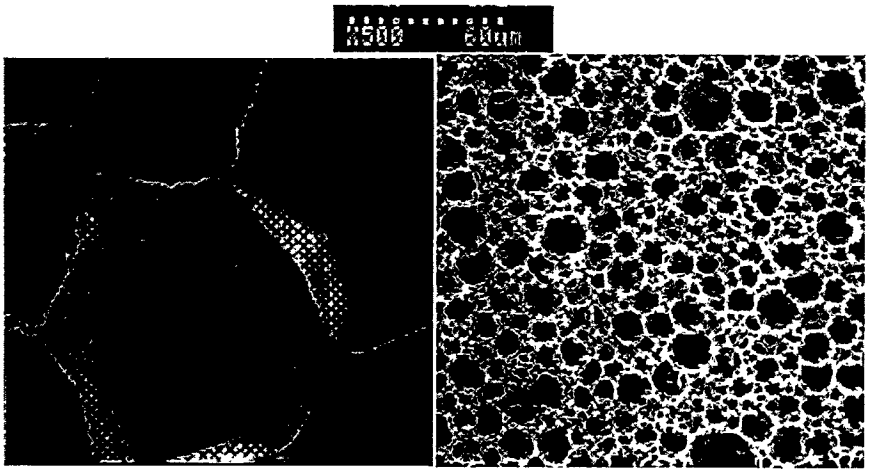
Our accomplishments during the last year include the following: (a) We deposited oriented films of zinc-oxide and silicon using a state-of-the-art ion gun and extensively characterized them; we found that the films had superior electrical and mechanical properties. (b) We modeled the performance of the ion gun with the 2-1/2-dimensional code MERLIN. (c) We began to develop intelligent process-control techniques with the aim of improving the quality and consistency of the product. In particular, we evaluated deposition parameters for use in adaptive-control techniques. (d) We developed a one-dimensional drift-diffusion code for use in simulating flat-panel displays. (e) We initiated a materials-modeling activity to study the properties of thin-film semiconductors. (f) On the theoretical side, we modeled the ion-beam and deposition conditions, as well as materials and devices.

Development of Structural Materials Exhibiting Dielectric and Magnetic Loss at Radio Frequencies

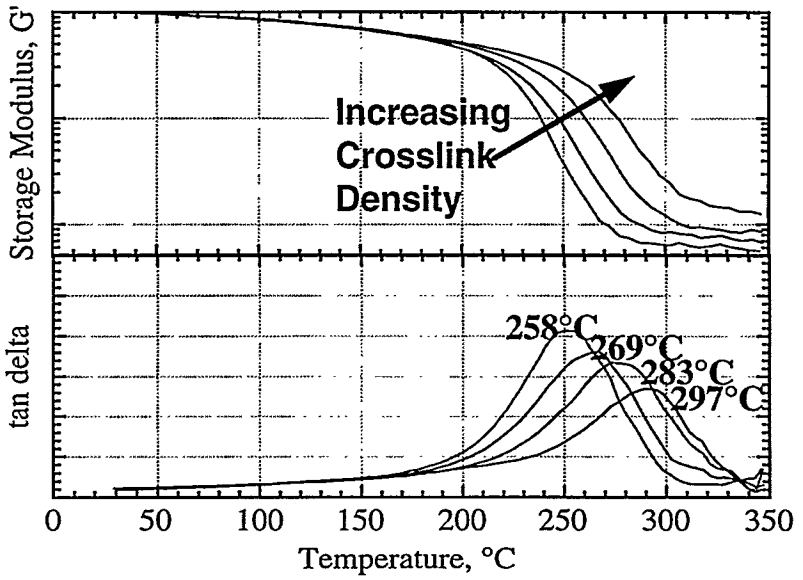
Joseph Duke

Reduced signature technologies and their incorporation into low-density structural materials for military aircraft has been of critical interest to the Department of Defense for the past twenty years. Unfortunately, the conventional radar-absorbing materials (RAM) in use today are structurally parasitic and reduce the range and performance of an aircraft by adding significant weight.

We have produced foams that have properties that exceed both the mechanical and thermal requirements for composite aircraft part manufacture. In our research, we varied processing parameters and chemical compositions and evaluated their effects on the mechanical and thermal properties of the foams (see figures). These ultralow-density polymeric foams are capable of meeting aircraft structural requirements as well as being modified with RAM systems. We developed two methods of incorporating RAM into these foams. Using radio frequency (RF) testing, we demonstrated that the RF properties of the foams could be tailored over the useful range of properties for bulk absorbers (stealthy materials). These new technologies allow for the incorporation of radar-absorbing structures into existing and future aircraft designs. These structures could provide benefits in aircraft performance, survivability, manufacturing, and costs in comparison with existing technologies. Further development of process scaleup and property optimization is needed at this point in our research.



Scanning electron microscopy photomicrograph comparison of commercial blown foam with the Los Alamos' high-internal-phase emulsion (HIPE) foam.



Dynamic mechanical analysis of high-temperature foams with increasing crosslinking densities.

Structure Versus Properties in High-Temperature Superconductors

James Smith

High-temperature superconductivity (HTS) has a myriad of potential applications in both electric-power and electronic-device areas; however, it has a complex physical behavior. Optimization of these important materials requires a very high level of understanding of fundamental relationships between structural and superconducting properties. Our effort relied on our expertise and facilities in scanning tunneling microscopy (STM), nuclear magnetic resonance (NMR), and theoretical modeling to further discern the underlying basis for HTS to improve the materials.

We have shown the STM to be very useful in characterizing HTS at the very high resolutions required to observe the magnetic-flux pinning tracks caused by proton bombardment and to determine thin-film microstructures. We used NMR to measure the temperature dependence of the nuclear spin-lattice relaxation rates for anisotropic planar oxygens with both the normal and superconducting states of an aligned powder of $YBa_2Cu_3O_{6.96}$ enriched with 17 oxygen atoms. Corresponding studies of the relationship between structural modulations and phase separation in oxygen doped $La_2CuO_{4+\delta}$ indicated that oxygen ordering occurs on a microscopic scale.

We successfully employed a combination of analytical and numerical many-body techniques to study several important aspects of HTS. The inelastic neutron-scattering results are consistent with our theoretical interpretations developed in collaboration with Egami et al. (at the University of Pennsylvania). This project has provided the technical bridge between the basic and applied research that has placed Los Alamos National Laboratory in an international leadership role in developing HTS materials.

Publications

Abrams, E., J.R. Schrieffer, D.J. Scalapino, et al., "Properties of Odd Gap Superconductors," *Phys. Rev. B* **52,** 1271 (1995).

Balatsky, A.V., "Impurities and Conductivity in a d-Wave Superconductor," in *Strongly Correlated Electronic Materials*," K. Bedell et al., Eds. (Addison-Wesley, Reading, Massachusetts, 1994), p. 551.

Balatsky, A.V. and M.I. Salkola, "Impurity Induced Virtual Bound States in d-wave Superconductor" (submitted to *Phys. Rev. Lett.*).

Balatsky, A.V., D. Pines, and P. Monthoux, "The Influence of Imperfections on the Low Temperature Properties of a d-Wave Superconductor," *Phys. Rev. B* **50,** 582 (1994).

Balatsky, A.V., A. Rosengren, and B.L. Altshuler, "Impurities and Quasi-One Dimensional Transport in a d-Wave Superconductor," *Phys. Rev. Lett.* **73,** 720 (1994).

Balatsky, A.V., M.I. Salkola, and A. Rosengren, "Impurity Induced Bound States in d-Wave Superconductor," Phys. *Rev. B* **51,** 15547 (1995).

Bishop, A.R., "Lattice and Multiband Electronic Effects in High-Temperature Superconductors, in *Strongly Correlated Electronic Materials*, K. Bedell et al, Eds. (Addison-Wesley, Reading, Massachusetts, 1994), p. 374.

Bishop, A.R., "Local Polarizability, Structure, and Charge-Transfer in HTC Superconductors" (to be published in *J. Superconductivity*).

Bonca, J. and A.V. Balatsky, "Composite Operators for BCS Pairing," *ZhETP Letters* **59,** 202 (1994).

Bussmann-Holder, A., and A.R. Bishop, "Anharmonicity in the c-direction of High-Tc Oxides," *Phys. Rev. B* **51,** 6640 (1995).

Hammel, P.C., B.W. Statt, R.L., Martin, et al., "Localized Holes in Superconducting Lanthanum Cuprate" (submitted to *Phys. Rev. Lett.*).

Martindale, J.A., P.C. Hammel, W.L. Hults, et al., "Temperature Dependence of the Anisotropic Planar Oxygen Nuclear Spin-Lattice Relaxation Rate in $YBa_2Cu_3O_{6.96}$" (submitted to *Phys. Rev. Lett.*).

Matveenko, S., A.R. Bishop, and A. Balatsky, "Superconductivity Fluctuations in a 1-dimensional, 2-band Electron-Phonon Model with Strong Electron-Electron Repulsion" (submitted to *Phys. Rev. B*).

Mustre de Leon, J., I. Baristic, A.R. Bishop, et al., "Reply to Comment on Polaron Origin for Anharmonicity of the Axial Oxygen in $YBa_2Cu_3O_7$," *Phys. Rev. Lett.* **75,** 584 (1995).

Salkola, M.I. and A.V. Balatsky, "Superconducting Fluctuations in Multi-band ID Hubbard Model," *Phys. Rev. B* **51,** 15267 (1995).

Salkola, M.I., A.R. Bishop, J. Mustre de Leon, et al., "Dynamic Polaron Tunneling in $YBa_2Cu_3O_7$: Optical Response and Inelastic Neutron Scattering," *Phys. Rev. B(RC)* **49,** 3671 (1994).

Salkola, M.I., A.R. Bishop, S.A. Trugman, et al., "Correlation-Function Analysis of Coupled Electron-Phonon Systems: Signatures of Polaron Tunneling," in *Anharmonic Properties of High Tc Cuprates*, P. Chu, Ed. (World Scientific, River Edge, New Jersey, 1994), p. 256.

Salkola, M.I., A.R. Bishop, S.A. Trugman, et al., "Correlation-Function Analysis of Nonadiabatic and Nonlinear Systems: Polaron Tunneling," *Phys. Rev. B* **51**, 8878 (1995).

Statt, B.W., P.C. Hammel, Z. Fisk, et al., "Oxygen Ordering and Phase Separation in $La_2CuO_{4+\delta}$" (to be published in *Phys. Rev. B*).

Engineering and Base Technologies

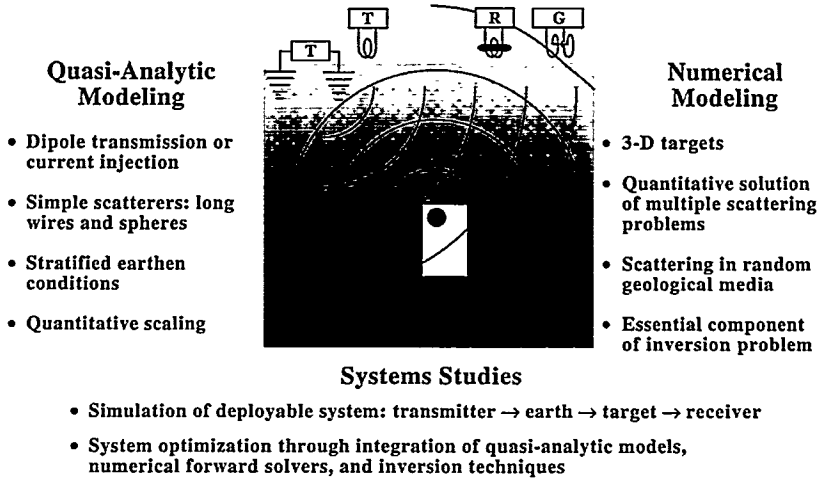
Detection of Underground Structures and Tunnels

Joseph Mack

The rapid political and social changes occurring around the world make it necessary for the United States and its allies to monitor a vast international array of clandestine threats. Modern surveillance technologies (for example, satellite surveillance) have forced clandestine operations to go underground; the profound complexity of underground detection gives those who hide and work underground a significant advantage. Because of worldwide variations in terrain and soil condition, there is no known technology that can detect underground clandestine operations in all situations; the prudent course to maintain national security is to develop a variety of systems that push the physical and technological limits of underground detection.

We have initiated a project to evaluate improved electromagnetic scattering (EMS) and gravity gradient (GG) underground detection methods. We wish to establish a common set of performance criteria for both methods using baseline experiments, verified semi-analytical theory, and numerical modeling (see figure). Work performed on this project will enhance our ability to verify underground structures and tunnels on-site or remotely by using improved geophysical methods. This verification capability is one of the highest priorities of the Department of Defense.

The primary objective of this project is to assess EMS and GG concepts and to develop selected approaches into fieldable systems able to detect and map underground structures and tunnels at 10- to 50-m depth. Properly configured electric- and magnetic-dipole techniques previously used in the mining industry are well-matched to our needs; GG methods complement EMS methods. Also, new superconducting quantum interference detection (SQUID) systems could significantly improve GG and EMS sensitivity. The detection problem requires progress in miniaturization and deployment; high-temperature SQUIDs may offer advantages in these areas. We are also evaluating how to engineer and characterize airborne platforms and how to use the global positioning system for ultra-accurate positioning and timing. Other objectives include developing a verified modeling ability, adapting EMS methods to underground communication requirements, and detecting unexploded ordinance.



Our collaborative theory and modeling effort provides an ability to assess and optimize several detection technologies.

Accelerator-Driven Transmutation of High-Level Waste from the Defense and Commercial Sectors

Charles Bowman

Our project aims to design a system for the accelerator transmutation of nuclear waste (ATW). Our ATW method will be applied to destroying plutonium from dismantled weapons and spent reactor fuel, as well as to producing energy from the thorium cycle, without producing a long-lived radioactive waste stream.

We have identified and quantified the unique qualities of subcritical systems and their capabilities in bringing about the complete destruction of plutonium, and we have continued our design work aimed at selecting the main components of an ATW system (see figure). Our base-design for a 500-MW_t system consists of (1) a 15-mA beam of 800-MeV protons, (2) a spallation target of flowing lead-bismuth eutectic (generating over 30 neutrons per incident GeV neutron), (3) a graphite moderator/reflector to achieve the optimum neutron spectrum for near-complete destruction of plutonium, (4) a molten fluoride-salt (LiF-BeF_2) blanket in which a subcritical amount of fissile material is dissolved with an effective multiplication factor of 0.95, (5) a reductive-extraction separations system for removing fission products after neutron irradiation, and (6) a steam-generating power system to generate electric power. For ATW, the spent reactor fuel will first undergo a preparation process consisting of hydrofluorination followed by electrowinning to separate out uranium, zirconium, and fission product metals.

Although these subcritical systems are a radical departure from traditional nuclear reactor concepts, ATW systems are based on extrapolations of existing technology. Such systems strive to keep the best that nuclear technology has developed over the years within a conservative design envelope and eventually to offer a safer and more environmentally sound approach to nuclear power.

Publications

Beard, C.A., and V.I. Belyakov-Bodin, "Comparison of Energy Deposition Calculations by the LAHET Code System with Experimental Results," *Nucl. Sci. Eng.* **119**, 87 (1995).

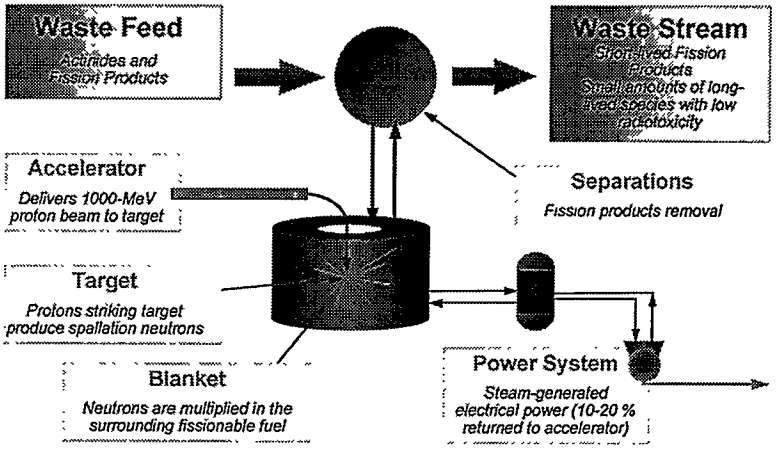
Beard, C.A., J.J. Buksa, M.W. Cappiello, et al., "Neutronics and Engineering Design of the Aqueous-Slurry Accelerator Transmutation of Waste Blanket," *Nucl. Technol.* **111**, 122 (1995).

Beard, C.A., J. Davidson, et al., "Parametric Systems Studies of the Aqueous-Based (Slurry) Blanket Concept for Accelerator Transmutation of Waste," *Nucl. Technol.* **110**, 321 (1995).

Krakowski, R.A., "Accelerator Transmutation of Waste Economics," *Nucl. Technol.* **110**, 295 (1995).

Olson, K.R., D.L. Henderson, et al., "Preliminary Investigation of Actinide and Xenon Reactivity Effects in Accelerator Transmutation of Waste High-Flux Systems," *Nucl. Technol.* **110**, 115 (1995).

Sailor, W.C., C.A. Beard, et al., "Review of Nuclear Waste Transmutation and Comparison of Accelerator-Based with Reactor-Based Transmutation Schemes," *Prog. Nucl. Energy* **28**, 359 (1994).



Principal components of the Los Alamos design for an accelerator-driven transmutation system for burning high-level nuclear waste (ATW) while generating useful nuclear power.

Feasibility of Microwave Interferometry and Fourier Transform Infrared (FTIR) Spectrometry for High-Spectral-Resolution Sensing

Joseph Giles and Siegfried Gerstl

The objective of this project was to determine the feasibility of new ideas based on high-spectral-resolution instruments and methods in satellite remote sensing. We performed field experiments with a Fourier transform infrared (FTIR) spectrometer to measure sensitivity, signal-to-noise ratios, and temperature dependencies when detecting gases in controlled plumes from various observation distances.

We remotely measured absorption spectra for ethylene, *n*-butanol, carbon tetrachloride, and other gases at a distance of 500 m. We found that the critical parameter determining detectability was the temperature difference between the plume and its background, which ranged from 15 K to 4 K in our field tests. These FTIR measurements proved the feasibility of measuring the presence and amounts of gases in a defined plume whose temperature differs significantly from that of the ambient atmosphere.

We also tested the feasibility of using microwave interferometry to determine the existence and extent of water-vapor irregularities in the atmospheric boundary layer. Knowledge of water-vapor distributions in the free atmosphere enables much improved atmospheric correction algorithms for remotely sensed surface images. Present indications are that the microwave interferometric technique works and that it is likely to be more accurate than other methods presently used.

Performance Monitoring for Plume Remediation and Containment Actions

Pat Unkefer

Bioremediation is a promising alternative to conventional cleanup technologies because of its relative speed, safety, and cost. However, current methods for measuring and evaluating the performance of bioremediation are inadequate. A key goal for future long-term bioremediation research is the development of both a basic understanding of, and methods for, assessing bioremediation performance. An improved understanding of the pathways and genes employed by bacteria in the catabolism of pollutants in actual field situations will

- improve our confidence in extrapolating genetic and physiological information from the laboratory to contaminated field sites,
- provide a basis for testing whether suspected biodegradative processes are actually occurring at field sites,
- aid in predicting the fate of pollutants, and
- assist in the development of inoculants for bioremediation.

Our project has focused on developing robust methods for detecting and monitoring bacterial populations which degrade toluene, an EPA priority pollutant. Toluene is catabolized in bacteria by one of five known pathways, each of which utilizes a distinct multicomponent oxygenase enzyme in aromatic-ring cleavage. Our objective is to develop the capability to detect, in both isolates and directly in environmental samples, genetic and metabolic markers of these pathways with the ultimate goal of quantifying their relative importance in the field and detecting possible new pathways for toluene catabolism. During this year, at a gasoline- and diesel-contaminated site, we have developed improved polymerase-chain-reaction-based methods for detecting and distinguishing indigenous toluene-degrading bacteria and their toluene catabolic pathways. In addition, we developed microcosm models to validate our molecular and chemical techniques for application at field sites.

Publications

Herrick, J.B., K.S. Harris, and J.R. Brainard, "Rapid Fingerprinting of Bacteria Using ERIC PCR Primers," in *PCR: Essential Techniques*, J.F. Burke, Ed. (Bios Scientific Publishers, Oxford, England, in press).

Megagauss Technology and Pulsed-Power Applications

Irvin Lindemuth

Magnetic-flux-compression techniques make it possible to produce ultrahigh magnetic fields and to generate ultrahigh-energy, pulsed electrical currents. Magnetic-flux compression permits access to a variety of extreme matter conditions and high-energy-density physics regimes.

Potential applications of magnetic-flux-compression technology include high-field and high-temperature superconductivity, the Faraday effect, cyclotron resonance, isentropic compression of solid materials, magneto-optical properties, plasma physics (including plasma confinement, plasma diagnostics, plasma production, fusion reactions, fluid properties, and plasma power supplies and energy storage), radiation sources for radiation-physics studies, astrophysics, energy research, and related endeavors. The world leader in flux compression is the All-Russian Scientific Research Institute of Experimental Physics (VNIIEF), Russia's premier nuclear weapons design laboratory.

Through this project Los Alamos has established a formal collaboration with VNIIEF, and the United States is acquiring unique Russian magnetic-flux-compression technology. Joint Los Alamos/VNIIEF experimental campaigns were conducted at Arzamas-16 in September 1993, April 1994, August 1994, February 1995, August 1995, and September 1995 and at Los Alamos in December 1993 and October 1994. The figures show experimental data from this collaboration.

The September 1993 experiment was the first-ever scientific experiment performed jointly by scientists from the nuclear weapons design laboratories of the United States and the Russian Federation. In addition to providing scientific benefits which accrue to both nations, the collaboration serves as a symbol that the two nations are beginning to "beat swords into plowshares" and has received extensive favorable coverage in the Russian and U.S. news media. This collaboration, and new ones modeled after it, represent a very effective way to prevent the proliferation of nuclear weapons by providing a scientific motivation and stabilizing influence.

Publications

Bykov, A., et al., "Complex Conductivity and Phase Diagram of $YBa_2Cu_3O_7$ in Magnetic Fields up to 500 T," *Supercon.: Phys., Chem., Tech.* 8, 37 (1995).

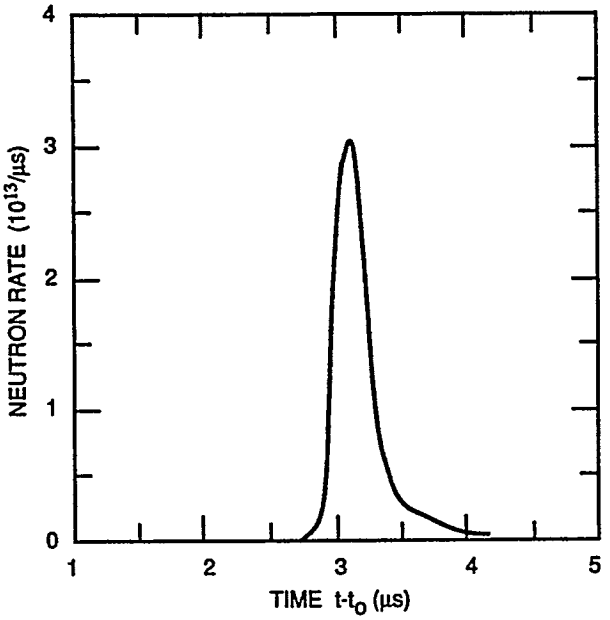
Bykov, A., M. Dolotenko, C. Fowler, et al., "Complex Microwave Conductivity of $YBa_2Cu_3O_7$ in Ultrahigh Magnetic Fields up to 500 T," *Physica B* **211**, 248 (1995).

Druzhinin, V., O. Tatsenko, A. Bykov, et al., "Nonlinear Faraday Effect in CdS Semiconductor in a Ultra High Magnetic Field," *Physica B* **211**, 392 (1995).

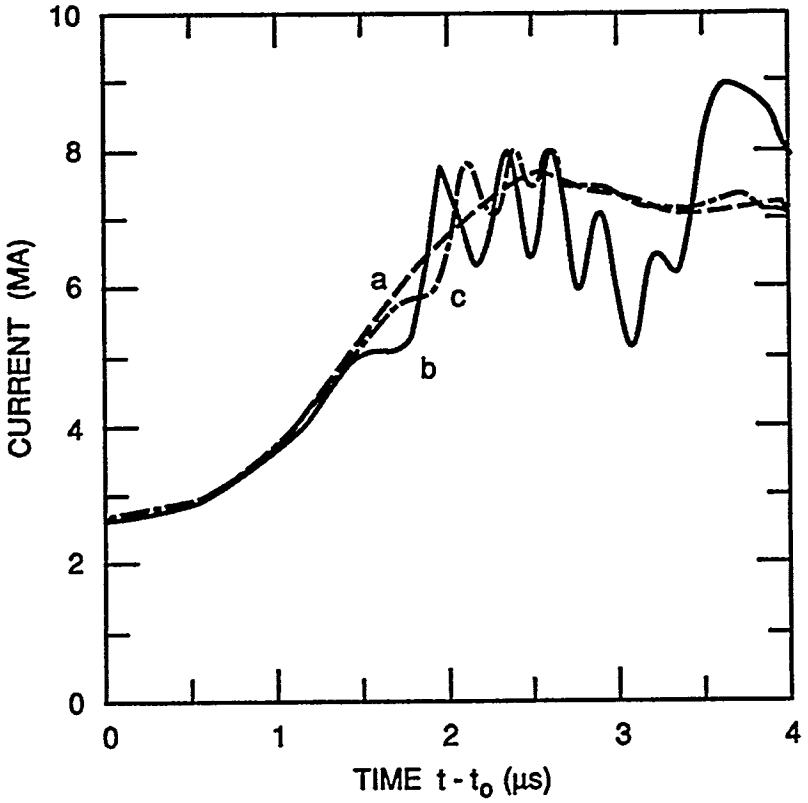
Goettee, J., Yu. Kudasov, W. Zerwekh, et al., "Complex Microwave Conductivity of $YBa_2Cu_3O_7$ in Magnetic Fields up to 500 T," *Physica C* **235-40**, 2090 (1994).

Lindemuth, I., et al., "Target Plasma Formation for Magnetic Compression/Magnetized Target Fusion (MAGO/MTF)," *Phys. Rev. Lett.* **75**, 1953 (1995).

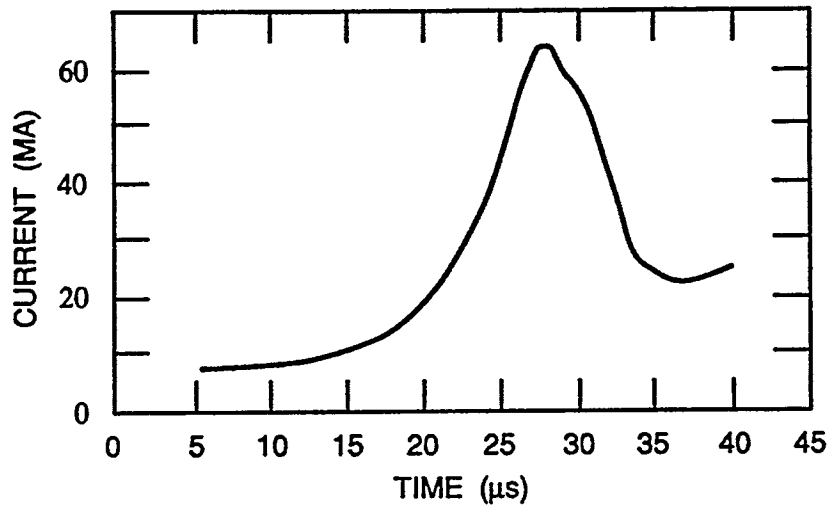
Sheehey, P., "Magnetized Target Fusion," *The World and I*, May 1995.



The deuterium-tritium thermonuclear-neutron pulse measured in the joint U.S./Russian MAGnitnoye Obzhatiye (MAGO, or magnetic-compression) magnetized-target-fusion plasma-formation experiment at Los Alamos in October 1994. The 10^{13} neutrons were the most ever produced at Los Alamos in a single pulse.



Los Alamos 2-D magnetohydrodynamic (MHD) computations are in good agreement with the current measured during the MAGO plasma-formation experiment at Los Alamos in October 1994: (a) chamber input current, (b) chamber-inductive-probe measured signal, and (c) chamber-inductive-probe computed signal. The computations predict that thermonuclear-fusion ignition can be achieved if the plasma is subsequently imploded in a magnetized-target-fusion (MTF) context.



The electrical current delivered by a Russian Disk Explosive Magnetic Generator to an imploding solid liner intended to form a "plasma bubble" source of soft x-rays. The current delivered in a February 1995 joint U.S./Russian experiment at Arzamas-16 exceeds existing U.S. "off-the-shelf" capability.

Advanced Satellite Sensors: Low-Energy Neutral Atom (LENA) Imager

Herbert O. Funsten

The terrestrial magnetosphere is immersed in the tenuous neutral atom geocorona, and plasma ions can be neutralized through charge exchange with geocoronal atoms. The neutralized plasma ions, which follow trajectories that are not affected by magnetic or electric fields, can be remotely detected, revealing detailed information about the source plasma. Collectively, these measurements provide global imaging of the structure and dynamics of the magnetosphere and are the next major scientific step in magnetospheric physics. The bulk of the neutralized plasma ions, or LENAs, resides at energies of 1–30 keV.

Although the field of magnetospheric imaging is quite new and the next NASA opportunity for flying a LENA imager is years away, we have developed and designed a potential flight LENA imager. The key aspect of the imager involves separating the LENAs from the enormous flux of ultraviolet (UV) radiation (to which the LENA detectors are sensitive) without losing trajectory and energy information carried by the LENA. We investigated two technologies: (1) gold transmission gratings, in which LENAs transited the grating while UV radiation was blocked (primarily by the waveguide effect) and (2) LENA ionization by transmission through an ultrathin (50 Å) carbon foil and subsequent electrostatic deflection into the LENA detector.

After performing complete theoretical and laboratory analyses of both techniques, we determined that the foil method was the most technologically mature. Furthermore, after performing detailed modeling and simulation of anticipated LENA images, we derived complete designs for hardware, electronics, and system integration. Los Alamos is now prepared to construct and fly the first LENA imager on an available ride of opportunity and to obtain the first global images of the terrestrial magnetosphere.

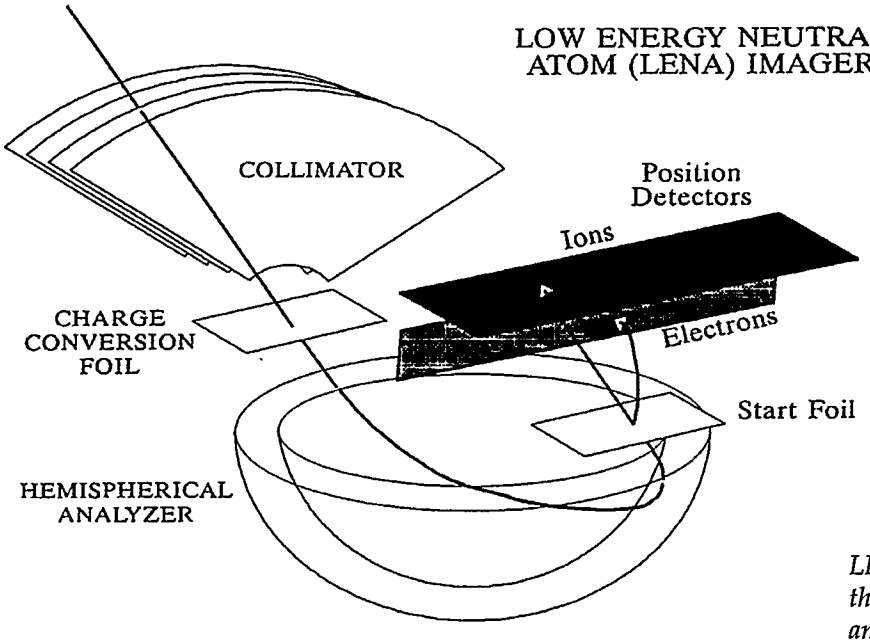
Publications

Funsten, H.O., D.J. McComas, K.R. Moore, et al., "Imaging of magnetospheric dynamics using low energy neutral atom detection," in *AGU Monograph No. 84: Solar System Plasma Physics: Resolution Processes in Space and Time*, J.L. Burch and J.H. Waite, Eds. (American Geophysical Union, Washington, 1994), p. 275.

Funsten, H., D. McComas, and E. Scime, "Low Energy Neutral Atom Imaging for Remote Sensing of the Magnetosphere" (to be published in *J. of Spacecraft and Rockets*).

Scime, E., E. Anderson, D. McComas, et al., "Extreme-Ultraviolet Polarization and Filtering with Gold Transmission Gratings," *Appl. Opt.* **34**, 648 (1995).

Scime, E., H. Funsten, D. McComas, et al., "Three Dimensional Neutral Atom Imaging of Tokamak Plasmas," *Rev. Sci. Instrum.* **66**, 336 (1994).



LENA imager for global imaging of the magnetospheric plasma structure and dynamics.

Thermoacoustic Natural Gas Liquefier

Gregory Swift

Our objective is to perform fundamental research to enable the development of a natural-gas-powered, natural gas liquefier that has no moving parts, requires no electrical power, has high efficiency, is maintenance-free, and is portable and environmentally benign. The thermoacoustic natural-gas liquefier (TANGL) is based on our recent invention of the first cryogenic refrigerator with no moving parts, which uses acoustic phenomena to produce refrigeration from heat. The refrigerator's experimental success on a small scale in earlier projects led us to propose a more ambitious application: large-scale liquefaction of natural gas that uses combustion of natural gas as the energy source.

Our efforts were instrumental in establishing a three-way partnership (Los Alamos, National Institute of Standards and Technology, and Cryenco, Inc.) that is developing a 500-gal./day TANGL prototype. We have designed and built a half-scale experimental model of the liquifier portion of the prototype. Results from our model provide data in the same sense that wind-tunnel tests with scale-model airplanes give exact information on the performance of the full-size airplane. The 500-gal./day prototype, which is being constructed by Cryenco, Inc., is large enough to illuminate all the issues of a large-scale TANGL without undue cost. The prototype is also appropriate for application to small fleet-vehicle fuel stations. Our completed two-year LDRD effort was instrumental in securing follow-on DOE programmatic support for continued research with our scale model. This research will continue to provide the performance data required to improve the technology's efficiency.

Publications

Swift, G.W., "Thermoacoustic Engines and Refrigerators," *Phys. Today* 48, 22 (1995).

A Predictive Ocean Oil Spill Model

James Sanderson

The major oil and gas companies of the United States are now exploring in deep offshore shelf areas. Detailed knowledge of the ocean's currents from surface to sea bottom are essential to model deep-water oil spills. In particular, ocean currents or eddies in selected geographic areas must be better understood. Ocean eddies can be thought of as hurricanes in the ocean and are of special importance. They are often localized and their effects can be devastating, especially on anchored exploration platforms. The Eddy Joint Industry Project (EJIP) consortium has been sampling eddies in the Gulf of Mexico for a number of years and would like to compare their data with computer model output.

The central theme of our project is to use output from the Laboratory's global ocean model to look in detail at ocean currents in selected geographic areas of the world. Once ocean currents are well understood, this information can be used to create oil spill models, improve the design of offshore exploration and drilling equipment, and aid in the design of semipermanent offshore production platforms.

Our work focused on making available three-dimensional, time-dependent ocean current data for the Gulf of Mexico. We have developed a graphics program that allows EJIP members to extract any geographical area around the world and to display and manipulate the area's full topography, particularly its ocean bottom topography. We have also developed graphical user interfaces to view model output in a time-dependent fashion so that a fully three-dimensional current profile could be animated in real time. Finally, we sponsored a workshop at Los Alamos to show EJIP representatives how to use the state-of-the-art graphics tools involved in analyzing model output.

Advanced Tunable Laser Source for DoD Applications

Nigel Cockroft

Recent initiatives in environmental monitoring, nuclear nonproliferation, battlefield chemical- or biological-agent detection, air-traffic safety, narcotics interdiction, and improved military systems have stimulated major interest in light-detection-and-ranging (LIDAR) research. Optimization of many of these applications will require laser transmitters that are not yet commercially available. Specifically, the sensitivity and selectivity of laser-based remote-sensing techniques are greatly increased by using compact solid-state lasers whose wavelengths can be tuned to the atomic resonances of specific chemical species.

The objective of this project is to develop a new, broadly tunable laser for LIDAR and other applications using the chromium-doped lithium strontium aluminum fluoride (Cr:LiSAF) crystal. No group has previously fully configured this emerging laser technology for LIDAR applications. This versatile laser also has many applications to military imaging and defensive optical countermeasures.

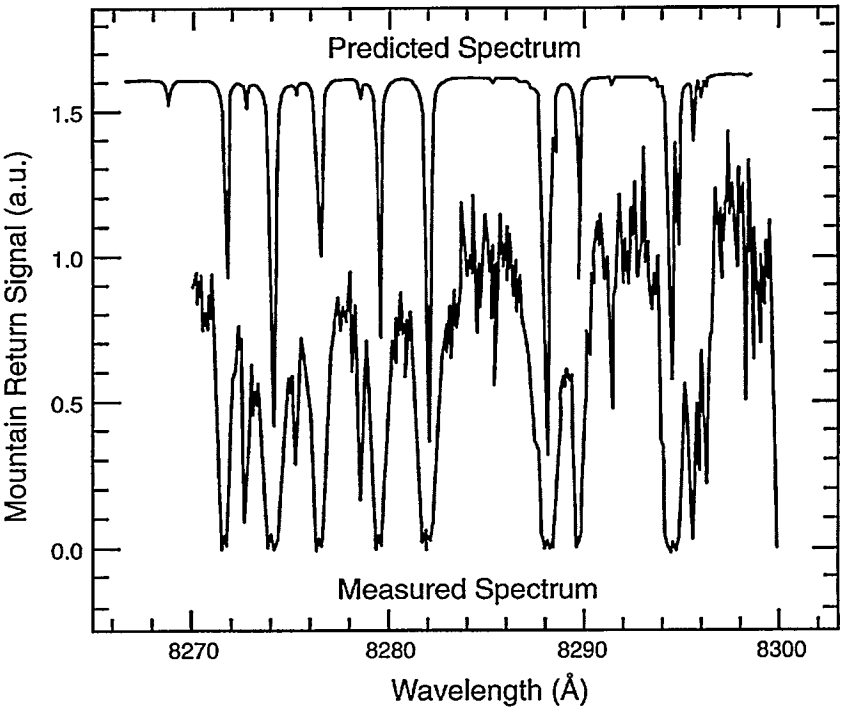
Within this project we have determined many relevant design parameters of this new laser medium and have developed a prototype laser with record efficiency, record average power, record Q-switched pulse energy, and narrow linewidth. We used this laser to perform the first field demonstrations of remote-sensing LIDAR measurements (see figure).

Recent activities include developing a high-power LIDAR system; using injection seeding to tune narrow-linewidth semiconductor-diode lasers; remote-sensing measurements of water vapor, uranium, nitric oxide, and ammonia; and atmospheric temperature measurements. We have coordinated relevant technical activities in materials development, chemical sensing, atmospheric measurements, and military applications with researchers at universities, companies, NASA, and the U.S. Army.

Publications

Shimada, T., J. Early, C. Lester, et al., "Repetitively-Pulsed Cr:LiSAF Laser for LIDAR Applications," in *Proceedings of the OSA Advanced Solid-State Lasers Meeting, 1994*, Ty. Fan and B. Chai, Eds. (Optical Society of America, Washington, DC, 1994), p. 188.

Early, J., C. Lester, C. Quick, et al., "Continuously-Tunable, Narrow-Linewidth, Q-Switched Cr:LiSAF Laser for LIDAR Applications," in *Proceedings of Advanced Solid-State Laser Meeting, 1995*, B. Chai and S. Payne, Eds. (Optical Society of America, Washington, DC, 1995), p. 9.



Comparison of LIDAR-measured water vapor spectrum (lower curve) with the predicted spectrum (upper curve).

Establishing the Operational Durability of Polymer Light-Emitting Diodes

Ian Campbell

Recently discovered polymer light-emitting diodes (PLEDs) have the potential to revolutionize display technology. In the near future displays are expected to be major drivers in both the computer and high-definition television industries. At Los Alamos we are developing PLEDs in collaboration with Hewlett-Packard Company, Uniax Corporation, the University of Texas at Dallas, and the University of California at Santa Barbara.

Our collaborative research has shown that PLEDs have all the necessary device attributes—efficiency, emission colors, and operating voltage—required for a successful display technology. In order to control device reliability and ultimately produce a viable commercial product, we must now establish device operating lifetimes and understand PLED failure mechanisms.

For this purpose we have set up a PLED lifetime testing facility and are measuring changes in PLED light output and drive voltage at constant current as functions of time for different currents, operating temperatures, and device (polymer) thicknesses. This work has just begun, but the dominant failure mechanism of the PLEDs has already been identified as delamination of the electron-injecting metal contact, which occurs at less than 1000 hours of operation.

Publications

Campbell, I.H., D.L. Smith, and J.P. Ferraris, "Electrical Impedance Measurements of Polymer Light-Emitting Diodes," *Appl. Phys. Lett.* **66**, 3030 (1995).

Davids, P., A. Saxena, D.L. Smith, et al., "Bipolaron Lattice Formation at Metal-Polymer Interfaces" (submitted to *Phys. Rev. B.*).

McBranch, D., I.H. Campbell, D.L. Smith, et al., "Optical Determination of Chain Orientation in Electroluminescent Polymer Films," *Appl. Phys. Lett.* **66**, 1175 (1995).

Development of a High-Count-Rate Neutron Detector with Position Sensitivity and High Efficiency

Ronald O. Nelson

Future advances in neutron-scattering science depend on the development of new thermal-neutron detection schemes and ideas. At pulsed sources the present detector systems are not adequate to accept high thermal-neutron fluxes. At LANSCE (the Los Alamos Neutron Science Center), the low-Q diffractometer is saturated with rates of 30 kHz, and the high-intensity powder diffractometer has neutron pile-up events at rates of 100 kHz per detector.

Worldwide there are numerous efforts directed at neutron detector research. Our project goal is to identify which emerging technology best matches LANSCE requirements and offers the possibility of commercial success. We explored the various neutron technologies under development during the past several years and assessed the requirements at LANSCE. Our research focused on literature and contacts with staff at other laboratories in the United States and Europe.

From a wide array of detector technologies (e.g., microstrip, gas-linear with position sensitivity, gas area, scintillation, and solid-state area), we identified two technologies that offer the maximum benefit for projected LANSCE research: gas microstrip and solid-state area.

The work performed in this project has application to radiation instrumentation, neutron physics, and material structures.

Development of a Low-Level In-Line Alpha Counter (LLILAC)

Russell Gritzo

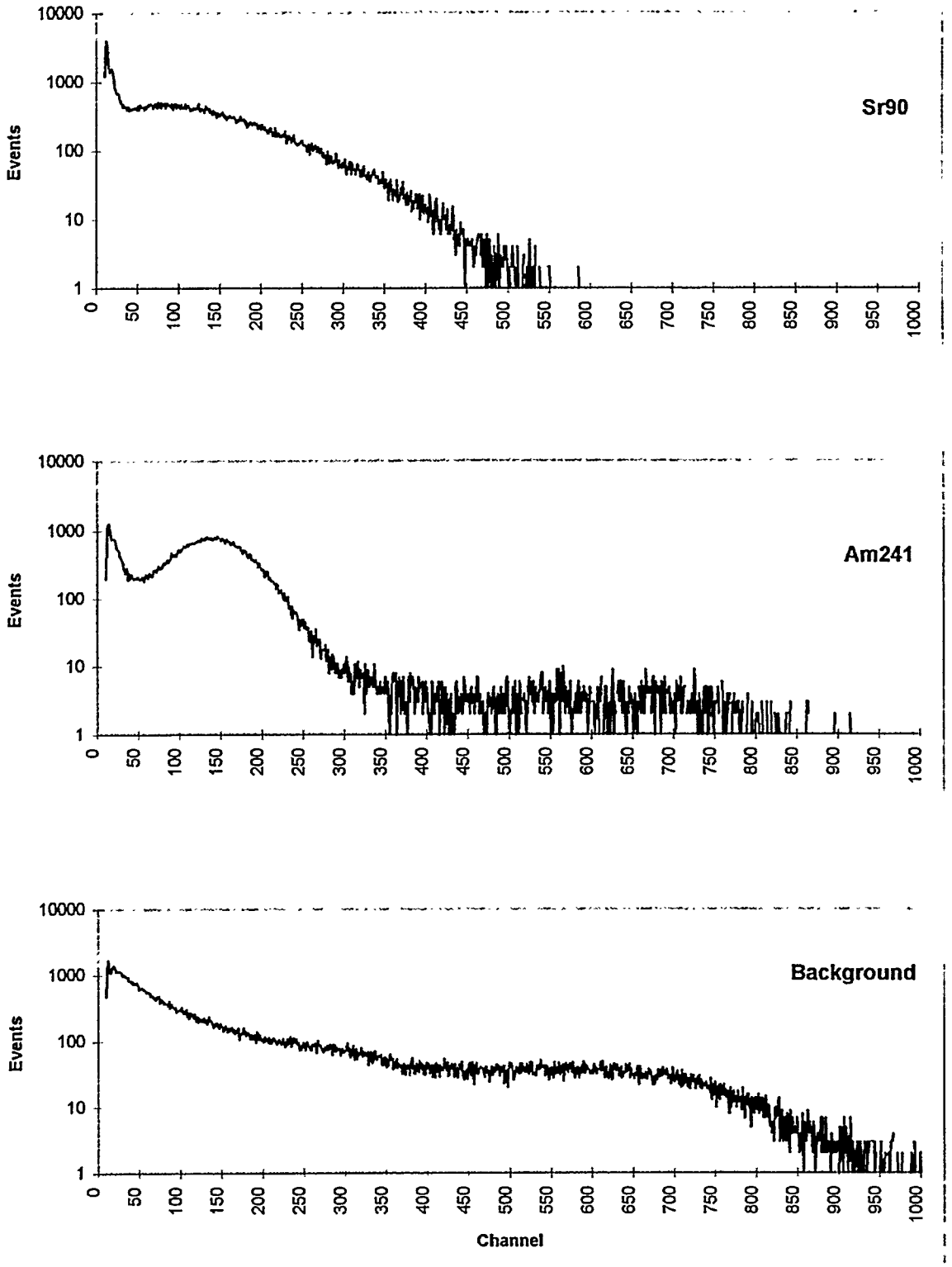
Many processes in the DOE complex and in the commercial sector involve aqueous streams containing radioactive materials. Examples of activities that produce such streams include fuel reprocessing, waste treatment facilities, and remediation activities. Increasing awareness of water contamination issues in the environment and rising consequences of any form of contamination are placing increased demands on effluent monitoring. In particular, monitoring for the presence of any radioactive material is paramount. One of the more challenging on-line instrumentation needs is for monitoring alpha-emitting radionuclides in aqueous process streams. Requirements to reduce analytical cost and response time make existing off-line batch sampling techniques unfavorable when compared with on-line instruments that can yield near-real-time analytical results.

The Low-Level In-Line Alpha Counter (LLILAC) addresses the need for on-line, near real-time monitoring of alpha-emitting radionuclides in aqueous streams. Although primarily designed as an on-line instrument for real-time applications, the detector can also be used for long-term, in situ post-closure monitoring. LLILAC operates by allowing the aqueous stream to come in contact with a large number of small rods or tubes made of scintillating material. By maximizing the surface-to-volume ratio of the scintillator, we favor the detector's response to alpha particles over other types of radiation. Several configurations of scintillator and light collection schemes have been investigated to optimize detection efficiency. We have written several Monte Carlo codes to help to predict and understand detector performance.

The accompanying figure shows the detector's response to a high-energy beta-emitting nuclide (strontium-90) and an alpha-emitting nuclide (americium-241), along with the detector's background response. In the figure, counting was done so that there are the same number of counts in each spectrum, making the statistical uncertainty in each spectrum similar. For strontium-90, a typical smooth beta spectrum is produced except for a low-energy peak corresponding to single photoelectron production. For americium-241, there is a fairly broad peak due to 5.4-MeV alpha emission, and again there is the low-energy peak associated with single photoelectron detection.

From these measurements, we can estimate the relative light production from alpha and beta radiation. For strontium-90, with a maximum energy of 2.2 MeV, the response extends out to channel 500, corresponding to about 50 photoelectrons (p.e.) or about 23 p.e/MeV. For the alpha particles (americium-241), the peak is at channel 150, corresponding to about 15 p.e. or about 2.7 p.e./MeV. This relative light production is typical of plastic scintillators and indicates that the detector should be better at detecting beta particles than alpha particles. We compensate for this by using very thin scintillators so that although the alpha particles will lose all of their energy in the detector, beta particles will leave only a small fraction of their energy.

We have measured a detection efficiency of about 3% for a detector made with small tubes. This measured value is in good agreement with our Monte Carlo estimates. Our current detector has an active volume of only about 30 cm^3 and a background of about 18 counts/s. We can estimate the detection sensitivity by calculating the concentration of alpha-emitting activity in the counter's active volume necessary to have an alpha count rate equal to the background. For the current detector, the concentration would be about 580 nCi/L. This concentration can be significantly reduced by building a larger detector and by keeping only those counts with energies corresponding to alpha events. Our approach to a novel alpha monitor has been shown to be workable and has both adequate detection sensitivity and design flexibility to be useful for a number of applications.



LLILAC detector's response to strontium-90 and americium-241 and its background; we can see activity above background levels and photomultiplier-tube thermal noise.

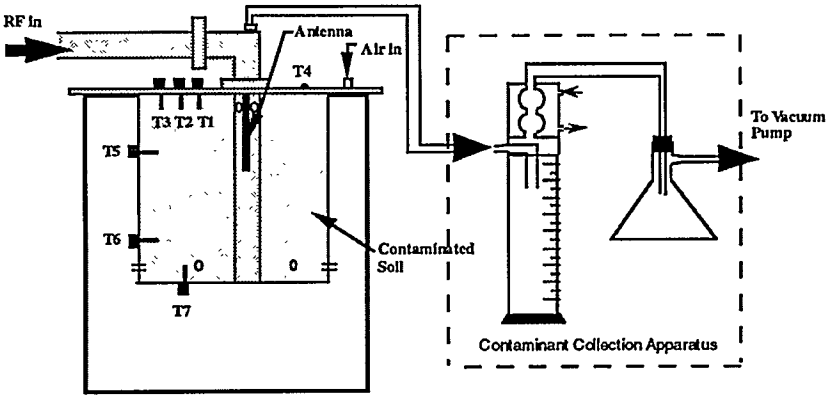
In Situ Microwave-Energy-Based Soil Remediation

Amy Regan

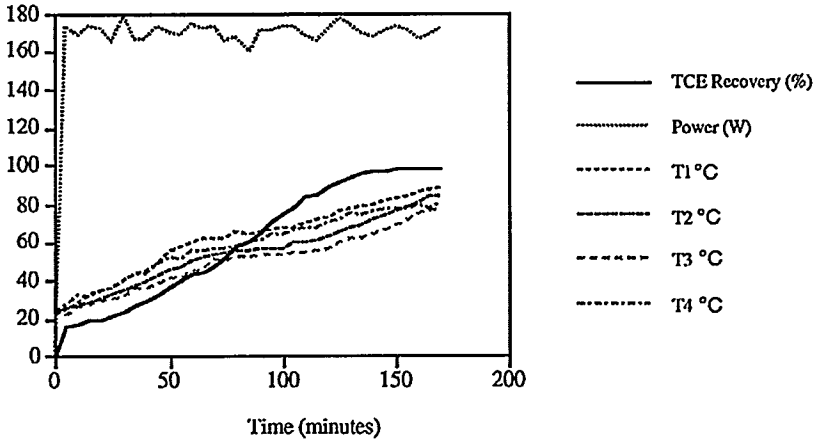
Contaminant plumes are significant waste problems that require remediation in both the government and private sectors. We are developing an in situ process that uses RF- or microwave-energy stimulation to remove pollutants from contaminated soils. This process is more efficient than existing technologies, creates less secondary pollution, and is applicable to situations that are not amenable to treatment by existing technologies.

Our in situ remediation process, based on RF- or microwave-energy stimulation, removes dense, nonaqueous-phase liquid (DNAPL) pollutants. RF energy applied to the contaminated soil raises the temperature to a point higher than the boiling point of the DNAPL yet lower than that of water. This past year we have defined an in situ microwave-energy-based soil remediation process, measured relevant RF or microwave characteristics of various soils, and developed two small-scale test chambers.

To date, we have been working primarily with an Air Force base soil sample provided to us by a potential cooperative research and development agreement (CRADA) partner, Montgomery Watson, a large environmental remediation company. We contaminated this soil with a DNAPL (CCl_4) and exposed it to RF energy. We volatilized the contaminant and achieved 90%–100% recovery of the DNAPL at relatively low soil temperatures (~70°C). Residual-gas analysis verified that we are not creating harmful byproducts. With a test chamber as depicted in the accompanying figure, we have shown the ability to use a downhole antenna to deliver RF energy into a contaminated volume of soil and, together with vapor extraction, have recovered >95% of the contaminant. The accompanying graph displays data measured from a test run on our apparatus.



Our second experimental setup—a volume of contaminated soil heated by RF energy applied via an antenna with stripping gas flowing as anticipated in the field demonstration.



A plot of RF power delivered, temperature as measured at different points of the test chamber, and the amount of contaminant recovered relative to the length of time of RF exposure for indigenous soil contaminated with trichloroethane (TCE).

Russian Collaborations on Lasers and Advanced Optics

James Munroe

There are several areas of technology where Russian work is judged to be far ahead of comparable work done in the West. The Russians are ahead in these areas because they have successfully pursued technologies and approaches different from those of their counterparts in the West.

High-power nonlinear optics and millimeter-wave radar are two of these areas, and there are undoubtedly more. Partnering with the Russians on applications involving such technologies would allow Los Alamos to effectively expand its technology base with a minimal investment. Because Russian costs are relatively low, a Los Alamos sponsor would receive more value for his dollar by incorporating Russian work into his project. The objective of our project was to match appropriate Russian technologies to potential Los Alamos sponsors and, for a particular technology, to bring the combination of Russian technology and Los Alamos sponsor to the attention of the appropriate Los Alamos program managers.

Three general programmatic areas were identified in our project: space debris, environmental remote sensing, and military applications. Because of policy sensitivities here and in Russia to military collaboration, we decided to eliminate the third category and to emphasize the first two. We find ourselves well on track for our first-year objectives, with several potential sponsors and programmatic areas identified.

Directed Light Fabrication—A Laser Metal-Deposition Process for Fabrication of Near-Net-Shape Components

Gary Lewis

Directed Light Fabrication (DLF)—a process invented and under development at Los Alamos—fuses layers of powdered metals in the focal zone of a laser. By successively building up fused layers, we fabricate a free-form metal part. With this capability we can eliminate conventional metal-working processes such as forging, stamping, casting, machining, and welding.

The goal of this project is to model the thermal gradients in DLF-rod and -plate formation, to verify those models experimentally, and to use the model data to modify process-control commands and to predict solidification behavior. Our approach to gain improved control, hence greater accuracy, over the DLF process is to model and measure the dynamics of the molten pool and how the molten pool solidifies.

The choice of process and process equipment must be based on laser power, speed, and mass input. We have developed thermal models for rod and plate deposits and have made experimental thermocouple and infrared measurements of both deposit processes. The thermal models for the DLF deposits agree with experimental measurements made during deposition. Use of the modeling data will provide a means to alter DLF process parameters for better control over deposit uniformity and microstructure. We also designed gas control, powder delivery, and powder recycling systems for a 5-axis DLF system.

Publications

Lewis, G., "Directed Light Fabrication—A Direct Laser Metal Deposition Process for Fabrication of Near Net Shape Components," *Mater. Technol.* **10**, 51 (1994).

Development of a High-Gradient Magnetic Separator Using High-Temperature Superconductors

F.C. Prenger

High-gradient magnetic separation (HGMS) is used for the separation of solids from other solids, liquids, or gases. Superconducting magnet technology has made it possible to separate more than half of the elements in the periodic table using this method. Recent advances in high-temperature superconducting (HTS) magnet development have made it possible to build an HGMS system using an HTS magnet.

Our objective is to develop a conductively cooled HGMS system using an HTS magnet, as shown schematically in our first accompanying figure. The design includes HTS current leads, which are shown in our second figure. The system will operate without the need for liquid cryogens, will be portable, and will be used to demonstrate both HTS and HGMS technologies.

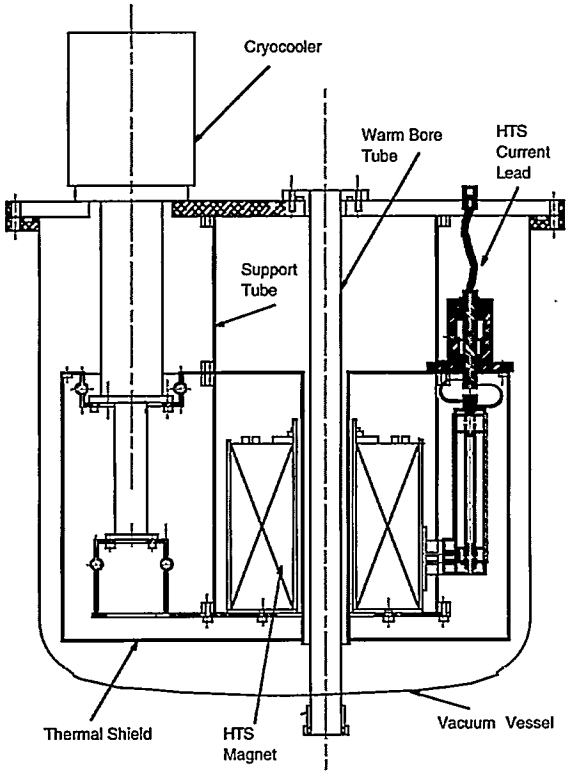
Currently the HGMS technology employs low-temperature superconducting magnets. Although more cost effective than electromagnets, low-temperature superconducting magnets must be operated at 4 K and typically require submersion in liquid helium. By using a high-temperature superconducting magnet, we can operate at 25 K—which will simplify the system design considerably and result in a more portable and robust system.

We have completed the design of the HGMS system using an HTS magnet. The system components have been fabricated and final assembly is in progress. The high-gradient magnetic separation system will be, to the best of our knowledge, the first conductively cooled HTS magnet to perform with the full fields required for an industrially viable magnetic separation system.

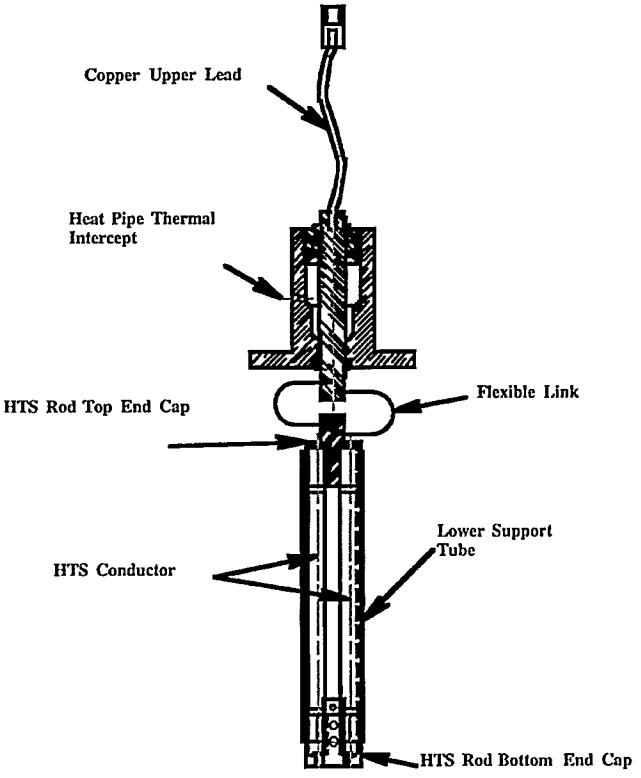
Publications

Daugherty, M.A., F.C. Prenger, D.D. Hill, et al., "HTS Current Lead Using a Composite Heat Pipe," *IEEE Trans. Appl. Superconductivity* 5, 773 (1995).

Daugherty, M.A., D.E. Daney, F.C. Prenger, et al., "Assembly and Testing of a Composite Heat Pipe Thermal Intercept for HTS Current Leads" (to be published in *Adv. Cryogenic Eng.*).



High-gradient magnetic separator.



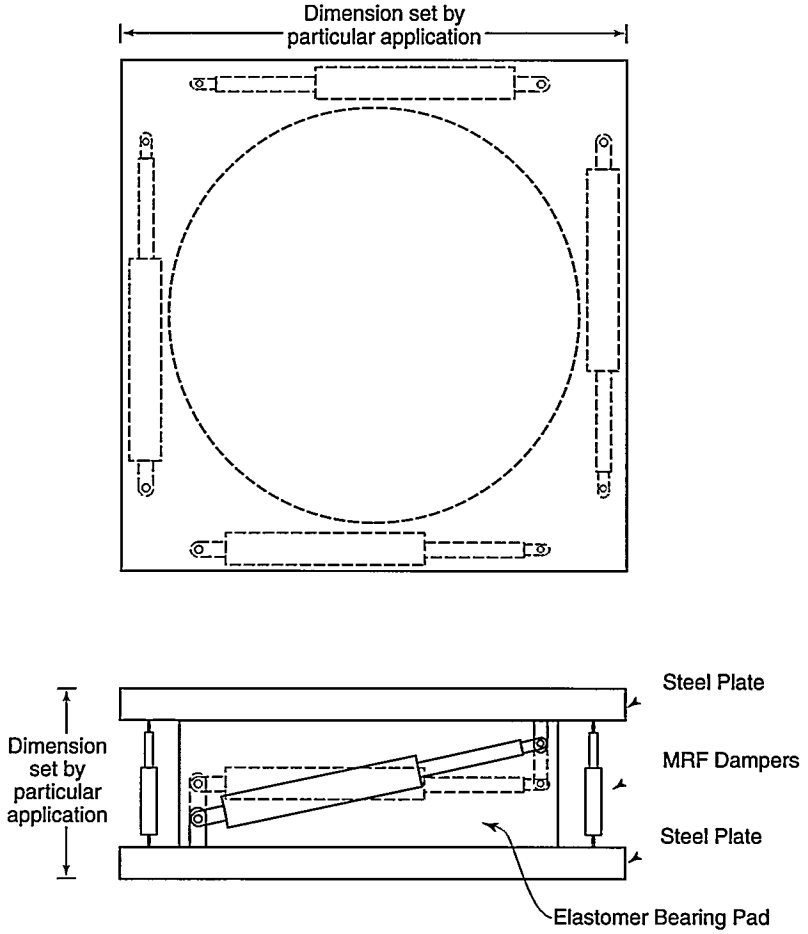
High-temperature superconducting current lead assembly.

Active Vibration Control of Civil Structures

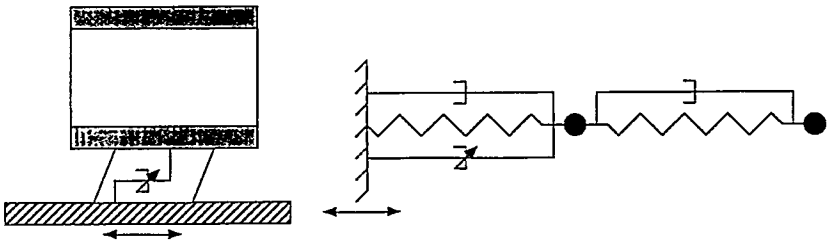
Charles Farrar

In this project, we investigated one of the rapidly advancing areas of engineering research: active vibration control of structural and mechanical systems. In the first phase of this research effort, we completed a thorough review of the literature pertaining to active vibration control of civil engineering structures, with particular emphasis on the use of magnetorheological fluid (MRF) dampers. In the second phase, we established a conceptual design using an active control system that can be used as a retrofit option or can be used in new construction (see figures).

The results we obtained show that a vibration isolator based on an actively controlled magnetorheological fluid-filled damper has the potential to offer enhanced vibration mitigation over passive dampers. The proposed design can be adapted to large civil structures or smaller mechanical systems and will mitigate vibrations caused by seismic events as well as those caused by impulsive-type loading. Our review of the literature shows that the application of an MRF damper to civil engineering systems is unique. The Advanced Research Project Agency is interested in funding the actual development and testing of an isolator system based on the technology produced during this project.



Vibration isolator based on magnetorheological fluid-filled dampers.



Structural Parameters: (for 32 isolators)

Mass of the Roof	=1,775,000 lbm
Mass of the Floor	=1,665,000 lbm
Structural Stiffness	=100,000 lbs/in
Isolator Stiffness	=70,400 lbs/in
Structural Damping	=5%
Isolator Damping	=10%
Max MRF Damping Force	=1,760,000 lbs (55,000 lbs each)

Idealization of an isolated structure.

Hydrogen Fueling Station Development and Demonstration

Fred Edeskuty

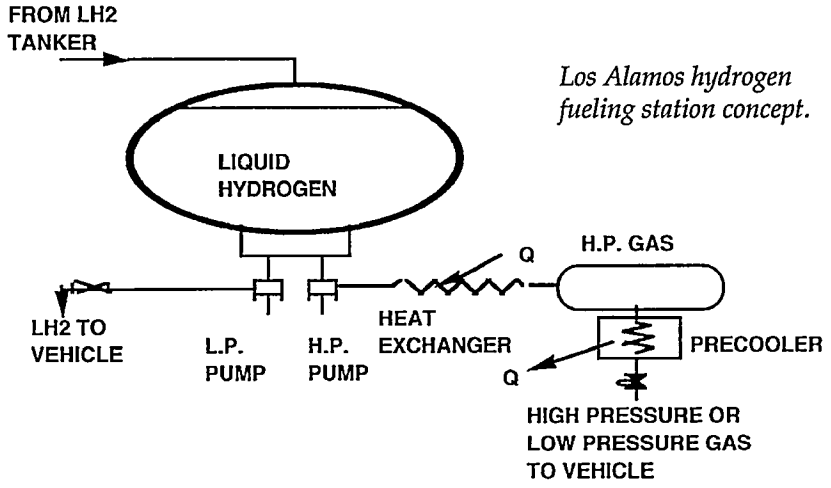
Because of the need to improve urban air quality, hydrogen-fueled vehicles have become a subject of increasing interest in recent years; in fact, a number of demonstration projects are planned or in progress around the world. Hydrogen fueling stations are essential to a practical demonstration of these vehicles. Furthermore, only a practical demonstration can accurately and convincingly address a number of issues such as safety, efficiency, design, and operating procedures. Regardless of whether the vehicle is powered by an internal combustion engine or fuel cell, or how hydrogen is stored on-board, the fueling station is the critical technology that links the local hydrogen storage facility and the vehicle (see first figure).

The goal of our project is to develop and demonstrate a hydrogen fueling station for vehicles. In the past year, we developed a conceptual design of the fueling station to serve as the basis for modeling liquid and gaseous transfer, safety analysis, and identification and pricing of major components. We also developed a hydrogen-transfer model as a design tool. Finally, we constructed a complementary model of vehicle fuel efficiency as a function of the on-board storage method (liquid, compressed gas, or hydride—see second figure) to specify design parameters for the hydrogen delivery system. Our research found that refueling hydrogen-powered vehicles in less than five minutes (without venting of the hydrogen) is feasible with a properly designed fueling station (see third figure).

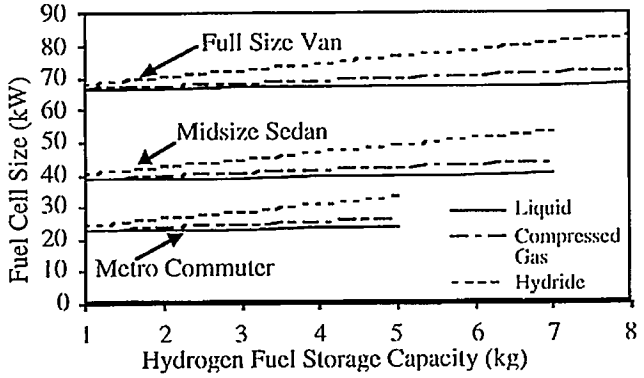
Publications

Daney, D.E., F.J. Edeskuty, M.A. Daugherty, et al., "Hydrogen Vehicle Fueling Station," in *Advances In Cryogenic Engineering*, Peter Kittel Ed. (Planum Press, New York, in press).

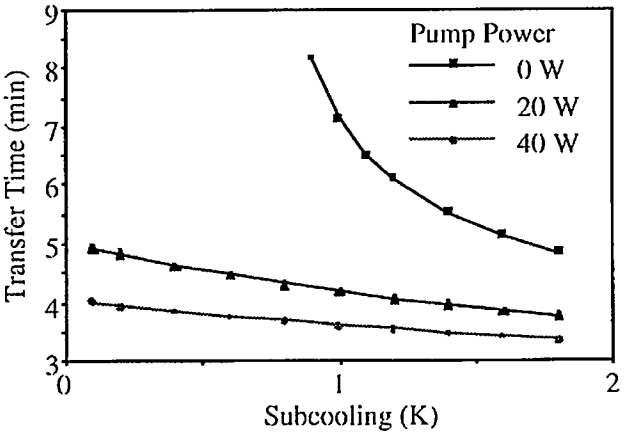
Daugherty, M.A., F. Prenger, D. Coyne, et al., "A Comparison of Hydrogen Vehicle Storage Options Using the EPA Urban Driving Schedule," in *Advances in Cryogenic Engineering*, Peter Kittel Ed. (Plenum Press, New York, in press).



Los Alamos hydrogen fueling station concept.



Fuel cell size as a function of hydrogen storage capacity.



Effect of transfer-pump power on calculated LH2 transfer time for no-vent transfer. Initial pressure difference is 1.0 bar. Initial vehicle tank pressure is 1.0 bar, and line inside diameter is 10.9 mm.

Night Vision Device Technology Development

Herbert Funsten

Night vision devices utilizing image-intensification tubes—the type used extensively by the military—have two significant problems that can critically compromise their operation: the field of view is restricted because of abberations introduced by the flat image plane and by gain loss (i.e., loss of light sensitivity) when a bright light source is within the field of view. A wide field of view is critical to aviators, who need peripheral vision for motion cues and for viewing nearby obstacles or aircraft, and bright-spot suppression is crucial to night missions performed in an urban or lighted environment (from streetlights, flares, or headlights, for example).

We have developed two technologies to overcome these problems. First, we are designing a curved image plane using recently developed detector technology for a wide field of view. We have performed optical and electro-optical simulations that enable fields of view of up to 80 degrees. And second, we have designed segmented microchannel plates and associated independent gain-control circuitry to suppress gain in the segment illuminated by a bright light source and retain full gain across all other segments so that dim objects within the field of view remain visible.

We have also initiated a collaborative effort with an industrial partner to develop proof-of-principle protoypes and to evaluate the possibility of retrofitting our technologies into existing night vision devices. Patents for these technologies are currently being pursued.

The Application of Microrobotics in Warfare

Johndale C. Solem

Progress in the development of microlithographic techniques for fabricating motors, pumps, flexors and other actuators, as well as chemical, electromagnetic, and mechanical sensors, has stimulated much speculation about the application of such devices in warfare. One area of speculation and research has dealt with construction of small (nearly undetectable by dint of size) sensor packages and their use in collecting intelligence concerning troop movements and other activities within enemy territory. These nonmotile sensing robots could be dispersed by a low-observable unmanned air vehicle and could be interrogated from time to time by the same aircraft.

A second area of speculation and research has dealt with construction of microrobots capable of moving themselves. An underlying premise is that these devices could be manufactured in large quantities and at low cost, much the way integrated circuits are manufactured today. A high probability of mission success could be ensured by using many identical devices programmed to accomplish the same task. The most important consideration for the motile microrobot is the energetics of its locomotion.

After considerable study, we decided that the near-term objective of the project was to develop a microscale flying device for surveillance and counter-proliferation. Rather than immediately pursuing the microlithographic fabrication techniques and using electrostatic motors, which are natural to the microlithography scale, we chose to investigate gram-scale devices using electromagnetic motors. We analyzed several alternative designs for microflyers, including some lighter-than-air devices, and also evaluated some rotary-wing lifting systems. We found that the rotary-wing systems were capable of kilometer-scale missions, if a high-rate lithium battery technology was employed. Lighter-than-air vehicles were considerably more complex but were capable of missions of indefinite duration.

Publications

Solem, J.C., "The Motility of Microrobots," in *Artificial Life III, SFI Studies in the Sciences of Complexity,* C. Langton, Ed. (Addison-Wesley, Reading, MA, 1994), p. 359.

Electromagnetic Targeting of Guns

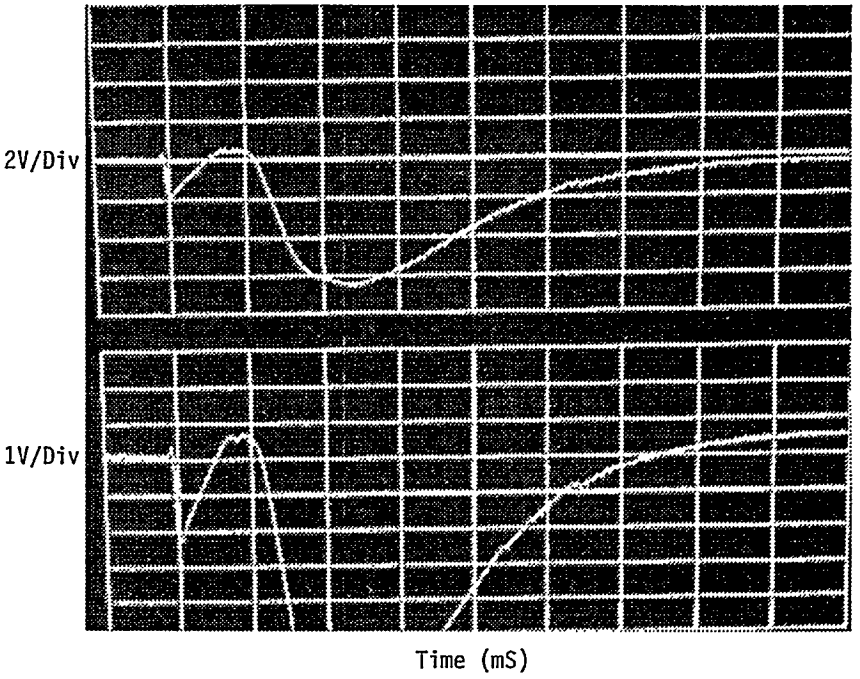
Edward Pogue

Radio-frequency (RF) signals produced by detonating energetic materials have been reported in the literature for the last fifty years. The research objective of this project is to establish the existence and nature of RF emissions produced by firing various weapons, including rockets, rifles, and heavy guns. The goal is to see if we can use these signals to detect and locate enemy weapons at the speed of light.

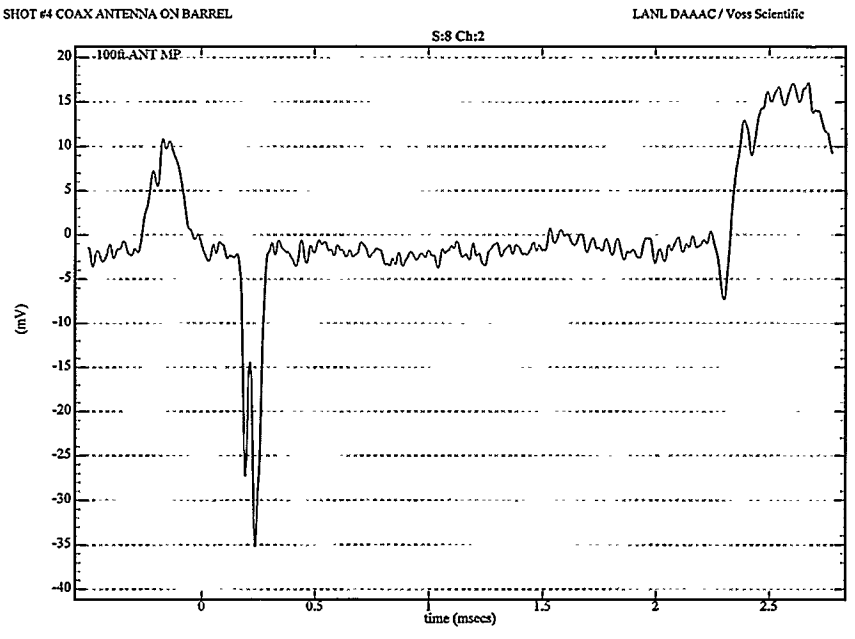
For each weapon tested we fielded many antennas and field monitors around the weapon and recorded signals on digital oscilloscopes when the weapon was fired (see figures). We triggered the oscilloscopes with various sensors, including infrared detectors, light screens, and foil switches at the muzzle of the weapon. The signals were subsequently analyzed for frequency content and compared to background measurements and the antenna response curve.

The major result of our study is that we found signals for every weapon tested. Rapid changes in the electric field produced by the weapons were seen in virtually all cases, but not all of these changes occurred on a short enough time scale to cause measurable RF emissions.

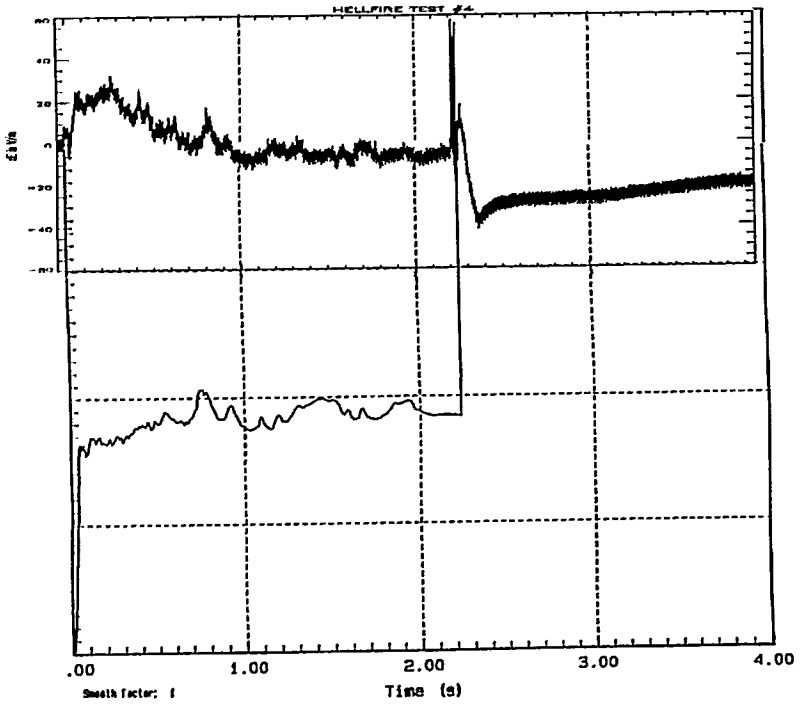
We have concluded, at this time in the project, that this phenomenon occurs for many weapons systems and that multiple mechanisms combine to produce these signals.



The signal from a military rifle. Both traces are the same signal on different scales.



The signal from a 30-mm experimental cannon. Zero time is when the bullet leaves the muzzle.



Data from an antitank rocket motor. The top trace is the electric field; the bottom trace is the thrust. The rocket exploded at 2.2 seconds.

Remote Moving Target Indication Assessment

Gregory H. Canavan

Moving target indication (MTI) sensors on remotely piloted vehicles, aircraft, or satellites could detect moving vehicles against cluttered backgrounds. Our project produced designs for the sensor and its computer and ideas on how to modify satellite remote sensors and computers to function as MTI sensors. The designs could be tested and prototyped rapidly, important advances for defense and counterproliferation work.

MTI sensors integrate multiple, low-signal infrared observations (unresolved points of light) to pull moving targets out of noise. The integration reduces the required signal-to-noise ratio per detection, which reduces the size, weight, and cost of optical components. Simplifying the optics increases the computation rates required, but these rates are within the capability of current flight computers with straightforward track assembly—and are even lower with neural net or Viturbi algorithms. Balancing optical simplification against computational complexity, which makes MTI sensors feasible, is not generally appreciated. It reduces the optical components to the levels of those we have flown on related programs while maintaining the computational burden at the level of flight computers in development.

Our project sketched out the changes needed to use existing remote-sensing cameras and flight computers for MTI. The deliverables were an assessment of alternative designs, the design for a proof-of-principle experimental sensor, and the results of analytic evaluation, which have been disseminated through publications.

Publications

Canavan, G.H., "Alternative Architectures," in *New World Vistas* (Air University Press, Montgomery, Alabama, in press).

Canavan, G.H., "Survivability of Space Systems," in *New World Vistas* (Air University Press, Montgomery, Alabama, in press).

Canavan, G.H., and S.P. Worden, "Space in the Next Century" (to be published in *Air University Rev.*).

Autonomous Biomorphic Robots as Platforms for Sensors

Mark Tilden

Our project focused on developing autonomous robots that could ultimately carry sensors for various applications. Our goal was to build machines that could survive in realistic environments and then use these machines to do useful work, such as mine clearing or remote sensing. The machines themselves were built using simple, processorless control structures that functionally mimic the neural controls of simple animals. So far several successful walking robots have been built in this way. We have concentrated on refining these devices and on using them in a particular application—the remediation of unexploded ordnance. We have built simple solar-powered walking devices and tested them in the field. The control structures seem adequate, but better walking mechanisms are needed, as well as better power sources.

The work performed in this project has application to treaty compliance and verification issues (including both remote and on-site inspection), and measures for long-term land restoration following radioactive contamination or chemical or thermal pollution. Our work may also apply to land use and reclamation and to the understanding of processes, activities, and functions of parts of living systems.

Plasmas, Fluids, and Particle Beams

Contamination and Uniformity Control in Plasma Processing Tools

Gary Selwyn

In this project we have collaborated with industry to build a laboratory to study plasma processing, a highly developed technology used in semiconductor fabrication to clean and decontaminate surfaces without chemicals that pollute the environment. This surface-cleaning technique uses short-lived, gaseous reactants in place of chemical solvents and avoids problems of waste disposal and minimizes the byproducts of decontamination.

We have performed experiments and developed computer models to understand how complex substrate geometries affect plasma electrical properties (see figure) and to demonstrate the feasibility of generating metastable molecular oxygen in a plasma. This metastable molecule, a reactive form of oxygen, can be used as an environmentally safe "dry" cleaning agent which degrades harmlessly to ordinary oxygen gas in less than 0.2 second at atmospheric pressure.

Our plasma-processing laboratory and nearly all of the associated equipment required for this work were made possible by a $750,000 equipment donation from IBM Corporation. A U.S. small business interested in our work donated additional plasma-processing equipment worth $150,000. The plasma-processing laboratory is now operational; it was built without any Los Alamos capital equipment funds.

Publications

Lapenta, G., F. Iinoya, and J.U. Brackbill, "Particle in Cell Simulation of Glow Discharges in Complex Geometries," *IEEE Trans. Plasma Sci.*, **23**, 769 (1995).

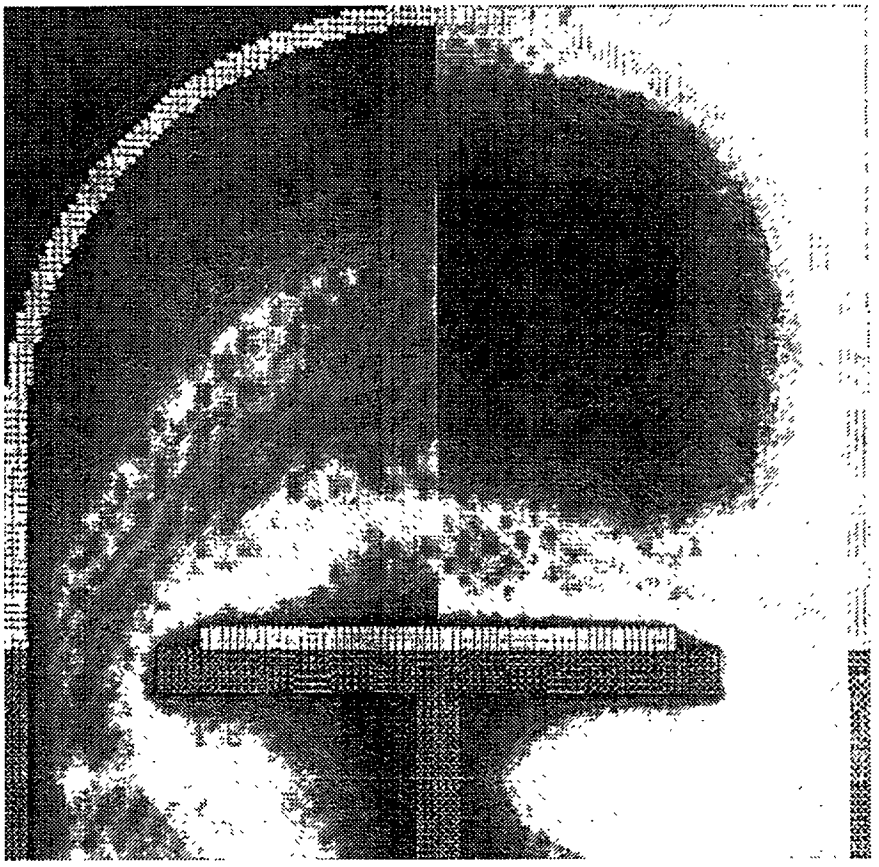


Illustration of our ability to model how complex substrate geometries affect plasma properties. Left side of figure: calculated electrostatic potential without plasma. Right side of figure: calculated electrostatic potential with plasma. The containment vessel is quartz. The chuck at the center of the vessel is a conductor with a silicon wafer on the top surface (not to scale).

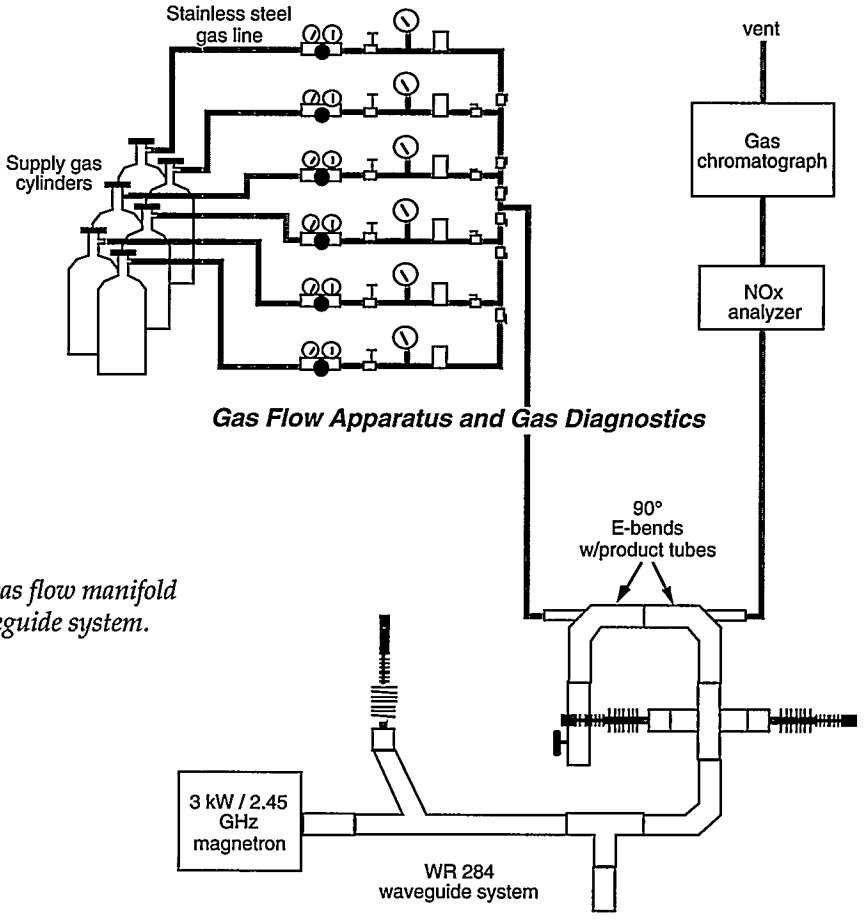
Advanced Technology for Nitrogen Oxide (NO_x) Abatement in Flue Gas Using Microwave Irradiation of Coal Char

Michael Fazio

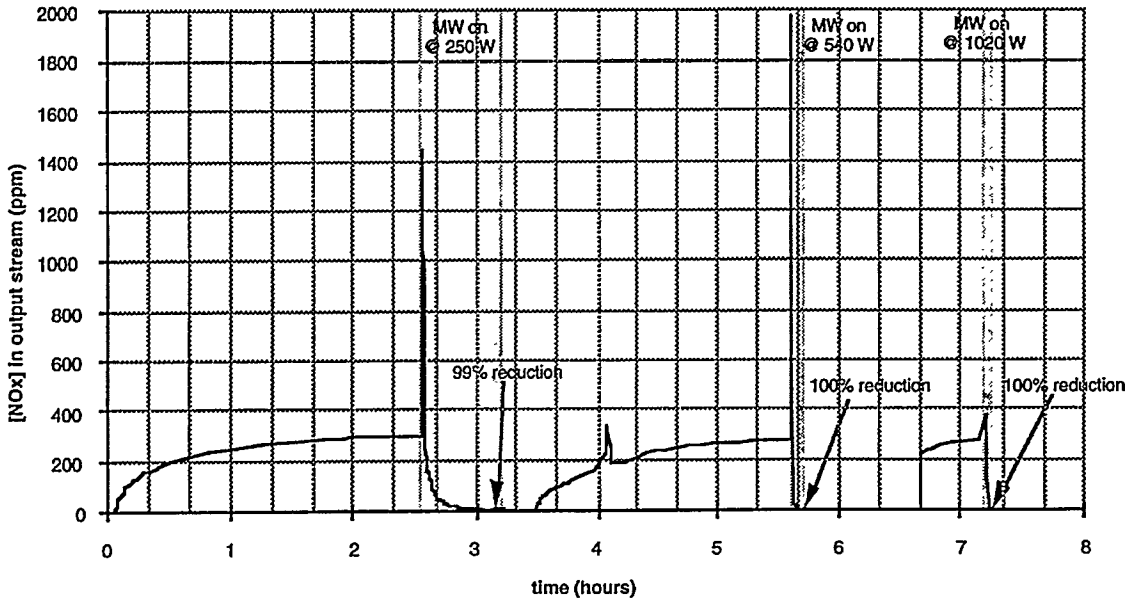
Nitrogen oxides (NO_x) emitted into the air by combustion-based power generation, manufacturing, and transportation are a significant air-pollution problem leading to photochemical smog, street-level ozone, and acid rain. The Clean Air Act Amendment of 1990 mandates a substantial improvement in air quality by 1997 that cannot be economically met with existing technologies. An exciting new approach to this problem was first demonstrated by Dow Chemical Company and Cha Corporation in a bench-scale study in which NO_x was removed from a waste-gas stream using coal-char filter beds. Subsequent microwave irradiation of the NO_x-loaded char safely decomposed the adsorbed NO_x with 98% efficiency.

Our research objective has been to gain an understanding of the underlying chemistry and operative microwave/material interactions in order to develop and optimize the process for commercial use. Our approach has been to bring together a multidisciplinary team with capabilities in high-power microwaves, microwave/materials interactions, chemistry, and chemical engineering to confirm and optimize the process.

Achievements in the past year include a demonstration of 100% removal and destruction of NO_x from a helium carrier gas, 80% removal and destruction from realistic exhaust-gas streams (gas mixtures containing O_2, CO_2, water, hydrocarbons, etc.), and minimization of the char consumption rate and of unwanted byproducts. The work performed in this project has application to nitrogen oxide abatement in coal and oil-fired power plants, industrial NO_x emitters, and mobile air polluters such as automobiles. The accompanying figures show our experimental apparatus and sample data.



Experimental apparatus combining the gas flow manifold and gas diagnostics and microwave waveguide system.



Data on NO_x abatement. The three sets of data correspond to incident microwave power levels of 250, 540, and 1020 W.

Waste Minimization in Chrome Plating

Jay Scheuer

Traditional electroplating, routinely applied to improve the lifetime of machine tooling, uses toxic materials and poses environmental hazards. The goal of this project is to reduce the chrome-plating waste stream by developing plasma source ion implantation (PSII). PSII is an economical technology for the formation of low-friction, high-strength, corrosion-resistant surfaces. It is a non-line-of-sight ion implantation technique that reduces the complexity and cost of traditional beam implantation.

We are developing and demonstrating PSII on a scale that would allow treatment of very large parts. This technology could revolutionize manufacturing, allowing the use of high-performance machinery while reducing (or eliminating) hazardous wet chemical processes. We are using the Laboratory's PSII facility, the largest ion implanter in the world, to modify and then measure the surface properties of steel manufacturing equipment. Work includes defining material systems and performing characterization and wear tests of implanted parts.

Progress during the reporting period includes the following. First, a comparative PSII study using ammonia-, methane-, and oxygen-implanted chromium showed increased surface hardness and wear resistance through the formation of hard compounds: CrN, Cr_3C_2, and Cr_2O_3. Ammonia-implanted chromium had a 4-times-longer wear lifetime and a 25% increase in hardness. Second, components were processed in collaboration with International Paper (IP), J.I. Case, GM Electromotive, and Alcoa. One component, a 3- × 8-ft IP press plate, represents the world's largest ion-implanted surface. Processed parts are currently being field-tested by our partners.

Publications

Walter, K., J. Scheuer, P.C. McIntyre, et al., "Increased Wear Resistance of Electrodeposited Chromium Through Applications of Plasma Source Ion Implantation Techniques" (to be published in *Surface Coatings Technol.*).

Plasma Source Ion Implantation for Advanced Manufacturing

Jay Scheuer

Research in the past few years has led to an experimental facility at Los Alamos for plasma-source ion implantation (PSII). In the PSII process we apply high-voltage pulses to a target immersed in a plasma. Plasma ions are accelerated by the electric field and buried in the target surface. The implanted ions change the surface chemistry and microstructure of the target surface and improve its surface properties, such as hardness, fatigue life, corrosion resistance, friction, and wear resistance. Compared to conventional ion-implantation technology, the PSII process provides more uniform implantation on complex-shaped components and higher throughput at lower cost. It is also an environmentally conscious alternative to wet-chemical plating. PSII has defense and civilian applications in many areas, including manufacturing, transportation, aerospace, electronics, environmental, biomedical, and energy.

The purpose of this project is to perform research and development in the areas of plasma and high-voltage technology, modeling, analysis, and assessment. This research will enable us to develop and demonstrate PSII on an industrially relevant scale. Specifically, this project targets R&D in five thrust areas: (1) investigating process windows to ensure successful scale-up demonstrations by industrial partners, (2) developing prototype components, (3) developing user-friendly systems-analysis models tailored to specific applications and evaluating the environmental impact of PSII and its influence on energy and transportation issues, (4) using existing supercomputer modeling to compute plasma dynamics, continuum mechanics, and surface-mechanical properties on an atomic scale, and (5) investigating materials design and analyses, including chemical, microstructural, and surface-mechanical properties.

We have achieved significant progress toward our goals in all five project areas. Nine industrial partners are now field-testing scale-up demonstrations on components of interest to them; we are assembling a new experimental deposition system at Los Alamos; we have designed and are now constructing a prototype solid-state PSII modulator; we have developed a generic model to calculate the cost-per-part for PSII; and we have performed molecular-dynamics modeling of the wear process for a model system (our plasma modeling has concentrated on magnetic insulation of secondary electrons during PSII).

Publications

Walter, K., J. Scheuer, P.C. McIntyre, et al., "Increased Wear Resistance of Electrodeposited Chromium Through Applications of Plasma Source Ion Implantation Techniques" (to be published in *Surface Coatings Technol.*).

Hammerberg, J.E., B.L. Holian, and S.J. Zhou, "Studies of Sliding Friction in Compressed Copper," in *Shock Compression of Condensed Matter—1995*, S.C. Schmidt and W.C. Tao, Eds. (American Institute of Physics, Woodbury, New York, in press).

Advanced Ignition of Jet Turbine Engines

James Kennedy

This collaborative project between industry and Los Alamos is relevant to research into reduced emissions from high-altitude aircraft, improved fuel efficiency for jet turbine applications, and expanded flight performance envelope for commercial and military aircraft. Such improvements are made possible by advances in engine ignition achieved with the use of microwave and laser technologies. The primary goal of our research is to demonstrate the possibility for unobtrusive fuel ignition within the primary fuel-flow region located at the center of the turbo-jet combustor.

We have succeeded in generating high-energy free-standing microwave plasmas both in a commercial General Electric J79 combustor and in a smaller combustor designed at Los Alamos in such a way that it could be installed in a jet engine. The power input required by the combustor is equal to that required by an ordinary home microwave oven; the possibility for inexpensive commercialization is thus greatly enhanced. BF Goodrich and Los Alamos have jointly applied for two patents on this technology.

We have also evaluated two laser-induced ignition concepts in an experimental program to initiate Jet A fuel aerosols produced by a commercial turbo-jet forced-air atomizer. Using a relatively simple, compact laser light source (single-pulse Q-switched Nd:YAG), we have successfully demonstrated efficient and reliable ignition of jet fuel aerosols at realistic fuel compositions and flow rates. A dual-pulse laser ignition concept, which had previously been disclosed by Los Alamos for patent coverage, has provided reliable ignition over a wider range of fuel compositions at equivalent total laser-energy requirements. Los Alamos researchers successfully demonstrated proof-of-principle for this concept.

INTEGRATED TREATMENT FOR MIXED/LEGACY WASTES CONTAINING METALS AND ORGANIC COMPOUNDS

Nancy Sauer

Heterogeneous wastes (HWs)—defined here as wastes containing bulk solids contaminated with one or more components subject to the Resource Conservation and Recovery Act (RCRA), the Comprehensive Environmental Response, Compensation, and Liability Act (CERCLA), and the Toxic Substances Control Act (TOSCA) or subject to radiation restrictions—are difficult to treat by any single conventional or developing technology. Most HWs generated now are either stored on-site or sent for landfill disposal. However, these alternatives are not satisfactory as long-term solutions because of their high cost and potential for environmental contamination.

Effective treatment of HWs includes

- destruction of toxic and hazardous organic compounds,
- removal, concentration, and recycling (or immobilization) of toxic and radioactive metals, and, if feasible,
- volume reduction of bulk materials.

Our goal is to develop and implement integrated chemical and biological treatment technologies to accomplish these three treatment objectives for HWs. We have demonstrated our approach at bench and small pilot scales on paint stripper waste (PSW). This legacy waste was generated at many DOE facilities during actinide processing and facility decontamination and decommissioning. It contains large volumes of cellulosic materials (rags, cheesecloth) and toxic metals (Cr and Pb), and it is suspected of containing radioactive metals (U, Pu, and Am). Los Alamos National Laboratory alone has approximately 200 drums, 55 gal. each, of this waste for which no permitted treatment technology is available. To treat HWs, we have coupled two accepted and proven waste treatment technologies—metal extraction chemistry and biological degradation of organic compounds.

To treat PSW, we use defined microbial consortia for destruction of volatile organic solvents, extracellular enzymes for destruction of cellulosic material and overall volume reduction, and water soluble chelators for selective removal and recovery of metals. The sequence of steps in this process is not static—indeed, some processes can occur simultaneously. The advantage of our modular approach is that it allows tailoring of the treatment system for each particular waste stream.

We have also worked with a regional small business to apply a portion of our technology to solve an increasingly common problem in sanitary-waste treatment systems: contamination and resulting kill of activated sludge systems by RCRA organic compounds. We have demonstrated increased resistance of an activated sludge system to inhibition by RCRA organic compounds, particularly substituted benzenes, when the sludge was bioaugmented with a microbe we have isolated to specifically degrade these RCRA organic compounds.

Publications

Vanderberg-Twary, L., R.K. Grumbine, M.N. Taylor, et al., "Evidence for Three Different Pathways in Toluene Utilization by Rhodococcus Rhodochrous Strain OFS"(submitted to *Appl. Environ. Microbiol.*).

Separations Technology Development for Accelerator Transmutation Technology Concepts

Francesco Venneri

Physical and chemical separation processes are essential elements of accelerator-driven transmutation technology (ADTT) systems. The goals of this project were to explore and develop processes for fuel preparation and cleanup.

Molten-salt hydrofluorination followed by electrowinning are processes we have identified to prepare spent nuclear waste for neutron irradiation in the ADTT blanket (see first figure). Using favorable differences in electrochemical potential, electrowinning extracts uranium and zirconium from the spent fuel without separating the plutonium and fission products. This robust process is applicable to any kind of plutonium-bearing waste, from spent reactor fuel to plutonium residues to weapons-grade plutonium.

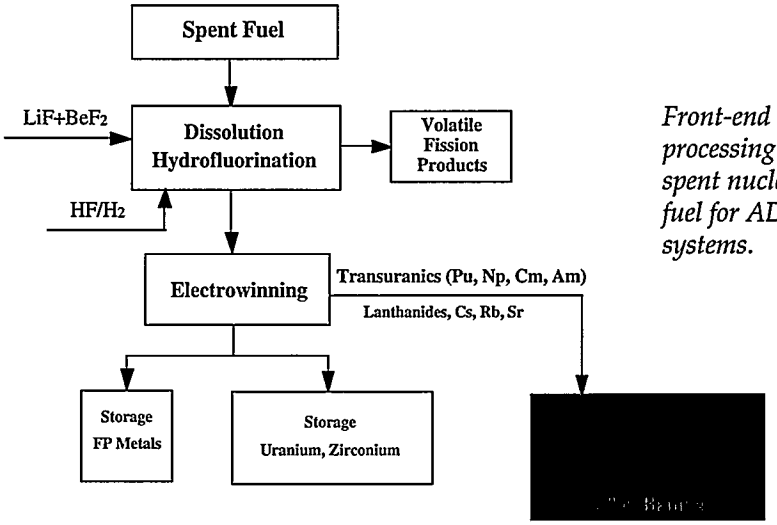
While no actinide separation from the fuel is needed for ADTT operation and all actinide isotopes are fissioned and used for their energy content, the by-products of fission must be removed from the fuel. The fission by-products in molten salt can be extracted by three processes:

1. Volatile species and noble gases will be removed by helium flow or sparging.

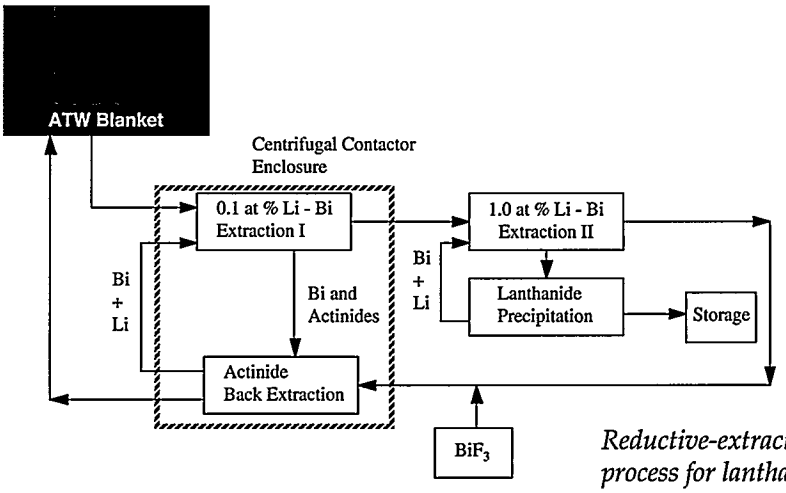
2. Noble and seminoble metals have low solubility in the salt and will plate-out on internal surfaces.

3. The remaining by-products, including the rare earths, stay in the salt solution but increase in concentration. Lanthanides and other nonvolatile species will be removed using a lithium-bismuth reduction process, possibly followed by liquid centrifugation and precipitation (see second figure).

Whereas the first two processes could be performed continuously, the lanthanides could be removed at intervals of as long as 5 to 10 years, as they accumulate in the fuel. With these three processes, ADTT systems now appear to preclude nuclear proliferation and diversion.



Front-end processing of spent nuclear fuel for ADTT systems.



Reductive-extraction process for lanthanide separation.

Publications

Li, N., R. Camassa, et al., "Centrifugal Separation for Miscible Solutions: Fundamentals and Applications to Separation of Molten Salt Nuclear Materials," in *Proc. Intl. Conf. on Accelerator Driven Transmutation Technologies and Applications* (American Institute of Physics, New York, 1995), p. 799.

Li, N., R. Camassa, et al., "Solutal Separation under Centrifugation" (submitted to *Int. J. Heat Mass Transport*).

Decontamination of Radioactive Liquids by Freeze Concentration and Fractional Precipitation

Ann Schake

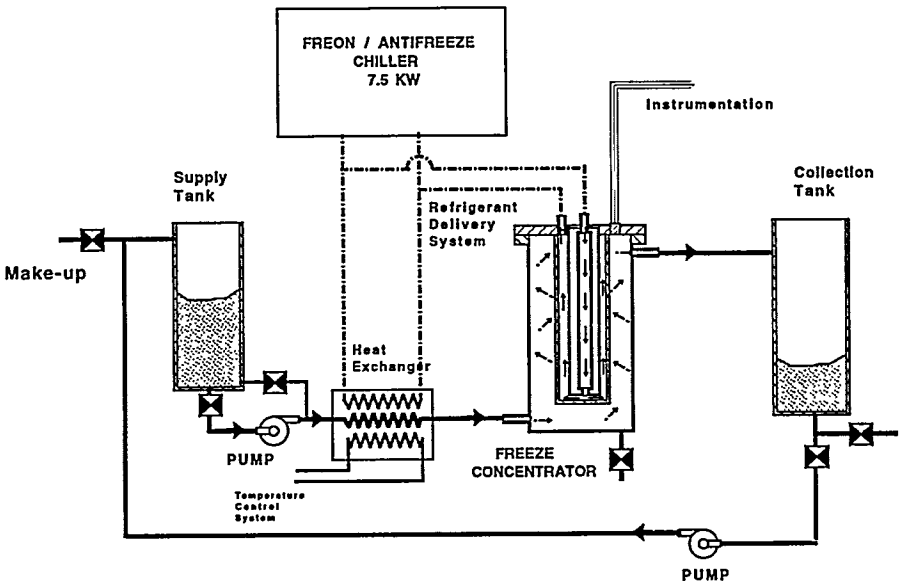
The purpose of this project is to use freeze concentration and fractional precipitation in combination to efficiently decontaminate radioactive solutions while selectively separating radioactive solutes from nonradioactive ones. We will develop and demonstrate low-temperature fractional precipitation for plutonium solutions for the first time and integrate this process with the freeze-concentration process.

Low-temperature solubility data for solutions pertinent to this work does not currently exist; however, we can obtain this data with simple low-temperature differential-scanning-calorimeter (DSC) measurements. For this purpose we will use a Netzsch thermogravimetric analyzer DSC upgraded for low-temperature operation.

Thus far in the project we have fabricated and used a low-volume batch-freeze concentrator operating in an isochoric-limited ice-growth mode to define the optimum coolant temperature and cooling rate for efficient separations. Preliminary results are shown in the accompanying table. We have also designed a second freeze-concentration/fractional-precipitation apparatus which operates in the static-concentration, continuous mode (see figure). We will test the performance of this instrument with nonradioactive materials; these tests will allow us to define the maximum decontamination factors.

Sample ID	Element	Initial Concentration (ppm)	Final Concentration (ppm)	Decontamination Factor (initial/final)
C104	Na	1.69×10^4	2.6	6.5×10^3
C105	Na	1.23×10^4	0.97	1.3×10^4
R101	Na	2.58×10^4	2.5	1.0×10^4
R102	Na	2.14×10^4	48	1.8×10^4
F104	Na	1.86×10^4	48	389.1
	Ca	1.02×10^4	7.3	140.1
	Zr	132.7	15	8.84
	La	81.3	5	16.3

Analytical data from freeze-concentration experiments on nitrate salts using a batch-freeze concentrator operating in an isochoric-limited ice-growth mode.



Schematic of the design for a freeze-concentration/freeze-precipitation apparatus that will operate in the preferred static-concentration, continuous mode.

Radionuclide Separations Using Pillared Layered Materials

Norman Schroeder

The goal of this project is to develop porous pillared layered materials (PLMs) that can efficiently sorb radionuclides from liquid nuclear wastes stored in underground tanks at DOE facilities (e.g., the Hanford Site, Oak Ridge National Laboratory, and Savannah River Plant) and from mixed wastes stored at Los Alamos. Our initial research is on sorbers that are designed to remove strontium-90 because separation of strontium from the bulk-waste constituents would significantly lower the radiological hazard of low-level waste forms, and a recent study of 60 sorbers for radionuclides in Hanford wastes concluded that an efficient strontium sorber must be developed. Subsequent research will focus on the extraction of other radionuclides such as cesium-137, technetium-99, or actinides and of other species that require separation but for which an efficient, selective technology has not been developed.

The PLMs of interest to us are inorganic ion exchangers propped apart by metal oxide pillars; these PLMs can be designed to selectively sorb specific metal cations. Pillaring is a technique that exchanges the layered material's charge-balancing interlayer cations, such as Na^+ or Ca^{2+} ions, for large metal oxohydroxide cations. Subsequent calcination drives off water to create metal oxide pillars; protons released from the cations remain in the cavities to balance the layer charge. The result is a greatly expanded clay structure with large channels and cavities of fixed size and a reservoir of exchangeable protons. This morphology permits metal ions to readily enter the material and undergo ion exchange.

During the past year, we synthesized and characterized a variety of PLMs that used chromium, silicon, zirconium, aluminum, and titanium pillaring species and montmorillonite, saponite, phlogopite, $HTaWO_6$, $H_3Sb_3O_6(PO_4)_2$, $HSb(PO_4)_2$, $H_2Ti_4O_9$, $H_2Ti_3O_7$, $H_4Ti_9O_{20}$, $H_xTi_{2-x/4}O_4$, $H_2Ti_5O_{11}$, and $H_2Ti_6O_{13}$. Using batch experiments with waste simulant solutions, we tested these PLMs for strontium uptake; some examples of testing results are shown in the accompanying table. A collaboration was set up with Texas A&M University for preparing a variety of PLMs including several silica-pillared titanates. These materials showed exceptional affinities for strontium, with distribution coefficients (K_d values) in excess of 100,000 mL/g in a 5-M $NaNO_3$ + 1-M NaOH solution. We will continue to prepare and optimize PLMs for strontium uptake, determine their exchange capacities, and test them using two Hanford waste simulants—double shell slurry feed (DSSF) and complexant concentrate (CC)—as well as real waste.

Material	Strontium K_d (mL/g)
Cr-pillared $HTaWO_6$	55,000
Zr-pillared $HTaWO_6$	18,100
Ti-pillared $HTaWO_6$	>61,000
Si-pillared $HTaWO_6$	1,100
Unpillared $HTaWO_6$	90
Cr-pillared $H_3Sb_3O_6(PO_4)_2$	3,100
Cr-pillared $HSb(PO_4)_2$	840
Al-pillared montmorillonite	970
Al-pillared saponite	830
Zr-pillared saponite	13,600
Cr-pillared saponite	4,300
Zr-pillared phlogopite	4,500

Examples of strontium K_d values (for a 1-h period) for a variety of PLMs using DSSF alkaline supernate waste simulant.

Chemical Conversions in Supercritical Media: Environmentally Sound Approaches to Processes and Materials

Steven Buelow

Our project evaluated the potential of supercritical fluids (SCF) as reaction media for chemical synthesis in an effort to develop new, environmentally-friendly methods for chemical synthesis or processing. The use of novel media creates the possibility of opening up substantially different chemical pathways, increasing selectivity (eliminating waste by-products), and enhancing reaction rates (decreasing hold-up times and saving energy). In addition, the use of SCF as reaction media facilitates downstream separations and mitigates or eliminates the need for hazardous solvents on scales from benchtop to production.

We chose to investigate three research areas (metal-catalyzed polymerizations, radical polymerizations, and synthetic organic chemistry) because they provided the highest potential for success, addressed critical need areas for potential industrial partners, and focused the capabilities and interest of the Laboratory. Our research successfully demonstrated both radical- and metal-catalyzed polymer production and the production of acrylate foams in supercritical carbon dioxide. Our efforts also validated the concept of conducting nucleophilic substitution reactions between ionic species and aromatic substrates in supercritical water.

The capabilities and results produced by this project have resulted in a cooperative research agreement with a U.S. polymer manufacturer and complementary work for the Environmental Protection Agency. Our work has applications in waste minimization, clean manufacturing, economic competitiveness, and energy efficiency.

Publications

Morgenstern, D., W. Tumas, R.M. LeLacheur, et al., "Supercritical Carbon Dioxide as a Substitute Solvent for Chemical Synthesis and Catalysis" (to be published in *Am. Chem. Soc. Symp. Ser.*).

Catalysis for the Utilization of Carbon Dioxide as an Alternative Chemical Feedstock

Kevin Ott

Finding alternative chemical feedstocks for chemical processing can potentially realize significant savings in energy and waste generation. We are examining the chemical catalysis of carbon dioxide conversion to useful chemicals—specifically replacing expensive syngas technologies with thermodynamically favorable processes based on carbon dioxide reduction with hydrogen or with alkanes and alkenes. This research, if successful, would lead to more energy-efficient production of chemicals such as methanol and acetic acid.

We have investigated the synthesis and reactivity of novel oxidation catalysts consisting of microporous zeolites having a small fraction of tetrahedral sites replaced with redox-active transition metal ions, titanium and vanadium in particular. We have studied solid-state titanium nuclear magnetic resonance (NMR) as a developmental tool to describe the chemistry of the active sites of the titanazeolites. Using multinuclear NMR techniques coupled with careful characterization (via x-ray diffraction, diffuse-reflectance spectroscopy, infrared spectroscopy, and thermal analysis) of the samples, we have made progress in determining that a significant number of observations in the literature regarding the phase behavior of prototypical titanazeolite, are likely to be in error. This information will clarify the catalytic activity of these samples and will substantially improve the general knowledge of this class of technologically important materials. Ongoing work will focus on a search for new catalysis involving direct activation of molecular oxygen as the terminal oxidant.

Chelating Water-Soluble Polymers for Waste Minimization

Barbara Smith

Our integrated project in ligand-design and separations chemistry has developed and evaluated a series of water-soluble chelating polymers for recovery of actinides and toxic metals from a variety of process streams. Specifically, we have developed and demonstrated a technology for recovering and recycling metal ions from electroplating rinse waters.

Polymer Filtration (PF) uses water-soluble chelating polymers in combination with ultrafiltration for the selective recovery and concentration of metal ions in aqueous solutions. Separation is based on size-exclusion—the polymer-metal complex is physically too large to pass through the ultrafiltration membrane (retentate), but unbound species readily pass through the membrane (permeate). The polymer-metal complex can then be concentrated by simple ultrafiltration. Once concentrated, the metal ions can be selectively released from the polymer (by adjusting the pH, for example) and collected in a concentrated form. The metal-free polymer is readily recycled for additional metal-ion binding.

This project builds on the successes of PF technology, expanding its range of applications to include a variety of solids, waters, and wastewater types for quality production, waste minimization, pollution prevention, and resource recovery. We are investigating the use of PF to selectively precipitate metal ions from acidic mine drainage, remove arsenic from drinking water, remove and recover mercury from solid waste, recover metals from mining ores, recover copper and other precious metals from catalytic materials, and remove plutonium and americium from nuclear materials processing wastewater.

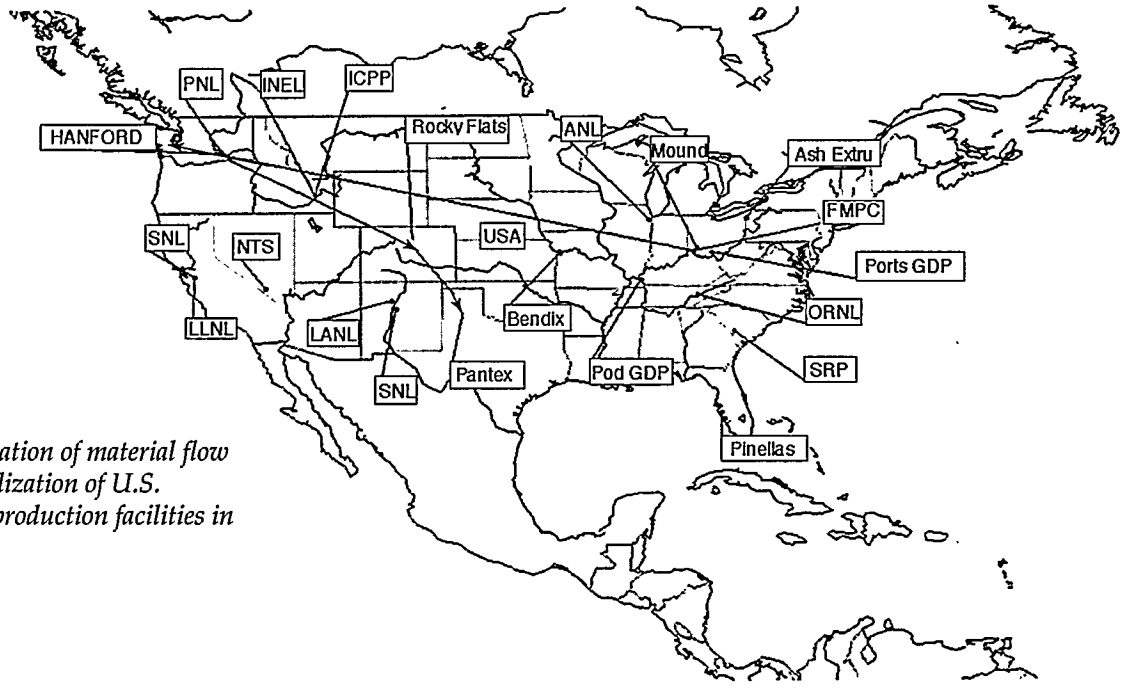
Mathematics and Computational Science

Global Nuclear Material Flow Model

Jared S. Dreicer

The global nuclear material flow model (GNMFM) project characterizes and models, from a global perspective, the management, control, and flow of weapons-grade nuclear material (plutonium and highly enriched uranium). This model provides a computer-based tool capable of many different functions. It captures and enumerates information and data concerning the global inventory of nuclear weapons material, and it provides a global view of the management and control of nuclear material, including resource and accounting requirements. The GNMFM model also undertakes macrosystem simulations of safeguards accounting surety and safeguards resource estimation to manage and control nuclear material. It visually represents information related to both intercountry and intracountry nuclear material flow (e.g., management and control, quantity, location, and transit) and supports the development of other pertinent algorithmic capabilities necessary to undertake further global nuclear-material-related studies (see accompanying figure).

Using the GNMFM model, we have partially enumerated the quantity of plutonium that exists globally by country and site and developed a visual representation of the previous characterization from a global perspective. We initiated characterization and development of safeguards management; material protection, control, and accounting; and disposition and proliferation algorithms. We have also developed a prototype of the fundamental computer-based framework necessary to undertake global nuclear-material-management studies.



Representation of material flow and visualization of U.S. weapons production facilities in the past.

Intelligent Controllers for Battlefield Simulations

Phillip Stroud

Intelligent objects can be treated as black boxes that take inputs, use the inputs to evaluate rule-based controllers, and then return outputs. These objects can be structured so that the mapping from input to output depends on a set of parameters. Our main objective is to find ways for obtaining useful transformations from a rule-based controller to a parameterized mapping.

The performance of an intelligent object can be evaluated within a simulation environment. When the intelligent object is represented by an appropriate parameterized mapping, alternative intelligent objects can be easily obtained by adjusting the parameters. The second aim of this research project is an investigation into methods for evolving intelligent objects within the context of a simulation-based performance evaluation. The simulation package called ELASTIC, that is, evolutionary Los Alamos simulation-based training for intelligent controllers, was built as a part of this project. It provides a flexible capability to simulate the operation of various airborne laser flight and fire controllers in a theater simulation environment.

We investigated a new approach for the fire controller; it is based on an extended version of a multilinear network. We also characterized several training methods and demonstrated automated controller learning. We constructed a rule-based flight controller and developed a new approach for transforming it into a parameterized mapping. Using evolutionary programming and simulation-based performance evaluation, we demonstrated automatic production of improved controllers. Furthermore, we also demonstrated the translation of knowledge obtained by the automatic evolutionary process into modifications of the rule-based controller.

Publications

Stroud, P., "An Adaptive Airborne Laser Flight Controller" (submitted to *IEEE Trans. Systems, Man, and Cybernetics*).

Stroud, P., "Anisoplanatism in Adaptive Optics Compensation of a Focused Beam Using Distributed Beacons" (to be published in *J. Opt. Soc. Am. A*).

Stroud, P., "Characterization of Production Training Methods for an Airborne Laser Adaptive Fire Controller" (submitted to *IEEE Trans. Neural Networks*).

Stroud, P., "Statistics of Intermediate Duration Averages of Atmospheric Scintillation" (to be published in *Opt. Eng.*).

Process Simulation, Control, and Optimization for Industrial Energy Efficiency

Edward Joyce

Detailed predictive tools that relate business performance to manufacturing conditions are not readily available but are recognized to be of great importance. The purpose of this project is to demonstrate a proof-of-principle capability for constructing a fully integrated, intelligent system simulation and control model of a complete industrial process. The fully integrated model consists of coupled hierarchical layers that span the industry's entire scope of activities necessary to production. The layers range from the enterprise level (the business models), to the manufacturing level (the unit operations models), to the molecular level (the physical models). Each hierarchical layer consists of a set of component processes, a method of control and integration, a source of intelligent decision support, and a means of coordination with the other layers. This project provided the foundation, for the formation of the (virtual) Center for Materials Process Modeling, which was established to coordinate and focus activities related to system, process, and materials modeling.

We have developed flowsheet scenarios for five steel manufacturing methods. We developed the overall simulation framework, improved the process/unit operation models, and incorporated them into the simulation. Contacts with several potential partners and sponsors were made. Additionally, we made a significant contribution to the Department of Energy Steel Industry Vision of the Future document. In 1996, we will extend the methodology to the processess and enterprises in the chemical industry. The results of this project can also be used to study and improve the efficiency of DOE facility operations throughout the DOE complex.

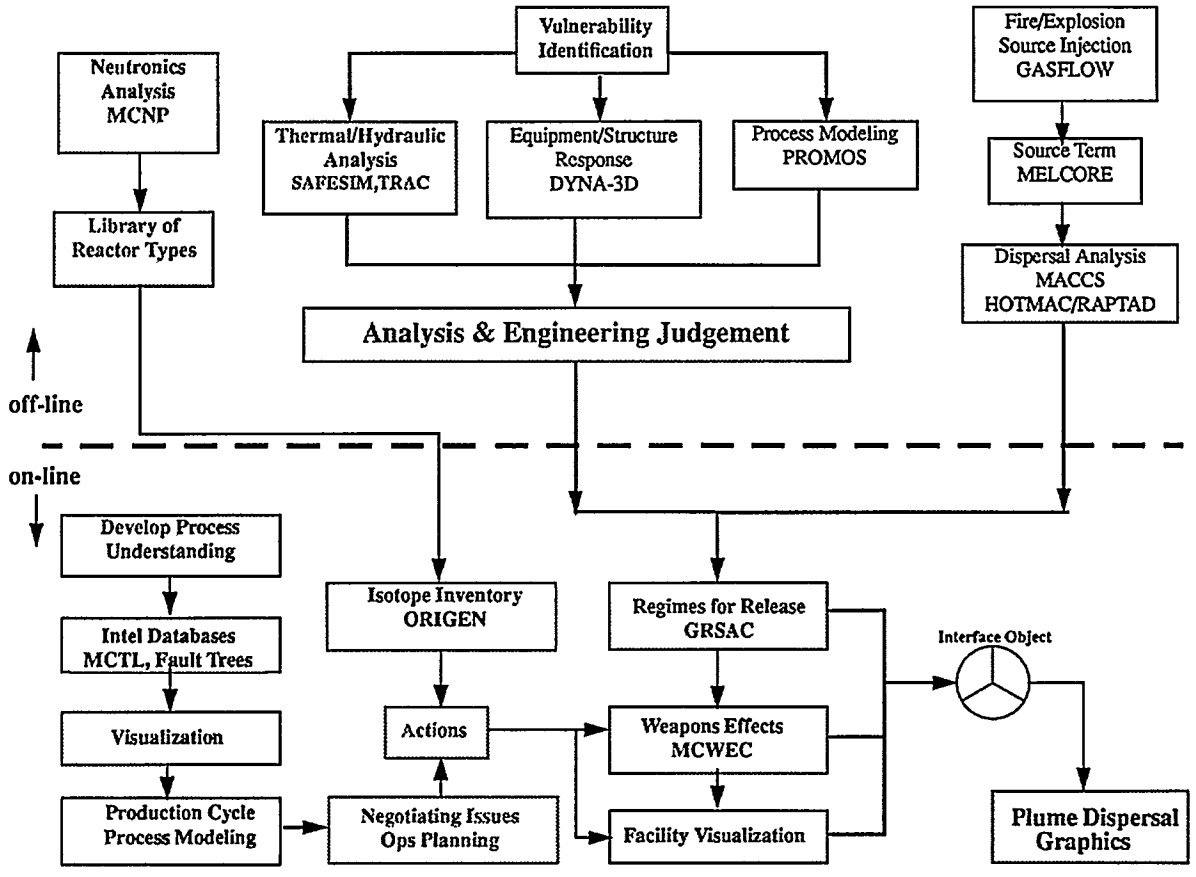
Nonproliferation/Counter-proliferation Synthetic Wargaming Environment

James Doyle

Nonproliferation and counter-proliferation (NP/CP) analysis requires using many diverse tools, data, and expertise. The broad spectrum of issues to be addressed by the NP/CP community range from interdiction analysis and consequence analysis to process modeling, facility/results visualization, isotope production, etc. These broad analysis requirements suffer from the inability to readily incorporate the functional output of one analysis tool into another set of tools to easily span the spectrum of analysis requirements.

This project involves a NP/CP simulation and analysis environment that would maximize the domain expertise across the range of analysis requirements. We have based this system upon a unifying framework defined and used by a multilaboratory NP/CP consortium, and we have integrated it with many other existing simulation models, databases, and decision support tools. Our system uses hyperlinked and object-oriented techniques to support planning, analysis, and policy development for deterring the proliferation of weapons of mass destruction (see the accompanying diagram).

Our efforts have so far defined the scope of the framework and have produced a preliminary version of the analysis environment with the following capabilities: counter-proliferation assessment capability, nuclear reactor isotopic calculations, fault-tree analysis output, plume dispersal graphics, and production cycle modeling.



Pilar prototype of our nonproliferation/counter-proliferation analysis environment.

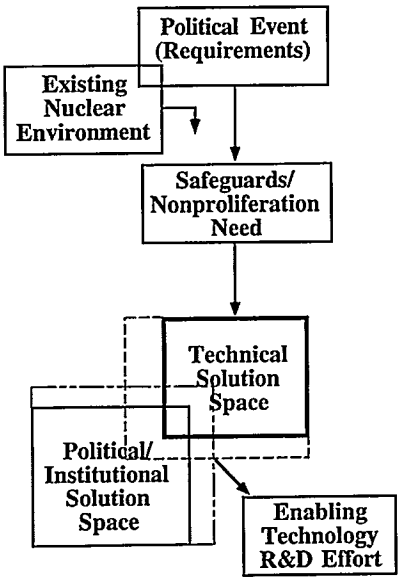
A Systems Framework for Defining Nonproliferation Program Technology Requirements

Chad Olinger

International safeguards and nonproliferation regimes are rapidly changing. Over the next few years, changes in the scope of nonproliferation activities will bring an overall larger fraction of the world's nuclear material under international inspection. Our objectives are to anticipate and develop an improved understanding of future needs in nonproliferation-enabling technology.

We are developing a systems framework for identifying nonproliferation needs. In this systems framework, we view political events such as domestic restructuring, international treaties, bilateral agreements, and unilateral initiatives as establishing policy requirements. These events, in conjunction with the existing nonproliferation environment, result in global safeguards and nonproliferation requirements. Political and institutional settings establish constraints for implementing technical solutions. Enabling technologies can then be developed to meet identified needs (see the accompanying figure). As one example, our systems framework identified the need to focus on unattended remote monitoring to detect the diversion of nuclear materials at nuclear facilities.

We further focus our efforts in identifying capabilities at Los Alamos that could meet multiple customer needs that are consistent with existing competencies or direct extrapolations of our capabilities. We have identified nonproliferation areas where the scientific infrastructure at Los Alamos could significantly contribute to advance nonproliferation goals. These nonproliferation areas include (1) continuous unattended remote monitoring of storage and material processing, (2) improved response to nuclear material diversion, (3) improved detection of clandestine nuclear material production, and (4) improved detection of nuclear explosions with very small yields.



Development of a systems framework for nonproliferation research and development. The overlapping portions of the possible technical and political/ institutional solutions represent areas where effort should be directed.

Modeling and Simulation for the Semiconductor and Optoelectronic Industries

David Cartwright

The cost and complexity of manufacturing integrated circuits have reached the point at which applying advanced modeling and simulation tools is a business imperative. The objective of this project was to investigate selected fundamental scientific issues which will determine the feasibility of building a suite of predictive design tools for use by the semiconductor industry in the technical thrust areas of topography, bulk processing, and grids and computational science. A truly predictive capability in these three areas will reduce the need for costly and time-consuming laboratory experiments to empirically develop new technology generations. The ultimate goal for the semiconductor industry is an improved ability to model and simulate semiconductor materials, devices, systems, and manufacturing processes for 0.1-micron technology by the year 2002.

Our work in topography focused on evaluating the basis for developing a fully three-dimensional (3-D) modeling of feature evolution by either deposition or etch processing. We benchmarked density functional approaches for computing thermochemical properties of Si-H-Cl molecules and found that gradient-corrected functionals are capable of giving more accurate thermochemical information than are traditional quantum chemical approaches. Calculations on $Si_xH_yCl_z$ molecules were carried out using all-electron and valence-electron techniques. Scaling tests on Si_9H_{14} and $Si_{21}H_{26}$ cluster models were

performed on IBM and Hewlett-Packard workstation clusters. Calculations on hydrogen and chlorine binding to clusters from Si_9H_{14} through $Si_{49}H_{44}$, which represent the Si(100) surface, were carried out using semiempirical techniques.

In the area of bulk processing, we completed all-electron, full-potential total-energy calculations of the vacancy formation energy in 64-atom supercells of silicon. Calculations of the vacancy formation energy in 128-atom silicon cells are in progress. Also in progress are calculations of lattice relaxation and relaxation energy around arsenic and phosphorus impurities and calculations of the energy of a silicon interstitial along the tetrahedral-hexagonal path.

Version 2.0 of the UT-Marlowe ion implanation code was released to more than 150 users at industrial research organizations, universities, and national laboratories; we played a substantial role in improving this code before its release. We installed the Mocabulk Monte Carlo electron-hole transport code from the University of Illinois and have linked it to the Los Alamos 3-D graphics/analysis system using a standard data output library developed for CRADA applications.

Our work in the area of grids and computational science focused on developing utilities for mesh generation, adaptive mesh refinement, dynamic mesh reconnection, and moving adaptive mesh algorithms for the Laboratory's X3D software package. We developed new algorithms to implement sheet surfaces, applied structured programming standards to critical parts of X3D, continued the specification of a test suite to be used to verify the code, and improved 3-D (error-gradient) smoothing algorithms and two-dimensional elliptical smoothing algorithms.

Based on these studies, it appears technically feasible to construct simulators that will meet industry needs by the year 2002.

Publications

Gronbech-Jensen, N., T. Germann, et al., "Molecular Reconnaissance," *Comput. Sci. Engin.* **2**, 4 (1995).

Visualization Capability for Nonproliferation and Emergency Training: A "Poor Man's" Virtual Reality System

George Papcun

A "poor man's" virtual-reality system is one in which viewers can observe a virtual-reality environment, such as a plant for processing nuclear materials, on the screen of a low-cost computer. Creating a scene in our virtual-reality environment is inexpensive. By integrating the mathematics of photogrammetry with a proper set of assumptions and computational tools, we have provided technicians with the means to build a virtual-reality environment directly from a photograph; this process takes only hours or days, rather than the weeks or months that would be required without our system. We have also made certain extensions to the previously known mathematics of photogrammetry so that the system can handle objects of various shapes (cylinders, cones, and spheres). Viewers can "enter" the environment, that is, they can "fly through" the environment. If they are wearing special glasses, the environment will appear to be in three dimensions.

Our virtual-reality system can be used in training inspectors or others in environments that are inaccessible for numerous reasons, such as political and safety ones. For example, if inspectors with the International Atomic Energy Agency cannot visit a site because of political reasons, they can effectively practice inspecting the site through a virtual-reality environment developed with our inexpensive and efficient system. At the same time, our system can be used for virtual inspections of radioactive, or otherwise dangerous, locations. Considering that it allows virtual-reality environments to be created quickly, our system shows promise for effective use in contingency planning or operational mission training.

It is important to emphasize the significance of photogrammetry, which distinguishes our approach from cruder techniques in which the user iteratively fiddles objects on the screen until they fit the scene. Once the vanishing points are calculated and the camera parameters are defined by photogrammetric techniques, our technique makes everything fit into the virtual-reality environment.

Image Processing Technology

Edward Van Eeckhout

The primary objective of this project is to advance image processing and visualization technologies for environmental characterization at DOE, Department of Defense, and other agencies. This will be effected by developing and implementing analyses of remote sensing data from satellite and airborne platforms and by demonstrating the analyses' effectiveness in visualizing environmental problems.

Digital computer technologies (commercial and noncommercial) are used to visualize two- and three-dimensional changes in environmental conditions (see figure). This data is processed using a desktop-based Geographic Information System that can be easily transported.

Specific accomplishments during the review period include the following:

1. Imagery for Los Alamos and Eglin Air Force Base has been collected with the help of DOE/Headquarters and the Environmental Research Institute of Michigan (ERIM).

2. Potential sources for depleted uranium at Eglin Air Force Base have been identified and visualizations provided to personnel on-site.

3. Historical photographs have been collected for a landfill site near Las Cruces for characterization purposes.

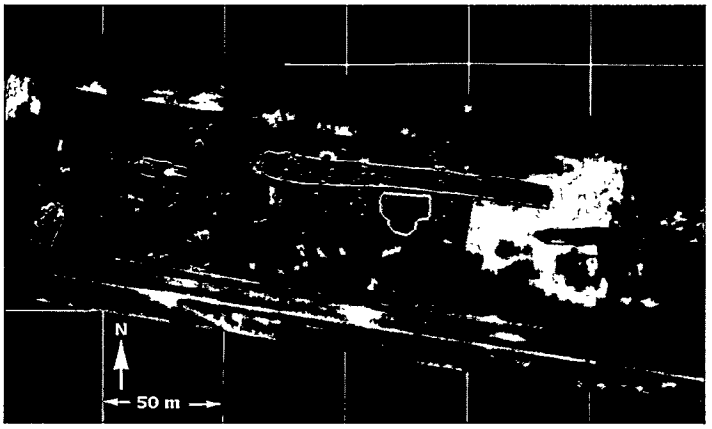
4. An EG&G overflight of Los Alamos for multispectral and radiation data was completed. We coordinated the flight, and the data from it is now being analyzed.

5. We have written visualization codes on the Silicon Graphics machine purchased last year.

6. We have collaborated with ERIM, which is funded by the Morgantown Energy Technical Center, to evaluate the feasibility of remote sensing for environmental purposes at Los Alamos.

Publications

David, N., W. Ginsberg, E. Van Eeckhout, et al., "Remote Sensing Characterization of Selected Waste Sites at the Los Alamos National Laboratory" (to be published in *Environ. Geosci. J. AAPG*).



Example of visualization of various data sources to better delineate historical waste trenches and their contents at Los Alamos. Suspected trenches are outlined on a 1958 aerial photograph (one additional "disturbed area" where trench material was stored is shown in white). A magnetic survey conducted in the gray area shows further detail of metal objects that are clustered in some of the trenches. This survey was conducted before analyses of historical photographs, which defined the trench boundaries. The magnetic survey is now being extended to the east.

Nanoscience and Technology: Self-Assembling Nanoscale Quantum Devices

Gary Doolen

Despite a strong desire for continued progress in microelectronics miniaturization, the means for achieving feature sizes below about 0.1 micron do not exist. Traditional, very large scale integrated circuit technologies are expected to dominate the market for the next 10–20 years, after which novel—and presently undemonstrated—techniques will be required. Two complementary projects address the development and demonstration of nanometer-scale components, circuits, techniques, and systems—that is, terascale integration (10^{12} components per chip)—and the opportunities and limitations associated with their use. To achieve this level of integration with the precision necessary for comput-

ing, the circuits must be self-assembled. Since self-assembly takes place at the nanoscale, we focused our efforts on self-assembled nanoscale electronics, in which device behavior and system performance are governed (and constrained) by quantum mechanics.

Our general objectives are to pursue the self-assembly of wires, active gain devices, and larger error-tolerant ensembles that memorize and compute and to explore self-assembly as a powerful alternative to technologies used currently by the semiconductor and micromachining industry. This new technology is clearly on the cusp of a revolution in how we make small devices and will have global impact. Our specific objectives involve theoretical and experimental research in Coulomb blockade devices, resonant tunneling systems, and self-assembled systems.

Semiconductor GaP and GaAs Coulomb blockade devices may be the basis for a room-temperature "quantum transistor." We have prepared well-characterized 1- to 3-nm nanoclusters, have developed nanoclusters that are soluble and stable in organic solutions, and have given them to others for study. We have prepared ultrasmooth gold substrates but are not yet successful at attaching clusters to them. We have developed a detailed model that describes how electrons tunnel between a source and a nanostructure and that leads to specific and accurate predictions. Resonant tunneling devices are the basis for multifunction compact devices, and we have progressed at understanding the effects of applied stress and sound waves on the internal electric fields and optical properties of double barrier systems and multiple quantum wells.

Nanoscale architecture deals with the means to assemble and operate nanocomputers. We learned how internal electric fields affect self-assembly via the use of Laplacian growth formalisms and operator gases (a simplified form of molecular dynamics). We applied the latter to the role of errors and programming languages in nanoarchitectures and learned about related issues in nonlinear dynamics. We initiated studies and modeling of biological systems—cytoskeletons, bacteria, and proteins—to better understand how nature does self-assembly.

Publications

Albrecht, J.D., L. Cong, P.P. Ruden, et al., "Resonant Tunneling in (001) and (111) Oriented III-V Double Barrier Heterostructures Under Transverse and Longitudinal Stresses" (submitted to *J. Appl. Phys.*).

Bonca, J., and S.A. Trugman, "The Effect of Inelastic Processes on Tunneling" (to be published in *Phys. Rev. Lett.*).

Campbell, I.H., M.P. Joswick, et al., "Observation of Piezoelectric Effects in Strained Resonant Tunneling Structures Grown on (111)B GaAs," *Appl. Phys. Lett.* **66**, 988 (1995).

Cong, L., J.D. Albrecht, M.I. Nathan, et al., "Piezoelectric Effects in Double Barrier Resonant Tunneling Structures," *Appl. Phys. Lett.* **66**, 1358 (1995).

Davids, P.S., L. Wang, et al., "Inelastic Neutron Scattering and Magnetic Collective Response of Mesoscopic Carbon Structures" (to be published in *Phys. Rev. B*).

Kogan, Sh.M., "Theoretical Study of a Quantum-Point-Contact," *Phys. Rev. B* **23**, 17230 (1994).

Mineev-Weinstein, M.B., "Conservation Laws in Field Dynamics Or Why Boundary Motion Is Exactly Integrable" (submitted to *Phys. Rev. Lett.*).

Mineev-Weinstein, M.B., "Noise, Fractal Growth, and Exact Integrability in Non-equilibrium Pattern Formation,"in *Proceedings of the International Conference on Noise and Fluctuations* (Springer-Verlag, Berlin, in press).

Mineev-Weinstein, M.B., and F.J. Alexander, "Conserved Moments in Nonequilibrium Field Dynamics," *J. Stat. Phys.* **79**, 1013 (1995).

Smith, D.L., Sh.M. Kogan, et al., "Acousto-Optic Modulation of III-V Semiconductor Multiple Quantum Wells" (submitted to *Phys. Rev.*).

Trugman, S.A., "Complex Scattering Dynamics and the Quantum Hall Effect," *Physica D* **83**, 271 (1995).

Wang, L., and A.R. Bishop, "Spin-Density-Wave Instabilities on a Graphite Nanotube" (to be published in *Phys. Rev. B*).

Wang, L., J.K. Zhang,and A.R. Bishop, "Conductance of Electron Tunneling Through a Quantum Dot," *Physica D* **83**, 271 (1995).

Wang, L., J.K. Zhang, and A.R. Bishop, "Microscopic Theory for Conductance Oscillations of Electron Tunneling Through a Quantum Dot," *Phys. Rev. Lett.* **73**, 585 (1994).

Wang, L., J.K. Zhang, and A.R. Bishop, "Theory of Quantized Dynamic Capacitance Charging Spectroscopy in Nanostructures," *Phys. Rev. Lett.* **74**, 4710 (1995).

Yang, R., P.P. Ruden, and D.L. Smith, "Coulomb Effects Between Electrons in Quantum Box Structures," *Phil. Mag.* **B71**, 359 (1995).

Zang, J., J.L. Birman, et al., "Resonant Tunneling and Population Inversion in Double Quantum Dots" (to be published in *Phys. Rev. B*).

High-Performance Computing for Simulation of Domestic Petroleum Reservoirs

George Zyvoloski

Unstructured numerical meshes, consisting of triangles in two dimensions and tetrahedrals in three dimensions, are becoming increasingly popular in oil reservoir simulations because of their ability to model complex phenomena such as faults and nonvertical wellbore systems. Our research interests included three areas related to unstructured grids:

- developing software to add unstructured meshes to existing meshes,
- benchmarking the performance of unstructured meshes against structured meshes, and
- developing linear-equation solvers for use with unstructured grids.

We developed the add-mesh capability because of a need in the oil industry to model reservoirs with highly deviated and even horizontal wellbores. We produced a meshing code that can combine a grid accurately reflecting the tortuous path of a wellbore with a pre-existing reservoir model that may have many stratigraphic boundaries to be maintained. The challenge has been to regulate the amount of "excavated " grid when it is added to the wellbore mesh. This technology will allow oil companies to evaluate the potential of long-reach horizontal wells for many applications where small surface facilities are demanded because of cost (off-shore) or environmental concerns (wildlife refuges).

Linear-equation solvers are extremely important for unstructured grids. In order to take advantage of the solid modeling capability of unstructured grids, the coupled linear equations resulting from the material balance equations must be solved with an efficiency approaching that of structured grids. We have improved our unstructured linear-equation solvers and have made them available for benchmarking to our university and industrial collaborators. We have also developed a massively parallel version of the equation solvers that is competitive with structured grid solvers in the parallel environment.

Prototype Demonstration of Radiation Therapy Planning Code System

Robert Little

Radiation therapy for cancer patients is based on several modalities, such as conventional (photon/electron) radiotherapy, stereotactic radiosurgery, conformal therapy, neutron therapy, and brachytherapy. Each of these modalities requires accurate and efficient schemes for radiation therapy planning so that a protocol can be developed to deliver sufficient radiation dose to the entire tumor while minimizing the dose to healthy tissue. Most radiation therapy planning suffers from inaccuracies in modeling patient anatomy and radiation transport.

The technical goal of this project was to demonstrate applicability of Los Alamos software (primarily the three-dimensional [3-D] Monte Carlo radiation transport code MCNP) for radiation dose calculations necessary for therapy planning.

In collaboration with colleagues from the Radiation Oncology Department at the University of California, Los Angeles, we linked patient-specific data (geometry, material composition) from computed tomography (CT) scans to MCNP; improved and benchmarked physics models used in MCNP electron transport; improved the efficiency of MCNP for patient dose calculations; performed dose calculations with actual patient geometries; developed visualization techniques for displaying the 3-D results; and demonstrated the applicability of MCNP to CT design and analysis. Sample results are shown in the accompanying figure.

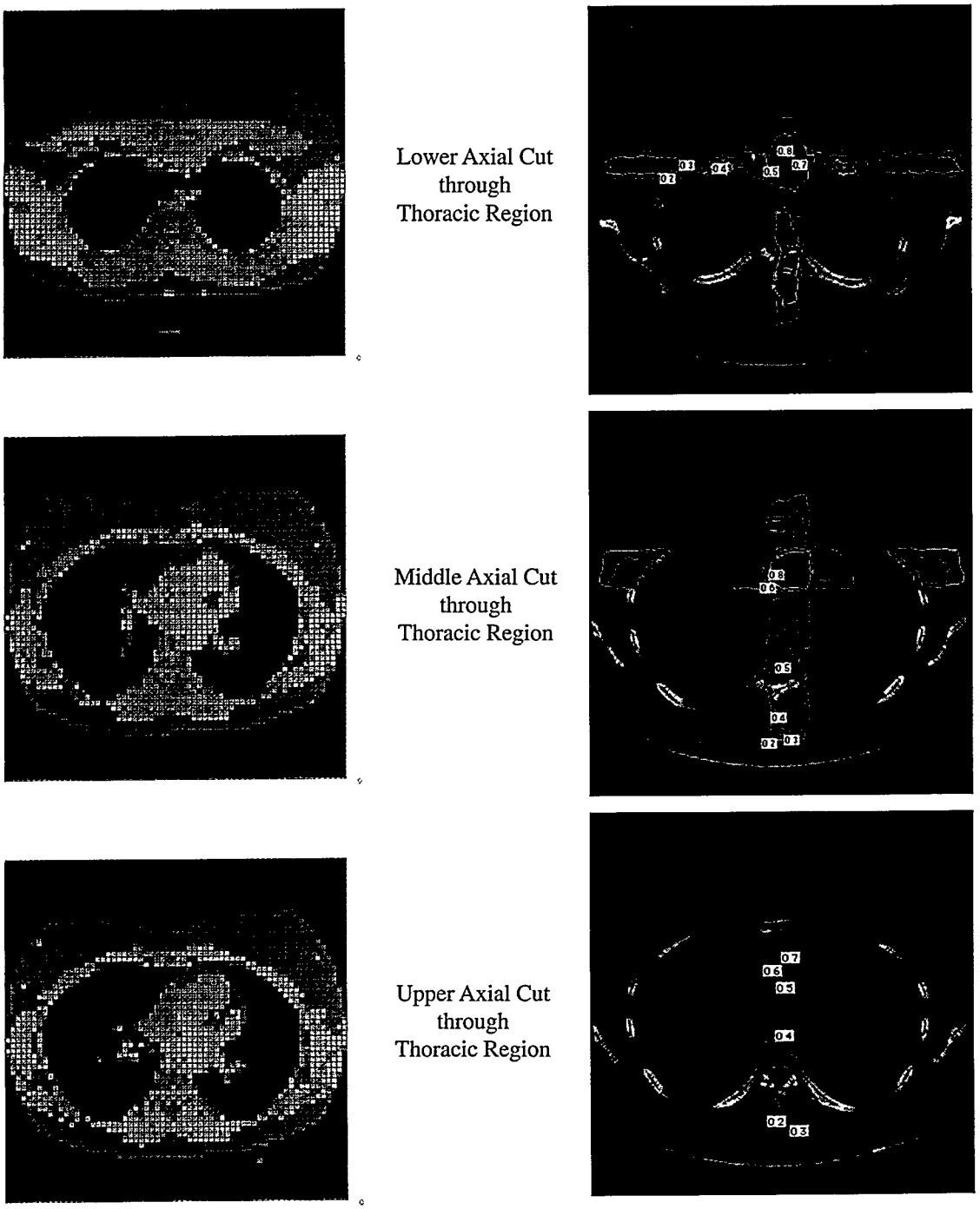
Publications

Adams, K.J., G.P. Estes, H.G. Hughes, et al., "The Use of MCNP in Conventional Radiotherapy Planning," *Medical Phys.* 22 (9), 1546 (1995).

Adams, K.J., and M. Hart, "Multigroup Boltzmann Fokker Planck Electron-Photon Transport Capability in MCNP," *Trans. Am. Nucl. Soc.* **73**, 334 (1995).

Hills, C.R., R.C. Brockhoff, and G.P. Estes, "CT Scan Simulation with the MCNP Monte Carlo Code," *Medical Phys.* **22** (9), 1534 (1995).

Hughes, H.G., "Status of Electron Transport in MCNP," *Trans. Am. Nucl. Soc.* **73**, 333 (1995).



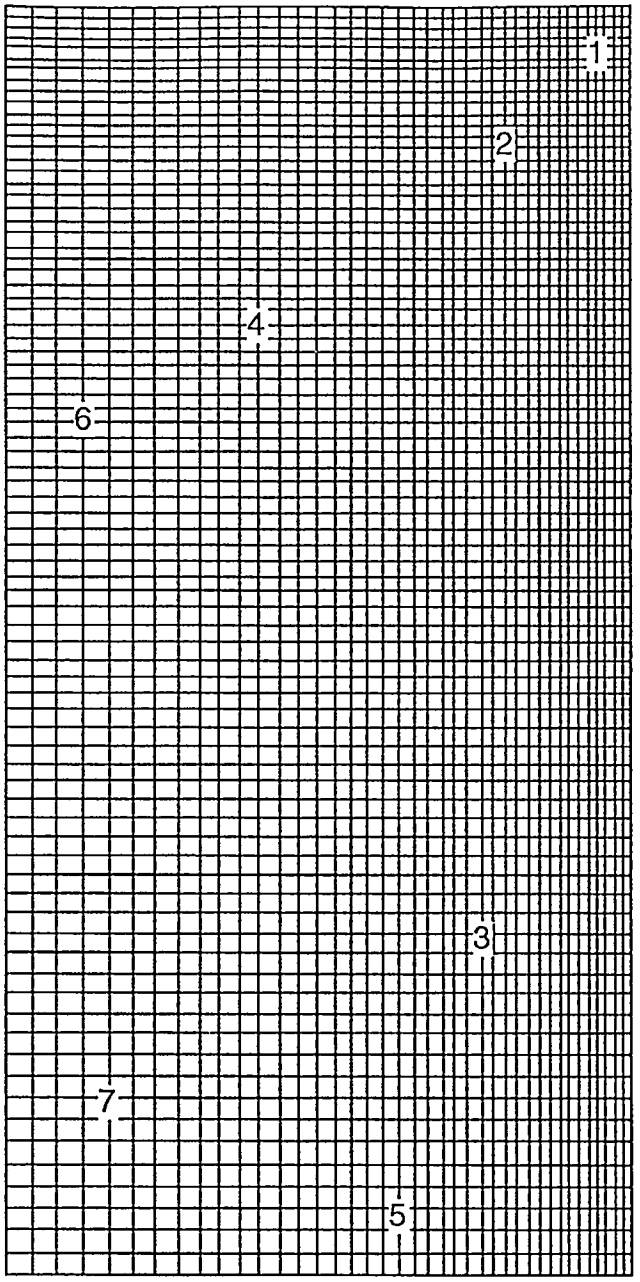
Sample MCNP patient geometries from CT scans (left); isodose contours calculated with MCNP superimposed on the CT images (right).

Industrial Applications for the Los Alamos Materials Modeling Platform

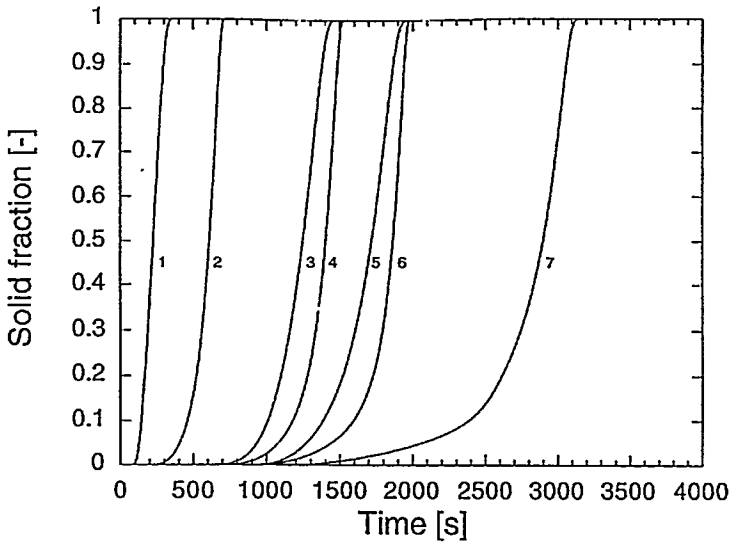
Richard Lesar

Casting and solidification of molten metals and metal alloys are critical steps in the production of high-quality metal stock and in the fabrication of finished parts. However, major problems with the quality of cast stock or finished parts can arise because of (1) the difficulty in preventing variations in the alloy content, (2) the generation of porosity or poor surface finish, and (3) the loss of microstructure-controlled strength and toughness resulting from the poor understanding and design of the mold filling and solidification processes. In this project, our objective was to create new applications for the Los Alamos Materials Modeling Platform (LAMMP). We focused on developing better and more-robust computer programs for casting, with emphasis on incorporating better materials models.

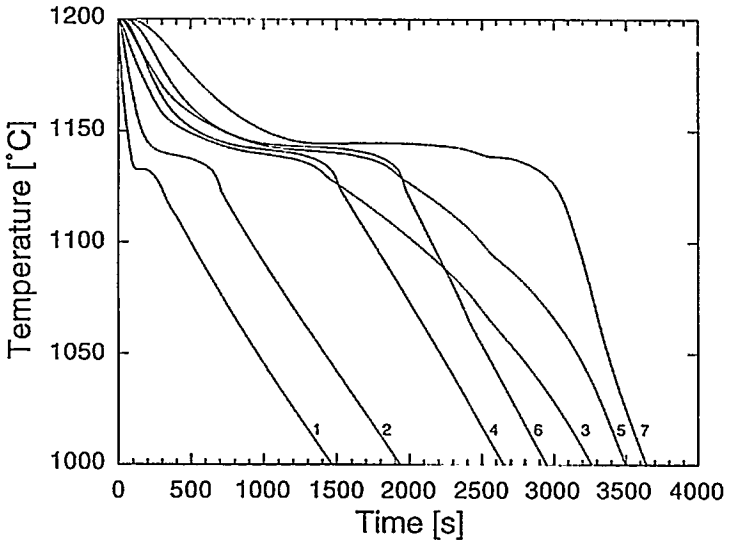
There were two main thrusts to this project. First, we developed new, improved microstructurally based models for solidification (see first two figures). Specifically, we created a fully coupled heat flow/solidification model for equiaxed, eutectic solidification. Second, we implemented solidification models within a new casting code, TELLURIDE, which is the first LAMMP application. We added two sets of models to TELLURIDE; the models describe isothermal solidification for both pure materials and alloys. This work represents the first implementation of a source-based enthalpy method for alloy solidification in a modern (i.e., parallel, FORTRAN 90), three-dimensional unstructured grid simulation tool (see third figure).



Mesh used in calculation of a fully coupled model for equiaxed, eutectic solidification. Adiabatic boundary conditions are present on the left and bottom, and a heat flux of -6000 W/m^2 is present on the top and right. The numbers indicate mesh points used in the second figure.

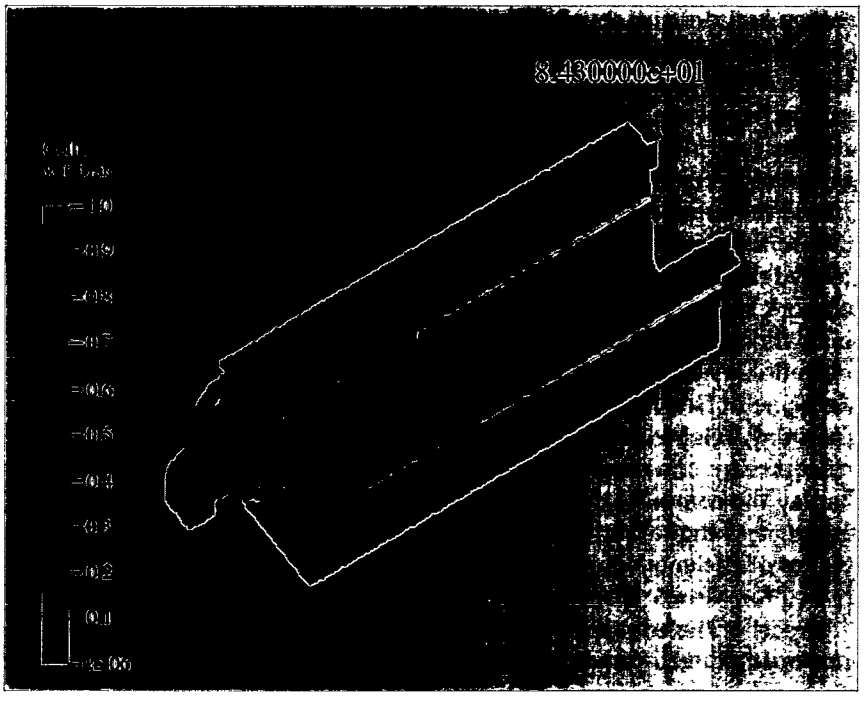


(a)



(b)

Solid fraction (a) and temperature (b) versus time at the mesh points indicated in the first figure.



Solidification in Al-4.5%Cu alloy in an Alcoa part, which is cooled from the bottom. The dark gray areas indicate solid, light gray indicates fluid, and intermediate gray shades indicate a mixture of solid and fluid (i.e., the mushy zone).

Low-Speed Flow Hydrodynamics

John H. Cerutti

Our project is focused on the development and application of a new three-dimensional (3-D), multifluid, low-speed flow model, called TELLURIDE, for simulating casting processes. We accomplished several TELLURIDE development efforts in the areas of physical model development, numerical algorithm formulation and development, and source code design and implementation.

We developed and implemented physical models for heat transfer and for solid-liquid phase changes in pure metals, binary alloys, and eutectic alloys. Our phase-change algorithm, which can model either solidification or melting, is based on an improved source-based enthalpy model. We validated both the heat conduction and the phase-change models against theory and, using a complex unstructured mesh, applied them to a real casting scenario. We have also implemented models for surface tension and for tracking free surfaces (important for mold filling), but we have yet to couple them with our fluid-flow algorithm, which is currently under development. To date, we have performed extensive tests and simulations of our fluid-flow algorithm in two dimensions, and we are currently extending the algorithm to the 3-D unstructured meshes in TELLURIDE.

We have fully implemented a novel interface-tracking algorithm. Currently being tested on simple and complicated meshes, this complex algorithm gives TELLURIDE the ability to model mold filling with much greater accuracy than existing tools. We have written an efficient, robust linear solver library that features all of the popular Krylov-subspace methods in use today and should easily solve the linear equations in a TELLURIDE casting simulation. We have created and integrated into TELLURIDE an efficient parallel gather-scatter library called PGSLIB, which is based on the message-passing library. PGSLIB will enable efficient parallelization of arbitrary unstructured meshes. We have also been building the various tools needed in the (unstructured grid) finite volume solution of our partial differential equations. Finally, we have begun implementing a massless tracer algorithm, which will be valuable in analyzing mold filling, melt convection, and material response (i.e., residual stress and porosity growth).

Publications

Kothe, D.B., and W.J. Rider, "Comments on Modeling Interfacial Flows with Volume-of-Fluid Methods" (submitted to *J. Comput. Phys.*).

National Information Infrastructure Applications

David Forslund

The goal of the Sunrise project at Los Alamos has been to develop a fully integrated prototype of the National Information Infrastructure (NII) by developing a common infrastructure driven by a suite of applications. We have largely succeeded in this goal. We have developed a fully functional distributed-object system whose security is based on the industry-standard Common Object Request Broker Architecture specification. The system supports multimedia data in a distributed object-oriented database for which security is applied object by object. We have successfully demonstrated the functionality of the distributed database system, called TeleMed, over a wide area network between Los Alamos and the National Jewish Center for Immunology and Respiratory Medicine in Denver, Colorado. In use today, TeleMed allows doctors to acquire (over a network) and display the complete treatment records and digital radiographic images of patients who are being treated for chronic illnesses.

As part of the advanced research supporting development of the TeleMed system, we have also evaluated asynchronous transfer mode networking for providing the support for the movement of multimedia database information. In addition, we have developed new algorithms for searching image databases, comparing multidimensional data, and compressing the data; these algorithms allow large data sets to be moved efficiently over low-bandwidth networks. Three-dimensional visualization of the data is handled in a portable way, reducing the requirement of high-performance hardware on users' desktops. In the past year, we focused on completing the TeleMed 2.0 software infrastructure and have demonstrated its full functionality.

We have explored extending the Sunrise/TeleMed technology to other applications, including engineering and manufacturing. This extension is called TeleFlex. Our success in constructing a usable NII has been validated by the NII Testbed choosing TeleMed as the base technologies of one of the healthcare applications to be deployed in its upcoming testbed.

Atomic and Molecular Physics

Measurement Criteria Analysis for Krypton, Xenon, and Hydrogen (Hydrogen/Deuterium/Tritium) Isotopes and Concentration Variability at Distance

Bryan Fearey

The importance of measuring xenon and krypton isotopes (as well as tritium abundances) to detect clandestine nuclear activities has increased substantially. Unfortunately, a complete systems analysis and simulation of the production and subsequent dilution of noble gas fission isotopes and tritium production gases have not been done. Specific questions of interest include the relative isotopic variation as a function of nuclear fuel composition, neutron flux, burnup duration, and fuel-rod position for different types of nuclear reactors. Other important questions involve defining the measurement accuracies required to extract operational parameters not only from nuclear reactors but also from clandestine reprocessing activities. Measuring hydrogen isotope ratios may also allow us to detect illicit tritium production and recovery, or detect gas leakage from nuclear weapons activities.

This project will allow us to theoretically determine and quantitatively analyze these isotopic parameters. The ability to quantify these parameters is particularly important to establish current and future measurement requirements for state-of-the-art instrumentation and determine how it might be deployed.

We have made substantial progress in many areas. We have encouraging results showing the dependence of noble gas ratios as a function of burnup, reactor, and fuel types. The value of measuring hydrogen isotope ratios for detecting illicit activities strongly depends on assumed operational scenarios. We have focused on high-payoff, critically important application scenarios to validate our effort. In addition, we have performed extensive transport and burnup calculations to yield the noble gas ratios and production for a variety of reactors under different burnups. We have used detailed atmospheric dispersion modeling to estimate isotope dilution factors at varying distances, and we have also begun a detailed data analysis and regression algorithm which should help us evaluate analysis needs and capabilities.

GEOSCIENCE, SPACE SCIENCE, AND ASTROPHYSICS

ADVANCED LASER REMOTE SENSING

John Schultz

Lidar research is a rapidly growing field with civilian and national-security applications. For some applications, lidar is an operational tool, and the development of improved lidar techniques and technologies is the focus of the research, while for other applications lidar is a critical tool used in support of other research objectives. At present, there are no real-time, three-dimensional, wind-measurement techniques that are practical for many applications. We investigated novel lidar wind-sensing techniques to fill this void. We devoted most of our effort to the aerosol-drift technique, which uses an elastic-backscatter lidar and advanced signal-processing techniques to identify and track aerosol patterns in the atmosphere and to calculate three-dimensional wind velocities from changes in the positions of the aerosol patterns.

One of the major obstacles to widespread use of lidar technology for military and civilian applications is the potential for exposing personnel to harmful levels of laser light. The wavelength range of choice for a wide variety of lidar applications lies between 1.5 and 1.7 μm. Unfortunately, there are no suitable lasers that operate efficiently between 1.5 and 1.7 μm. Therefore, the second objective of our project was evaluation and development of new, solid-state eyesafe lasers for lidar applications.

The third objective of this project was to study the feasibility of using lidar to measure atmospheric parameters such as winds, humidity, and temperatures that are related to the transport of airborne materials within the planetary boundary layer. Los Alamos' interest is related to the transport of effluents from activities related to proliferation of chemical, biological, and nuclear weapons, and is related to long-standing NASA interests but has significantly different measurement requirements. We studied measurement requirements, potential operational platforms, and lidar techniques and technologies.

We modified existing algorithms and wrote simple processing codes in the Mathcad and C languages. We generated data sets both artificially and experimentally with an existing elastic-backscatter lidar for use with the processing codes referred to above. We also used the experimental data sets to conduct speed tests with the codes written in C, and we developed refinements to the algorithms and codes. We also established contact with Professor Edward Eloranta of the University Wisconsin-Madison (UW-M), who developed the original algorithms.

Based on this exploratory work, we determined that we could most efficiently accomplish the development of three-dimensional, real-time algorithms that are compatible with operational platforms through an active collaboration with Professor Eloranta. We therefore established a contract with UW-M to jointly develop the algorithms, use an existing UW-M lidar to take sample data sets of a type that is compatible with moving operational platforms, and use the data sets to test and refine the algorithms. This work is not complete, but Professor Eloranta has developed initial versions of the new algorithms and has taken several lidar data sets.

We conducted an objective evaluation of the merits of all state-of-the-art eyesafe laser technologies that may be applicable to Laboratory lidar interests through literature searches and contact with workers in the field. We chose two promising technologies that are not being adequately pursued elsewhere, "cascade lasing" in erbium materials and development of lasers based on chromium^{4+}-doped laser materials, for experimental evaluation and development at Los Alamos under this project.

We demonstrated a significant improvement in the eyesafe, 1.6-μm laser output of erbium-doped crystals using a novel "cascade lasing" scheme. In this scheme we pump the erbium ions to high energy levels using 0.97-μm commercial laser diodes. In normal erbium lasers only a small fraction of this energy decays, by phonon processes that heat the crystal, to the initial state of the 1.6-μm transition. In the cascade scheme, we adopted a cavity that provides optical feedback at the 2.8-μm as well as the 1.6-μm wavelength. The 2.8-μm laser process channels energy by photon processes to the initial level for 1.6-μm lasing. Besides improving the laser efficiency, this process reduces the very detri-

mental heating process common in erbium lasers.

During our research, we improved the slope efficiency of 0.19% for "normal" erbium lasing to 7% through cascade lasing. Rate-equation modeling confirmed that if losses are reduced we might obtain even greater improvement. Our results demonstrate the excellent feasibility of developing compact, efficient eyesafe transmitters. Industrial interest in this technology is high.

We acquired and evaluated experimental laser crystals with special charge-compensating dopant combinations that stabilize the tetravalent state of chromium. This was the first objective comparison of Russian- and (new) American-grown laser crystals. The advantage of chromium ions is that they are tunable in the 1.3- to 1.6-μm spectral range. We obtained laser powers that approached 1 W from the best crystals when they were pumped by a 1-μm Nd:YLF laser. This demonstrated good improvement in material quality over previous reports. Feedback presented to US suppliers has helped them enhance the quality of their material to approximately match the Russian crystals.

We considered access to proliferation sites, potential lidar platforms, and probable measurement requirements in our effort to determine the constraints on the problem of predicting transport of effluents from proliferation activities. Due to a combination of peacetime restrictions on airspace violation and the probable need for both a measurement grid covering hundreds of square kilometers and frequent revisit times, we determined that satellites are the most promising platform. However, wind patterns are strongly dependent on the time of day, particularly in complex terrain and along coastlines. Because the time between each satellite view of a site is generally longer than the time scale of daily changes in wind patterns, it became apparent that the measured data may have to be used in conjunction with mesoscale modeling.

We studied the extensive literature on meteorological applications of lidar to determine probable constraints on the number of measurements that can be made around a specific site in a satellite pass and to select candidate lidar techniques. We rejected the aerosol-drift wind-measurement technique because it required too much laser energy to make a single wind measurement from space that would result in too sparse a grid to be very useful. If used at CO_2-laser wavelengths of approximately 10 μm, the heterodyne or "coherent" doppler-wind-measurement technique would probably provide the necessary wind measurements, but this wavelength range is not suitable for water vapor or temperature measurements that may also be required for this application. Based on these considerations, we chose "incoherent" doppler-wind-measurement techniques that measure the doppler shift with edge filters or Fabry-Perot interferometers at laser wavelengths between 0.3 and 1.6 μm as the top candidates for further development. We are writing a report on this study.

During a visit to NASA's Langley Research Center, we identified a common interest in Cr:LiSAF lasers based on their potential suitability for lidar measurement of a wide variety of atmospheric parameters, and we executed a joint Cr:LiSAF laser demonstration at Los Alamos in August 1995. A joint team assembled laser hardware drawn from both organizations in a configuration traceable to lidar applications. Several performance records for Cr:LiSAF lasers were established, and at the conclusion of the effort the laser system was installed in a Los Alamos lidar system. We made some water-vapor measurements, but, due to equipment failures, the lidar data obtained is of marginal utility. We are also preparing a report on this effort.

Prestack Migration of Three-Dimensional Seismic Data

Michael Fehler

Because foreign oil is cheaper than new domestic oil, U.S. producers are looking for ways to lower their exploration and production costs and to more fully exploit their existing reservoirs. To achieve these ends, they need improved ways of imaging the earth's subsurface. The ability to acquire and process three-dimensional (3-D) seismic data is a key component of such imaging, but the data's volume requires substantial computing power to process it. Conventional computing is no longer able to provide the required throughput or raw computing power. Although massively parallel processing (MPP) can handle the data, implementing MPP requires more resources than many companies can afford.

This project explored a method called prestack migration, the most sophisticated way to process 3-D seismic data, converting the data into information on the geometric and physical properties of the strata being imaged. Given the high cost of drilling new wells, oil companies are interested in the most detailed knowledge of the subsurface as possible. Our project

originally aimed at implementing 3-D prestack migration on an MPP system, the Thinking Machines model CM-5; however, industry interest led us to work in the distributed parallel-computing environment of the Cray Research T3D.

We implemented 3-D prestack migration on a single computer and are now working on extending it to the parallel environment. In addition, we developed two methods for calculating the travel times of seismic waves in complex media. The first method is slow but always gives the correct answer; the second is a fast calculation of both the travel time and strength of a signal. Both methods are important to 3-D stack migration and will allow improved subsurface imaging.

Publications

Cheng, N., and L. House, "Minimum Travel Time Calculation in 3D by Graph Theory," (submitted to *Geophys.).*

Cheng, N., L. House, and M. Fehler, "Amplitude and Traveltime Calculation Using Higher-order Parabolic Equations" (submitted to *Bull. Seismol. Soc. Am.).*

Coupled Transport and Chemical Interactions in Petroleum Reservoirs: Multicomponent-Tracer Large-Scale Application Demonstration

David R. Janecky

Injection of chemical tracers into natural reservoirs is a direct method for characterizing how fluids move and interact during petroleum production. Existing tracer technology uses a limited number of tracer chemicals and relies heavily on radioactive materials. A large increase in the number of tracers and simultaneous improvements in analytical approaches are critical to utilization for improved reservoir management, characterization of enhanced production operations (for example, water and CO_2 flooding), and validation/development of significantly enhanced computer models. Using expertise developed through applications of chemical, analytical, and geologic science to Los Alamos testing, alternative energy, and environmental programs, we have defined new classes of conservative and reactive nonradioactive tracers for both laboratory and field experiments. This project focused on initial experiments necessary to demonstrate that the multicomponent tracers and analytical methods were applicable and valuable in large-scale reservoir systems.

We demonstrated a field tracer experiment in the Salt Creek Field Unit in West Texas. Our purpose was to characterize a section of the reservoir during waterflooding. During a large-scale, multiwell, multitracer test of reservoir flow and connectivity, we demonstrated an initial robust set of tracers and gained experience in the application, field behavior, and operation of the tracers. The results of such experiments provide a major step toward significantly enhanced characterization of reservoir flow paths. In effect, the results allow minimizing unconstrained terms in mathematical/computational models of the reservoir by providing substantial increases in spatial and temporal information on the results of transport processes—geochemical tomography. Demonstration and development of this multicomponent-tracer approach has provided technology interchange with benefits to the US petroleum industry and energy supplies. Simultaneously, the capabilities developed have application to geothermal reservoir, environmental, and defense systems.

Hyperspectral Scanner Design and Analysis

Gregory H. Canavan

Recognizing that hyperspectral sensors could be deployed on satellites to measure crop stress and maturity, Motorola, Inc., provided the opportunity for Los Alamos to include such a sensor on their Comet satellite. To seize this opportunity we had to design, fabricate, and test the sensor in three months. Its main components are a telescope, CCD camera, and wedge filter, which together produce the hyperspectral resolution (i.e., contiguous 10-nm resolution), and our R3000 flight computer, which compresses data into the memory available for storage and transmission.

What made the tight schedule feasible was the availability of the R3000 computer, which we had developed for the satellite attack warning and assessment flight experiment (SAWAFE). Its processor, memory, and power boards could be used directly. We had to build the data compression, camera, and modulator interface boards. We identified the appropriate compression chips and produced preliminary designs for the interface circuits. We were able to purchase chips and circuits and reprogram the computer in time to meet Motorola's launch schedule.

We fabricated the sensor in one month and calibrated it to essentially a flat response across the visible and near-infrared in a second month. After being used to take, compress, and transmit images of test scenes in the laboratory, the sensor was installed on the booster and retested there, where it met all optical and electrical performance specifications. It has remained aligned and adjusted for four months while the launch has been delayed by booster problems. The sensor's success through integration and checkout has served as a proof-of-principle demonstration for follow-on efforts both here and at other laboratories. Development of small hyperspectral sensors is now viewed as important for defense and commercial applications.

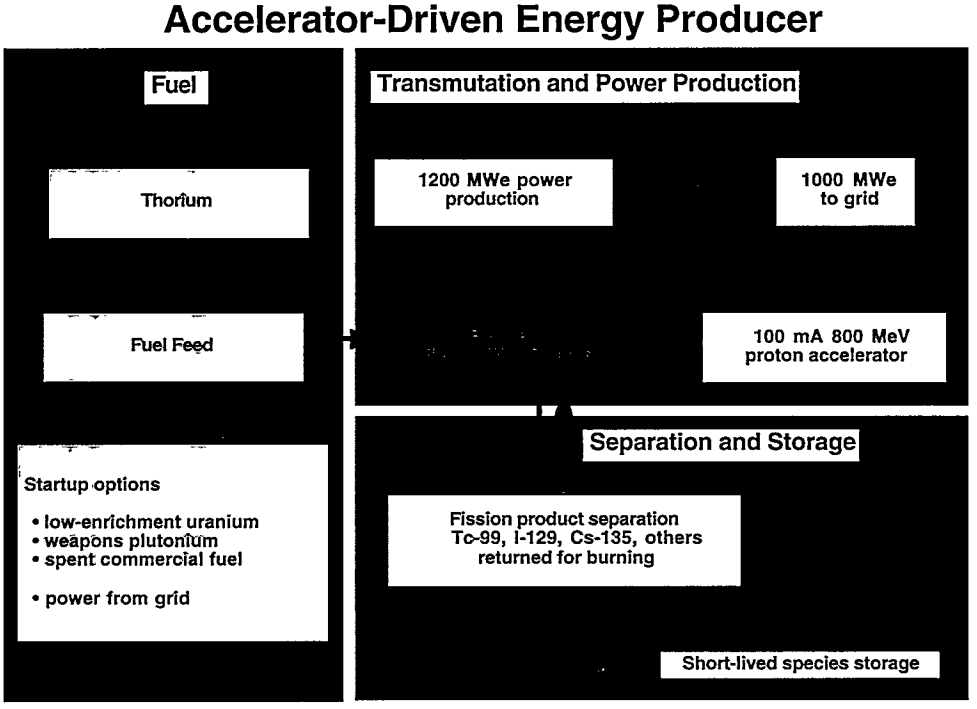
Nuclear and Particle Physics

Development of the Accelerator-Driven Energy Production Concept

Francesco Venneri

We established the basic design for an Accelerator-Driven Energy Producer (ADEP) based on the thorium cycle (see figure). The system uses a molten-salt-based, graphite-moderated blanket similar to the molten-salt breeder design of Oak Ridge National Laboratory. However, the subcritical nature of ADEP allows for relaxation from the demanding chemical reprocessing that characterizes the Oak Ridge design. For example, the actinide protactinium is never removed from the salt. At the front end, pure thorium fluoride is fed into the molten-salt blanket for neutron irradiation. To build up the inventory of uranium-233 in the fissile material within the blanket at the start of the ADEP process, the proton accelerator may need to generate an initial supplemental neutron flux. The back-end separation processes are similar to those derived for the Los Alamos systems for accelerator-transmutation of nuclear waste (ATW) and accelerator-based conversion of plutonium.

Economic studies suggest that electricity generated by ADEP systems might be more expensive than that produced by equivalent-sized conventional nuclear reactors. However, other factors not considered, such as the systems' elimination of fuel fabrication and waste disposition, could tilt the balance in favor of ADEP. Additionally, ADEP systems would preclude production and release of the vast amounts of plutonium now generated during nuclear power production. The isotopic composition of ADEP's very small amount of plutonium—with its large fractions of plutonium-238, -240, and -242—would be unattractive for weapons use. Our analyses also indicated that addition of as little as 5% uranium-238 to the initial thorium inventory would prevent production of weapons-grade uranium-233.



Schematic of the accelerator-driven energy producer based on the thorium cycle.

A High-Power Accelerator Driver System for Spallation Neutron Sources

Andrew Jason

The Los Alamos Neutron Science Center (LANSCE) uses a short-pulse spallation source (SPSS) of neutrons for materials research and other research requiring high neutron fluxes. Specialized nuclear reactors provide complementary neutron sources. Recently, international attention has focused on increasing the neutron fluxes of such sources. When the Advanced Neutron Source reactor project was cancelled, interest developed in building a long-pulse spallation source (LPSS) able to generate the neutron fluxes typical of a reactor. In this project we have studied issues related to increasing neutron fluxes by an order of magnitude over those of existing pulsed sources by upgrading the LANSCE proton linac.

Our goal has been to determine, in parallel with a target study, how to adapt the LANSCE proton linac for the requirements of a 1-MW LPSS and to devise a way to transport the proton beam to a spallation target in Area A at LANSCE.

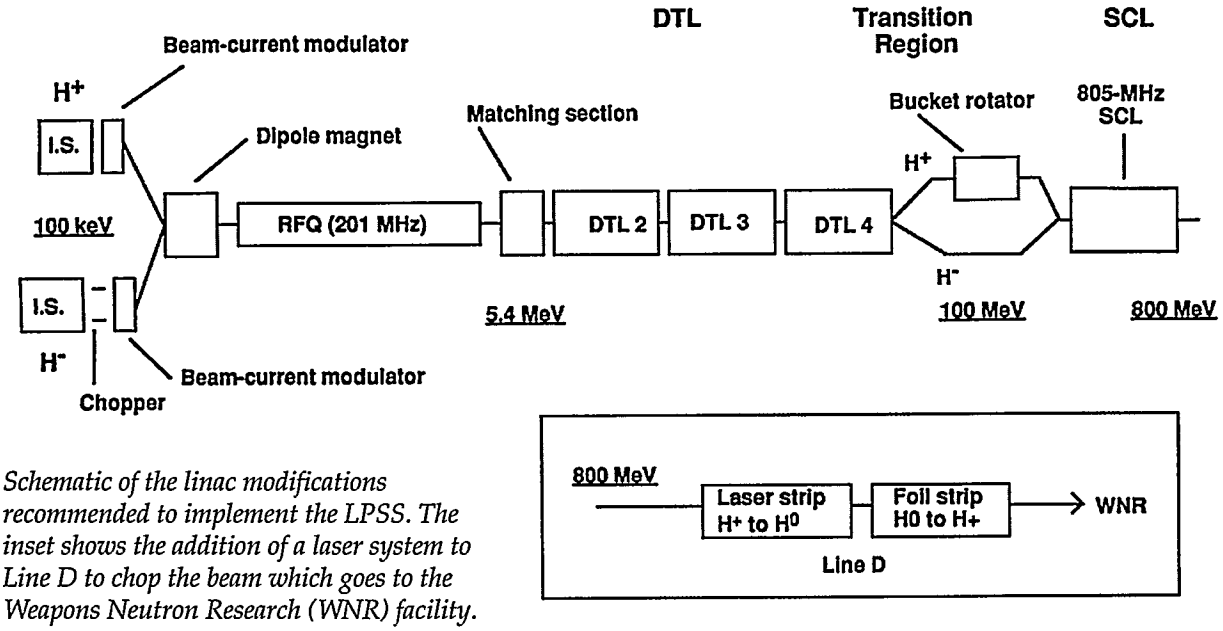
Our study has relied mainly on simulation, calculation, LANSCE operating experience, and brief experiments to be carried out during the linac upgrade. The scheme we have developed (see figure) requires installing a radio-frequency-quadrupole linac that will achieve the LPSS goals with high reliability and low nuclear activation of equipment. We have also developed a less expensive alternative that requires further study. We have concluded that a successful LPSS using LANSCE infrastructure can be achieved at low cost.

Publications

Barlow, D., A. Jason, F. Neri, et al., "Mirror-Field Magnet for Stripped Electron Sweeping" (to be published in *IEEE Trans. Magn.*).

Jason, A., B. Blind, T.-S. Wang, et al., "Minimization of First-Turn Losses by Excited Neutrals in Charge-Changing Injection of Accumulator Rings," in *Proceedings of the Fourth European Particle Accelerator Conference, London (1994)*, Vol. 2, V. Suller and Ch. Petit-Jean-Genaz, Eds. (World Scientific, River Edge, New Jersey, 1994), p. 1219.

Jason, A., and R. Woods, "The Los Alamos Study for a Next Generation Spallation-Neutron Source Driver," in *Proceedings of the Fourth European Particle Accelerator Conference, London (1994)*, Vol. 3, V. Suller and Ch. Petit-Jean-Genaz, Eds. (World Scientific, River Edge, New Jersey, 1994), p. 2684.



Schematic of the linac modifications recommended to implement the LPSS. The inset shows the addition of a laser system to Line D to chop the beam which goes to the Weapons Neutron Research (WNR) facility.

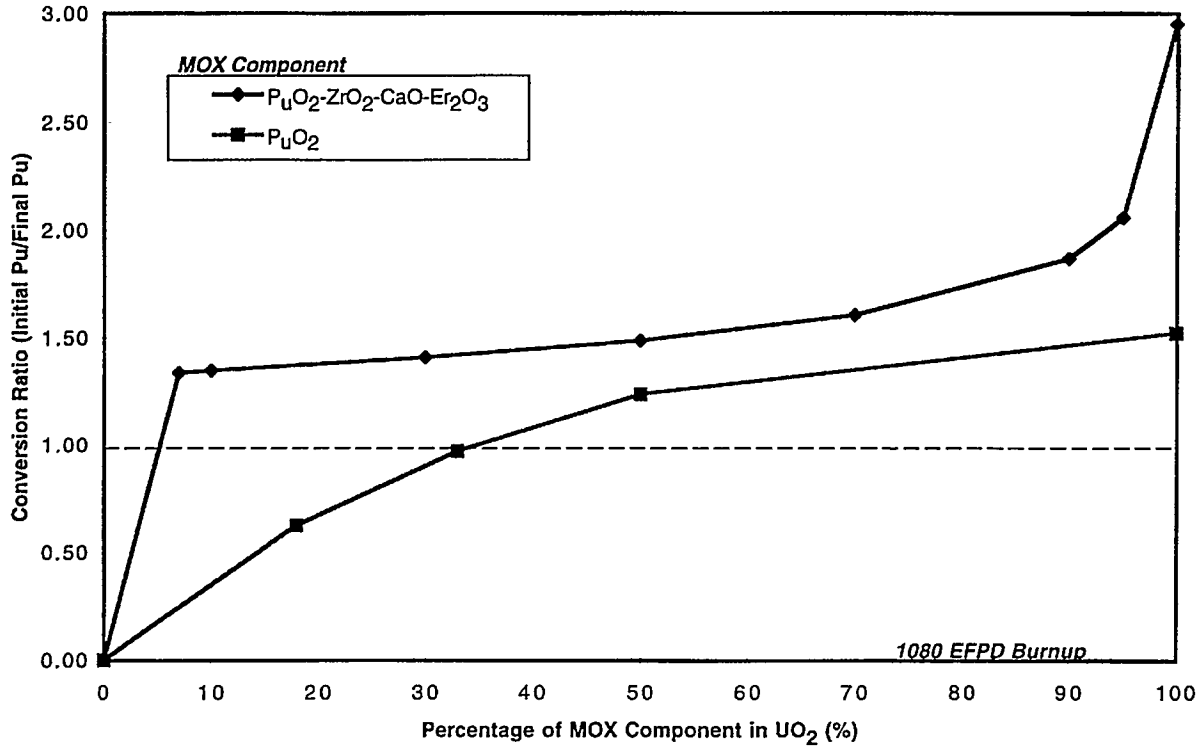
Disposition of Weapons Plutonium as Nonfertile Fuel for Light-Water Reactors

Kenneth Chidester

A nonfertile (inert) fuel offers several advantages over the mixed oxide (MOX) fuels currently being considered for the disposition of weapons plutonium. The most important advantage is that no plutonium is produced during irradiation because of the lack of uranium in the initial fuel form. Although the stockpile of plutonium in surplus weapons is an immediate issue, a need exists to address the broader issues involved with the global inventory of plutonium contained in spent reactor fuel.

For this study, we selected a nonfertile oxide fuel (plutonia-zirconia-calcia-erbia) for further analysis. First, we developed a fabrication process with which we can address issues such as material compatibility. The process involves preparing fuel pellets by using a plutonium surrogate (cerium), which also can be used to study the effects of fuel contaminants and additives. Second, we focused on using advanced computational models to assess the feasibility of using the fuel in reactors. Further efforts include (1) developing a strategy to facilitate a smooth transition from conventional to nonfertile cycles and (2) quantifying the effect the nonfertile cycles have on the global plutonium inventory.

In our fabrication effort, we are focusing on preparing the surrogate fuel. For the analysis effort, we developed physics models of pressurized water reactors (PWRs) and Canadian natural-uranium, heavy-water-moderated and -cooled power reactors. We have completed the initial calculations, including determining reactivity and fuel lifetime. The accompanying figure provides our preliminary results, showing the advantages, in terms of plutonium destruction in commercial PWRs, of a nonfertile MOX fuel compared with a conventional MOX fuel.



Conversion ratios for Pu-239 production/destruction using nonfertile Pu-MOX (PuO_2-ZrO_2-CaO-Er_2O_3) and conventional Pu-MOX (PuO_2) fuels.

Spallation Source Neutron Target Systems

Gary Russell

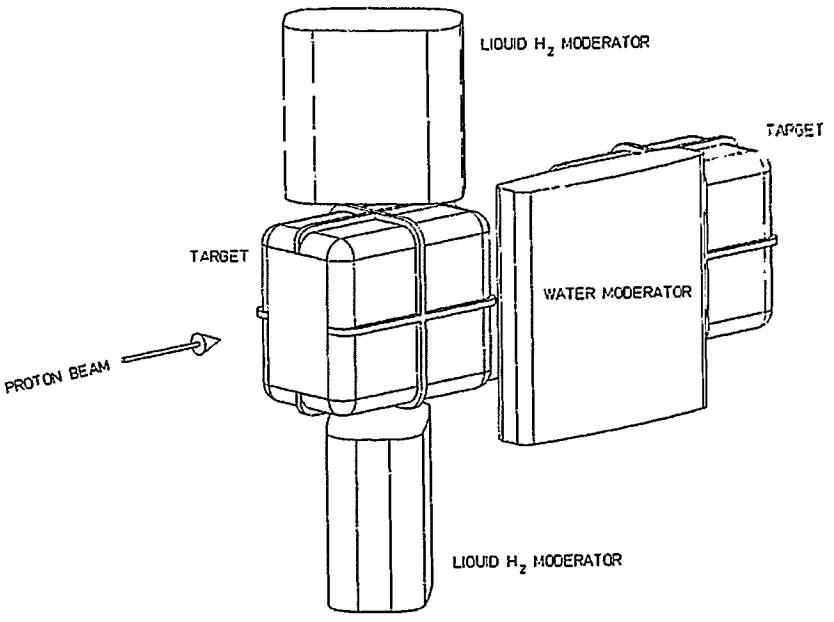
Recently it has been proposed that for a certain class of neutron-scattering instruments a long-pulse spallation source (LPSS) of neutrons driven by a 1-MW proton accelerator can deliver performance nearly equal to or better than that obtained at the world's most powerful neutron-scattering facility, the Institute Laue Langevin (ILL) in Grenoble, France. The purpose of this LDRD project was to perform a feasibility design and to generate a preliminary cost estimate for an LPSS target station to be placed in Area A of the Manual Lujan Jr. Neutron Scattering Center at the Los Alamos Neutron Science Center (LANSCE). The existing 1-mA, 800-MeV proton accelerator at LANSCE would drive the LPSS target system—that portion of the target station that produces potentially useful neutrons.

In addition to providing neutron beam lines that service neutron-scattering instruments, the LPSS facility would include a cell to test high-power spallation-target concepts, an ultracold neutron (UCN) source that would provide very-low-energy (~1 μeV) neutrons for fundamental physics experiments, a dedicated beam line for high-energy neutron radiography, and possibilities for materials irradiation and isotope production.

We have made a preliminary design for an LPSS target station with horizontal proton-beam insertion. The target system consists of a split tungsten target with two wing moderators and a single flux-trap moderator (see first figure). For servicing, the target is extracted horizontally into a hot cell located just downstream of the target station. The moderators and surrounding reflector are extracted vertically into a sealed cask, which is then transported by rail to the hot cell. The moderator assembly can then be lowered into the hot cell for servicing (see second figure).

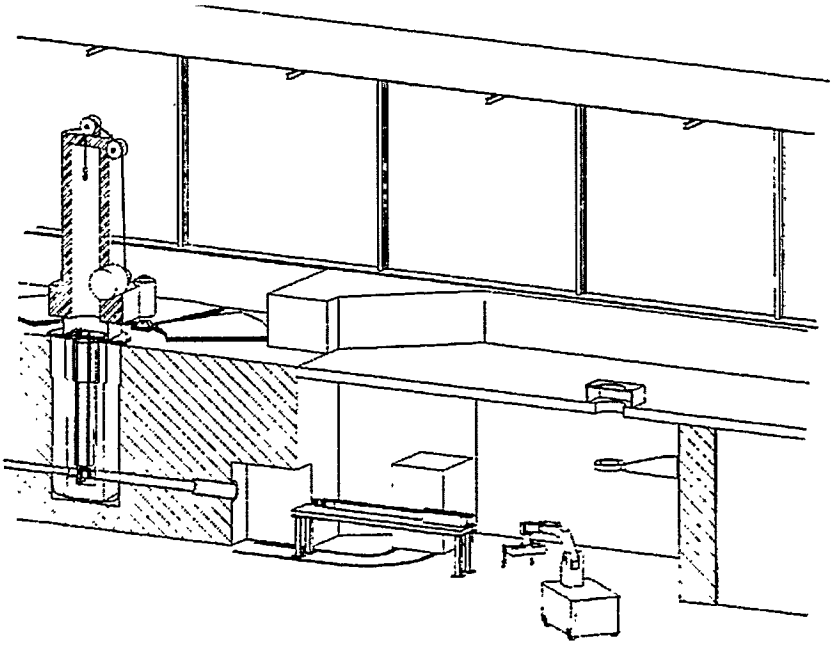
We also calculated the neutronic performance of the target system using the Los Alamos LAHET computer-code system. We found that for $5 \times 10 \times 10$ cm wing moderators and an all-beryllium reflector the calculated average source brightness is one-fourth that of the ILL liquid-deuterium source, CS-2 (see third figure).

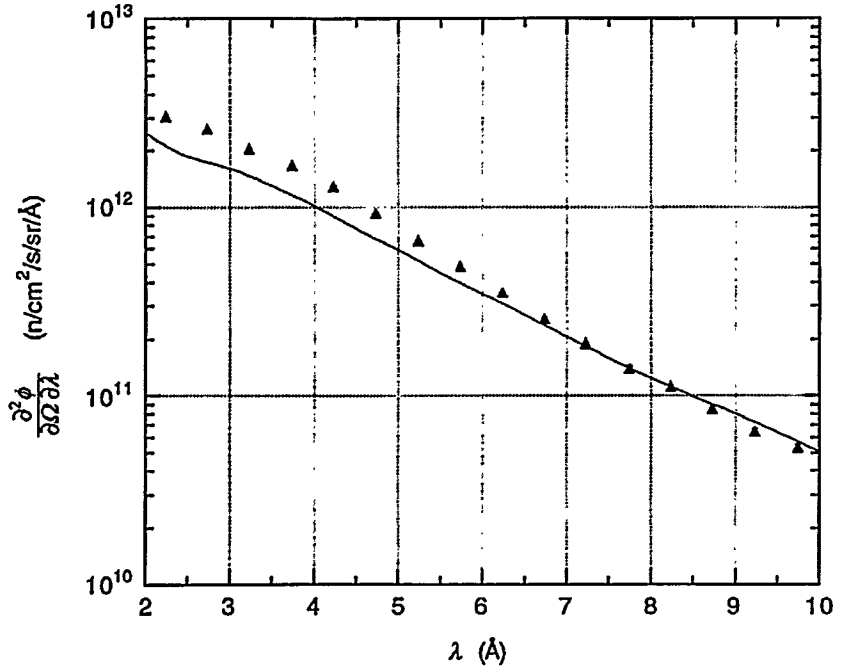
Preliminary estimates indicate that we can construct the LPSS at Los Alamos for a total cost of ~$95 million in 1995 dollars, with a 30% contingency factor. Current estimates indicate that we can design, fabricate, and commission the facility in three years.



LPSS target-moderator configuration.

Hot cell downstream of the LPSS shielding monolith. Here the horizontally extracted target module is shown lying on a table in the hot cell. The cask used to vertically withdraw the moderator and reflector components is also shown.





Calculated source brightness of the LPSS (triangles) compared to the calculated brightness of the ILL (solid line) at one-quarter of full power.

An Ultracold Neutron Facility at LANSCE

Thomas Bowles

The wavelengths of ultracold neutrons (UCNs) are sufficiently long (>500 Å) to allow total internal reflection of the neutrons from the surfaces of various materials. Therefore, it is possible to confine UCNs totally within a bottle for periods longer than 100 s and thus obtain a compact source of stored neutrons that can be used for fundamental physics measurements.

In the initial phase for a UCN source at the Los Alamos Neutron Science Center (LANSCE), we will install a beam guide, shielding, and a Doppler-shifted Bragg scattering converter on Flight Path 11 at 7 m from the present cold moderator. Based on emittance measurements of the present LANSCE moderator and reasonable conversion efficiencies, we expect to produce densities of about 10 ultracold neutrons per cubic centimeter. We are also collaborating on studies using a frozen deuterium converter, which will allow significantly higher UCN densities. Future plans call for moving the source to an optimized moderator that is in the planning stages for LANSCE and will allow an increase of 2 to 3 times in UCN density. In this way, the UCN facility at LANSCE would reach an international standard of excellence.

We have completed the engineering design for the UCN source and will assemble the source at LANSCE in the next year. The UCN source at Los Alamos will be the only operational facility of this kind in the United States and will fulfill a need expressed in the Nuclear Science Advisory Panel's long-range plans of 1989 and 1995. Once the source is operational, we expect to begin a research effort that will use the UCN source.

A CONSORTIUM FOR BIOMEDICAL APPLICATIONS OF SINGLE MOLECULE DETECTION

Richard Keller

We are exploring applications of ultrasensitive fluorescence detection technology for use in basic research and industry.

In the past year, we

- Expanded the range of DNA fragments we can size to include fragments ranging from 550 to 167,000 base pairs, a significant improvement over our previous range of 1500 to 50,000 base pairs.
- Developed a combination near-field optical microscope and atomic force microscope with single-fluorochrome sensitivity. We have used our microscope to detect single molecules of rhodamine-6G and to observe photobleaching and to measure fluorescence lifetimes of single molecules. We have also used it to image single, fluorescently stained DNA strands, single chromosomes, and protein fragments.
- Demonstrated that photobleaching can be used to remove fluorescent contaminants from buffer and enzyme solutions, which improves the efficiency for detection of single molecules in bioassays.
- Improved the detection efficiency of small analyte molecules in hydrodynamically focused flows by combining the analyte molecules with high-molecular-weight adducts to reduce diffusional defocusing.
- Demonstrated sizing of cosmids for characterization of DNA libraries, which has led to a joint project with the Human Genome Program at Los Alamos.
- Began a collaborative project with researchers from the University of New Mexico Medical School to size lipid vesicles by measuring the amount of incorporated fluorescent dye.
- Began investigating the use of photochemical pattering to develop enzyme-based microbiosensors.
- Noted the first observation of photon antibunching from single molecules adsorbed on a silica surface at room temperature and excited with far-field emissions. Photon antibunching is a fundamental photophysical property associated with the detection of emission from single molecules.

Publications

Goodwin, P.M., R.L. Affleck, W.P. Ambrose, et al., "Detection of Single Fluorescent Molecules in Flowing Sample Streams," in *Computer-Enhanced Analytical Spectroscopy: Recent Advances*, Vol. 5, Steven Brown, Ed. (John Wiley and Sons, Chichester, New York, 1995).

Goodwin, P.M., W.P. Ambrose, J.C. Martin, et al., "Spatial Dependence of the Optical Collection Efficiency in Flow Cytometry," *Cytometry* **21**, 133 (1995).

Keller, R.A., W.P. Ambrose, P.M. Goodwin, et al., "Ultrasensitive Fluorescence Analysis in Solution" (to be published in *Appl. Spectrosc.*).

Petty, J.T., M.E. Johnson, P.M. Goodwin, et al., "Characterization of DNA Size Determination of Small Fragments by Flow Cytometry," *Anal. Chem.* **67**, 1755 (1995).

Cancer Risk Assessment

Bruce Lehnert

The objective of this project is to develop new mechanistically based biotechnological methods for assessing the risk of cancer development in individuals who have been or may be exposed to environmental carcinogens. Estimates of cancer risk in response to carcinogens currently are based on empirical evidence of cancer incidence and are generally applicable to the human population as a whole. More individualized cancer risk assessment through the identification of biomarkers of susceptibility has not been possible previously because of major gaps in the understanding of the basic mechanisms involved in carcinogenesis.

The scientific focus of this project is to identify those critical genes and gene products that render seemingly normal individuals more susceptible to exposures to carcinogens, especially those genes that are involved in cell-cycle regulation and DNA repair. The specific aims of the effort are to identify and characterize potential cancer-susceptibility genes, to develop advanced flow cytometric assays for detecting susceptibility genes and gene products on a cell-by-cell basis, to determine relationships between variations in susceptibility-gene products and cancer risk, and to develop user friendly bioassays for cancer susceptibility genes.

Our accomplishments include (1) the development and application of new phase-sensitive detection flow cytometry for biomarker analyses, (2) studies involving concurrent flow cytometric analysis of potential cancer-susceptibility genes and cell-cycle analysis following exposures to low- and high-linear-energy-transfer ionizing radiation, (3) further characterizations of a variety of DNA repair genes, and (4) the establishment of collaborations with other institutions investigating cancer risk assessment.

Publications

Amundson, S.A., and D.J. Chen, "Ionizing Radiation Induced Mutation of Human Cells with Different DNA Repair Capacities" (submitted to *Adv. Space Res.*).

Chen, F., S. Peterson, M. Story, et al., "Distribution of DNA-PK in Ku80 Mutant Xrs-6 and the Implications in DNA DSB Repair" (to be published in *Mutat. Res.*).

Crissman, H., and A. Nastasi, "Cell Cycle and Cell Proliferation Markers" (to be published in *Prog. Flow Image Cytom.*).

Deka, C., L.S. Cram, R. Habbersett, et al., "Simultaneous Dual-Frequency Phase-Sensitive Flow Cytometric Measurements for Rapid Identification of Heterogeneous Fluorescence Decays in Fluorochrome Labeled Cells and Particles" (to be published in *Cytom.*).

Deshpande, A., D. Archuleta, Y.Valdez, et al., "Tumor Necrosis Factor-Alpha Production by Alveolar Macrophages during the Early Development of Phosgene-Induced Lung Injury" (to be published in *Inhal. Toxicol.*).

Gadbois, D., B. Lehnert, S. Wang, et al., "Alterations in Cell Cycle Traverse after Exposure to Alpha Particles and Gamma Rays" (submitted to *Rad. Res.*).

Gadbois, D., S. Peterson, E.M. Bradbury, et al., "CDK4/Cyclin D1/PCNA Complexes During Staurosporine-Induced G1 Arrest and G0 Arrest of Human Fibroblasts" (to be published in *Exp. Cell Res.*).

Knauf, J., M. MacInnes, B. Marrone, et al., "Regions within the XPG Protein that are Involved in its Intranuclear Localization and UV Response" (submitted to *In Vitro Cell. Dev. Biol.*).

Kunz, L., and J. Freyer, "Adaptation of an Automated Selective Dissociation Procedure to Multicellular Spheroids of Oncogene-Transformed Fibroblasts" (to be published in *In Vitro Cell. Dev. Biol.*).

Park, M.S., "Expression of Human RAD52 Confers Resistance to Ionizing Radiation in Mammalian Cells," *J. Biol. Chem.* **270,** 15467–15470 (1995).

Park, M., J. Knauf, G. Strniste, et al., "Nuclear Localization and UV Response of a Human DNA Excision Repair Protein, Xeroderma Pigmentosum G (XPG) Endonuclease" (submitted to *J. Cell Sci.*).

Peterson, S.R., A. Kurimasa, M. Oshimura, et al., "Loss of the 350-kd Catalytic Subunit of the DNA-Dependent Protein Kinase in DNA Double-Strand Break Repair Mutant Mammalian Cells," *Proc. Natl. Acad. Sci. U.S.A.* **89,** 11920 (1995).

Stackhouse, M.A., B.L. Marrone, D. Grady, et al., "Regional Assignment of the Human DNA Repair Gene (XRCC4L) to the 5q13-14 Boundary by Fluorescence In Situ Hybridization," *Genomics* **27,** 215 (1995).

Wharton, W., "Cell Cycle Constraints of Peroxide- and Radiation-Induced Inhibitory Checkpoints" (to be published in *Cancer Res.*).

Yamada, Y., M. Park, and D. Chen, "Molecular Analysis of Radiation-Induced Large Deletions Containing the HPRT Locus in Normal Human Fibroblasts" (to be published in *Rad. Res.*).

Molecular Medicine for the 21st Century: A Computational Basis for Design and Critique of Vaccines and Therapeutics

Alan Lapedes

The motivation for this project is the crisis in health care that is the consequence of newly evolved pathogens and the enhanced transmission of infectious diseases. A critical need exists for computational and theoretical efforts aimed at assimilating, integrating, and interpreting vast collections of scattered biomedical information. Our objective is to develop a comprehensive, integrated approach to bring the great wealth of experimental data currently being generated into a comprehensible framework that would allow reasoned selection of vaccine candidates and therapeutic agents, rapid evaluation of changes in pathogens that display drug resistance, and the development of new means to overcome this resistance. We will closely coordinate this effort with our partnered pharmaceutical companies and other laboratories that engage in accumulating data and developing drugs.

Nature published our work on understanding the dynamics of the body's response to the HIV virus in its January 1995 issue. The article received widespread attention that included a front-page story in the New York Times and other major media outlets. In collaboration with scientists from GlaxoWellcome, we have analyzed experimental data from molecular-diversity experiments and have successfully predicted peptides that have higher affinity for an antibody than any previously known. We have been instrumental in forming a consortium, the Diversity Biotechnology Consortium, which includes four corporate laboratories in addition to academic laboratories and Los Alamos National Laboratory. We organized two workshops—one on molecular diversity, one on sequencing and informatics for sexually transmitted disease pathogens.

Publications

Farmer, A.D., C.E. Calef, K. Millman, et al., "The Human Papillomavirus Database," *J. Biomed. Sci.* **5,** 90 (1995).

Gupta, G. and G. Myers, "Analyses of Various Folding Patterns of the HIV-1 Loop," *in Peptides: Design, Synthesis and Biological Activity,* C. Basava and G. M. Anantharamiah, Eds. (Birkhauser, New York, 1994), pp. 259–277.

Ho, D.D., A.U. Neumann, A.S. Perelson, et al., "Rapid Turnover of Plasma Virions and CD4 Lymphocytes in HIV-1 Infection," *Nature* **373,** 123 (1995).

Huynen, M.A., A.S. Perelson, W.A. Vieira, et al., "Base Pairing Probabilities in a Complete HIV-1 RNA" (submitted to *J. Comp. Biol.*).

Kober, B.T.M., E.E. Allen, A.D. Farmer, et al., "Heterogeneity of HIV-1 and HIV-2," *AIDS* **9 (Suppl. A),** s5 (1995).

Macken, C.A. and A.S. Perelson, "Protein Evolution on Partially Correlated Landscapes," *Proc. Natl. Acad. Sci.* **92,** 9657 (1995).

Myers, G., "HIV: Between Past and Future," *AIDS Research and Human Retroviruses* **10,** 1317 (1994).

Myers, G., "Molecular Investigation of HIV Transmission," *Ann. Intern. Med.* **121,** 889 (1994).

Pennypacker, C., A.S. Perelson, N. Nys, et al., "Localized or Systemic Heat-Inactivation of Human Immunodeficiency Virus: A Mathematical Analysis," *AIDS* **8,** 321 (1995).

Safe Extension of Red Blood Cell Storage Life at 4°C

Mark Bitensky

This project focuses on developing technology to safely extend the storage life of red blood cells. With current storage practices blood is properly considered unusable after six weeks at 4°C and must be discarded as toxic waste. This practice results in the loss of more than 2 million units of blood each year in the United States. An autologous (self) donor cannot set aside blood for storage more often than once every 10 days without severely depleting the body's reserves of red blood cells. Because blood can be stored safely for only 42 days, by the time a patient can donate a fourth unit, the first unit has already begun to deteriorate.

The alternatives to refrigerated storage are still experimental. The most promising of these methods is to freeze red blood cells in glycerol, but this method is rarely used, and it is prohibitively expensive: costs approach $1,000 per unit of blood (not including the cost of maintaining the blood at –80°C). Freezing blood in glycerol, removing the glycerol, and preparing red blood cells for

transfusion are complex, labor-intensive tasks which involve the loss of up to 25% of the cells and require expensive, complicated instrumentation. Other alternatives to refrigerated storage include the use of liposome-encapsulated hemoglobins, cross-linked hemoglobins, and freeze-dried red blood cells. At present none of these techniques is even marginally successful.

Our studies of human erythrocytes (red blood cells) have allowed us to explain, in biochemical terms, specific pathological changes that occur to red blood cells during prolonged refrigerated storage. For example, we have learned that it is essential to stabilize or protect hemoglobin against oxidative damage that, paradoxically, increases at low temperatures. This and other experimental insights have allowed us to develop a new red-blood-cell storage protocol which has the potential to more than double present refrigerated-storage times and has greatly improved the quality of stored red blood cells. This storage technique, which we have patented, has important applications in combat-casualty care and in preplanned surgery for which longer term storage makes autologous transfusion more practicable.

Human Brain Mapping: Experimental and Computational Approaches

Charles Wood

Based on recommendations of the National Academy of Sciences, a consortium of federal agencies has developed the Human Brain Project to stimulate the integration of noninvasive brain-imaging techniques with advanced computer modeling, visualization, and database techniques. Our project combines the strengths of Los Alamos and its collaborators in noninvasive brain imaging and high-performance computing to contribute significantly to the Human Brain Project.

The experimental component of our project emphasizes optimizing spatial and temporal resolution of functional brain imaging by combining (a) structural magnetic resonance imaging (MRI) measurements of brain anatomy; (b) functional MRI (fMRI) measurements of blood flow, oxygenation, and volume; and (c) magnetoencephalography (MEG) measurements of neuronal population currents. The computational component of the project emphasizes the development of a high-resolution 3-dimensional volumetric model of the brain—based on anatomical MRI—in which structural and functional information from multiple forms of brain imaging can be integrated into a single computational framework for modeling, visualization, and representation in a distributed database form.

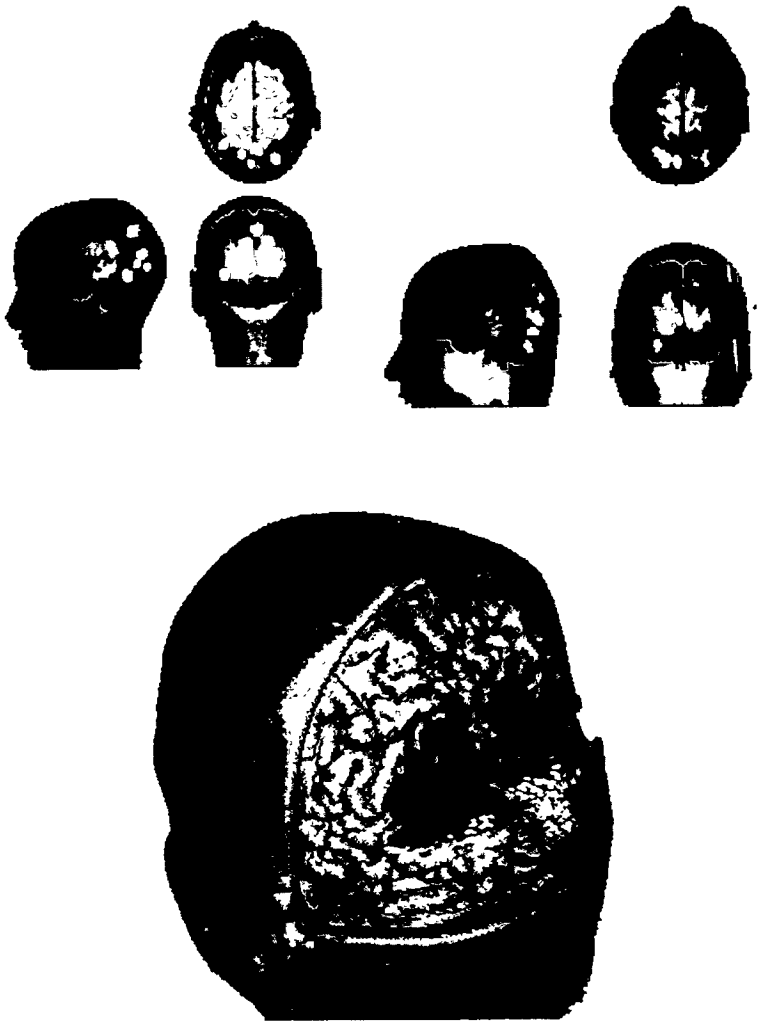
We have (a) begun experimental comparisons of fMRI and MEG estimates of brain activation of the human visual system using comparable visual stimulation, (b) extended tools for volume visualization and anatomical segmentation based on MRI data, and (c) explored alternative mathematical approaches to integration of fMRI and MEG estimates of brain activation.

This work will contribute significantly both to a basic understanding of brain structure and function and to improved noninvasive diagnosis in neurology, neurosurgery, and psychiatry.

Publications

Aine, C.J., J.S. George, et al., "Differences in temporal dynamics of visual evoked neuromagnetic activity" (to be published in *Cerebral Cortex*).

George, J.S., C.J. Aine, et al., "Mapping Function in the Human Brain with MEG, Anatomical MRI, and Functional MRI," *J. Clinical Neurophysiology* **12**, 406 (1995).



Magnetoencephalography (MEG) and functional magnetic resonance imaging (fMRI) responses to a visual stimulus—a region of checkerboard placed in the lower-right quadrant of the subject's visual field. We used anatomical MRI to obtain head and brain-surface renderings of the subjects. Upper figure: *comparison of functional maps of brain activation (white regions) by visual stimulation. The left panel shows five sources identified from MEG field maps collected 80–160 ms after introducing the visual stimulus. The right panel shows regions of apparent activation indicated by blood flow and blood oxygenation in an fMRI study using comparable visual stimulation.* Lower figure: *probable source locations (white regions) determined from combined MEG and MRI data. The dark gray regions are where the rendered brain surface has been cut away to disclose underlying anatomy. We used Bayesian decision theory to map (1) possible source locations from MRI data, (2) probable source locations from functional fMRI data, and (3) estimates of detailed spatial locations of the sources and their activation strengths as functions of time from MEG data.*

Deformable Human Body Model Development

William O. Wray

Existing state-of-the-art human body models were developed primarily for ergonomic analysis. These models have accurate external geometry and can exhibit realistic joint movements and body configurations. Less-sophisticated crash victim simulator (CVS) models based on rigid body mechanics are used to simulate the responses of occupants to vehicular collisions.

We are developing a much more useful deformable human body model (DHBM) by incorporating realistic constitutive relations for soft tissue into one of the advanced ergonomic analysis or CVS models. In addition, we are incorporating the following into the DHBM: (1) accurate bone-geometry representations of body areas such as the back and buttocks whose comfort is affected by contact-pressure distributions and (2) realistic hard-tissue constitutive relations in areas such as the head, thorax, and pelvis, which are commonly subjected to injury. We have also developed a nonlinear, viscoelastic constitutive model for automobile seat-cushion foam. This model provides a good foundation for the development of constitutive relations for soft human tissue.

The DHBM will be applicable to the analysis of occupant safety and comfort in automobiles, the fit and function of prosthetic and orthotic devices, and battlefield injuries incurred by soldiers wearing body armor.

Development of Experimental Techniques to Study Protein and Nucleic Acid Structures

Jill Trewhella

We are developing experimental tools for structural biology, specifically those applicable to three-dimensional (3-D) biomolecular structure analysis. Since most biological systems function in solution environments, the ability to study proteins and polynucleotides under physiologically relevant conditions is of paramount importance.

We are focusing on studies of protein-nucleic acid complexes and DNA hairpin structures important for understanding the regulation of gene expression, as well as the fundamental interactions that allow these complexes to form. An understanding of how genetic information is expressed will be a major factor in interpreting the information now being obtained through the Human Genome Project.

We have adopted a three-pronged approach that involves crystallography and nuclear magnetic resonance (NMR) spectroscopy to study protein and DNA structures at high (atomic) resolution and neutron (and x-ray) scattering techniques to study the complexes they form in solution. We are also using isotope labeling to expand the range of molecules we can investigate using NMR and neutron scattering.

For several decades crystallography was the only method for obtaining complete 3-D, high-resolution structures of biomolecules. It remains one of the most powerful approaches, and recent developments in synchrotron facilities and Laue diffraction methods have opened new horizons for time-resolved studies of biomolecules. Over the past decade, there has also been a revolution in NMR applications to biomolecular structure analysis—uniform ^{13}C and ^{15}N labeling coupled with three- and four-dimensional NMR methods has made NMR spectroscopy competitive with x-ray crystallography for studying the high-resolution structures of small biological molecules, and it has facilitated detailed comparisons between crystal and solution forms.

Neutron scattering techniques complement these other approaches: biomolecular complexes often function in large assemblies that are not suited to study by crystallography or NMR spectroscopy. For such complexes in solution, neutron scattering provides information on the overall structures and relative dispositions of their components. This capability arises from the radically different neutron scattering properties of ^{1}H and ^{2}H, and it depends upon measuring neutron scattering data from a complex whose components have different mean neutron scattering densities and can be dissolved in solvents with different D_2O:H_2O ratios.

The nucleosome core particle is the fundamental repeating unit of chromosomes in higher organisms. It is composed of a core of protein subunits (the histone octamer) surrounded by double-stranded DNA. The histone proteins are subject to chemical modification in the form of reversible N-acetylation of specific lysine residues located in their N-terminal tail regions. This acetylation has long been associated with transcriptional activity.

We have completed neutron scattering experiments that show the histone tails contribute significantly to the radius of gyration of the histone octamer in the intact core particle. At the same time, the shape of the DNA component seems to be altered by the loss of the histone tails. The main interactions of the histone tails appear to be in the regions of DNA beyond the 146 base pairs associated with the histone core and acetylation may modulate that interaction. We also studied nucleosomes reconstituted with a minor variant histone, H2B0, associated with human sperm chromatin. There is a substantial difference in the structure of the particle with the substitution of H2B0 histone, which has significant implications about the role of minor variant histones in chromatin function.

Identifying sequences of human DNA that are unusually regulated or especially prone to breakage will be one of the many payoffs from the Human Genome Project. The so-called "fragile-X" repeat is a three-nucleotide sequence associated with the *fmr-1* gene and involved in certain mental disorders. This repeat has the potential to expand—once expanded it is fragile, which can lead to DNA breakage. Once expanded, it can also be methylated, which turns off the *fmr-1* gene, leading to mental disorders.

We have determined the structures formed by the fragile X repeat using multidimensional NMR techniques and find that they form "hairpin" structures. These hairpin structures suggest a mechanism of how these repeats can extend during replication, leading to DNA breakage or methylation.

We further showed that chromomycin-A3, a nonintercalative drug specific for GC base pairs, binds only the Watson-Crick DNA duplex and not the hairpin structures adopted independently by G- and C-rich strands. Therefore, this drug is capable of blocking the transition from the Watson-Crick heteroduplex to the

self-assembled hairpin structures in the fragile-X repeat. In addition, the Watson-Crick DNA duplex of the fragile-X repeat in the methylated form shows stronger binding to Chromomycin-A3, thereby offering a diagnostic tool for discriminating the methylated and unmethylated forms of this repetitive DNA. The selective preference of this drug for the methylated form of the fragile-X repeat could be utilized for diagnosis of such repeats in the chromosomal DNA.

A critical component of this project was to establish NMR capabilities for biomolecular structure analysis. Three high-field, high-resolution NMR instruments are now in use for structural biology studies. We also collected our first multidimensional NMR spectra of proteins (ubiquitin and the muscle protein complex troponin C/troponin I [residues 96–115] in which the troponin C component was isotopically labeled).

Stable isotope labeling is the key to full utilization of multidimensional NMR methods for structure analysis. Uniform labeling with ^{13}C and ^{15}N has permitted us to solve the solution structure of proteins up to ~30 kilodaltons. (The size limitation arises from the fact that both the proton resonance line width and the absolute number of protons increase in proportion to the molecular weight, resulting in severe spectral overlap problems for most globular proteins greater than 20 kilodaltons.)

Protons are relaxed primarily by dipole-dipole interactions with other protons, which, because of the long correlation times associated with large proteins, can yield broad resonances. The α-carbon in amino acids is a stereochemical center, making the β-methylene protons inequivalent and causing them to give rise to separate NMR signals. Because dipolar relaxation is strongly dependent on the interproton distance ($1/r^6$), methylene protons that are close in space (1.8 Å) can broaden each other significantly. This relaxation mechanism is removed by stereoselective replacement of one of the methylene protons with deuterium (see figure). The remaining proton is relaxed by protons that are more distant (2.3–3.1 Å), which significantly sharpens the resonance. To counter the effects of dipolar relaxation, we developed three approaches for stereospecific deuteration at the β-methylene position of amino acids.

In conjunction with representatives from academia and industry, we held a workshop on "Stable Isotope Labeling in Biomolecular Structure and Mechanisms" in March 1994. The more than 100 attendees included the leading biomolecular NMR spectroscopists from the U.S., Europe, Japan, and Australia. We edited and published the conference proceedings, which is now an important reference document for the field.

Publications

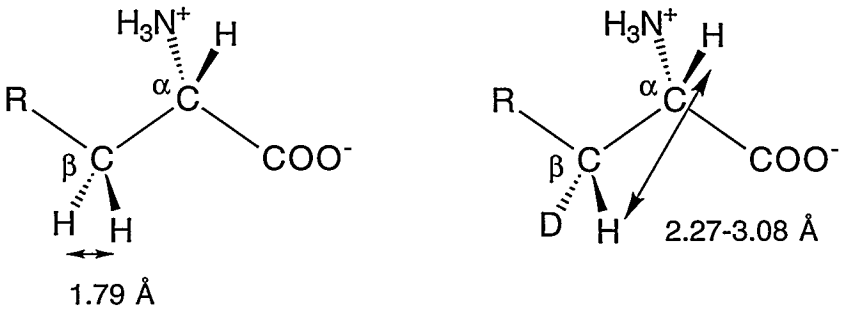
Catasi, P., G. Gupta, A. Garcia, et al., "Unusual Structures of the Tandem Repetitive DNA Sequences Located at Human Centromeres," *Biochem.* **33**, 3819 (1994).

Gupta, G., A. Garcia, P. Catasi, et al., "Stem-Loop Structures of the Repetitive DNA Sequences Located at Human Centromeres" in *Structural Biology: The State of the Art*, R.H. Sarma and M.H. Sarma, Eds. (Adenin Press, New York, 1994), Vol. 2, p. 137.

Kelly, J., D.A. Ashburn, R. Michalczyk, et al., "An Improved Synthesis of [Amino-^{15}N]Adenine; Useful in the Large Scale Synthesis of 2'-Deoxy[Amino-^{15}N]Adenosine," *J. Labelled Compds. Radiopharm.* **36**, 631 (1994).

Silks, L.A., E. Dunkle, C.J. Unkefer, et al., "A Reinvestigation of the Synthesis of [$^{15}N_2$]Hydroxymethylimidazole: Useful in an Improved Synthesis of (D,L)-$^{15}N_2$Histidine" (to be published in *J. Labelled Compds. Radiopharm.*).

Trewhella, J., T.A. Cross, and C.J. Unkefer (Eds.), *Stable Isotope Applications in Biomolecular Structure and Mechanisms* (Los Alamos National Laboratory, Los Alamos, NM, 1995).



Stereospecific deuteration at the β-methylene position of amino acids improves the resolution of multidimensional NMR spectra. Because dipolar relaxation is strongly dependent on the interproton distance ($1/r^6$), methylene protons that are close in space (1.8 Å) can broaden each other significantly. This relaxation mechanism is removed by stereoselective replacement of one of the methylene protons with deuterium. The remaining proton is relaxed by protons that are more distant (2.3–3.1 Å), which significantly sharpens the resonance.

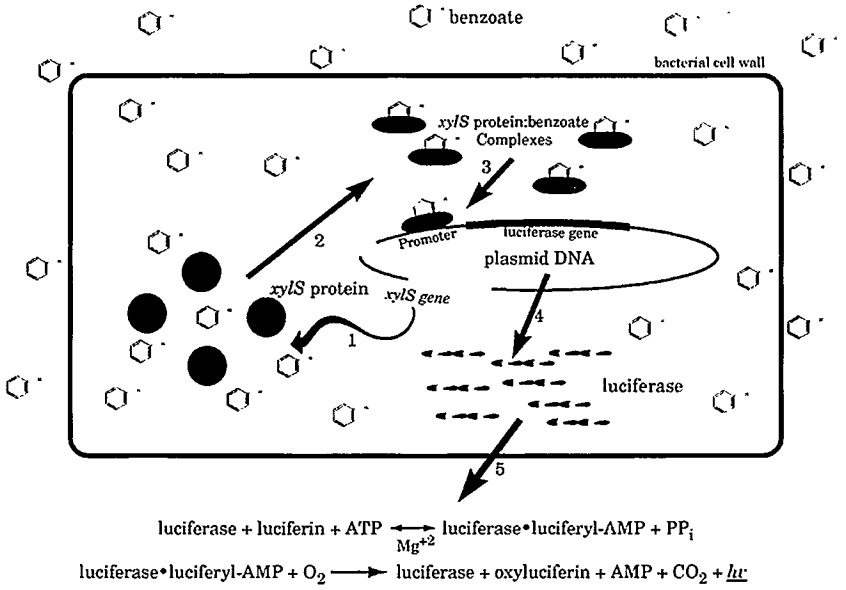
Development and Testing of Biosensors that Quantitatively and Specifically Detect Organic Contaminants

Paul Jackson

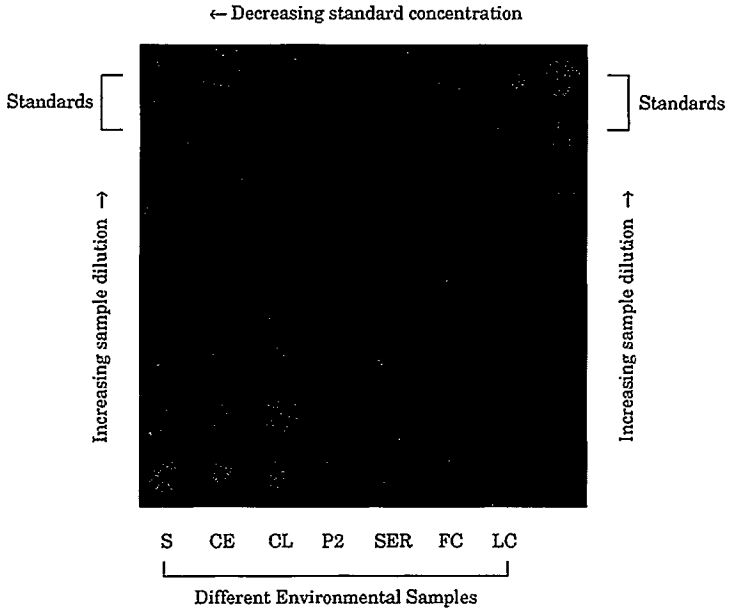
Assaying complex environmental samples for organic contaminants is costly and labor intensive—a more sensitive and less expensive method of detecting organic contaminants is needed.

We have developed sensitive microbial biosensors that detect specific organic contaminants in complex waste mixtures without prior separation from other components of the waste. Some soil microbes degrade organic compounds that contaminate the environment. These bacteria sense minute quantities of particular organic compounds, and then respond by activating genes encoding enzymes that degrade these contaminants (see schematic). We have genetically manipulated these gene-regulatory processes to develop bacterial biosensors that use sensitive biochemical assays to detect specific organic compounds.

We have constructed, laboratory tested, and deployed to a field site two biosensors that detect different xylene compounds (see figure). Our results demonstrate that these biosensors sensitively detect targeted compounds in complex environmental solutions. The cost of these biosensor assays is at least 100-fold less than other methods, allowing more rapid and extensive testing and site characterization.



Schematic of biosensor design and function. The xylS gene produces xylS protein (1), which binds to benzoic acid entering the cells (2). This complex binds to the promoter (3), activating the luciferase gene (4). Luciferase produces light (5) when provided with the appropriate reagents.



Photograph of biomonitor bioluminescence induced by exposure to waste samples. Samples from different waste streams were tested using the benzoic acid biomonitor to determine the amount of this compound. S, CE, CL, P2, SER, FC, and LC are different environmental samples. Different dilutions of each sample were assayed. High concentrations of some samples inhibited the reaction (LC). Benzoic acid standards were included (top two rows).

Neutron Scattering and Nuclear Magnetic Resonance (NMR) Spectroscopy Structural Studies of Protein-DNA Complexes

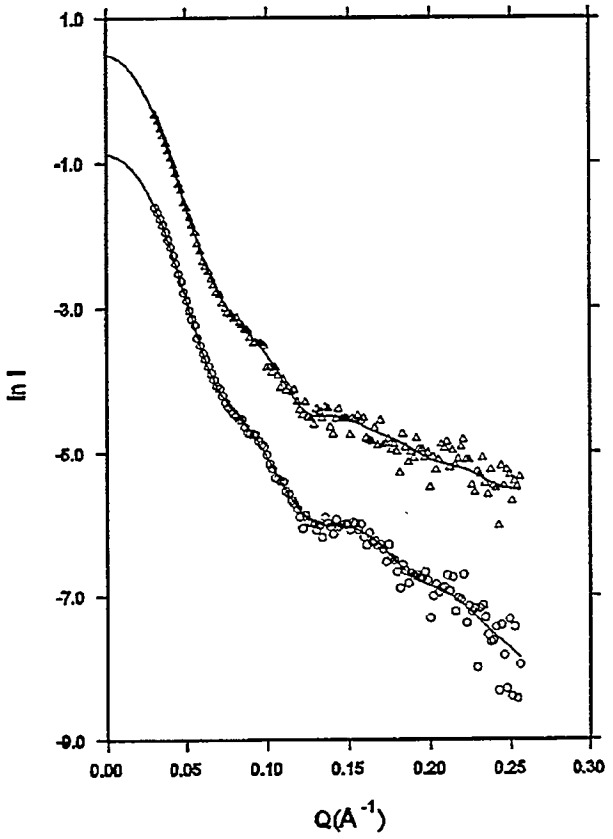
E. Morton Bradbury

Virtually all of the DNA in eukaryotic genomes, which includes the human genome, is packaged into a repeating subunit called a nucleosome. Nucleosomes consist of a 195-bp (base pair) segment of DNA coiled twice around an octamer of histone proteins and completed by the binding of histone H1. All aspects of DNA processing (DNA replication, transcription, and spermiogenesis) are strictly associated with the reversible acetylations of lysine residues in the histone octamer.

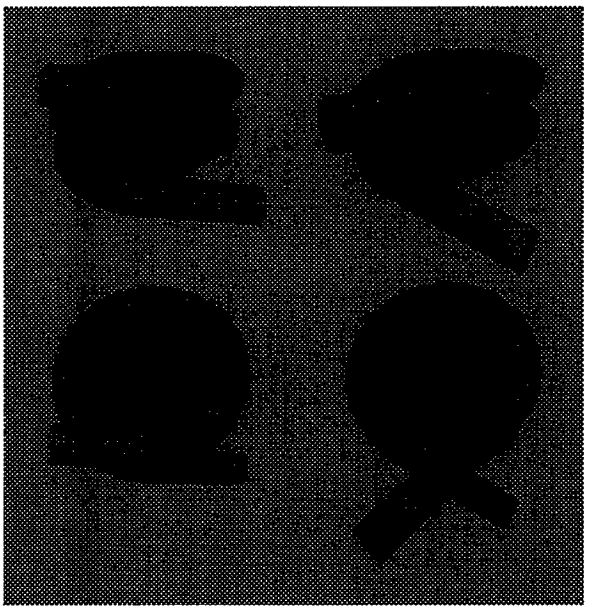
Our x-ray scattering studies of 195-bp control and acetylated nucleosome particles have, for the first time, demonstrated an effect of histone acetylation on nucleosome structure (see figure showing scattering data). The acetylation of histone H4 releases 0.17 turns of the DNA previously constrained by the nucleosome particle (see three-dimensional representation). Such a release facilitates the unfolding of chromatin to allow transcription and replication factors access to the DNA.

Inherited neuromuscular disorders have been associated with the abnormal expansion of DNA triplets. Using NMR spectroscopy, we determined that the single strands $(CCG)_n$ and $(GGC)_n$ form stem-loop DNA structures. In Fragile-X patients, the expanded triplet $(CCG)_n$ is hypermethylated, which is thought to silence the FMR-1 gene, causing the onset of the disease.

We have shown that the stem-loop or hairpin structure formed by $(CCG)_n$ is a much better substrate for human methyl



Small-angle scattering data and corresponding best-fit curves for nonacetylated and tetra-acetylated 195-bp nucleosomes.



Three-dimensional representations of the model used to generate the best-fit P(r) functions to the measured P(r) functions.

transferase than the Watson-Crick double-stranded DNA structure, thus providing a basis for understanding the disease. The Human Genome Project has identified a repeated centromeric DNA sequence, which we determined forms stem-loop structures that may function in cell division by providing binding sites for proteins in the spindle apparatus.

Publications

Catasti, P., G. Gupta, A.E. Garcia, et al., "Unusual Structures of the Tandem Repetitive DNA Sequences Located at Human Centromeres," *Biochem.* **33**, 3819–3830 (1994).

Chen, X., S.V.S. Mariappan, P. Catasti, et al., "Hairpins Are Formed by the Single DNA Strands of the Fragile X Triple Repeats," *Proc. Natl. Acad. Sci. U.S.A.* **92**, 5199–5203 (1995).

Mariappan, S.V.S., P. Catasi, X. Chen, et al., "Solution Structure of the Fragile X DNA Triplet Repeats, (GCC)n•(GGC)n: NMR Studies of the Individual Strands" (submitted to *J. Biol. Chem.*).

Computational and Theoretical Aspects of Biomolecular Structure and Dynamics

Angel Garcia

The relationship of structure and function in biomolecules is strongly linked to the dynamics and stability of the molecules in solution. Previous workers have used computational methods to describe the dynamics and energetics of biomolecules. In our work we have calculated biomolecular dynamics and solvation free energies.

Dynamics

Simulations of biomolecular dynamics are commonly interpreted in terms of harmonic or quasi-harmonic models which assume that the biomolecule oscillates around a single energy minimum. However, spectroscopic data on myoglobin suggest it has a broad distribution of energy barriers; this behavior has been seen in other biomolecular systems. To study protein dynamics, we performed a 1.2-ns molecular-dynamics trajectory calculation of crambin in aqueous solution. This trajectory sampled multiple local energy minima.

Collective motions of amino acids over long distances lead to transitions between local energy minima. We have shown that nonlinear motions produce most of the atomic fluctuations of the protein. These fluctuations are not well described by large motions of individual atoms or by a small group of atoms; they are well described by concerted motions of many atoms. These nonlinear motions produce transitions between different basins of attraction. Signatures of these motions appear in local and global structural variables.

We have also developed a way to extract molecule optimal dynamic coordinates (MODC); we have used a generalization of this method to identify small (1–3) dimensional subspaces of the configuration space which describe the dynamics of the protein in the context of a nonlinear multibasin system.

We model the dynamics of biomolecules with an open Newtonian system (the protein) coupled to a stochastic system (the solvent). Autocorrelation functions of the displacements along relevant MODC show that the protein loses memory of its position within a few picoseconds.

We also find that the diffusion of the protein in configuration space is anomalous: the time dependence of its mean-square displacement is not proportional to time, but to t^{2H_D}, where $2H_D$ is a nontrivial fractional exponent; transitions among energy minima far apart in configuration space show a stretched-exponential time dependence which scales as $t^{-2H_D}\exp(-t^{-2H_D})$, with $H_D < 0.5$. This picture is consistent with a model suggested by Frauenfelder and collaborators to explain multiple-timescale relaxation processes observed in myoglobin.

Theory of Solvation. We have analyzed and implemented a continuum dielectric model for solvation of electrostatic interactions in aqueous solutions. The method developed to solve the requisite macroscopic Poisson equation is essentially a boundary-element method, but it differs from previous numerical algorithms used for this problem by sampling the molecular surface with quasi-random-number series. This approach allows us to explicitly demonstrate numerical convergence and to systematically use coarse-grained results.

We tested this method by applying it to a range of solvation problems in aqueous solutions, including obtaining the potentials of mean force for (a) NaCl, (b) the SN2 reactive system chloride-methylchloride, and (c) the SN2 reactive system hydroxide-formaldehyde. When we analyzed the results of these tests, we determined that the success of the dielectric model results from a solvation stabilization of ionic

fragments that is physically reasonable.

The success of the dielectric model encouraged us to study the molecular theory for the model in more depth. As a result we developed new theory. Our analysis of the new theory and testing it with molecular simulation data has provided a basic understanding of the conventional parameterizations of the dielectric model.

Free Energy Calculations

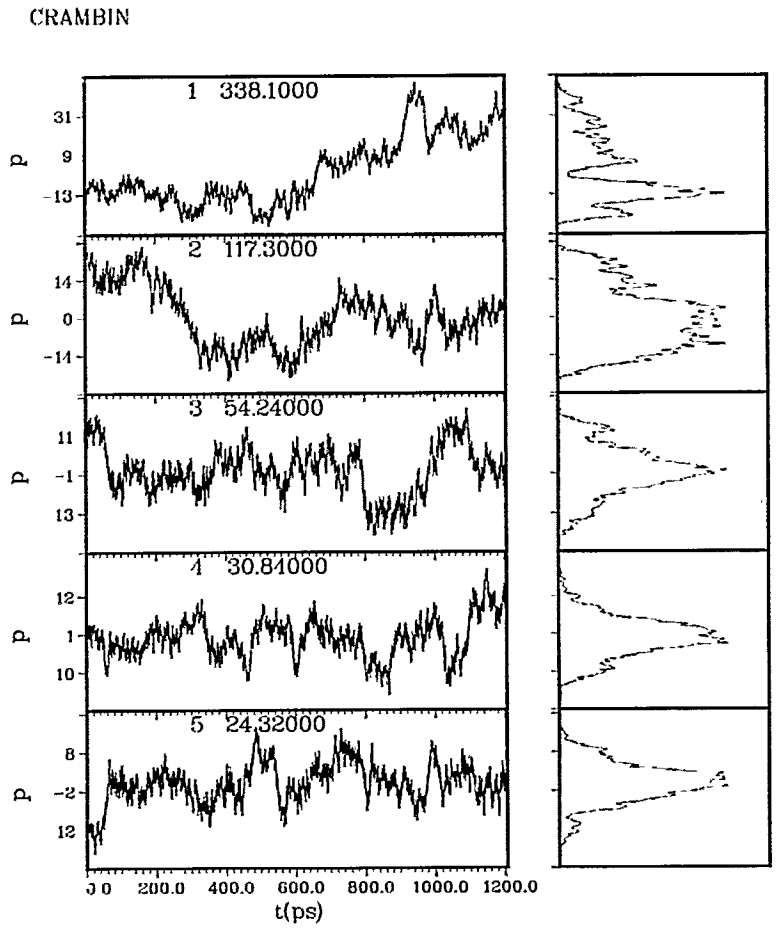
Ionic Hydration. The hydration free energies of ions depend on the ionic charge in an approximately quadratic fashion, as predicted by the Born model. We have analyzed this behavior using second-order perturbation theory.

Our analysis provides an effective way to calculate free energies from equilibrium computer simulations. The average and the fluctuations of the electrostatic potential at charge sites appears as the first coefficients in a Taylor expansion of the free energy of charging. Combining data from different charging states allow us to calculate free-energy profiles as functions of ionic charge. We accurately calculated the first two coefficients of the Taylor expansion from equilibrium simulations, but these calculations were affected by a string system size dependence. We applied corrections for these finite-size effects by using Ewald lattice summation and adding self-interactions consistently. We have published results using this technique for a model ion with methane-like Lennard-Jones parameters in simple-point-charge (SPC) water model.

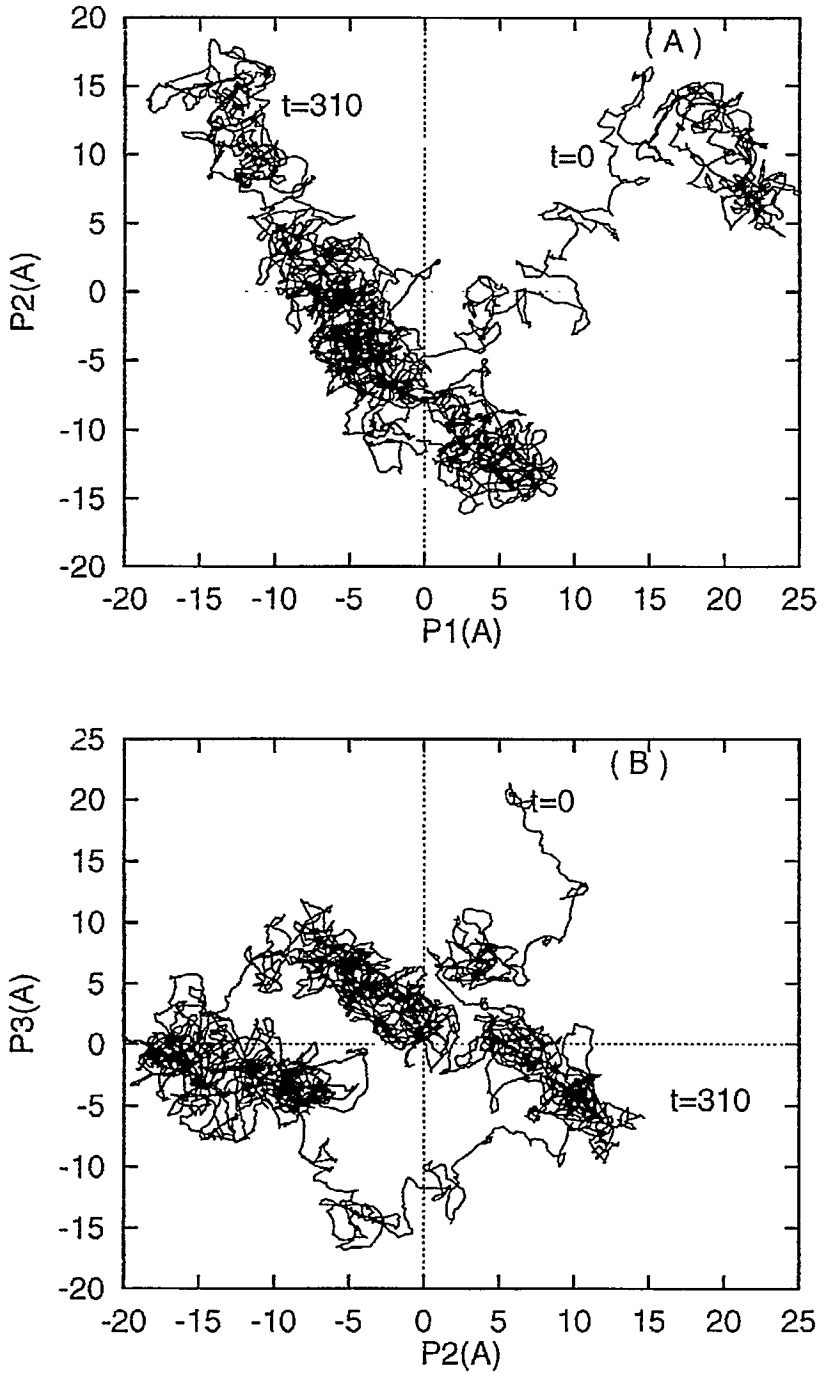
We found two approximately quadratic regimes with different parameters for positive and negative ions. Negative ions are more strongly solvated than positive ions of equal size, as is determined by the solvation free energies. We ascribed this preference of negative ions to their strong interaction with water hydrogens. We consistently found a positive electrostatic potential at the center of uncharged Lennard-Jones particles, which also favorably affects the free energy of solvation of negative ions.

Hydration Free Energy of Water. Using perturbation theory we studied the chemical potential of water as a function of charge. By calculating the electrostatic-energy fluctuations of two states (fully charged and uncharged), we were able to accurately determine the dependence of the chemical potential on charge. We obtained identical results for the chemical-potential difference of fully charged and uncharged water from overlapping-histogram and acceptance-ratio methods and by smoothly connecting the curves of direct exponential averages.

Our results agreed well with those published by Rich and Berne with respect to both the chemical-potential difference and its dependence on the charge-coupling parameter. We also observed significant deviations from simple Gaussian fluctuations statistics. The dependence on the coupling parameter is not quadratic, as would be expected from linear-continuum methods of electrostatics.



Projections $p_i(t)$ of the 1200-ps molecular-dynamics trajectory along the five principal molecule optimal dynamic coordinates (MODC) are shown in the plots on the left. The plots on the right are histograms of the frequency of occurence of all values of $p_i(t)$ for the corresponding vector. The units for $p_i(t)$ are angstroms; the units for time are picoseconds. The labels at the top of each curve show the eigenvalues, from large to small, in Å^2.



Projections for the first 310 ps of the molecular-dynamics trajectory on the plane spanned by directions (A) m_1 and m_2 and (B) m_2 and m_3. The initial (t = 0) and final (t = 310 ps) positions of this trajectory on the plane are labeled in the figures. The distribution of sampled conformations shows four basins of attraction. These basins are densely sampled during the simulation.

Publications

Garcia, A.E., "Multi-Basin Dynamics of a Protein in Aqueous Solution," in *Nonlinear Excitations in Biomolecules*, M. Peyrard, Ed. (Springer, Berlin, 1995), p. 191.

Garcia, A.E., and J.G. Harman, "Simulations of CRP:(cAMP)2 in Non-Crystalline Environment Show a Transition from the Open to Closed Conformation" (to be published in *Protein Science*).

Garcia, A.E., R. Blumenfeld, G. Hummer, et al., "Diffusion of a Protein in Configuration Space" in *Proceedings of the 9th Conversation in Biomolecular Stereodynamics*, R.A. Sarma, Ed. (Adenine Press, Schenectady, New York, in press).

Garde, S., G. Hummer, L.R. Pratt, et al., "Information Theory Modeling of Hydrophobicity" (submitted to *J. Phys. Chem.*).

Gu, W., and B.P. Schoenborn, "Molecular Dynamics Simulation of Hydration in Myoglobin," *Proteins: Structure, Function & Genetics* **22,** 20 (1995).

Gu, W., A.E. Garcia, and B.P. Schoenborn, "Understanding Water Interactions with Myoglobin by Molecular Dynamics Simulations," in *Neutrons in Biology*, B.P. Schoenborn and R. Knott, Eds. (Plenum Press, New York, in press).

Hummer, G., "Electrostatic Potential of a Homogenously Charged Square and Cube in Two and Three Dimensions" (to be published in *J. Electrostatics*).

Hummer, G., "The Numerical Accuracy of Truncated Ewald Sums for Periodic Systems with Long-Range Coulomb Interactions," *Chem. Phys. Lett.* **235,** 297 (1995).

Hummer, G., L.R. Pratt, and A.E. Garcia, "On the Free Energy of Ionic Hydration" (to be published in *J. Phys. Chem.*).

Hummer, G., L.R. Pratt, and A.E. Garcia, "The Hydration Free Energy of Water," *J. Phys. Chem.* **99**, 14188 (1995).

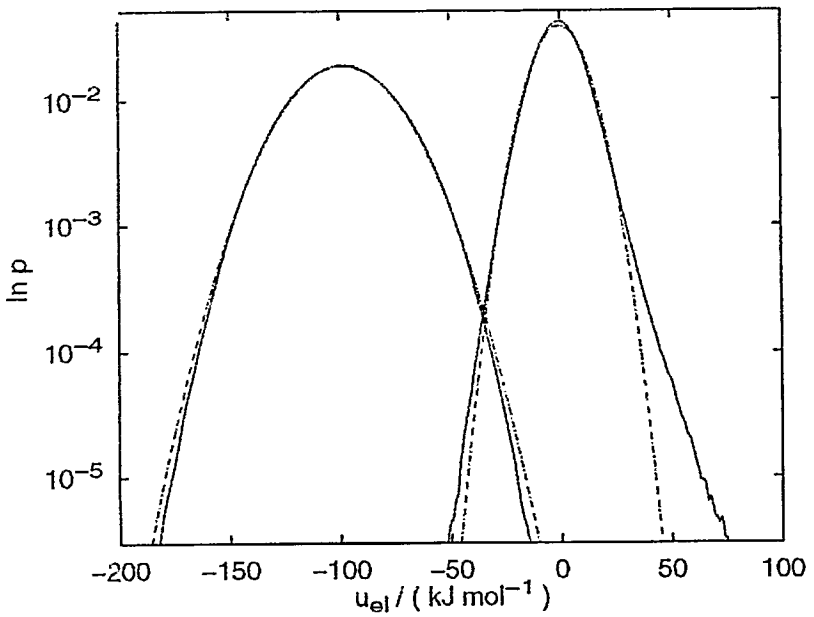
Oprea, T.I., and A.E. Garcia, "Three-Dimensional Quantitative Structure Activity Relationship of Steroid Aromatase Inhibitors. Multiple Validation of a 3d-Qsar Mode" (submitted to *J. Computer-Aided Mol. Design).*

Pratt, L.R., G.J. Tawa, G. Hummer, et al., "Boundary Integral Methods for the Poisson Equation of Continuum Dielectric Solvation Models" (to be published in *J. Phys. Chem.*).

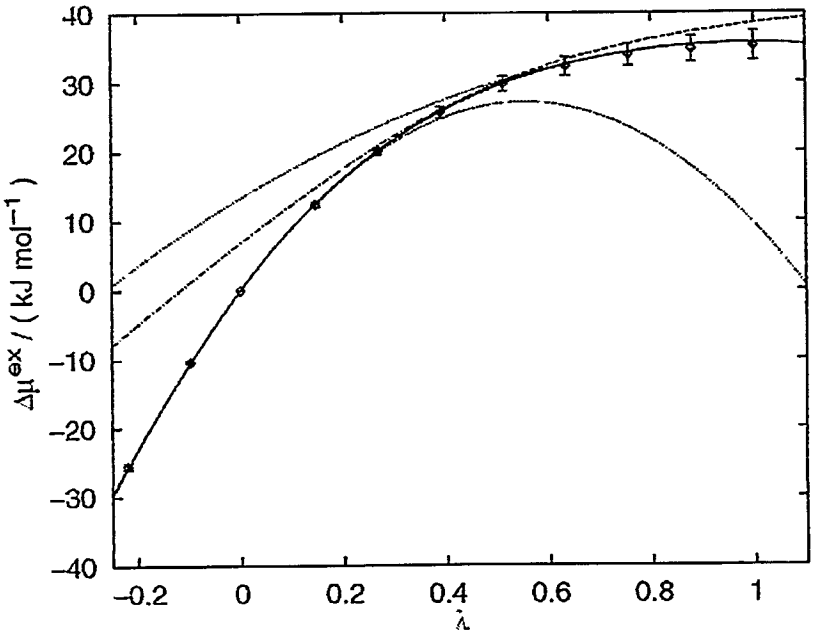
Ritchie, J.P., and A.S. Copenhaven, "Comparison of Potential-derived Charge and Atomic Multipole Models in Calculating Electrostatic Potentials and Energies of Some Nucleic Acid Bases and Pairs," *J. Comp. Chem.* **16**, 777 (1994).

Schlichting, I., J. Berendzen, G.N. Phillips, et al., "Crystal Structure of an Intermediate of CO Binding to Myoglobin," *Nature* **371**, 808 (1994).

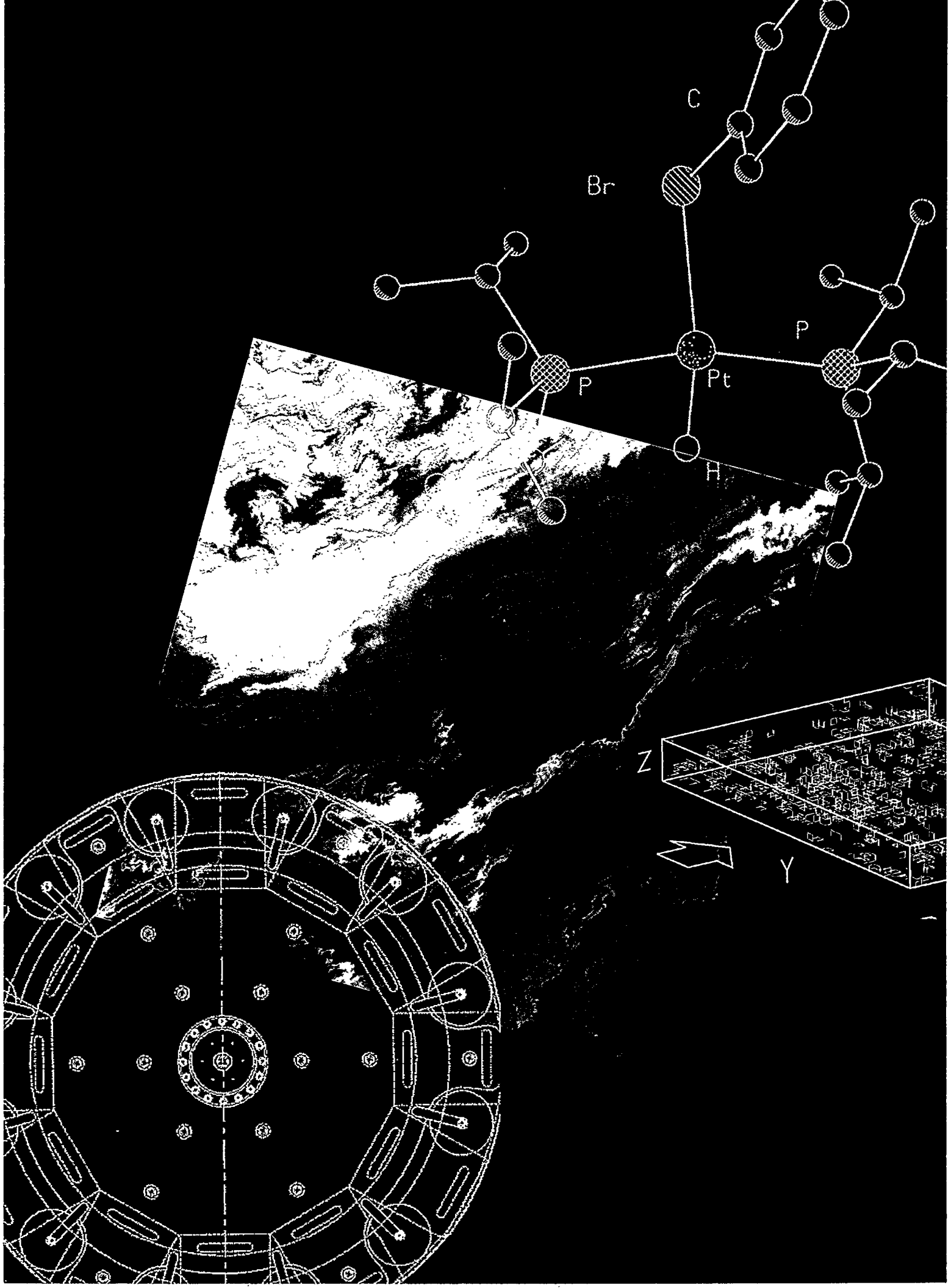
Tung, C.-S., T.I. Oprea, G. Hummer, et al., "Three Dimensional Model of a Selective Theophylline-Binding RNA Molecule" (to be published in *J. Mol. Recognition*).



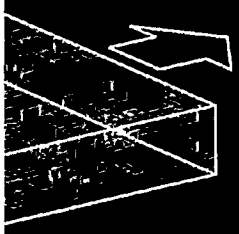
Probability density of the electrostatic energy U_{el} of a water molecule with full charge (centered near –100 kJ/mol) and zero charge (centered near 0 kJ/mol). The probabilities are shown on a logarithmic scale; Gaussians appear as parabolas. Also shown are Gaussian distributions (dashed lines),with mean and variance equal to distributions calculated from Monte Carlo simulations using 216 water molecules with Ewald summation. The curves do not include corrections for self-interactions.



The chemical potential $\Delta\mu^{ex}$ of water as a function of its charge λ. The fully charged and uncharged states are given by λ = 0 and λ = 1, respectively. Solid lines are eighth-order polynomials fitted to the cumulants of $C_{1,1}$, $C_{2,1}$, $C_{3,1}$, and $C_{4,1}$ of the electrostatic potential distributions for λ = 0 and λ = 1. The curves for Ewald-summation and generalized-reaction-field (GRF) data are practically indistinguishable. The data of Rick and Berne are shown as symbols with bars. The results from direct calculations are also shown. The expansions around the charged (λ = 0) and uncharged (λ = 1) states are shown with dashed and dot-dashed lines, respectively. Both cases use data from Ewald-summation simulations. The dotted lines represent quadratic expansions around λ = 0 and λ = 1 using mean and variance of the Ewald-summation data and assuming Gaussian statistics.


C
Br
P
P
Pt
H
Z
Y





INDEX OF PRINCIPAL INVESTIGATORS

Index of Principal Investigators

A

Abdallah, Jr., J. 96
Adams, T. 218
Agrawal, D. 223
Aidun, J.B. 185
Albers, R.C. 183
Altherr, M. 150
Aubrey, J. 258

B

Baldridge, W.S. 226
Barlow, D. 195
Bartlett, R.J. 93
Bedell, K. 22, 187, 222
Benjamin, R.F. 195
Berkbigler, L.W. 42
Birn, J. 120, 231
Bishop, A. 81, 178, 227
Bitensky, M. 321
Bocian, D.F. 205
Borovsky, J. 123
Bossert, J. 110
Bourke, M. 168
Bowles, T. 129, 318
Bowman, C. 264
Bowman, J.D. 137
Bradbury, E.M. 327
Bronisz, L. 44
Brown, D. 76
Buelow, S. 293
Burns, C. 57, 64

C

Camassa, R.A. 75
Campbell, I. 271
Canavan, G.H. 281, 312
Carlsten, B. 47
Cartwright, D. 298
Casperson, D. 121
Castro, A. 147
Cerutti, J.H. 306
Chen, S. 82
Chen, W. 88
Chidester, K. 315
Clark, T. 51
Cockroft, N. 270
Collins, L.A. 91
Conradson, S. 93
Cooke, D.W. 16
Cort, B. 184
Cram, L.S. 237
Cranfill, C. 210
Cremers, D.A. 36
Cross, J. 255

D

Daemen, L. 10
Darling, T. 40
Dixon, R. 18
Doering, C. 160
Doggett, N. 140, 226
Donohoe, R. 7, 16, 205
Doolen, G. 220, 300
Doyle, J. 297
Dreicer, J.S. 295
Duke, J. 259
Dye, R. 250
Dyer, R.B. 141

E

Ecke, R. 45
Eckert, J. 183
Edeskuty, F. 278
Epstein, R. 214

F

Faber, V. 84, 220
Farrar, C. 35, 212, 277
Fasel, J. 223
Fazio, M. 38, 56, 284
Fearey, B. 307
Federspiel, F. 136
Fehler, M. 121, 310
Fenimore, E. 103
Fitzsimmons, M. 171
Flynn, E.R. 197
Foltyn, S. 247
Forslund, D. 306
Frauenfelder, H. 207, 239
Freyer, J. 148
Fry, H. 98
Funk, D. 197
Funsten, H. 268, 279

G

Gac, F. 258
Garcia, A. 139, 328
Garzon, F.H. 42
Gerstl, S. 236, 265
Giles, J. 265
Glatzmaier, G.A. 101, 216
Goff, F. 103
Goldman, T. 137
Goldstone, J.A. 19, 164
Goodwin, E. 149
Gosling, J. 109
Gosnell, T.R. 28, 99
Gottesfeld, S. 37
Gray III, G. 11
Gritzo, R. 272
Gubernatis, J. 213
Gupta, G. 153
Gupta, R. 132
Guthrie, Jr., G.D. 108
Guzik, J. 122

H

Hagan, P. 77
Hahn, H.A. 230
Hamkalo, B. 237
Hammel, P.C. 252
Hasslacher, B. 85
Hawley, M. 190
Heffner, R. 177, 251
Heighway, E. 1
Henriksen, A. 40
Hermes, R.E. 68
Hersman, L. 236
Hickmott, D.D. 104
Hills, J.G. 128
Hixson, R. 14
Hjelm, R. 179, 182
Hoffbauer, M. 30
Hoffman, C. 132
Holm, D. 87, 208
Huling, J. 257
Hyman, J. 76, 77, 86, 90

J

Jackson, P. 326
Janecky, D.R. 311
Jarvinen, G. 172
Jason, A. 314
Jen, E. 80
Johnson, J.N. 185
Johnston, R. 35, 43
Jones, M. 46
Joyce, E. 296

K

Kao, C.-Y.J. 118, 224
Keller, C. 218
Keller, R. 238, 319
Kennedy, J. 287
Kinnison, W. 133
Kirkpatrick, R. 199
Kocks, U.F. 160
Kraus, R. 36
Kubas, G. 66
Kwan,T. 49
Kyrala, G.A. 94

L

Lackner, K. 201
Lapedes, A. 230, 321
Laurich, B. 28
Lehnert, B. 320
Lesar, R. 304
Lewis, G. 41, 275
Lindemuth, I. 266
Little, R. 302
Lomdahl, P. 214
Lowe, T. 223

M

MacArthur, D. 256
Macinnes, M. 201
Mack, J. 263
Maggiore, C. 199
Mainieri, R. 79, 228
Maley, M. 248
Margolin, L. 217
Marrone, B. 144
Martin, R. 57
Mason, R. 52
Mattis, M. 133
McBranch, D. 72, 254
Middleditch, J. 106
Migliori, A. 14, 19
Miller, W. 104, 124
Mitchell, M 10
Mitchell, T. 191
Morel, J. 85, 222
Morris, C.L. 43
Mosteller, R. 231
Mottola, E. 135, 221
Mourant, J. 146
Mroz, E. 116
Muenchausen, R. 15
Munroe, J. 275

N

Nelson, R.O 271
Nguyen, D. 54
Nogar, N. 34, 203

O

Olinger, C. 298
Olivares, J. 32
Ott, K. 293

P

Pack, R.T. 59
Paffett, M. 204
Papcun, G. 299
Park, M.S. 152, 237
Peng, J.-C. 136
Phillips, D. 186
Pittman, P. 44
Pogue, E. 280
Poling, D. 207
Prather, K.A. 202
Pratt, L. 153
Prenger, F.C. 276

R

Regan, A. 274
Robinson, B. 108
Robinson, J.M. 115, 202
Rose, H. 114
Rosocha, L. 196
Roussel-Dupré, R.A. 112
Russell, G. 316
Ryne, R. 200

S

Saltzman, J. 84, 211
Sanderson, J. 269
Sandford, M. 86
Sauer, N. 289
Schake, A. 291
Scheuer, J. 53, 285, 286
Schiferl, D. 122
Schmidt, S. 63
Schoonover, J. 70
Schroeder, N. 292
Schultz, J. 309
Schwarz, R.B. 171
Scott, M. 254
Scovel, J. 83
Scripsick, R. 170
Selwyn, G. 283
Shankland, T. 188
Shi, N. 162
Silks, L. 149
Sinnis, C. 135
Smith, B. 294
Smith, D. 22, 174
Smith, G. 173, 174, 182
Smith, J. 260
Smith, P. 60
Solem, J.C. 279
Soll, W. 88
Sonek, G. 238
Spriggs, G. 34
Strauss, C.E.M. 99
Stroud, P. 296
Suszcynsky, D. 114
Swanson, B. 73
Swift, G. 269
Sze, R. 37

T

Taylor, A. 25, 39
Taylor, C. 247
Terwilliger, T. 152
Thode, L.E. 47
Thompson, J. 235
Thompson, J.D. 163, 166, 257
Thomsen, M. 118
Tilden, M. 282
Torney, D. 147, 227
Trewhella, J. 240, 242, 324
Trugman, S. 177
Tumas, W. 65
Tung, C.-S. 142
Tuszewski, M. 48

U

Unkefer, C. 140
Unkefer, P. 265

V

Van Eeckhout, E. 300
Venneri, F. 290, 313
Vieira, D. 130
Von Dreele, R. 161, 167
Voter, A. 69

W

Wagner, H. 55
Wang, T.-S. 54
Warnock, T. 78
Watkin, J. 59, 61, 71
Watkins, D. 30
West, G. 134
Wills, C. 226
Wills, J. 159, 186
Winske, D. 125, 235
Wood, C. 322
Woodruff, W. 69, 145, 238
Wray, W.O. 323
Wu, X.D. 250

Z

Zawodzinski, T. 62
Zurek, W.H. 126
Zweig, G. 89
Zyvoloski, G. 302

This report has been reproduced
directly from the best available copy.

It is available to DOE and DOE
contractors from the Office of
Scientific and Technical Information,
P.O. Box 62,
Oak Ridge, TN 37831.
Prices are available from
(615) 576-8401.

It is available to the public from the
National Technical Information
Service,
US Department of Commerce,
5285 Port Royal Rd.
Springfield, VA 22616.